Residency and trafficking of ILC2s in steady state and Th2 induced inflammatory conditions

Maxime Petit

Université de Paris

École doctorale BioSPC - ED562

Unité Lymphopoïèse / Inserm U1223 – Institut Pasteur

Residency and trafficking of ILC2s in steady state and Th2 induced inflammatory conditions

Préparée par **Maxime PETIT**

Thèse de doctorat d'Immunologie

Dirigée par Rachel GOLUB

Présentée et soutenue publiquement à l'Institut Pasteur - Paris le 17 Décembre 2019

Président du jury :	EBERL Gérard / Professor / Institut Pasteur
Directeur de thèse :	GOLUB Rachel / Professor / Université Paris Diderot
Rapporteur :	GIRARD Jean-Philippe / Professor / Université Toulouse III
Rapporteur :	BJORKSTROM Niklas / Professor / Karolinska Institutet Medical University
Examinateur :	JABRI Bana / Professor / University of Chicago
Examinateur :	DALMAS Élise / Chargé de Recherche / Sorbonne Université
Membre invité :	GUY-GRAND Delphine / Chercheur Émérite / Institut Pasteur

ACKNOWLEDGMENT

Tu n'as pas pu me soutenir durant ces 3 années, mais tu me soutenais plus que quiconque. Tu as été plus fier que toute autre personne avant même le commencement de ma thèse. Tu es resté et tu resteras toujours présent dans ma vie.

Ainsi, tu es le premier à qui je dédie cette thèse.

Je dédie cette thèse à tous ceux qui ont compté, participé et soutenu, de près ou de loin, à sa réalisation.

Tout d'abord, je remercie les différents membres de l'unité lymphopoïèse, notamment Ana Cumano pour m'avoir accueilli et soutenu toutes ces années au sein du laboratoire.

Je remercie ma directrice de thèse, Rachel Golub, de m'avoir accueilli il y a si longtemps au sein de son équipe, tout d'abord en stage de master puis de m'avoir fait confiance pour effectuer un doctorat sur un sujet si particulier. Je la remercie pour toutes les expériences que j'ai vécues ces dernières années et qui m'ont permis d'évoluer.

Je remercie tout particulièrement Delphine Guy-Grand, qui m'a permis de beaucoup évoluer après des heures de discussion, animées ou non, et toujours sincères et amicales. Tu as toujours été présente pour moi, comme la grand-mère que je n'ai jamais eu, à m'inviter dans ta si belle maison, et nous avons pu développer plus qu'une relation professionnelle épanouissante.

Je remercie Odile pour tout le travail important au quotidien au laboratoire, et sans qui beaucoup de choses essentielles ne seraient pas faites.

MC, je te remercie pour ton travail et ton investissement afin d'aider tous les membres du laboratoire, pour ta bonne humeur et le soutien dont tu fais preuve au quotidien.

Je remercie tous les étudiants avec qui j'ai vécu ces dernières années : Sylvestre Chea pour ce qu'il nous a transmis, aussi bien scientifiquement, humainement, que techniquement. Damien Garidot, qui a fait partie de mes premières rencontres au laboratoire et avec qui nous avons passé des moments riches en rigolades. Claire Berthault qui a laissé un vide à la fin de sa thèse. Je remercie Junjie, pour toute sa bonne humeur quotidienne malgré toutes les difficultés que tu as pu traverser. Merci également à Francisca pour toutes ces histoires vécues ensemble et sans qui beaucoup de moments n'auraient pas été les mêmes. Je te dirai seulement : Éo so stupide. Je remercie Ramy pour tout ce que tu nous apportes, beaucoup de légèreté au quotidien et toutes ces discussions ouvertes d'esprit.

Je remercie Lucia et Elena, avec qui nous avons vécu beaucoup d'heures de travail, souvent très efficaces, mais surtout toujours rendues si drôles et uniques, et qui ont laissé un vide à leur départ. Tous les étudiants que nous avons pu encadrer de près ou de loin, au

cours de ces années ; Mélissa, Émilia, Ioana, Florian, Sarah, Youssef, Amélie et tous les autres avec qui nous avons généralement passé de nombreuses heures à s'amuser, au labo et en dehors.

J'en arrive à deux personnes particulières du laboratoire : Sylvain, avec qui je passe énormément de temps depuis ces deux dernières années. Je te remercie d'avoir été présent pour moi depuis ton arrivée, professionnellement et humainement ; et Thibaut, avec qui nous avons fait les 400 coups à l'Institut Pasteur et en dehors depuis mon arrivée en master. Cela fait bien longtemps et nous avons vécu tout ce qui est possible de vivre, en bien comme en mal, au sein d'un laboratoire, ensemble. La fin est enfin arrivée pour nous deux mais ces nombreux moments resteront gravés.

Durant ces années, j'ai eu la chance de faire beaucoup de rencontres à l'Institut. Je remercie tous les membres du département d'immunologie, ainsi que toutes personnes d'autres départements, pour les moments vécus ensemble, qu'il soit cité ici ou non. Je remercie tout d'abord François Huetz, que je considère comme un mentor, tu le sais, pour toutes ces discussions que nous avons pu avoir. Tu m'as transmis le poste de technicien informatique de Delphine, mais tu as surtout toujours été de bon conseil et une personne de confiance pour moi. Je remercie également Myriam qui m'a soutenu et guidé pendant une bonne partie de la thèse.

Je remercie Erminia, Melania et Thomas, pour tous ces instants vécus ensemble.

Suryia, Nicolas, Hanane et Claire, des visages du quotidien qui me manqueront beaucoup.

Je remercie Philippe Bousso, qui m'a permis de passer de nombreuses heures dans son laboratoire, au sein duquel je tiens à remercier Jeremy, une personne formidable qui m'a beaucoup fait rire ; Sacha, je pense qu'il est essentiel d'avoir un soutien quotidien, qui redonne le sourire en toutes circonstances, et tu es de ces personnes, un véritable maitre pour nous ; Fabrice, qui participe toujours en binôme avec Sacha à redonner le sourire ; et finalement

Marine, Margot et Morgane avec qui nous vivons également beaucoup de moments. Idan, je te remercie de ta bonne humeur constante.

Je remercie Ophélie, la meilleure des ingénieures et une joueuse de pétanque hors pair ; Pablo, avec qui discuter est toujours un grand plaisir, nous amenant à des conversations pas toujours faciles à suivre tant elles sont folles. Je remercie Éva et Bianca, qui, après une rencontre due au hasard dans un train, m'ont souvent accueillies dans leur laboratoire.

Merci à Joy, qui n'est plus à l'institut mais qui a partagé avec Jeremy beaucoup de son temps pour développer les relations entre étudiants du département. Estelle, toujours cachée derrière une porte, qui a rendu mes visites au quatrième très surprenantes.

Je remercie Nicolas, Dylan et Angélique qui partagent cette si particulière passion des ILCs.

Je remercie tous les membres de la plateforme, Mamie Sophie, Sandrine, Pierre-Henry et toutes ces heures folles passées ensemble en pièce de tri, et Seb, ce grand fou.

J'ai pu rencontrer à la Stapa de nombreuses personnes avec qui j'ai développé une amitié et passer de magnifiques moments : Nicolas, Alexis, Crispin, Pedro, Caris, Javier, Sol, et tous les autres, merci.

Je vous souhaite à tous le meilleur.

Je dédie cette thèse à tous les membres de ma famille, présents ou non au quotidien, mais qui me soutiennent et me soutiendront toujours. Je tiens énormément à chacun d'entre eux.

Je tiens à dédicacer cette thèse à une poignée de personnes très proches de moi, me soutenant le plus au quotidien et avec qui je vis tellement de choses.

Malgré tout ce qui a pu être difficile entre nous, en master et en thèse, je remercie Zu de tout mon cœur pour tout ce qu'elle m'a apporté et tous ces moments magiques que nous avons vécus. Tu as fait de moi quelqu'un de meilleur, et je tiendrai toujours autant à toi.

Poulet, on a vécu l'année la plus difficile ensemble. On continue nos soirées traditionnelles, et on les continuera longtemps encore ! Je t'embrasse, on a encore beaucoup de choses à fêter ensemble.

À Bernardo, après toutes ces années, tes silences sont d'or et ta présence toujours aussi rassurante. Me supporter démontre ta force, et nous continuerons à vivre de nombreux moments idiots ensemble.

Killer, moins silencieux mais tout aussi présent, notre amitié t'a même convaincu de te mettre au rugby. Avec ton optimisme, tu deviendras solide j'en suis sûr ! Plus sérieusement, ces années de thèse sans toi auraient été si ce n'est futile, beaucoup moins marantes et faciles. On continuera à vivre beaucoup de choses ensemble, surtout des voyages de bons vivants.

Mademoiselle Parfaite, compliquée et facile à la fois, tout est mieux de jours en jours. Il n'y a pas plus à dire que tu ne saches déjà. Tu es un soutien inébranlable et j'espère que cela durera longtemps.

ABSTRACT

ILC2s are found in mucosal tissues as lung and intestine, in lymph nodes, and in metabolic tissues such as the adipose tissues. They play important role in maintaining or inducing type-2 immune responses as innate equivalent of Th2 lymphocytes. They are activated by alarmins (IL-25 and IL-33) and by external activators (allergens, metabolites and neuromediators). ILC2s are secreting type-2 cytokines to facilitate the activation of other cells and to induce an important repair program. Their activation allows large type of events as diverse as myeloid cells recruitment and activation, mucus production, muscle contractility and tissue repair. They have key role in lung and adipose tissue development and maintain their homeostasis by early responding against parasitic pathogens. Abnormal activation of ILC2s is also participating to chronic diseases.

ILCs are mostly considered as resident cells. However, different studies suggested that migration could be important for the maturation of their effector capacities and to correctly target the injured tissue. Circulation and trafficking of ILC subsets is still unclear. No mechanism is yet available to explain the turnover of ILC2s and how they can act in many tissues following *stimuli*.

We found that large numbers of mature and immature ILC2s could be collected in the thoracic duct lymph of mice perfused over several hours, showing that ILC2s are in fact actively circulating through the hemo-lymphatic circuit. Furthermore, circulating mature ILC2s could be separated into three distinct subsets depending on their pattern of receptor and adhesion molecule expression. Cell transfer experiments proved that specific patterns are representative of specific tropism for gut, lung and adipose tissues.

To analyse ILC2 behaviour in the context of a type-2 response, we injected IL-25 and IL-33 before lymph collection. IL-33 stimulation largely enhanced the number of circulating ILC2s in the lymph. These different ILC2 tissue targeted subsets responded differently to IL-33. Specifically, gut-trafficking ILC2s were mainly stimulated to proliferate whereas lung and adipose tissue subsets were stimulated to produce IL-13, IL-5 and Areg. This suggests that, in ILC2s, specific tissue targeting is associated with already imprinted functions while transiting through the hemo-lymphatic system. We confirmed these functions of circulating ILC2 subsets in more physiological context by mimicking allergy and helminth infection (stimulation by papain and succinate) where specific migration to lungs and intestine play important roles in mounting the type-2 response by IL-5/IL-13 secretion, and also initiating tissue repair by Areg production. Interestingly, we showed that lung migrating ILC2s participated to resident pool renewal that main function is Areg production. Finally, we characterized important trafficking of ILC2 at different stages of *Nippostrongulus brasiliensis* infection, confirming the functional relevance of ILC2 trafficking.

Keywords : ILC2 ; Circulation ; Thoracic Duct ; Lymph ; Homeostasis ; Intestine ; Lungs ; *Nippostrongulus brasiliensis*

RÉSUMÉ

Les ILC2s sont retrouvées au niveau des muqueuses comme les poumons et l'intestin, ainsi que dans divers ganglions et organes liés au métabolisme comme les tissus adipeux (ATs). Elles jouent un rôle important dans l'induction des réponses immunitaires de type Th2 comme équivalents innées dans lymphocytes Th2. Elles sont activées par des alarmines (IL-25 et IL-33) et des activateurs environnementaux (allergènes, métabolites et neuromédiateurs). Les ILC2s sécrètent des cytokines de type Th2 permettant de recruter et d'activer des cellules myéloïdes, d'augmenter la production de mucus et la contraction musculaire, ainsi que d'initier la réparation et le renouvellement des tissus. Cependant, une activation non contrôlée des ILC2s participe au développement de maladies chroniques.

Les ILCs sont généralement considérées comme des cellules résidentes. Cependant, plusieurs études ont suggéré que la migration pourrait être un processus important pour la maturation des capacités effectrices. La circulation des ILCs reste peu documentée, et aucun mécanisme n'est pour l'instant capable d'expliquer le renouvellement des ILC2s pour agir dans de nombreux tissus suite à une stimulation.

Nous avons montré que des quantités significatives d'ILC2s matures et immatures peuvent être collectées dans la lymphe du canal thoracique de souris canulées durant plusieurs heures. Les ILC2s circulantes forment 3 groupes distincts avec des expressions de molécules d'adhésion et récepteurs de migration spécifiques. Nos expériences de transferts cellulaires montrent que ces groupes spécifiques de molécules exprimées sont liés à des tropismes particuliers pour l'intestin, les poumons ou les ATs.

Pour analyser le comportement des ILC2s dans un contexte de réponse de type Th2, nous avons injecter les cytokines IL-25 et IL-33 et étudié la lymphe de ces souris. La stimulation à l'IL-33 augmente le nombre de cellules ILC2s circulants dans la lymphe. Les différents groupes d'ILC2s montrent des réponses différentes à l'IL-33. Ainsi, les ILC2s migrants vers l'intestin sont majoritairement prolifératives tandis que le groupe migrant vers les poumons et les ATs secrètent de l'IL-5, de l'IL-13 et de l'Areg. Cela suggère que les ILC2s migrants de façon spécifique possèdent une empreinte fonctionnelle. Nous confirmons les fonctions des groupes d'ILC2s circulants en utilisant des modèles plus physiologique mimant des réactions allergiques et des infections parasitaires (stimulation par la papaïne et le succinate). Les migrations vers l'intestin et les poumons jouent un rôle primordial dans l'induction de réponse de type Th2 par sécrétion d'IL-5 et d'IL-13, et à l'initiation de la réparation tissulaire par production d'Areg. De façon intéressante, les ILC2s migrants vers les poumons participent au renouvellement des populations résidentes participant principalement à la production d'Areg. Finalement, nous caractérisons un rôle important du trafic des ILC2s à différents temps suivant l'infection par *Nippostrongulus brasiliensis*, confirmant la fonction des ILC2s migrantes.

Mots-clés : ILC2 ; Circulation ; Canal Thoracique ; Lymphe ; Homéostasie ; Intestin ; Poumons ; *Nippostrongulus brasiliensis*

LIST OF ABBREVIATIONS

6-OHDA : 6-hydroxydopamine
AA : allergic asthma
AC : adenylate cyclase
AD : Atopic dermatitis
AHR : airway hyper-responsiveness
AR : androgen receptor
Areg : amphiregulin
Arg1 : Arginase 1
ATs : Adipose Tissues
APC : Allophycocyanin
BAT : brown adipose tissue
Bcl11b : B-Cell Lymphoma/Leukemia 11B
BCR : B Cell Receptor
BCS : blood circulatory system
BM : Bone Marrow
bmAT : bone marrow adipose tissue
CCR9 : C-C motif chemokine receptor 9
CF : cystic fibrosis
CFTR : CF transmembrane conductance regulator
ChILP : Common helper ILC Precursor
CLA : cutaneous lymphocyte antigen
CLP : Common Lymphoid Progenitor
COPD : obstructive pulmonary disease
CRS : chronic rhinosinusitis
DC : dendritic cells
DHT : 5α-dihydrotestosterone
dILC2 : dermal ILC2
DSS : dextran sodium sulfate
DSS : dextran sulfate sodium
E2A : E-box transcription factors
EGF : epidermal growth factor
EILP : Early Innate Lymphoid Progenitor
EOMES : Eomesodermin
EPO : erythropoietin
Esr : oestrogen receptor
ETP : Early Thymic Progenitors
FCS : Fetal Calf Serum
FDC : Follicular Dendritic Cells
FL : Fetal Liver
FRCs : fibroblastic reticular cells
FS : Fetal Spleen
GALT : gut-associated lymphoid tissue
GI : gastrointestinal

GPCRs : G protein–coupled receptors
HBSS : Hank's Balanced Salt Solution
HDAC : histone desacetylase
HDM : House Dust Mite
HEV : High endothelial vessels
HFD : high fat diet
HIF1α : hypoxia- inducible factor 1α
HLH : helix-lool-helix
IAV : Influenza A virus
ICAM-1 : intercellular adhesionmolecule-1
Icos : inducible T cell costimulatory
Ih2 : Innate Helper 2
iILC2 : inflammatory ILC2s
IL-1RAcP : IL- 1 receptor accessory protein
IL-5R : IL-5 receptor
ILC1P : intermediate ILC1 Precursor
ILC1s : group 1 ILCs
ILC2P : ILC2 Precursor
ILC2s : group 2 ILCs
ILC3s : group 3 ILCs
ILCP : ILC precursor
ILCs : Innate lymphoid cells
KLRG-1 : Killer cell lectin-like receptor subfamily G member 1
LFA1 : lymphocyte function associated antigen 1
Lin- : Lineage negative
LMPPs : Lymphoid Multipotent Progenitor
LNs : Lymph nodes
LP : L*amina Propria*
LPL : *Lamina Propria* lymphocytes
LT : leukotrienes
LTi : Lymphoid Tissue inducers
MAdCAM1 : mucosal addressin cell adhesion molecule 1
mesLNs : mesenteric LNs
MetEnk : methionine-enkephalin
N.b. : *Nippostrongulus brasiliensis*
NHCs : Natural Helper Cells
nILC2 : natural ILC2
NK : Natural Killer
NKP : NK Progenitor
NMU : Neuromedin U
NP : Nasal Polyposis
PA *: Pseudomonas aeruginosa*
PBS : Phosphate Buffered Saline

Pcsk1 : proprotein convertase subtilisin/ kexin 1
PD-1 : Programmed death 1 (CD279)
PE : Phycoerythrin
PG : prostaglandins
PNAD : peripheral node addressin
PP : Peyer's patches
Pro-Areg : glycoprotein precursor
PSGL1 : P-selectin glycoprotein ligand 1
PTX : pertussis toxin
RA : Retinoic acid
RBC : Red blood cells
RORE : ROR elements
RORα : retinoic acid-related orphan receptors alpha
RSV : respiratory syncytial virus
RTE : recent thymic emigrants
RV-16 strain : Rhinovirus
S1P : sphingosine 1- phosphate
S1PR5 : lysosphingolipid sphingosine 1-phosphate
SA *: Staphylococcus aureus*
SCFA : short chain fatty acid
SCS : subcapsular Sinuses
SI : small intestine
SMCs : smooth muscle cells
SNC : central nervous system
SPF : specific pathogen-free
SRC : non-receptor tyrosine kinases
sWAT : subcutaneous WAT
TCR : T Cell Receptor
TD : thoracic duct
TF : transcription factor
Th : T helper
TSA : trichostatin A
TSLP : Thymic Stromal LymphoPoietin
uILC2s : uterus resident ILC2s
VAT : visceral adipose tissue
VCAM1 : vascular cell adhesion molecule 1
vWAT : visceral white adipose tissue
WAT : white adipose tissue
α7nAChR : α7-nicotinic acetylcholine receptor
β2AR : β2 adrenergic receptor
γc : common gamma chain

TABLE OF CONTENTS

ACKNOWLEDGMENT .....

ABSTRACT .....

RÉSUMÉ .....

LIST OF ABBREVIATIONS .....

TABLE OF CONTENTS .....

TABLE OF ILLUSTRATIONS .....

INTRODUCTION *1*

I. Innate lymphoid cells : not so young **2**

A. A recent discovery 2

B. The T cell redundancy case 2

II. Innate lymphoid cells : derived from the lymphoid lineage **4**

A. CLP, CHILP, EILP and other ILCPs : a little bit of complexity 4

1. Common Lymphoid Progenitor : CLP 4
2. Early Innate Lymphoid Progenitor : EILP 5
3. ILC Progenitor : ChILP and ILCP 5
4. NK and ILC1 development : Not so simple 6
5. ILC3Ps et LTiP : A question of timing 6

B. ILC2 progenitor : a special development 7

1. Different stages 7
2. ILCs transcription factors 8
   a. Id2 8
   b. Gata3 8
   c. Bcl11b 9
   d. RORα 9
3. One other important pathway : Notch2 9

C. The niches question : ILC and environment 10

III. Group 2 innate lymphoid cells : the mothership **12**

A. Origins : long live the king 12

1. Fetal development 12
2. Perinatal stage 12
3. Adult renewal 13

B. ILC2 functions at homeostasis 15

1. All about localization 15
   a. Lung 16
   b. Small intestine 16
   c. Healthy fat metabolism : adipose tissues 18
   d. Pancreas 20
   e. Skin 20
2. Interactions with environment : a strong imprinting 22
   a. ILC2 activating cytokines 22
      IL-33 : the key cytokine 22

IL-25 : a redundant Th2 molecule ? 23
IL-18 : specific to the skin ? 24
b. Co-stimulatory signals of ILC2 activation 25
TSLP : lung and skin 25
IL-2 26
IL-7 26
c. Direct receptor interactions 26
Icos / Icos ligand 27
PD-1 / PDL-1/2 27
KLRG-1 / E-Cadherin 27
MHC-II / TCR 27
d. Sex sensitivity : Roles of hormones 28
e. Role of alimentary nutrients 28
f. Regulation by neuropeptides 29
3. Innate secreting helper cells 31
a. IL-4 31
b. IL-5 31
c. IL-9 32
d. IL-13 32
e. Amphiregulin 32
4. Memory ILC2s : remember me 33
C. ILC2s : important regulation for functions in diseases 36
1. Homeostatic and regulated functions 36
a. Metabolic troubles : Obesity and diabetes 36
b. Helminth infection 38
Lung infections : early stage 39
Intestinal infection : late stage 39
2. Loss of control and chronic disease 41
a. Airways diseases 41
Allergic lung diseases and asthma 41
Viral infections 42
b. Skin diseases : Dermatitis 42
c. Gastrointestinal tract : Colitis 44

IV. Immune cells migration and surveillance : the hemolymphatic system 45

A. The blood : a tissue of life 45
B. The thoracic duct lymph : from periphery to global circulation 45
1. Lymph 45
a. Lymph formation 46
b. Molecular composition at homeostasis 47
c. Molecular composition under pathologic conditions 47
2. Cellular composition of the thoracic duct lymph 48
3. Lymphatic vessels to lymph nodes 48
C. Lymph nodes (LNs) : stock and passage 50
1. LNs architecture : precise compartments for specific functions 50
2. Special organization of vessels for immune cells migration 51
a. High endothelial vessels (HEV) 51

b. Afferent lymphatic vessels 52
c. Efferent lymphatic vessels 54
D. Immune cells : a controlled migration 55
1. Chemokines 55
2. Integrins 57
3. Selectins 60
4. Markers of residency are highly expressed by ILCs 62
E. Studying circulation : not so easy 63
1. Parabiosis : the limitation of a powerful technic 63
2. Adoptive transfers or mice reconstitution : different questions 64
F. About ILCs ? 65
1. Proof of residency phenotype 65
2. But not only, the ILC2 case 66
G. Importance of circulation : a different point of view 67
1. Homeostasis : day and night variations concern 68
2. Circulation in pathology and inflammation : target for treatments 70

GOALS ***73***

MATERIALS AND METHODS ***75***

Mice 76
Technics 76
Cannulation of the thoracic duct 76
Organ dissociations 76
Cell culture 77
Adoptive transfer and reconstitution 77
In vivo mAb treatment 78
N.b. infection 78
Flow cytometry and cell sorting 78
Antibodies 78
Bioinformatics 79
Statistics 79

RESULTS ***80***

I. In steady state, different subtypes of ILC2 circulate through the hemolymphatic circuit. 81

II. Circulating ILC2 subsets have specific tropism at homeostasis 84

III. IL-25 and IL-33 alarmins are strong modulators of ILC2 circulation 88

IV. Inter-tissue ILC2 homing is finely regulated 92

V. Specific migrations of iILC2 subsets following lung or intestinal inflammation 95

VI. Specific migrations of ILC2 subsets at different stages of *N.b.* infection 100

DISCUSSION ***101***

Differences nILC2/KLRG1$^-$ ILC2s : regulation of ILC2s 106

MadCAM1 as central receptor for ILC2 migration **107**
Neonatal and foetal *vs* adult MadCAM1 expression 107
Pancreas migration 107
Liver inflammation and MadCAM1 107
Skin migration **108**
Importance of stimulatory signals **108**
Redundancy between IL-25/IL-33 109
RA 109
Notch2 110
Epigenetic, imprinting and memory **110**
Mobilisation of ILC2s and treatment to control migration **111**
***N.b.* infection** **112**
CONCLUSION ***117***
ILC circulation as a system **118**
Other works **119**
BIBLIOGRAPHY ***121***
ANNEX ***146***

TABLE OF ILLUSTRATIONS

FIGURE 1 : T CELL AND ILC REDUNDANCY 2
FIGURE 2 : ILC LINEAGE DEVELOPMENT 4
FIGURE 3 : DIFFERENT STAGES OF ILC2 DIFFERENTIATION 7
FIGURE 4 : ILC2 WAVES OF COLONIZATION 12
FIGURE 5 : ILC2S ARE HETEROGENEOUS RESPONDERS 15
FIGURE 6 : ANATOMY OF INTESTINAL MUCOSA 17
FIGURE 7 : INTESTINAL LYMPHATIC VASCULATURE 18
FIGURE 8 : HETEROGENEITY OF ADIPOSE TISSUES IN HUMANS 19
FIGURE 9 : ANATOMY OF THE SKIN 20
FIGURE 10 : REGULATION OF ILC2 ACTIVATION AND EFFECTOR FUNCTIONS OF ILC2-DERIVED CYTOKINES 22
FIGURE 11 : ILC2S AS SECRETOR CELLS 31
FIGURE 12 : MEMORY ILC2S VS TRAINED IMMUNITY 34
FIGURE 13 : ILC2S COMMUNICATION WITH OTHER CELL TYPES 36
FIGURE 14 : IFN-Γ COUNTERPART IL-33 MEDIATED ACTIVATION OF ILC2S 38
FIGURE 15 : INTESTINAL EFFECTOR FUNCTIONS OF ILC2S 39
FIGURE 16 : INTERACTION OF ILC2S WITH THE PULMONARY ENVIRONMENT 41
FIGURE 17 : SKIN ORGANIZATION AT HOMEOSTASIS AND FOLLOWING INFLAMMATION 43
FIGURE 18 : MIGRATORY ROUTES OF T CELLS 50
FIGURE 19 : LNS ARE COMPARTMENTALIZED ALLOWING LYMPH FILTRATION 51
FIGURE 20 : MULTI STEP ADHESION CASCADES ON HEVS 52
FIGURE 21 : DCS AND T CELLS TRAFFICKING THROUGH LNS 53
FIGURE 22 : MECHANISM OF LYMPHOCYTES EGRESS FROM LNS 55
FIGURE 23 : ROLES OF CHEMOKINES AT HOMEOSTASIS 56
FIGURE 24 : INTEGRIN FAMILY AND AB COUPLES 58
FIGURE 25 : INSIDE-OUT ACTIVATION OF INTEGRINS 59
FIGURE 26 : EXPRESSION OF SELECTINS BY IMMUNE CELLS 60
FIGURE 27 : SELECTIN-DEPENDENT INTERACTIONS 61
FIGURE 28 : CD69-MEDIATED INHIBITION OF S1PR1 62
FIGURE 29 : T-CELL TRAFFICKING PATTERNS 63
FIGURE 30 : REGULATION OF ADAPTIVE IMMUNITY IN THE LYMPH NODE IN MICE 68
FIGURE 31 : INTEGRINS AS THERAPEUTIC TARGETS 71
FIGURE 32 : ILC SUBSETS ARE CIRCULATING IN TDLS 81
FIGURE 33 : ILC2S SUBSETS IN CIRCULATION 82
FIGURE 34 : ILC2 PHENOTYPES COMPARISON IN TDL, BM AND LP 82
FIGURE 35 : SPECIFIC CIRCULATING ILC2S IN TISSUE AND THEIR CYCLING STAGE 83
FIGURE 36 : ILC2 HETEROGENEITY IN TISSUES 84
FIGURE 37 : CIRCULATING MOLECULES PHENOTYPES OF ILC2S 86
FIGURE 38 : CIRCULATING ILC2S CAN RECONSTITUTE PERIPHERAL POOLS OF ILC2S 87
FIGURE 39 : CIRCULATING ILC2 SUBSETS IN TDL FOLLOWING CYTOKINE STIMULATIONS 88
FIGURE 40 : ILC2S FROM BM AND LP ARE DIFFERENTIALLY RESPONDING TO ALARMINS 89
FIGURE 41 : TRILC2S ARE FROM PERIPHERAL ORIGIN AND DIFFERENTIATE TO IILC2S 90
FIGURE 42 : SECRETORY AND DIVIDING PHENOTYPE OF ILC2 SUBSETS 91
FIGURE 43 : DIFFERENT ILC2 SUBSETS HAVE SPECIFIC POTENTIAL OF MIGRATION 92
FIGURE 44 : ILC2 SUBSETS HAVE SIMILAR SPECIFIC POTENTIAL OF MIGRATION AT HOMEOSTASIS 93
FIGURE 45 : INTEGRIN-BLOCKADE ANTIBODIES SHOW SPECIFICITY OF SUBSETS TO TISSUES 94
FIGURE 46 : SPECIFIC TRANSFER OR IILC2 SUBSETS SHOW AN IMPORTANT INTESTINAL STAGE TO GENERATE $\alpha4\beta7^{-/LO}$ IILC2S 94
FIGURE 47 : SPECIFIC CIRCULATING ILC2 SUBSETS INCREASED DEPENDING ON STIMULATION 95
FIGURE 48 : IMPORTANT ROLE OF MIGRATING ILC2S AS TYPE-2 SECRETOR CELLS 96
FIGURE 49 : SUCCINATE SHOW SPECIFIC MIGRATION OF AN INTESTINAL IILC2 SUBSET 97
FIGURE 50 : IMPORTANCE OF ILC2 MIGRATION FOR MUCUS PRODUCTION IN INTESTINE 99
FIGURE 51 : SPECIFIC CIRCULATING ILC2 SUBSETS INCREASED DEPENDING ON STAGE OF N.B. INFECTION 100
FIGURE 52 : NILC2S AND TRILC2S ARE DIFFERENT ILC2 STAGES 106
FIGURE 53 : ILC2S HAVE ACTIVATED PHENOTYPES IN NOTCH2 DELETED MICE 110
FIGURE 54 : ILC2 ACTIVATION INDUCE IMPORTANT EPIGENETIC MARKS 111
FIGURE 55 : SCHEME OF HOMEOSTATIC TURNOVER OF ILC2S 115
FIGURE 56 : SCHEME OF ILC2 ACTIVATION AND TURNOVER DURING INFLAMMATION 116

INTRODUCTION

I. Innate lymphoid cells : not so young

A. A recent discovery

Innate lymphoid cells (ILCs) are lymphoid cells lacking T and B antigen specific receptors, so called T cell receptor (TCR) and B cell receptor (BCR). They are largely tissue resident and are involved in numerous processes including tissues homeostasis. Their discovery and investigation started a decade ago and changed our concepts about immune regulation and how immune cells maintain tissue homeostasis especially in the mucosal environments. ILCs contribute to different immune pathways by producing cytokines. They provide strong protection of mucosal barriers, enhance adaptive immunity and regulate tissue inflammation as well as wound healing.

ILCs are the innate counterparts of T lymphocytes and are classified in 5 different groups : NK cells, ILC1s, ILC2s, ILC3s and LTi (Artis and Spits, 2015; Spits et al., 2013; Vivier et al., 2018). Natural Killer (NK) are lymphocytes with innate cytotoxic ability against tumoral cells (Herberman et al., 1975; Kiessling et al., 1975). Lymphoid tissue inducers (LTi) were discovered as a discrete subset of lymphoid cells with a key function in peripheral lymph nodes and Peyer's patches development during embryonic life (Mebius et al., 1997). Finally, ILC1s, ILC2s and ILC3s are non-T, non-B lymphocytes called helper ILCs with differences in ontogeny, localisation, functions and regulatory transcriptional networks.

B. The T cell redundancy case

Due to similar functions, ILC1s, ILC2s, and ILC3s are innate equivalent to CD4⁺ T helper (Th)1, Th2, and Th17 respectively. NK cells functions of mirror CD8⁺ cytotoxic T cells (cTL) (**Figure 1**). On top of a role in homeostasis maintenance, ILCs and T cells are important contributors in orchestrating appropriate immune responses to danger. Intracellular pathogens, such as viruses or bacteria, and tumors are linked to NKs, ILC1s and Th1 cells responses; ILC2s as well as Th2 cells play key functions against large extracellular parasites and allergens; and ILC3s and Th17 cells combat extracellular microbes, such as

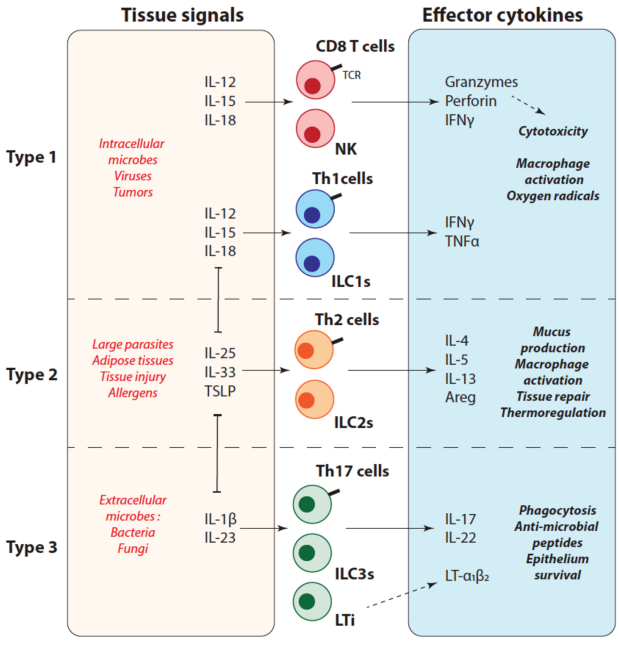

Figure 1 : T cell and ILC redundancy **(adapted from Eberl et al., 2015).** The different ILC subsets show redundant functionality compare to T lymphocytes. They are involved in similar responses against pathogens or following activating signals.

bacteria and fungi. As for T cells, ILCs are instructed by myeloid and non-hematopoietic cells as stromal cells and *epithelia*. They are regulated *via* positive and negative feedbacks through immune regulatory and effector functions (**Figure 1**).

Recent studies discussed the functional redundancy between T cells and ILCs (**Figure 1**)(Vivier et al., 2016). More specifically, the lack of disease associated with ILC deficiency in humans give evidence on a dispensable role of ILCs (Vély et al., 2016). However, it remains unclear whether the absence of observable disease should be considered as the only proof of concept, as ILCs have been described as pivotal for development of inflammation in gut and skin for ILC3s (Buonocore et al., 2010; Tait Wojno and Artis, 2012) and lung for ILC2s (Scanlon and McKenzie, 2012). The impact of ILC deficiency could also disrupt homeostasis, with impact on long-term metabolism and increased susceptibility to chronic diseases.

II. Innate lymphoid cells : derived from the lymphoid lineage

To better understand ILC turnover in adult, it is important to know their tissue of origin and their ontogeny. ILC development comprises several intermediate stages and takes place in different places during different stages of life. ILC waves of progenitors were described from the fetal liver (FL) stage, the neonatal stage in to a less extent from the adult bone marrow (BM) stage. Most studies on ILC2 functions have been performed in the adult where maturation of precursors in peripheral tissues could still be observed. Except for the characterisation of specific intermediate stages, the ILC development has been well documented in mice this last decade (**Figure 2**)(Cherrier et al., 2018; Zook and Kee, 2016). It is proposed that newly generated tissue ILC2 will participate to the replenishment of peripheral ILCs by *in situ* BM differentiation or following their migration to the tissue of destination.

A. CLP, CHILP, EILP and other ILCPs : a little bit of complexity

1. Common Lymphoid Progenitor : CLP

The bone marrow adult CLP was first described as Lin⁻ cell, corresponding to cells that bore no B, T or myeloid markers, which expresses IL-7Rα and lower levels of c-kit and Sca-1 (Cumano et al., 2019; Kondo et al., 1997). Its FL counterpart is also comprised within the Lin⁻ IL-7Rα⁺ fraction and express high levels of c-kit. The CLP is a multipotent lymphoid progenitor and clonal assays proved B, T, and NK cell potential with lack of myeloid potential. Fetal c-kit^{hi} CLP have enriched multipotent potential compare to BM CLP (Cumano et al., 2019). Indeed, the fetal CLP compartment is heterogeneous, comprising a α4β7⁺ population that countains a LTi, T, and DC but no B potentials (Kondo et al., 1997).

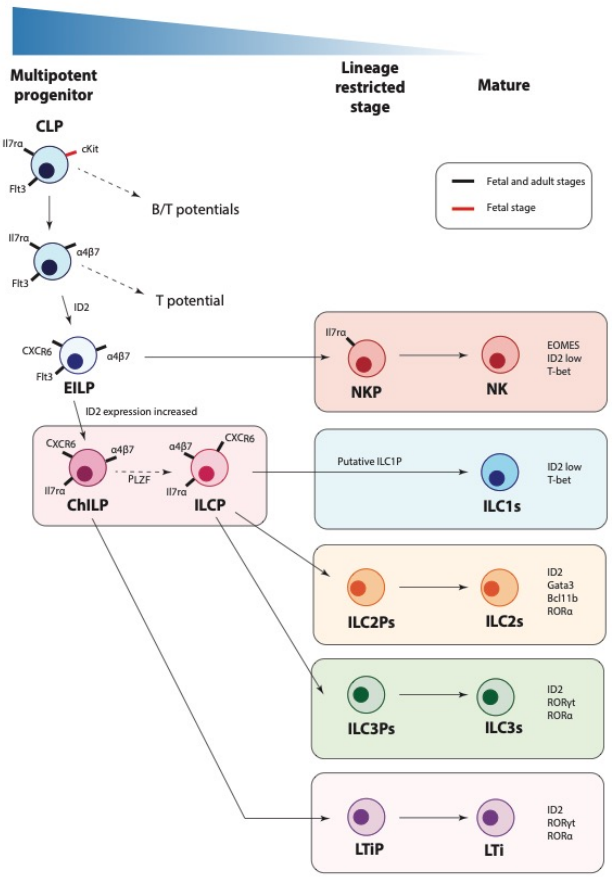

Figure 2 : ILC lineage development **(adapted from Zook and Kee, 2016).** During ILC differentiation, different precursors will be involved, losing differentiation potentials to finally commit to specific subsets. To give all ILC lineages, CLP is differentiating to EILP, ChiLP and ILCP, before acquisition of committed features for each subset. Only ILC1P has not yet been characterized.

Fetal and adult ILCs differentiate from CLPs (Possot et al., 2011; Cherrier et al., 2012) through a

loss of B cell potential concomitant with an upregulation of α4β7 expression. Further expression of CXCR6 marks the loss of T cell potential and passage to an early innate lymphoid progenitor (EILP) stage (Harly et al., 2018; Possot et al., 2011).

2. Early Innate Lymphoid Progenitor : EILP

Using *in vitro* clonal assays, around 60% of EILPs are able to generate all ILC lineages (ILC1, ILC2 and ILC3) and cNK cells, while T and B potentials are lost. EILPs are essentially not expressing IL-7Rα, unlike upstream CLP and downstream progeny (Klose et al., 2014; Yang et al., 2015). Recent studies showed that EILPs derive from CLPs (Harly et al., 2018), suggesting rapid changes in IL-7Rα expression during ILC lineage commitment to a more restricted precursor. Innate cell development initiates with the expression of Id2, that inhibits E-box transcription factors (such as E2A) important for T cell development (Yokota et al., 1999). In an Id2 reporter mouse model, it gives rise to both IL-7Rα$^+$ NK Progenitor (NKP) (Carotta et al., 2011) and Id2-GFP$^+$ CXCR6$^+$ α4β7$^+$ CLPs that lose Flt3 and have been described as common helper ILC precursor (ChILP) in adult (**Figure 2**).

3. ILC Progenitor : ChILP and ILCP

ChILPs appeared as a heterogeneous population able to generate all ILCs *in vivo* and *in vitro* in mice, including LTi cells but not cNK cells, high levels of Id2 expression concurs with the loss of NK potential (Klose et al., 2014). Subsequent upregulation of Zbtb16 is concomitant to the loss of LTi potential (Constantinides et al., 2014; Ishizuka et al., 2016). A PLZF reporter and fate map mouse line mark a majority of mature ILCs but only a small fraction of cNK and LTi cells, thus defining the ILC precursor (ILCP) as a PLZF$^+$ α4β7$^+$ FLT3$^-$ CLP (**Figure 2**) (Constantinides et al., 2014; Ishizuka et al., 2016).

The transcriptional profile expressed in ILCPs includes *Zbtb16* and *Id2*, and also *Tcf7*, *Gata3* and *Tox* (Aliahmad et al., 2010; Mielke et al., 2013; Yagi et al., 2014). Inactivation of any of these genes profoundly affects the development of all ILC lineages (**Figure 2**). Before *Id2* expression, a transient expression of *Nfil3* and TCF-7 expression during thymic development are essential and regulated by Notch1 signalling (Yagi et al., 2014). In contrast, Notch signalling appears dispensable in FL ILCPs for the expression of transcription factors and α4β7, which marks bias in ILC commitment (Chea et al., 2016b, 2016a; Possot et al., 2011). Of note, only an α4β7$^+$ subset with ILC2 genes expression get affected by inactivation of the Notch pathway (Chea et al., 2016a). Importantly, ILC1s, ILC2s, and ILC3s transcriptional programs initiate in multipotent ILCP. These profiles are found co-expressed before being segregated, a process described to occur in the periphery with specific precursors for each lineage (Bando et al., 2015; Cherrier et al., 2018; Ishizuka et al., 2016).

4. NK and ILC1 development : Not so simple

NK cells and ILC1s are high producers of type 1 cytokines (including TNF-α and IFN-γ) in a T-bet-dependent fashion, as deficient production has been reported in Tbx21$^{-/-}$ mice (Klose et al., 2014; Townsend et al., 2004). Levels of T-BET expression differentially impact NK cell and ILC1 homeostasis as partial *Tbx21* repression is observed during NK cell development but its overexpression decreases cNK at the expense of ILC1s (Daussy et al., 2014). Runx3 expression is essential for generation of T-BET^{+} NK cells and ILC1s (Ebihara et al., 2015), and has been described as a downstream target of *Tbx21* in NK cells, ILC1s and Th1 cells (Djuretic et al., 2007).

T-bet is not the only important transcription factor (TF), as cNK cells require several additional TFs not shared with ILC1s. The major factor required for NK development is the well-known Eomesodermin (EOMES), already expressed in NKPs but not in ILCPs (Male et al., 2014). In an Eomes deleted mouse model, whereas ILC subsets are unaffected, NKPs fail to mature into NK cells, identifying EOMES as a critical regulator of NK cell differentiation (**Figure 2**)(Gordon et al., 2012; Klose et al., 2014).

NK cell maturation and egress of the bone marrow through expression of the lysosphingolipid sphingosine 1-phosphate (S1PR5) needs Zeb2, induced by T-BET (van Helden et al., 2015). It remains unclear whether ILC1s come from an intermediate ILC1 Precursor (ILC1P) stage (**Figure 2**), neither if they colonize peripheral tissues at fetal stages with long-term maintenance nor if ILC1 differentiation still occurs in adult BM. However, ILC1s are lowly detected in circulation and fail reconstitution in parabiotic models (Gasteiger et al., 2015).

5. ILC3Ps et LTiP : A question of timing

RORγt TF is essential for generation of all group 3 ILCs produced during fetal and adult life (Cording et al., 2014). *Rorc*, coding for RORγt, is activated via retinoic acid (RA) receptor signalling (Van De Pavert et al., 2014). RORγt bind DNA, interact with non-receptor tyrosine kinases (SRC) family co-activators for transcription activation (Ciofani et al., 2012), while RA signals later act on gut migration by inducing expression of gut-homing receptors such as C-C motif chemokine receptor 9 (CCR9) (Ciofani et al., 2012; Kim et al., 2015). Similarly to Th17 cell polarization, role for RORγt appears essential in ILC3 differentiation. Indeed, RORγt mutations that cripple Th17 cell polarization also induce loss of LTi-dependent Peyer's patches and secondary lymphoid organs as lymph nodes (LNs) (He et al., 2017).

Clonal differentiation potential coupled to single-cell transcriptional analyses confirmed that the fetal LTi cell precursor (LTiP) and the ILCP are separated. The ChILP could be then considered as their common precursor (Ishizuka et al., 2016), and only LTi progenitors commit before the ILCP stage (**Figure 2**).

B. ILC2 progenitor : a special development

1. Different stages

Concerning ILC2 differentiation, key TFs are well characterized and include ID2, RORα, TCF-1, BCL11b, and GATA-3 in an ILC2 Precursor (ILC2P) lineage-restricted stage (**Figure 3**) (Califano et al., 2015; Hoyler et al., 2012; Klein Wolterink et al., 2013; Walker et al., 2015; Wong et al., 2012; Yu et al., 2016). How these TFs really promote ILC2P differentiation has not yet been described. Although, as previously mentioned, TCF-7 (a potential Notch target) can induce *Gata3* and *Bcl11b* expression (Weber et al., 2011). Recently, using Bcl11b-Tomato mice, Il-7rα^{+} Flt3^{-} α4β7^{+} Id2^{+} Bcl11b^{+} ILCPs have been described as restricted to ILC2 lineage *in vitro* (**Figure 3**)(Xu et al., 2019). *In vitro* assays with stromal cells expressing ligands of the Notch receptors family, supplemented with IL-2, IL-7 and the ligand for the stem-cell-factor-receptor c-Kit, or IL-7 and IL-33, demonstrated an expansion of ILC2Ps and ILC2 populations (Wong et al., 2012). Notch is important for the ILC2 lineage expansion as shown by the decrease of ILC2P proliferation and transcriptional profile variations if the Notch pathway is inactivated from the lymphoid stage (Chea et al., 2016a; Zook and Kee, 2016).

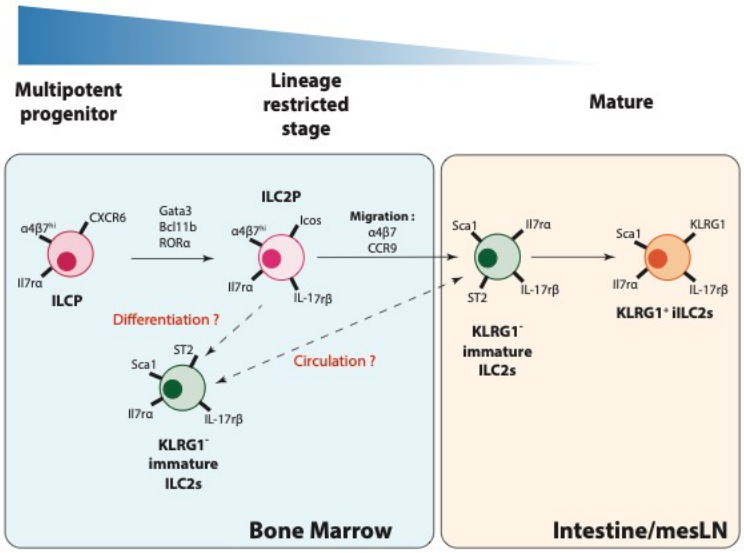

Figure 3 : Different stages of ILC2 differentiation. From ILCP, a commitment due to increased Gata3, RORα and BCL11B expressions is giving rise to ICL2P characterized by high expression of α4β7 and CCR9. After migration to intestinal mucosa, they give rise to Sca1^{+} KLRG1^{-} immature ILC2s than will mature and express KLRG1. It is still not clear in *in situ* differentiation occur in BM or if immature ILC2s circulate between tissues.

Gata3 and *Bcl11b*, primed by high amounts of TCF-7, may bias ILC progenitors to the ILC2 lineage. It is well known that GATA-3 activates type-2 cytokines, due to its ability to bind and induce the transcription of *Il5* and *Il13* promoters (Zhang et al., 1997). For BCL11B, it appears to influence ILC2 differentiation through regulation of Il17rβ (IL-25R) expression (**Figure 3**)(Yu et al., 2016).

Together, these TFs ensure productive ILC2 differentiation plus coordinate expression of ILC2-specific effector functions and responsiveness to ILC2-dependent homeostatic cytokines or alarmins.

2. *ILCs transcription factors*

a. Id2

ID2 belongs to the inhibitor of DNA binding family, comprising 4 TFs named Id1-4. They share a highly conserved helix-loop-helix (HLH) domain that can form heterodimers with HLH domain contained in other TFs, inhibiting their ability to bind DNA (Sun et al., 1991). This negative regulation is well described in ILC development as ID2 is a key TFs for ILC lineage commitment (Yokota et al., 1999). During hematopoietic development, an upregulation of ID2 and ID3 by EILPs partially inhibits E2A activity, leading to the down-regulation of Notch1 expression, which is important for T cell commitment, and as a consequence to the loss of T cell potential (Ji et al., 2008; Yagi et al., 2014). Then, ID2 deficiency results in the loss of all mature ILCs *in vivo* (Yokota et al., 1999). In ID2 deficient mice, E2A inactivation partially rescues secondary LN structures and LTi development, indicating the important role of ID2 in E2A inhibition for ILC lineage commitment (Boos et al., 2007). More mechanistic studies showed importance of ID2 level of expression on other TFs regulation, as for $Id2^{hi}$ vs $Id2^{lo}$ expression that respectively inhibits or allows GATA1-PU.1 interaction, known as important for NK cells (Ji et al., 2008)

Even if environmental signals of *Id2* expression in ILCs remain unclear, studies deciphered TCF-7 involvement on ID2 maintenance during ILC2 development and functions (Zook et al., 2016), and both its regulation and functions studied on other immune or non-immune populations as in dendritic cell development of keratinocyte proliferation (Memezawa et al., 2007; Murphy, 2013).

b. Gata3

GATA3 is then well described as a key TF for development and maintenance of mature ILCs, plus an important regulator of ILC2 functions. It belongs to the GATA TFs family of proteins with two zinc finger DNA binding domains that recognize GATA sequence (Boos et al., 2007). GATA3 is an already well characterized TF required for T and ILC development (De Obaldia and Bhandoola, 2015; Yagi et al., 2014). Conditional deleted mouse models targeting HSC stage show alteration of all IL-7rα^{+} ILC development (Serafini et al., 2014; Yagi et al., 2014). In line with its expression in ILCPs, GATA3 is needed for EILP differentiation (**Figure 3**)(Constantinides et al., 2014). GATA3 specific deletion in ID2 expressing cells affected ILC2 maintenance and functions but without effect on other ILC populations (Yagi et al., 2014). This depletion in ILC2s induced complete loss of IL-13 production and loss of ILC2 related genes expression (Liang et al., 2012; Yang et al., 2013a).

c. Bcl11b

B-Cell Lymphoma/Leukemia 11B (BCL11B) or BAF Chromatin Remodeling Complex Subunit, is a Kruppel-like C_2H_2 type zinc finger transcription proteins (Kominami, 2012). It contains six zinc-finger domains that can bind DNA. It has several target genes as Zbtb7b and Runx3, both important in ILC development (**Figure 2**)(Kastner et al., 2010). Its regulation is quite unknown, but BCL11B may be regulated by the Notch signalling pathway as it is upregulated during T cell (Avram and Califano, 2014) and ILC2 differentiation (Walker et al., 2015; Yu et al., 2015), both lymphoid subsets depending on the Notch pathway. ILC2 functions are also impacted as Bcl11b$^{-/-}$ ILC2s fail to response to IL-25 or IL-33 stimulations but ILC3 phenotype and function are normal in Bcl11b$^{-/-}$ mice after IL-23 treatment (Califano et al., 2015).

d. RORα

The retinoic acid-related orphan receptors alpha (RORα) is part of the ROR family, composed of 3 members : RORα, RORβ and RORγ. RORα, encoding by *RORa* gene, is composed of two zinc finger DNA binding domains. Specific association to ROR elements (RORE) in regulatory regions is necessary for RORα's function as a transcriptional activator. RORα achieves this by specific binding to a consensus core motif in RORE (Cook et al., 2015). Several studies show important role of RORα both in ILC2 development and functions, as they are impaired in RORα deficient mice when it doesn't impact T cells and ILC3s development (Halim et al., 2012a, 2018; Rajput et al., 2017; Wong et al., 2012).

3. One other important pathway : Notch2

Notch2 is part of the Notch family, comprising 4 Notch receptors (Notch1-4) with well five known ligands of the DSL (Delta, Serrate, Lag-2) family: Jagged ligands (JAG1 and JAG2), and Delta-like ligands (DLL1, DLL3 and DLL4) (D'Souza et al., 2010). Both Notch receptors and ligands are transmembrane proteins that enable cell signalling between neighbouring cells. Notch signalling has been widely described for about a century as a key-signalling pathway that regulates numerous biological processes as far as differentiation, proliferation and apoptosis. Although the very core of the signalling is really well characterized and simple, numerous modifications can alter its activation, and the outcome of Notch signalling highly depends on the cellular context.

Notch signalling, in combination with IL-7 and IL-33, is required *in vitro* to derive ILC2s from CLPs. IL-7 alone on OP9 or OP9-DL1 stromal cells fails generating ILC2s, whereas IL-7 and IL-33 combination on OP9-DL1 cells showed Lin$^-$ Icos$^+$ ST2$^+$ cells (Wong et al., 2012). Moreover, similar cell cultures without IL-33 could also give rise to Icos^{hi} α4β7$^+$ ILCPs (Constantinides et al., 2014) or GATA-3$^+$ ILC2s (Klose et al., 2014). Blocking of Notch signalling by retroviral transduction in early progenitors resulted in failure of reconstitution of ILC2 compartment, suggesting that Notch signalling may act upstream

of TCF-7 in ILC2 development. Also, blocking Wnt signalling pathway, one of the pathways induced by Notch activation, show that TCF-7 does not require Wnt signalling to generate ILC2 (Yang et al., 2013a). More recent works on the fetal ILC development show that among ILCp only the fraction enriched in ILC2Ps is affected by inactivation of the Notch pathway, (Chea et al., 2016a) and variations on strength and time of Notch contact with its ligand could have an effect on T, B, NK or ILC2s biased development of CLPs (Koga et al., 2018).

C. The niches question : ILC and environment

We described ILC development as long process with lot of intermediate multipotent stages. However, last precursors are engaged toward a specific lineage (lineage commitment) and needs final activation to be mature productive ILCs. Niches are well characterized for T cell development in the thymus contrasted with the lack of data for early progenitors and for mature ILCs development. It is quite unclear whether FL or BM has all the required signals for final ILC development. In the BM, it has been demonstrated that ILC3 commitment was impossible and that ILCP are migrating toward the intestine to further express RORγt and finally differentiate into ILC3 (Possot et al., 2011). Moreover, during fetal life, only very few cells are able to express RORγt contrary to ILC from fetal peripheral organs (spleen, lymph nodes and intestine). Except for immature NK cells (van Helden et al., 2015), no study proved final steps of FL or BM precursor local functional maturation, and the concept is that ILCs circulate at the stage of precursors and reach peripheral tissues for final maturation (Lim et al., 2017). Recent studies showed that BM retention of ILCps is linked to increased expression of CXCR4 and that BM ILC2p subsets are retained in BM of CXCR6 deficient mice (Chea et al., 2015; Stier et al., 2018). Moreover, a proof of peripheral differentiation has been made at fetal stages, as LTiP are detected in fetal spleen (FS), and are not impacted by the loss of Notch signalling to generate mature LTi (Chea et al., 2016a).

More specifically, according to the level of gut tropic α4β7 and CCR9 molecules biased and unbiased ILCPs (Cherrier et al., 2018; Possot et al., 2011), ILCPs migrate toward the gut mucosa to further differentiate in situ and to be primed by external cytokine *stimuli* (Bando et al., 2015; Cherrier et al., 2018; Ishizuka et al., 2016). Finally, they may recirculate through the hemo-lymphatic system to colonize other peripheral tissues and reside as activated cells.

Accessibility to signals, as specific cytokines, is more prevalent in peripheral tissues with high stimulations of immune cells as showed for ILC2 from peripheral mesenchymal cells of fetal mesentery tissue (Koga et al., 2018). Indeed, interactions with specific populations of stromal or epithelial cells is mandatory, and alarmins like IL-25 or IL-33 plus co-stimulatory signals are important factors for ILC2 maturation (Walker and McKenzie, 2013). These cytokines are poorly described in primary lymphoid tissues as

BM, but mostly described as expressed in the periphery by the intestinal tuft cells or by epithelial and endothelial cells (Gronke and Diefenbach, 2016; Von Moltke et al., 2016).

Following differentiation, ILCs are important regulators of homeostasis, creating an important link between environmental modifications and physiologic adaptation of metabolic or other major systems, as ILC2s do in adipose tissues (ATs) and lungs (Bénézech and Jackson-Jones, 2019; Huang et al., 2018; Kredel and Siegmund, 2014). The formation of new ILC2 for adult turnover remains poorly described, and the trafficking of ILC2Ps or differentiated ILC2s may play an important role for continuously generating new pools of ILC2s.

III. Group 2 innate lymphoid cells : the mothership

A. Origins : long live the king

Recent studies in adult mice showed waves of peripheral ILC2 colonisation with foetal, perinatal or adult origins, questioning the turnover of ILC2s through life. Using Arg1-driven or Id2-driven inducible fate mapping mouse models, they induced fate mapping at foetal, perinatal or adult stages and followed ILC2 turnover over time (**Figure 4**)(Schneider et al., 2019). Arg1 is a metabolic enzyme constitutively expressed by lung and intestinal ILC2s. Where ILC2 differentiation occurs and the impact of aging and environment on ILC2 renewal is still an open question. It is important to determine the origin of ILC2 found in peripheral tissues during life and understands their circulating mechanism.

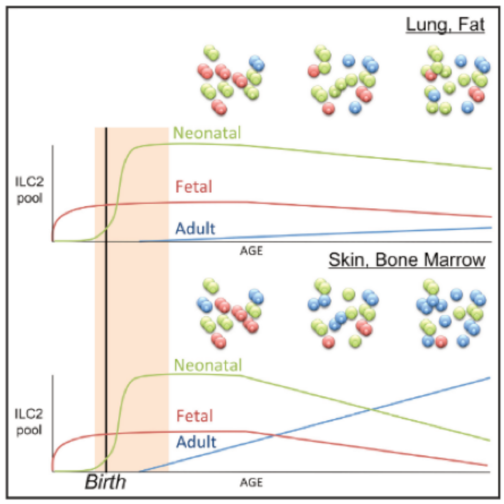

Figure 4 : ILC2 waves of colonization **(adapted from Schneider et al., 2019).** Perinatal pool of ILC2s highly participate to tissue resident cells in adult. They are slowly replaced by adult waves with *de novo* ILC2 generation. Interestingly, intestine, BM and skin show higher rate of replacement and ILCs from different origin than lung and fat. Fetal period is rapidly replaced.

1. Fetal development

Many innate tissue-resident cells, including tissue resident macrophages, are seeded during fetal development (Ginhoux and Guilliams, 2016). ILC2 development during embryonic life has largely been reviewed, and according to urea cycle enzyme Arginase 1 (Arg1)-YFP reporter mice, positive ILCP were described in fetal intestine (Bando et al., 2015). Arg1 has been described as expressed by BM, lung, adipose tissue, majority of intestinal and a minority of skin CD25$^+$ Id2-GFP$^+$ ILC2s, corroborating heterogeneity in Arg1 expression among adult ILC2 subsets from different tissues (Ricardo-Gonzalez et al., 2018; Schneider et al., 2018, 2019). Prenatal studies characterized the role of peripheral PDGFRα$^+$ gp38$^+$ mesenchymal cells as drivers of fetal liver–derived ILC2 differentiation in mesenteric tissues (Koga et al., 2018). Finally, colonisation of E17.5 lungs, intestine and skin by CD25$^+$ Arg1-RFP$^+$ ILC2 populations contributes to resident ILC2 pools able to respond in adult life following helminth infections (**Figure 4**)(Schneider et al., 2019).

2. Perinatal stage

Neonatal ILC2s are important modulators of tissue homeostasis and defences (Yu et al., 2018). IL-33-driven ILC2 responses is largely reported and reviewed as a key modulator of airway responses to asthma and during allergic responses by type-2

cytokines secretion mediating myeloid recruitment (Coquet et al., 2015; Endo et al., 2015; Guo et al., 2015; Mindt et al., 2018). However, it was largely not described why young babies are highly susceptible to become sensitized by allergen. Using house dust mite (HDM) stimulation, mimicking allergy, studies on neonatal mice showed strong IL-33 mediated accumulation of ILC2s (de Kleer et al., 2016). This high production of ILC2s during neonatal period is known and its importance for tissue development already discussed in lung with important role of IL-13 production by ILC2s and mast cells to drive lung development (Cohen et al., 2018; de Kleer et al., 2016; Scott and Guilliams, 2018).

In Arg1-driven or Id2-driven inducible fate mapping mouse models, staining respectively a majority and all ILC2s, neonatal ILC2 development appear to be a major contributor of peripheral tissues (**Figure 4**)(Schneider et al., 2019). This Arg1-driven increased labelling of neonatal ILC2s compare to prenatal (more than 2 fold change) corroborate with importance of ILC2s in mucosal tissues like lung and intestine. As Arg1 is constitutively expressed by lung and intestinal ILC2s, and as birth goes with crucial activation of respiratory and digestive tracts, it suggests an important role of postnatal period for ILC2 activation and dissemination to participate to peripheral tissue pool. Moreover, no ILC2Ps in the adult BM remained labelled in adult life in Arg1 fate mapping model. It suggests that post-birth BM Arg1$^+$ ILC2s have an origin temporally distinct from and without contribution from prenatally derived ILC2s. Finally, adult ILC2s from skin are only labelled by Id2-driven fate mapping, showing a distinct origin of dermal ILC2s without any role of Arg1 expression for constituting this pool (Schneider et al., 2019).

3. Adult renewal

The current statement on adult ILC2s describe low ILC2 turnover in peripheral tissues, with low or almost no circulating ILC2s in adult (Gasteiger et al., 2015; Schneider et al., 2019). However, *Nippostrongulus brasiliensis (N.b.)* infection of parabiotic mice induced significant increased ILC2 circulation to the lung of parabionts (Gasteiger et al., 2015). In helminth infection, essential intestinal IL-17rb$^+$ "inflammatory" ILC2 (iILC2s) were migrating to the lung in a S1P-dependant manner, as blocking S1P using FTY720 treatment prevents iILC2 accumulation. Deletion of iILC2 migration increased the death susceptibly of *N.b.* infected mice (Huang et al., 2015, 2018). Migratory ILC2s have also been described using in CCR10 double deficient and GFP reporter mice, showing a CCR10-dependant migration for skin (Yang et al., 2016b). Inversely, CXCR4 downregulation is needed for BM egress and migration to the lung following IL-33 stimulation (Stier et al., 2018). ILC2 turnover is low but still efficient since more than 90% of skin, LP and BM ILC2s are from adult origin in 32 weeks old mice (**Figure 4**)(Schneider et al., 2019).

Several waves of ILC2s have been described, with a main adult origin for BM, LP and skin and a main neonatal origin for lung and fat. All IC2 subsets are increased

following *N.b.* infection independently of their origin, showing long lifespan of ILC2s (Schneider et al., 2019). The high fetal *versus* neonatal origin heterogeneity described in adult ILC2s relates to their role in tissues. As dependant of environmental signals, ILC2 dissemination and priming occur following stimulation due to important external variations, such as such as birth and weaning. These variations induce peripheral imprinted cytokine production abilities and appear as a key step for ILC2s (Ricardo-Gonzalez et al., 2018; Zhu, 2018). Fate-mapping models gave clues on ILC2 turnover during life, but the localisation of ILC2 development for the renewal of peripheral tissues, and the mechanisms behind ILC2s circulation and fate, remain still unclear and are important points to be questioned.

B. ILC2 functions at homeostasis

ILC2s were first described in several tissues by different groups that gave them different names: nuocytes *in vitro* and in intestine, mesLNs and BM after adoptive transfers (Neill and McKenzie, 2011; Neill et al., 2010), Natural Helper Cells (NHCs) in Adipose Tissues (ATs) (Moro et al., 2010) and Innate Helper 2 (Ih2) in intestine, mesLNs, liver and spleen (Price et al., 2010). A consensus for homogeneous classification came later in 2010 (Saenz et al., 2010) and the definition of ILC groups in 2013 revised in 2018 (Spits et al., 2013; Vivier et al., 2018). Since when, studies on ILC2s heterogeneity never stopped to characterize specific functions of different ILC2 populations, with intermediate classification depending on the cytokines and localisation of their activation (**Figure 5**). Indeed, natural ILC2s (nILC2s) are the most immature KLRG1^{-} cells characterized by IL-33 receptor (T1-ST2 or ST2) expression in lung and iILC2s are mature KLRG1^{+} cells expressing IL-17rβ, the receptor of IL-25 in intestine (**Figure 5**)(Huang and Paul, 2016). They can also bore other receptors to respond to TSLP (TSLPR) (Kim et al., 2013) or IL-18 (IL-18r1) (Ricardo-Gonzalez et al., 2018)(**Figure 5**). They respond to other type of simulation as metabolites or neuropeptides, directly or by non-immune cells mediation, giving them the potential to sense environmental modifications.

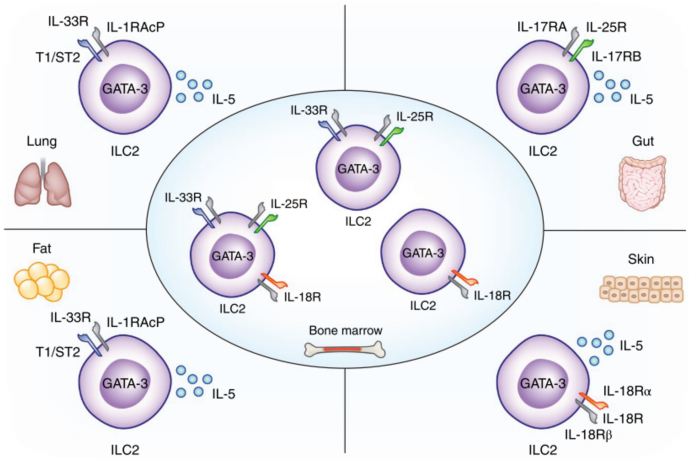

Figure 5 : ILC2s are heterogeneous responders **(from Zhu, 2018).** IL-33 and IL-25 are critical cytokines for ILC2 activation. Gut ILC2s express preferentially IL-17rβ whereas lung and fat ILC2s express mostly ST2. Interestingly, skin iLC2s are expressing IL-18R and not IL-33R or IL-25R. In BM, majority of ILC2s co-express ST2 and IL-17rβ, a small population also express IL-18R, and another IL-18R alone.

ILC2s are plastic populations and respond to a large variety of *stimuli* by adapting their phenotype (Zhu, 2018). Understanding if that adaptation of ILC2s involve trafficking of immature or mature cells needs to first describe the types of modification ILC2s can pass by.

1. All about localization

Single-cell sequencing analyses of ILC2s at steady state in the small intestine showed that ILC2 are heterogeneous and several subgroups with different gene expression patterns were identified (Gury-BenAri et al., 2016). But no known surface markers or characteristics that define ILC2s at one site are absent or not inducible at any other sites, questioning the link between ILC2 pools in different locations, and their possible migration. It is important to better characterize ILC2 localizations within tissues

as well as their functions and how they can answer activation signals in different sites or during diseases.

a. Lung

About 40 distinct cell populations are interacting in the lungs (Reid et al., 2005). To provide barriers to potential pathogens and allergens, the tightly organized respiratory immune system and surrounding lung cells are a unique microenvironment for ILC2s.

Pulmonary ILC2s were first defined thanks to the use of type-2 cytokine reporter mice. They were defined in IL-4 (4get) and IL-13 (YetCre-13) reporter mice (Price et al., 2010). Interestingly, ILC2s are the predominant ILC population in the lungs at steady state (Monticelli and Artis, 2012). Later on, ILC2s were described in non-reporter wild-type mice with variable gating strategies, generally defined as lineage negative cells and expressing Thy1, Sca-1, GATA-3, T1/ST2, inducible T cell costimulatory (Icos), CD44, CD25, IL-7Rα, KLRG1, and c-kit low to positive (Chang et al., 2011; Van Dyken et al., 2014; Halim et al., 2012b; Hoyler et al., 2012; Monticelli and Artis, 2012).

Il5 is expressed at steady state in lung, whereas *Il13* is only inducible in pulmonary ILC2 upon challenge (Nussbaum et al., 2013).

Using an IL-5 reporter mouse, the first report on the localization of pulmonary ILC2s identified them in collagen rich structures, close to airways at steady state (Nussbaum et al., 2013). This location was better defined as close to the epithelium and small conducting airways (Molofsky et al., 2015).

In summary, ILC2 are highly represented in lung and located at peripheral and central sites of the lungs at steady state. ILC2 clusters both interrogate whether ILC2s actively proliferate at these locations due to stimuli or/and if they result from constant migration from other peripheral locations both at steady state and in case of infections. They actively contribute to the homeostasis of the lungs by secreting type 2 cytokines.

b. Small intestine

ILCs are enriched at mucosal sites, but the only one site comprising all 3 groups of ILC populations is the gut mucosa. Due to its essential functions as a barrier with external environment, the intestine plays an important role in host protection and immune system modulation.

The functions of the gastrointestinal (GI) tract are vital and comprise absorbing nutrients and immune-surveillance of the gut bacteria. Many publications have detailed the influence of intestinal microbiota on body homeostasis and diseases (**Figure 6**)(Belkaid and Hand, 2014; Mayer et al., 2015). Food absorption, with contained antigens, and the intestinal microbiota has probably resulted in stromal adaptation, with

development of specialized fibroblasts, blood endothelial cells (Kamba et al., 2006; Powell et al., 2011; Yang et al., 2013b), lymphatic vessels (**Figure 7**)(Bernier-Latmani and Petrova, 2017), and an evolution of gut immune cells for tolerance maintenance and responses against infections (MacDonald et al., 2011; Powell et al., 2011). In mammals, the small intestine is covered by finger like *villi* into the lumen. The colon, where *villi* are absent and replaced by a flat luminal surface (**Figure 6**), is the site for liquid absorption from faeces and also possess the majority of commensal bacteria, which are essential for mammals health. Intestinal crypts, embedded in the submucosa between *villi*, contain intestinal stem cells that participate to maintain the epithelium by migrating from the crypt to the villus (**Figure 6**)(van der Flier and Clevers, 2009). Intestinal stem cells also give rise to all differentiated cells including: enterocytes, responsible for nutrient absorption, Paneth cells, important for anti-microbial defence, mucus-producing goblet cells, tuft cells and enteroendocrine cells, which secrete hormones (**Figure 6**)(van der Flier and Clevers, 2009).

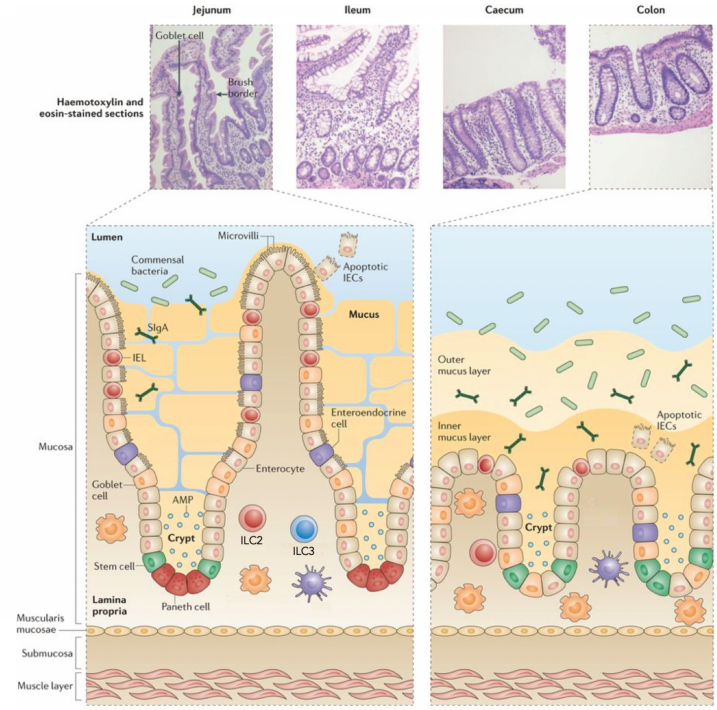

Figure 6 : Anatomy of intestinal mucosa **(adapted from Mowat and Agace, 2014).** Mouse intestine is separated in several part, jejunum, ileum, caecum and colon. *Villi* are long in the beginning of intestine while they are almost not existing in colon. A lot of cells compose intestinal barrier, and ILC2s are present in Lamina Propria and in theepithelium, playing important functions at homeostasis or to mount type-2 responses to parasites.

The intestinal lamina propria underlies epithelial cells, contains blood and lymphatic vessels, enteric nerves, as well as fibroblasts and smooth muscle cells (SMCs) (Powell et al., 2011). The lamina propria is a dense tissue, with high amounts of immune cells, making the intestine one of the main immunological organ in the body (**Figure 6**)(MacDonald et al., 2011; Powell et al., 2011).

The intestine also contains organized gut-associated lymphoid tissue (GALT), comprising Peyer's patches, aggregates of lymphoid follicles and isolated lymphoid follicles (crypto-patches) (Eberl and Lochner, 2009). Then, a thin layer of smooth muscle, the muscularis mucosae, separates the mucosa from the dense connective tissue of the submucosa, containing blood and lymphatic vessels plus a plexus of para-sympathetic nerves. Two muscle layers, formed by either circular or longitudinally aligned SMCs, line

the submucosa. The serosa, composed of loose connective tissue and covered by mesothelial cells, form the outer layer of the intestine. The serosa is continuous with a thin membrane supporting the intestine and the peritoneum called mesentery (**Figure 6**).

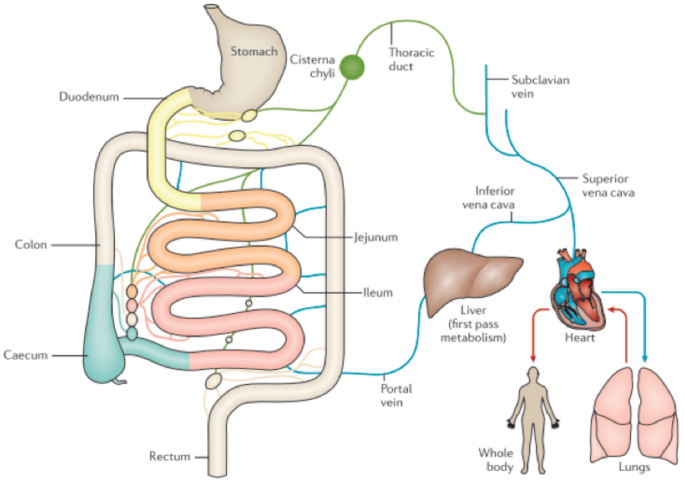

Figure 7 : Intestinal lymphatic vasculature **(adapted from Bernier-latmani and Petrova, 2017).** All different parts of intestinal mucosa are drained by different mesenteric lymph nodes that from a chain. From intestinal mucosa, lymphatic vessels passing through mesLNs join the thoracic duct at *Cisterna chyli* level, before going back in the general blood circulation.

In mice, ILC2s are typically identified by the expression of CD25, KLRG1, Icos, or ST2. However, gut ILC2s specifically express IL-17rβ, contrary to their lung counterparts. Moreover, *Il5* and *Il13* are constitutively expressed at steady state by intestinal ILC2s (Nussbaum et al., 2013). The first report on the localization of gut ILC2s identified them in the lamina propria, in close localization with EpCAM$^+$ epithelial cells, maintaining epithelium homeostasis and modulating remodeling by type-2 cytokines secretion. Following stimulation, mature KLRG1$^+$ ILC2s gain the ability to enter in intestinal lymphatic vessels (Huang et al., 2018). This is a first direct clue of ILC2 trafficking from the periphery and question on the role of mature intestinal ILC2 circulation.

c. Healthy fat metabolism : adipose tissues

ILC2s are found in important non-mucosal metabolic tissues, as adipose tissues. Indeed, the storage of energy as lipids is a highly conserved mechanism shared by unicellular and multicellular organisms across evolutionary phylogeny. In mammals, two principal types of adipose tissue exist, white (WAT) and brown (BAT) (**Figure 8**)(Frontini and Cinti, 2010; Rosen and Spiegelman, 2014). BAT develops embryonically and is derived from mesodermal precursors expressing *Myf5* and *Pax.* These precursors can also give rise to skeletal muscle cells and a portion of white adipocytes (Lepper and Fan, 2010; Sanchez-Gurmaches et al., 2012; Seale et al., 2008; Wang and Seale, 2016). Brown adipocytes, in majority contained in the interscapular region for rodents, possess multilocular lipid droplets and high numbers of mitochondria, and have as main function to dissipate stored energy in the form of heat (**Figure 8**). Recent studies suggested that some adipocytes, possessing characteristics of both brown and white adipocytes (known as "beige" or "brite" adipocytes), may be more common in adults than had been previously appreciated (**Figure 8**)(Wang and Seale, 2016). However, the majority of

adipose tissue in mammals, including adult humans, is WAT composed of large adipocytes harbouring single lipid droplet and less mitochondria than brown adipocytes (**Figure 8**).

WAT principal function is to control energy homeostasis *via* the storage and release of lipids in response to systemic nutritional and metabolic needs. WAT is distributed throughout the body in several distinct depots. They include visceral depots (vWAT), which in humans include omental, mesenteric, retroperitoneal, gonadal, and pericardial WAT (Seale et al., 2008), which are commonly associated to metabolic disorders so called diabetes and cardiovascular disease (Seale et al., 2008). Another studied depot is subcutaneous WAT (sWAT), located in several locations under the skin (Kwok et al., 2016). Clinically and extensively reviewed, sWAT confer beneficial effects on metabolism (Rosen and Spiegelman, 2014; Tchkonia et al., 2013; Tran et al., 2008). In addition to major WAT depots, discrete tissue-associated adipose depots are broadly distributed across the body. Finally, a bone marrow adipose tissue (bmAT) is thought to be distinct from either WAT or BAT (Horowitz et al., 2017).

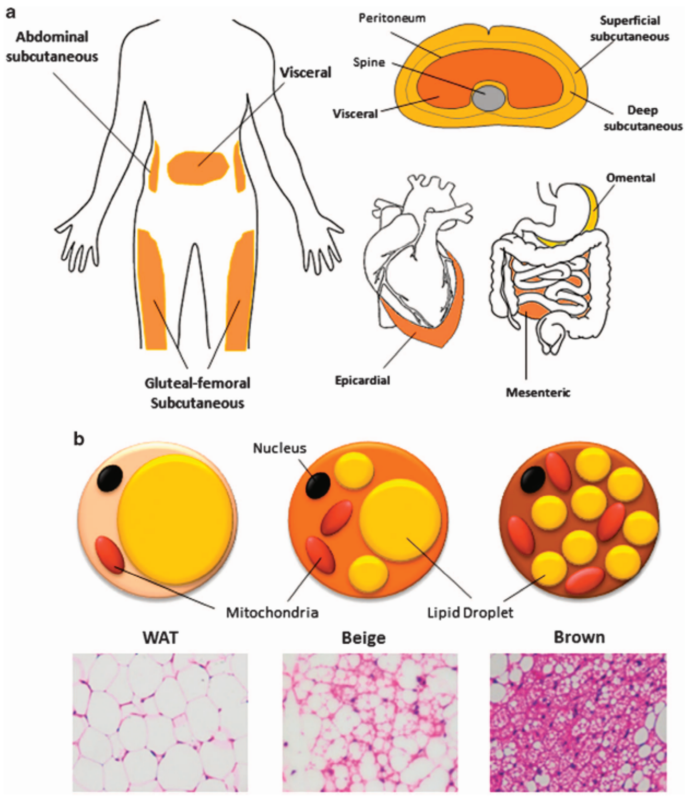

Figure 8 : Heterogeneity of adipose tissues in humans **(from Kwok et al., 2016). A.** ATs are located at different localisations : subcutaneous and visveral ATs are major ATs from the body. Visceral ATs as mesenteric are in the peritoneal cavity and subcutaneous are located bellow the skin. **B.** ATs are divided in white (WAT) and brown ATs (BAT). They play different fucntions as stockage of lipids for WAT, with a lot of lipid droplets, and dissipate stocked energy for BAT, due to high number of mitochondria and multilocular lipid droplets. Some beige adipocytes possess characteristic of both WAT and BAT.

Adipose tissues contain many types of immune cells, which reside among the adipocytes. Recent studies demonstrated a role for ILC2s in the maintenance of metabolic homeostasis by supporting the type-2 immune environment characteristic of the adipose tissue in lean individuals. ILC2s reside constitutively in visceral adipose tissue (VAT), maintained by IL-33 production, are IL-5 and IL-13 producers (Brestoff et al., 2015). ILC2s appear to regulate adiposity and caloric expenditure through several different mechanisms. In fact, reports demonstrate that IL-4 and IL-13 productions induce pre-adipocyte differentiation into beige adipocytes (Lee et al., 2015). Additionally, ILC2s have been shown to express the endopeptidase proprotein convertase subtilisin/ kexin 1 (Pcsk1), which can process the proenkephalin A produced by ILC2s to create methionine-enkephalin (Met-Enk) peptides, inducing UCP1 and adipocyte beiging, thus increasing

caloric consumption (Brestoff et al., 2015). Brown adipose tissue can then transfer energy from food into heat, potentially protecting hosts against obesity and more generally metabolic disorders by increasing caloric expenditure.

d. Pancreas

Pancreas has two types of tissues, an exocrine component (including acinar cells, centro-acinar cells, and ducts) that count for 95% of pancreas mass and secretes digestive enzymes into the intestine, and 5% of endocrine component (comprising islets of Langerhans) that secretes hormones into the blood stream (insulin and glucagon for glucose regulation), with entirely different morphologies.

ILC2s are rare cells in pancreas, as few as 1 to 2% of $CD45^+$ cell in pancreatic islet. The physiological contribution of IL-33 stimulated ILC2 is to elicit secretion of retinoic acid (RA) by macrophages and dendritic cells (DCs) thanks to IL-13 production, which in turn promotes the secretion of insulin by β cells in pancreatic islets, and then glucose regulation (Dalmas et al., 2017).

Few is known about pancreatic ILC2s, and it will be of great interest to better characterize ILC2s functions in this major metabolic tissue.

e. Skin

The skin is the largest barrier separating the body from the outside environment. It is composed of 2 main layers, the epidermis, the external one, and the dermis, with hair follicles, sweat and sebaceous glands, both on top of a subcutaneous adipose tissue (**Figure 9**).

As many physical, chemical and microbial injures occur in the skin, main goals of this tissue are to protect the internal organs from external dangers, going from sun light containing UVs, but also maintaining a stable temperature against external variations thanks to adipose tissue beiging to warm up and sebaceous glands to cool down. Various immune cell types reside in or are recruited to the skin upon inflammatory challenges. The recruitment is then mediated *via* the blood vessels present in dermis and adipose tissue, and draining lymph nodes allowing immune cells of infected

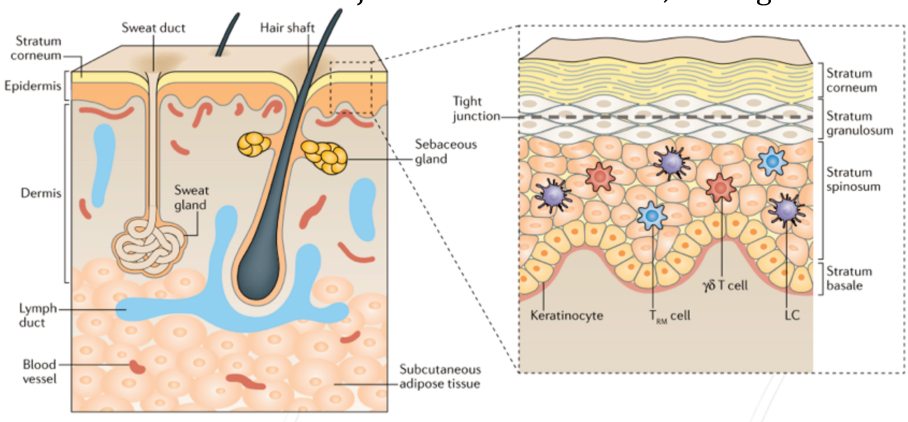

Figure 9 : Anatomy of the skin **(from Kabashima et al., 2018).** Skin is the largest barrier in the organism, composed of different layers and a large variety of cells. Immune cells are present in the *Stratum spinosum*, including dermal ILC2s that correspond to a specific subset responding to IL-18. Skin is irrigated by blood vessels and drained by lymphatic vessels, correlated with high turnover of ILC2s showed in adult mice.

skin to promote adaptive immunity after migration through lymphatic vessels (**Figure 9**)(Kabashima et al., 2018).

Among this large variety of immune cells, the first evidence of ILC2 population in mouse skin was reported as a population of Lin $^{-}$ CD25^{+} ST2^{+} c-Kit^{+} IL-7Rα $^{+}$ ICOS^{+} cells (Kim et al., 2013) expressing RORα and GATA-3 (Salimi et al., 2013). Potential immuno-surveillance activity of ILC2 in mouse skin has been reported as a unique and abundant population of CD45^{+} CD11b^{-} CD90^{hi} CD3^{-} CD2^{-} c-Kit^{-} ILC2s in the dermis of naïve mice so called 'dermal ILC2' (dILC2), not dependent on IL-25. dILC2s represent 5-10% of CD45^{+} dermal cells and express integrin αEβ7 (CD103). Using dual IL-13-dsRed and IL-4-Amcyan reporter mice, dILC2 are shown to be the main cells controlling homeostasis of the skin at steady state by IL-13 production (Roediger et al., 2013).

Furthermore, intravital multiphoton microscopy showed that CXCR6^{+} ILC2s are mainly aggregated close to blood vessels. They are constantly patrolling in skin local microenvironment as rapid migrated cells and they intermittently interact with dermal mast cells to regulate them through IL-13. Anti-CD90.2 antibody ILC2s depletion in mice are successful (Kim et al., 2013; Salimi et al., 2013) but not for CD103^{+} dILC2 from the skin (Roediger et al., 2013). Only the ILC2 population in the spleen was depleted, suggesting that CD103^{+} dILC2 population might represent a distinct sub-population of resident ILC2 in the skin. dILC2s were recently characterize as a specific subset not any more responsive to IL-33 or IL-25, but to IL-18 secreted in the skin and mediated by *Il18r1* expression, characterizing this subset with a specific tissue imprinting (Ricardo-Gonzalez et al., 2018).

ILC2 isolated from skin draining lymph nodes express skin homing markers cutaneous lymphocyte antigen (CLA), CCR10 precursors, suggesting that similar to other organs, bone marrow derived ILC2 probably circulate and can directly migrate to the skin (Yang et al., 2016b). The exact mechanism remains unclear and needs further investigations on mechanism and stages used by ILC2s for circulation.

2. *Interactions with environment : a strong imprinting*

ILC2s are highly influenced and shaped by their respective microenvironment for its immune response profile at steady state as well as upon immune challenge.

Activating cytokines, considered as strong activators for ILC2s, include IL-33, IL-25, and IL-18. These cytokines induce rapid proliferation and cytokine production from ILC2s, mainly via NF-κB and MAPK signalling pathways. Responsiveness to these cytokines is somehow different depending on the tissue, and in some cases, on the expression of co-stimulatory cytokines (**Figure 10**). Their role on peripheral ILC2 turnover is still poorly deciphered, but roles of such stimulations will be central for ILC2s trafficking.

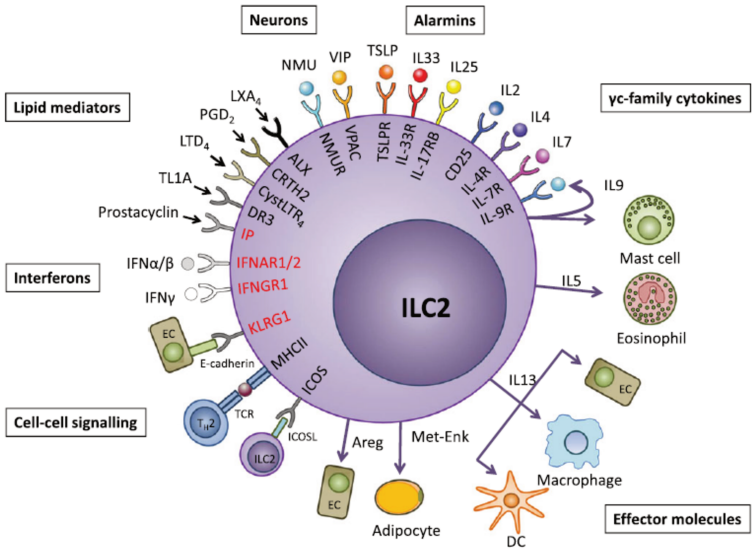

Figure 10 : Regulation of ILC2 activation and effector functions of ILC2-derived cytokines **(from Schuijs and Halim, 2016).** ILC2 integrate multiple signals. They are mainly regulated by IL-18, IL-25, IL33 and TSLP, but their activation is strongly influenced by a variety of other signals : γc-dependant cytokines, lipid- and neuro-mediators and cell-to-cell interactions. It allows activation and secretion of type-2 cytokines such as IL-5 and IL-13, but also other molecules as Met-Enk. In red : receptors inducing inhibitory signal.

a. ILC2 activating cytokines

IL-33 : the key cytokine

IL-33 is an alarmin cytokine of the IL-1 family, corresponding to endogenous molecules that act as danger signals and are generated as a result of non-programmed cell death (Yang et al., 2017). IL-33 is constitutively expressed at high levels in the *nuclei* of various cellular types such as epithelial, endothelial, and mesenchymal cells. Following tissue injury and/or cellular activation through ATP signalling, these cells promptly release IL-33. Released full-length IL-33 is rapidly cleaved by protease derived from neutrophils, mast cells, or environmental allergens as papain, to become mature IL-33, a 30-fold more potent molecule for ILC2s activation (Cayrol and Girard, 2014; Cayrol et al., 2018; Lefrancais et al., 2014; Liew et al., 2016). IL-33 plays important roles in type-2 innate immunity, and after parasitic (*N.b.*) and viral infections (influenza virus), it mediates strong activation of ILC2s (see *ILC2s : important regulation for functions in diseases* part below).

IL-33 binds to a heterodimeric receptor formed by T1/ST2 and the IL-1 receptor accessory protein (IL-1RAcP)(**Figure 10**), leading to NF-κB and MAPK (ERK, p38, JNK) signalling pathways activation via MyD88 (Liew et al., 2016). More precisely, p38 MAPK activation induces GATA3 phosphorylation and promotes GATA3 binding to the IL-5 and IL-13 promotor regions of ILC2s. Also, IL-33 induces IL-6 production by ILC2s but as a GATA3 independent process (Furusawa et al., 2014). Target cells include ILC2s, mast cells and their progenitors, basophils, eosinophils, Th2 cells, regulatory T cells, NKT and NK cells (Griesenauer and Paczesny, 2017). However, it exists a soluble decoy receptor lacking transmembrane and cytoplasmic domains contained on ST2 and instead contains a unique nine amino acid C-terminal sequence, called sST2 (Gächter et al., 1996). This sST2 is enhanced by pro-inflammatory cytokines (IL-1β and TNFα) and participates to the inhibition of IL-33 effects, decreasing the production of the type-2 cytokines IL-4 and IL-5 but not the type-1 cytokine IFN-γ (Oshikawa et al., 2002). Then, sST2 may be an important soluble factor to modulate systemic propagation and effects of IL-33, and understanding its production in different tissues questioned.

IL-33 serves as a critical cytokine for the activation of mouse and human ILC2s by induction of intense proliferation and type 2 cytokines production (IL-5, IL-6, IL-13, GM-CSF, and amphiregulin), chemokines (such as eotaxin), and peptides (like Met-Enk, an endogenous opioid-like peptide)(Cayrol and Girard, 2014). The responsiveness of ILC2s to IL-33 is controlled by Gfi1, a TF regulating ST2 surface expression on ILC2 surface (Spooner et al., 2013). Interestingly, the responsiveness to IL-33 and the cytokine production profiles differ depending on tissue and species (Halim et al., 2012b; Mjösberg et al., 2011; Moro et al., 2010). For example, blood human ILC2s but also mouse new-born and fetal mesentery ILC2s do not respond well to IL-33-stimulation alone, whereas a combination of IL-33 with other "co-stimulatory cytokines" such as IL-2, IL-7, and TSLP potently activate them (Koga et al., 2018; Mjösberg et al., 2011).

Collectively, these findings suggest that IL-33 effects, specifically on ILC2s, differ depending on tissue, but also on timing and type of inflammation. These differences might be due to other local mediators, which modify the function and phenotype of ILC2s. IL-33 remains central for ILC2 functions, and it will be an important cytokine to study turnover of ILC2s, independently from the replenishment of peripheral ILC2s.

IL-25 : a redundant Th2 molecule ?

IL-25, also named IL-17E, is part of the IL-17 family of cytokines. At steady state, IL-25 is constitutively expressed by tuft cells, a specific population of epithelial cells in the intestine (Gronke and Diefenbach, 2016; Von Moltke et al., 2016) but also salivary gland, in the respiratory tract (trachea) and other tissues (Liu et al., 2018; Sato, 2007).

Tuft cells were initially considered as important for chemosensory role involved in transduction of bitter and umami tastes (Howitt et al., 2016; Sato, 2007), but recent

studies using IL-25 reporter mice have revealed that tuft cells constitute the primary source of IL-25 in the intestine after parasite infections (Gerbe et al., 2016; Gronke and Diefenbach, 2016; Howitt et al., 2016; Von Moltke et al., 2016). Surprisingly, after inflammation or allergen stimulation, IL-25 could also be expressed at low levels in other cell types such as Th2 cells, mast cells, alveolar macrophages, basophils, and eosinophils, even if the functional role of this expression remains unclear (Fort et al., 2001; Ikeda et al., 2003; Kang et al., 2005; Wang et al., 2007). Parasitic infections mediated tuft cells hyperplasia, thus increasing IL-25 production in the gut mucosa. It remains to be elicited whether specific infections at other location (as for lung) increases rare IL-25 producing tuft-like cells described in trachea (Von Moltke et al., 2016).

IL-25 binds to a heterodimeric receptor consisting of IL-17Rα and IL-17Rβ (**Figure 10**). It activates MAPK (JNK and p38) and NF-κB pathways, as IL-33, but here mediated *via* TRAF6 and Act-1 on IL-17Rα chain (Petersen et al., 2012). However, IL-25 alone has limited effect *in vitro* on ILC2s activation. The combination of IL-25 and IL-2 induces a rapid proliferation and type-2 cytokine production by ILC2s (Moro et al., 2010). Similarly, as IL-33, IL-2 plus IL-25 activate p38 MAPK, promoting GATA3 phosphorylation in ILC2s (Furusawa et al., 2014). In mice, intranasal administration of IL-25 alone induces weak ILC2-mediated type-2 inflammation in the lung (Barlow et al., 2012, 2013). Using IL-25$^{-/-}$ mice, IL-25 has been described as an important cytokine for type-2 immune response in murine asthma model (Suzukawa et al., 2012) but no direct local production and effect has been showed. In fact, propagation of IL-25, or migration of IL-25 stimulated cells from other tissues may impact lung immunity. Then, it remains important to understand if IL-25 alone is able to drive ILC2 response *in vitro* and *in vivo* or if other cells are needed to secrete the co-stimulatory cytokines such as IL-2 producing T cells *in vivo*. Conversely to IL-25, the intranasal administration of IL-33 was more potent to increase lung ILC2 number, coupled with type-2 inflammation in the lung (Barlow et al., 2012, 2013).

Less efficient than IL-33 to activate ILC2s, IL-25 role may be to induce specific stimulations of ILC2 subsets or restricted functions (see *ILC2s : important regulation for functions in diseases* part below). Moreover, characterization of the tissues where IL-25 is directly stimulating immune cells needs to be questioned.

IL-18 : specific to the skin ?

IL-18 belongs to the IL-1 family of cytokines, as IL-33 and IL-1α. IL-18 is produced as a "pro-IL-18" that needs a cleavage from cysteine protease caspases 1 to generate a mature active form (Nakanishi, 2018). The receptor for IL-18 (IL-18R) is selectively expressed by skin ILC2 and BM ILC2Ps at steady state (**Figure 10**). IL-18 is functionally important for the optimal activation and proliferation of ILC2s during the development of atopic dermatitis induced by an analog of vitamin D3 in mice (Ricardo-Gonzalez et al., 2018). More importantly, both IL-18Rα and IL-18Rβ, subunits of the functional receptor

for IL-18 (IL-18R), are expressed by skin ILC2s. These dILC2s constitutively express IL-5 even in absence of IL-33-, IL-25-, or TSLP-mediated signalling pathways, but they remain able to produce type-2 cytokines, including IL-13, after stimulation with IL-18. IL-18R-expressing ILC2s have also been described in human peripheral blood, and they can produce type-2 cytokines in response to stimulation with IL-7 and IL-18 (Simoni et al., 2017). IL-18 might facilitate type-2 responses by stimulation of basophils and mast cells to produce type-2 cytokines (Nakanishi, 2018). IL-18 seems specific to skin ILC2 stimulation, and reinforce the idea than IL-18 and IL-25 may specifically induce certain type of ILC2 functions by different pools.

b. Co-stimulatory signals of ILC2 activation

"Co-stimulatory cytokines" promote activation of ILC2s along with activating cytokines, and comprise members of the common gamma chain (γc) family of cytokines (**Figure 10**). γc family cytokines signal through JAK/STAT pathways and play critical roles in survival, development, and also maintenance of ILC2s. They are definitively important signals to specify ILC2 functions in different situations.

TSLP : lung and skin

TSLP (for thymic stromal lymphopoietin) plays a critical role in the induction of type 2 inflammations in various allergic diseases. It is mainly produced by epithelial cells, fibroblasts, and stromal cells (Ziegler, 2012). The TSLP receptor is closely related to the IL-7 receptor and consists of IL-7Rα and TSLPR (**Figure 10**). It activates STAT5 through JAK1 and JAK2 (Ziegler et al., 2013). TSLP signalling pathways analysis show that TSLP is able of activating not only STAT5 but STAT1, STAT3, STAT4, STAT6, PI3K/Akt, SRC, NK-κB, and MAPK (ERK, JNK, p38) pathways (Zhong et al., 2014). TSLP assists ILC2s survival similarly to IL-2 and IL-7. TSLP stimulation alone does not induce type-2 cytokine production from lung ILC2s (Mohapatra et al., 2016).

However, TSLP along with IL-33 has a synergistic effect on both proliferation and type-2 cytokine production of mouse and human ILC2s (Camelo et al., 2017; Halim et al., 2012b; Mohapatra et al., 2016). TSLP induces a corticosteroid resistance of mouse and human ILC2s, by STAT5-activation of an anti-apoptotic molecule, Bcl-xL, in mice, contributing to pathologic functions of ILC2s in allergies (Kabata et al., 2013). Besides, a combination of TSLP with IL-33 induces IL-9 production from ILC2s *via* interferon regulatory factor 4 (IRF4) (Mohapatra et al., 2016).

Collectively, the function of TSLP resembles that of "co-stimulatory cytokines" such as IL-2 and IL-7 as a STAT5-inducing cytokine rather than of activating cytokines such as IL-33 and IL-25.

IL-2

As for T cells, IL-2 promotes the proliferation and survival of ILC2s. Isolated ATs ILC2s can survive and proliferate slowly during several weeks in response to IL-2 and feeder cells without any phenotype modifications (**Figure 10**)(Moro et al., 2010). In addition, IL-2 leads to the corticosteroid-resistance of ILC2s *in vitro*, reversing corticosteroid induced apoptosis of ILC2s (Kabata et al., 2013). In fact, ILC2s produce small amounts of type 2 cytokines and expand slowly in response to IL-2 alone, whereas combination of IL-2 with IL-25 and IL-33 induces the production of high amounts of type-2 cytokines and rapid proliferation of ILC2s (Moro et al., 2016). Also, IL-2 modifies the cytokine production from ILC2s. Indeed, added IL-2 specifically induces IL-9 production by lung ILC2s *in vitro* (Wilhelm et al., 2011). Furthermore, a study shows that a combination of IL-2 and IL-33 allows induction of IL-10 production by ILC2s (Wilhelm et al., 2011), showing ILC2 adaptation to different signals.

Finally, IL-2 has a function to enhance cell survival and modify the cytokine production from ILC2s.

IL-7

IL-7 is a critical cytokine for the development of lymphoid cells including ILC subsets, as shown by the significant reduction of ILCs in IL-7- or IL-7Rα-deficient mice (Moro et al., 2010). IL-7 is produced in several tissues by stromal cells, epithelial cells and fibroblasts, it binds to IL-7Rα and γc (**Figure 10**), to activate JAK/STAT (STAT1, STAT3, and STAT5), PI3K/Akt, SRC, and MAPK pathways (Moro et al., 2010). As for IL-2, IL-7 strongly activates STAT5 and is involved in the development, maturation, and survival of ILC2s (Xue et al., 2014). IL-7 alone is insufficient for proliferation and type-2 cytokines production of ILC2s. However, combination of IL-7 with other activating cytokine create synergistic effects on ILC2s as for IL-2 combination (Moro et al., 2016). Finally, it has been demonstrated that IL-7 also induces a corticosteroid-resistance of ILC2s *in vitro*, limiting treatment in refractory asthmatic patients (Kabata et al., 2013).

c. Direct receptor interactions

Group 2 innate lymphoid cells express various surface molecules that can interact with their respective ligands using *trans* and *cis* cellular interactions. However, only a small number of *trans* ILC2s cellular interaction have been studied so far. ILC2s can then be regulated by cell-to-cell interaction in local tissues, but interaction with other cell type would be important during trafficking of ILC2s, as circulation allow lots of interaction with a large variety of cells from different environments (**Figure 10**).

Icos / Icos ligand

Inducible T cell co-stimulator (CD278) belongs to the CD28 family. It is described as an important regulatory molecule in T cell signalling transduction (Leconte et al., 2016; Yoshinaga et al., 1999). Icos is expressed in both mouse and human ILC2s independently to their location, at steady state and following stimulation (**Figure 10**). Deficiencies of Icos or its ligand IcosL lead to reduced numbers of lung and intestinal ILC2s and a decreased expression of KLRG1 (Paclik et al., 2015). Intranasal IL-33 stimulation or Alternaria-induced lung inflammation don't recover pulmonary ILC2s in these same Icos and IcosL deficient mice (Maazi et al., 2015; Paclik et al., 2015). Again in the lung, Icos deficient ILC2s is linked to reduced survival, cytokine production, and reduced pSTAT5 levels, all keys for efficient function and signal transduction in ILC2s (Maazi et al., 2015).

PD-1 / PDL-1/2

Programmed death 1 (CD279 or PD-1) is another member of the CD28 family that is an important negative regulator of T cells. PD-1 treatment has been successfully used in cancer therapy (Sharpe and Pauken, 2018). The two PD-1 ligands, PD-L1 and PD-L2, are expressed on several immune and non-immune cells (Sharpe and Pauken, 2018). Importantly, ILC2s have recently been shown as influenced by PD-1-ligands interaction (**Figure 10**). PD-1 is first a key factor for ILC2 development and function as it is expressed on both mature ILC2s and ILC2 progenitors (Taylor et al., 2017; Yu et al., 2016). PD-1 regulates ILC2s by inhibiting STAT5 phosphorylation, leading to reduced ILC2 proliferation and cytokine production (Eastman et al., 2017).

KLRG-1 / E-Cadherin

Killer cell lectin-like receptor subfamily G member 1 (KLRG-1) is expressed on mature activated T cells and NK cells but also on mature ILC2s (**Figure 10**). KLRG-1 binds to cadherins (E, N, and R) expressed by epithelial cells. In contrast to N- and R-cadherins, which are expressed by the nervous system, E-cadherin are found on epithelial cells and Langerhans cells (Henson and Akbar, 2009). Indeed, pulmonary KLRG1$^+$ ILC2s may interact with E-cadherin expressed on lung epithelial cells, located basolateraly, just next to intercellular tight junctions formed by the lung epithelium (Hartsock and Nelson, 2008; Metzger et al., 2008). However, the exact mechanisms and the KLRG1 downstream signalling pathways within ILC2s after interaction with its ligand are still not understood. Moreover, whether KLRG1$^+$ ILC2s are able to interact with N- and R-cadherins expressed by the nervous system *via* KLRG1 still remains elusive and need to be documented.

MHC-II / TCR

ILC2s have been reported to express and/or upregulate MHC-II upon activation (**Figure 10**)(Mebius et al., 1997; Neill et al., 2010). The role of MHC-II activation for ILC2

functions has been deciphered using MHC-II$^+$ ILC2s *in vitro* co-culture with T cells and MHC-II deficient mice (Mirchandani et al., 2014; Oliphant et al., 2014). ILC2s express MHC-II at homeostasis or following systemic IL-33 activation to various extent depending on their location, for example, pulmonary ILC2s show less MHC-II expression compared with small intestinal ILC2s (Oliphant et al., 2014). ILC2s express functional MHC-II molecule that are completely able to process and present antigens. However, MHC-II expression on ILC2s stay stable *in vivo* whereas ILC2s downregulate MHC-II cell surface expression after *ex vivo* cultures (Oliphant et al., 2014). In addition to systemic administration, intra-nasal IL-33 increased MHC-II expression on a subpopulation of pulmonary iILC2s (Oliphant et al., 2014).

d. Sex sensitivity : Roles of hormones

Sex hormones include androgen and oestrogen that are well known as regulators for the development and functions of multiple immune cell types (**Figure 10**)(Kovats, 2015; Laffont et al., 2017). Female mice exhibit increased numbers of ILC2s in the lungs, visceral adipose tissues, and mesLNs compared to those in male mice (Laffont et al., 2017). In fact, endogenous androgen in males suppresses ILC2 development and activation. Conversely, female oestrogen is related to the maintenance of uterus-resident ILC2s (Bartemes et al., 2018). Oestrogen signalling does not affect lung ILC2s. Indeed, uILC2s are significantly decreased following ovariectomy and increased after oestrogen administration, when lung ILC2s are unaffected under these treatments. In addition, uILC2s are shown as reduced in oestrogen receptor-deficient mice (Bartemes et al., 2018). Thus, these data show new heterogeneity of ILC2s as oestrogen exerts different effects on ILC2s depending on the tissue. A similar signal can then have different effects depending on ILC2 localisation, and an the quantity of accessible molecules and expressed receptors are then central for the orientation of ILC2 response.

e. Role of alimentary nutrients

Butyrate constitutes a short chain fatty acid (SCFA), mainly end product of dietary fiber fermentation of anaerobic bacteria. SCFAs, comprising propionate and butyrate for example, have protective role on intestinal inflammation through a direct action on regulatory T cells (Furusawa et al., 2013). In mouse and human, butyrate inhibits ILC2 proliferation, Gata3 expression and decreases their production of type-2 cytokine (**Figure 10**). Butyrate, as well as trichostatin A (TSA) used as control, are histone desacetylase (HDAC) inhibitors that are suppressing the ILC2-mediated lung inflammation that follows IL-33 and Alternaria stimulations, decreasing epigenetic modification of ILC2 mandatory for adaptation to environment (Thio et al., 2018; Toki et al., 2016). SCFAs can directly pass through the intestinal barrier and reach lymph, LNs and circulation, where activation of ILC2s can then occur.

Retinoic acid is the biologically active metabolite form of vitamin A. In human, IL-2, IL-7, TSLP, IL-33, or IL-25 together with RA induces type-2 cytokine production from ILC2s. IL-2 plus RA induces expression of the gut-homing integrin, α4β7, on human ILC2s (**Figure 10**)(Ruiter et al., 2015). Conversely, in mice, RA is promoting gut-homing receptors on ILC1s and ILC3s but not ILC2s. Hence ILC2s migration to the gut is not regulated by RA signalling (Kim et al., 2015). Importantly, lack of RA promotes ILC2 proliferation and cytokine production (Spencer et al., 2014). Thus, RA effects on ILC2s are probably species-dependent but differences could be explained by *in vitro* experiments on human *versus in vivo* experiments on mice.

Lipid mediators come from arachidonic acid metabolites and include leukotrienes (LT) and prostaglandins (PG). They play critical roles at homeostasis and under inflammation. Leukotrienes and prostaglandins are respectively generated from arachidonic acid by 5-lipoxygenase and cyclooxygenase. Each mediator is further processed to give downstream metabolites by different enzyme cascades. Lipid mediators used during *in vitro* cultures of ILC2s or *in vivo* administration in mice showed that LTB4, LTC4, LTD4, LTE4, and PGD2, are positively regulating ILC2s, whereas LXA4, PGE2, and PGI2 are negative regulators (**Figure 10**). Lipid meditors act by binding G-protein coupled receptors. Positive regulators increase the intracellular levels of Ca^{2+}, leading to ILC2s activation (Doherty et al., 2013; Oguma et al., 2008; Pettipher, 2008; Singh et al., 2010; Xue et al., 2014). In contrast, negative regulators such as PGE2 and PGI2 activate adenylate cyclase (AC) and cAMP/PKA pathways by suppressing IL-33 or Alternaria-induced activation of ILC2s through the decreased expression of GATA3 and ST2 or CD25 (Maric et al., 2018; Zhou et al., 2016). Lipid mediators are then in close localisation to ILC2s in metabolic tissues and act as important regulators.

f. Regulation by neuropeptides

Multiple interactions occur between nervous system and immune system. Several studies recently revealed roles for neuropeptides produced by peripheral neurons on the function of ILC2s in local tissues, specifically in the lung and intestine.

Neuromedin U (NMU) is a neuropeptide ubiquitously distributed in peripheral neurons and central nervous system (SNC). NMU bore two G-protein coupled receptors, NmUR1 and NmUR2, that activate the MAPK pathway (ERK1/2) and induces increased Ca^{2+} influx (Brighton et al., 2004). Three reports revealed that ILC2s selectively express NmUR1 at steady state and following inflammatory conditions (**Figure 10**)(Cardoso et al., 2017; Klose et al., 2017; Wallrapp et al., 2017). NMU directly induces ILC2 proliferation and production of IL-5, IL-9, IL-13, and Areg. Inhibitors of ERK, Gq protein, calcineurin, and NFAT inhibits NMU effect, indicating that NMU activates ILC2s via both ERK signalling and Ca^{2+}-NFAT patways through the Gq protein (Cardoso et al., 2017; Klose et al., 2017). In HDM-induced lung inflammation, type-2 cytokine production by ILC2s is again

decreased in NmuR1-deficient mice (Wallrapp et al., 2017). Therefore, NMU is and activator of ILC2s via Ca^{2+}-NFAT and MAPK pathways.

Vasoactive intestinal peptide (VIP) is a neuropeptide part of the secretin family expressed by neurons in the gut and pancreas. VIP receptors are G-protein coupled receptors named VPAC1 and VPAC2 that activate the AC/cAMP/PKA pathway and phospholipase C, inducing an increase of intracellular Ca^{2+} levels (Dickson and Finlayson, 2009). ILC2s express VPAC2 (**Figure 10**) and then VIP induces IL-5 production in presence of IL-7. As quantity of blood eosinophils and levels of type-2 cytokine expressing ILC2s are affected by food intake and circadian rhythm, it strongly suggests that VIP, an important regulator of the circadian cycle in the brain, might regulate the change of blood eosinophils through activation of ILC2s (Nussbaum et al., 2013). Circulation is directly regulated by day and night rhythm, and VIP could then directly impact ILC2 activation and trafficking.

3. *Innate secreting helper cells*

Group 2 innate lymphoid cells actively shape their microenvironment by the release of several different cytokines, mainly IL-4, IL-5 and IL-13 but also IL-9, IL-10, and amphiregulin (Areg)(**Figure 11**). The secretion of these immune mediators can be beneficial or detrimental for the host and therefore a well-balanced and fine-tuned release of cytokines by ILC2 cells is needed.

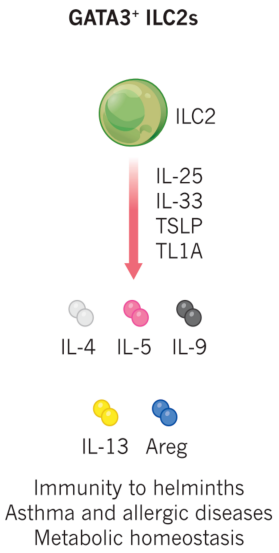

***Figure 11 : ILC2s as secretor cells* (adapted from Artis and Spits, 2015).** ILC2s are major producers of type-2 cytokines to promote immune responses.

a. IL-4

IL-4 is a key cytokine for the differentiation of Th2 cells but also for stimulation of B cells to produce IgE antibodies. IL-4 is mainly produced by T cells, NKT cells, basophils, and mast cells (Walford and Doherty, 2013). It binds to the IL- 4 receptor, constituted by IL-4Rα chain (CD124) and γc, and it activates STAT6 and IRS-2 via JAK1 and JAK3. IRS-2 further activates PI3K/AKT and NF-κB pathways. IL-4Rα is able to form a different type of receptor as a complex with IL-13Rα1, which can bind both IL-4 and IL-13. It also enhances STAT6 via JAK1 and TYK2/JAK2 (Kandasamy et al., 2010).

IL-4 promotes type-2 cytokine production and maintains ILC2 phenotype that bore its receptors. In mice, secreted IL-4 rapidly stimulate ILC2s to produce IL-5, IL-9, IL-13, CCL3, CCL5, and CCL11 *in vitro*, and a synergistic effect exist with the addition of IL-33 (Kandasamy et al., 2010).

b. IL-5

IL-5 signals lead to maintenance of survival and functions of B cells and eosinophils. IL-5 acts on target cells by binding to its specific IL-5 receptor (IL-5R) that consists of two distinct subunits α and β, and it specifically binds to the IL-5Rα subunit. It transduces a signal through JAK–STAT, Btk, and Ras/Raf-ERK signalling pathways (Takatsu, 2011).

Upon activation, ILC2s are able to secrete IL-5 (**Figure 11**), which is important for eosinophil homeostasis and B cell function (Hamza et al., 2010; Moro et al., 2010). The production of IgA upon co-culture of mesenteric ILC2s and splenic B cells is described as IL-5 dependent (Moro et al., 2010). In addition, proliferation as well as IgA, IgM, IgE, and IgG1 secretion by B-1 and B-2 cells by peripheral (peritoneal cavity, spleen) and pulmonary ILC2s was observed in *ex vivo* co-culture experiments (Drake et al., 2016). However, how B cells and ILC2s interact within their environment *in vivo* still needs further investigation.

Future experiments will be needed to decipher both cellular and molecular signalling cascades triggered by IL-5 to support tissue restoration and homeostasis.

c. IL-9

IL-9 stimulates various types of cells including lymphocytes, mast cells, and epithelial cells. Several immune cell types as T cells, mast cells, NKT cells, and ILC2s are able to produce it (**Figure 11**)(Goswami, 2017). The IL-9 receptor is composed of IL-9R and γc. IL-9 binding is strongly activating STAT5 via JAK1 and JAK3. In addition, IL-9 is also capable of activating STAT1, STAT3, PI3K/Akt, MAPK, and NF-κB pathways (Goswami, 2017).

IL-9 enhances the survival of ILC2s and induces their production of type-2 cytokines. IL-9 activates an anti-apoptotic protein named Bcl-3 (Turner et al., 2013), and induces the corticosteroid-resistance of ILC2s *in vitro* although this effect is relatively weak compared to that of IL-2, IL-7, or TSLP (Kabata et al., 2013). IL-9 directly induce IL-5 and IL-13 productions *in vitro* by lung ILC2s isolated from helminth-infected mice (Wilhelm et al., 2011).

ILC2s are also IL-9 producers in response to IL-2 or a combination of IL-2 with IL-33, IL-7 with IL-33, and TSLP with IL-33 via IRF4 signalling pathway (Mohapatra et al., 2016). In fact, IL-9-deficient ILC2s show impaired production of IL-5 and IL-13 in response to IL-33 plus TSLP *in vitro*, suggesting that an IL-9 autocrine loop plays an important role for the function of ILC2s (Mohapatra et al., 2016).

d. IL-13

IL-13 belongs to the class of type I cytokines and shares 25% homology with IL-4. In fact, IL-13 and IL-4 share the IL-4rα to signal. More precisely, IL-13 possesses 2 specific receptors, IL-13rα1 and IL-13rα2. When a dimeric receptor made of IL-4Rα and IL-13rα1 can signal through JAK–STAT pathway and specifically STAT6, IL-13rα2 has been described in a soluble decoy form in circulation *in vivo* (Khurana Hershey, 2003).

By secretion of IL-13, ILC2s are able to target both non-immune and immune compartment in several tissues. IL-13 releasing ILC2s (**Figure 11**) can initiate mucus secretion, induce goblet cell hyperplasia and induce smooth muscle contraction helping to homeostatic process of digestion or under infectious diseases (Doeing and Solway, 2013; Morimoto et al., 2006). However, the exact pattern of IL-13 receptors on cells at steady state and during immune challenges is not yet fully clear.

e. Amphiregulin

Amphiregulin (Areg) is a member of the epidermal growth factor (EGF) family. Areg is transcribed as a transmembrane polarized glycoprotein precursor (Pro-Areg) and the mature soluble Areg (containing the EGF) motif is produced following proteolytic

cleavage of pro-Areg. Areg signalling depends on the processing and trafficking of the protein, and can be triggered in different manners : juxtacrine, autocrine, paracrine, by intracellular nuclear translocation, and by its inclusion in exosomes. The juxtacrine and autocrine/paracrine signalling mediated by pro-Areg and Areg depends mainly on the binding and activation of EGFR (Berasain and Avila, 2014). EGFR has been reported to be expressed by all cells including hematopoietic cells (Zaiss et al., 2015). Downstream receptor activation trigger multiple intracellular signalling pathways, including Ras/MAPK, PI3K/AKT, mTOR, STAT and PLCγ, modulating gene expression and eliciting multiple cellular responses such as proliferation, survival, invasiveness, mobility and angiogenesis (Berasain and Avila, 2014).

Diverse stimuli have been associated with production of Areg by leukocytes. For ILC2s (**Figure 11**), IL-33 exposure stimulates Areg expression in lung, intestine and skin. As such, innate Areg expression by ILC2s constitutes a primordial mechanism to promote wound healing and tissue homeostasis after pulmonary, dermal or intestinal challenges.

4. Memory ILC2s : remember me

Immunological memory has first been described as a property of the adaptive immune system resulting from potent responses on exposure to an antigen encountered previously. After re-encounter with the same antigen, memory cells specific to the antigen respond faster and more efficiently than naïve cells. Antigen specificity has long been considered an essential feature of immunological memory (Ahmed and Gray, 1996; Swain et al., 1996; Zinkernagel, 2000).

Recently, discovery of memory NK cells have shown that innate lymphocytes also have specific memory (Sun et al., 2009). Recent studies have also suggested that macrophages bore some features of memory. β-glucan-mediated activation of macrophages results in their differentiation into highly functional macrophages that live up to 4 weeks (Quintin et al., 2012). This memory has been named “trained immunity” (**Figure 12**), with antigen specificity, and is mediated by epigenetic modifications rather than genetic changes (Netea et al., 2016; Saeed et al., 2014).

One study shows that ILC2s can remember previous activation, and then they are able to respond more efficiently following second challenge with allergens in the lung and lung-draining lymph nodes (Martinez-Gonzalez et al., 2016). As already discussed, ILC2s do not recognize specific antigens but are directly activated by alarmins, and therefore their memory is not antigen specific. Nevertheless, ILC2s show an enhanced response similar to T cells. Analyses of their phenotype and functions after a long time demonstrated that they acquire immunological memory. Indeed, intranasal papain, fungal protease or IL-33 injections into naïve mice induced a 10- to 100-fold increase of lung ILC2s number (Gold et al., 2014; Halim et al., 2012b; Martinez-Gonzalez et al., 2016). Then,

the resolution of inflammation and a contraction phase was observed, as showed in trained immunity.

Moreover, lung ILC2 numbers in challenged mice remained higher than in naïve mice for several months, suggesting that pre-activated ILC2s persist for a long period of time. Lung ILC2s labelled with BrdU were detected for more than 2 months, indicating long live of the same ILC2s that get activated. The lung-draining LNs contain few ILC2s in naïve mice, but this population expand, activate, and then encounter a contraction phase similarly to lung ILC2s (**Figure 12**). Whether the activated lung ILC2s are migrating to the draining LNs remains unclear, and relationship between these populations have to be understood (Martinez-Gonzalez et al., 2016).

Last proof of memory phenotype is the increased capacity of these ILC2s to respond to inflammation. Allergens- or IL-33-challenged mice were boosted with an unrelated allergen several months later. Lung ILC2s from challenged mice responded more intensely than those of naïve mice. More precisely, 'trained' ILC2s are more proliferative and produce greater quantities of IL-5 and IL-13 compared to naïve ILC2s (**Figure 12**). Lung-ILC2s are surprisingly capable of "remembering" a first activation when they become "long-lived" or "memory" ILC2s (6 months or longer in mice) (Martinez-Gonzalez et al., 2016).

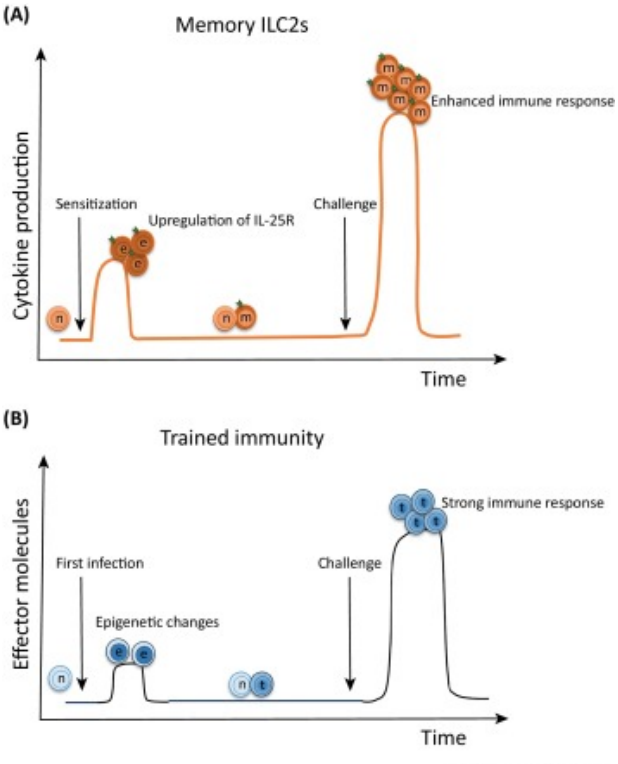

Figure 12 : Memory ILC2s vs trained immunity **(from Martinez-Gonzalez et al., 2017). A.** Model of memory ILC2s response following sensitization, contraction phase and second activation called challenge. **B.** Memory ILC2 model is based on trained immunity model, that also show a stronger immune response after a secondary stimulation of memory cells.

To conclude, both ILC2s respond to a primary stimulus and increase in number either by proliferation or by recruitment. They are able to remember the state of activation, they become long lived immune cells in tissues, and following a second stimulus, they respond more intensely (**Figure 12**). However, ILC2s are already committed to specific functions in their naïve state (Martinez-Gonzalez et al., 2016). It remains to be studied whether ILC2 memory also involves epigenetic changes, Studying their surveillance ability as recirculating or tissue resident cells compare to other ILC2 pools, important characteristic of memory cells, may give information on ILC2 memory cells.

Now, immunological memory, at least for innate immunity, can be defined as the ability of immune cells to remember information from a previous activation and to show stronger and faster effector functions than during the primary challenge. Future research will have to focus on the factors important for memory ILC2s appearance, as well as potential memory of other ILC subsets, to better understand the concept of immune memory. The trained-immunity has been proposed for this form of immune memory, and shows similarities with the adaptive memory.

C. ILC2s : important regulation for functions in diseases

Following their discovery in gut-associated tissues, it has become evident that ILC2s may be involved in other innate type-2 immune processes. To date, ILC2s have been implicated or associated with an increasing list of functions in diseases. Importantly, ILC2s also function in other type-2 cytokine-driven processes such as lipid metabolism and thermogenesis in adipose tissue and metabolic trouble regulation in adipose tissues and pancreas. They play important roles in maintenance of homeostatic conditions of lung or intestine, where dysregulation induce severe chronic allergies or colitis. They respond to viral infections or environmental modifications, with variable roles from eosinophil homeostasis, development of alternatively activated macrophages or anti-helminth major mediators. Furthermore, innate IL-5-producing cells are present in the liver, uterus, heart, kidney and brain of naive mice (Nussbaum et al., 2013), suggesting potential roles of circulating ILC2s in these organs, free of ILC2s at homeostasis. The main function of ILC2s is communication with other immune or non-immune cell types, either to activate them, to recruit them or to have broader impact on healing tissues. More precisely, ILC2s can impact on many other cell types, as all innate and adaptive immune cells. They also send signals to all non-immune cells, enhancing activation and responses, differentiation and maintaining or recover homeostatic conditions (**Figure 13**). These interactions are central for ILC2 local adaptation to tissues, and specifically following migration of different ILC2 pools in new tissues.

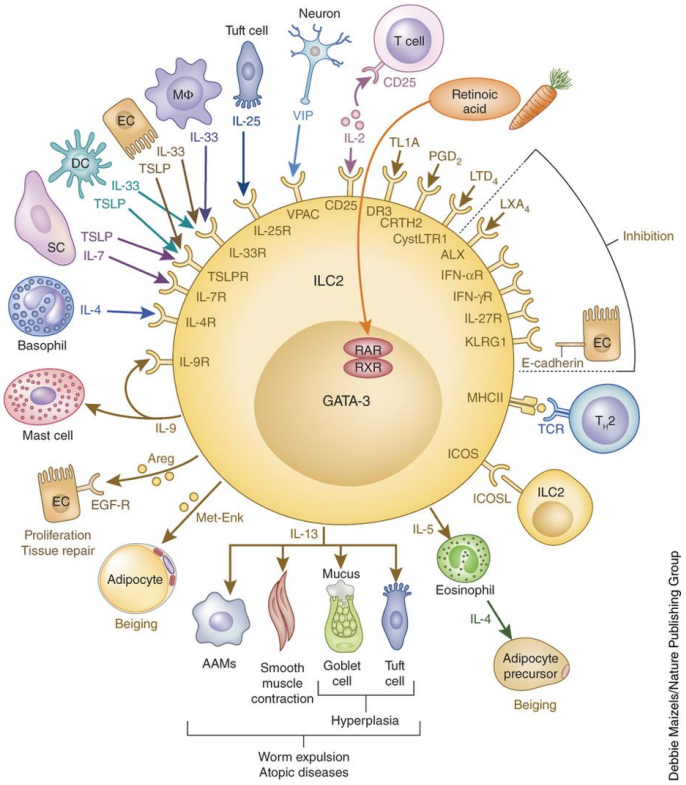

Figure 13 : ILC2s communication with other cell types **(from Klose and Artis, 2016).** ILC2s express an array of activatory and inhibitory receptors that allows them to interact with a large variety of cells. Then, they receive signals to be negatively regulated or to be enhanced and secrete molecules participating to type-2 defences.

1. Homeostatic and regulated functions

a. Metabolic troubles : Obesity and diabetes

Although it has been quite reviewed that genetic and environmental factors were the major influence on the development of obesity and diabetes, many recent data have shown that immunological factors are also important contributors to the pathogenesis of

obesity and linked diabetes comprising insulin-resistance and decreased production of insulin. Then, several immune cell types have been recognized as critical regulators of metabolic homeostasis (Jin et al., 2013; Osborn and Olefsky, 2012), and crosstalks involving different immune cells to low grade inflammation in many organs as adipose tissues, pancreas, liver and intestines, are now consider as characteristics and potentially regulatory actors behind the development of obesity (Osborn and Olefsky, 2012; Winer et al., 2016).

ILCs are now recognized as new regulators involved in both adipose tissue and metabolic homeostasis maintenance (Bostick and Zhou, 2016; Yang et al., 2016a). Most of the studies on ILC roles in metabolism are focused on ILC2s, reported to play a role in maintaining metabolic homeostasis. ILC2s and eosinophils are predominantly resident in lean adipose tissues, and are 'upstream' regulators of M2 macrophages in adipose tissues (Hams et al., 2013). With the cooperation of eosinophils and M2 macrophages, ILC2s have been shown to regulate obesity and beiging of white adipose tissue with beige fat biogenesis (Brestoff et al., 2015; Hashiguchi et al., 2015; Molofsky et al., 2013). The production of IL-5 and IL-13 from VAT ILC2s is essential for eosinophil and M2 macrophage differentiation and activation, both important regulators of obesity (Molofsky et al., 2013). Moreover, lack of ILC2s in $Rag1^{-/-}$ mice resulted in significant decreased number of eosinophils and M2 macrophages, showing that ILC2s can promote the development of eosinophils and M2 macrophages of adipose tissues and regulating homeostasis or development of obesity (Brestoff et al., 2015; Molofsky et al., 2013). IL-33 is an important inducer of ILC2s and can *de facto* influence the development of obesity. Recent studies showed that ILC2s with a role on VAT biogenesis depending on IL-33 stimulation (Brestoff et al., 2015; Lee et al., 2015) and might regulate obesity. In addition, ILC2s were decreased in obese murine epididymal adipose tissues, as for human abdominal subcutaneous WATs (Brestoff et al., 2015). In fact, IL-33 knock-out mice had weight gain and reduction in both frequency and absolute numbers of ILC2s, even under normal diet conditions (Brestoff et al., 2015). Indeed, this situation is reversible as administration of IL-33 led to increased numbers of ILC2s, consequently promoting the recovery of M2 macrophage numbers (**Figure 14**)(Brestoff et al., 2015).

In counterpart, roles of cNK cells and ILC1s in obesity have also been demonstrated. One important recent study showed that large quantities of IFN-γ, which could trigger M1 macrophages in VAT, may be derived from cNK cells under high fat diet

(HFD)-induced obesity (**Figure 14**)(Wensveen et al., 2015). Moreover, systemic depletion of NK1.1^{+} and NKp46^{+} cells decreased diet-induced insulin resistance by restriction of the M1 macrophages polarization, but did not decrease obesity, suggesting that cNK cells are affecting inflammation-related insulin resistance but not directly metabolism (Lee et al., 2016; Wensveen et al., 2015). Adoptive transfer of splenic NK cells into the VAT of IFN-γ knock-out mice restore insulin resistance following HFD given to mice (Wensveen et al., 2015), showing that this cell type may be an important regulator of insulin resistance. Recently, tissue resident group 1 ILCs have also been reported to contribute to obesity-associated insulin resistance independently of the influence by T and/or NKT cells (O'Sullivan et al., 2016). IL-12, upstream signals and cellular sources, can activate adipose ILC1s, inducing the production of IFN-γ and the polarization of M1 macrophages in adipose tissue at early stages of HFD (O'Sullivan et al., 2016). Mirroring the cellular Th1-Th2 balance, IFN-γ, partly derived from ILC1s, counteract the IL-33 function and interfere with the activation of ILC2s of infected/inflamed tissues, as well as healthy adipose tissues (**Figure 14**)(Molofsky et al., 2015). Therefore, type-1 immunity and ILC1s may indirectly affect ILC2-mediated regulation of obesity and of general activation of ILC2s.

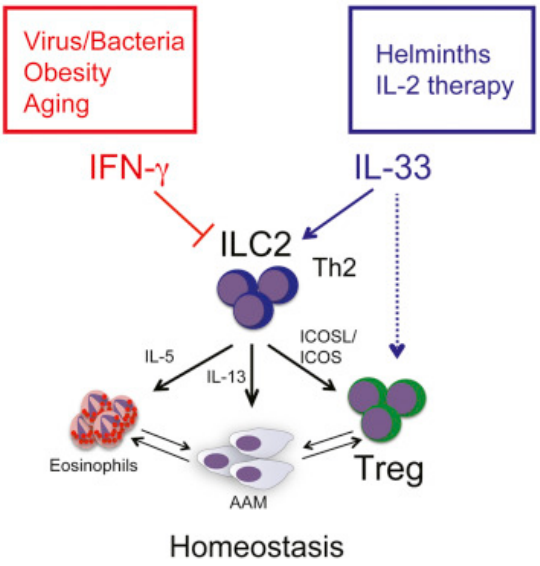

Figure 14 : IFN-γ counterpart IL-33 mediated activation of ILC2s **(from Molofsky et al., 2015).** ILC2s and regulatory T cells participate to helminth infection responses and sustain metabolic homeostasis. Here, IL-33 and IFN-γ counter regulate ILC2 activation to control Treg and type-2 immune response.

b. Helminth infection

Helminth infections are the most common infections worldwide with approximately one-fourth of the world's population (about 1.5 billion people) affected (WHO official information – 2019 statistics). The majority of helminth infections are not life threatening in humans, but they represent a massive health and economic burden. Type-2 immune responses are essential to efficiently expel the worm and then protect from re-infections. ILC2s were shown to participate and amplify the immune responses.

Nippostrongylus brasiliensis (*N.b.*), a natural rodent helminth, is often used as a model of helminth infections. After subcutaneous injection of mice with worm larvae (L3), the larvae migrate into the lungs, molt during the 3 first days, get coughed up, swallowed and then reach the intestine before elimination after about 15 days (Camberis et al., 2003; Jarrett et al., 1968; Taliaferro and Sarles, 1939).

Lung infections : early stage

ILC2s were initially identified in studies using *N.b.* as a helminth infection model. Early on during the infection, ILC2s are induced and responsible for the induction of type-2 signature cytokines, especially IL-13 (Moro et al., 2010; Neill et al., 2010; Price et al., 2010). IL-13 released by ILC2s is essential for clearance of the parasitic infection as IL-13 deficiency results in inefficient worm expulsion. Transfer of wild-type ILC2s into these IL-13-deficient mice allow good recovering of worm clearance (Neill et al., 2010). In addition, eosinophil counts significantly increase in the lungs upon *N.b.* infection (Hung et al., 2013; Neill et al., 2010; Price et al., 2010). At early stage of infection, the lung tissue is extremely fragile, with increase of red blood cells in the bronchiolar alveolar lavage (Chen et al., 2012; Hung et al., 2013). Using reporter mice, pulmonary ILC2s were detected and described as early sources of IL-13 and IL-9 during *N.b.* infection (Nussbaum et al., 2013; Price et al., 2010; Turner et al., 2013). As IL-9 is regulating fitness of ILC2s, ILC2s and eosinophils numbers are decreased in IL-9 receptor-deficient mice (Turner et al., 2013).

Intestinal infection : late stage

Three days are sufficient for *N.b.* clearance from lungs, but from the second day until about 15 days post-infection, eggs in feces and larvae in intestine can be detected (Jarrett et al., 1968) showing the main localization of the infection. As already said, at late stages, ILC2s play important role in parasitic clearance as IL-13 deficiency results in inefficient worm expulsion (**Figure 15**). Transfer of wild-type ILC2s into these IL-13-deficient mice allow good recovering of worm clearance (Neill et al., 2010). ILC2 secreting IL-13 play important role in goblet cell hyperplasia and induce smooth muscle contraction allowing worm expulsion (**Figure 15**). Recently, tuft cells have been described as critical players in induction of intestinal type-2 immune responses to helminths (*N.b.*) and protists (*Tritrichomonas muris*) (Gerbe et al., 2016; Howitt et al., 2016; Von Moltke et al., 2016). In IL-25-reporter-floxed mice, tuft cells are shown as a constitutive and major, and probable only, source of IL-25 in intestine. Following intestinal helminth infection, IL-25 stimulates lamina propria ILC2s to secrete IL-13 allowing amplification of the circuit by an action on tuft cells and goblet cells differentiation to expand them (Von Moltke et al., 2016). Requirement for tuft cells in these IL-25/IL-13 cytokine loop was also demonstrated using Pou2f3$^{-/-}$ tuft deficient mice in which helminth expulsion is delayed (Gerbe et al., 2016).

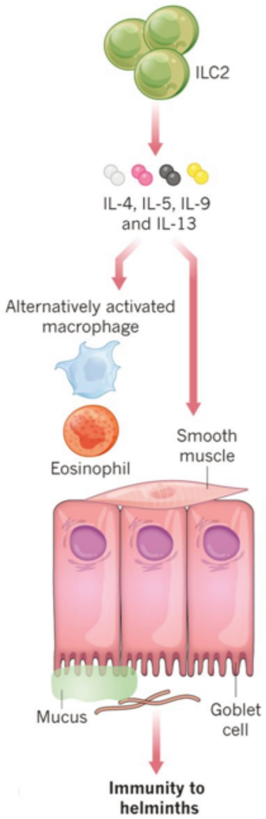

Figure 15 : Intestinal effector functions of ILC2s **(adapted from Artis and Spits, 2015).** By secretory functions, ILC2s participate to macrophage activation, eosinophil recruitment, smooth muscle contraction and goblet hyperplasia to participate to anti-helminth immunity.

Recent studies have identified succinate as a potent agonist of tuft cells (Lei et al., 2018; Nadjsombati et al., 2018; Schneider et al., 2018). It acts via GPR91 (SUCNR1) expression by small-intestinal tuft cells (Bezençon et al., 2008; Haber et al., 2017). Succinate given in the drinking water was sufficient to promote small-intestine tuft cell expansion, ILC2 proliferation, and IL-13 expression in an IL-25- and POU2F3-dependent manner. Germfree mice mono-colonized with *Tritrichomonas muris* accumulated succinate in the intestinal lumen (Schneider et al., 2018), activating the the all immune system response by GPR91-signalling (Nadjsombati et al., 2018). Alteration of the bacterial microbiota by streptomycin or polyethylene glycol 3350 treatments promotes a succinate-producing flora that also triggers GPR91 (Lei et al., 2018). *N.b.* infected Trpm5$^{-/-}$ tuft lacking mice, the chemosensory receptor TRPM5 as a mediator of tuft cell expansion in a *Tritrichomonas*-mediated manner, showed deficient ILC2 responses (Howitt et al., 2016). Surprisingly, both tuft cell expansion and worm clearance remain normal in *N.b.* infected Sucnr1$^{-/-}$ mice, suggesting alternative or redundant pathways in helminth-driven circuit activation of type-2 immunity (Lei et al., 2018; Nadjsombati et al., 2018). Interestingly, the activation of the circuit did not impact *Tritrichomonas* loading, suggesting that this pathway for luminal detection may facilitate mutualistic responses to luminal patho-symbionts with tissue remodeling to facilitate energy homeostasis (Schneider et al., 2018). Chronic activation of the circuit showed that the associated small-intestine remodeling impairs helminth parasitism, suggesting a concomitant immunity activation (Schneider et al., 2018). Of note, small-intestine circuit activity can also be influenced depending on the diet (Aladegbami et al., 2017; Wilen et al., 2018), strongly suggesting additional actors that will need extensive investigation.

Recent studies identified KLRG1^{-} nILC2s and mature KLRG1^{+} iILC2s in the lungs. They are both induced upon *N.b.* infection but appear with different kinetics : iILC2s are induced early on and nILC2 are dominant in the lungs at late timepoints post-infection. It was suggested that iILC2s may act as transient progenitors of nILC2s in this setting (Huang et al., 2015), but it is still unclear whether they can adapt in the tissue after migration. Moreover, they are described as originating from intestine, and experiments with blocked iILC2 circulation increases severity of worm infection. Then characterization of circulating features becomes central to understand the role of ILC2s as anti-helminth responders.

2. *Loss of control and chronic disease*

a. Airways diseases

Lung diseases, comprising infections and abnormal immune responses, are the most prevalent responses and represent a significant disease burden (Mizgerd, 2006). Respiratory virus infections have elevated infection and mortality rate worldwide with influenza virus infections as the most prevalent with approximately 250,000 deaths each year (WHO official information).

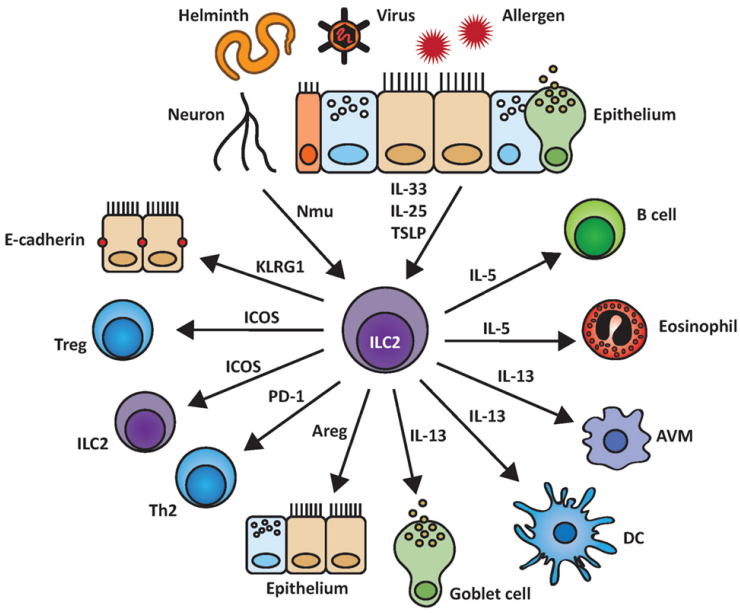

***Figure 16 : Interaction of ILC2s with the pulmonary environment* (from Mindt et al., 2018).** All features of ILC2 functions are present in the lung environment. ILC2s participate, with positive or negative effects, to type-2 immune responses against helminth, viruses and allergens. It is mediated by interactions with the large variety of lung cells that allow their activation (IL-33, IL-25, TSLP and Nmur) or their inhibition (KLRG1 and PD1). Then they are secreting type-2 cytokines.

Infections with respiratory viruses can affect the upper airway as for rhinovirus and respiratory syncytial virus (RSV) and the lower respiratory tract with influenza viruses, and these infections are frequently combinate to asthma or asthma exacerbations (**Figure 16**)(Carroll and Hartert, 2008).

Allergic lung diseases and asthma

Since ILC2s are present in lungs and rapidly secreting type-2 cytokines after activation, their role in pulmonary allergic reactions and asthma models has been extensively studied. Several models exist, and 2 allergens composed of proteases are extensively used : house dust mite (HDM) and papain. Mice receive intranasal administration to induce allergic reactions and are then used as a model for cellular and molecular mechanism study of allergic asthma (AA) (**Figure 16**).

Papain is a cysteine protease extracted from papaya (and other fruits such as pineapple). It has been used in alimentary and drug industries as meat tenderizer and in toothpaste. In these industries, after long-term exposure to papain powder, workers developed papain induced asthma combined with papain specific IgE antibody responses (**Figure 16**)(Novey et al., 1979). Papain induces IL-33- and TSLP-dependent type-2 immune responses with eosinophilia independently of adaptive immune cells in mice (Hoyler et al., 2012; Oboki et al., 2010). Indeed, TSLP levels in broncho-alveolar fluid are correlated with the corticosteroid-resistance of ILC2s in asthmatic patients. Rapidly after intranasal papain administration, pulmonary ILC2s are the main source of IL-5 and IL-13

(Halim et al., 2012b). As for HDM, the amount of papain and the number of administrations modulate the number of detected NKT and T cells in the lungs, but it is independent of the pulmonary ILC2 fitness in a model of unresponsive ILC2s (Yu et al., 2014). Dendritic cell-dependent priming of Th2 cells by ILC2-derived IL-13 appear if administration of papain combined early (day 0 and 1) and late (day 13 and 20) intranasal injections (Halim et al., 2014). Thus, papain is an important model to study IL-33-dependent ILC2 functions in the pulmonary environment (Halim et al., 2012b). Specifically, a recent study showed an important function of IL-33 as protease sensor that detected proteolytic activities associated with various environmental allergens, including papain protease as efficient at low concentration (10-30µg/mL *in vitro*). Full-length IL-33 is then cleaved and activated, thus participating to ILC2 activation (Cayrol et al., 2018). Role of specific nILC2 and iILC2 pools during allergic responses, as described in lungs of *N.b.* infected mice, remains not elucidated.

Viral infections

Studying respiratory virus infections in mice is in general induced by intranasal administration to anesthetized mice. Importantly, ILC2s are induced upon viral infections in mice and humans, as for example Influenza A virus (IAV), Rhinovirus and RSV (**Figure 16**)(Beale et al., 2014; Chang et al., 2011; Duerr et al., 2016; Hong et al., 2014; Jackson et al., 2014; Monticelli and Artis, 2012; Moro et al., 2016) and they induce an asthma-like reaction in mice even in the absence of adaptive immunity (Chang et al., 2011).

b. Skin diseases : Dermatitis

Atopic dermatitis (AD) is a chronic, relapsing inflammatory skin disease characterized by hypersensitivity reactions to common environmental allergens. It is the most common chronic inflammatory skin disease with a prevalence of 20% during lifespan (Moreno and Peiró, 2000). It bores several clinical manifestations depending on age and severity as seborrheic dermatitis, allergic contact eczema, psoriasis, etc characterized by skin inflammation and immune infiltration. AD can appear at any age, with an onset before 6 years of age in 80% of patients (Moreno and Peiró, 2000). With high levels of type-2 cytokines secretion, as IL-13, IL-4 and IL-5, during acute atopic eczema lesions, due to increased production of IL-33, IL-25 and TSLP production, ILC2s are major contributors of atopic dermatitis pathogenesis (**Figure 17**). Indeed, ILC2s are in higher proportions in the lesions of atopic dermatitis patients with similar frequency of cells in the blood of both healthy and the atopic individuals (Kim et al., 2013; Salimi et al., 2013). ILC2s from atopic lesions had activated phenotype with higher expression of cytokine receptors, IL-17Rβ, ST2 and TSLPR. Also in human, ILC2s showed higher expression of *Il17rb*, *Il1rl1*, *Tslpr*, *Ptgdr2* (coding for CRTH2), *Rora* and *Areg* in lesional skin biopsies of AD patients (Salimi et al., 2013). Interestingly, similar ILC2s infiltration were detected in subcutaneous administration of HDM extract in mice, showing a

response to allergen challenge in allergic individuals. Then a mechanism of skin barrier sensing was described for activated ILC2s accumulating in atopic dermatitis lesions (**Figure 17**). Local application of calcipotriol (MC903, a form of vitamin D3) induced ear thickening, dry skin (xerosis) and histopathological changes similar to AD lesions and is now used as a mouse model of AD. An increased infiltration of ILC2s was observed in the ear skin and draining lymph nodes of treated WT and Rag1$^{-/-}$ mice (Kim et al., 2013; Salimi et al., 2013). The real implication of ILC2s induced by epithelial cytokines IL-25, IL-33 and TSLP was established using Il17rβ$^{-/-}$, Il1rl1$^{-/-}$ and Tslpr$^{-/-}$ back-crossed to BALB/c and C57BL/6 strain. In BALB/c deficient mice, the greatest protection against calcipotriol induced AD-like inflammation was observed in mice lacking IL-25Rβ followed by ST2 deficient mice. Reduction in ear thickness correlated with a decreased frequency of ILC2s in ear skin and draining lymph nodes. TSLPR deficient BALB/c mice showed a modest reduction in ILC2 numbers and ear inflammation. Very surprisingly, the C57BL/6 strains showed greater effect on TSLP signalling pathway deficiency, with a lower but still significant role of IL-25 and IL-33 pathways to induce AD-like inflammation (Salimi et al., 2013).

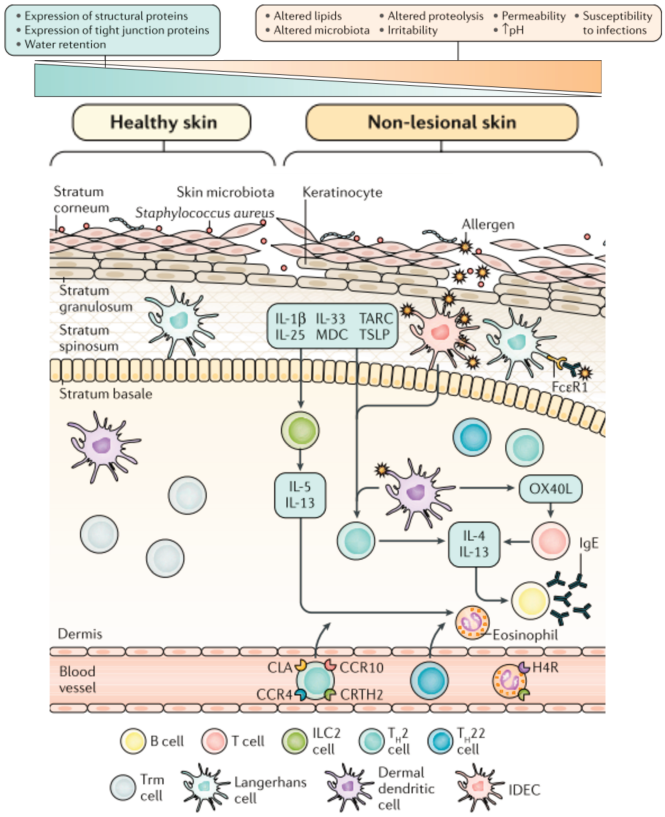

Figure 17 : Skin organization at homeostasis and following inflammation **(from Moreno and Peiró, 2000).** Epidermal barrier disruption stimulates keratinocytes *via* allergens to produce chemokines and cytokines as CCL17/22, IL-1β, IL-33 and TSLP. These mediators will recruit and activate ILC2s to mediate immune responses by IL-5 and IL-13 secretion. It participates to eosinophil recruitment and to their activation along with B cell.

ILC2s up-regulated KLRG1 in response to stimulation in the skin. KLRG1 ligation to E-cadherin in a plate-bound assay inhibited production of IL-13 and IL-5 (**Figure 17**), and decreased Areg and Gata3 expression (Salimi et al., 2013). In healthy tissues, E-cadherin expression and ligation to KLRG1 probably regulates ILC2 responses. In AD lesions, a significant down-regulation of E-cadherin by keratinocytes may reduce inhibitory signals to ILC2s and allow production of type-2 cytokines. Then, the type-2 cytokines can contribute to cutaneous inflammation by down-regulating anti-microbial peptides production (Leung et al., 2004).

These data remind the phenotype of iILC2s accumulating in lungs of helminth-infected mice. dILC2s do not express KLRG1 and IL-17rβ at homeostasis, and accumulated

ILC2s have different origin from resident ones, coming from circulation to play functions in inflamed-skin.

c. Gastrointestinal tract : Colitis

Recent studies on murine and human intestinal ILC subsets demonstrated that ILC2s have higher abundance compared to ILC1s but lower than ILC3s (Forkel et al., 2017; Krämer et al., 2017; Spencer et al., 2014), and possess important functions during intestinal inflammation. Intestinal ILC2s are mainly described as important mediators to clear helminth infection from the intestine (*cf.* "*Helminth* infection" part above). Following activation, intestinal ILC2s express IL-5 and IL-13 that respectively participate to recruitment of other immune cell types as eosinophils and stimulation of mucus production by goblet cells (**Figure 15**)(Moro et al., 2010; Neill et al., 2010; Price et al., 2010) to prevent the breakdown of the intestinal barrier and development of colitis (Bergstrom et al., 2010; Johansson et al., 2014). Intestinal ILC2s do not only contribute to anti-helminth immunity, but also in the maintenance of the intestinal barrier. However, ILC2s exact role in this maintenance remains controversial.

A study using oxazolone-mediated colitis in mice demonstrated that ILC2 derived IL-13 expression is enhanced in response to IL-25 stimulation. Inflammation of the colon was there associated to significant decrease of the colon length. In contrast, antibody-dependent ablation of IL-25 showed a reduction in IL-13 expression by ILC2s and limited infiltration of tissues by $Gr1^{+}$ macrophages. It correlates with limited disease pathology, and it was suggested that IL-25 promotes colitis by subsequent and continuous activation of ILC2s (Camelo et al., 2017).

In another hand, intestinal inflammation mediated by dextran sodium sulfate (DSS) revealed an IL-33-dependent expansion of intestinal ILC2s following tissue damages. Expanded ILC2s expressed Areg and allowed limited intestinal insult as more pronounced disease pathology were present in Areg-deficient mice (Monticelli et al., 2015). Both exogenous injection of IL-33 for *Areg* expression in ILC2s or direct treatment with Areg allowed significant reduction of the inflammation score, suggesting a protective role for intestinal ILC2s during colitis (Monticelli et al., 2015).

Then ILC2s play important roles participating to type-2 responses in diverse situations. A tight control of their functions is needed during inflammation. It allows a balance between sufficient but regulated response, avoiding over activation of ILC2s but participation to the different stages that correspond to acute response and tissue repair to recover homeostatic conditions. The role of ILC2 circulation remains not characterized in this precise control of ILC2 functions.

IV. Immune cells migration and surveillance : the hemolymphatic system

A. The blood : a tissue of life

The blood is the main body fluid in humans and other animals, representing about 7% of the body mass in human. The blood circulatory system (BCS) is composed of the heart and blood vessels running through the entire body. The arteries carry the blood away from the heart while the veins carry it back to the heart.

The blood is considered as the fluid of life that delivers nutrients, oxygen, hormones or numerous signalling molecules, to all tissues and cells. Blood also participates to metabolic waste products and carbon dioxide evacuation from those same tissues and cells to the lungs and kidneys. Nutrients comprise metabolites, lipids, glucids and proteins, obtained from digestion or storage tissues and used as energy sources, whereas hormones from exocrine glands circulate in blood to transmit signals for nutrients storage or release regulation.

Blood carries another important role in health, as all the hematopoietic cells and different members of the immune system (as for complement or antibodies) are circulating or recirculating through blood until they get activated to respond against potential threat diseases in peripheral tissues.

Blood can be in four main parts is composed of plasma, red blood cells, platelets and white blood cells or leucocytes. Cells and platelets make up about 45% of human blood, while plasma makes up the 55%.

B. The thoracic duct lymph : from periphery to global circulation

1. Lymph

The lymph is the biological fluid deriving from the interstitial fluid with products of tissue metabolism and catabolism, apoptotic cells, cellular debris, and circulating immune cells (Santambrogio, 2011). Lymph is carrying the global tissue proteomic signature plus invading pathogens to the draining lymph nodes in both physiological and pathological conditions. It is then not surprising that lymph plays a central role in every immunological processes, including maintenance of immunological tolerance to our cells and microbiota, immunity against pathogens, autoimmune responses, inflammation, and cancer (Santambrogio, 2011).

It is only recently that the composition of the lymphatic fluid, that was virtually unknown or poorly described, started to be detailed, and it was generally quite accepted that the lymph and blood composition overlapped, as the lymph somehow join blood in subclavian vein just before heart (Tilney, 1971).

This lack of knowledge was mostly due to the technical difficulty in cannulating lymphatic vessels and the small amount of collected fluid in rodents. These technical problems prevented an in-depth analysis of the lymph-circulating immune cells as well as any biochemical–biophysical analysis aimed at analysing the lymph composition for cells or nutrients. Over time, most of the technical issues have been solved and lymph biology progressively received more attention, allowed by "omic" analysis of cellular and molecular lymph composition in physiological and pathological conditions.

a. Lymph formation

Blood plasma that escapes from the blood vessels is absorbed into the surrounding tissues and form interstitial fluid. From the lymph tubes, the interstitial fluid returns to the blood after passing through a lymph node. If a blister is broken, lymph can be seen as a colorless, slightly sticky liquid.

Lymph is an important part of the circulatory system. It aids the body's absorption of nutrients and helps to remove waste from tissues and then deposits it in a lymph node as it passes through.

Blood circulating in capillaries is obviously not directly in contact with the cellular layers of parenchymal tissues, and then the different elements as proteins, lipids, and other molecules have to be transported from the intravascular to the extravascular space to deliver nutrients and hydration to each cell (Bird et al., 2009; Leak et al., 2004; Levick and Michel, 2010; Rockson, 2007). The intravascular hydrostatic pressure creates a molecule ultrafiltration which drives proteins and other molecules from the capillary bed into the extracellular space (Levick and Michel, 2010). The molecular movement is then controlled protein filtration according to their molecular size (Levick and Michel, 2010). More precisely, water and small molecules easily pass through the vessels when proteins and bigger molecular complexes have to move across the endothelial barrier through openings or pores (Levick and Michel, 2010).

To avoid formation of tissue edema, the interstitial fluid needs to be reabsorbed into the blood circulation. In fact, there are several important reasons why the interstitial fluid is not directly absorbed back into the general blood circulation but is directed through the lymphatic system. In blood, the fluid volume, osmolality, protein concentration, pH, and electrolytes are very tightly controlled, since even the slight modification in any of these parameters has critical consequences on the body homeostasis. Contrasting with blood, the composition of the lymphatic fluid can range widely in lipid and protein concentration, electrolytes, pH, and overall cellular composition without harming the organ homeostasis (Aukland et al., 1984). As such the lymph functions is to accommodate the metabolic and catabolic needs of each parenchymal organ, without compromising body homeostasis, clearance of tissue invading by pathogens, and carries products of tissue remodelling, cellular

secretion/processing, and cellular debris to immune cells in lymph nodes, ensuring that the immune system is constantly exposed to the tissue self-antigens for maintenance of peripheral tolerance (Clement et al., 2010, 2013; Goldfinch et al., 2008). The interstitial fluid, present in every parenchymal organ, seems to be the "precursor" of the lymph.

b. Molecular composition at homeostasis

As a consequence, proteomic analyses on bovine, ovine, rodent, and human lymph under physiological and pathological conditions have shown that the lymph fluid collects the "omic signature" of parenchymal organs from which it drains (Clement et al., 2010, 2013; Veenstra et al., 2005). Although plasma albumin and serum globulins constitute the majority of lymph proteins, tissue-specific proteins are also highly represented in the lymph proteome when compared to the plasma proteome. The greatest differences between lymph and plasma proteomes are extracellular matrix (ECM) proteins and the products of their processing that are derived from tissue growth and remodelling. They are highly represented in the lymph in comparison to plasma, as for proteins resulting from cellular metabolic/catabolic activities in each parenchymal organ, and intracellular proteins released by apoptotic cells. In another hand, proteins important for maintenance of the intra-capillary osmotic pressure (albumin, α1-, α2- and β-globulins) and clotting factors are more highly represented in the plasma than the lymph proteome (Goldfinch et al., 2008; Meng and Veenstra, 2007; Mittal et al., 2008; Nguyen et al., 2010). Finally, lipoproteins are among the most abundant proteins in the lymph, and HDL and cholesterol were significantly higher in the interstitial fluid and lymph, indicating that the lymph is the primary egress for HDL-bound cholesterol reverse transport from the periphery to the bloodstream and liver (Randolph and Miller, 2014).

c. Molecular composition under pathologic conditions

The lymph composition vary between homeostatic and pathological conditions, and it reflects the molecular signature of pathological conditions such as infections, inflammation or traumatic events (trauma/haemorrhagic shock) (Goldfinch et al., 2008; Mittal et al., 2008; Zhang et al., 2014).

Hundreds of different specific proteins were mapped in the mesenteric lymph collected following cecal ligation and puncture, an animal model of septic peritonitis, compared to healthy animals (Zhang et al., 2014). Lymph collected from animals infected with anthrax showed a different proteome compared with lymph collected from control animals (Popova et al., 2014). These observations in different animal models was also confirmed following analyses of human mesenteric lymph collected during surgery for abdominal trauma (Clement et al., 2013).

Thus, lots of studies showed that the lymph is the biological fluid that mostly mirrors the molecular signature of physiological and pathological conditions in

parenchymal organs. Quantitative proteomic analyses have shown that tissue-specific antigens are 100 to 500 times more represented in the lymph than in the plasma. Lymph analyses in different animal models and in various human pathologies strongly indicate that the lymph is a unique biological fluid, with a different proteomic composition compared to plasma, and with better potential for biomarker and antigen discoveries. Indeed, the use of lymph samples as liquid biopsy for a range of human diseases may be considered to discover early pathological markers.

2. Cellular composition of the thoracic duct lymph

The thoracic duct (TD) lymphatic drains the lower part of the body, including hind footpads, organs from pelvic and abdominal cavities, and it empties into the subclavian vein. The lymphatics of the small intestine (SI) and the colon, of Peyer's patches (PP) and mucosal isolated lymphoid follicles, are drained into the afferent lymphatics of the mesenteric lymph node chain (mesLNs), and the mesenteric efferent lymphatics enter TD (Tilney, 1971). Lymphatics arise as blind-ended capillaries in the intestinal mucosal lamina propria (LP) (Bernier-Latmani and Petrova, 2017).

The large majority of lymphocytes which circulate between lymph and blood are T cells (74%) and B cells (18%) (Guy-Grand et al., 1974). They are very numerous and in mice, it was calculated that 7 millions lymphocytes circulate per hour in the TD (Gesner and Gowans, 1962). They mainly belong to a pool of lymphocytes which continuously patrol through the body, circulating about one or two times a day at homeostasis. Very few populations of recently activated effector cells circulate and they mostly home in different tissues having less than 3 days of recirculation (Gowans, 1959; Gowans and Knight, 1964; Griscelli et al., 1969; Guy-Grand et al., 2013).

In the TD, rare populations are also detected such as dendritic cells (Milling et al., 2010), NK cells (Vosshenrich et al., 2006), hematopoietic cell progenitors (Massberg et al., 2007) and mucosal mast cell precursors (Guy-Grand et al, 1984). ILC subsets were suggested as possibly migrating at low frequency. However, we here bring direct proof of their presence and will characterize them into detail.

3. Lymphatic vessels to lymph nodes

Networks of open-ended lymphatic capillaries, which collect the interstitial fluid, are present in every parenchymal organ. The lymphatic capillaries are composed of a single thin and incomplete layer of LYVE1^{+} lymphatic endothelial cells (LEC) (Tammela and Alitalo, 2010; Tammela et al., 2005).

Under physiological conditions, a lymph flow running at about 1–5 mL/h was reported in the sheep. However, the differences are important according to the location of lymph flow measurement, animal body mass, and physiological state. For example, in the mesentery of fasting rats, afferent lymph flow has been calculated to be around

15µL/h, and the efferent lymph flow around 1.3 mL/h (Dixon et al., 2006). However, during the peak of lipid absorption the flow in the mesenteric duct can increase up to 13mL/h (Tso et al., 1985). In contrast, under inflammatory conditions with pathogen invasion or sterile inflammation as under autoimmune diseases, an increased lymph formation is observed, due to increased tissue edema formation. This increased amount of interstitial fluids, and consequently of lymph fluid, is also associated with neo-lymphangiogenesis, a generation of new lymphatic vessels from existing ones, increased immune cell trafficking from the periphery to the draining lymph nodes, and increased production of proinflammatory mediators, which alter lymphatic permeability and contractility (Cromer et al., 2014; Girard et al., 2012; Rahbar et al., 2014; Swartz and Randolph, 2014). Finally, measurements of thoracic duct lymph flow estimates that 3 to 4L of protein-enriched interstitial fluid are formed everyday under physiological conditions in the human body. However, since lymph fluid has to be reabsorbed in lymph nodes and then returned to the general circulation, it appears that an additional 3–4L of interstitial fluid are likely formed daily (Kramer et al., 1986; Levick and Michel, 2010; Squire et al., 2001).

The control of lymph flow toward the node is also facilitated by layers of valves organized by connective tissue from LEC (Schmid-Schonbein, 1990; Vittet, 2014). The valves are unidirectional with the lymph flow and are placed at anatomical intervals along the collectors.

Thus, an essential physiological question is why the interstitial fluid is not directly taken up at the venule end of the capillary network but will form lymphatic fluid drained by one or more of the about 450-700 lymph nodes distributed throughout the human body, before emptying into the thoracic duct and the *vena cava*.

C. Lymph nodes (LNs) : stock and passage

While LNs collect cells in lymph drained from tissues through their afferent lymphatic, they release immune cells from the LNs through efferent lymphatic vessels disperses lymphocytes back into the bloodstream, by often passage through additional LNs arranged in chains (**Figure 20**)(Braun et al., 2011). LNs are strategically positioned collecting stations for antigens that are present in peripheral tissues.

LNs possess several important functions in the immune system : recruitment of large numbers of naive lymphocytes from the blood, collecting antigen and DCs from peripheral tissues, providing an environment for antigen-specific tolerance or productive primary and secondary effector responses, modulation of the homing characteristics of effector or memory T cells that will target tissues that contain their specific antigen, and last but not least providing a place of activation for central memory cells (**Figure 18**). For these diverse functions, cells must migrate into the LNs and find their correct place within them. The role of LNs in the immune system involve a tight organization of the vessels and different compartments, with good trafficking signals production, and all of that make these organs a crucial interface between the innate and adaptive cellular components of the immune system (Von Andrian and Macley, 2000).

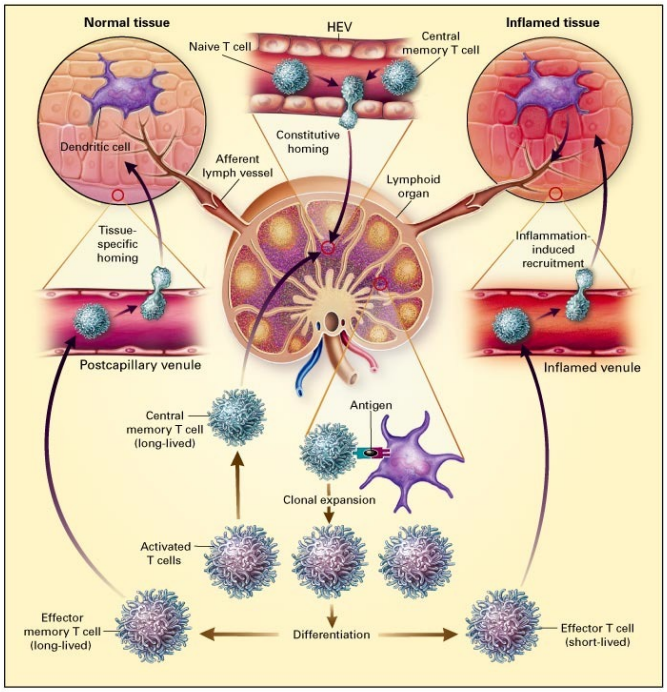

Figure 18 : Migratory routes of T cells **(from Von Andrian and Macley, 2000).** 3 different routes are used by immune cells. Naive T cells circulate from the blood to lymph nodes and other secondary lymphoid tissues using HEV that express molecules for the constitutive recruitment of lymphocytes. Lymph are draining tissues and coming from afferent vessels. Dendritic cells are mobilized to carry antigen to lymph nodes, where they stimulate antigen-specific T cells. After activation, effector T cells express receptors that enable them to migrate to sites of inflammation. At the same time, memory cells are subdivided into two populations on the basis of their migratory ability : effector memory cells migrate to peripheral tissues and central memory cells express a repertoire of circulating molecules similar to that of naive T cells and stay in circulation in hemolymphatic system. The migration to peripheral tissue is organ-specific and is modulated by inflammatory mediators.

1. LNs architecture : precise compartments for specific functions

Two main regions can be distinguished histologically in LNs, the cortex and the medulla. The cortex is then further divided into the paracortex or T-cell area, and the more

superficial B-cell area that consists of primary follicles and germinal centres following antigen challenges (**Figure 19**)(Von Andrian and Mempel, 2003). B-cell follicles are the main sites of humoral responses, whereas the paracortex is the site where circulating lymphocytes enter the LNs (Marchesi and Gowans, 1964) and where T cells interact with DCs (Mondino et al., 1996). The medulla is a constituted of lymph-draining sinuses separated by medullary cords, containing many plasma cells, some macrophages and memory T cells (**Figure 19**).

The fine architecture of the LN cortex is complex (Fossum and Ford, 1985; Pabst and Binns, 1989). Nevertheless, common structural features have been identified. According to electron-microscopy images, paracortex is arranged in paracortical cords that originate between or below the B-cell follicles and get extensions towards the medulla where they merge into medullary cords (**Figure 19**)(Fossum and Ford, 1985). At the center of each paracortical cord is an HEV surrounded by pericytes known as fibroblastic reticular cells (FRCs)(**Figure 19**). A space between the basal membrane of the HEV and pericytes form the perivenular channel that may receive lymph from the FRC conduit. Networks of FRCs around the HEVs enclose 10–15µm corridors along which lymphocytes are thought to migrate (Fossum and Ford, 1985; Gowans and Knight, 1964; Marchesi and Gowans, 1964). The lymph enters from afferent lymph vessels into the subcapsular sinus, a space below the fibrous capsule that covers the LN, and exit by efferent vessels, so called cortical sinuses, after exploring lymph node for about several hours (**Figure 19**). Of note, a single inguinal mouse LN recruits ~2% of the recirculating pool per day (Von Andrian, 1996).

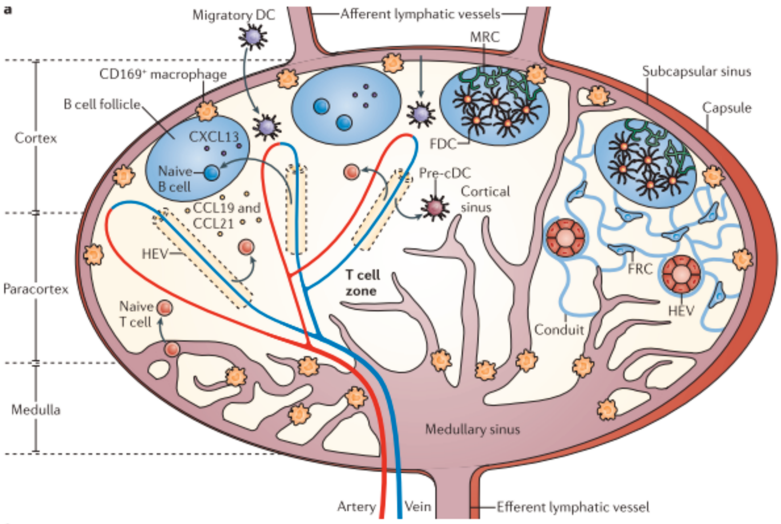

***Figure 19 : LNs are compartmentalized allowing lymph filtration* (from Girard et al., 2012).** LNs possess 3 main different compartments : the cortex, the para cortex and the medulla. Migrating cells arrive from HEV and afferent vessels and exit through cortical sinuses, medullar sinuses and efferent vessels in the medulla.

2. Special organization of vessels for immune cells migration

a. High endothelial vessels (HEV)

HEVs are only found in secondary lymphoid tissues (**Figure 19**)(Girard and Springer, 1995). The composition and distribution of lymphocyte traffic molecules on HEVs vary between LNs, and both presence and function of HEVs is regulated throughout life. For instance, HEVs in the LNs of newborn mice all express mucosal addressin cell-

adhesion molecule 1 (MadCAM1), a ligand for α4β7 integrin (Berlin et al., 1993), but not the peripheral node addressin (PNAD), ligand of L-Selectin (also known as CD62L). The adult PNAD$^+$ MadCAM$^-$ LN-specific HEV phenotype is only gradually acquired after birth (Mebius et al., 1996). The maintenance of MadCAM expression is only true for mucosal LNs, such as mesenteric LNs (mesLNs), and intestinal associated lymphoid tissues in adult mice, important to specifically direct the migration toward the intestine. HEVs express specific genes that are not expressed by other endothelial blood cells, allowing specific migration of immune cells into LNs.

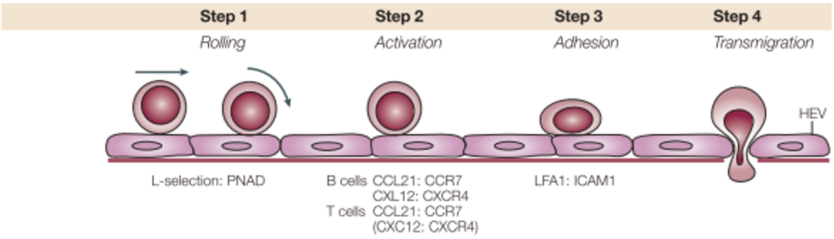

Figure 20 : Multi step adhesion cascades on HEVs **(from Von Andrian and Mempel, 2003).** To pass through HEVs, immune cells initiate rolling by L-selectin binding to its ligand PNAD. HEVs present chemokines as CCL21, CCL19 and CXCL12 to CCR7 and CXCR4 on immune cells. That activates LFA-1-mediated arrest on endothelial expressing ICAM1 and ICAM2. Finally, arrested cells pass through HEVs by transmigration.

The interactions of lymphocytes with HEVs start by the lymphocyte homing receptor CD62L, which mediates the first phase of lymphocytes rolling along HEV walls (**Figure 20**)(Von Andrian and Mempel, 2003; Rosen, 2004). Naive B and T cells enter LNs through a well-known multistep adhesion and migration cascade (**Figure 20**). Lymphocytes first undergo chemokine-induced activation of their integrins, mediating lymphocyte arrest on the HEV wall. Different chemokines CC-chemokine ligands (CCL) expressed at homeostasis by FRCs, Follicular Dendritic Cells (FDCs) in follicles and endothelial cells, are crucial factors for lymphocyte extravasation through LNs HEVs (see "*Chemokines*" part below). Then, the integrin lymphocyte function associated antigen 1 (LFA1 or αLβ2 integrin), which binds to intercellular adhesion molecule 1 (ICAM1) and ICAM2 expressed by endothelial cells, is the major integrin for B and T cell arrest in the HEVs of peripheral lymph nodes. This is contrasting with the essential role of integrin α4β7 also important for lymphocyte arrest in mesLNs (**Figure 20**)(Von Andrian and Mempel, 2003; Miyasaka and Tanaka, 2004; Shamri et al., 2005).

b. Afferent lymphatic vessels

Some immune cells also enter lymph nodes via afferent lymphatics and not through HEVs. They use the lymphatic system as a rapid and direct circulatory way between the parenchymal organs and the LNs (Randolph et al., 2008, 2017). The lymphatic capillaries from tissues fuse into increasingly larger vessels, known as lymphatic collectors. The collectors are formed by a thicker and more organized basal membrane that is supporting the LEC (Tammela and Alitalo, 2010). Dispersed into the surrounding ECM, the lymphatic collectors are lymphatic muscle cells and fibroblasts,

with characteristics of both smooth and striatal muscles, and are fundamental to move the lymph flow toward the draining LN (Gashev, 2008, 2010).

The entry and migratory routes of DCs in lymphatic vessels have been well described (Alvarez et al., 2008; Förster et al., 2012; Randolph et al., 2005), and evidence proved that naïve, effector and memory T cells also enter LNs through afferent lymphatics (Braun et al., 2011; Förster et al., 2012).

DCs enter into terminal lymphatics in a CCR7-dependant manner at both homeostasis and inflammatory conditions. Also, CCR8 and its ligand CCL1 have been suggested to contribute to the homing of DCs into the LN, when integrins, important for entrance by HEV, are dispensable for this process (Qu et al., 2004). In fact, β1, β2 and β7 integrins deficiency in DCs didn't restrict migration to LNs and accumulation in T cell areas compare to wild-type DCs (Lämmermann et al., 2008).

Memory T cells collected were isolated from afferent lymph vessels from popliteal LNs in sheep (Mackay et al., 1990). It is important to remember that LNs are mostly arranged in chains and that cells leaving LNs through efferent lymphatics (see below) will enter a new LN *via* an afferent lymphatic. It has been recently shown in mice that after microinjection of naive T cells into the afferent lymphatic vessel of a popliteal LN, the transferred cells do not only migrate to the T zone but also to the T areas of other LNs located further downstream as the medial iliac LN (Braun et al., 2011; Tilney, 1971). Then, using "kaede" photoconvertible mice, naive T cells have been shown to migrate from one LN to another *via* lymphatics (**Figure 21**)(Tomura et al., 2008).

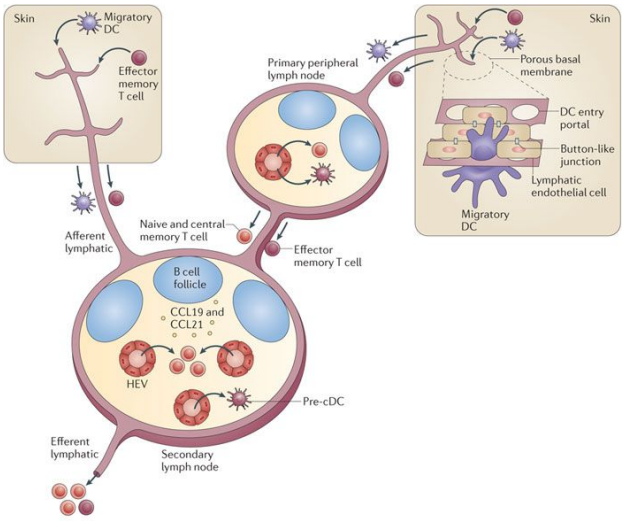

Figure 21 : DCs and T cells trafficking through LNs **(from Girard et al., 2012).** In peripheral tissues, as for skin here, lymphatic vessels collect interstitial fluids and immune cells. They enter in LNs by afferent vessels and circulate through a chain of different LNs. Cells are then often migrating in a second or several LNs to optimise specific immune cells to enconter activating signals.

Finally, afferent lymph-derived DCs and T cells use different routes to enter LNs. While DCs transmigrate through the floor of the subcapsular sinuses (SCS), naive T cells enter through the medullary sinuses (**Figure 19**). Naive T cells can not only enter lymph nodes via HEVs, but after leaving a first LN through efferent lymphatics, they may circulate in lymph, together with effector and effector memory T cells, and enter another LN via afferent lymphatics (**Figure 21**).

c. Efferent lymphatic vessels

After several minutes to few hours, naive lymphocytes that didn't encounter a specific antigen leave the LN through efferent lymphatics. Migration of lymphocytes into efferent lymph is also a highly regulated process that involves coordination of signals from CCR7 and the G protein-coupled receptor called sphingosine phosphate receptor 1 (or S1PR1) (**Figure 21**)(Cyster and Schwab, 2012).

S1P and S1PR1 are required for both B and T cells egress from LNs (Bajénoff et al., 2006; Cyster and Schwab, 2012). S1P receptors are heterotrimeric G protein–coupled receptors (GPCRs) comprising S1PR1 (or S1P1), S1PR2 (Edg-5 or S1P2), S1PR3 (Edg-3 or S1P3), S1PR4 (Edg-6 or S1P4), and S1PR5 (Edg-8 or S1P5) (Chun et al., 2010; Lee et al., 1998) with different nanomolar affinities for Sphingosine-1-phosphate (or S1P). S1P has roles as an extracellular signalling molecule, a potent bioactive sphingolipid metabolite, and may be an intracellular signalling molecule (Serra and Saba, 2010; Spiegel and Milstien, 2011).

S1P was first implicated in the exit of lymphocytes from LNs during homeostasis, when it was discovered that an immunosuppressive drug FTY720 (called fingolimod), an agonist of S1P receptors, induces lymphocytes sequestration by inhibition of their exit into lymph (Mandala et al., 2002). More precisely, FTY720 acts by induction of the S1PR1 expression downregulation on lymphocytes, showing its important role for LNs exit (Matloubian et al., 2004).

In another hand, S1P is produced *in vivo* by sphingosine kinases expression, and genetical inactivation these kinases in LECs reduces S1P levels in lymph and impaired lymphocyte egress from LNs (Pham et al., 2010). S1P gradients are important for egress, as inhibition of S1P lyase, important for degradation of S1P in LNs to maintain low S1P levels, also resulted in lymphocyte sequestration (Schwab et al., 2005). The two-photon intravital imaging showed that B and T cells are exiting LNs through cortical sinuses in a multistep process (Grigorova et al., 2009; Sinha et al., 2009). Some migrating T cells entered into contact with LYVE1$^+$ cortical sinuses in interfollicular areas for few minutes, and a good proportion of wild-type but no S1PR1-deficient T cells crossed the lymphatic endothelium and entered the sinuses at multiple locations (Grigorova et al., 2009). ILC2s

and ILC3s reside in interfollicular spaces of mesLNs and are probably similar to those migrating T cells (Mackley et al., 2015).

In a similar manner, B cells were exiting LNs by migration from the B cell follicles into adjacent cortical sinuses, and the use of FTY720 showed that B cells failed to enter into the sinus lumen in absence of S1PR1. S1PR1 signalling mainly acts by bypassing retention mediated by Gαi-coupled receptors as CCR7 and CXCR5 (**Figure 22**)(Pham et al., 2008, 2010; Sinha et al., 2009). Interestingly, S1PR1-deficient T cells (Pham et al., 2008) and S1P-deficiency in lymphatic endothelium (Pham et al., 2010) treated with pertussis toxin, which inactivates Gαi and retention by CCR and CXCR molecules, completely restored T cells egress through cortical sinuses.

Although cortical sinuses appear to be the major sites of lymphocyte egress from LNs, medullary sinuses and the SCS may also serve as exit sites (Grigorova et al., 2009; Pham et al., 2008; Sinha et al., 2009). After egress from LNs, high levels of S1P in blood and lymph induce the rapid downregulation of S1PR1 expression on B and T cells through receptor internalization (Lo et al., 2005; Park et al., 2012).

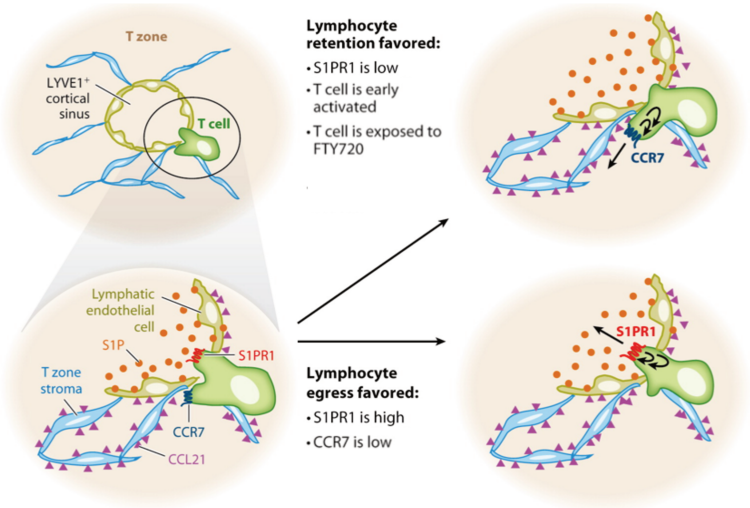

Figure 22 : Mechanism of lymphocytes egress from LNs **(adapted from Cyster and Schwab, 2012).** To egress LNs, lymphocytes are dependent on S1P-S1PR1 and CCR7 expression. When cells express high levels of CCR7 of low levels of S1PR1, it induces retention in LNs. S1P is more expressed in lymph than in LN, and when cells upregulate S1PR1 and downregulate CCR7, they egress from LNs to enter circulation.

Interestingly, the egress rates of lymphocytes from LNs critically influence entry through HEVs. Lymphocytes sequestration in LNs trough specific inactivation of S1PR1 inhibited the income of blood-circulating lymphocytes that where accumulated in near HEVs. HEVs then function as traffic checkpoints to maintain LN cellularity at steady state (Mionnet et al., 2011).

To conclude, S1P–S1PR1 signalling allows lymphocytes to exit through cortical sinuses and regulate the egress of lymphocytes from LNs by overcoming retention signals from Gαi-coupled receptors.

D. Immune cells : a controlled migration

1. Chemokines

Chemokines are a large family of small, secreted chemotactic cytokines, which are defined by their primary amino acid sequence and the arrangement of specific

structurally important cysteine residues within the mature protein. They consist of a central three-stranded β-sheet, an overlying C-terminal α-helix, and a short unstructured N-terminus that plays a critical role in receptor activation. Variations in the configuration of the two cysteines close to the N-terminus allow chemokines to be split into four subfamilies: CC, CXC, CX3C, and XC. In CC chemokines, the cysteines are directly juxtaposed, while CXC chemokines have a single variable amino acid between them. The CX3C chemokine has three amino acids between these two cysteines, while XC chemokines, of which there are two forms in humans and one in mice, lack first cysteine of the motif (Hughes and Nibbs, 2018).

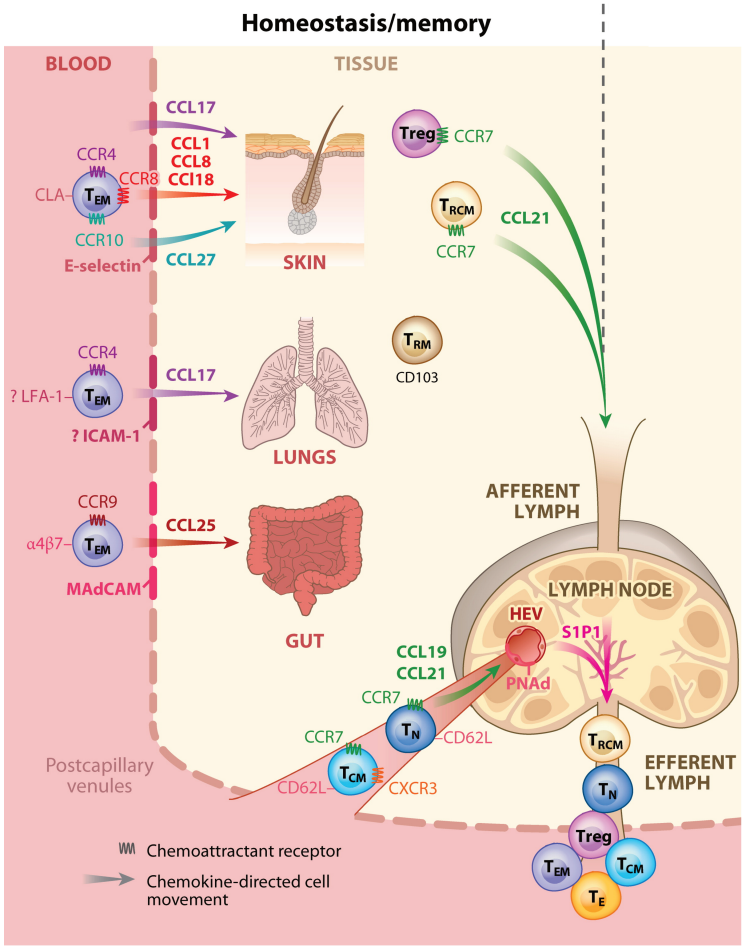

Figure 23 : Roles of chemokines at homeostasis **(adapted from Griffith et al., 2014).** Naive T cells (T_N) and central memory T cells (T_{CM}) express CCR7 and CD62L and migrate between the blood and LN, attracted by CCL19, CCL21, and PNAd presented on HEVs. Activated effector and effector memory T cells (T_E and T_{EM}) are found in the blood and are characterized by a lack of CCR7 expression. They are imprinted for tissue-homing according to the chemokine receptors and adhesion molecules they express. These trafficking molecules allow specific migration of activated lymphocytes into various tissues based on each unique chemokine and adhesion molecule expression. Resident-memory T cells (T_{RM}) express CD103 and are resident for long periods within the tissues. Recirculating memory T cells (T_{RCM}) enter the tissues but then return to the LNs in a CCR7-dependent manner. Regulatory T cells (Treg) appear to have a similar distribution to effector and memory T cells and likely form populations that are both tissue resident and recirculating.

Chemokines constitute the largest family of cytokines with about 50 endogenous chemokine ligands described in humans and mice. In another part, chemokine receptors are part of the γ subfamily of rhodopsin-like seven-transmembrane receptors, and constitute the principal group of molecules in this family. They are differentially expressed on all leukocytes and are divided into two distinct groups : G protein–coupled chemokine receptors, signalling by activation of pertussis toxin (PTX)-sensitive Gi-type G proteins, and the second group made of atypical chemokine receptors that shapes chemokine gradients and signal inflammation using scavenging chemokines in a G protein–independent manner. 20 chemokine receptors induce a signalling pathway whereas 5 others are non-signalling chemokine receptors.

Chemokines control the migratory patterns and tissue positioning of immune cells. All immune cell types need chemokine functions for migration at homeostasis and for peripheral recruitment and retention of activated cells, but chemokine signals are also required for immune cell development and for the generation of primary and secondary cellular and humoral immune responses. It can also mediate pathologic recruitment of immune cells in diseases (Griffith et al., 2014).

In lymphocytes, chemokines promote recruitment into lymphoid tissues where optimal priming occurs by good co-localization with dendritic cells (DCs) (Bromley et al., 2008; Groom et al., 2012). This priming in lymphoid tissues induces a switch of chemokine receptor expression in T cells leading to expression of distinct combinations of tissue homing chemokine receptors by the different effector and memory lymphocytes. These specific homing receptor switches will then limit the ability of lymphocytes to interact with micro-vessels present in distinct anatomical compartments, inducing at the same time the acquisition of tissue-specific tropism.

Naive T cells express CCR7 and CXCR4. CCR7 binds to CCL21, produced by HEVs, and to CCL19, produced by the FRC network and transcytosed across HEVs (Förster et al., 2008; Nakano et al., 1997). CXCR4 on naive T cells also promotes LN entry by binding to CXCL12 produced by the FRCs. They will then induce retention and upregulation of other chemokines mediating lymphocyte residency as CXCR6 (**Figure 20, 21 and 23**)(Von Andrian and Mempel, 2003; Förster et al., 2008; Miyasaka and Tanaka, 2004).

It has been described that T cell subsets expressing CCR4, CCR8 and CCR10 home and persist into skin compare to other tissues, as their ligands CCL17, CCL18, CCL22 and CCL27 are expressed by skin endothelial cells and keratinocytes (**Figure 23**) (Campbell et al., 1999; Reiss et al., 2001). In fact, in a more general way, skin-, lung-, and inflammation-homing chemokine receptors may be mediated by a chemokine receptors CXCR3, CCR2, CCR4, CCR5, CCR6, and CCR8 (**Figure 23**) (Grindebacke et al., 2009; Islam et al., 2011; Lim et al., 2006; Mikhak et al., 2013) for specific migration, with variable expressions in different immune subtypes, as for Th2 cells that highly express CCR4, CCR8, CX3CR1.

On the other hand, the CCR9 ligand, CC motif chemokine ligand (CCL)-25, is expressed by gut endothelial and epithelial cells, contributing to the homing of effector T cells that prevalently express CCR9 along with the other gut homing receptor, as the integrin α4β7 (**Figure 23**) (Mora and von Andrian, 2006; Rot and von Andrian, 2004; Svensson et al., 2002).

2. Integrins

The integrins are a superfamily of cell adhesion receptors that recognize mainly the extracellular matrix and the cell-surface ligands, even if soluble ligands have been

identified (Hynes, 2002). They are transmembrane αβ heterodimers, with at least 18 α and 8 β subunits known in humans (Shimaoka and Springer, 2003).

Integrin functions as traction receptors that can both transmit and detect changes in mechanical force acting on the extracellular matrix. Integrins can be broadly grouped depending on their ligand specificity. The ligand binding and intercellular adhesion is done through the I-domain (for insertion/interaction or A-domain) for the α integrins that contains one (with α1, α2, α10, α11, αM, αL, αD, αX and αE), through the recognition of RGD motifs (α4β1, α5β1, αVβ1, αVβ3, αVβ5, αVβ6, αVβ8, and αIIbβ3) or through the interaction with laminin (α1β1, α2β1, α3β1, α6β1, α7β1, and α6β4) and collagen (α1β1, α2β1, α3β1, α10β1, and α11β1)(**Figure 24**) (Takada et al., 2007). The I-domain can be present in either an open (active) or a closed (inactive) conformation (**Figure 24 and 25**). These are major conformational changes that affect ligand binding affinity and nature, and appear to regulate the degree and kinetics of cell adhesion. Integrins can be activated intracellularly by signals from G-protein-coupled receptors, called inside-out signals, which finally lead to phosphorylation of the cytoplasmic domain of the β subunit. The association of the α and β cytoplasmic tails is required to maintain their inactive state and it is disrupted by chemokine or agonists treatment that are known to cause integrin activation *via* G-protein-coupled receptors (Ley et al., 2016).

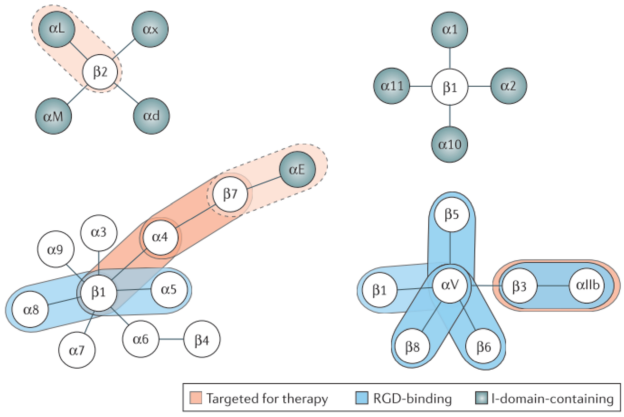

Figure 24 : Integrin family and αβ couples **(from Ley et al., 2016).** Integrins are heterodimers comprised of one α and one β subunit (black ovals). Integrins targeted for therapy are circled in red and the dotted red circle indicates past therapeutic use (for αLβ2 integrin) or unknown effects (for αEβ7 integrin). Integrins that bind to RGD are circled in blue and I-domain-containing integrin-α subunits are grey.

Upon binding an extracellular ligand, integrins generate an intracellular signal, called outside-in signal (**Figure 25**), whereas their function is regulated by intrinsic signals. Extracellular ligation of integrins triggers a large variety of signal transduction events modulating cell behaviour such as adhesion, proliferation, survival or apoptosis, shape, polarity, mobility, haptotaxis, gene expression, and differentiation, mostly through effects on the cytoskeleton.

Some integrins are only expressed by leukocytes, as for subunits αL, αM, αD, and αX, while others are also expressed by platelets and endothelial cells like the αIIb, α6, α4, αV and β3.

β2 chain (also known as CD18) is common to the αLβ2 (or LFA1 for lymphocyte function-associated antigen 1 or CD11a/CD18), αMβ2 (or Mac1 for Macrophage 1 antigen or CD11b/CD18), αxβ2 and αdβ2 integrin. Leukocyte integrins have a prominent role in

inflammation and immunity. Specifically, LFA1 is required for the formation of the immunological synapse (Grakoui et al., 1999). αL-deficient mice have reduced lymphocyte numbers in their secondary lymphoid organs and a mild defect in inflammation (Henderson et al., 2001), showing its importance for lymphocyte migration into LNs. Mac1 has a major role in host defence, especially against bacterial and fungal infections, and is an important molecule in the recognition of complement C3bi-opsonized particles allowing complement mediated-cytotoxicity of NK cells and complement phagocytosis by macrophages and neutrophils.

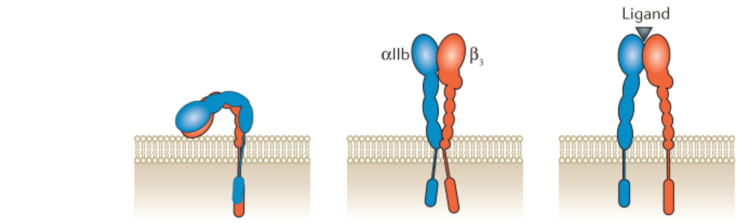

Affinity	Low	Intermediate	High
Conformation	Bent	Extended	Open
Outside-in signalling	No	No	Yes

Figure 25 : Inside-out activation of integrins **(from Ley et al., 2016).** The bent (left), extended (middle) and extended-open (right) conformations (αIIbβ3 integrin here). The α subunit is shown in blue, and the β subunit is shown in red. The ligand-binding site is indicated by a grey triangle in the extended-open integrin. Upon integrin activation, it induces a movement of the transmembrane and cytoplasmic domains.

αVβ3, widely expressed in proliferative endothelial cells, where it has been implicated in aspects of angiogenesis, and in vascular smooth muscle cells, monocytes, macrophages and some tumour cells (Cheresh et al., 1993), can interact with many of RGD-containing adhesive proteins and with a number of non-RGD-containing proteins in the extracellular matrix. Studies on neutralizing antibodies showed a role of αVβ3 on pulmonary T lymphocytes infiltration during primary pulmonary fibroblasts stimulated (Luzina et al., 2009).

α4 is common to α4β7 and α4β1 integrins that don't contain an I-domain. α4β7 binds predominantly to mucosal addressin cell adhesion molecule 1 (MAdCAM1), which is expressed on endothelial cells of tissues in the gastrointestinal tract, and allows specific homing of lymphocytes to the gut (Berlin et al., 1993). α4β1 integrin, also called very late antigen-4 (VLA4 or CD49d/CD29)(Hemler et al., 1987) as it was originally identified on lymphocytes that were activated for extended periods, binds to vascular cell adhesion molecule 1 (VCAM1)(Cybulsky and Gimbrone, 1991) and other ligands on endothelial cells as intercellular adhesionmolecule-1 (ICAM-1) and -2, is involved in adhesion of effector, effector-memory and central-memory cells to tissues at homeostasis and many, if not all, inflamed organs (Xu et al., 2003).

Both α4β7 and α4β1 are shown as upregulated after cell activation. Whereas the exact signalisation for α4β1 expression is still few documented, RA regulates α4β7 upregulation on activated lymphocytes. More precisely, RA increased α4 that resulted in higher levels of α4β7, showing a privileged dimerization of α4 with β1 as free β7 molecules are available for pairing with α4 (DeNucci et al., 2010). However, a balance

between β1 and β7 chains occurs. After activation, dividing lymphocytes increased β1 expression correlated with a progressive loss of β7 on cell surface. Overexpression of β1 induced suppression of α4β7 expression *in vitro*, even in presence of overexpressed α4 that usually results on α4β7 upregulation (DeNucci et al., 2010). Finally, while $\beta7^{-/-}$ mice show no differences of α4 and β1 expressions, $\beta1^{-/-}$ mice have permanent increased α4β7 expression on splenic $CD4^+$ T cells. Moreover BM T cells are decreased, and an accumulation in payer's patches is observed, according to the higher potential of migration due to α4β7 (DeNucci et al., 2010). Together, these findings show important balance between β1 and β7 integrins for new activated lymphocytes migration. Moreover, α4β7 is expressed on dividing lymphocytes, when α4β1 progressively increased during divisions and high expressions are observed on undividing cells. A link between specific functions and couple of integrins could then happen, but still need to be characterized.

Integrin affinity for their ligands is directed by chemokine signals. After first contact between integrins and ligands with a low affinity, specific chemokine signals on migrating cells result in increased affinity of integrin by conformational modification. For example, CCL17-CCR4 couple increase α4β1-VCAM1 affinity. As $\alpha4\beta7^{hi}$ cells lacking CCR9 migrate to intestinal LP, it is still unclear if CCL25 activation of CCR9 on $\alpha4\beta7^{hi}$ cells is needed for increased affinity of α4β7 for MadCAM1. CCR9 could then be an important factor to determine LP versus intra-epithelial localisation of cells in the intestinal mucosa (Guy-Grand et al., 2013). However, the increased affinity is still a crucial step for endothelial extravasation of migrating cells, and variable affinities has been showed for α4β7. Under CCL25-CCR9, α4β7 have high affinity for MadCAM1, when following CXCL10-CXCR3 activation, the affinity is switched to VCAM1 (Sun et al., 2014), questioning the mechanism behind α4β7 activation.

Selectin	Cell/tissue	Expression pattern
L-selectin	Myeloid cells	Constitutive
	Naive T cells	Constitutive
	Effector T cells	Low/negative
	Effector memory T cells	Absent
	Central memory T cells	Re-expressed or retained
E-selectin	Skin endothelium	Constitutive
	Inflamed endothelium	Inducible in most organs
P-selectin	Choroid plexus	Constitutive
	Lung endothelium	Constitutive
	Platelets	After activation
	Platelet-derived microparticles	Constitutive
	Peritoneal macrophages	Constitutive
	Inflamed endothelium	Inducible in most organs

***Figure 26 : Expression of selectins by immune cells* (from Ley and Kansas, 2004).** Table of selectins expression patterns depending on cell types and tissues.

3. Selectins

The selectins are a family of three C-type lectins expressed exclusively by bone-marrow-derived hematopoietic cells and endothelial cells. They are classified as L for leukocyte (L-selectin or CD62L), E for endothelial cell (E-selectin or CD62E), and P for platelet (but also endothelial) cell (P-selectin or CD162) (**Figure 26**). Selectins consist in an amino-terminal lectin domain, one EGF-like domain, several consensus repeats with homology to complement regulatory proteins, a single membrane-spanning domain and a carboxy-terminal cytoplasmic domain (Kansas, 1996; Ley, 2003; Vestweber and Blanks, 1999). The main physiological function of all selectins is leukocyte adhesion under blood flow, but both selectins and their ligands also trigger signalling functions (Crockett-Torabi, 1998). L-selectin is expressed by all myeloid cells,

naive T cells, and some activated and memory T cells. P-selectin is expressed in secretory granules of platelets and platelet surface after activation. E-selectin is expressed by acutely inflamed endothelial cells in most organs and in non-inflamed skin microvessels (**Figure 26**). P-selectin is constitutively expressed on the endothelium of lung (Kivisäkk et al., 2003), and is inducible on inflamed endothelial cells in many diseases or inflammatory conditions (Ley and Kansas, 2004; Vestweber and Blanks, 1999). Selectin interactions with their ligands have been assessed by testing *in vitro* the rolling of leukocytes on endothelial cells or on recombinant molecules in micro-fluidic chamber systems (**Figure 27a**), and *in vivo* on micro-vessels or other cell types expressing ligands (**Figure 27b**).

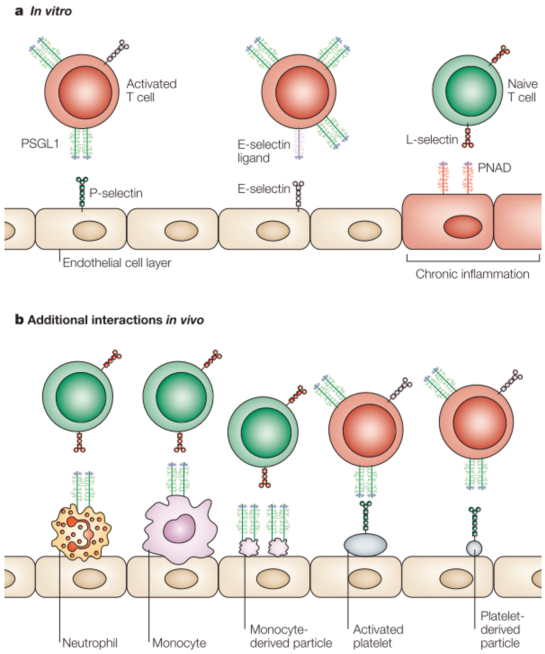

Figure 27 : Selectin-dependent interactions **(from Ley and Kansas, 2004). A.** T cell/endothelial-cell interactions studied in flow chamber systems *in vitro*. P-selectin/PSGL1; E-selectin/E-selectin ligand(s) and L-selectin/PNAd. **B.** T cell to other cell types interactions studied *in vivo*. At sites of inflammation, neutrophils and monocytes or their specific secreted particle interact with the inflamed endothelium and present functional PSGL1. This PSGL1 can interact with L-selectin on naive or central memory T cells. Activated platelets and their derived particles are also interact and present P-selectin to T cells.

Their ligand are carbohydrate-containing molecules and comprise P-selectin glycoprotein ligand 1 (PSGL1 or CLA) that directly participate in P-, but also L- and in a less extent E-selectins binding (Somers et al., 2001). PSGL1 is not the main E-selectin ligand, and the other E-selectin ligands remain poorly defined and contain ESL-1 glycoprotein and CD44 (Ellies et al., 2002; Hidalgo et al., 2007). In addition to PSGL1-binding, L-selectin also binds to endothelial ligands, most of which are known as peripheral node addressins (PNADs), including CD34 or MadCAM-1 (Rosen, 2004).

All T cells express PSGL1 protein, with different levels of glycosylation that modulate its binding and could explain why naive T cells cannot bind selectins. However, activated and effector memory T cells express glycosyltransferases that modify PSGL1 and enable binding to the three selectins. Selectins interaction with PSGL1 could have a role in T-cell homing to extra-lymphoid sites as homing to the skin, lung or inflamed tissues (Kivisäkk et al., 2003; Lim et al., 1999; Massaguer et al., 2002; Wolber et al., 1998; Xu et al., 2003).

L-selectin, altogether with CCR7, allow naïve T cells circulation through the hemo-lymphatic system and more specifically, for the entrance into LNs. Under chronic inflammation, the L-selectin–PNAD system in combination with inflammatory chemokine

receptors, enable these cells to enter inflammatory sites expressing ligands such as PNAD, confirming functionality in lymphocyte recruitment to non-lymphoid tissues as lung and intestine (Michie et al., 1995; Xu et al., 2003).

Finally, glycolipids have the ability to bind to selectins and the main role on lymphocyte migration seem to be supporting the rolling of leukocytes under flow (Alon et al., 1995).

4. *Markers of residency are highly expressed by ILCs*

CD69 is a membrane-bound, type II C-lectin receptor and a classical early marker of lymphocyte activation due to its rapid expression on the cell surface after stimulation (Cibrián and Sánchez-Madrid, 2017). When cells express high levels of CD69, CD69 association with S1PR1 causes modulation of S1PR1 on the cell surface through a mechanism requiring S1PR1 ligand binding pocket and Gα protein–coupling ERY motif (Bankovich et al., 2010). CD69 engagement then locks S1PR1 in an active ligand-bound state conformation and promotes internalization and degradation (**Figure 28a**). However, when S1PR1 is more expressed than CD69, low expression of CD69 on cell surface is shown (**Figure 28b**) (Bankovich et al., 2010; Shiow et al., 2006). By inhibiting S1PR1, CD69 blocks lymphocyte egress from inflamed LNs is blocked by CD69, then contributing to a local accumulation of circulating cells to increase chances of a productive response (Shiow et al., 2006). Following migration to peripheral inflamed tissues, CD69 is rapidly upregulated to maintain activated lymphocytes in a local resident state (**Figure 28b**) (Mackay et al., 2015).

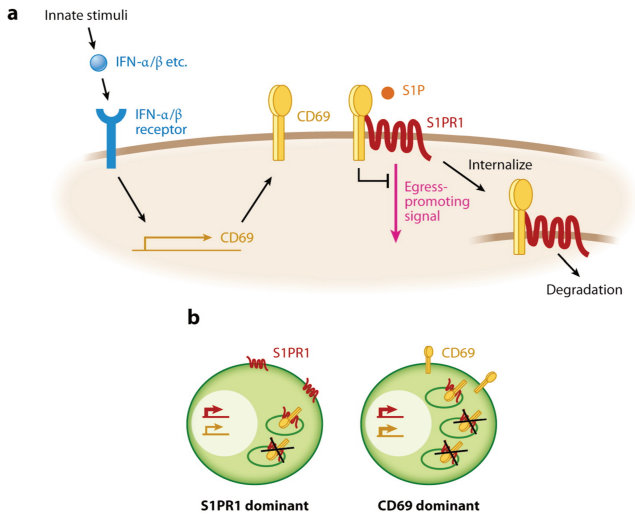

Figure 28 : CD69-mediated inhibition of S1PR1 **(adapted from Cyster and Schwab, 2012). A.** Upon exposure to type-I IFNs, lymphocytes rapidly upregulate CD69, which becomes physically associated with S1PR1, inhibiting its signalling function and promoting its internalization and degradation. It blocked the egress-promoting signal and lymphocyte egress from LN. **B.** In naive lymphocytes, S1PR1 is abundant on cell surface while some associates with the basally expressed CD69, which retains and degrades linked S1PR1 (black cross)(*left*). In lymphocytes activated by innate *stimuli* (IFN-α/β and TLR ligands), and possibly after weak or transient antigen receptor stimulation, CD69 is rapidly induced, causes S1PR1 removal from the surface and its degradation (*right*).

It has also been reviewed that CD69 does not interact with the function of S1PR3 or S1PR5 (Bankovich et al., 2010; Jenne et al., 2009), as NK cells migration could be done by activated CD69⁺ NK to leave LNs (Jenne et al., 2009).

CD103, or αEβ7 integrin, binds to E-cadherin, a cellular adhesion molecule, expressed mostly by epithelial cells and is thought to be involved in localizing

intraepithelial lymphocytes near or inside the epithelial monolayer that lines the intestine and the skin. It has also recently been implicated in residency of tissue resident memory cells (Masopust et al., 2010) and is expressed by resident localization of lymphocytes and dendritic cells in intestine, but also in skin and lungs (Mueller and Mackay, 2015; Schenkel and Masopust, 2014; Woodberry et al., 2005).

E. Studying circulation : not so easy

For immune cells, circulation is the process referring to cell egress from the tissue producing them such as the bone marrow. Circulation corresponds to the passage through the blood while recirculation is through the hemolymphatic vessels until cells are activated. Recently activated cells or cells primed and expressing homing markers of destination will then migrate and do a limited number of turn to home to the tissue they are able to reach and respond against injuries or activation signals mediated by inflammation (**Figure 29**). The scheme well characterized for T lymphocytes can be similar of ILC subsets.

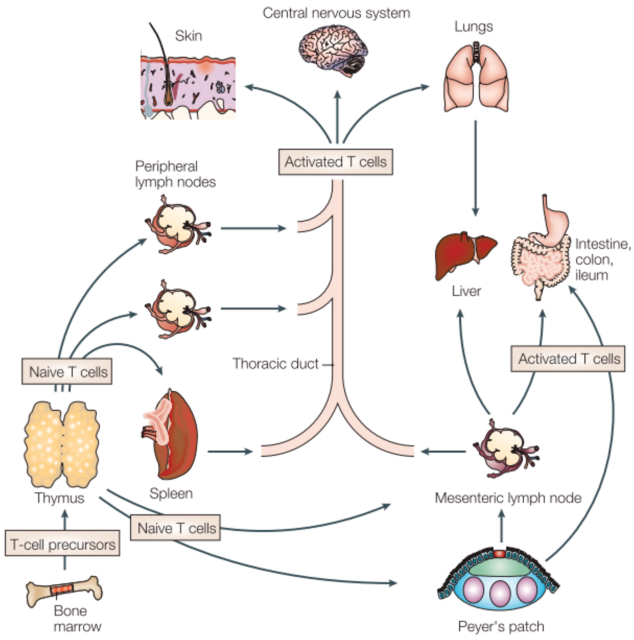

Figure 29 : T-cell trafficking patterns **(from Ley and Kansas, 2004).** T cells originate from BM precursors that mature into naive T cells in the thymus. Naive T cells traffic to peripheral and mesenteric LNs, Peyer's patches and the spleen, where they might encounter antigen and become polarized into Th1, Th2 and other effector T cells. They are collected in efferent lymphatics of LNs and enter the circulation through the thoracic duct (TD). Activated T cells traffic to extralymphoid organs, including the uninflamed lungs, skin, central nervous system and gastrointestinal organs. Many activated T cells ultimately migrate to the liver to undergo apoptosis. Activated T cells can home to almost all inflamed organs and tissues.

Studying circulation then means characterizing the activation stages of the immune cell types with their migratory or residency markers. It is important to determine the tissues where they received the stimulation, either tissue they pass through during migration, lymph, LNs and blood), or tissues where they are homing to. We need to study the balance between naïve and activated stages in lymphocyte and to determine their functions, as they might become new effectors or memory resident cells.

1. Parabiosis : the limitation of a powerful technic

Parabiosis were described long time ago to create an exchange of nutrients by establishing a common circulatory system, and so that a more or less extended physiological and pathological connection results from the vascular connection (Bert,

1864). It was used time to time and good reviews describe historical used of parabiosis for different homeostatic aspects (Conboy et al., 2013).

Parabiosis consists in linking the circulatory systems of two individuals in order to compare systemic or circulatory factors and cells from one animal affecting the other animal after homogenisation of their circulation, as homeostatic turnover of circulating cells and molecules or also the effects of a certain treatment given to one parabiont on both sides. The most valuable advances given by parabiosis studies were on aging research, by joining young and old mice, called heterochronic parabiosis, in search of answers regarding the degree to which aging is influenced by a changing balance of signals in the bloodstream (Conese et al., 2017).

This model also assessed lymphocytes turnover in tissues (Gowans and Knight, 1964). Residency was characterized as a lack of exchanges between parabiotic mice, and corresponds to maintenance of a cell into a certain peripheral tissue for long term. Parabiosis showed that peripheral tissues contain resident lymphocytes persisting for a very long time in tissues, as for lymphocytes and ILCs in intestine (Gasteiger et al., 2015; Klonowski et al., 2004). Even if circulating naïve lymphocytes reach a full equilibrium in circulation and in LNs, specific lymphocytes migration to tissues showed a low turnover from the parabiotic mouse. Two types of lymphocytes were originally described migrating in the lymph : 1) a majority of small lymphocytes, described as recent differentiated lymphocytes (RTE for recent thymic emigrants) found in LNs following congenic transfer, and 2) blast cells expressing homing molecules and incorporating tritiated thymidine, migrating to peripheral tissues as intestine following transfer to persist as resident cells (Gowans and Knight, 1964; Griscelli et al., 1969; Guy-Grand et al., 2013). These two circulating populations were later confirmed using parabiotic models, where blasts were absent from the thoracic duct lymph of the parabiont, but also from peripheral tissues as the intestine (Tyler and Everett, 1972).

This low frequency of migrating blast found in the second mouse during parabioses shows low or no recirculation of resident cells, and rapid migration of activated cells that express homing molecules. A last important point should be taken into account when parabiosis are used. When the circulatory systems of the two mice are linked together, it has been determined that the linked vessels and skin were in an inflammatory traumatic stage (Eichwald et al., 1959), increasing circulatory perturbation and adhesive molecules expression by endothelial cells (Aird, 2003; Huber-Lang et al., 2018), allowing exit of migrating cells from blood to inflamed skin.

2. Adoptive transfers or mice reconstitution : different questions

Another method to study circulation consists in adoptive transfer. This cell transfer to congenic mice corresponds to injection of migrating cells or progenitors into

mice Alternatively, transferred cells could express a reporter gene such as GFP or RFP. Finally, the transferred cells are analysed in a short period of times (or more than few days) to observe specific migration potential. The use of reconstitution experiments with the use of congenic "progenitors" allows looking for progeny migration and differentiation and requires a first step of engraftment. Depending on the stage of the progenitor, the kinetic of reconstitution could vary from less than one week to months.

The transfer can be combined with analyses of cell properties as cell division or changes in phenotypes. CFSE stainings have often been used to follow the cell division potential over time, and the number of divisions after becoming resident (Jaroszeski and Heller, 1997) but show limitation as secreting cells are not incorporating it. Blocking antibody stainings before reinjection of circulating cells allow the identification of important receptors for specific migration into tissues, and agonist blockade antibodies should be daily reinjected before analysis, as it has been done for $\alpha4\beta7^{hi}$ $V\gamma7^{+}$ T cells specific migration to the intestine (Guy-Grand et al., 2013).

In blocking transfer experiments, blocked cells, which are not able to migration in their specific tissues, will accumulate in highly irrigated tissues as lungs, liver or spleen, and die within 4-5 days, as it has already been showed for $CD69^{+}$ or $CD103^{+}$ resident cell transfers. It is probably due to lack of signals that cells should receive when migrating through vessels and becoming resident in the tissues they home to, questioning the relevance of $CD69^{+}$ intestinal resident iILC2s transferred that showed migration to the lung (Huang et al., 2018).

F. About ILCs ?

The TD circulation of ILCs has not been studied and these lymphocytes has been described as nearly exclusively resident thanks to parabiosis (Gasteiger et al., 2015). Nevertheless, the relevance of parabiosis experiments can be discussed since it has been shown that blast cells do not recirculate to cross the junction between the mice (Tyler and Everett, 1972) and since the permeability of the parabiotic anastomose can be questioned (Aird, 2003; Kotas and Locksley, 2018). As a matter of fact, ILC2s have been visualized in the lymphatic vessels of the SI *villi* (Huang et al., 2018), and IlC2s and ILC3s have been shown to migrate from LP to mesLNs (Mackley et al., 2015), suggesting that they could follow the hemo-lymphatic circuit. By collecting the TD lymph in mice, we will try to evidence this circuit for ILC and assign it a role in the body distribution of ILC2 subsets.

1. Proof of residency phenotype

Apart of NK cells, all ILC populations are considered as resident cells. Using parabiosis approaches, no significant numbers of ILC2s from the parabiont host were found in the peripheral tissues as intestine or lungs within 4 months of parabiosis (Gasteiger et al., 2015). Even after one-week post *N.b.* infection, a majority or even only

host ILC2s were detected in the lungs, underlining the tissue residency of ILC2s. However, two weeks post-infection by *N.b.*, a significant increase of donor-derived ILC2s was detected in lungs, small intestine, and mesLNs of parabiont, while no repartition change was observed for ILC3s in the small intestine.

In another study, parabiotic pairs after more than one month of shared circulation were analysed for ILC2 and eosinophils at steady state and up to one-week post-intratracheal IL-33 challenge. Whereas T cells and eosinophils are present from donor and host, ILC2 exchanges were not detected (Moro et al., 2016), suggesting that ILC2s remain local and could not migrate to parabiotic host.

Both reports show that ILC2s are tissue-resident cells that retain their tissue residency at steady state and following immune challenges. Interestingly, during development of the mouse lungs, ILC2s accumulate with number peak around two weeks after birth (de Kleer et al., 2016; Steer et al., 2017). ILC2s of immature mice have increased levels of intracellular cytokines in comparison with adult stage ILC2s that are dependent on IL-33.

Further studies are needed to be able to understand how ILC2s are directed to find their respective tissue niches during ontogeny and accumulation. Moreover, since ILC2s are observed in tissues at steady state and upon challenges or diseases, the question remains on the tissue of origin, how ILC2s take part to tissue surveillance and what is needed to support their functions and numbers in acute and chronic diseases.

2. But not only, the ILC2 case

Recent studies showed a low turnover of recently produced ILC2s compared to pre-existing fetal or neonatal populations, and reveal the importance of ILC circulation in mice (Schneider et al., 2019). It will then be of great interest to understand how and under which circumstances ILC2 egress from the bone marrow or LNs and the way they circulate and home between distinct peripheral tissues.

A first study unlighted the migratory ability of IL-17rβ$^+$ CD25$^+$ IL-7rα$^+$ BM ILC2s under IL-33 stimulation. IL-33- and ST2-deficient mice show similar ILC2 phenotype to wild-type mice. However increased numbers with ILC2s retained in the BM combined to higher expression of CXCR4 show important role for IL-33 in ILC2 egress from the BM (Stier et al., 2018). In addition, parabiosis with IL-33 stimulation of the host showed that ILC2s have the ability to migrate and populate ILC2 niches of parabiont tissues.

Another study using parabiotic mice identifies iILC2s able to migrate from the small intestine to the lungs upon systemic IL-25 administration or following helminth infection (Huang et al., 2018). It shows circulating ILC2s are not only originating from egress of BM ILC2s, as specific intestinal iILC2s have the potential to migrate. Under FTY720 treatment, absence of iILC2 accumulation in the lungs shows the regulation by

S1P-S1PR1 to exit LNs and enter the hemolymphatic system. Moreover, nILC2s reside in a different location in lungs, the alveolar space, in contrast to iILC2s that seem confined to the vascular space, according to their circulation origin. In addition, S1PR1 and CD62L were expressed in naïve lung ILC2s and decreased following IL-33 challenges, corresponding to a loss of circulatory phenotype following activation (Martinez-Gonzalez et al., 2016). ILC2s are detected in mesLNs upon systemic challenges (Neill and McKenzie, 2011) and in mediastinal draining LNs upon intranasal administration of IL-33 or papain (Martinez-Gonzalez et al., 2016), in accordance with the idea of naïve ILC2s awaiting stimulation for recruitment. It could be due to either local proliferation of resident ILC2s or/and mediated by active ILC2s migration. However, the homing ability of ILC2s from distal sites, such as the lung or small intestinal tissue, to the respective draining LNs is only beginning to be understood (Germain and Huang, 2019).

The first study on migration of ILC2s used Kaede transgenic mice, where cells can be tracked *via* a photoconvertible fluorescent protein, revealing that all ILC populations constitutively traffic from the small intestine to the draining mesLNs (Mackley et al., 2015). Interestingly, the report showed that the migration is only dependent on the CCR7 for LTi-like ILC3s, but not for ILC1s or ILC2s (Mackley et al., 2015). Moreover, RA regulates α4β7 expression by ILC1s and ILC3s from mesLNs for migration to the intestine. ILC2s don't need RA and would rather directly migrate from BM to intestine (Kim et al., 2015), eliciting that different homing programs exist for the different ILC subsets, at least for intestine homing. Importantly, recent 3D-immunofluorescence analyses revealed that ILC2 where located in the lymphatic vessels of intestinal *vili* under IL-25 treatment, showing migration of ILC2s to draining mesLNs (Huang et al., 2018). On another hand, ILC2s from skin draining LNs express skin homing markers CLA and CCR10 for localization to the skin, suggesting that ILC2s probably circulate and can traffic between draining LNs and the skin (Yang et al., 2016b), in accordance with different homing programs of specific imprinted ILC2 pools.

Indeed, under specific circumstances these studies show that ILC2s are trafficking, conversely to their tissue-resident definition. Migrating ILC2s were identified in these reports by their expression of the IL-25R that is expressed by ILC2Ps in the bone marrow (Yu et al., 2016) but limits detection to iILC2 subset showed migrating from the intestine to the lungs (Huang et al., 2015) as well as memory ILC2s characterized in the lungs (Martinez-Gonzalez et al., 2016, 2017). If circulation concerns all ILC2s, no study has identified circulating nILC2s or ILC2Ps from the lymphatic circuit.

G. Importance of circulation : a different point of view

Other important factors have not been addressed as circulation related topics but they are important to take into account. Circulation is linked to other systems in the organism, has blood vessels pressure, metabolic statues and signals from the central

nervous system. All processes are tightly regulated in the organism and impact cells of the immune system and immune responses. One important daily environmental variation that also impact immune system and homeostatic immune cell circulation is the circadian rhythm.

Also, studies using drugs succeeded to treat severe diseases using blocking or enhancing of circulation.

1. Homeostasis : day and night variations concern

Daily circadian rhythms concern almost all life forms on Earth. Circadian rhythms are driven by cell-autonomous biological clocks, which allow organisms to anticipate any temporal changes in the environment (Arjona et al., 2012; Curtis et al., 2014; Dibner et al., 2010; Labrecque and Cermakian, 2015; Man et al., 2016; Scheiermann et al., 2013, 2018). In the mammalian circadian system, peripheral clocks are maintained by daily exposure to the light–dark cycles. This photic entrainment pathway operates via retinal innervation of a specialized neural circadian pacemaker of around 20,000 neurons (Dibner et al., 2010).

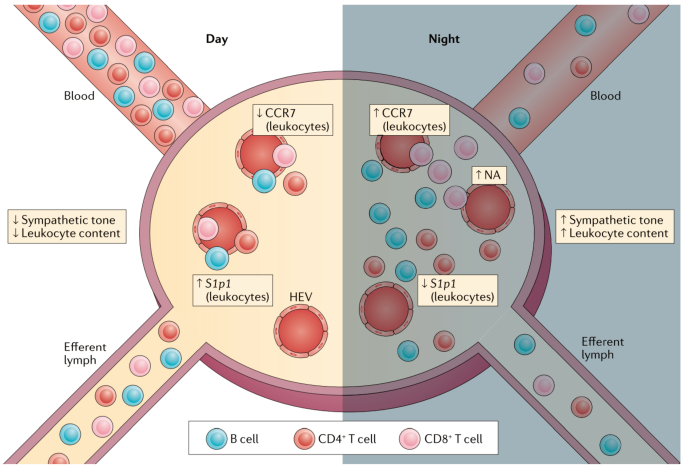

Figure 30 : Regulation of adaptive immunity in the lymph node in mice **(from Scheiermann et al., 2018).** A coordinated oscillation in pro-migratory factors drives leukocyte oscillations in blood, LNs and lymph. During the active phase, sympathetic tone and concentrations of CCL21 are high in the LNs. In addition, CCR7 expression is at its peak on T and B cells. The combination of high receptor expression on the cells and high chemokine production in the LN provides a strong attraction signal, leading to increased LN cellularity during this phase. During the rest phase, CCL21 and CCR7 expression decrease and retention signals are reduced. Leukocytes begin to upregulate expression of the S1PR1, a critical mediator of cell egress. Finally, the reduction in sympathetic tone and homing drive coupled with an increased egress potential lead to an emptying of the LN during the day.

The number of leukocytes present in circulation varies throughout the day and night, reflecting BM output and LNs egress for migration to blood and in tissues (Casanova-Acebes et al., 2013; Druzd et al., 2017; Nguyen, 2013; Scheiermann et al., 2012; Shimba et al., 2018; Suzuki et al., 2016). Then, oscillations in pro-migratory factors for specific vascular beds and individual leukocyte subsets migration vary depending on the circadian cycle.

The number of leukocytes circulating in blood is largely dependent on two factors : mobilization into blood from organs, which increases cellularity in blood (input); and emigration from blood into organs, decreasing cellularity in blood (output). Variations of immune cell circulation have been linked to circadian cycle. More precisely, T and B lymphocytes exhibit strong circadian oscillations in the blood, with peak numbers during the respective behavioural rest phase of the organism (corresponding to the day in mice

and night in humans) (**Figure 30**)(Druzd et al., 2017; Lange et al., 2010; Suzuki et al., 2016). In fact, oscillations are linked to modulations of migration markers such as CXCR4 and CX3CR1 expression that are regulated by glucocorticoids and catecholamines (Besedovsky et al., 2014; Dimitrov et al., 2009), as well as hypoxia-inducible factor 1α (HIF1α) signalling (Zhao et al., 2017). At steady-state, lymphocytes in LNs also exhibit circadian oscillations in mice, with the highest numbers present at the beginning of the active phase, at night in mice (Besedovsky et al., 2014; Druzd et al., 2017; Shimba et al., 2018). These higher numbers were not due to local proliferation but depended on cycling homing and egress of cells from blood in LNs and from LNs into efferent lymph. CCR7, important for LNs migration and lymphocyte circulation in the hemo-lymphatic system, exhibited diurnal oscillations in both T and B cells, with an expression peak correlated with CCL21 levels on HEVs of LNs (**Figure 30**)(Druzd et al., 2017), whereas B cells also rely on additional receptors such as CXCR4 and CXCR5 (Förster et al., 2008). These peak expression levels of CCR7 and CCL21 were observed around night onset, correlated with the highest recruitment of B cells, $CD4^+$ and $CD8^+$ T cells (**Figure 30**)(Druzd et al., 2017). This process is linked to the microenvironment and lymphocyte modifications. With T cell-specific genetic deletion of the circadian clock regulator BMAL1, the time-dependent difference in LNs homing and cellularity disappeared (Druzd et al., 2017). In parallel, the egress of cells into efferent lymphatics was also dependant on circadian cycle, with lymphocyte counts highest in lymph just before night-time that was dependent on rhythmic expression of S1P1R-S1P (**Figure 30**). Interestingly, cells that migrated into the LNs at night also stayed longer within these tissues than the fewer cells that migrated during the day, a mechanism dependant on lymphocyte expression of β2-adrenergic receptors, linking the nervous sympathetic system, which react to day time, and immune system (Nakai et al., 2014). Indeed, β2-Adrenergic-receptor-deficient lymphocytes transited through LNs more quickly and did not show any diurnal pattern (Suzuki et al., 2016). It clearly indicates that enhanced sympathetic signals and activation of the β2-adrenergic receptors during night time induced cells residency in LNs compartments, by increasing lymphocyte expression of CCR7 and CXCR4 (Nakai et al., 2014). This longer residency in LNs show an important role in generating good adaptive immune responses (Druzd et al., 2017; Suzuki et al., 2016). Thus, time of day dictates expression of critical pro-migratory factors on lymphocytes and endothelial cells and modulates the trafficking of lymphocytes into the hemo-lymphatic system.

In contrast, innate immunity and myeloid-specific ablation of the circadian gene *Bmal1* leads to a general pro-inflammatory phenotype in mice (Nguyen, 2013). ILCs are known to be dependent on environmental variations, and ILC2s specifically express neurotropic receptors as β2-adrenergic receptor that negatively regulates them (Moriyama et al., 2018) and are innate equivalent of lymphocytes. Time of the day impacts

on their responses, and more precisely on their ability to migrate and circulate remain not elucidated and should be assessed.

2. Circulation in pathology and inflammation : target for treatments

Immune cell circulation plays critical role in peripheral responses against dangers as well as negative effects in autoimmune diseases. Playing on specific migration of lymphocytes could enhance their responses during infections or limit exaggerated-responses in inflammatory diseases. Several clinical trials tested potential treatment impacting specific migration, either targeting activation of lymphocytes to increase specific responses, but also chemokines, selectins or integrins, important mediators of homing, to decrease over-activated lymphocytes or re-orient their specific migration.

First, pertussis toxin (PTX) is a toxin that blocks Gαi-coupled receptor signalling as chemokine receptor signalling by catalysing ADP ribosylation of the Gαi subunit. It has been shown that PTX treatment blocked T cells egress from the thymus, showing the involvement of a Gαi-coupled receptor (Chaffin and Perlmutter, 1991). Moreover, experiments on S1PR1-deficient T cells and on mice with deficient production of S1P by lymphatic endothelial cells (Pham et al., 2008, 2010) demonstrated that the PTX-treatment restores T cells egress through LNs cortical sinuses even in the absence of S1P–S1PR1 signalling.

This S1P-S1PR1 signalling can also be inhibited using an immunosuppressive drug FTY720 (or fingolimod). FTY720 is an agonist of S1P receptors that induces the sequestration of lymphocytes in LNs by inhibiting their egress from sinus lumen to lymph (Mandala et al., 2002). The mechanism of FTY720 inhibition is a down-regulation of S1PR1 expression by B and T lymphocytes required for their egress from LNs (Matloubian et al., 2004). FTY720 therapeutic effects in multiple sclerosis patients are not fully understood. Although, it remains possible that the drug sequesters in LNs the newly generated auto-reactive effector T cells and central memory T cells (Mandala et al., 2002), and may increase regulatory T cell functions (Sawicka et al., 2005). In allergic and infectious diseases, intratracheal administration of FTY720 protected against asthma (Idzko et al., 2006) and suppressed cytokine-mediated inflammation during influenza infection (Teijaro et al., 2011), whereas systemic FTY720 treatment shown prevention of autoimmune diabetes, thyroiditis, uveitis and rheumatoid arthritis when was begun prior to disease onset (**Figure 22**)(Commodaro et al., 2010; Tsunemi et al., 2010; Yang et al., 2003).

Both PTX treatment, that targets all chemokine receptors, and FTY720 that blocks the general circulation of lymphocytes in the hemo-lymphatic system need better characterisation to be used as safe treatments. Using treatment that impacts on immune

cell migration should target more precisely the subsets directly involved in the inflammatory processes.

To do so, targeting leukocyte integrins is an application used in several diseases such as multiple sclerosis, Crohn disease and ulcerative colitis. In fact, only four combinations of integrins expressed by leukocytes can be targeted by antagonist monoclonal antibodies and they have been already investigated in patients : αLβ2, α4β1, α4β7 and αEβ7 integrins (or their ligands VCAM1 and MadCAM1)(**Figure 31**).

The first important observation was that antibodies against α4β1 integrin can abrogate in mice the autoimmune encephalomyelitis (EAE) (Yednock et al., 1992), a preclinical mouse model of multiple sclerosis, which spawned the clinical development of α4 subunit antagonists. Then, α4β1 was targeted by the humanized recombinant antibody natalizumab, a monoclonal antibody that binds to α4-containing integrins and blocks the binding of their potential physiological ligands (α4β7 to MadCAM1 and VCAM1 and α4β1 to VCAM1)(**Figure 31**). It is a treatment indicated in multiple sclerosis (MS)(Balcer et al., 2007) and Crohn disease (Sandborn et al., 2005; Targan et al., 2007). However, some patients treated with natalizumab developed fatal brain infection, progressive multifocal leuko-encephalopathy (PML)(**Figure 31**)(Berger and Houff, 2010), inducing temporary and voluntary withdrawal of the drugs from the market between 2005 and 2006.

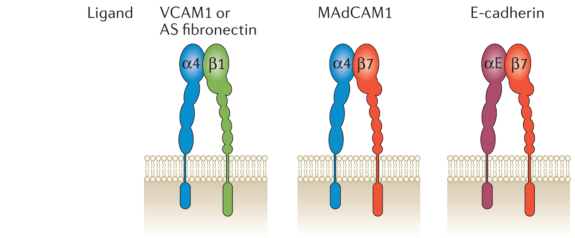

Natalizumab	Yes	Yes	No	Yes
Vedolizumab	No	Yes	No	Not observed
Etrolizumab	No	Yes	Yes	Unknown

Figure 31 : Integrins as therapeutic targets **(from Ley et al., 2016).** The α4 subunit (blue) is targeted by natalizumab : impacting α4β1 and α4β7 integrins. The β7 subunit (red) is targeted by etrolizumab, impacting α4β7 and αEβ7 integrins. Vedalizumab and AMG-181 recognize an epitope formed by both α4 and β7 and thus are monospecific. Natalizumab induces PML in patient treated.

α4β7 integrin is targeted by another antibody, vedolizumab, a humanized IgG1 monoclonal antibody that recently proved good effects for the treatment of inflammatory bowel diseases (IBDs), including Crohn disease and ulcerative colitis (**Figure 31**)(Sandborn et al., 2013). α4β7 integrin is also targeted by another antibody : the abrilumad (AMG181), another monoclonal antibody. The risk of PML is the limiting factor for the use of natalizumab, and then vedolizumab effectively replaced natalizumab in clinical practice for the treatment of Crohn disease and ulcerative colitis. MadCAM1 is expressed in the chronically inflamed livers of patients with primary sclerosing cholangitis (Grant et al., 2001), and studies for new indications for vedolizumab and or drugs that affect β7 integrin are actually done. The other antibody produced against α4β7, the AMG181, had same effects in patients with ulcerative colitis and Crohn disease, and

published data compared potential similarities or differences in binding sites between AMG181 and vedolizumab.

Etrolizumab, a humanized IgG1 monoclonal antibody that is directed against the β7 integrin subunit, is targeting both αEβ7 and α4β7 integrins, blocking their interactions with MAdCAM1 and E-cadherin, respectively (**Figure 31**). Etrolizumab is in late stage clinical development for IBDs and ulcerative colitis treatments, with increased clinical remission at week 10 compared to placebo.

The αL integrin subunit is the target of efalizumab, previously used for psoriasis but withdrawn in 2009 because of PML. A topical αLβ2 integrin inhibitor, lifitegrast, blocked αLβ2-ICAM1 interaction and limited inflammation due to ICAM1 overexpression in corneal and conjunctival tissues of patients with dry eye disease.

Another strategy involved drugs targeting integrin ligands, and then, MAdCAM1 is the target of a new antibody to treat IBD. Two antibodies were tested, PF00547659 is a fully humanized IgG2κ monoclonal antibody that binds specifically to human MAdCAM1 and gave good results against IBD (Reinisch et al., 2015), and PF00547659 that gave discussed results (Vermeire et al., 2017). Other ligands including ICAM1 and VCAM1 could be targeted, but targeting ICAM1 with a monoclonal antibody did not show effective responses in a clinical trial.

The development and demonstrated efficacy of these different strategies showed importance of circulation in immune responses. Indeed, integrin antagonists are the most promising targets for therapeutic treatments, as all approved drugs prevent the target integrin from binding to ligands and, except for natalizumab that carries a risk of PML, integrin-targeting drugs are until now remarkably safe and effective.

Circulation of ILC2s is not well characterized. They play important functions dependant on integrins for cell accumulation, such as lungs or intestine. We described their high potential to react to after a lot of micro-environmental signals. They are migrating between tissues, and characterization of the precise mechanisms used by ILC2s during my PhD is important if we want to understand and impact on specific functions in tissues.

GOALS

ILCs are hematopoietic cells produced in the BM. As for all immune cells they will have to migrate to peripheral tissues to react in immune responses.

ILC2s are type 2 secretor cells, innate equivalent of Th2 lymphocytes, playing important functions in lung or adipose tissue development and homeostasis, but also in good immune responses against pathogens or during several diseases, interacting with a high number of different other cell types. To do so, they are resident cells in periphery and are key sensors of many environmental perturbations and signals, from neural peptides to external helminthic damages mediating activation by alarmins. They are tissue-specific adapted cells, with tight imprinting, dividing ILC2s in several groups as skin-resident ILC2s, intestine-resident iILC2s, nILC2 or ILC2Ps in the BM and lung-, adipose tissue-, and other peripheral tissue-resident ILC2s.

Playing so many functions in several tissues need a permanent presence of ILC2s in these different environments, and questioned ILC2s turnover in periphery. ILC2s have several origins through life, with 3 main waves : one fetal, a second during neonatal period, and the last one during adult life. ILC2s can then be produced in hematopoietic tissues, fetal liver or bone marrow, or turnover can be mediated through continuous and discrete migration of ILC2s from and between peripheral tissues. First evidences of ILC2 circulation in the hemolymphatic system have been published, describing important markers with BM and intestinal origin of lung pools, and CCR10-dependant skin migrating-ILC2s.

But important questions remain not elicited and questioned for ILC2 turnover during adult life. What is the origin of ILC2s in adult ? It could then be precursors or specific other stages of ILC2s that may circulate and differentiate in BM or in periphery. To understand their origin, it is necessary to characterize molecules important for specific migration in peripheral tissues and how these homing markers are modulated.

iILC2s have been described as migrating cells from intestine to the lung, but the mechanism and the role of migrating cells in comparison to resident cells was not explained. Are they migrating as immature or activated mature ILC2s ? The turnover and potential migration of nILC2s was also not questioned. Answering these questions would allow characterizing and picturing the ILC2s circulating system and turnover between organs.

During my PhD, I tried to picture this circulating system of ILC2s using thoracic duct cannulation and comparison of resident *versus* circulating ILC2s at homeostasis, but also following several type-2 inflammations. I described how ILC2s migrate in systemic IL-33 and IL-25 stimulations, and used these descriptions to characterize migratory functions in tissue-specific inflammations mediated by papain and succinate models. Finally, I confirmed the importance of ILC2 migration in a physiological model of *N.b.* infection at different stages.

MATERIALS AND METHODS

Mice

CD45.2 C57BL/6 mice were purchased from Envigo. CD45.1 C57BL/6 mice were purchased from Charles River. Il7rα^{cre}-Fucci2a, CXCR6^{GFP}, Kaede, Rag2$^{-/-}$, Rag2$^{-/-}$ Il2rγc$^{-/-}$ C57BL/6 mice were back crossed to obtain good genotypes. All animal experiments were approved by the Pasteur Institute Safety Committee in accordance with French Agriculture Ministry and the European Union guidelines.

Technics

Cannulation of the thoracic duct

7-10 wks old mice were anesthetized and their thoracic ducts were exposed behind the left kidney. A carefully heat-curved polythene catheter (*0.40 mm ID, 0.80 OD; Portex UK*) was inserted into the duct beneath the diaphragm, glued with Histoacryl (*Braun*), and exteriorized at the lower part of the ventral incision. Mice received 0.7 ml phosphate-buffer-saline per hour, via the tail vein, using an infusion pump (*Harvard Apparatus*). Lymph was collected in ice-cold culture medium containing heparin. The average number of TDLs recovered during 4-6h was 20×10^6 (±10) per mouse, and 15–60×10^6 TDLs were intravenously injected in the recipients.

Organ dissociations

Lymph, blood, adipose tissues, bone marrow, lymph nodes, spleens, and lamina propria were harvested, dissociated, and resuspended in Hanks' balanced salt solution (*HBSS, Gibco*) supplemented with 1% fetal calf serum (*FCS; Gibco*).

Blood : Blood samples were harvested using a 1-ml syringe (*BD Plastipak*) and laid on Ficoll Paque Plus (*GE Healthcare*). After centrifugation at 600 g for 20 min at 20°C, the cell at the interface were washed in HBSS containing 1% FCS and recovered.

Lung : After heart flushing with 5-10mL of PBS to eliminate circulating cells from the blood, lung were harvested in 4mL of RPMI 1640 (*Gibco*) with DNase (*50 µg/mL, Roche*) and type IV collagenase (*1 mg/mL, Gibco*) contained in C tube gentleMACS (*Miltenyi*) and dissociated on gentleMACS dissociator (*Miltenyi*). After 45 min incubation at 37°C and a second round of dissociation on gentleMACS dissociator (*Miltenyi*), lungs are resuspended in 10mL of RPMI 1640 supplemented with 2% FCS, repeatedly passed through a 10-ml syringe for 5 min and then filtered through a 40-mm cell strainer (*BD Biosciences*) and collected by centrifugation. The cell pellet was resuspended in 44% Percoll (*GE Healthcare*), laid over 67% Percoll, and centrifuged at 600g for 20 min at 20°C. Cells at the interface were collected, washed in HBSS containing 1% FCS, and recovered.

Adipose tissues : The different ATs were isolated and incubated RPMI 1640 (*Gibco*) with type I collagenase (*1 mg/ml; Sigma-Aldrich*) and were shaken for 1h at 37°C. Red

blood cells were lysed by incubation with ammonium chloridepotassium bicarbonate solution (*ACK solution*).

Small Intestine : To isolate LPLs, the small bowel was flushed with phosphate-buffered saline (PBS) and the conjunctive tissue and Peyer's patches were carefully removed. The intestine was opened and cut into 1-cm pieces. To collect and/or eliminate epithelial cells and intraepithelial lymphocytes, these fragments were incubated at 37°C in 50 ml of RPMI 1640 (*Gibco*) containing 10% FCS and 10 mM Hepes buffer under strong agitation for 30 min, which was followed by vortex treatment for 4 min. For LPL isolation, the remaining fragments were incubated in identical medium to which was added type VIII collagenase (*0.5 mg/ml; Sigma-Aldrich*) and were shaken for 30 min at 37°C. To complete digestion, the suspension was repeatedly passed through a 10-ml syringe for 5 min and then filtered through a 40-mm cell strainer (*BD Biosciences*) and collected by centrifugation. The cell pellet was resuspended in 44% Percoll (*GE Healthcare*), laid over 67% Percoll, and centrifuged at 600g for 20 min at 20°C. Cells at the interface were collected, washed in HBSS containing 1% FCS, and recovered.

Bone marrow : BM were flushed out of femurs and tibias; red blood cells were lysed by incubation with ACK solution. Cells were depleted of Lin+ cells by staining with biotinylated-conjugated antibodies specific for lineage markers, CD3ε, CD5, CD8α, CD11c, CD19, Ter119, Gr-1, NK1.1, TCRβ, and TCRγδ, followed by incubation with anti-biotin microbeads (*Miltenyi Biotec*). Depletion was performed on LS MACS columns (*Miltenyi Biotec*) from which the negative fraction was recovered.

Cell culture

OP9 stromal cells were plated one day prior to culture experiment in culture medium: OPTIMEM, 10% FCS, *β*-Mercaptoethanol (*500 µM, Gibco*), penicillin (*5 U/mL, Gibco*), and streptomycin (*5 µg/mL, Gibco*). Bone marrow ILC2s were FACS sorted in 400 µL of culture medium and plated on OP9 cells at 50 cells per well. Medium was complemented with in-lab produced cytokines (IL-7, c-KitL and Flt3-L) with or without IL-33 (*10ng/mL, Biolegend*). Cells were cultured for 7 days at 37°C and 5% CO2 and then harvested and stained for analysis

Adoptive transfer and reconstitution

Recipient Ly5.1 or Ly5.1 Rag2$^{-/-}\gamma c^{-/-}$ mice were used for injection. Total lymph or specific sorted ILC2 subpopulations from donor Ly5.2 in PBS were *i.v.* injected into the retro-orbital vein. Reconstituted mice were analyzed after 18h, 5 days or 10 days after transfer. Cells from the recipient mice were CD45.1^{+} CD45.2^{-}, whereas migratory cells (kaede or wild-type C57BL/6) were CD45.1^{-} CD45.2^{+} or expressing GFP.

In vivo mAb treatment

Anti-α4β7 and –β1 purified mAb (*BD and Biolegend*) were used for their blockade capacities. TDLs were incubated for 30 min with 100 µg of the mAb, and the preparation was injected into the recipients.

N.b. infection

Infections were done in Germany in collaboration with Georg Gasteiger lab. 6-8 week-old Female C57BL/6 mice were injected subcutaneously (s.c.) with 350 L3 *Nippostrongylus brasiliensis* (*N.b.*) larvae that were cultured and delivered by David Voehringer's lab. L3 larvae were extensively washed with pre-warmed PBS to eliminate culture contaminants and further incubated at 37°C water bath for 1h and the viable larvae, defined as able to migrate through a paper filter, were collected and used for infection. Injections were carried out using a 23G needle with a total of 350 L3 *N.b.* in 200uL of sterile PBS. Mice were anesthetized with intraperitoneal injection of ketamine (70 mg/kg) and xylazine (10 mg/kg) before infection. Analyses were done 2-3days or 10days pot-infection.

Flow cytometry and cell sorting

Flow cytometry data were acquired using a BD LSRFortessa or BD Symphony (*Becton Dickinson*) and analyzed with FlowJo software (*Tree Star*). Dead cells were eliminated by propidium iodide or Dead-Live staining (*Thermo Fischer*) exclusion. Cells were stained intracellularly after permeabilization and fixation with True Nuclear Transcription Factor Fixation/Permeabilization Concentrate and Diluent (*Biolegend*). Sorted cells were purified with a FACSAria III (*Becton Dickinson*). Cells were recovered in Eppendorf tubes.

Antibodies

All antibodies were from BD Biosciences, eBioscience, BioLegend, Cell Signalling Technology, or R&D Systems. Antibodies were biotinylated or conjugated to fluorochromes [fluorescein isothiocyanate, phycoerythrin (PE), PECy5, PerCPCy5.5, PECy7, allophycocyanin (APC), Alexa Fluor 647, APCCy7, Pacific Blue, BV421, eFluor450, V500, BV510, BV605, BV655, BV711, BV786, BUV395, BUV496, BUV563, BUV661, BUV737 and BUV805] and were specific for the following mouse antigens: Ter119 (TER119), Gr-1 (RB6-8C5), CD4 (GK1.5), CD8α (53-6.7), CD8β (53-5.8), CD11c (HL3), CD3ε (145-2C11), CD5 (53-7.3), CD19 (6D5), NK1.1 (PK136), IL-7Rα (A7R34), c-Kit (2B8), Sca1 (D7), RORγt (AFKJS-9), α4β7 (DATK32), Flt3 (A2F10), CD8α (53-6.7), TCRβ (H57-597), TCRγδ (GL3), CD4 (GK1.5), CD25 (PC61), CD44 (IM7), Thy1.2 (53-2.1), NKp46 (29A1.4), GATA3 (L50-823), ICOS (C398.4A), CD27 (LG.3A10), T1/ST2 (DIH9), CD45.1 (A20), CD45.2 (104), CD45 (30-F11), CD49a (HMa1), CD49b (DX5), CD11b (M1/70),

EOMES (Dan11mag), KLRG1 (2F1), IL-17rβ (MUNC33), IL-18R1 (BG/IL18RA), CD69 (H1.2F3), CD62L (MEL14), MHC-II (M5/114.15.2), CD49d (9C10), CD29 (HMβ1-1), CD51 (RMV-7), CD61 (HMβ3-1), LFA-1 (H155-78), PSGL-1 (4RA10), CCR4 (2G12), CCR8 (SA214G2), CCR9 (9B1), IL-5 (TRFK5), IL-13 (13A), Areg (Poly), and SiglecF (E50-2440). Antibody against Ki-67 (B56) was obtained from BD Pharmingen**.**

Bioinformatics

t-SNE representation : For visualization, the dimensionality of the datasets was further reduced using the "Barnes-hut" approximate version of t-SNE. This was implemented using the Rtsne function from the Rtsne R package using 800 iterations and a perplexity setting that varied from 10 to 30 depending on the size of the dataset. PhenoGraph takes as input a matrix of N single-cell measurements and partitions them into subpopulations by clustering a graph that represents their phenotypic similarity.

Automatic clustering : PhenoGraph builds this graph in two steps. First, it finds the k nearest neighbours for each cell (using Euclidean distance), resulting in N sets of k-neighbourhoods. Second, it operates on these sets to build a weighted graph such that the weight between nodes scales with the number of neighbours they share. The Louvain community detection method is then used to find a partition of the graph that maximizes modularity. Given a dataset of N d-dimensional vectors, M distinct classes, and a vector providing the class labels for the first L samples, the PhenoGraph classifier assigns labels to the remaining N_L unlabelled vectors. First, a graph is constructed as described above. The classification problem then corresponds to the probability that a random walk originating at unlabelled node x will first reach a labelled node from each of the M classes. This defines an M-dimensional probability distribution for each node x that records its affinity for each class.

Statistics

Statistical analysis was performed with the Mann-Whitney nonparametric test where appropriate. These tests were performed with Prism software (*GraphPad*). Graphs containing error bars show means ± SD. Statistical significance is represented as follows: *P < 0.05, **P < 0.01, and ***P < 0.001, and ns= not significant.

RESULTS

I. In steady state, different subtypes of ILC2 circulate through the hemolymphatic circuit.

Immune cells recovered from the TDL of adult WT mice are composed by half of CD4$^+$ T cells as previously shown (**Figure 32A**). Hematopoietic progenitors, NK and ILC subsets are contained in the lineage negative (Lin$^-$) fraction that represents less than 1% of circulating leukocytes (**Figure 32A and B**). The most frequent subset among Lin$^-$ cells is NK determined as NK1.1$^+$ NKp46$^+$ CD49b$^+$ Eomes$^+$ cells, a *bona fide* circulating subset (**Figure 32A and C**). In steady state, ILC1, ILC2 and ILC3 subsets are very rare populations represented in equivalent frequency in the TDL (**Figure 32A**). ILC1s are determined as NK1.1$^+$ NKp46$^+$ CD49a$^+$ CD49b$^-$ Eomes$^-$ cells (**Figure 32C**). Other ILC subsets have been determined using specific combinations markers or specific reporter mice from the Lin$^-$ IL7Rα^+ fraction (**Figure 32A, D and E**). ILC3s were characterized using the Rorγt^{GFP} reporter mouse model as Lin$^-$ Il7rα^+ Thy-1$^+$ GFP$^+$ cells with a majority of them being CD4$^-$ cells. Similar results were found using Rorγt^{GFP}x Rag2$^{-/-}$ mice devoid of any possible T cell contamination (**Figure 32D**).

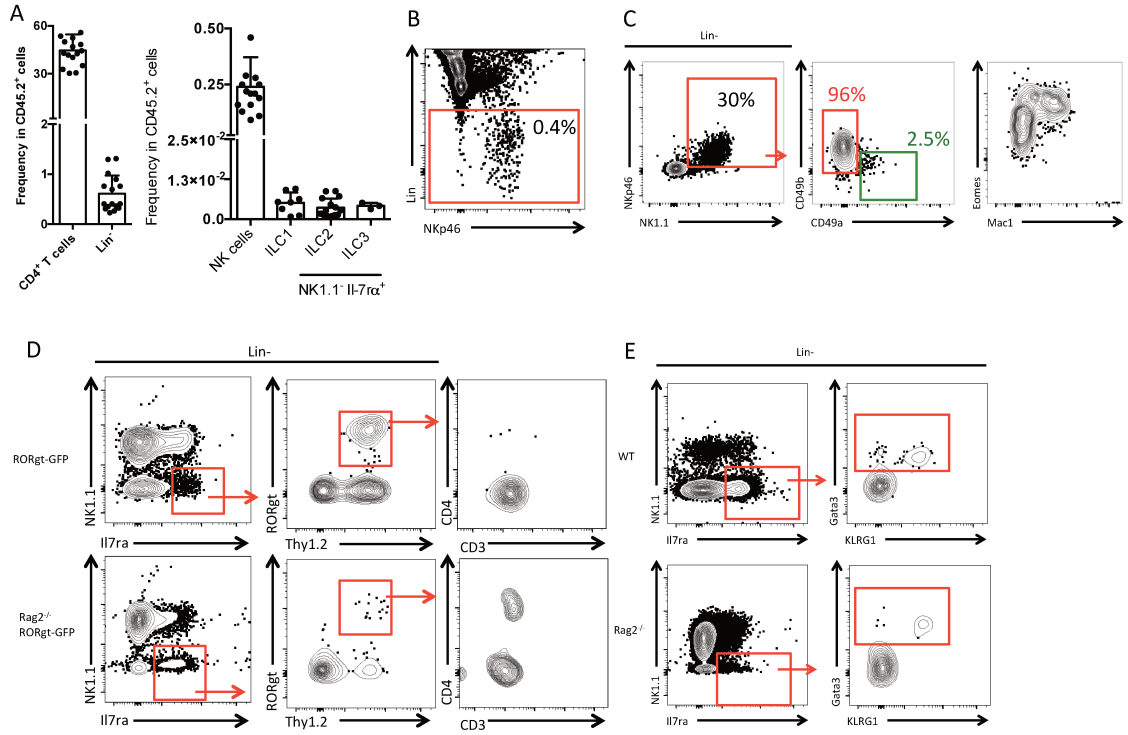

Figure 32 : ILC subsets are circulating in TDLs. **A.** Frequency of Lin$^-$ comparatively to CD4$^+$ T cells in CD45$^+$ cells (*left panel, representative of 16 mice in 8 individual experiments*). Frequency of innate lymphoid cells substets in total CD45.2$^+$ cells in WT mice (*right panel, representative of 15 mice for ILC group 1 and 2 and 3 mice for ILC group 3, respectively in 8 and 2 individual experiments*). **B.** Lineage gating strategy. Lineage comprise *CD3ε, CD5, CD8α, CD11c, CD19, Ter119, Gr-1, NK1.1, TCRβ, and TCRγδ.* **C.** CD45$^+$ Lin$^-$ NKp46$^+$ NK1.1$^+$ are separated into type 1 (CD49a$^+$) and NK cells (CD49b$^+$). Eomes level are checked by comparison with Mac1. **D.** CD45$^+$ Lin$^-$ ILC3 are shown as NKp46$^-$ NK1.1$^-$ Il7rα^+ RORγt$^+$ Thy1.2$^+$ in RORγt-GFP reporter mice and Rag2$^{-/-}$ RORγt-GFP mice (*representative plots of the experiments in A*). **E.** CD45$^+$ Lin$^-$ ILC2 are shown as NKp46$^-$ NK1.1$^-$ Il7rα^+ Gata3$^+$ in WT and Rag2$^{-/-}$ mice (*representative plots of the experiments in A*).

Characterized by their expression of Gata3, ILC2s were detected both in normal and Rag2$^{-/-}$ mice TDL (**Figure 32E**) and separated into two subsets depending on the expression of KLRG1. The TDL KLRG1^{+} subset could be further separated into a4b7^{hi} and a4b7$^{-/lo}$ populations (**Figure 33**).

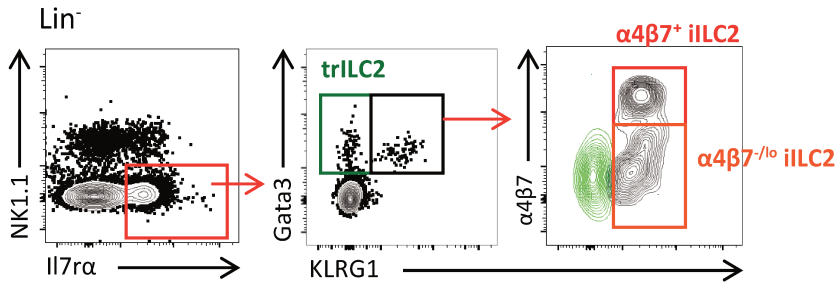

Figure 33 : ILC2s subsets in circulation. CD45^{+} Lin^{-} ILC2s are shown as NKp46^{-} NK1.1^{-} Il7rα^{+} Gata3^{+} in WT mice. They are KLRG1^{+} (black) or KLRG1^{-} (green). KLRG1^{+} were divided into 2 subsets according to α4β7 expression.

ILC2s have been previously divided into natural (nILC2) and inflammatory (iILC2) lung subtypes according to the combination of KLRG1, Thy1, ST2 and IL17rβ expression (Huang and Paul, 2016). We added to our phenotypic panel the IL18r1 marker as it is expressed from the ILC2 progenitor stage and was shown to be important for the migration toward the skin (Ricardo-Gonzalez et al., 2018). Here, we determine that according to the expression of these markers, a TDL "transitory" ILC2 (trILC2) subset could be defined as composed of Thy1.2^{hi} KLRG1^{-}IL17Rβ^{+} ST2$^{-/lo}$ cells. TDL trILC2s are quite similar to its bone marrow or intestinal LP counterpart, except for the ST2 levels that are clearly negative in the LP (**Figure 34A and B**). trILC2 subset constitutes half of ILC2s from TDL (**Figure 34A**). Defined as KLRG1^{+} cells, TDL iILC2s are heterogeneously composed of a4b7^{lo} and a4b7^{hi} subsets with similar expression of cytokine receptors (ST2^{-} IL17rβ^{med} IL18r1^{lo}).

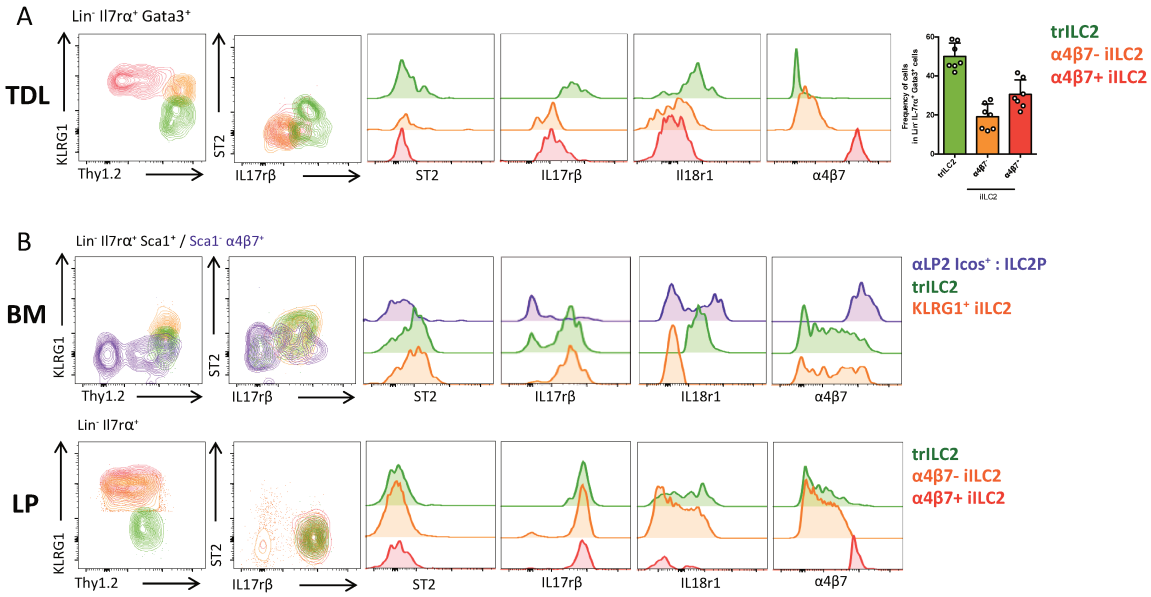

Figure 34 : ILC2 phenotypes comparison in TDL, BM and LP. **A.** KLRG1, Thy1.2, ST2, IL17rβ, IL18r1 and α4β7 phenotypes of TD KLRG1^{-} ILC2s (green), KLRG1^{+} α4β7$^{-/lo}$ iILC2s (orange) and KLRG1^{+} α4β7^{hi} iILC2s (red)(*left panels*). Frequency of the different subsets of ILC2 (*right panel*) analysed by flow cytometry (*concatenate of 3 samples and representative of 10 individual samples*). **B.** KLRG1, Thy1.2, ST2, IL17rβ, IL18r1 and α4β7phenotypes of Sca1^{+} α4β7^{+} Icos^{+} ILC2Ps (violet), KLRG1^{-} trILC2s and KLRG1^{+} α4β7$^{-/lo}$ iILC2 (orange) from BM and trILC2s (green), KLRG1^{+} α4β7$^{-/lo}$ iILC2s (orange) and KLRG1^{+} α4β7^{hi} iILC2s (red) from LP ILC2s subsets analysed by flow cytometry (*representative of 10 individual samples*).

Differential levels of Thy1.2 are associated to each iILC2 subset (Thy1.2^{+} for the α4β7^{lo} and Thy1.2$^{-/lo}$ for α4β7^{hi} iILC2s, **Figure 34A**). Respectively, these subsets represent 20% and 30% of the TDL ILC2s (**Figure 34A**). Importantly, we also show that in steady state, the bone marrow is devoid of the α4β7^{hi} iILC2 subset while intestinal LP contains all equivalent of TDL ILC2 subsets (**Figure 34A and B**). A small subset expressing mild levels of KLRG1 is detected in steady state bone marrow and called "iILC2" (**Figure 34B**). This fraction is ST2^{+} IL17rβ^{+} IL18r1^{-} with a diffuse α4β7 expression from negative to medium levels (**Figure 34B**). The BM trILC2 like population is KLRG1^{-} with most cells being ST2^{+} IL17rβ^{+} IL18r1^{+} and a similar diffuse expression of α4β7 (**Figure 34B**). The earliest committed ILC2 precursors (ILC2Ps) are detectable from WT mice as Lin^{-} IL7Rα^{+} α4β7^{+} Sca1^{-} Icos^{+} cells. These precursors contain a majority of cells that are already highly expressing the IL17Rβ and α4β7 but are mostly ST2$^{-/lo}$ (**Figure 34B**). A cluster of these precursors expresses high levels of IL18r1 (**Figure 34B**).

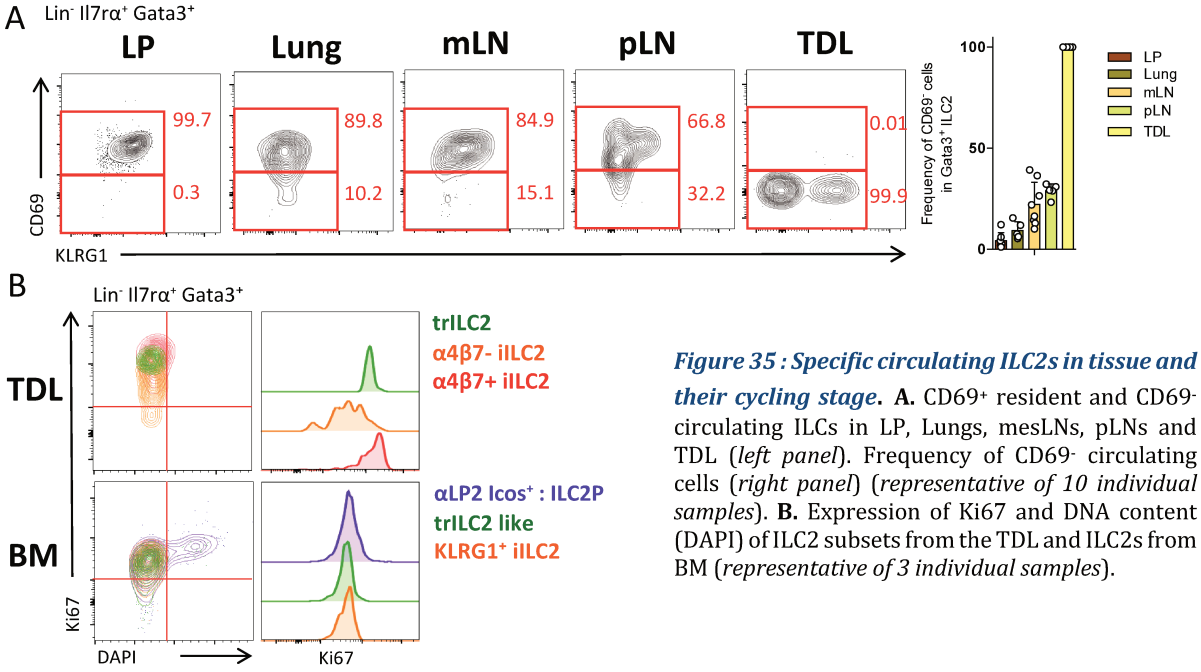

Figure 35 : Specific circulating ILC2s in tissue and their cycling stage. **A.** CD69^{+} resident and CD69^{-} circulating ILCs in LP, Lungs, mesLNs, pLNs and TDL (*left panel*). Frequency of CD69^{-} circulating cells (*right panel*) (*representative of 10 individual samples*). **B.** Expression of Ki67 and DNA content (DAPI) of ILC2 subsets from the TDL and ILC2s from BM (*representative of 3 individual samples*).

As expected for circulating cells, TDL ILC2s are CD69^{-}, while CD69^{-} ILC2s are exceptional in the gut LP, rare in the lung and easily detectable in lymph nodes (**Figure 35A)**. Most TDL ILC2s are cycling even if higher Ki-67 expression is found for trILC2s and a4b7^{hi} iILC2s than for α4β7^{lo} iILC2s suggesting that α4β7^{lo} iILC2s are probably less poised to divide (**Figure 35B)**. In BM, all ILC2s are similarly cycling and ILC2Ps are also actively dividing (Ki67^{+} DAPI^{+}) as expected for precursors (**Figure 35**).

In conclusion, three subtypes of ILC2s are found in circulation at steady state. Comparative analyses of these TDL ILC2 populations allow us to determine them as trILC2s and iILC2s subsets that could have different functions and circulatory characteristics.

II. Circulating ILC2 subsets have specific tropism at homeostasis

We used 11 different markers known to be expressed by ILC2 among different organs on top of our usual basic staining for lineage, CD45 and CD4 markers to phenotype ILC2s across 10 different tissues in steady-state : BM, intestinal LP and Intra-Epithelial Lymphocytes (IEL), mesenteric lymph nodes (mesLN), lung, inguinal lymph nodes, subcutaneous (sc), perigonadic (pg) and mesenteric (mes) adipose tissues (ATs), blood and lymph. Using unsupervised automatic clustering by "phenograph", a bioinformatic method with t-SNE dimensional reduction representation implemented in R software, we were able to obtain 15 different clusters of ILC2 based on their differential phenotypes (Amir et al., 2013; Levine et al., 2015)(**Figure 36**). The 15 generated clusters were kept for further analyses as they all contain more than 1% of total cells (**Figure 36B**). The most representative cluster per tissue is indicated by a coloured rectangle with the indication

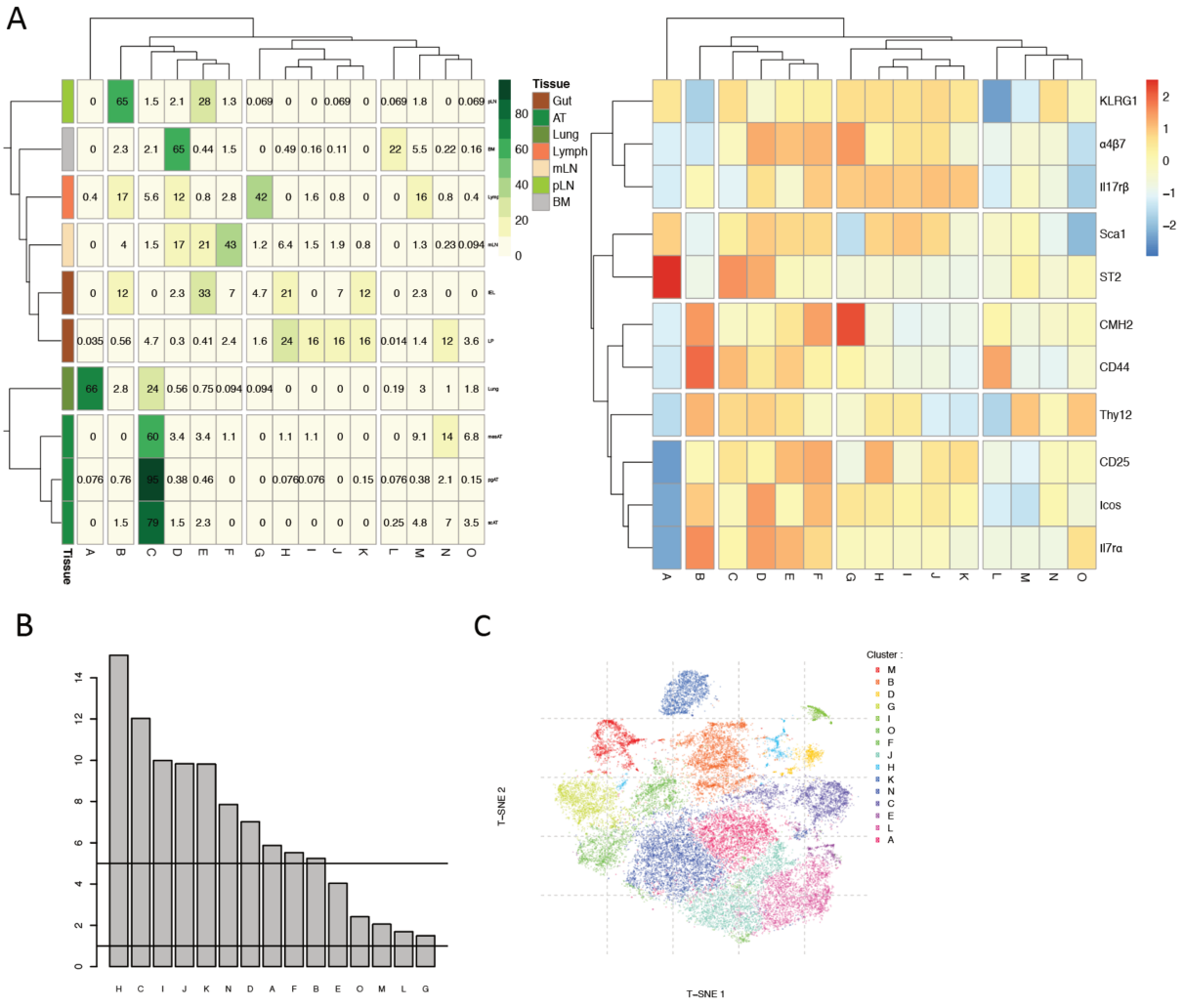

***Figure 36 : ILC2 heterogeneity in tissues*. A.** Phenograph algorithm clustering performed and plotted on t-SNE graph, showing 15 different clusters among ILC2 from lamina propria (LP), intestine epithelium (IEL), mesenteric lymph nodes (mesLN), inguinal lymph nodes (pLN), visceral adipose tissues (pgAT), subcutaneous AT (scAT), mesenteric AT (mesAT), TD lymph, lung (BALT) and bone marrow (BM). Heatmap with unsupervised hierarchical clusters of markers selected in panel expressed by phenograph clusters (left panel). Heatmap with unsupervised hierarchical clusters of ILC2s' tissue origins present in phenograph clusters (right panel). **B.** Histogram representing frequency of ILC2 from different tissues grouped in each cluster. **C.** ILC2 from WT mice origins are represented in small t-SNE graphs with clusters showed in individual colors. Each cluster groups cells from several origins depending on their phenotype.

of the representative frequency in the tissue of interest. The second hierarchical clustering examines the mean expression of these 11 markers per ILC2 cluster. Globally, we observed that ILC2 clusters are specific of each organ reflecting the early tissue imprinting of ILC2 (Ricardo-Gonzalez et al., 2018). The fact that tissues also contain at low frequency subsets specific of other tissues suggests a migratory capacity of all tissue clusters in homeostatic conditions (**Figure 36A**).

H and C clusters are the most abundant subsets in terms of number of cells and they correspond to specific gut and adipose tissue subsets (**Figure 36A and B**). trILC2 TDL are composed of 3 clusters (B, D and M) that are respectively specific of pLN, BM and TDL. It confirmed that KLRG1- trILC2 are mostly represented among circulating ILC2s (45% of ILC2) in steady state. The M cluster corresponds to the circulating $\alpha4\beta7^{-}$ trILC2 fraction and could be isolated from all tissues suggesting a capacity for this cluster to recirculate (**Figure 36A**). C, F and G clusters represent TDL $KLRG1^{+}$ iILC2 subsets. The most representative TDL subset (G:42%) is distinguishable by its high expression of MHCII and correlates with our previously defined $\alpha4\beta7^{hi}$ iILC2s as it expresses the highest mean for $\alpha4\beta7$ expression (**Figure 36A**). This cluster is only found in the digestive area representing 4.7% and 1.6% of gut IEL and LP ILC2s and 1.2% of mesLN ILC2s (**Figure 36A**). The F cluster mostly fits with the $\alpha4\beta7^{lo}$ iILC2 TDL subset determined as expressing mild $\alpha4\beta7$ expression levels, similarly to E and D clusters, all representative of mesLN ILC2s (**Figure 36A**). Finally, C cluster corresponds to the typical $\alpha4\beta7^{-}$ iILC2s from ATs (**Figure 36A**). The most representative subset of the lung (A) is found in very rare frequencies in the lymph reflecting the fact that lymph collected from the thoracic duct collects circulation of the bottom part of the body, but could correspond to contaminated cells as expressing to low levels of IL7Rα and Thy1.2, which are characteristic of lung ILC2s. However, it should be noted that clusters B and C that are also detectable in small proportion in the lungs are found in higher frequencies in the lymph indicating circulation to all tissues. The phenograph study specifically allocates these clusters to pLN and adipose tissue (**Figure 36A**).

These observations suggest a regulated migration of ILC2 subsets between organs. Hence, the expression of tropic molecules from TDL ILC2 was studied. First, all ILC2 subsets express at similar levels the cell adhesion molecule CD44 (**Figure 37A**). All TDL ILC2 express PSGL1 and LFA1, despite modulation of levels by the $\alpha4\beta7^{hi}$ iILC2s show increased levels of PSGL1 and decreased levels of LFA1 (**Figure 37A**). The $\alpha4\beta7$ integrin is known to be expressed on T-cells (like the $V\gamma7^{+}$ T cell subset) for their homing into gut-associated lymphoid tissues through the binding to MadCAM1, which is present on high endothelial venules of mucosal lymphoid organs (**Figure 37B**) (Berlin et al., 1993). As defined in figure 1 and 2A, we determined that only one of the $KLRG1^{+}$ subsets (red subset) express very high levels of $\alpha4\beta7$ integrin despite higher levels of $\alpha4$ integrin

expression by the other iILC2s (orange) subset constituted of a mix of α4β7^{-} and α4β7^{lo} clusters (**Figure 37A**).

We determined that the α4β7^{lo} iILC2 TDL subset expresses high levels of the α4β1 integrin (**Figure 37A**). The α4β1 integrin is important for cell adhesion of numerous immune populations and is essential during inflammation for leukocyte movement due to its interaction with diverse ligands such as VCAM1 and fibronectin (Cybulsky and Gimbrone, 1991). While the β3 chain is commonly expressed by all TDL ILC2, only iILC2 subsets also express the αv chain (**Figure 37A**). The integrin αvβ3 is known to be able to bind to extracellular matrix proteins such as vitronectin and fibronectin. trILC2s, contrary to iILC2s, have no clear integrin combination However, only trILC2 contains a cluster of CD62L^{+} cells (**Figure 37A**).

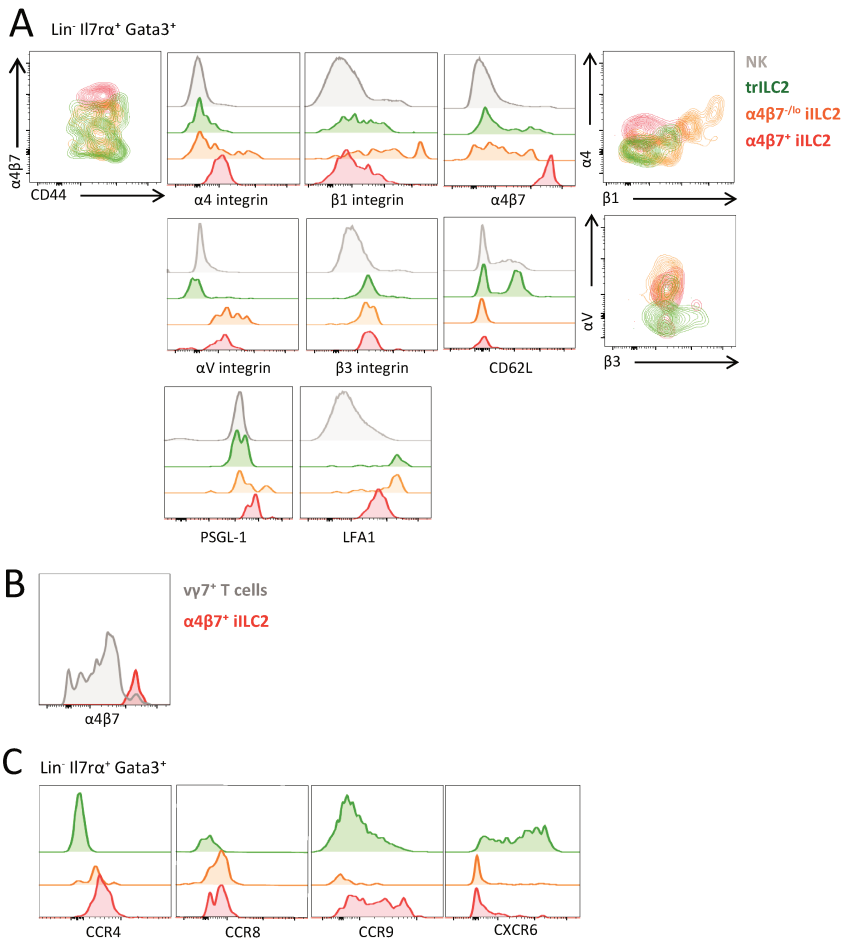

Figure 37 : Circulating molecules phenotypes of ILC2s. **A.** Expression of CD44, CD62L, α4β7, α4, β1, αV, β3, PSGL1 and LFA1 in trILC2 (green) and α4β7$^{-/lo}$ (orange) or α4β7^{hi} (red) iILC2s (lin^{-} CD45^{+} NKp46^{-} NK1.1^{-} IL-7rα^{+} Gata3^{+} cells) from the TD lymph of WT mice (*representative of 3 experiments*). **B.** Comparison of α4β7 level in trILC2 (red) and vγ7+ T cells (grey) from TDL. **C.** Expression of CCR4, CCR8, CCR9 and CXCR6 in trILC2s (green), KLRG1^{+} α4β7$^{-/lo}$ iILC2 (orange) and KLRG1^{+} α4β7^{hi} iILC2 (red) from the TD lymph of PBS or IL33 injected WT mice.

The regulation of immune cell trafficking is also related to their expression of chemokines. CCR4 and CCR8 are type-2 chemokine receptor types (Griffith et al., 2014). CCR4 binds CCL17 and CCL22 in inflamed tissues and CCR8 binds CCL18, constitutively expressed in the lung (Chenivesse and Tsicopoulos). While trILC2s from TDL express no clear CCR4 and CCR8 levels, iILC2 are all positive (**Figure 37C**). CCL25, the CCR9 ligand, is specifically expressed by the small bowel epithelium (Campbell and Butcher, 2002); accordingly CCR9 is expressed by the TDL α4β7^{hi} iILC2s and a cluster of trILC2s (**Figure 37C**). CXCR6, a typical marker of BM ILC progenitors (Possot et al., 2011) is expressed by the largest TDL trILC2 cluster (**Figure 37C**).

To study the potential of TDL ILC2 in colonizing the gut and other peripheral tissues, total lymph from CD45.2$^+$ WT mice were congenitally transferred to CD45.1$^+$ non-irradiated Rag2$^{-/-}\gamma c^{-/-}$ mice (**Figure 38A**). According to their panel of tropic molecules, donor derived TDL ILC2s were found 5 days after transfer in all analysed organs. CD45.2$^+$ ILC2 were detected in small intestine LP, as well as lung, adipose tissues and blood confirming the potential of ILC2 subsets to reach all tissues and to home (**Figure 38A**). Spleen was nearly devoid of donor derived ILC2 (**Figure 38B**). We confirmed that homing of ILC2s to the different organs is undergone by multiple clusters. Donor derived ILC2s have tissue signatures as shown by the typical combination of Thy1.2, KLRG1, ST2 and IL17rb phenotype of donor derived ILC2s (**Figure 38A**). Indeed, iILC2s (defined as KLRG1$^+$ Thy1$^-$ cells) express IL17rβ in the intestinal LP but ST2 in the lung and adipose tissues (**Figure 38A**). trILC2, defined as KLRG1$^-$ Thy1$^+$ cells, are mostly recovered in LP and express IL17rβ as expected for this organ (**Figure 38A**). The different tissue frequencies are indicated in figure 2E. The preferential homing to the adipose tissues is explained by the use of recipient Rag2$^{-/-}\gamma c^{-/-}$ mice that are devoid of all LN and consequently could accumulate ILC subsets in the adipose tissues (**Figure 38A and B**).

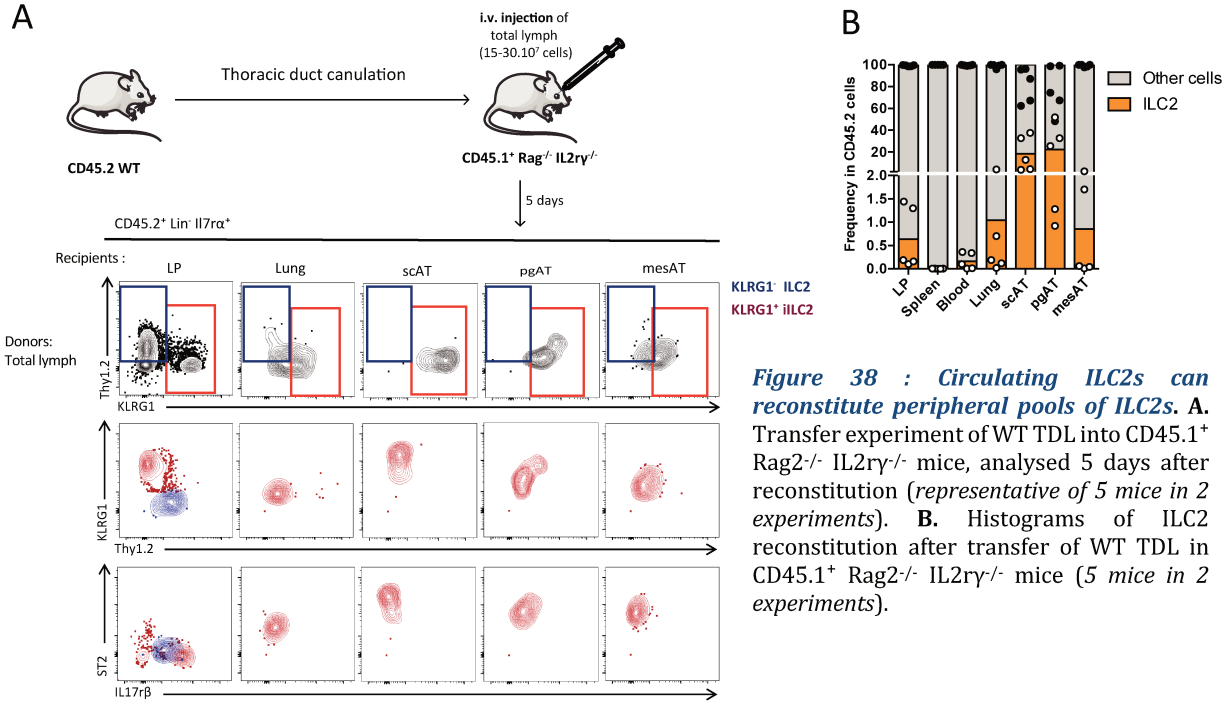

Figure 38 : Circulating ILC2s can reconstitute peripheral pools of ILC2s. **A.** Transfer experiment of WT TDL into CD45.1$^+$ Rag2$^{-/-}$ IL2rγ$^{-/-}$ mice, analysed 5 days after reconstitution (*representative of 5 mice in 2 experiments*). **B.** Histograms of ILC2 reconstitution after transfer of WT TDL in CD45.1$^+$ Rag2$^{-/-}$ IL2rγ$^{-/-}$ mice (*5 mice in 2 experiments*).

In conclusion, circulation of ILC2 between tissues is possible in steady state conditions. Different ILC2 subsets are circulating in homeostatic conditions with different tropism for each target tissue. We show that most TDL ILC2 clusters are tissue-derived and thus already having imprinted features. However, five days may be enough time for circulating trILC2 to adapt their phenotype to the homing tissue. The main trILC2 cluster is BM-derived and it could be found in small frequencies in intestinal LP, lung and adipose tissue. Another trILC2 cluster is a recirculating population patrolling through the body.

III. IL-25 and IL-33 alarmins are strong modulators of ILC2 circulation

Endogenous molecule recognized by the immune system as danger signals include cytokines that passes from an intracellular localization to an outside release during inflammatory processes. To mimic the danger signals released in case of a Th2 bias immune response, we daily injected either IL-25 or IL-33 to WT mice for 3 days (**Figure 39A**). Both alarmins are already known to stimulate ILC2 *in vivo* (Camelo et al., 2017; Gronke and Diefenbach, 2016; Hodzic et al., 2017; Howitt et al., 2016; Martin and Martin, 2016; Von Moltke et al., 2016; Nadjsombati et al., 2018; Schneider et al., 2018).

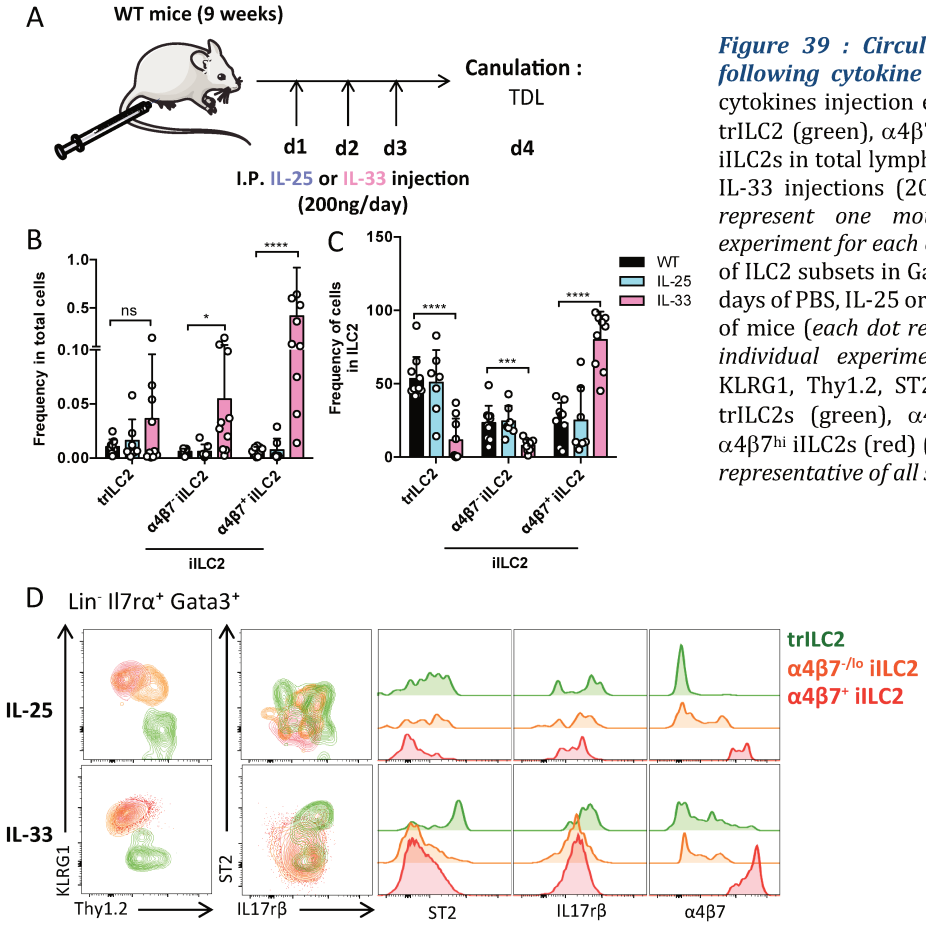

Figure 39 : Circulating ILC2 subsets in TDL following cytokine stimulations. **A.** Scheme of cytokines injection experiments. **B.** Frequency of trILC2 (green), α4β7$^{-/lo}$ (orange) or α4β7^{hi} (red) iILC2s in total lymph after 3 days of PBS, IL-25 or IL-33 injections (200ng/day) of mice (*each dot represent one mouse, at least 3 individual experiment for each condition*). **C.** Same frequency of ILC2 subsets in Gata3^{+} circulating ILC2s after 3 days of PBS, IL-25 or IL-33 injections (200ng/day) of mice (*each dot represent one mouse, at least 3 individual experiment for each condition*). **D.** KLRG1, Thy1.2, ST2, IL17rβ phenotypes of TD trILC2s (green), α4β7$^{-/lo}$ iILC2s (orange) and α4β7^{hi} iILC2s (red) (*concatenate of 3 samples and representative of all samples*).

Contrary to IL-25 administration, IL-33 treated mice showed an increase of TD circulating iILC2 subset frequencies (**Figure 39B**). While moderately increased for the α4β7$^{-/lo}$ ILC2 subset, the frequency of the α4β7^{hi} iILC2 subset is increased by 40 (**Figure 39B**). When ILC2 subset frequencies are reported among total ILC2s, the α4β7^{hi} subset is expanded in favour of all TDL ILC2 (**Figure 39C**). In contrast, IL-25 administration did not affect ILC2 subset distribution (**Figure 39C**). IL-25 and IL-33 treatments show different and redundant effects (**Figure 39C**). In both conditions of alarmin treatment, phenotypic modifications could be observed for TDL ILC2 with a common decrease in Thy-1 expression and an ST2 upregulation by trILC2 and α4β7$^{-/lo}$ iILC2s (**Figure 39D**). IL-25

can efficiently activate TD ILC2s by increasing IL17rβ levels from all ILC2 clusters. IL-33 upregulates low levels of ST2 by TDL α4β7^{hi} iILC2s (**Figure 39D**).

In the intestinal LP, both alarmins upregulate levels of KLRG1 at the surface of iILC2s (**Figure 40A and B**). This effect is also detectable in the bone marrow where iILC2s present higher levels of KLRG1 than in steady state and all cells become ST2$^+$ IL17rβ$^+$ α4β7$^+$ (**Figure 40A and B**). KLRG1$^+$ cells in the bone marrow are mature recirculating cells as previously shown, and after type-2 alarmin treatment, they share a common activated phenotype (**Figure 40A and B**).

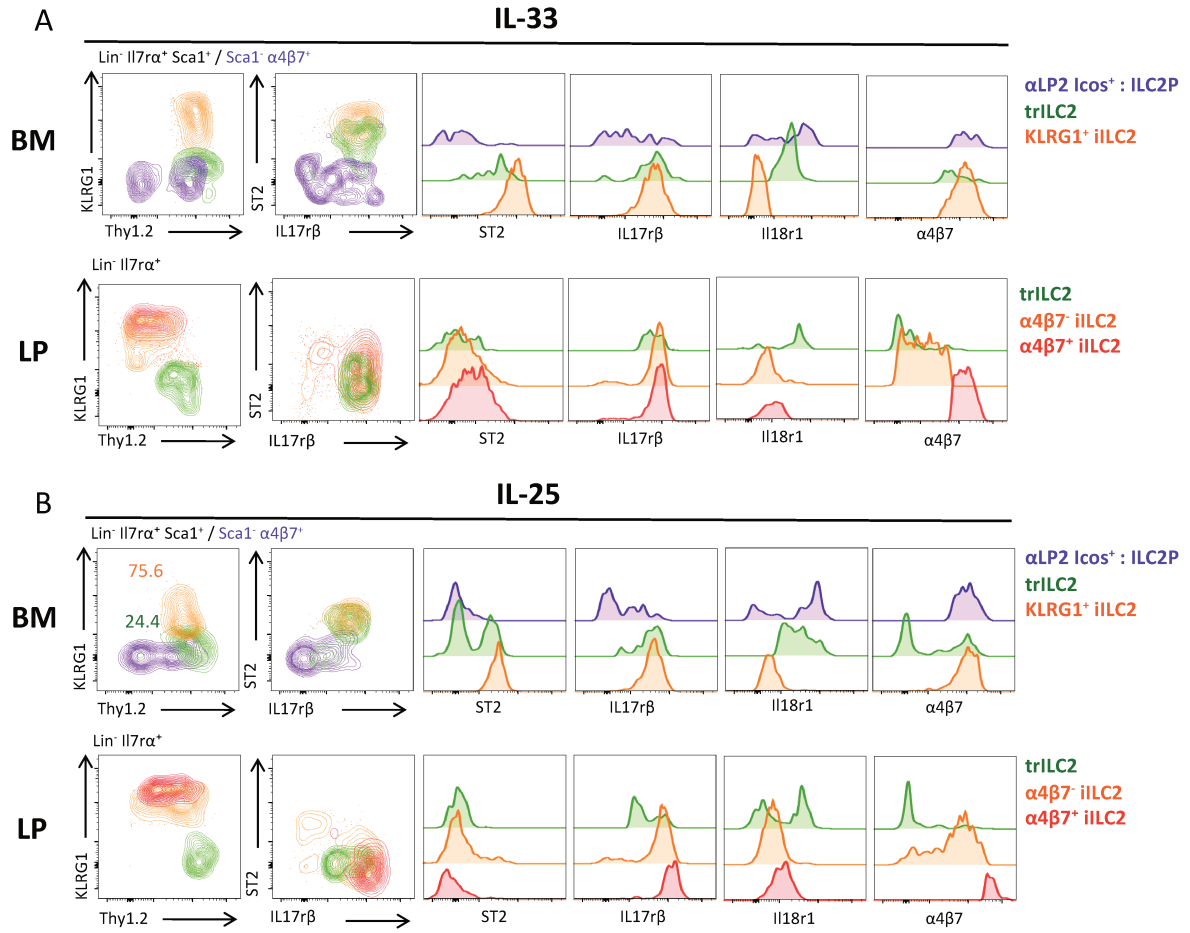

Figure 40 : ILC2s from BM and LP are differentially responding to alarmins. **A.** KLRG1, Thy1.2, ST2, IL17rβ and IL18r1 phenotypes of Sca1$^+$ α4β7$^+$ Icos$^+$ ILC2Ps (violet), KLRG1$^-$ trILC2s and KLRG1$^+$ α4β7$^{-/lo}$ iILC2 (orange) from BM and trILC2s (green), KLRG1$^+$ α4β7$^{-/lo}$ iILC2 (orange) and KLRG1$^+$ α4β7^{hi} iILC2 (red) from LP ILC2s subsets analysed by flow cytometry in IL-33 injected mice (*representative of 10 individual samples*) and **B.** in IL-25 injected mice (*representative of 10 individual samples*).

Only IL-33 treatment increase ST2 levels at the surface of the intestinal iILC2 subsets (**Figure 40A**). Both alarmins increase the α4β7 expression levels but on different intestinal iILC2 subsets, respectively α4β7$^{-/lo}$ for IL-25 and α4β7^{hi} for IL-33 (**Figure 40A and B**). The ILC2P fraction is quite unchanged in the bone marrow after alarmin treatment (**Figure 40B**). The BM trILC2 equivalent is slightly modified by the IL-25 treatment with a small increase of ST2 levels (**Figure 40B**). In case of IL-33 treatment,

ST2 and IL17rβ are increased on bone marrow trILC2s and all cells become α4β7⁺ (**Figure 40A**).

Using Kaede transgenic mice (Tomura et al., 2008), we photoconverted mesLNs with U.V. light for 60s after 2 days of PBS or IL-33 treatment. After a third injection of PBS or IL-33, we analysed BM of the photoconverted mice the day after. The only photoconverted population found coming back in BM ILC2 populations was KLRG1⁻ trILC2s, showing their accumulation from periphery and not from a local differentiation of ILC2Ps (**Figure 41A**). To test whether α4β7 upregulation could result from a direct IL-33 action on BM trILC2, the levels of α4β7 expression were compared after culture of BM trILC2 complemented or not with IL33 (**Figure 41B**). The MFI of α4β7 is significantly increased after IL33 addition as well as the division of the cells in culture (**Figure 41B**), and BM α4β7⁺ KLRG1⁺ iILC2s originate from stimulated immature KLRG1⁻ ILC2s.

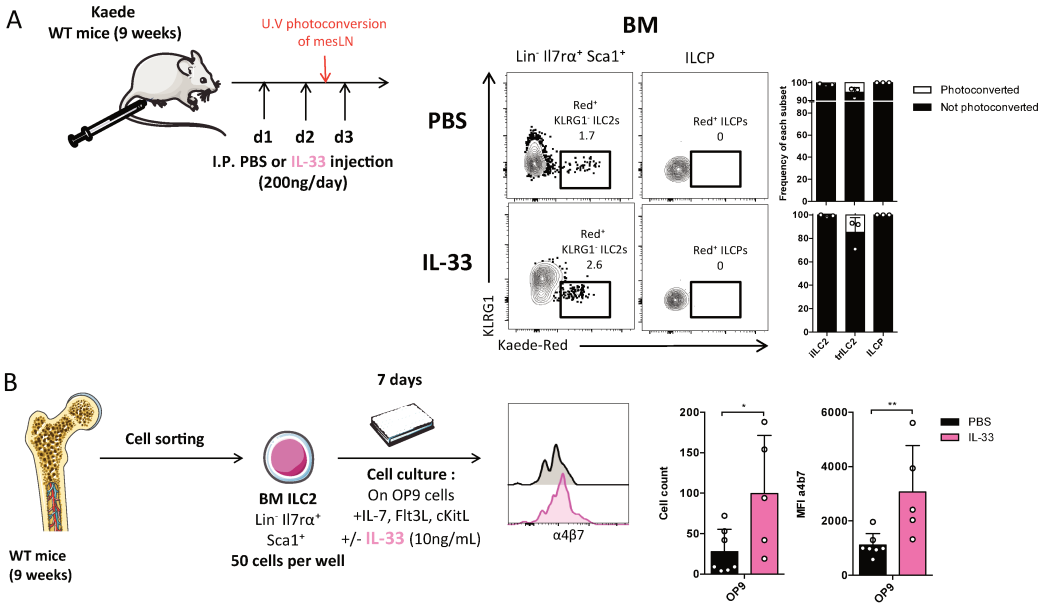

Figure 41 : trILC2s are from peripheral origin and differentiate to iILC2s. **A.** mesLNs of Kaede transgenic mice were photoconverted with 395nm U.V. LED for 60s after 2 days of IL-33 treatment. One day after the 3rd injection, BM of photoconverted mice showed Kaede-red⁺ photoconverted (Ph) cells or Kaede-green⁺ not photoconverted (Not Ph) cells in KLRG1⁺ iILC2, KLRG1⁻ trILC2 of Sca1⁺ α4β7⁺ ILCP compartment (*each dot represents one mouse from 3 individual experiments*). **B.** Cell culture of BM Sca1⁺ KLRG1⁻ trILC2s after 7 days with or without IL-33 stimulation. Numbers and α4β7 expression were assessed using flow cytometry (*representative of 2 experiments*).

In steady state, all TDL ILC2 subsets are poorly dividing with a majority of cells being in cycle (G1 state). In response to IL33 stimulation, the α4β7^{hi} iILC2 subset highly divides (**Figure 42A**), whereas its α4β7$^{-/lo}$ counterpart increases the frequency of IL-5/IL-13 producing cells (**Figure 42C**). The cell cycle status was analysed for ILC2s from peripheral and mesLN and intestinal LP (**Figure 42B**). The active division of α4β7^{hi} iILC2s is significantly observed in mesLN and also enhanced in the intestinal LP (**Figure 42B**). It is important to note that among circulating α4β7$^{-/lo}$ iILC2, cells are either secreting or cycling (**Figure 42D**). This is coherent with the significant loss of cells in G1 state among the α4β7$^{-/lo}$ iILC2s subset in mesLN and LP (**Figure 42B**). Indeed, secreting ILC2s have

left the G1 state and significantly accumulate in the G0 state both in mesLN and LP (**Figure 42B**). Interestingly, circulating iILC2s have anticipatory functions in circulation and appear to be actively secreting or dividing.

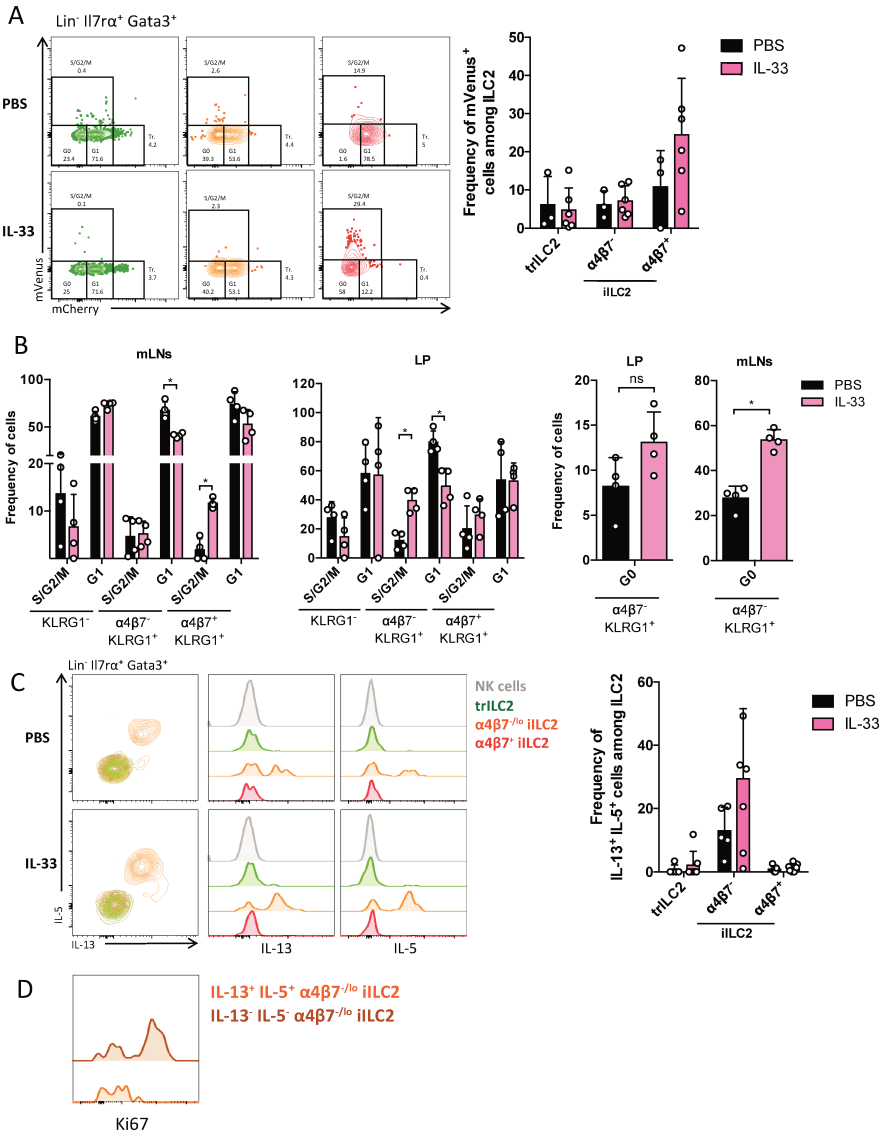

***Figure 42 : Secretory and dividing phenotype of ILC2 subsets*. A.** TD trILC2s (green), α4β7$^{-/lo}$ iILC2s (orange) and α4β7^{hi} iILC2s (red) cells division using Fucci2a mouse model. mVenus represent the S/G2/M phase and mCherry the G1 phase for positive cells or transitory to S/G2/M phase for high expressing cells. Histogram represent the frequency of cells in S/G2/M phase (active division) (*representative of 3 experiments*). **B.** G1 and S/G2/M dividing trILC2s, α4β7$^{-/lo}$ iILC2s and α4β7^{hi} iILC2s from mesLNs and LP (*representative of 2 individual experiments*) (*left panels*) and α4β7$^{-/lo}$ iILC2s in G0 from mesLNs and LP (*representative of 2 individual experiments*)(*right panels*) using Fucci2a mice. **C.** Expression of IL-5 and IL-13 in NK cells (grey), trILC2s (green), α4β7$^{-/lo}$ iILC2s (orange) and α4β7^{hi} iILC2s (red) from the TD lymph of PBS or IL-33 injected mice. Histogram represent the frequency of IL-5 and IL-13 double producers without previous *ex vivo* stimulation (*representative of 3 experiment*). **D.** Ki67 expression by IL-5^{+} IL-13^{+} and IL-5^{-} IL-13^{-} α4β7$^{-/lo}$ iILC2 (*representative of 2 experiments*).

In conclusion, IL33 treatment is significantly increasing the frequency KLRG1^{+} α4β7^{hi} iILC2 subset in the circulation and this subset is found as actively dividing in the digestive tract. On top of increasing the level of alarmin receptor expression, IL33 also promotes the expression of the α4β7gut homing integrin from medullar trILC2s. The α4β7$^{-/lo}$ iILC2 subset increases its ability to secrete type-2 cytokines but is not able to divide. IL25 and IL33 alarmins differently activate circulating ILC2 subsets with a recirculation of activated iILC2 homing back in the bone marrow as newly activated cells.

IV. Inter-tissue ILC2 homing is finely regulated

Short adoptive transfer of total lymph cells from IL-33 treated mice to non-irradiated WT congenic mice were performed to decipher the different migrative capacities of TDL ILC2. The homing of donor circulating subsets and their phenotype were analysed 18h after their transfer of IL-33 stimulated or normal TDL (**Figure 43A and Figure 44**). We show here a specific trafficking to all tissues, with a detection of ILC2s in the intestinal LP and their associated mesLN, lungs and ATs and very few cells in pLN (**Figure 43A and 44**). Donor ILC2s were absent from liver, spleen or blood of recipient mice. iILC2 subsets are found in all organs (except pLN) and in higher proportions than trILC2 subsets consistent with the fact that IL33 increase the circulation of iILC2 subsets over trILC2. The phenotype of donor iILC2s in tissues is specific of the circulating subset and has not yet been able to adapt to the seeded tissue phenotype (**Figure 43A**). Indeed, the donor intestinal LP iILC2 and trILC2 subset resemble more TDL ILC2 subsets (**Figure**

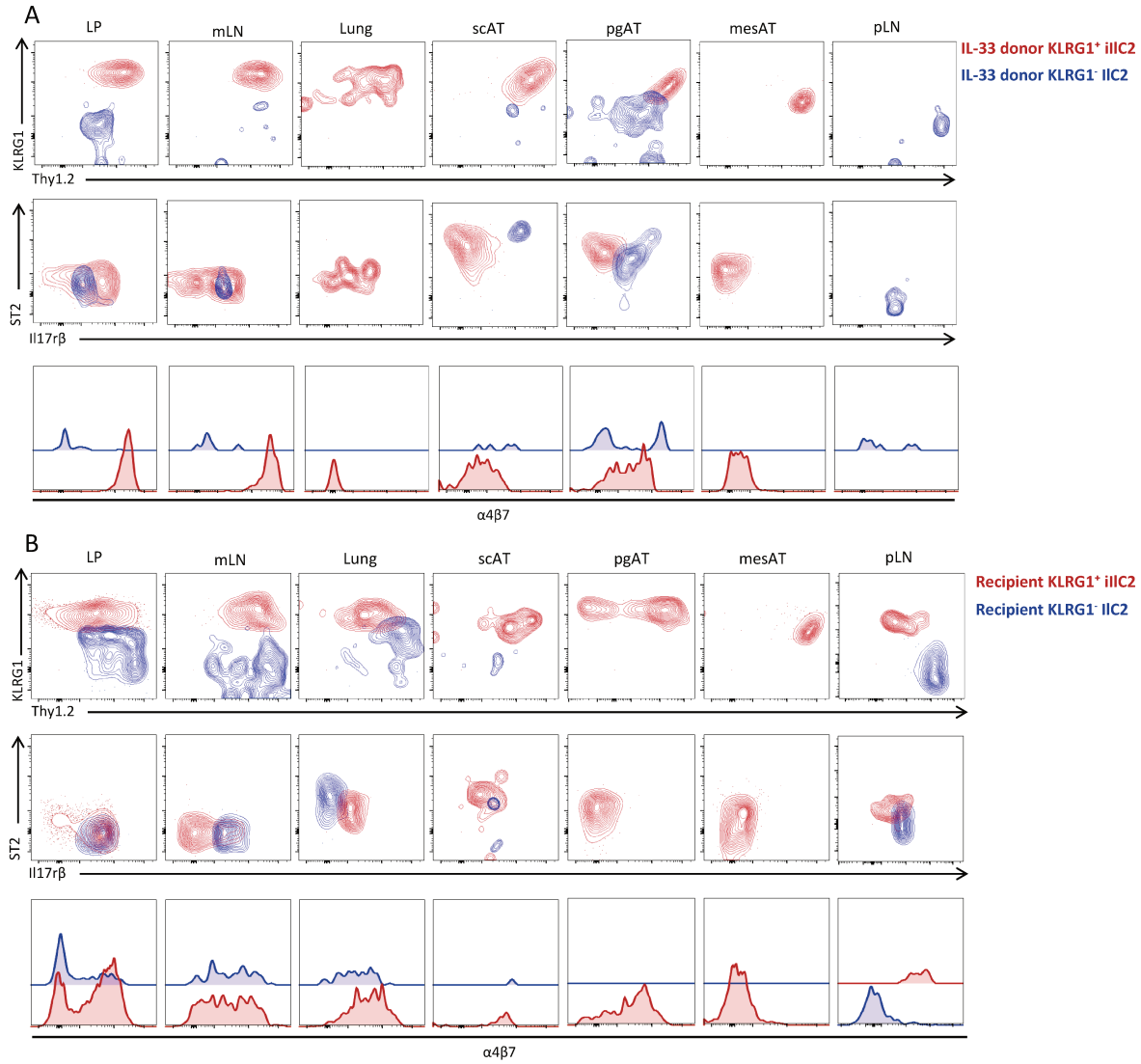

Figure 43 : Different ILC2 subsets have specific potential of migration. **A.** Transfer experiment of IL-33 injected TDL into WT mice, analysed 18h after injection (*representative of 3 mice in 3 experiments*). Phenotypic analysis of KLRG1- or + ILC2s in LP, mesLNs, Lung, pLN and ATs (subcutaneous, perigonadal and mesenteric) and **B.** of resident KLRG1- or + ILC2s in LP, mesLNs, Lung, pLN and ATs (subcutaneous, perigonadal and mesenteric).

39D) than their recipient tissue equivalents (**Figure 43B**). Moreover, the α4β7 levels are still very high in donor iILC2s from gut related tissues compared to endogenous levels (**Figure 43A and B**) confirming their recent emigration. It is interesting to note that the lung and ATs are only colonized by α4β7^{-} iILC2 clusters suggesting that iILC2s dedicated to the intestinal area (α4β7^{hi}) are really migrating in intestine (**Figure 43A and 44**).

trILC2 are found in the digestive area and few in pLN (**Figure 43A and 44**). This is consistent with the existence of TDL CD62L^{+} recirculating clusters that could express or not the α4β7 integrin as previously shown in figure 2.

To confirm that α4β7 expression by circulating ILC2 is related to their specific

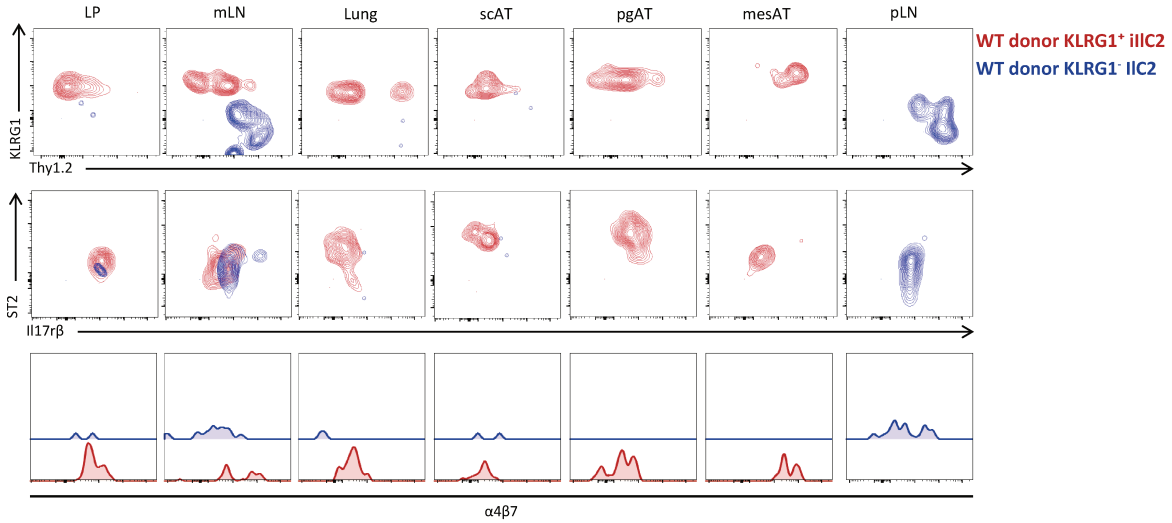

Figure 44 : ILC2 subsets have similar specific potential of migration at homeostasis. Transfer experiment of WT injected TDL into WT mice, analysed 18h after injection (*representative of 3 mice in 3 experiments*). Phenotypic analysis of transferred KLRG1- or + ILC2s in LP, mesLNs, Lung, pLN and ATs (subcutaneous, perigonadal and mesenteric).

homing to the digestive tract, we performed short adoptive transfer experiments of TDL into WT congenic recipient mice using or not anti-α4β7 or anti-β1 blocking antibodies (**Figure 46**). ILC2 reconstitution of the different organs (LP, mesLN, pLN, pgAT, scAT and lung) is indicated as a ratio of the reconstitution with blocking antibodies treated lymph versus untreated lymph (**Figure 46**). Then, the ratio value is 1 when the blockade of α4β7 has no effect on trafficking to the tissue (**Figure 46**). Hence, whereas α4β7 is not necessary to reach pLN, AT and lungs, we demonstrate that trafficking to intestinal LP and mesLN is highly dependent on α4β7 expression as its blockade nearly abrogates TDL ILC2 abilities to home to these tissues (**Figure 46**). Alternatively, the ILC2 trafficking toward AT and lung is highly dependent on the β1 expression (**Figure 46**).

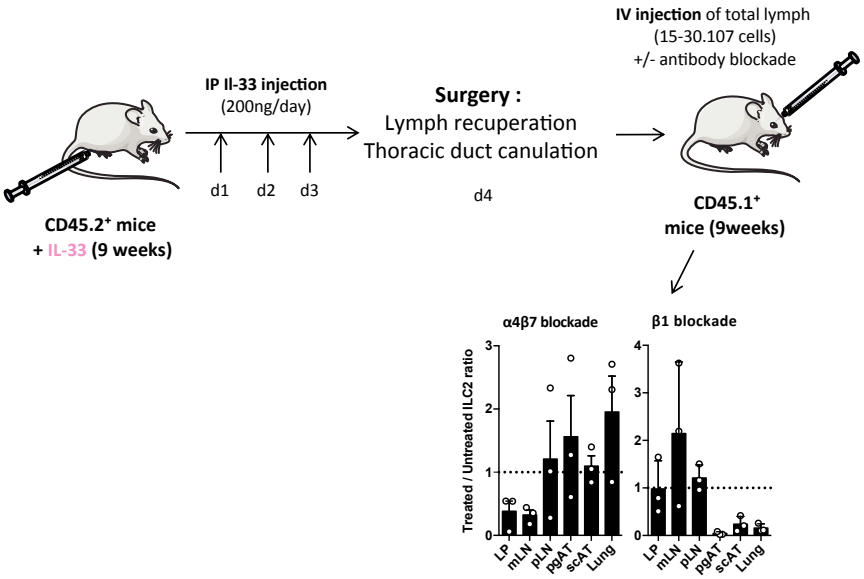

Figure 46 : Integrin-blockade antibodies show specificity of subsets to tissues. Experiment scheme of blockade experiment. IL-33 injected TDL into WT mice after α4β7 or β1 blockade antibody staining of TDL before injection. Transfer experiment of IL-33 injected TDL into WT mice after α4β7 or β1 blockade antibody staining of TDL before injection. Each IL-33 TDL were plated in 2, one stained with antibody and the other with isotype control antibody, and injected in 2 different CD45.1+ mice. Histogram of Il33 transferred treated ILC2s/untreated ILC2s ratio (*3 individual experiments*).

To confirm that α4β7$^{-/lo}$ and α4β7^{hi} CD69^{-} iILC2 subsets have different migratory route, they were sorted from mesLN of congenic mice and adoptively transferred for 18h and 10 days in Rag2$^{-/-}$ recipient (**Figure 45**). We observe here that while α4β7^{hi} iILC2 subset is only populated intestinal LP and mesLNs at 18h, lung and pgAT can equally receive ILC2s from α4β7$^{-/lo}$ and α4β7^{hi} iILC2 subsets origin after 10 days (**Figure 45**).

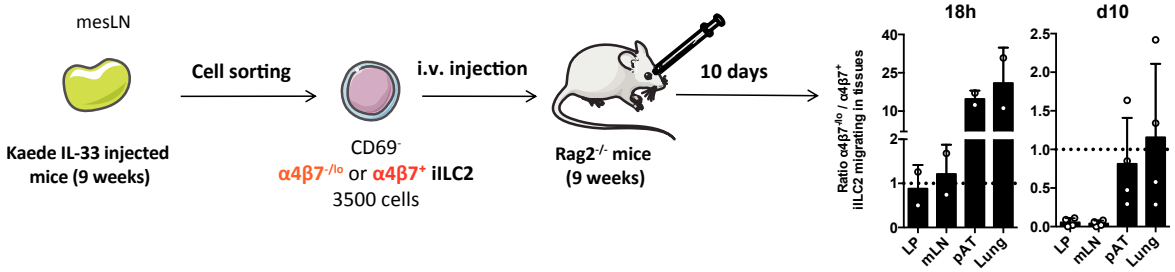

Figure 45 : Specific transfer or iILC2 subsets show an important intestinal stage to generate α4β7$^{-/lo}$ iILC2s. Sorted α4β7^{hi} or α4β7$^{-/lo}$ iILC2s from mesLNs transfer in Rag2$^{-/-}$ mice and analysed 18h or 10 days following transfer (*representative of 2 experiments*).

In conclusion, we demonstrate that the diverse ILC2 clusters from the TD have specific migratory abilities to reach non-lymphoid tissues. The trafficking of ILC2 depends on integrin combination with α4β7 as a specific gut homing molecule contrary to α4β1 that is essential for AT and lung homing. While IL-33 is increasing the frequencies of gut homing iILC2 subsets, capacities of ILC2 migration are mostly similar between steady-state and alarmin treated mice.

V. Specific migrations of iILC2 subsets following lung or intestinal inflammation

By using intranasal administration of papain allergen or adding succinate to the drinking water, we respectively stimulated lung and intestinal inflammation of WT mice. Both inflammatory models are more physiologically activating ILC2 than single alarmin injections. We compared the circulation capacities of these ILC2 subsets activated by tissue specific inflammatory processes (**Figure 47A and B**). TD cannulations of papain and succinate treated mice show that activation concerns different ILC2 subsets using different migratory mechanisms (**Figure 47C and D**). In case of papain induced lung inflammation, the $\alpha4\beta7^{-/lo}$ iILC2 subset is increased among circulating cells while its $\alpha4\beta7^{hi}$ iILC2 counterpart is increased after succinate induced intestinal inflammation. For both type of inflammation, the TDL iILC2 subsets are increased in favour of the trILC2 subsets (**Figure 47C and D**). As observed for IL-25 and IL-33 treatment, ST2 upregulation is observed on the $\alpha4\beta7^{-/lo}$ TDL iILC2 6 days after the first papain challenge (**Figure 47E**).

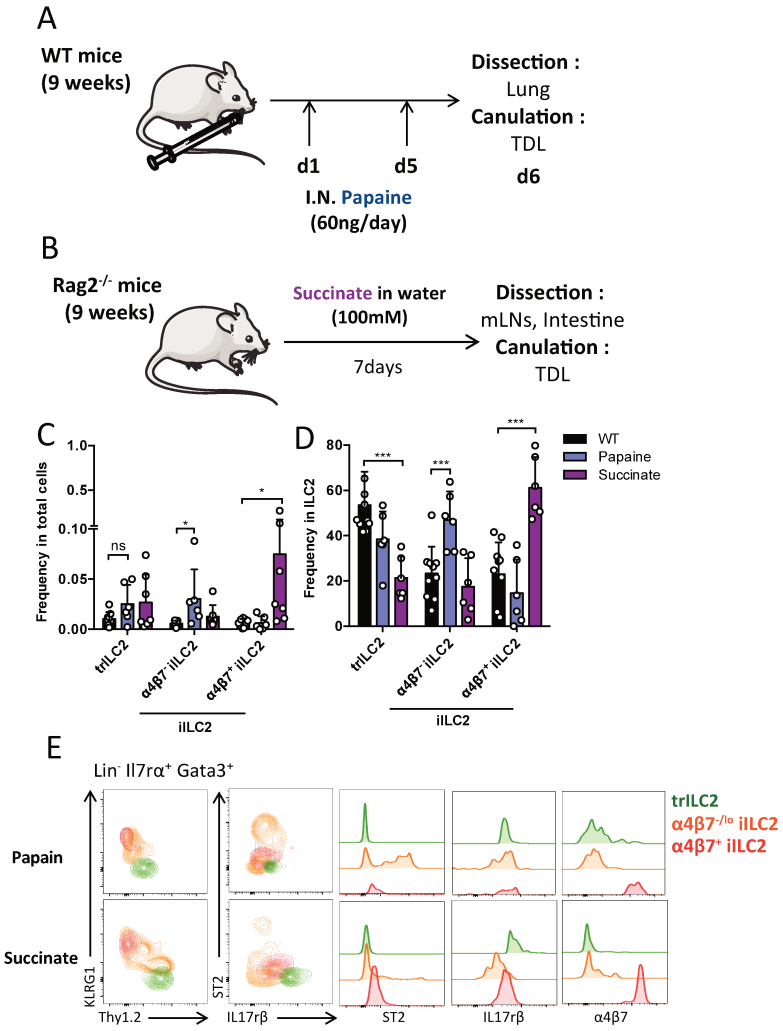

Figure 47 : Specific circulating ILC2 subsets increased depending on stimulation. **A.** Scheme of papain experiments. Intra-nasal injections of papain (60ng/day) at d1 and d5 and mice analysed at d6 for migrating ILC2s in TDL and tissues. **B.** Scheme of succinate experiments. Water or water supplemented with succinate (100mM) given 7days before analysis for migrating ILC2s in TDL and tissues. **C.** Frequency of trILC2 (green), $\alpha4\beta7^{-/lo}$ (orange) or $\alpha4\beta7^{hi}$ (red) iILC2s in total lymph after 7 days of water or succinate (100mM) and PBS vs papain inhalation (60ng/day) by mice (*each dot represent one mouse, at least 3 individual experiment for each condition*) and **D.** in $Gata3^+$ circulating ILC2s after 7 days of Water or Succinate (100mM) and PBS vs papain inhalation (60ng/day) by mice (*each dot represent one mouse, at least 3 individual experiment for each condition*). **E.** KLRG1, Thy1.2, ST2, IL17rβ phenotypes of TD trILC2s (green), $\alpha4\beta7^{-/lo}$ iILC2s (orange) and $\alpha4\beta7^{hi}$ iILC2s (red) (*concatenate of 3 samples and representative of all samples*).

In the lung treated with papain allergen, an accumulation of ILC2s is observed for both $ST2^+$ $KLRG1^-$ nILC2s and IL-$17r\beta^+$ $KLRG1^+$ iILC2 subsets. This last population is very rare in steady-state lungs (**Figure 48A**). The $ST2^+$ nILC2 subset is called resident as most cells are $CD69^+$ (**Figure 48C**). The $\alpha4\beta7^{-/lo}$ iILC2 subset is increased

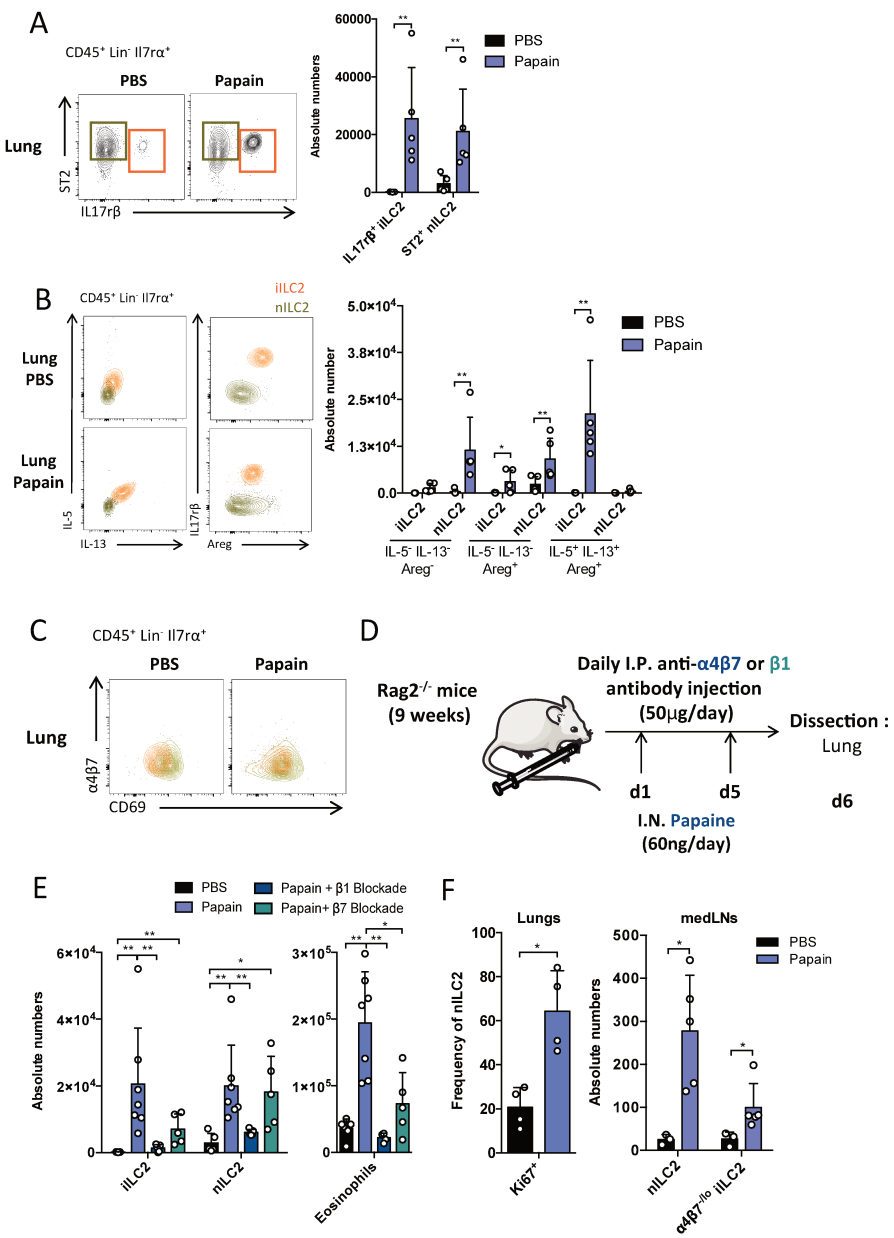

Figure 48 : Important role of migrating ILC2s as type-2 secretor cells. **A.** Selection of ILC2s in lung (*left panel*). Histogram of ST2⁺ and IL17rβ⁺ ILC2s absolute numbers from PBS and Papain treated mice (*right panel*) (*each dot represents one mouse, representative of 4 individual experiments*). **B.** Dot plots representing IL-5, IL-13 and Areg secretion by ILC2s from lung in PBS or Papain conditions (*left panel*). Histogram representing numbers of Areg single producers or IL-5, IL-13 and Areg triple producers in Lung of PBS or Papain mice (*right panels*) (*each dot represents one mouse, representative of 4 individual experiments*). **C.** CD69 and α4β7 expression by ST2⁺ or IL17rβ⁺ ILC2s from lungs of PBS or Papain mice. **D.** Scheme of papain experiment with antibody blockade. Intra-nasal injections of papain (60ng/day) at d1 and d5 and mice analysed at d6 for migrating ILC2s in TDL and tissues. Rag2$^{-/-}$ mice with papain and antibody blockade were daily injected with 50µg of anti-α4β7 or β1 blockade antibody. **E.** Histogram of eosinophils, ST2⁺ and IL17rβ⁺ ILC2s absolute numbers from PBS, Papain + isotype controls and Papain + I.P. anti-α4β7 or β1 blockade antibody treated mice (*each dot represents one mouse, representative of at least 2 individual experiments*). **F.** Histogram of Ki67⁺ cells in nILC2 frequencies from lungs and nILC2s and IL17rβ⁺ α4β7⁻ iILC2s absolute numbers from medLNs of PBS and Papain treated mice (*each dot represents one mouse, representative of 2 individual*

in the TDL of papain-treated mice and could directly reach the lung as proven by previous antibody blocking experiments (**Figure 46**). Short adoptive TDL transfer proved that lung is colonized by α4β7⁻ circulating subsets. Concerning the IL-17rβ⁺ KLRG1⁺ iILC2 subset, it results from the incoming of α4β7$^{-/lo}$ IL-17rβ⁺ KLRG1⁺ shown to be actively secreting in IL-33 conditions (**Figure 42C**). Moreover, the IL17rβ⁺ iILC2 subset is able to secrete IL-5, IL-13 and Areg (**Figure 48B**) contrary to the ST2⁺ nILC2 that is only capable to secrete Areg (**Figure 48B**).

Both increased subsets could be attributed to an active income of circulating cells, as β1 antibody blockade treatment abolished accumulation of ILC2 subsets (**Figure 48E**). However, it is also probable that the increase of ILC2 subset in lungs results from *in situ* proliferation under papain stimulation as small increase is observed even after treatment (**Figure 48E and F**). As we previously showed, ILC2 subsets are either secreting or proliferating (**Figure 42D**) explaining that the loss of Areg⁺ cells among nILC2 in papain

conditions may be due to their proliferation (**Figure 48B**). When ILC2s where blocked using anti-α4β7 antibody, only the IL17rβ^{+} iILC2 accumulation decreased, confirming a constant renewal from α4β7^{hi} iILC2 subset differentiation after migrating to intestine (**Figure 48E**). In both conditions, decreased production of type-2 cytokines by iILC2s strongly impacted eosinophils accumulation in lungs of treated mice (**Figure 48E**). As iILC2s accumulate from intestinal origin, it questioned nILC2s origin that did not migrate from lymph during transfer experiments but need α4β1 for migration. nILC2 have been described as deriving from iILC2s (Huang et al., 2015, 2018), but accumulation of nILC2s in mediastinal draining LNs let also suppose a local renewal of resident nILC2s and migration from draining lymph nodes of new generated nILC2s (**Figure 48E and F**).

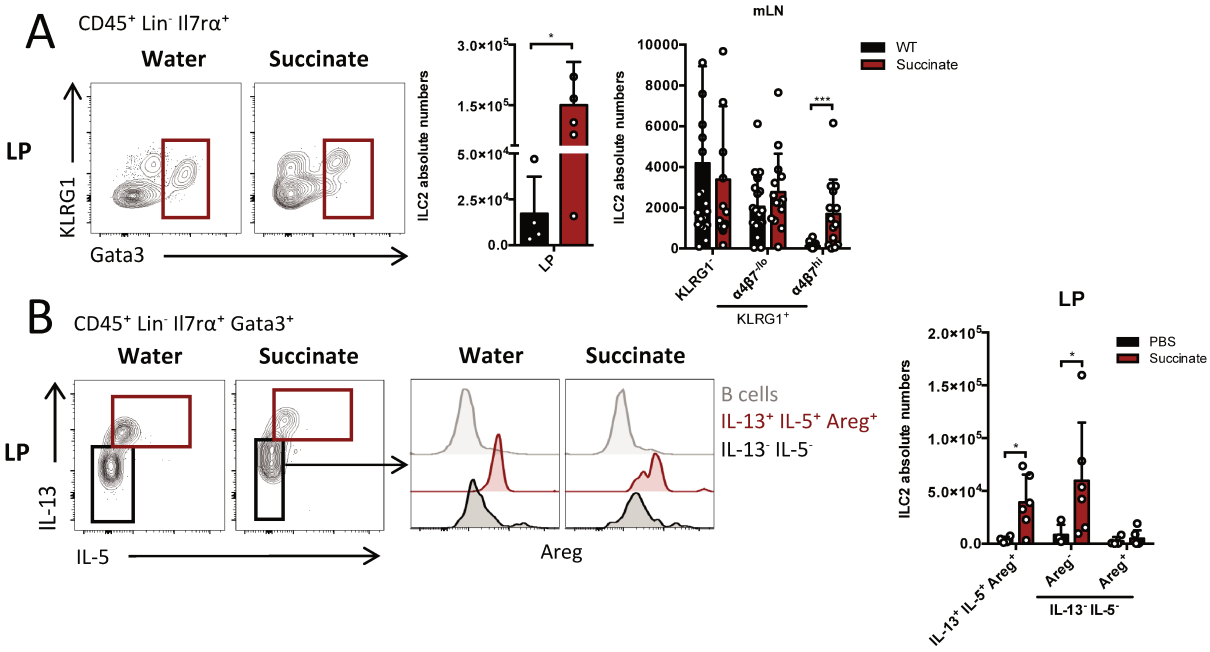

Figure 49 : Succinate show specific migration of an intestinal iILC2 subset. **A.** Selection of ILC2s in lamina propria (*left panel*). Histogram of LP ILC2s numbers from Water and Succinate mice (*central panel*). Histogram representing numbers of trILC2 (green), α4β7^{-} (orange) or α4β7^{hi} (red) iILC2s from mesLNs in water and succinate conditions (*right panel*). **B.** Dot plots representing IL-5, IL-13 and Areg secretion by ILC2s from lung in Water or Succinate conditions (*left panel*). Histogram representing numbers of no cytokine producers, Areg single producers or IL-5, IL-13 and Areg triple producers in LP of Water or Succinate mice (*right panels*) (*each dot represents one mouse, representative of 4 individual experiments*).

In case of succinate-stimulated intestinal inflammation, ILC2s are increased in both the intestinal LP and the mesLNs (**Figure 49A**). The increased ILC2 subset in the LP results in an increase of functional ILC2 that are IL-5/IL-13/Areg triple producers (**Figure 49B**). The decrease of Areg^{+} single producing cells ILC2 that are in proliferative state is a phenomenon already observed for lung trILC2 under inflammation (**Figure 49B**). To definitely prove that in case of inflammation functional ILC2s are coming from circulating iILC2s, we used anti-α4β7 blocking antibodies on succinate-treated Rag2$^{-/-}$ mice (**Figure 50A**). As we showed previously, the α4β7 is absolutely needed to recruit new iILC2 in the intestinal area (**Figure 50B**). We proved that the anti-α4β7 blocking antibodies, only impact and block the α4β7^{hi} iILC2 subset from the mesLN (**Figure 50B**).

Then, intestinal mucus and number of goblet cells are strongly decreased in succinate-treated mice with anti-α4β7 blocking antibodies (**Figure 50C and D**)**.** Indeed, the number of goblet cells producing mucus return to the steady state basal level despite succinate treatment demonstrating that preventing the $\alpha4\beta7^{hi}$ iILC2s to reach the intestine results in the loss of gut IL-13 producing ILC2s in intestinal inflammation (**Figure 50C and D**).

In conclusion, the specific blockade of circulating iILC2s under inflammation conditions demonstrates that circulation of ILC2s is crucial to recover functional cells in the damaged tissue and contribute to local inflammation and stimulation of other actor of type-2 immune response.

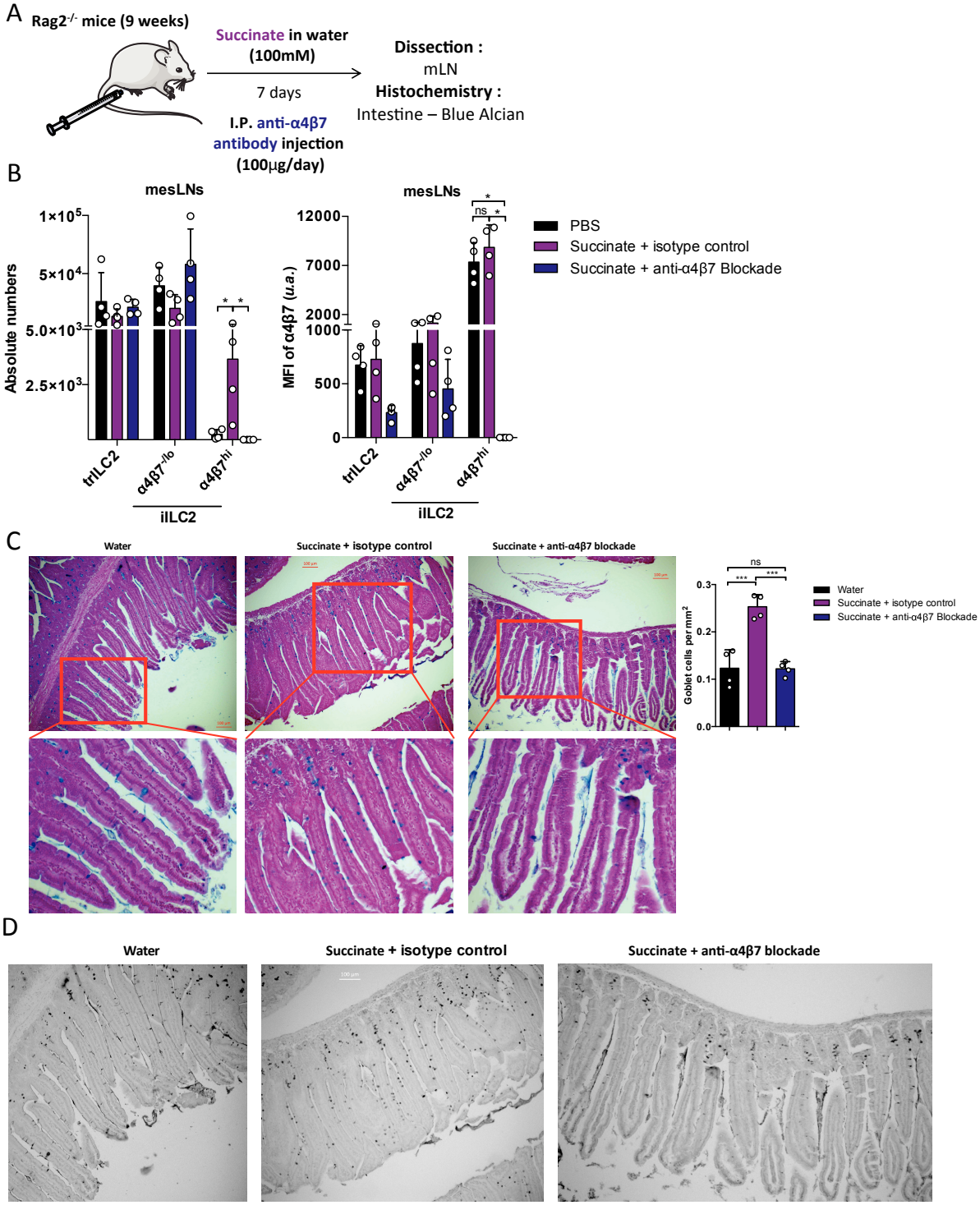

Figure 50 : Importance of ILC2 migration for mucus production in intestine. **A.** Scheme of succinate experiments with antibody blockade. Water or water supplemented with succinate (100mM) given 7 days to Rag2$^{-/-}$ mice with or without intra-peritoneal anti-α4β7-blockade antibody or isotype control injections (50µg/day). Intestine where then analysed by histology with blue alcian stainings and mesLNs by flow cytometry to check α4β7 blockade efficiency. **B.** Histogram representing absolute numbers and α4β7 level of expression by ILC2 subsets in mesLNs in the 3 different conditions (*each dot represents one mouse, representative of 2 individual experiments*). **C.** Images of intestinal histological cut from Water, Succinate + I.P. isotype control, or succinate + I.P. anti-α4β7-blockade antibody in Rag2$^{-/-}$ mice (Blue Alcian staining, blue dot represent goblet cells)(*left panels*). Histogram of goblet cells number per mm^2 in the 3 conditions (*right panel*) (*each dot represents one mouse, representative of 2 individual experiments*). and **D.** Levels of grey images of blue colour from histological cut of intestines from Water, Succinate + IP isotype control, or Succinate + IP anti-α4β7 blockade antibody injected mice (Blue Alcian staining, black dots represent goblet cells).

VI. Specific migrations of ILC2 subsets at different stages of *N.b.* infection

By using *N.b.* infection of mice, we were able to compare with alarmin stimulation and understand the important subsets to respond at early and late stages of infection. We compared the circulation capacities of the ILC2 subsets activated at lung and intestinal stages of *N.b.* infection. TD cannulations after 2 days and 10 days of infection show that activation concerns different ILC2 subsets using specific migratory mechanisms (**Figure 51A and 51B**). In case of early lung stage, the trILC2 and $\alpha4\beta7^{-/lo}$ iILC2 subsets are increased among circulating cells while it is both $\alpha4\beta7^{-/lo}$ and $\alpha4\beta7^{hi}$ iILC2 subsets that are increased during intestinal stage (**Figure 51A and B**). Then, d2 post-infection resemble lung inflammation with increased migration of $\alpha4\beta7^{-/lo}$ iILC2s while d10 show equivalent response from $\alpha4\beta7^{hi}$ iILC2s as for succinate, confirmation the good mimicking of that model for helminth infection (**Figure 47 and 51**). As observed for IL-25 and IL-33 treatment, but also during papain inflammation, ST2 upregulation is observed on the $\alpha4\beta7^{-/lo}$ TDL iILC2 2 and 10 days after infection (**Figure 51**).

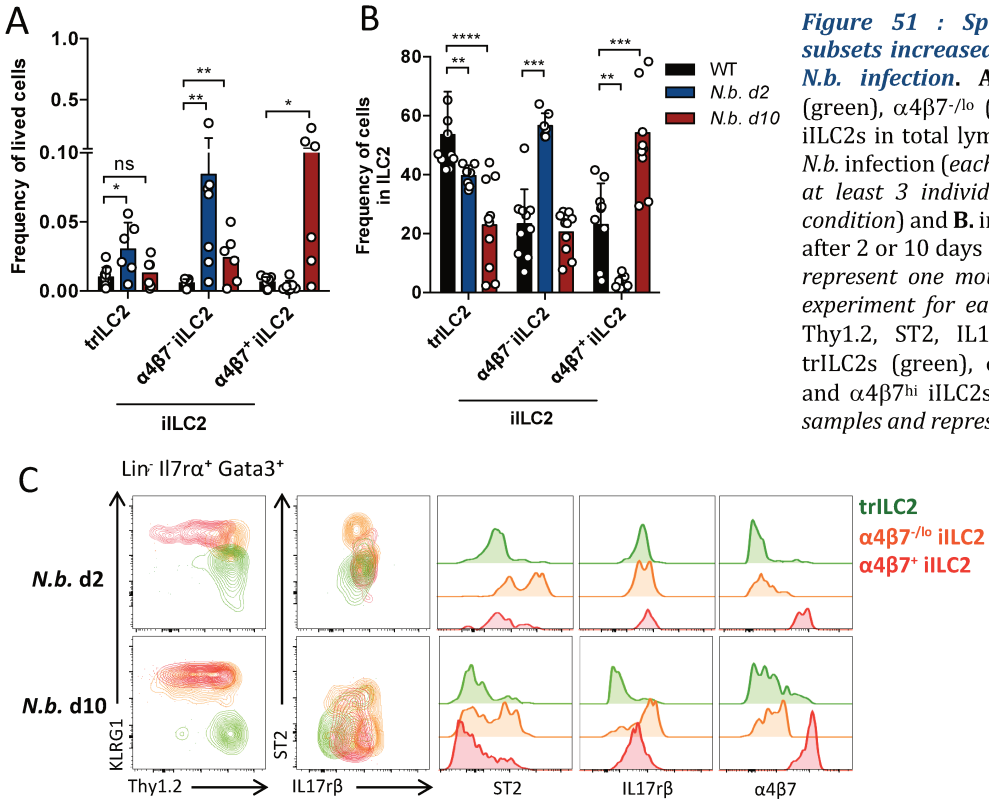

Figure 51 : Specific circulating ILC2 subsets increased depending on stage of N.b. infection. **A.** Frequency of trILC2 (green), $\alpha4\beta7^{-/lo}$ (orange) or $\alpha4\beta7^{hi}$ (red) iILC2s in total lymph after 2 or 10 days of *N.b.* infection (*each dot represent one mouse, at least 3 individual experiment for each condition*) and **B.** in $Gata3^{+}$ circulating ILC2s after 2 or 10 days of *N.b.* infection (*each dot represent one mouse, at least 3 individual experiment for each condition*). **C.** KLRG1, Thy1.2, ST2, IL17rβ phenotypes of TD trILC2s (green), $\alpha4\beta7^{-/lo}$ iILC2s (orange) and $\alpha4\beta7^{hi}$ iILC2s (red) (*concatenate of 3 samples and representative of all samples*).

In conclusion, the specific circulating subsets have importance at different stages of *N.b.* infection. Similar phenotypes with papain and succinate inflammation demonstrate that circulation of ILC2s is crucial to recover functional cells in the damaged tissue and contribute to local inflammation and stimulation of other actor of type-2 immune response, mediating worm expulsion from lung and intestine.

DISCUSSION

In immunology, the circulation is usually viewed as a process of surveillance by immune cells. Cells are ready to become functional following activation and specific signals drive the upregulation of their homing markers. These molecules will allow a rapid migration of specific subsets to seed the appropriate tissue restricting their number of turns in the hemolymphatic system. ILC2s are described as mostly long-lived resident cells, that have reached the tissues early in life with anticipatory functions (Ricardo-Gonzalez et al., 2018; Schneider et al., 2019). Using parabiosis, it was shown that in case of parasitic infections, ILC2 could circulate (Gasteiger et al., 2015; Huang et al., 2015, 2018). However, the stage of differentiation of the circulating ILC2 subsets, the molecular mechanisms used to migrate as well as ILC2 circulating functions are still unknown. It is also unclear whether ILC2 subsets could circulate in homeostatic conditions. Data on trafficking of ILC2 and their progenitors are needed to understand how the adult ILC2 peripheral turnover is carried out in both steady-state and inflammatory conditions. Adult wave contribution to the ILC2 turnover was analysed during adult life using fate-mapping mouse models (Schneider et al., 2019). They showed that about 10 to 20% of ILC2 from most tissues are able to derive from the adult wave within 4 weeks. Moreover, the turnover is very slow since it takes more than 30 weeks to replace 90% of ILC2 peripheral pools (Schneider et al., 2019). Hence, circulating ILC2s could either derive from proliferating cells that locally maintain, or from newly generated BM progenitors and/or from peripheral ILC2 recirculation (**Figure 52**). BM is the source of adult lymphoid progenitors and BM ILCPs can migrate to the intestine where they can differentiate into immature and probably to effector ILC subsets following stimulation (Bando et al., 2015; Possot et al., 2011). Committed BM ILC2Ps have been identified as a fraction contained among BM ILCPs that all express high levels of α4β7 and CCR9 (**Figure 52**)(Cherrier et al., 2018; Kim et al., 2015; Walker et al., 2019).

Our investigation of the circulating lymph composition revealed that ILC2s are circulating as a lymphoid population *via* the LN circuit to connect different tissues in homeostatic conditions (**Figure 55**). Interestingly, different ILC2 subsets circulate in the adult mice at very low frequencies in steady-state situations. We defined 3 circulating subtypes of ILC2s depending on KLRG1 and α4β7 expression levels. Phenotypic analyses determined that KLRG1/Thy1.2 ratio expression could distinguish inflammatory ILC2s (iILC2s) in the TD similarly to their first description as IL25 responsive lung KLRG1^{+} Thy1.2^{lo} iILC2s (Huang et al., 2015)(**Figure 55**). These iILC2 were defined as circulating cells that could be found in close contact to Lyve1^{+} lymphatics from the intestine in case of inflammation (Huang et al., 2018). TD iILC2s were also ST2^{-} but expressed only low levels of IL-17Rβ compared to their lung iILC2 counterparts. As receptors for cytokine may be differentially modulated depending on the tissue of residency, we decided to keep the iILC2 nomenclature for these KLRG1^{+} subsets. We further subdivided TD iILC2s into two populations depending on their respective levels of the surface integrin α4β7 (α4β7^{hi}

and $\alpha4\beta7^{-/lo}$ subsets). Comparative bioinformatic analyses of ILC2 phenotypes among tissues allowed to correlate $KLRG1^+$ circulating subsets to those present in the peripheral tissues known as already imprinted subsets (Ricardo-Gonzalez et al., 2018). We also showed and proved that while the $KLRG1^+$ $\alpha4\beta7^{hi}$ subset is restricted to the intestinal area, its $KLRG1^+$ $\alpha4\beta7^{-/lo}$ counterpart is dedicated to the lung and adipose tissues. Devoid of β7 chain expression, $KLRG1^+$ $\alpha4\beta7^{-/lo}$ ILC2 maintained the α4 chain expression and formed a surface α4β1 integrin complex instead (**Figure 55**).

The third remaining TD $KLRG1^-$ $Thy1.2^{hi}$ ILC2 subset resembles the previously defined lung resident nILC2 based on the KLRG1/Thy1.2 expression (Huang et al., 2015). However, this TD subset was not called nILC2 as it was found to be the most frequent circulating ILC2 subset in the steady-state and as it expressed high levels of IL-17Rβ. This third circulating subset was named transitional ILC2 (trILC2) instead (**Figure 55**). Devoid of α4 and αv integrin expression, this subset contains a large $CD62L^+$ recirculating population. The phenograph related trILC2 to $ST2^+$ $ICOS^+$ BM-derived ILC2P and to ILC2 subsets from LN (**Figure 52**). trILC2 was also found in small frequencies in all peripheral tissues studied LP, lung and ATs.

To prove that iILC2 subsets were specifically targeted for different organs, we performed TD transfer experiments and specifically blocked the integrins on the circulating ILC2s. We demonstrated the essential role of α4β7 as an ILC2 specific gut homing molecule whereas α4β1 was essential for trafficking toward AT and lung (**Figure 55**).

To understand whether specific signals could drive ILC2 subsets to change their migratory circuit from the steady state context, we first used simple models of i.p. injections of IL-33 or IL-25. We observed that the migratory capacities of TD ILC2 subsets were mostly conserved after inducing inflammation in mice (**Figure 55**Figure 56). It was the nature and the location of the stimulus that was specifically promoting the enrichment of the "integrin-targeted" subset of ILC2 over the others. Indeed, IL-25 and IL-33 i.p. stimulations only mildly changed the phenotype of TD iILC2 subsets with a common downregulation of Thy1.2 and a slight increase of the respective cytokine receptors. It appears that IL25 or IL-33 stimulation does not really change the expression of iILC2 migratory molecules. α4β7 levels only increased for the $\alpha4\beta7^+$ iILC2 subset after IL-33 stimulation and consequently was reinforcing its intestinal homing ability (Figure 56). On the contrary, type 2 stimulations decreased the surface levels of α4β7 for trILC2 with a clear-cut effect of IL-25 in the abrogation of the α4β7 expression. This result in avoiding this subset to reach the intestinal area and to be preferentially addressed to other tissues. This trILC2 is considered as the most immature circulating ILC2 subset, enriched in BM ILC2P that left the BM as $\alpha4\beta7^+$ $Icos^+$ $IL\text{-}18R1^{hi}$ ILCP and are maintained as an immature precursor population in the periphery. As we found this subset back in the BM after

photoconversion of mesLN from kaede mice. Moreover, we demonstrated that BM ILC2 populations such as ILC2P could upregulate α4β7 at the surface when IL-33 is added to the culture media (Figure 56). Hence, it appears trILC2 are mostly coming back from the periphery as they are $\alpha4\beta7^{lo}$ after IL-33 stimulation. However, we showed *in vitro* that IL-33 could directly upregulate the α4β7 integrin at the surface of BM ILC2P to promote their homing to the intestinal area. Surprisingly, systemic IL-25 did not trigger frequency differences of ILC2 subsets in circulation.

Following intraperitoneal IL-33 treatment, the two circulating iILC2s subsets were significantly increased in frequency. However, they behaved differently to the stimulation. The increase of $\alpha4\beta7^{hi}$ iILC2 frequency was due to an active proliferation in circulation, whereas unable to divide the $\alpha4\beta7^{-/lo}$ iILC2s were only accumulating (Figure 56). However, $\alpha4\beta7^{hi}$ iILC2 were unable to be functional while $\alpha4\beta7^{-/lo}$ iILC2 showed an increased ability to secrete type-2 cytokines demonstrating that iILC2 have to choose between proliferation and secretive functions. Then, we demonstrated by specifically transferring individual iILC2 subsets that the increased frequency of $\alpha4\beta7^{-/lo}$ iILC2s resulted from the $\alpha4\beta7^{hi}$ iILC2 differentiation in the intestine. Indeed, $\alpha4\beta7^{hi}$ iILC2 were directly homing to the intestine and after several rounds of division, decreased their surface levels of α4β7 to become effector intestinal iILC2s that could further recirculate through the hemolymphatic system (Figure 56).

We used inflammatory models that stimulate the release of a complex mix of Th2 alarmins. In these contexts, homing iILC2s were strong producers of cytokines demonstrating their functional importance for the tissue local response. Tissue ILC2 subsets resulting from migratory iILC2 were IL-5, IL-13 and Areg triple producers in lungs during papain challenges and also in the intestine of succinate treated mice (Figure 56). Moreover, blockade of their specific circulation under inflammation conditions demonstrated that ILC2 trafficking is crucial to recover enough functional cells in the damaged tissues. α4β1 blockade abrogated the accumulation of both iILC2 and nILC2 subsets in the lungs of papain challenged mice in agreement with the previous data showed by Huang et al. that iILC2 are precursors of lung nILC2 and that they differentiate in situ (Huang et al., 2015). The strong decrease of IL-5 production in this blockade context resulted in an absence of eosinophil recruitment (Figure 56). Interestingly, α4β7 blockade limited the specific recruitment of secretor iILC2s in the same papain inflammation, whereas it totally blocked iILC2 accumulation in intestine of succinate mice, with inactivity of goblet cells to secrete mucus. This observation confirmed that iILC2 reaching the intestine as $\alpha4\beta7^{hi}$ subsets are the precursors of lung $\alpha4\beta1^{+}$ iILC2 as previously suggested by our blockade model in IL-33 injected mice (Figure 56). Moreover, even if iILC2 are thought to differentiate into resident $ST2^{+}$ nILC2, the remaining trILC2 may be a good precursor for that specific subset either in the medLN or the lung itself.

BM ILC2P fractions and TD $\alpha4\beta7^{hi}$ iILC2s upregulated the $\alpha4\beta7$ in intestinal inflammatory succinate fed mice or after IL33 injections confirming that cells (iILC2 or ILC2P) migrate to the intestine where they can further differentiate into $\alpha4\beta7^{-}$ iILC2s secretor cells, becoming either resident or re-circulating cells depending on the presence of other co-stimulatory signals. Then, intestine would play a role of privileged site for ILC differentiation (ILC2P) and maturation (iILC2)(Figure 56). In case of more physiological inflammation (allergen and metabolite stimulations or helminth infection), the presence of continuous co-stimulatory signals is also probably acting on survival and maturation into different subsets.

We explained here that iILC2s have already tissue-imprinted functions linked to their migratory specificities whereas circulating trILC2 have the potential of a typical ILC2P monitoring any possible tissue anomalies to further differentiate in situ in any type of ILC2 subset (**Figure 52**).

N. b. infection triggers similar modifications of circulating ILC2 subset frequencies depending on the kinetic of the infection. 2 days post *N.b.* infection is restricted to the lungs without any passage of *larvae* to the intestine. TD subsets show an increase of $\alpha4\beta7^{-/lo}$ iILC2s in circulation as for the papain model. However, the intestinal stage at 10 days post-infections showed increased circulation to intestine with an increased frequency of $\alpha4\beta7^{hi}$ iILC2s in circulation.

Here we discuss the relevance of our findings in regards to the current knowledge and the questions that this study raises with a personal point of view.

Differences nILC2/KLRG1^{-} ILC2s : regulation of ILC2s

Two distinct populations are described in lung following *N.b.* infection (Huang and Paul, 2016; Huang et al., 2015), an iILC2 subset, which secrete IL-5/13 and Areg (**Figure 48**), and a nILC2, only producing Areg but not IL-5 and IL-13 (**Figure 48**). This nILC2 subset resembles the circulating KLRG1^{-} trILC2 population. The intestinal Areg^{-} KLRG1^{-} ILC2 subset is most likely immature ILC2s. The trILC2 subset may receive different signals than nILC2 due to different location in the lung. In close contact with the epithelium (Molofsky et al., 2015), nILC2 may originate from active iILC2s receiving inhibitory signals by KLRG1/E-cadherin interactions to regulate them, inducing KLRG1 downregulation (**Figure 52**). This KLRG1/E-cadherin inhibition of ILC2s was already described in a plate-bound assay that showed diminished production of IL-13 and IL-5, and decreased Areg and Gata3 expression (Salimi et al., 2013). It appears seducing to correlate position of ILC2s among the tissue to their functions. Areg would be produced next to the lung epithelium by nILC2s whereas IL-5/13 by migrating cells close to the vessels of the tissue where they accumulate and can increase the myeloid attraction/activation with a larger propagation of cytokines in the micro-environment (*e.g* : induce mucus production by goblet cells at different localisations)(Molofsky et al., 2015). During resolution phase, long-lived accumulated iILC2s could then participate to tissue repair as Areg^{+} nILC2s following this inhibition. This suggest an important role for ILC2 localisation to enhance their functions, but would also characterise ILC2 migration and chemokine/cytokine receptors as important mediators of ILC2 functional regulation to avoid over-production of type-2 cytokines as well as tissue damages.

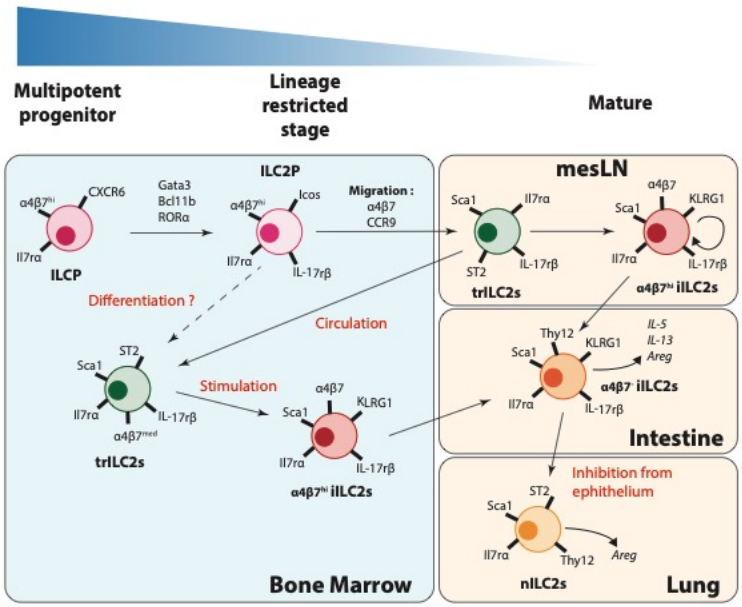

Figure 52 : nILC2s and trILC2s are different ILC2 stages. From ILC2P, all ILC2 stages are generated. Differentiation into trILC2s occur in periphery (mesLN/LP), but it is still unknown if local differentiation exist. Then trILC2s will generate proliferative α4β7hi iILC2s. In intestine, following migration, they give rise to local active ILC2s and to recirculating α4β7-/lo iILC2s. In the lungs, they are secreting type-2 cytokines, and may receive inhibitory signals, inducing their last step of differentiation as nILC2s.

MadCAM1 as central receptor for ILC2 migration

Neonatal and foetal *vs* adult MadCAM1 expression

Contrary to the adult, MadCAM1 is expressed by several tissues during foetal and neonatal life, including intestine, thymus, skin and all LNs (Iizuka et al., 2000; Salmi et al., 2001). trKLRG1$^-$ ILC2s are absent in FL but present in the BM at homeostasis. We can then postulate that early colonisation of tissues by ILC2s, or more generally by all ILC subsets generated from FL $\alpha4\beta7^+$ ILCP, is taking place early in life using the $\alpha4\beta7$/MadCAM1 axis considering that ILC populations have a long-term maintenance in peripheral tissues due to high survival potential. It could explain the slow turn-over of ILC2 and very gradual replacement from BM progenitors, with a late accumulation of trILC2 in BM from peripheral tissues. Then, FL $\alpha4\beta7^+$ ILCP can migrate into all tissues, waiting for specific signals to differentiate into ILC1s, ILC2s or ILC3s (Bando et al., 2015; Possot et al., 2011). This early generation of ILC2s in periphery can explain the heterogeneity of ILC2 subsets, with specific adaptation to activating signals from the different tissues, as for example IL-18 on dILC2s in skin or IL-25 in the intestine. This concept is in accordance with early imprinting of ILC2s for specific tissues, *via* an early colonisation of the tissues (Ricardo-Gonzalez et al., 2018; Schneider et al., 2019).

Pancreas migration

ILC2s are found to play a major role in pancreas, where they promote insulin production by β-cells of pancreatic islets (Dalmas et al., 2017). Similarly to intestinal migration, the pancreas could be early colonized by ILC2 and being replaced in a continuous fashion during adult life as the adult pancreatic endothelial cells are constitutively expressing MadCAM1 (Hanninen et al., 1998). $\alpha4\beta7^{hi}$ iILC2s circulate at low frequency at homeostasis, and only 1-2% of ILC2s are found in the pancreas. However, the accumulation of ILC2s inside pancreatic islets following IL-33 treatment was observed, and beneficial- or detrimental-role of their accumulation in the pancreas, both at homeostasis and during inflammation, could be important (Dalmas et al., 2017). Since $\alpha4\beta7^{hi}$ iILC2s are highly increased in circulation following IL-33, the specific functional role of this iILC2 subset in pancreas following inflammation may be deciphered to check whether resident versus inflammatory subsets have a similar preferential subdivision, functions and locations as we showed here in intestine and lungs.

Liver inflammation and MadCAM1

Peripheral tissues increased the MadCAM1 expression on their endothelial cells following inflammation. Liver is a good example as MadCAM1 is expressed during chronic inflammation of patients with primary sclerosing cholangitis (Grant et al., 2001). Type-2 fibrosis is important in the etiology of this disease and could be related to the increased

migration of $\alpha4\beta7^+$ immune cells, including $\alpha4\beta7^+$ iILC2s. Then, terminal differentiation of ILC2s will induce long-lived secreting ILC2s that will adapt to the liver environment and participate to the induction of chronic inflammation.

Skin migration

Another important tissue with a different resident subset of ILC2s that could be stimulated is the skin. Dermal ILC2s showed a different ontogeny as this subset is not derived from the neonatal wave in Arg1 fate mapping experiments (Schneider et al., 2019). A different mechanism for colonisation of skin could then explain the difference of phenotype in this population, and induce a different turnover of ILC2 from the skin. We did not check for skin ILC2 migration, as it would be difficult to detect any accumulation of ILC2s without a localised inflammation allowing migration to a small piece of skin. However, accumulation of IL-17rβ^+ KLRG1$^+$ ILC2s, absent at homeostasis, in the skin of atopic dermatitis (Kim et al., 2013; Salimi et al., 2013) correlate with the phenotype of migrating ILC2 subsets in the lungs and ATs. This skin subset might be generated in intestine and need for a certain co-stimulatory signal to be able to migrate to the skin. These newly recruited ILC2s are responding to different signals than the one induced locally : IL-18 for dILC2s and IL-33 or TSLP for the new accumulated ILC2s.

Importance of stimulatory signals

We can postulate that local signals, which are different between tissues, trigger variable activation of ILC2s. For example, papain *vs* succinate stimulations are inducing production of different alarmins and co-stimulatory signals to induce immune system activation. Indeed, stimulation of the intestinal ILC2s is increasing their ability to replenish LP and activate ILC2s by local high production of IL-25, IL-33 and specific local co-stimulatory signals as TSLP, neuromodulators … Conversely, lung inflammation could lead to similar local activation, and in parallel, a systemic dissemination of low quantities of signals (hormones, cytokines, chemokines, …) reaching the intestinal environment inducing migration of lung-targeted $\alpha4\beta7^{-/lo}$ iILC2 subset. These signals may contain Nmur (derived from nervous system) that participates to activate lung ILC2s (Klose et al., 2017), and would then play a paracrine signal in the intestinal *mucosa* to orient activation and migratory functions of ILC2 subsets. Hence, ILC2s could be considered as having anticipatory functions since their specific activating signals, direct their migration with an imprinting activity in these different tissues (Ricardo-Gonzalez et al., 2018).

It is then true but incomplete to describe an intestinal subset migrating to the lung, as cells are first migrating to the intestine before adapting phenotype and recirculating to home to the lung (Huang et al., 2018).

Redundancy between IL-25/IL-33

One other point to better understand differences between human and mouse ILC2s concerns IL-25 as it was not studied in human. This cytokine is localized to intestinal mucosa as secreted by tuft cells. IL-25 specifically activate intestinal ILC2s, allowing the local control of their secretory functions

Studying ILC2 migration in mice with increased type-2 immunity at homeostasis, as in BALB/c mice, in humanized mice or in human lymph could allow to have different results in the control of ILC2 migration by different types of stimulation. It would be an important way to understand the potential differences in ILC2 turnover between human and mice and transpose our data and model to a human level.

RA

First studies showed that α4β7 expression by ILC1 and ILC3 is induced by RA thanks to a stimulation in the mesLNs (Kim et al., 2015). However, the RA was not demonstrated as efficient for ILC2. Immature BM KLRG1$^-$ ILC2s are receiving a specific signal, different form RA, mediated by IL-33 to upregulate α4β7 (**Figure 41**). They will then be able to migrate to intestine and adapt their phenotype to secretor cells. Mice lacking RA showed increased and dysregulated ILC2 proliferation and cytokine production (Spencer et al., 2014). As a matter of fact, RA balance the type of ILC response that occur in intestinal mucosa at any moment, allowing tight control of type-1/3 *vs* type-2 responses on innate cells.

RA induces type-2 cytokine production and expression of the gut-homing integrin α4β7 on human ILC2s (**Figure 10**)(Ruiter et al., 2015). IL-25 has not yet described as important for ILC2 activation in humans, and it is suggested that type-2 immunity may be beneficial for human at homeostasis. More precisely, in mice, IL-10 is considered to be a Th2 cytokine, when both Th1 and Th2 cells can make IL-10 in humans (Del Prete et al., 1993). Then, human immune cells are more prompt to produce type-2 cytokines in comparison with mice. These differences correlate with a different regulation of ILC2 activation and then migration in human compared to mice, due to different immune status. Human ILC2s are then tightly but less controlled than mice ILC2s, and a continuous stimulation of intestinal homing by RA is probably happening in human, at higher frequency compared to mice.

Notch2

Notch2 signal has been shown as important for ILC2 development during embryogenesis promoting the proliferation of ILC2Ps in the fetal liver (Chea et al., 2016a). IL-33 is described as inhibiting the Notch signalling pathway in intestinal the case of the epithelial cells development (Mahapatro et al., 2016). Data from my group on the role of Notch2 in peripheral control of ILCs show increased ILC2 activation and migration in IL-7rα^{cre} Notch2$^{Fl/Fl}$ mice, with specific increase of α4β7^{+} ILC2s in mesLNs, levels of α4β7 expression were similar to those promoted by an IL-33 stimulation (**Figure 53**). This is suggesting a role of Notch2 pathway in the peripheral regulation of ILC2s, like balancing IL-33 activation and allowing ILC2 activation. It remains unclear how it links to IL-25, but it is possible that a balance between IL-25, IL-33 and Notch signalling could regulate the type of ILC2 activation and migration through the hemolymphatic system, as they differentially impact ILC2 trafficking. In our data, LP ILC2s are resident cells and possess an activated phenotype in IL-7rα^{cre} Notch2$^{Fl/Fl}$ compared to control mice (**Figure 53**). Notch2 signals could regulate a control point of the passage from ILC2P to trILC2 such as generating a privileged activation of ILC2s to either become resident in intestinal mucosa or migrate to lungs, ATs, BM or other tissues. This will underline the importance of specific co-stimulatory signals to mediate intestinal residency by accumulation of new incoming ILC2 and recirculation to replenish lungs, ATs or skin. They also accumulate in the BM as trILC2s and iILC2s and Notch signalling seems important for inhibition of cytokinic production by ILC2s following helminth infection in intestine.

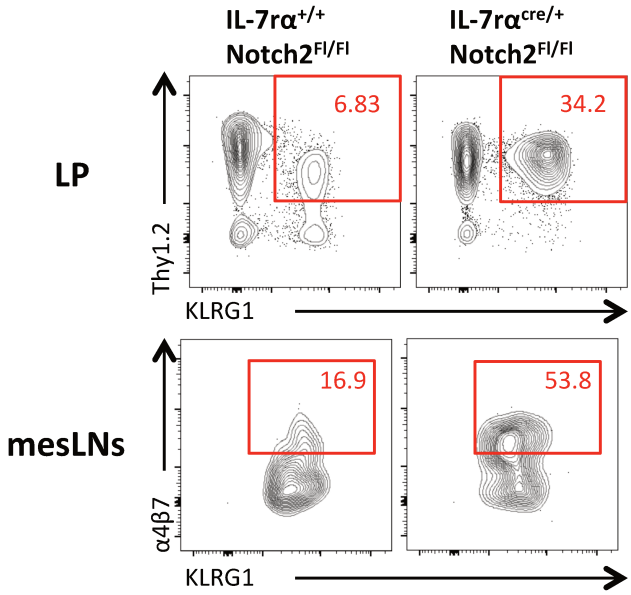

Figure 53 : ILC2s have activated phenotypes in Notch2 deleted mice. Analyses of LP and mesLNs ILC2s deficient for Notch2. In this model, other lymphocytes are shown as poorly affected by Notch2 depletion, while ILC2s have severe activated phenotype.

Epigenetic, imprinting and memory

Imprinting of circulatory ILC2s was described before colonizing tissues as a link between a specific signal of activation received by ILC2s and ILC2 colonisation and functions in a certain tissue. In our context, it will be the migration to a specific tissue or/and long-lived effector cells. Preliminary data showed importance of epigenetic marks on histone, mediated by Kdm6b enzyme, a histone demethylase, to allow the final maturation and activation of ILC2s. We showed that BM, AT and lung ILC2s have

increased Kdm6b expression. It allows demethylation of trimethyl-H3K27, that we show as taking place following IL-33 activation of BM immature KLRG1^{-} ILC2s (**Figure 54A**). Without possibility to modify epigenetic marks in IL-7rα^{cre} Kdm6b$^{Fl/Fl}$ mice, a strong diminution of ILC2s is observed in ATs, lungs and peripheral tissues were active ILC2s should be detected (**Figure 54B**). It would suggest that following activation, ILC2s proceed to epigenetic modifications to mark a probable irreversible activated stage, and this "imprinting" will allow long-lived secretor phenotype of ILC2s in tissues, with a survival for weeks and coming back to normal in months. It remains unclear whether this "imprinting" is not an essential part of memory ILC2 generation following several stimulations of the same cell, and studying its role in ILC2 circulation and migration to specific tissue would be of great interest.

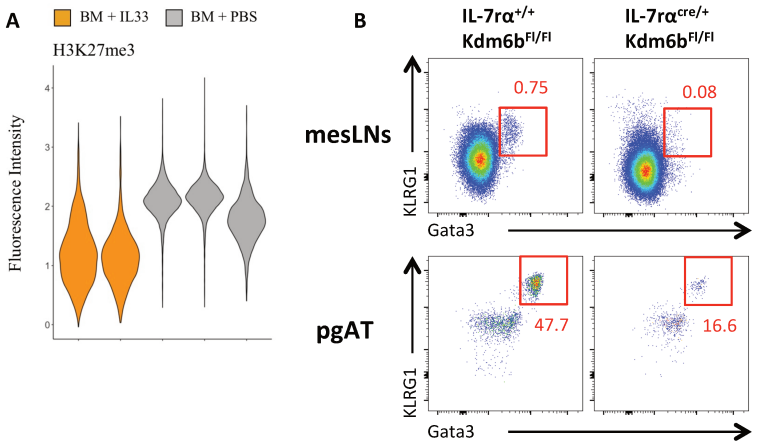

Figure 54 : ILC2 activation induce important epigenetic marks. ILC2s depleted for Kdm6b are not detected anymore in mesLNs and peripheral tissues as pgAT. Further investigation may characterize the role of epigenetic marks for peripheral ILC2s.

Mobilisation of ILC2s and treatment to control migration

To have a possible therapeutic action on ILC2 functions, we need to completely understand the ILC2 turnover and processes of activation is important before expecting any type of treatment involving their specific activation or inhibition. Over activation of ILC2 induces severe diseases as asthma, allergies or fibrosis driven by type-2 chronic inflammations. ILC2s are also important in the development of diabetes and obesity, as important role at homeostasis in balancing the macrophage orientation and immune responses has been showed as crucial in ATs and pancreas (Dalmas et al., 2017; Molofsky et al., 2015). We showed that specific ILC2 activation allow their migration toward different tissues.

ILC2s increase in circulation and accumulate in several tissues following stimulation or during the inflammatory processes. Mice show increased ILC2s accumulation in ATs following helminth infection, without any type of stimulation or inflammation from these ATs (Molofsky et al., 2015). During my PhD, we used integrin treatment to inhibit the accumulation of ILC2s and their specific functions, such as eosinophil attraction and goblet cells stimulation, respectively decreased in papain and succinate induced inflammation. These treatments could allow the characterization of specific signals important for ILC2 tissue accumulation.

For instance, cumulating different treatments could be used on allergic or obese mice to reverse diseases. For example, we can imagine the use of IL-33 treatment, continuously or at several time points to have prime/boost effect, will increase ILC2 turnover. Cumulated together with integrin blockade antibody treatment would allow manipulation of homing to the lungs or ATs and avoid over-accumulation of ILC2s after a certain time of treatment. During development of diabetes or obesity, IFNγ has been showed as balancing the immune response by decreasing IL-33 effect on ILC2 functions in homeostasis of pancreas and AT (Dalmas et al., 2017; Molofsky et al., 2015). A combination of IL-33 plus anti-IFNγ treatments could show promising results to recover ATs homeostasis and block the evolution of the diseases by accumulation of ILC2s. In pancreas, increasing or reducing ILC2 accumulation would probably trigger important signals to macrophages, major mediator of insulin secretion at homeostasis and of insulin resistance in advanced diabetes. In the lung, blocking ILC2s accumulation would allow a decrease of the increased type-2 response but not damage the repair process that us provided by local resident ILC2s. Finally, treatment for intestinal inflammation, using IL-33 with anti-β1 treatment can limit side effects due to plasticity of new accumulated intestinal ILC2 toward α4β1 migratory iILC2s, as development of skin or lung allergies, and allow specific step of ILC2s accumulation. Short treatment with α4β7-blockade antibody will also limit liver and intestinal chronic inflammation, and probably promote a timeframe for tissue-repair and a better control of the immune response.

From our studies, we now understand how to modulate ILC2 functions thanks to modulation of their circulatory features and the specific functions of the circulatory subsets. Our anti-integrin based treatments are more specific than FTY720, used to block all circulation during *N.b.* infection (Huang et al., 2018). Anti-α4β7 and anti-α4β1 antibodies are already used as treatments for human diseases, as chronic intestinal inflammations and multiple sclerosis (Balcer et al., 2007; Sandborn et al., 2013). As anti-α4β1 antibody induce sever secondary effects in long term treatments of multiple sclerosis, α4β1 blockade should be carefully controlled, used in short term treatments and anti-α4β7 antibodies may be privileged.

N.b. infection

Finally, our data are in line with the more recent studies on the role of ILC2s during *N.b.* infection. Our studies bring new data that evidence mechanisms of circulation. ILC2s participate to lung response against *N.b.* early during infection by secretion of IL-13 and IL-9 in lungs (Nussbaum et al., 2013; Price et al., 2010; Turner et al., 2013). At homeostasis, resident lung ILC2s are not expressing IL-13 (Nussbaum et al., 2013), and we show that recruited ILC2s generate an important source of type-2 cytokines in the lung and correlate with eosinophil recruitment (**Figure 48**).

Resident ILC2 are also increasing due to proliferation in the tissue and in the draining mediastinal LNs (medLNs) few days after papain and *N.b.* infection. In papain induced inflammation, we showed that β1 blockade abolished both nILC2 and iILC2 pulmonary accumulation, whereas β7 blockade only impacted iILC2 accumulation, confirming that $\alpha4\beta7^{-/lo}$ iILC2 arriving to the lungs are derived from the $\alpha4\beta7^{hi}$ iILC2 subset that has first reached the intestine. Accumulating nILC2s are derived from iILC2s, but could also come from local proliferation of $Areg^{-}$ nILC2s in the lungs and medLNs, where they proliferate during *N.b.* infection and participate as an important source of nILC2s. Importantly, they would also need α4β1 integrin to circulate through the hemolymphatic system (**Figure 51**) and finally accumulate in lungs.

Important role of circulating iILC2s was shown in mice with the FTY720 blocking molecule (Huang et al., 2018). Infected mice treated with FTY720 showed lower survival, and after iILC2 transfer, good helminth expulsion was recovered. The exact mechanism of iILC2s role was not described, and our data give complementary information as these iILC2s mixture of $\alpha4\beta7^{-/lo}$ and $\alpha4\beta7^{hi}$ subsets give airway and intestinal protection against parasites.

Their high potential as migrating cells also explain the low passage between parabiotic mice (Gasteiger et al., 2015), as a combination of low frequency of circulating ILC2s and inflamed vasculature between mice is probably inducing extravasation of cells before they reach the parabiont. However, following *N.b.* infection, we suggest that differentiation of donor trILC2s in the host mice and the high increase of circulating ILC2s gives higher probability for ILC2s to reach and accumulate in the lungs of not infected parabiont, as already showed (Gasteiger et al., 2015). Similarly, high ILC2 turnover in peripheral tissues with cells from perinatal or adult origins was shown following *N.b.* infection, with an equivalent participation of both ILC2 pools (Schneider et al., 2019). The long-lived perinatal fate mapped ILC2s are then residing in peripheral tissues, as their progenitor colonised them early in life, and this is confirming our concept describing peripheral origin of ILC2 turnover in adult during type-2 responses.

It is important to underline that ILC2s are not the only innate population that can be important in our model, as mast cells show similar type-secretor profile and use same mechanism to migrate through hemolymphatic system and colonise intestine, especially after *N.b.* infection (Guy-Grand et al., 1984). However, their contribution seems poor compared to ILC2s that are secreting 3 to 4 fold more IL-13 than mast cells during infection (Neill et al., 2010).

Finally, we are now performing anti-integrin antibody blockade during *N.b.* infection in $Rag2^{-/-}$ mice. We expect an absence of ILC2 accumulation both in lungs and intestine from infected mice. This will prove the implication of circulation on ILC2 functions during a response to parasitic infections. Also, we will be able to confirm the

potential role of ILC2 in parasite clearance from the lung early on. The role of migrating ILC2s has recently been showed as essential for mucus production in lungs of helminth infected mice. Here, circulating IL-13^{+} iILC2s from intestinal origin were sufficient to restore mucosal production in lungs of immunodeficient mice (Campbell et al., 2019). We will then prove the crucial role of integrin during the migration of ILC2s and the intestine as a central organ for ILC2 maturation of functions. It will complete evidences showing that intestinal activation of ILC2s by *N.b.* infection cross protects lungs against *Trichinella spiralis* infection by induction of goblet cell hyperplasia in lungs (Campbell et al., 2019). It will decipher the importance of ILC2 subsets accumulation at early and late time of infection for *N.b.* clearance and development of tissue regeneration processes. One interesting possibility would be the generation of ILC2 memory that could be important in case of secondary infections. For example, comparison of secondary infection of previously infected mice and infected mice treated with integrin blockade of ILC2 and an anti-parasitic drug will allow comparison of ILC2 responses. In one case, ILC2 may keep a memory of the first infection, when naïve ILC2s from antibody treated mice will act as in a primary contact with the helminth. The already primed ILC2s could act faster and stronger due to the first ILC2 activation and accumulation in the lungs and intestine, and would act as memory ILC2s generated from helminth infection. In these conditions, it would be of great interest to study the circulation of ILC2 from both infected conditions, and we expect an increased circulation of activated ILC2s.

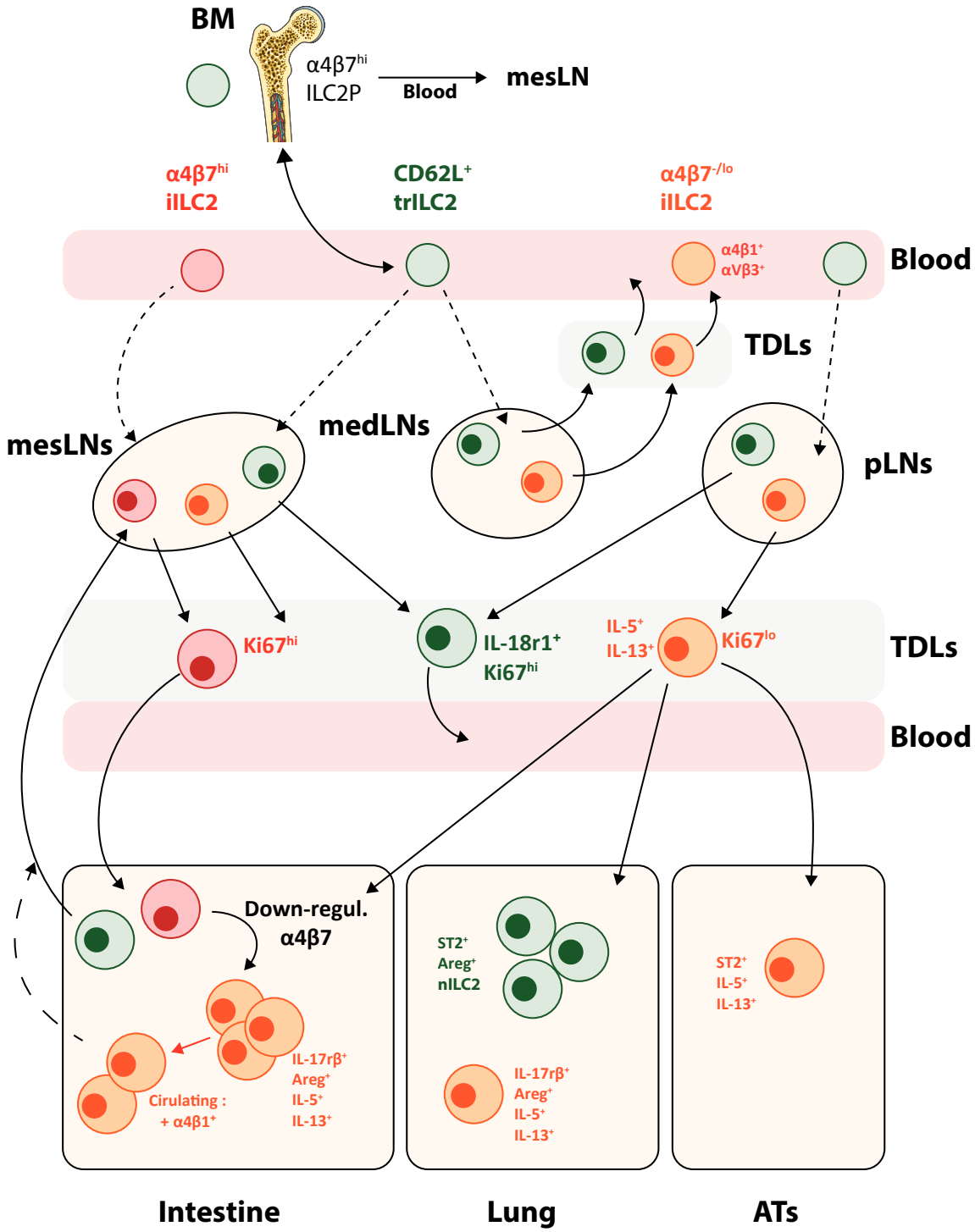

Figure 55 : Scheme of homeostatic turnover of ILC2s. In the hemolymphatic, we described 3 circulating subtypes of ILC2s depending on KLRG1 and α4β7 expression levels. KLRG1^{+} α4β7^{hi} subset is restricted to the intestinal area, its KLRG1^{+} α4β7$^{-/lo}$ counterpart is dedicated to the lung and adipose tissues and trILC2 contains a large CD62L^{+} recirculating population. trILC2s are present in LNs and BM. α4β7^{hi} ILC2s can differentiate in mesLNs and LP and generate α4β7$^{-/lo}$ subset that either secrete locally or can migrate to lungs and ATs as secretor cells.

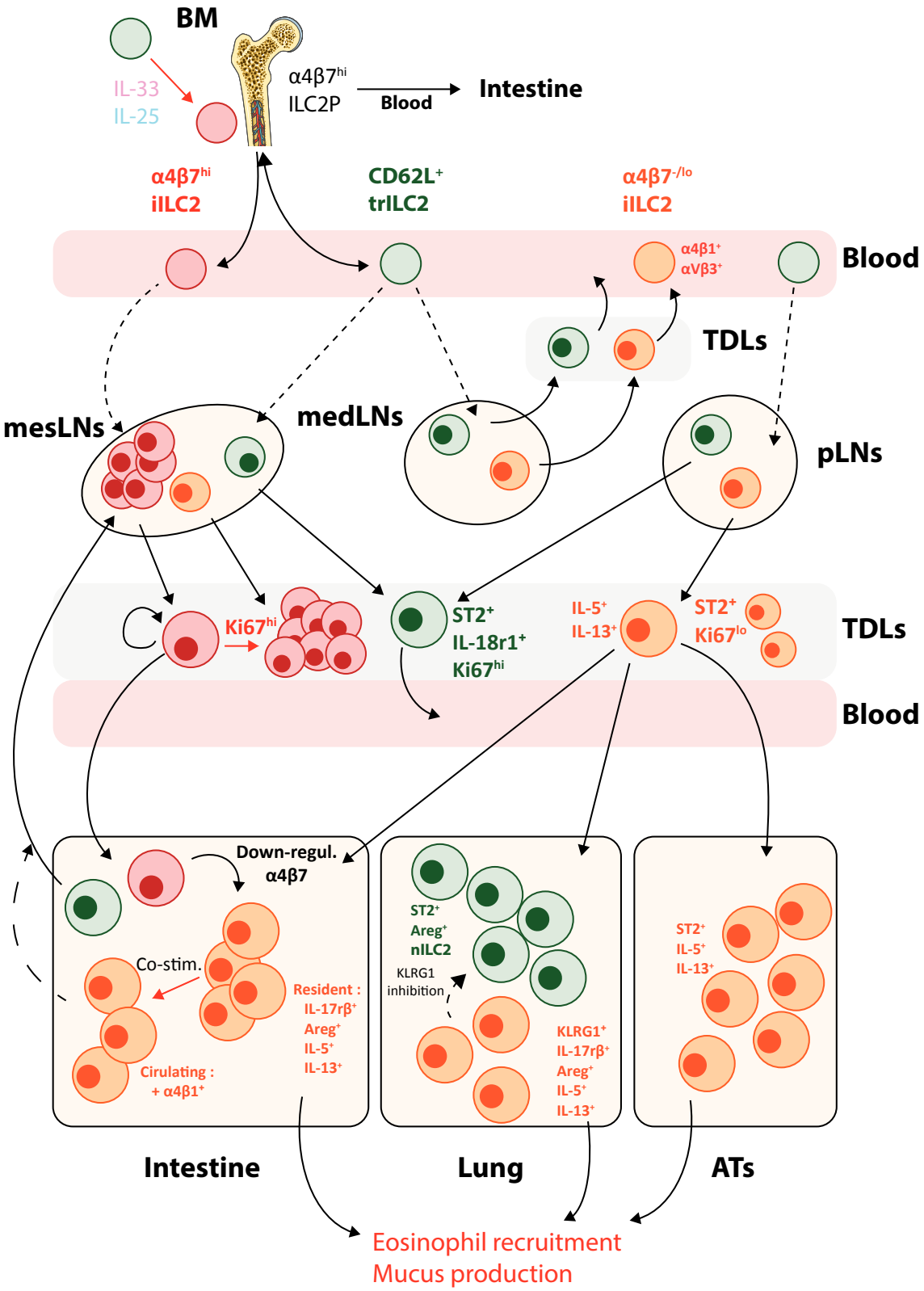

Figure 56 : Scheme of ILC2 activation and turnover during inflammation. In the hemolymphatic, we the 3 circulating subtypes of ILC2s described at homeostasis keep similar migratory phenotypes after stimulations. However, iILC2s are increasing in circulation. α4β7^{hi} subset is proliferating in mesLNs and TDL, and more α4β7$^{-/lo}$ secretor ILC2s are migrating to lungs and pgATs. trILC2s can generate α4β7^{hi} subset following stimulation. α4β7^{hi} ILC2s can differentiate in mesLNs and LP, where they downregulate α4β7 during division. The generated α4β7$^{-/lo}$ subset secrete locally type-2 cytokines or can migrate to lungs and ATs. Locally, they participate to type-2 responses by increasing mucus production and eosinophils recruitment. Finally, lung iILC2s entering tissues may receive inhibitory signals and generate local nILC2s, which are Areg producers or proliferative resident cells participating to tissue regeneration during tissue regeneration phase.

CONCLUSION

ILC circulation as a system

As I obtained a master degree with a mention in system biology, I would like to open the view of ILC2 circulation as an integrated system. A complicated system that starts early in life with layered processes allowing permanent renewal and control of ILC2 functions. This system is based on complicated levels of control, with importance of local micro environments dependant on ILC2 niches in periphery and on migratory stages to perform imprinting of specific subsets. The circulation is central to understand ILC2 turnover in peripheral tissues, and need a complete characterization of the different stages and subsets of for activation and maintenance as resident cells.

As ILC2 pools find in adult life starts in foetal life, competition with other precursors or immune populations for their own surveillance and turnover. It is a key momentum that starts our system. ILC2Ps are able to differentiate to the different pools of ILC2s in peripheral tissues, with the intestine as an important tissue for ILC differentiation and imprinting. We showed that recirculation will be confined to the intestinal barrier.

Then, a complex migratory system take place for ILC2 functions. We are the first one to show that 3 different subsets are circulating in hemolymphatic system at homeostasis and under inflammation. Through different stages, ILC2s differentiate and get activated to participate to ILC2 turnover. Following activation, they keep similar trafficking behaviours. Circulating ILC2s largely and rapidly expand, but also respond differently to *stimuli* for renewal of peripheral populations. Importantly, migrating ILC2s are the main ILC2 population secreting type-2 cytokines after migration. Such a number of stages to generate activated ILC2s allow tight control of their functions. We are first to describe links between these subsets to generate fully activated ILC2s. During helminth infection, a large number of newly generated ILC2s will then be able to initiate type-2 immune response. Then, a contraction phase comprising inhibition and slow diminution of these new ILC2s avoid any abnormal activation and type-2 chronical diseases. More details of ILC2 activating signals important for specific migration are still needed to understand specific behaviours. Computational analysis would allow generation of a complete model for ILC2 turnover in the different tissues, predicting the effect of specific activatory signals on a specific subset and its impact on the all population. It would allow prediction of a threshold for loss of control and participation to chronic disease apparition. Characterization of inhibitory signals features would balance our model, and these prediction may predict fate of treatment on ILC2 in diverse diseases.

ILC2 trafficking is controlled by a lot of external signals, mainly from other compartment. Impact of nervous system on ILCs is an important field impacting responses. Circadian rhythm is directly linked to neural signals, and all immune responses and immune cell circulation are directly linked to time of the day. In ILC2 circulation

system, circadian rhythm is an important factor of their turnover, and numbers of migrating ILC2s subsets may vary during the day. It would be an important factor to take into account for better characterization of ILC2 trafficking.

Lymph composition is variable and change depending on environmental status. As extremely sensitive to external signal, circulating ILC2s may be impacted by variation in metabolic and cytokinic modifications. For example, AT and pancreas migrating ILC2s may be impact by diet, alternatively activating different subsets.

Finally, studying ILC2 trafficking offer several perspectives to better characterize their development, their function and better understand impact of a large variety of activating signals

Other works

During my 2nd year of master and my PhD in the lab, I participated to several project and side projects.

My principal project, presented in this report, will be submitted soon.

I participated to several projects during the different internships I performed (bachelor and master degrees). Then I am included in the papers that are related to my PhD and to my participation as a member of the unit of lymphopoiesis. I participated mostly to projects done on ILC topic, giving me a large overview and expertise on these populations. First, I participated to three papers describing roles of Notch signalling pathway in group-3 ILC plasticity and in group-1 ILCs functions and their maintenance in periphery. It gave me knowledge on the importance of ILC response heterogeneity depending on the environments and the signals they are faced to. The third paper was dissecting the role of the Notch signalling in the heterogeneous responsiveness of fetal ILCPs, important evidences that will allow us to better understand the development of ILC2s and the role of Notch in that development and their functions in periphery.

I performed projects on ILCs circulation and residency characterizing the role of CXCR6 on ILCP retention in the BM, deeply impacting peripheral phenotypes with compensation by increased cell division in peripheral tissues, probably coming from fetal colonisation of intestine. Another paper is under submission and describes the absence of resident ILC2s in the lung, compensated by migrating ILC2s following local inflammation

I participated to experiments of mice reconstitution to characterize the inability of ILCPs to reconstitute peripheral tissues in the adult mice if they are not irradiated due to the competition with other local precursors in their niches.

I am able to perform computational analyses that I extensively used to analyses high dimensional panels of flow-cytometry, RNAseq or also multiplexed RT-qPCR data. I re-analysed biomark data from a collaboration with Jim Di Santo lab that demonstrated

that an Id2^{+} Zbtb16^{+} ILCP retain multi-potent abilities with NK potential in mice, redefining the development tree of ILC subsets. It also allowed me to participate to the last review from Ana Cumano in Annual review of immunology by re-analysing all the biomarks done by previous students to dissect hematopoietic scheme in an unsupervised way. Ana Cumano and her students could now use my R codes for their research and publications.

BIBLIOGRAPHY

Ahmed, R., and Gray, D. (1996). Immunological memory and protective immunity: Understanding their relation. Science (80-.). *272*, 54–60.

Aird, W.C. (2003). The role of the endothelium in severe sepsis and multiple organ dysfunction syndrome. Blood *101*, 3765–3777.

Aladegbami, B., Barron, L., Bao, J., Colasanti, J., Erwin, C.R., Warner, B.W., and Guo, J. (2017). Epithelial cell specific Raptor is required for initiation of type 2 mucosal immunity in small intestine. Sci. Rep. *7*, 1–10.

Aliahmad, P., De La Torre, B., and Kaye, J. (2010). Shared dependence on the DNA-binding factor TOX for the development of lymphoid tissue-inducer cell and NK cell lineages. Nat. Immunol. *11*, 945–952.

Alon, R., Feizi, T., Yuen, C.T., Fuhlbrigge, R.C., and Springer, T.A. (1995). Glycolipid ligands for selectins support leukocyte tethering and rolling under physiologic flow conditions. J. Immunol. *154*, 5356–5366.

Alvarez, D., Vollmann, E.H., and von Andrian, U.H. (2008). Mechanisms and Consequences of Dendritic Cell Migration. Immunity *29*, 325–342.

Amir, E.A.D., Davis, K.L., Tadmor, M.D., Simonds, E.F., Levine, J.H., Bendall, S.C., Shenfeld, D.K., Krishnaswamy, S., Nolan, G.P., and Pe'Er, D. (2013). ViSNE enables visualization of high dimensional single-cell data and reveals phenotypic heterogeneity of leukemia. Nat. Biotechnol. *31*, 545–552.

Von Andrian, U.H. (1996). Intravital Microscopy of the Peripheral Lymph Node Microcirculation in Mice. Microcirculation *3*, 287–300.

Von Andrian, U.H., and Macley, C.R. (2000). T-cell Function and Migration : Two Sides of the Same Coin. N. Engl. J. Med.

Von Andrian, U.H., and Mempel, T.R. (2003). Homing and cellular traffic in lymph nodes. Nat. Rev. Immunol. *3*, 867–878.

Arjona, A., Silver, A.C., Walker, W.E., and Fikrig, E. (2012). Immunity's fourth dimension: Approaching the circadian-immune connection. Trends Immunol. *33*, 607–612.

Artis, D., and Spits, H. (2015). The biology of innate lymphoid cells. Nature *517*, 293–301.

Aukland, K., Kramer, G.C., and Renkin, E.M. (1984). Protein concentration of lymph and interstitial fluid in the rat tail. Am. J. Physiol. Circ. Physiol. *247*, H74–H79.

Avram, D., and Califano, D. (2014). The Multifaceted Roles of Bcl11b in Thymic and Peripheral T Cells: Impact on Immune Diseases. J. Immunol. *193*, 2059–2065.

Bajénoff, M., Egen, J.G., Koo, L.Y., Laugier, J.P., Brau, F., Glaichenhaus, N., and Germain, R.N. (2006). Stromal Cell Networks Regulate Lymphocyte Entry, Migration, and Territoriality in Lymph Nodes. Immunity *25*, 989–1001.

Balcer, L.J., Galetta, S.L., Calabresi, P.A., Confavreux, C., Giovannoni, G., Havrdova, E., Hutchinson, M., Kappos, L., Lublin, F.D., Miller, D.H., et al. (2007). Natalizumab reduces visual loss in patients with relapsing multiple sclerosis. Neurology *68*, 1299 LP – 1304.

Bando, J.K., Liang, H.E., and Locksley, R.M. (2015). Identification and distribution of developing innate lymphoid cells in the fetal mouse intestine. Nat. Immunol. *16*, 153–160.

Bankovich, A.J., Shiow, L.R., and Cyster, J.G. (2010). CD69 suppresses sphingosine 1-phosophate receptor-1 (S1P1) function through interaction with membrane helix 4. J. Biol. Chem. *285*, 22328–22337.

Barlow, J.L., Bellosi, A., Hardman, C.S., Drynan, L.F., Wong, S.H., Cruickshank, J.P., and McKenzie, A.N.J. (2012). Innate IL-13-producing nuocytes arise during allergic lung inflammation and contribute to airways hyperreactivity. J. Allergy Clin. Immunol. *129*, 191-198.e4.

Barlow, J.L., Peel, S., Fox, J., Panova, V., Hardman, C.S., Camelo, A., Bucks, C., Wu, X., Kane, C.M., Neill, D.R., et al. (2013). IL-33 is more potent than IL-25 in provoking IL-13-producing nuocytes (type 2 innate lymphoid cells) and airway contraction. J. Allergy Clin. Immunol. *132*, 933–941.

Bartemes, K., Chen, C.-C., Iijima, K., Drake, L., and Kita, H. (2018). IL-33-Responsive Group 2 Innate Lymphoid Cells Are Regulated by Female Sex Hormones in the Uterus. J. Immunol. *200*, 229–236.

Beale, J., Jayaraman, A., Jackson, D.J., R Macintyre, J.D., Edwards, M.M.R.M.M.R., Walton, R.P., Zhu, J., Man Ching, Y., Shamji, B., Edwards, M.M.R.M.M.R., et al. (2014). Rhinovirus induced IL-25 in asthma exacerbation drives type-2 immunity and allergic pulmonary inflammation Europe PMC Funders Group. Sci Transl Med Oct. *1*, 256–134.

Belkaid, Y., and Hand, T.W. (2014). Role of the microbiota in immunity and inflammation. Cell *157*, 121–141.

Bénézech, C., and Jackson-Jones, L.H. (2019). ILC2 orchestration of local immune function in adipose tissue. Front. Immunol. *10*, 1–6.

Berasain, C., and Avila, M.A. (2014). Amphiregulin. Semin. Cell Dev. Biol. *28*, 31–41.

Berger, J.R., and Houff, S.A. (2010). Neurological infections: the year of PML and influenza. Lancet Neurol. *9*, 14–17.

Bergstrom, K.S.B., Kissoon-Singh, V., Gibson, D.L., Ma, C., Montero, M., Sham, H.P., Ryz, N., Huang, T., Velcich, A., Finlay, B.B., et al. (2010). Muc2 protects against lethal infectious colitis by disassociating pathogenic and commensal bacteria from the colonic mucosa. PLoS Pathog. *6*.

Berlin, C., Berg, E.L., Briskin, M.J., Andrew, D.P., Kilshaw, P.J., Holzmann, B., Weissman, I.L., Hamann, A., and Butcher, E.C. (1993). α4β7 integrin mediates lymphocyte binding to the mucosal vascular addressin MAdCAM-1. Cell *74*, 185–195.

Bernier-Latmani, J., and Petrova, T. V (2017). Intestinal lymphatic vasculature: Structure, mechanisms and functions. Nat. Rev. Gastroenterol. Hepatol. *14*, 510–526.

Bert, P. (1864). Expériences et considérations sur la greffe animale.

Besedovsky, L., Born, J., and Lange, T. (2014). Endogenous glucocorticoid receptor signaling drives rhythmic changes in human T-cell subset numbers and the expression of the chemokine receptor CXCR4. FASEB J. *28*, 67–75.

Bezençon, C., Fürholz, A., Raymond, F., Mansourian, R., Métairon, S., Le Coutre, J., and Damak, S. (2008). Murine intestinal cells expressing Trpm5 are mostly brush cells and express markers of neuronal and inflammatory cells. J. Comp. Neurol. *509*, 514–525.

Bird, N.J., Michell, A.R., and Peters, A.M. (2009). Accurate measurement of extracellular fluid volume from the slope/intercept technique after bolus injection of a filtration marker. Physiol. Meas. *30*, 1371–1379.

Boos, M.D., Yokota, Y., Eberl, G., and Kee, B.L. (2007). Mature natural killer cell and lymphoid tissue-inducing cell development requires Id2-mediated suppression of E protein activity. J. Exp. Med. *204*, 1119–1130.

Bostick, J.W., and Zhou, L. (2016). Innate lymphoid cells in intestinal immunity and inflammation. Cell. Mol. Life Sci. *73*, 237–252.

Braun, A., Worbs, T., Moschovakis, G.L., Halle, S., Hoffmann, K., Bölter, J., Münk, A., and Förster, R. (2011). Afferent lymph-derived T cells and DCs use different chemokine receptor CCR7-dependent routes for entry into the lymph node and intranodal migration. Nat. Immunol. *12*, 879–887.

Brestoff, J.R., Kim, B.S., Saenz, S.A., Stine, R.R., Monticelli, L.A., Sonnenberg, G.F., Thome, J.J., Farber, D.L., Lutfy, K., Seale, P., et al. (2015). Group 2 innate lymphoid cells promote beiging of white adipose tissue and limit obesity. Nature *519*, 242–246.

Brighton, P.J., Szekeres, P.G., and Willars, G.B. (2004). Neuromedin U and Its Receptors : Structure , Function , and Physiological Roles. Pharmacol. Rev. *56*, 231–248.

Bromley, S.K., Mempel, T.R., and Luster, A.D. (2008). Orchestrating the orchestrators: Chemokines in control of T cell traffic. Nat. Immunol. *9*, 970–980.

Buonocore, S., Ahern, P.P., Uhlig, H.H., Ivanov, I.I., Littman, D.R., Maloy, K.J., and Powrie, F. (2010). Innate lymphoid cells drive interleukin-23-dependent innate intestinal pathology. Nature *464*, 1371–1375.

Califano, D., Cho, J.J., Uddin, M.N., Lorentsen, K.J., Yang, Q., Bhandoola, A., Li, H., and Avram, D. (2015). Transcription Factor Bcl11b Controls Identity and Function of Mature Type 2 Innate Lymphoid Cells. Immunity *43*, 354–368.

Camberis, M., Le Gros, G., and Urban, J. (2003). Animal Model of Nippostrongylus brasiliensis and Heligmosomoides polygyrus . Curr. Protoc. Immunol. 1–27.

Camelo, A., Rosignoli, G., Ohne, Y., Stewart, R.A., Overed-sayer, C., Sleeman, M.A., and May, R.D. (2017). IL-33, IL-25, and TSLP induce a distinct phenotypic and activation profile in human type 2 innate lymphoid cells. Blood Adv. *1*, 577–589.

Campbell, D.J., and Butcher, E.C. (2002). Intestinal attraction: CCL25 functions in effector lymphocyte recruitment to the small intestine. J. Clin. Invest. *110*, 1079–1081.

Campbell, J.J., Haraldsen, G., Pan, J., Rottman, J., Qin, S., Ponath, P., Andrew, D.P., Warnke, R., Ruffing, N., Kassam, N., et al. (1999). The chemokine receptor CCR4 in vascular recognition by cutaneous but not intestinal memory T cells. Nature *400*, 776–780.

Campbell, L., Hepworth, M.R., Whittingham-Dowd, J., Thompson, S., Bancroft, A.J., Hayes, K.S., Shaw, T.N., Dickey, B.F., Flamar, A.-L., Artis, D., et al. (2019). ILC2s mediate systemic innate protection by priming mucus production at distal mucosal sites. J. Exp. Med. jem.20180610.

Cardoso, V., Chesné, J., Ribeiro, H., Garcia-Cassani, B., Carvalho, T., Bouchery, T., Shah, K., Barbosa-Morais, N.L., Harris, N., and Veiga-Fernandes, H. (2017). Neuronal regulation of type 2 innate lymphoid cells via neuromedin U. Nature *549*, 277–281.

Carotta, S., Pang, S.H.M., Nutt, S.L., and Belz, G.T. (2011). Identification of the earliest NK-cell precursor in the mouse BM. Blood *117*, 5449–5452.

Carroll, K.N., and Hartert, T. V. (2008). The Impact of Respiratory Viral Infection on Wheezing Illnesses and Asthma Exacerbations. Immunol. Allergy Clin. North Am. *28*, 539–561.

Casanova-Acebes, M., Pitaval, C., Weiss, L.A., Nombela-Arrieta, C., Chèvre, R., A-González, N., Kunisaki, Y., Zhang, D., Van Rooijen, N., Silberstein, L.E., et al. (2013). XRhythmic modulation of the hematopoietic niche through neutrophil clearance. Cell *153*, 1025.

Cayrol, C., and Girard, J.P. (2014). IL-33: An alarmin cytokine with crucial roles in innate immunity, inflammation and allergy. Curr. Opin. Immunol. *31*, 31–37.

Cayrol, C., Duval, A., Schmitt, P., Roga, S., Camus, M., Stella, A., Burlet-Schiltz, O., Gonzalez-De-Peredo, A., and Girard, J.P. (2018). Environmental allergens induce allergic inflammation through proteolytic maturation of IL-33. Nat. Immunol. *19*, 375–385.

Chaffin, K.E., and Perlmutter, R.M. (1991). A pertussis toxin-sensitive process controls thymocyte emigration. Eur. J. Immunol. *21*, 2565–2573.

Chang, Y.J., Kim, H.Y., Albacker, L.A., Baumgarth, N., McKenzie, A.N.J., Smith, D.E., Dekruyff, R.H., and Umetsu, D.T. (2011). Innate lymphoid cells mediate influenza-induced airway hyper-reactivity independently of adaptive immunity. Nat. Immunol. *12*, 631–638.

Chea, S., Possot, C., Perchet, T., Petit, M., Cumano, A., and Golub, R. (2015). CXCR6 Expression Is Important for Retention and Circulation of ILC Precursors. Mediators Inflamm. *2015*.

Chea, S., Schmutz, S., Berthault, C., Perchet, T., Petit, M., Burlen-Defranoux, O., Goldrath, A.W., Rodewald, H.R., Cumano, A., and Golub, R. (2016a). Single-Cell Gene Expression Analyses Reveal Heterogeneous Responsiveness of Fetal Innate Lymphoid Progenitors to Notch Signaling. Cell Rep. *14*, 1500–1516.

Chea, S., Perchet, T., Petit, M., Verrier, T., Guy-Grand, D., Banchi, E.G., Vosshenrich, C.A.J., Di Santo, J.P., Cumano, A., and Golub, R. (2016b). Notch signaling in group 3 innate lymphoid cells modulates their plasticity. Sci. Signal. *9*.

Chen, F., Liu, Z., Wu, W., Rozo, C., Bowdridge, S., Millman, A., Van Rooijen, N., Urban, J.F., Wynn, T.A., and Gause, W.C. (2012). An essential role for T H 2-type responses in limiting acute tissue damage during experimental helminth infection. Nat. Med. *18*, 260–266.

Chenivesse, C., and Tsicopoulos, A. (2018). CCL18 - Beyond chemotaxis. Cytokine *109*, 52–56.

Cheresh, D.A., Felding-Habermann, B., and Cheresh, D.A. (1993). Vitronectin and its receptors. Curr. Opin. Cell Biol. *5*, 864–868.

Cherrier, D.E., Serafini, N., and Di Santo, J.P. (2018). Innate Lymphoid Cell Development: A T Cell Perspective. Immunity 1091–1103.

Cherrier, M., Sawa, S., and Eberl, G. (2012). Notch, Id2, and RORγt sequentially orchestrate the fetal development of lymphoid tissue inducer cells. J. Exp. Med. *209*, 729–740.

Chun, J., Hla, T., Lynch, K.R., Spiegel, S., and Moolenaar, W.H. (2010). Pharmacology . LXXVIII . Lysophospholipid. J. Clin. Invest. *62*, 579–587.

Cibrián, D., and Sánchez-Madrid, F. (2017). CD69: from activation marker to metabolic gatekeeper. Eur. J. Immunol. *47*, 946–953.

Ciofani, M., Madar, A., Galan, C., Sellars, M., MacE, K., Pauli, F., Agarwal, A., Huang, W., Parkurst, C.N., Muratet, M., et al. (2012). A validated regulatory network for Th17 cell specification. Cell *151*, 289–303.

Clement, C.C., Cannizzo, E.S., Nastke, M.D., Sahu, R., Olszewski, W., Miller, N.E., Stern, L.J., and Santambrogio, L. (2010). An expanded self-antigen peptidome is carried by the human lymph as compared to the plasma. PLoS One *5*.

Clement, C.C., Aphkhazava, D., Nieves, E., Callaway, M., Olszewski, W., Rotzschke, O., and Santambrogio, L. (2013). Protein expression profiles of human lymph and plasma mapped by 2D-DIGE and 1D SDS-PAGE coupled with nanoLC-ESI-MS/MS bottom-up proteomics. J. Proteomics *78*, 172–187.

Cohen, M., Giladi, A., Gorki, A.D., Solodkin, D.G., Zada, M., Hladik, A., Miklosi, A., Salame, T.M., Halpern, K.B., David, E., et al. (2018). Lung Single-Cell Signaling Interaction Map Reveals Basophil Role in Macrophage Imprinting. Cell *175*, 1031-1044.e18.

Commodaro, A.G., Peron, J.P.S., Lopes, C.T., Arslanian, C., Rubens, B., Rizzo, L.V., and Bueno, V. (2010). Evaluation of experimental autoimmune uveitis in mice treated with FTY720. Investig. Ophthalmol. Vis. Sci. *51*, 2568–2574.

Conboy, M.J., Conboy, I.M., and Rando, T.A. (2013). Heterochronic parabiosis: Historical perspective and methodological considerations for studies of aging and longevity. Aging Cell *12*, 525–530.

Conese, M., Carbone, A., Beccia, E., and Angiolillo, A. (2017). The Fountain of Youth: A tale of parabiosis, stem cells, and rejuvenation. Open Med. *12*, 376–383.

Constantinides, M.G., McDonald, B.D., Verhoef, P.A., and Bendelac, A. (2014). A committed precursor to innate lymphoid cells. Nature *508*, 397–401.

Cook, D.N., Kang, H.S., and Jetten, A.M. (2015). Retinoic Acid-Related Orphan Receptors (RORs): Regulatory Functions in Immunity, Development, Circadian Rhythm, and Metabolism. Nucl. Recept. Res. *2*, 1–40.

Coquet, J.M., Schuijs, M.J., Smyth, M.J., Deswarte, K., Beyaert, R., Braun, H., Boon, L., Hedestam, G.B.K., Nutt, S.L., Hammad, H., et al. (2015). Interleukin-21-Producing CD4+ T Cells Promote Type 2 Immunity to House Dust Mites. Immunity *43*, 318–330.

Cording, S., Medvedovic, J., Cherrier, M., and Eberl, G. (2014). Development and regulation of RORγt+ innate lymphoid cells. FEBS Lett. *588*, 4176–4181.

Crockett-Torabi, E. (1998). Selectins and mechanisms of signal transduction. J. Leukoc. Biol. *63*, 1–14.

Cromer, W.E., Zawieja, S.D., Tharakan, B., Childs, E.W., Newell, M.K., and Zawieja, D.C. (2014). The effects of inflammatory cytokines on lymphatic endothelial barrier function. Angiogenesis *17*, 395–406.

Cumano, A., Berthault, C., Ramond, C., Petit, M., Golub, R., Bandeira, A., and Pereira, P. (2019). New Molecular Insights into Immune Cell Development. Annu. Rev. Immunol. *37*, 497–519.

Curtis, A.M., Bellet, M.M., Sassone-Corsi, P., and O'Neill, L.A.J. (2014). Circadian Clock Proteins and Immunity. Immunity *40*, 178–186.

Cybulsky, M.I., and Gimbrone, M.A. (1991). Endothelial expression of a mononuclear leukocyte adhesion molecule during atherogenesis. Science (80-.). *251*, 788–791.

Cyster, J.G., and Schwab, S.R. (2012). Sphingosine-1-Phosphate and Lymphocyte Egress from Lymphoid Organs. Annu. Rev. Immunol. *30*, 69–94.

D'Souza, B., Meloty-Kapella, L., and Weinmaster, G. (2010). Canonical and non-canonical notch ligands.

Dalmas, E., Lehmann, F.M., Dror, E., Wueest, S., Thienel, C., Borsigova, M., Stawiski, M., Traunecker, E., Lucchini, F.C., Dapito, D.H., et al. (2017). Interleukin-33-Activated Islet-Resident Innate Lymphoid Cells Promote Insulin Secretion through Myeloid Cell Retinoic Acid Production. Immunity *47*, 928-942.e7.

Daussy, C., Faure, F., Mayol, K., Viel, S., Gasteiger, G., Charrier, E., Bienvenu, J., Henry, T., Debien, E., Hasan, U.A., et al. (2014). T-bet and Eomes instruct the development of two distinct natural killer cell lineages in the liver and in the bone marrow. J. Exp. Med. *211*, 563–577.

DeNucci, C.C., Pagán, A.J., Mitchell, J.S., and Shimizu, Y. (2010). Control of α4β7 Integrin Expression and CD4 T Cell Homing by the β1 Integrin Subunit. J. Immunol. *184*, 2458–2467.

Dibner, C., Schibler, U., and Albrecht, U. (2010). The Mammalian Circadian Timing System: Organization and Coordination of Central and Peripheral Clocks.

Dickson, L., and Finlayson, K. (2009). VPAC and PAC receptors: From ligands to function. Pharmacol. Ther. *121*, 294–316.

Dimitrov, S., Benedict, C., Heutling, D., Westermann, J., Born, J., and Lange, T. (2009). Cortisol and epinephrine control opposing circadian rhythms in T cell subsets. Blood *113*, 5134–5143.

Dixon, J.B., Greiner, S.T., Gashev, A.A., Cote, G.L., Moore, J.E., and Zawieja, D.C. (2006). Lymph flow, shear stress, and lymphocyte velocity in rat mesenteric prenodal lymphatics. Microcirculation *13*, 597–610.

Djuretic, I.M., Levanon, D., Negreanu, V., Groner, Y., Rao, A., and Ansel, K.M. (2007). Transcription factors T-bet and Runx3 cooperate to activate Ifng and silence Il4 in T helper type 1 cells (Nature Immunology). Nat. Immunol. *8*, 145–153.

Doeing, D.C., and Solway, J. (2013). Airway smooth muscle in the pathophysiology and treatment of asthma. J. Appl. Physiol. *114*, 834–843.

Doherty, T.A., Khorram, N., Lund, S., Mehta, A.K., Croft, M., and Broide, D.H. (2013). Lung type 2 innate lymphoid cells express cysteinyl leukotriene receptor 1, which regulates TH2 cytokine production. J. Allergy Clin. Immunol. *132*, 205–213.

Drake, L.Y., Iijima, K., Bartemes, K., and Kita, H. (2016). Group 2 Innate Lymphoid Cells Promote an Early Antibody Response to a Respiratory Antigen in Mice. J. Immunol. *197*, 1335–1342.

Druzd, D., Matveeva, O., Ince, L., Harrison, U., He, W., Schmal, C., Herzel, H., Tsang, A.H., Kawakami, N., Leliavski, A., et al. (2017). Lymphocyte Circadian Clocks Control Lymph Node Trafficking and Adaptive Immune Responses. Immunity *46*, 120–132.

Duerr, C.U., Mccarthy, C.D.A., Mindt, B.C., Rubio, M., Meli, A.P., Pothlichet, J., Eva, M.M., Gauchat, J.F., Qureshi, S.T., Mazer, B.D., et al. (2016). Type I interferon restricts type 2 immunopathology through the regulation of group 2 innate lymphoid cells. Nat. Immunol. *17*, 65–75.

Van Dyken, S.J., Mohapatra, A., Nussbaum, J.C., Molofsky, A.B., Thornton, E.E., Ziegler, S.F., McKenzie, A.N.J., Krummel, M.F., Liang, H.E., and Locksley, R.M. (2014). Chitin activates parallel immune modules that direct distinct inflammatory responses via innate lymphoid type 2 and γδ T cells. Immunity *40*, 414–424.

Eastman, J.J., Cavagnero, K.J., Deconde, A.S., Kim, A.S., Karta, M.R., Broide, D.H., Zuraw, B.L., White, A.A., Christiansen, S.C., and Doherty, T.A. (2017). Group 2 innate lymphoid cells are recruited to the nasal mucosa in patients with aspirin-exacerbated respiratory disease. J. Allergy Clin. Immunol. *140*, 101-108.e3.

Eberl, G., and Lochner, M. (2009). The development of intestinal lymphoid tissues at the interface of self and microbiota. Mucosal Immunol. *2*, 478–485.

Eberl, G., Colonna, M., Di Santo, J.P., and McKenzie, A.N.J. (2015). Innate lymphoid cells: A new paradigm in immunology. Science (80-.). *348*, 6566.

Ebihara, T., Song, C., Ryu, S.H., Plougastel-Douglas, B., Yang, L., Levanon, D., Groner, Y., Bern, M.D., Stappenbeck, T.S., Colonna, M., et al. (2015). Runx3 specifies lineage commitment of innate lymphoid cells. Nat. Immunol. *16*, 1124–1133.

Eichwald, E.J., Lustgraaf, E.C., and Strainer, M. (1959). Genetic factors in parabiosis. J. Natl. Cancer Inst. *23*, 1193–1213.

Ellies, L.G., Sperandio, M., Underhill, G.H., Yousif, J., Smith, M., Priatel, J.J., Kansas, G.S., Ley, K., and Marth, J.D. (2002). Sialyltransferase specificity in selectin ligand formation. Blood *100*, 3618–3625.

Endo, Y., Hirahara, K., Iinuma, T., Shinoda, K., Tumes, D.J., Asou, H.K., Matsugae, N., Obata-Ninomiya, K., Yamamoto, H., Motohashi, S., et al. (2015). The Interleukin-33-p38 kinase axis confers memory T helper 2 cell pathogenicity in the airway. Immunity *42*, 294–308.

van der Flier, L.G., and Clevers, H. (2009). Stem Cells, Self-Renewal, and Differentiation in the Intestinal Epithelium. Annu. Rev. Physiol. *71*, 241–260.

Forkel, M., Berglin, L., Kekäläinen, E., Carlsson, A., Svedin, E., Michaëlsson, J., Nagasawa, M., Erjefält, J.S., Mori, M., Flodström-Tullberg, M., et al. (2017). Composition and functionality of the intrahepatic innate lymphoid cell-compartment in human nonfibrotic and fibrotic livers. Eur. J. Immunol. *47*, 1280–1294.

Förster, R., Davalos-Misslitz, A.C., and Rot, A. (2008). CCR7 and its ligands: Balancing immunity and tolerance. Nat. Rev. Immunol. *8*, 362–371.

Förster, R., Braun, A., and Worbs, T. (2012). Lymph node homing of T cells and dendritic cells via afferent lymphatics. Trends Immunol. *33*, 271–280.

Fort, M.M., Cheung, J., Yen, D., Li, J., Zurawski, S.M., Lo, S., Menon, S., Clifford, T., Hunte, B., Lesley, R., et al. (2001). IL-25 Induces IL-4, IL-5, and IL-13 and Th2-associated pathologies in vivo. Immunity *15*, 985–995.

Fossum, S., and Ford, W.L. (1985). The organization of cell populations within lymph nodes: their origin, life history and functional relationships. Histopathology *9*, 469–499.

Frontini, A., and Cinti, S. (2010). Distribution and Development of Brown Adipocytes in the Murine and Human Adipose Organ. Cell Metab. *11*, 253–256.

Furusawa, J. -i., Moro, K., Motomura, Y., Okamoto, K., Zhu, J., Takayanagi, H., Kubo, M., and Koyasu, S. (2014). Critical Role of p38 and GATA3 in Natural Helper Cell Function. J. Immunol. *193*, 1512–1512.

Furusawa, Y., Obata, Y., Fukuda, S., Endo, T.A., Nakato, G., Takahashi, D., Nakanishi, Y., Uetake, C., Kato, K., Kato, T., et al. (2013). Commensal microbe-derived butyrate induces the differentiation of colonic regulatory T cells. Nature *504*, 446–450.

Gächter, T., Werenskiold, A.K., and Klemenz, R. (1996). Transcription of the interleukin-1 receptor-related T1 gene is initiated at different promoters in mast cells and fibroblasts. J. Biol. Chem. *271*, 124–129.

Gashev, A.A. (2008). Lymphatic vessels: Pressure- and flow-dependent regulatory reactions. In Annals of the New York Academy of Sciences, pp. 100–109.

Gashev, A.A. (2010). Basic mechanisms controlling lymph transport in the mesenteric lymphatic net. Ann. N. Y. Acad. Sci. *1207*, 16–20.

Gasteiger, G., Fan, X., Dikiy, S., Lee, S.Y., and Rudensky, A.Y. (2015). Tissue residency of innate lymphoid cells in lymphoid and nonlymphoid organs. Science (80-.). *350*, 981–985.

Gerbe, F., Sidot, E., Smyth, D.J., Ohmoto, M., Matsumoto, I., Dardalhon, V., Cesses, P., Garnier, L., Pouzolles, M., Brulin, B., et al. (2016). Intestinal epithelial tuft cells initiate type 2 mucosal immunity to helminth parasites. Nature *529*, 226–230.

Germain, R.N., and Huang, Y. (2019). ILC2s — resident lymphocytes pre-adapted to a specific tissue or migratory effectors that adapt to where they move? Curr. Opin. Immunol. *56*, 76–81.

Gesner, B.M., and Gowans, J.L. (1962). The Output of Lymphocytes from the Thoracic Duct of Unanaesthetized Mice. Br. J. Exp. Pathol. *43*, 424–430.

Ginhoux, F., and Guilliams, M. (2016). Tissue-Resident Macrophage Ontogeny and Homeostasis. Immunity *44*, 439–449.

Girard, J.P., and Springer, T.A. (1995). High endothelial venules (HEVs): specialized endothelium for lymphocyte migration. Immunol. Today *16*, 449–457.

Girard, J.P., Moussion, C., and Förster, R. (2012). HEVs, lymphatics and homeostatic immune cell trafficking in lymph nodes. Nat. Rev. Immunol. *12*, 762–773.

Gold, M.J., Antignano, F., Halim, T.Y.F., Hirota, J.A., Blanchet, M.R., Zaph, C., Takei, F., and McNagny, K.M. (2014). Group 2 innate lymphoid cells facilitate sensitization to local, but not systemic, TH2-inducing allergen exposures. J. Allergy Clin. Immunol. *133*, 1142-1148.e5.

Goldfinch, G.M., Smith, W.D., Imrie, L., McLean, K., Inglis, N.F., and Pemberton, A.D. (2008). The proteome of gastric lymph in normal and nematode infected sheep. Proteomics *8*, 1909–1918.

Gordon, S.M., Chaix, J., Rupp, L.J., Wu, J., Madera, S., Sun, J.C., Lindsten, T., and Reiner, S.L. (2012). The Transcription Factors T-bet and Eomes Control Key Checkpoints of Natural Killer Cell Maturation. Immunity *36*, 55–67.

Goswami, R. (2017). Th9 Cells.

Gowans, J.L. (1959). The recirculation of lymphocytes from blood to lymph in the rat. J. Physiol. *146*, 54–69.

Gowans, J.L., and Knight, E.J. (1964). the Route of Re-Circulation of Lymphocytes in the Rat. Proc. R. Soc. London. Ser. B, Contain. Pap. *159*, 257–282.

Grakoui, A., Bromley, S.K., Sumen, C., Davis, M.M., Shaw, A.S., Allen, P.M., and Dustin, M.L. (1999). The immunological synapse: a molecular machine controlling T cell activation. Science (80-.). *285*, 221–227.

Grant, A.J., Lalor, P.F., Hübscher, S.G., Briskin, M., and Adams, D.H. (2001). MAdCAM-1 expressed in chronic inflammatory liver disease supports mucosal lymphocyte adhesion to hepatic endothelium (MAdCAM-1 in chronic inflammatory liver disease). Hepatology *33*, 1065–1072.

Griesenauer, B., and Paczesny, S. (2017). The ST2/IL-33 axis in immune cells during inflammatory diseases. Front. Immunol. *8*, 1–17.

Griffith, J.W., Sokol, C.L., and Luster, A.D. (2014). Chemokines and Chemokine Receptors: Positioning Cells for Host Defense and Immunity. Annu. Rev. Immunol. *32*, 659–702.

Grigorova, I.L., Schwab, S.R., Phan, T.G., Pham, T.H.M., Okada, T., and Cyster, J.G. (2009). Cortical sinus probing, S1P1-dependent entry and flow-based capture of egressing T cells. Nat. Immunol. *10*, 58–65.

Grindebacke, H., Stenstad, H., Quiding-Järbrink, M., Waldenström, J., Adlerberth, I., Wold, A.E., and Rudin, A. (2009). Dynamic Development of Homing Receptor Expression and Memory Cell Differentiation of Infant CD4 + CD25 high Regulatory T Cells . J. Immunol. *183*, 4360–4370.

Griscelli, C., Vassalli, P., and McCluskey, R.T. (1969). The distribution of large dividing lymph node cells in syngeneic recipient rats after intravenous injection. J. Exp. Med. *130*, 1427–1451.

Gronke, K., and Diefenbach, A. (2016). Tuft cell-derived IL-25 activates and maintains ILC2. Immunol. Cell Biol. *94*, 221–223.

Groom, J.R., Richmond, J., Murooka, T.T., Sorensen, E.W., Sung, J.H., Bankert, K., von Andrian, U.H., Moon, J.J., Mempel, T.R., and Luster, A.D. (2012). CXCR3 Chemokine Receptor-Ligand Interactions in the Lymph Node Optimize CD4+ T Helper 1 Cell Differentiation. Immunity *37*, 1091–1103.

Guo, L., Huang, Y., Chen, X., Hu-Li, J., Urban, J.F., and Paul, W.E. (2015). Innate immunological function of T <inf>H</inf>2 cells in vivo. Nat. Immunol. *16*, 1051–1059.

Gury-BenAri, M., Thaiss, C.A., Serafini, N., Winter, D.R., Giladi, A., Lara-Astiaso, D., Levy, M., Salame, T.M., Weiner, A., David, E., et al. (2016). The Spectrum and Regulatory Landscape of Intestinal Innate Lymphoid Cells Are Shaped by the Microbiome. Cell *166*, 1231-1246.e13.

Guy-Grand, D., Griscelli, C., and Vassali, P. (1974). The gut-associated lymphoid system: nature and properties of the large dividing cells. Eur. J. Immunol. *4*, 435–443.

Guy-Grand, D., Dy, M., Luffau, G., Vassalli, P., and Guy-Grand, D; Dy,M., Luffau,G., Vassalli, P. (1984). Gut mucosal mast cells. Origin, traffic, and differentiation. J Exp Med *160*, 12–28.

Guy-Grand, D., Vassalli, P., Eberl, G., Pereira, P., Burlen-Defranoux, O., Lemaitre, F., Di Santo, J., Freitas, A., Cumano, A., and Bandeira, A. (2013). Origin, trafficking, and intraepithelial fate of gut-tropic T cells. J. Exp. Med. *210*, 1839–1854.

Haber, A.L., Biton, M., Rogel, N., Herbst, R.H., Shekhar, K., Smillie, C., Burgin, G., Delorey, T.M., Howitt, M.R., Katz, Y., et al. (2017). A single-cell survey of the small intestinal epithelium. Nature *551*, 333–339.

Halim, T.Y.F., MacLaren, A., Romanish, M.T., Gold, M.J., McNagny, K.M., and Takei, F. (2012a). Retinoic-Acid-Receptor-Related Orphan Nuclear Receptor Alpha Is Required for Natural Helper Cell Development and Allergic Inflammation. Immunity *37*, 463–474.

Halim, T.Y.F., Krauß, R.H., Sun, A.C., and Takei, F. (2012b). Lung Natural Helper Cells Are a Critical Source of Th2 Cell-Type Cytokines in Protease Allergen-Induced Airway Inflammation. Immunity *36*, 451–463.

Halim, T.Y.F., Steer, C.A., Mathä, L., Gold, M.J., Martinez-Gonzalez, I., McNagny, K.M., McKenzie, A.N.J., and Takei, F. (2014). Group 2 innate lymphoid cells are critical for the initiation of adaptive T helper 2 cell-mediated allergic lung inflammation. Immunity *40*, 425–435.

Halim, T.Y.F., Rana, B.M.J., Walker, J.A., Kerscher, B., Knolle, M.D., Jolin, H.E., Serrao, E.M., Haim-Vilmovsky, L., Teichmann, S.A., Rodewald, H.R., et al. (2018). Tissue-Restricted Adaptive Type 2 Immunity Is Orchestrated by Expression of the Costimulatory Molecule OX40L on Group 2 Innate Lymphoid Cells. Immunity *48*, 1195-1207.e6.

Hams, E., Locksley, R.M., Mckenzie, A.N.J., and Fallon, P.G. (2013). IL-25 Elicits Innate Lymphoid Type 2 and Type II NKT Cells That Regulate Obesity in Mice. J. Immunol. *191*, 5349–5353.

Hamza, T., Barnett, J.B., and Li, B. (2010). Interleukin 12 a key immunoregulatory cytokine in infection applications. Int. J. Mol. Sci. *11*, 789–806.

Hanninen, A., Jaakkola, I., and Jalkanen, S. (1998). Mucosal addressin is required for the development of diabetes in nonobese diabetic mice. J. Immunol. *160*, 6018–6025.

Harly, C., Cam, M., Kaye, J., and Bhandoola, A. (2018). Development and differentiation of early innate lymphoid progenitors. J. Exp. Med. *215*, 249–262.

Hartsock, A., and Nelson, W.J. (2008). Adherens and tight junctions: Structure, function and connections to the actin cytoskeleton. Biochim. Biophys. Acta - Biomembr. *1778*, 660–669.

Hashiguchi, M., Kashiwakura, Y., Kojima, H., Kobayashi, A., Kanno, Y., and Kobata, T. (2015). IL-33 activates eosinophils of visceral adipose tissue both directly and via innate lymphoid cells. Eur. J. Immunol. *45*, 876–885.

He, Z., Ma, J., Wang, R., Zhang, J., Huang, Z., Wang, F., Sen, S., Rothenberg, E. V, and Sun, Z. (2017). A two-amino-acid substitution in the transcription factor ROR 3t disrupts its function in T H 17 differentiation but not in thymocyte development. Nat. Immunol. *18*, 1128–1138.

van Helden, M.J., Goossens, S., Daussy, C., Mathieu, A.L., Faure, F., Marçais, A., Vandamme, N., Farla, N., Mayol, K., Viel, S., et al. (2015). Terminal NK cell maturation is controlled by concerted actions of T-bet and Zeb2 and is essential for melanoma rejection. J. Exp. Med. *212*, 2015–2025.

Hemler, M.E., Huang, C., and Schwarz, L. (1987). The VLA Protein Family. J. Biol. Chem. *262*, 3300–3309.

Henderson, R.B., Lim, L.H.K., Tessier, P.A., Gavins, F.N.E., Mathies, M., Perretti, M., and Hogg, N. (2001). The Use of Lymphocyte Function–Associated Antigen (Lfa)-1–Deficient Mice to Determine the Role of Lfa-1, Mac-1, and α4 Integrin in the Inflammatory Response of Neutrophils. J. Exp. Med. *194*, 219–226.

Henson, S.M., and Akbar, A.N. (2009). KLRG1-more than a marker for T cell senescence. Age (Omaha). *31*, 285–291.

Herberman, R.B., Nunn, M.E., and Lavrin, D.H. (1975). Natural cytotoxic reactivity of mouse lymphoid cells against syngeneic and allogeneic tumors. I. Distribution of reactivity and specificity. Int. J. Cancer *16*, 216–229.

Hidalgo, A., Peired, A.J., Wild, M., Vestweber, D., and Frenette, P.S. (2007). Complete identification of E-selectin ligand activity on neutrophils reveals a dynamic interplay and distinct functions of PSGL-1, ESL-1 and CD44. Immunity *26*, 477–489.

Hodzic, Z., Schill, E.M., Bolock, A.M., and Good, M. (2017). IL-33 and the intestine: The good, the bad, and the inflammatory. Cytokine *100*, 1–10.

Hong, J.Y., Bentley, J.K., Chung, Y., Lei, J., Steenrod, J.M., Chen, Q., Sajjan, U.S., and Hershenson, M.B. (2014). Neonatal rhinovirus induces mucous metaplasia and airways hyperresponsiveness through IL-25 and type 2 innate lymphoid cells. J. Allergy Clin. Immunol. *134*, 429-439.e8.

Horowitz, M.C., Berry, R., Holtrup, B., Sebo, Z., Nelson, T., Fretz, J.A., Lindskog, D., Kaplan, J.L., Ables, G., Rodeheffer, M.S., et al. (2017). Bone marrow adipocytes. Adipocyte *6*, 193–204.

Howitt, M.R., Lavoie, S., Michaud, M., Blum, A.M., Tran, S. V, Weinstock, J. V, Gallini, C.A., Redding, K.,

Margolskee, R.F., Osborne, L.C., et al. (2016). Tuft cells, taste-chemosensory cells, orchestrate parasite type 2 immunity in the gut. Science (80-.). *351*, 1329–1333.

Hoyler, T., Klose, C.S.N.N., Souabni, A., Turqueti-Neves, A., Pfeifer, D., Rawlins, E.L., Voehringer, D., Busslinger, M., and Diefenbach, A. (2012). The Transcription Factor GATA-3 Controls Cell Fate and Maintenance of Type 2 Innate Lymphoid Cells. Immunity *37*, 634–648.

Huang, Y., and Paul, W.E. (2016). Inflammatory group 2 innate lymphoid cells. Int. Immunol. *28*, 23–28.

Huang, Y., Guo, L., Qiu, J., Chen, X., Hu-Li, J., Siebenlist, U., Williamson, P.R., Urban, J.F., and Paul, W.E. (2015). IL-25-responsive, lineage-negative KLRG1 hi cells are multipotential "inflammatory" type 2 innate lymphoid cells. Nat. Immunol. *16*, 161–169.

Huang, Y., Mao, K., Chen, X., Sun, M., Kawabe, T., Li, W., Usher, N., Zhu, J., Urban, J.F., Paul, W.E., et al. (2018). S1P-dependent interorgan trafficking of group 2 innate lymphoid cells supports host defense. Science (80-.). *359*, 114–119.

Huber-Lang, M., Lambris, J.D., and Ward, P.A. (2018). Innate immune responses to trauma. Nat. Immunol. *19*, 1–15.

Hughes, C.E., and Nibbs, R.J.B. (2018). A guide to chemokines and their receptors. FEBS J. *285*, 2944–2971.

Hung, L.-Y., Lewkowich, I.P., Dawson, L.A., Downey, J., Yang, Y., Smith, D.E., and Herbert, D.R. (2013). IL-33 drives biphasic IL-13 production for noncanonical Type 2 immunity against hookworms. Proc. Natl. Acad. Sci. *110*, 282–287.

Hynes, R.O. (2002). Integrins: Bidirectional, allosteric signaling machines. Cell *110*, 673–687.

Idzko, M., Hammad, H., Van Nimwegen, M., Kool, M., Müller, T., Soullié, T., Willart, M.A.M., Hijdra, D., Hoogsteden, H.C., and Lambrecht, B.N. (2006). Local application of FTY720 to the lung abrogates experimental asthma by altering dendritic cell function. J. Clin. Invest. *116*, 2935–2944.

Iizuka, T., Tanaka, T., Suematsu, M., Miura, S., Watanabe, T., Koike, R., Ishimura, Y., Ishii, H., Miyasaka, N., and Miyasaka, M. (2000). Stage-Specific Expression of Mucosal Addressin Cell Adhesion Molecule-1 During Embryogenesis in Rats. J. Immunol. *164*, 2463–2471.

Ikeda, K., Nakajima, H., Suzuki, K., Kagami, S.I., Hirose, K., Suto, A., Saito, Y., and Iwamoto, I. (2003). Mast cells produce interleukin-25 upon FcεRI-mediated activation. Blood *101*, 3594–3596.

Ishizuka, I.E., Chea, S., Gudjonson, H., Constantinides, M.G., Dinner, A.R., Bendelac, A., and Golub, R. (2016). Single-cell analysis defines the divergence between the innate lymphoid cell lineage and lymphoid tissue-inducer cell lineage. Nat. Immunol. *17*, 269–276.

Islam, S.A., Chang, D.S., Colvin, R.A., Byrne, M.H., McCully, M.L., Moser, B., Lira, S.A., Charo, I.F., and Luster, A.D. (2011). Mouse CCL8, a CCR8 agonist, promotes atopic dermatitis by recruiting IL-5+ T(H)2 cells. Nat. Immunol. *12*, 167–177.

Islam, S.A., Ling, M.F., Leung, J., Shreffler, W.G., and Luster, A.D. (2013). Identification of human CCR8 as a CCL18 receptor. J. Exp. Med. *210*, 1889–1898.

Jackson, D.J., Makrinioti, H., Rana, B.M.J., Shamji, B.W.H., Trujillo-Torralbo, M.B., Footitt, J., Del-Rosario, J., Telcian, A.G., Nikonova, A., Zhu, J., et al. (2014). IL-33-Dependent type 2 inflammation during rhinovirus-induced asthma exacerbations in vivo. Am. J. Respir. Crit. Care Med. *190*, 1373–1382.

Jaroszeski, M.J., and Heller, R. (1997). Flow Cytometry Protocols.

Jarrett, E.E.E., Jarrett, W.F.H.H., Urquhart, G.M., Jarrett, B.Y.E.E.E., Jarrett, W.F.H.H., Urquhart, G.M., Jarrett, E.E.E., Jarrett, W.F.H.H., and Urquhart, G.M. (1968). Quantitative studies on the kinetics of establishment and expulsion of intestinal nematode populations in susceptible and immune hosts. Nippostrongylus brasiliensis in the rat. Parasitology *58*, 625–639.

Jenne, C.N., Enders, A., Rivera, R., Watson, S.R., Bankovich, A.J., Pereira, J.P., Xu, Y., Roots, C.M., Beilke, J.N., Banerjee, A., et al. (2009). T-bet-dependent S1P5 expression in NK cells promotes egress from lymph nodes and bone marrow. J. Exp. Med. *206*, 2469–2481.

Ji, M., Li, H., Suh, H.C., Klarmann, K.D., Yokota, Y., and Keller, J.R. (2008). Id2 intrinsically regulates lymphoid and erythroid development via interaction with different target proteins. Blood *112*, 1068–1077.

Jin, C., Henao-Mejia, J., and Flavell, R.A. (2013). Innate immune receptors: Key regulators of metabolic disease progression. Cell Metab. *17*, 873–882.

Johansson, M.E. V, Gustafsson, J.K., Holmen-Larsson, J., Jabbar, K.S., Xia, L., Xu, H., Ghishan, F.K., Carvalho, F.A., Gewirtz, A.T., Sjovall, H., et al. (2014). Bacteria penetrate the normally impenetrable inner colon mucus layer in both murine colitis models and patients with ulcerative colitis. Gut *63*, 281–291.

Kabashima, K., Honda, T., Ginhoux, F., and Egawa, G. (2018). The immunological anatomy of the skin. Nat. Rev. Immunol.

Kabata, H., Moro, K., Fukunaga, K., Suzuki, Y., Miyata, J., Masaki, K., Betsuyaku, T., Koyasu, S., and Asano, K. (2013). Thymic stromal lymphopoietin induces corticosteroid resistance in natural helper cells during airway inflammation. Nat. Commun. *4*, 1–7.

Kamba, T., Tam, B.Y.Y., Hashizume, H., Haskell, A., Sennino, B., Mancuso, M.R., Norberg, S.M., O'Brien, S.M., Davis, R.B., Gowen, L.C., et al. (2006). VEGF-dependent plasticity of fenestrated capillaries in the normal adult microvasculature. Am. J. Physiol. Circ. Physiol. *290*, H560–H576.

Kandasamy, K., Sujatha Mohan, S., Raju, R., Keerthikumar, S., Sameer Kumar, G.S., Venugopal, A.K., Telikicherla, D., Navarro, D.J., Mathivanan, S., Pecquet, C., et al. (2010). NetPath: a public resource of curated signal transduction pathways. Genome Biol. *11*, 1–9.

Kang, C.M., Jang, A.S., Ahn, M.H., Shin, J.A., Kim, J.H., Choi, Y.S., Rhim, T.Y., and Park, C.S. (2005). Interleukin-25 and interleukin-13 production by alveolar macrophages in response to particles. Am. J. Respir. Cell Mol. Biol. *33*, 290–296.

Kansas, G.S. (1996). Selectins and Their Ligands: Current Concepts and Controversies. J. Am. Soc. Hematol. *9*, 3.

Kastner, P., Chan, S., Vogel, W.K., Zhang, L.J., Topark-Ngarm, A., Golonzhka, O., Jost, B., Le Gras, S., Gross, M.K., and Leid, M. (2010). Bcl11b represses a mature T-cell gene expression program in immature CD4+CD8+ thymocytes. Eur. J. Immunol. *40*, 2143–2154.

Khurana Hershey, G.K. (2003). IL-13 receptors and signaling pathways: An evolving web. J. Allergy Clin. Immunol. *111*, 677–690.

Kiessling, R., Klein, E., and Wigzell, H. (1975). „Natural" killer cells in the mouse. I. Cytotoxic cells with specificity for mouse Moloney leukemia cells. Specificity and distribution according to genotype. Eur. J. Immunol. *5*, 112–117.

Kim, B.S., Siracusa, M.C., Saenz, S.A., Noti, M., Monticelli, L.A., Sonnenberg, G.F., Hepworth, M.R., Van Voorhees, A.S., Comeau, M.R., and Artis, D. (2013). TSLP elicits IL-33-independent innate lymphoid cell responses to promote skin inflammation. Sci. Transl. Med. *5*.

Kim, M.H., Taparowsky, E.J., Kim, C.H., Elizabeth, J., Kim, C.H., Kim, M.H., Taparowsky, E.J., Kim, C.H., Kim Correspondence, C.H., and Kim, C.H. (2015). RetinOic Acid Differentially Regulates The Migration Of Innate Lymphoid Cell Subsets To The Gut. Immunity *43*, 107–119.

Kivisäkk, P., Mahad, D.J., Callahan, M.K., Trebst, C., Tucky, B., Wei, T., Wu, L., Baekkevold, E.S., Lassmann, H., Staugaitis, S.M., et al. (2003). Human cerebrospinal fluid central memory CD4 + T cells: Evidence for trafficking through choroid plexus and meninges via P-selectin . Proc. Natl. Acad. Sci. *100*, 8389–8394.

de Kleer, I.M., Kool, M., de Bruijn, M.J.W., Willart, M., van Moorleghem, J., Schuijs, M.J., Plantinga, M., Beyaert, R., Hams, E., Fallon, P.G., et al. (2016). Perinatal Activation of the Interleukin-33 Pathway Promotes Type 2 Immunity in the Developing Lung. Immunity *45*, 1285–1298.

Klein Wolterink, R.G.J., Serafini, N., Van Nimwegen, M., Vosshenrich, C.A.J., De Bruijn, M.J.W., Pereira, D.F., Fernandes, H.V., Hendriks, R.W., and Di Santo, J.P. (2013). Essential, dose-dependent role for the transcription factor Gata3 in the development of IL-5+ and IL-13+ type 2 innate lymphoid cells. Proc. Natl. Acad. Sci. U. S. A. *110*, 10240–10245.

Klonowski, K.D., Williams, K.J., Marzo, A.L., Blair, D.A., Lingenheld, E.G., and Lefrançois, L. (2004). Dynamics of blood-borne CD8 memory T cell migration in vivo. Immunity *20*, 551–562.

Klose, C.S.N., and Artis, D. (2016). Innate lymphoid cells as regulators of immunity, inflammation and tissue homeostasis. Nat. Immunol. *17*, 765–774.

Klose, C.S.N., Flach, M., Möhle, L., Rogell, L., Hoyler, T., Ebert, K., Fabiunke, C., Pfeifer, D., Sexl, V., Fonseca-Pereira, D., et al. (2014). Differentiation of type 1 ILCs from a common progenitor to all helper-like innate lymphoid cell lineages. Cell *157*, 340–356.

Klose, C.S.N., Mahlakõiv, T., Moeller, J.B., Rankin, L.C., Flamar, A.L., Kabata, H., Monticelli, L.A., Moriyama, S., Putzel, G.G., Rakhilin, N., et al. (2017). The neuropeptide neuromedin U stimulates innate lymphoid cells and type 2 inflammation. Nature *549*, 282–286.

Koga, S., Hozumi, K., Hirano, K.I., Yazawa, M., Terooatea, T., Minoda, A., Nagasawa, T., Koyasu, S., and Moro, K. (2018). Peripheral PDG FRa+gp38+ mesenchymal cells support the differentiation of fetal liver-derived ILC2. J. Exp. Med. *215*, 1609–1626.

Kominami, R. (2012). Role of the transcription factor Bcl11b in development and lymphomagenesis. Proc. Japan Acad. Ser. B Phys. Biol. Sci. *88*, 72–87.

Kondo, M., Weissman, I.L., and Akashi, K. (1997). Identification of clonogenic common lymphoid progenitors in mouse bone marrow. Cell *91*, 661–672.

Kotas, M.E., and Locksley, R.M. (2018). Why Innate Lymphoid Cells? Immunity *48*, 1081–1090.

Kovats, S. (2015). Estrogen receptors regulate innate immune cells and signaling pathways. Cell. Immunol. *294*, 63–69.

Kramer, G.C., Sibley, L., Aukland, K., and Renkin, E.M. (1986). Wick sampling of interstitial fluid in rat skin: Further analysis and modifications of the method. Microvasc. Res. *32*, 39–49.

Krämer, B., Goeser, F., Lutz, P., Glässner, A., Boesecke, C., Schwarze-Zander, C., Kaczmarek, D., Nischalke, H.D., Branchi, V., Manekeller, S., et al. (2017). Compartment-specific distribution of human intestinal innate lymphoid cells is altered in HIV patients under effective therapy. PLoS Pathog. *13*, 1–24.

Kredel, L.I., and Siegmund, B. (2014). Adipose-tissue and intestinal inflammation - visceral obesity and creeping fat. Front. Immunol. *5*, 1–12.

Kwok, K.H.M., Lam, K.S.L., and Xu, A. (2016). Heterogeneity of white adipose tissue: Molecular basis and clinical implications. Exp. Mol. Med. *48*, e215-12.

Labrecque, N., and Cermakian, N. (2015). Circadian clocks in the immune system. J. Biol. Rhythms *30*, 277–290.

Laffont, S., Blanquart, E., Savignac, M., Cénac, C., Laverny, G., Metzger, D., Girard, J.-P., Belz, G.T., Pelletier, L., Seillet, C., et al. (2017). Androgen signaling negatively controls group 2 innate lymphoid cells. J. Exp. Med. *214*, 1581–1592.

Lämmermann, Ti., Bader, B.L., Monkley, S.J., Worbs, T., Wedlich-Söldner, R., Hirsch, K., Keller, M., Förster, R., Critchley, D.R., Fässler, R., et al. (2008). Rapid leukocyte migration by integrin-independent flowing and squeezing. Nature *453*, 51–55.

Lange, T., Dimitrov, S., and Born, J. (2010). Effects of sleep and circadian rhythm on the human immune system: Annals of the New York Academy of Sciences. Ann. N. Y. Acad. Sci. *1193*, 48–59.

Leak, L. V., Liotta, L.A., Krutzsch, H., Jones, M., Fusaroa, V.A., Ross, S.J., Zhao, Y., and Petricoin, E.F. (2004). Proteomic analysis of lymph. Proteomics *4*, 753–765.

Leconte, J., Bagherzadeh Yazdchi, S., Panneton, V., and Suh, W.K. (2016). Inducible costimulator (ICOS) potentiates TCR-induced calcium flux by augmenting PLCγ1 activation and actin remodeling. Mol. Immunol. *79*, 38–46.

Lee, B.C., Kim, M.S., Pae, M., Yamamoto, Y., Eberlé, D., Shimada, T., Kamei, N., Park, H.S., Sasorith, S., Woo, J.R., et al. (2016). Adipose Natural Killer Cells Regulate Adipose Tissue Macrophages to Promote Insulin Resistance in Obesity. Cell Metab. *23*, 685–698.

Lee, M., Brocklyn, J.R. Van, Thangada, S., Liu, C.H., Hand, A.R., Menzeleev, R., Spiegel, S., and Hla, T. (1998). Sphingosine-1 – Phosphate as a Ligand for the G Protein – Coupled Receptor EDG-1. Science (80-.). *279*.

Lee, M.W., Odegaard, J.I., Mukundan, L., Qiu, Y., Molofsky, A.B., Nussbaum, J.C., Yun, K., Locksley, R.M., and Chawla, A. (2015). Activated type 2 innate lymphoid cells regulate beige fat biogenesis. Cell *160*, 74–87.

Lefrancais, E., Duval, A., Mirey, E., Roga, S., Espinosa, E., Cayrol, C., and Girard, J.-P. (2014). Central

domain of IL-33 is cleaved by mast cell proteases for potent activation of group-2 innate lymphoid cells. Proc. Natl. Acad. Sci. *111*, 15502–15507.

Lei, W., Ren, W., Ohmoto, M., Urban, J.F., Matsumoto, I., Margolskee, R.F., and Jiang, P. (2018). Activation of intestinal tuft cell-expressed Sucnr1 triggers type 2 immunity in the mouse small intestine. Proc. Natl. Acad. Sci. *115*, 5552–5557.

Lepper, C., and Fan, C.M. (2010). Inducible lineage tracing of Pax7-descendant cells reveals embryonic origin of adult satellite cells. Genesis *48*, 424–436.

Leung, D.Y.M., Nomura, I., Hamid, Q.A., Leung, D.Y.M., Boguniewicz, M., Howell, M.D., Nomura, I., and Hamid, Q.A. (2004). New insights into atopic dermatitis Find the latest version : Science in medicine New insights into atopic dermatitis. J Clin Invest. *113*, 651–657.

Levick, J.R., and Michel, C.C. (2010). Microvascular fluid exchange and the revised Starling principle. Cardiovasc. Res. *87*, 198–210.

Levine, J.H., Simonds, E.F., Bendall, S.C., Downing, J.R., Pe, D., Nolan, G.P., Levine, J.H., Simonds, E.F., Bendall, S.C., Davis, K.L., et al. (2015). Data-Driven Phenotypic Dissection of AML Reveals Progenitor-like Cells that Correlate with Prognosis Resource Data-Driven Phenotypic Dissection of AML Reveals Progenitor-like Cells that Correlate with Prognosis. Cell *162*, 184–197.

Ley, K. (2003). The role of selectins in inflammation and disease. Trends Mol. Med. *9*, 263–268.

Ley, K., and Kansas, G.S. (2004). Selectins in T-cell recruitment to non-lymphoid tissues and sites of inflammation. Nat. Rev. Immunol. *4*, 325–335.

Ley, K., Rivera-Nieves, J., Sandborn, W.J., and Shattil, S. (2016). Integrin-based therapeutics: Biological basis, clinical use and new drugs. Nat. Rev. Drug Discov. *15*, 173–183.

Liang, H.E., Reinhardt, R.L., Bando, J.K., Sullivan, B.M., Ho, I.C., and Locksley, R.M. (2012). Divergent expression patterns of IL-4 and IL-13 define unique functions in allergic immunity. Nat. Immunol. *13*, 58–66.

Liew, F.Y., Girard, J.P., and Turnquist, H.R. (2016). Interleukin-33 in health and disease. Nat. Rev. Immunol. *16*, 676–689.

Lim, A.I., Li, Y., Lopez-Lastra, S., Stadhouders, R., Paul, F., Casrouge, A., Serafini, N., Puel, A., Bustamante, J., Surace, L., et al. (2017). Systemic Human ILC Precursors Provide a Substrate for Tissue ILC Differentiation. Cell *168*, 1086-1100.e10.

Lim, H.W., Broxmeyer, H.E., and Kim, C.H. (2006). Regulation of Trafficking Receptor Expression in Human Forkhead Box P3 + Regulatory T Cells . J. Immunol. *177*, 840–851.

Lim, Y.C., Henault, L., Luscinskas, F.W., Lichtman, A.H., Wagers, A.J., and Kansas, G.S. (1999). Expression of functional selectin ligands on Th cells is differentially regulated by IL-12 and IL-4. J. Immunol. *162*, 3193–3201.

Liu, Y., Shao, Z., Shangguan, G., Bie, Q., and Zhang, B. (2018). Biological properties and the role of IL-25 in disease pathogenesis. J. Immunol. Res. *2018*.

Lo, C.G., Xu, Y., Proia, R.L., and Cyster, J.G. (2005). Cyclical modulation of sphingosine-1-phosphate receptor 1 surface expression during lymphocyte recirculation and relationship to lymphoid organ transit. J. Exp. Med. *201*, 291–301.

Luzina, I.G., Todd, N.W., Nacu, N., Lockatell, V., Choi, J., Hummers, L.K., and Atamas, S.P. (2009). Regulation of pulmonary inflammation and fibrosis through expression of integrins αVβ3 and αVβ5 on pulmonary T lymphocytes. Arthritis Rheum. *60*, 1530–1539.

Maazi, H., Patel, N., Sankaranarayanan, I., Suzuki, Y., Rigas, D., Soroosh, P., Freeman, G.J., Sharpe, A.H., and Akbari, O. (2015). ICOS: ICOS-Ligand Interaction Is Required for Type 2 Innate Lymphoid Cell Function, Homeostasis, and Induction of Airway Hyperreactivity. Immunity *42*, 538–551.

MacDonald, T.T., Monteleone, I., Fantini, M.C., and Monteleone, G. (2011). Regulation of homeostasis and inflammation in the intestine. Gastroenterology *140*, 1768–1775.

Mackay, C.R., Marston, W.L., and Dudler, L. (1990). Naive and memory t cells show distinct pathways of lymphocyte recirculation. J. Exp. Med. *171*, 801–817.

Mackay, L.K., Braun, A., Macleod, B.L., Collins, N., Tebartz, C., Bedoui, S., Carbone, F.R., and Gebhardt, T. (2015). Cutting Edge: CD69 Interference with Sphingosine-1-Phosphate Receptor Function Regulates Peripheral T Cell Retention. J. Immunol. *194*, 2059–2063.

Mackley, E.C., Houston, S., Marriott, C.L., Halford, E.E., Lucas, B., Cerovic, V., Filbey, K.J., Maizels, R.M., Hepworth, M.R., Sonnenberg, G.F., et al. (2015). CCR7-dependent trafficking of RORγ+ ILCs creates a unique microenvironment within mucosal draining lymph nodes. Nat. Commun. *6*, 5862.

Mahapatro, M., Foersch, S., Hefele, M., He, G.W., Giner-Ventura, E., Mchedlidze, T., Kindermann, M., Vetrano, S., Danese, S., Günther, C., et al. (2016). Programming of Intestinal Epithelial Differentiation by IL-33 Derived from Pericryptal Fibroblasts in Response to Systemic Infection. Cell Rep. *15*, 1743–1756.

Male, V., Nisoli, I., Kostrzewski, T., Allan, D.S.J., Carlyle, J.R., Lord, G.M., Wack, A., and Brady, H.J.M. (2014). The transcription factor E4bp4/Nfil3 controls commitment to the NK lineage and directly regulates Eomes and Id2 expression. J. Exp. Med. *211*, 635–642.

Man, K., Loudon, A., and Chawla, A. (2016). Immunity around the clock. Science (80-.). *354*, 999–1003.

Mandala, S., Hajdu, R., Bergstrom, J., Quackenbush, E., Xie, J., Milligan, J., Thornton, R., Shei, G., Card, D., Keohane, C., et al. (2002). Alteration of Lymphocyte Trafficking by Sphingosine-1-Phosphate Receptor Agonists. Science (80-.). *296*, 346–349.

Marchesi, V.T., and Gowans, J.L. (1964). The migration of lymphocytes through the endothelium of venules in lymph nodes: an electron microscope study. Proc. R. Soc. London. Ser. B. Biol. Sci. *159*, 283–290.

Maric, J., Ravindran, A., Mazzurana, L., Björklund, Å.K., Van Acker, A., Rao, A., Friberg, D., Dahlén, S.E., Heinemann, A., Konya, V., et al. (2018). Prostaglandin E2 suppresses human group 2 innate lymphoid cell function. J. Allergy Clin. Immunol. *141*, 1761-1773.e6.

Martin, N.T., and Martin, M.U. (2016). Interleukin 33 is a guardian of barriers and a local alarmin. Nat. Immunol. *17*, 122–131.

Martinez-Gonzalez, I., Mathä, L., Steer, C.A., Ghaedi, M., Poon, G.F.T., and Takei, F. (2016). Allergen-Experienced Group 2 Innate Lymphoid Cells Acquire Memory-like Properties and Enhance Allergic Lung Inflammation. Immunity *45*, 198–208.

Martinez-Gonzalez, I., Mathä, L., Steer, C.A., and Takei, F. (2017). Immunological Memory of Group 2 Innate Lymphoid Cells. Trends Immunol. *38*, 423–431.

Masopust, D., Choo, D., Vezys, V., Wherry, E.J., Duraiswamy, J., Akondy, R., Wang, J., Casey, K.A., Barber, D.L., Kawamura, K.S., et al. (2010). Dynamic T cell migration program provides resident memory within intestinal epithelium. J. Exp. Med. *207*, 553–564.

Massaguer, A., Perez-Del-Pulgar, S., Engel, P., Serratosa, J., Bosch, J., and Pizcueta, P. (2002). Concanavalin-A-induced liver injury is severely impaired in mice deficient in P-selectin. J. Leukoc. Biol. *72*, 262–270.

Massberg, S., Schaerli, P., Knezevic-Maramica, I., Köllnberger, M., Tubo, N., Moseman, E.A., Huff, I. V., Junt, T., Wagers, A.J., Mazo, I.B., et al. (2007). Immunosurveillance by Hematopoietic Progenitor Cells Trafficking through Blood, Lymph, and Peripheral Tissues. Cell *131*, 994–1008.

Matloubian, M., Lo, C.G., Cinamon, G., Lesneski, M.J., Xu, Y., Brinkmann, V., Allende, M.L., Proia, R.L., and Cyster, J.G. (2004). Lymphocyte egress from thymus and peripheral lymphoid organs is dependent on S1P receptor 1. Nature *427*, 355–360.

Mayer, E.A., Tillisch, K., Gupta, A., Mayer, E.A., Tillisch, K., and Gupta, A. (2015). Gut / brain axis and the microbiota Find the latest version : Gut / brain axis and the microbiota. J. Clin. Investiogation *125*, 926–938.

Mebius, R.E., Streeter, P.R., Michie, S., Butcher, E.C., and Weissman, I.L. (1996). A developmental switch in lymphocyte homing receptor and endothelial vascular addressin expression regulates lymphocyte homing and permits CD4+CD3- cells to colonize lymph nodes. Proc. Natl. Acad. Sci. U. S. A. *93*, 11019–11024.

Mebius, R.E., Rennert, P., and Weissman, I.L. (1997). Developing lymph nodes collect CD4+CD3- LTβ+ cells that can differentiate to APC, NK cells, and follicular cells but not T or B cells. Immunity *7*, 493–504.

Memezawa, a, Takada, I., Takeyama, K., Igarashi, M., Ito, S., Aiba, S., Kato, S., and Kouzmenko, a P. (2007). Id2 gene-targeted crosstalk between Wnt and retinoid signaling regulates proliferation in human keratinocytes. Oncogene *26*, 5038–5045.

Meng, Z., and Veenstra, T.D. (2007). Proteomic analysis of serum, plasma, and lymph for the identification of biomarkers. Proteomics - Clin. Appl. *1*, 747–757.

Metzger, R.J., Klein, O.D., Martin, G.R., and Krasnow, M.A. (2008). The branching programme of mouse lung development. Nature *453*, 745–750.

Michie, S.A., Streeter, P.R., Butcher, E.C., and Rouse, R. V. (1995). L-Selectin and α4β7integrin homing receptor pathways mediate peripheral lymphocyte traffic to AKR mouse hyperplastic thymus. Am. J. Pathol. *147*, 412–421.

Mielke, L.A., Groom, J.R., Rankin, L.C., Seillet, C., Masson, F., Putoczki, T., and Belz, G.T. (2013). TCF-1 Controls ILC2 and NKp46 + RORγt + Innate Lymphocyte Differentiation and Protection in Intestinal Inflammation. J. Immunol. *191*, 4383–4391.

Mikhak, Z., Strassner, J.P., and Luster, A.D. (2013). Lung dendritic cells imprint T cell lung homing and promote lung immunity through the chemokine receptor CCR4. J. Exp. Med. *210*, 1855–1869.

Milling, S., Yrlid, U., Cerovic, V., and MacPherson, G. (2010). Subsets of migrating intestinal dendritic cells. Immunol Rev *234*, 259–267.

Mindt, B.C., Fritz, J.H., and Duerr, C.U. (2018). Group 2 innate lymphoid cells in pulmonary immunity and tissue homeostasis. Front. Immunol. *in press*, 1–17.

Mionnet, C., Sanos, S.L., Mondor, I., Jorquera, A., Laugier, J.P., Germain, R.N., and Bajénoff, M. (2011). High endothelial venules as traffic control points maintaining lymphocyte population homeostasis in lymph nodes. Blood *118*, 6115–6122.

Mirchandani, A.S., Besnard, A.-G., Yip, E., Scott, C., Bain, C.C., Cerovic, V., Salmond, R.J., and Liew, F.Y. (2014). Type 2 Innate Lymphoid Cells Drive CD4+ Th2 Cell Responses. J. Immunol. *192*, 2442–2448.

Mittal, A., Middleditch, M., Ruggiero, K., Buchanan, C.M., Jullig, M., Loveday, B., Cooper, G.J.S., Windsor, J.A., and Phillips, A.R.J. (2008). The proteome of rodent mesenteric lymph. Am. J. Physiol. Liver Physiol. *295*, G895–G903.

Miyasaka, M., and Tanaka, T. (2004). Lymphocyte trafficking across high endothelial venules: Dogmas and enigmas. Nat. Rev. Immunol. *4*, 360–370.

Mizgerd, J.P. (2006). Lung infection - A public health priority. PLoS Med. *3*, 0155–0158.

Mjösberg, J.M., Trifari, S., Crellin, N.K., Peters, C.P., van Drunen, C.M., Piet, B., Fokkens, W.J., Cupedo, T., and Spits, H. (2011). Human IL-25-and IL-33-responsive type 2 innate lymphoid cells are defined by expression of CRTH2 and CD161. Nat. Immunol. *12*, 1055–1062.

Mohapatra, A., Van Dyken, S.J., Schneider, C., Nussbaum, J.C., Liang, H.E., and Locksley, R.M. (2016). Group 2 innate lymphoid cells utilize the IRF4-IL-9 module to coordinate epithelial cell maintenance of lung homeostasis. Mucosal Immunol. *9*, 275–286.

Molofsky, A.B., Nussbaum, J.C., Liang, H.E., Dyken, S.J.V., Cheng, L.E., Mohapatra, A., Chawla, A., and Locksley, R.M. (2013). Innate lymphoid type 2 cells sustain visceral adipose tissue eosinophils and alternatively activated macrophages. J. Exp. Med. *210*, 535–549.

Molofsky, A.B., Van Gool, F., Liang, H.E., Van Dyken, S.J., Nussbaum, J.C., Lee, J., Bluestone, J.A., and Locksley, R.M. (2015). InterleuKin-33 And Interferon-Γ Counter-Regulate Group 2 Innate Lymphoid Cell Activation During Immune Perturbation. Immunity *43*, 161–174.

Von Moltke, J., Ji, M., Liang, H.E., and Locksley, R.M. (2016). Tuft-cell-derived IL-25 regulates an intestinal ILC2-epithelial response circuit. Nature *529*, 221–225.

Mondino, A., Khoruts, A., and Jenkins, M.K. (1996). The anatomy of T-cell activation and tolerance. Proc. Natl. Acad. Sci. U. S. A. *93*, 2245–2252.

Monticelli, L. a., and Artis, D. (2012). Innate lymphoid cells promote lung tissue homeostasis following acute influenza virus infection. Nat. Immunol. *12*, 1045–1054.

Monticelli, L.A., Osborne, L.C., Noti, M., Tran, S. V., Zaiss, D.M.W., and Artis, D. (2015). IL-33 promotes

an innate immune pathway of intestinal tissue protection dependent on amphiregulin–EGFR interactions. Proc. Natl. Acad. Sci. *112*, 10762–10767.

Mora, J.R., and von Andrian, U.H. (2006). T-cell homing specificity and plasticity: new concepts and future challenges. Trends Immunol. *27*, 235–243.

Moreno, R.A., and Peiró, P.S. (2000). Atopic dermatitis. Med. Natur. *2000*, 112–121.

Morimoto, M., Morimoto, M., Zhao, A., Madden, K., Dawson, H., Finkelman, F., Mentink-Kane, M., Urban Jr, J., Wynn, T., and Shea-Donohue, T. (2006). Functional Importance of Regional Differences in Localized Gene Expression of Receptors for IL-13 in Murine Gut1. J. Immunol. *5*, 1–8.

Moriyama, S., Brestoff, J.R., Flamar, A.L., Moeller, J.B., Klose, C.S.N., Rankin, L.C., Yudanin, N.A., Monticelli, L.A., Putzel, G.G., Rodewald, H.R., et al. (2018). B2-Adrenergic Receptor-Mediated Negative Regulation of Group 2 Innate Lymphoid Cell Responses. Science (80-.). *359*, 1056–1061.

Moro, K., Yamada, T., Tanabe, M., Takeuchi, T., Ikawa, T., Kawamoto, H., Furusawa, J.-I.I., Ohtani, M., Fujii, H., and Koyasu, S. (2010). Innate production of TH 2 cytokines by adipose tissue-associated c-Kit+ Sca-1+ lymphoid cells. Nature *463*, 540–544.

Moro, K., Kabata, H., Tanabe, M., Koga, S., Takeno, N., Mochizuki, M., Fukunaga, K., Asano, K., Betsuyaku, T., and Koyasu, S. (2016). Interferon and IL-27 antagonize the function of group 2 innate lymphoid cells and type 2 innate immune responses. Nat. Immunol. *17*, 76–86.

Mowat, A.M., and Agace, W.W. (2014). Regional specialization within the intestinal immune system. Nat. Rev. Immunol. *14*, 667–685.

Mueller, S.N., and Mackay, L.K. (2015). Tissue-resident memory T cells: local specialists in immune defence. Nat. Rev. Immunol. *16*, 1–11.

Murphy, K.M. (2013). Transcriptional Control of Dendritic Cell Development (Elsevier Inc.).

Nadjsombati, M.S., McGinty, J.W., Lyons-Cohen, M.R., Jaffe, J.B., DiPeso, L., Schneider, C., Miller, C.N., Pollack, J.L., Nagana Gowda, G.A., Fontana, M.F., et al. (2018). Detection of Succinate by Intestinal Tuft Cells Triggers a Type 2 Innate Immune Circuit. Immunity *49*, 33–41.

Nakai, A., Hayano, Y., Furuta, F., Noda, M., and Suzuki, K. (2014). Control of lymphocyte egress from lymph nodes through β2-adrenergic receptors. J. Exp. Med. *211*, 2583–2598.

Nakanishi, K. (2018). Unique action of Interleukin-18 on T cells and other immune cells. Front. Immunol. *9*.

Nakano, H., Matsuzawa, A., Tamura, T., Yoshimoto, T., Nariuchi, H., Kakiuchi, T., Yagita, H., Miyasaka, M., and Butcher, E.C. (1997). Genetic defect in T lymphocyte-specific homing into peripheral lymph nodes. Eur. J. Immunol. *27*, 215–221.

Neill, D.R., and McKenzie, A.N.J. (2011). Nuocytes and beyond: New insights into helminth expulsion. Trends Parasitol. *27*, 214–221.

Neill, D.R., Wong, S.H., Bellosi, A., Flynn, R.J., Daly, M., Langford, T.K.A., Bucks, C., Kane, C.M., Fallon, P.G., Pannell, R., et al. (2010). Nuocytes represent a new innate effector leukocyte that mediates type-2 immunity. Nature *464*, 1367–1370.

Netea, M.G., Joosten, L.A.B., Latz, E., Mills, K.H.G., Natoli, G., Stunnenberg, H.G., ONeill, L.A.J., and Xavier, R.J. (2016). Trained immunity: A program of innate immune memory in health and disease. Science (80-.). *352*, aaf1098–aaf1098.

Nguyen, K.D. (2013). Circadian Gene Bmal1 Regulates Diurnal Oscillations of Ly6C. Science (80-.). *341*, 1483–1488.

Nguyen, V.P.K.H., Hanna, G., Rodrigues, N., Pizzuto, K., Yang, E., Van Slyke, P., Kim, H., Chen, S.H., and Dumont, D.J. (2010). Differential proteomic analysis of lymphatic, venous, and arterial endothelial cells extracted from bovine mesenteric vessels. Proteomics *10*, 1658–1672.

Novey, H.S., Marchioli, L.E., Sokol, W.N., and Wells, I.D. (1979). Papain-induced asthma-physiological and immunological features. J. Allergy Clin. Immunol. *63*, 98–103.

Nussbaum, J.C., Van Dyken, S.J., von Moltke, J., Cheng, L.E., Mohapatra, A., Molofsky, A.B., Thornton, E.E., Krummel, M.F., Chawla, A., Liang, H.-E., et al. (2013). Type 2 innate lymphoid cells control eosinophil

homeostasis. Nature *502*, 245–248.

O'Sullivan, T.E., Rapp, M., Fan, X., Weizman, O. El, Bhardwaj, P., Adams, N.M., Walzer, T., Dannenberg, A.J., and Sun, J.C. (2016). Adipose-Resident Group 1 Innate Lymphoid Cells Promote Obesity-Associated Insulin Resistance. Immunity *45*, 428–441.

De Obaldia, M.E., and Bhandoola, A. (2015). Transcriptional Regulation of Innate and Adaptive Lymphocyte Lineages. Annu. Rev. Immunol. *33*, 607–642.

Oboki, K., Ohno, T., Kajiwara, N., Arae, K., Morita, H., Ishii, A., Nambu, A., Abe, T., Kiyonari, H., Matsumoto, K., et al. (2010). IL-33 is a crucial amplifier of innate rather than acquired immunity. Proc. Natl. Acad. Sci. *107*, 18581–18586.

Oguma, T., Asano, K., and Ishizaka, A. (2008). Role of Prostaglandin D2 and Its Receptors in the Pathophysiology of Asthma. Allergol. Int. *57*, 307–312.

Oliphant, C.J., Hwang, Y.Y., Walker, J.A., Salimi, M., Wong, S.H., Brewer, J.M., Englezakis, A., Barlow, J.L., Hams, E., Scanlon, S.T., et al. (2014). MHCII-mediated dialog between group 2 innate lymphoid cells and CD4 + T cells potentiates type 2 immunity and promotes parasitic helminth expulsion. Immunity *41*, 283–295.

Osborn, O., and Olefsky, J.M. (2012). The cellular and signaling networks linking the immune system and metabolism in disease. Nat. Med. *18*, 363–374.

Oshikawa, K., Yanagisawa, K., Tominaga, S., and Sugiyama, Y. (2002). Expression and function of the ST2 gene in a murine model of allergic airway inflammation. Clin. Exp. Allergy *32*, 1520–1526.

Pabst, R., and Binns, R.M. (1989). Heterogeneity of Lymphocyte Homing Physiology: Several Mechanisms Operate in the Control of Migration to Lymphoid and Non-Lymphoid Organs In Vivo. Immunol. Rev. *108*, 83–109.

Paclik, D., Stehle, C., Lahmann, A., Hutloff, A., and Romagnani, C. (2015). ICOS regulates the pool of group 2 innate lymphoid cells under homeostatic and inflammatory conditions in mice. Eur. J. Immunol. *45*, 2766–2772.

Park, C., Hwang, I.Y., Sinha, R.K., Kamenyeva, O., Davis, M.D., and Kehrl, J.H. (2012). Lymph node B lymphocyte trafficking is constrained by anatomy and highly dependent upon chemoattractant desensitization. Blood *119*, 978–989.

Van De Pavert, S.A., Ferreira, M., Domingues, R.G., Ribeiro, H., Molenaar, R., Moreira-Santos, L., Almeida, F.F., Ibiza, S., Barbosa, I., Goverse, G., et al. (2014). Maternal retinoids control type 3 innate lymphoid cells and set the offspring immunity. Nature *508*, 123–127.

Petersen, B.C., Budelsky, A.L., Baptist, A.P., Schaller, M.A., and Lukacs, N.W. (2012). Interleukin-25 induces type 2 cytokine production in a steroid-resistant interleukin-17RB + myeloid population that exacerbates asthmatic pathology. Nat. Med. *18*, 751–758.

Pettipher, R. (2008). The roles of the prostaglandin D 2 receptors DP 1 and CRTH2 in promoting allergic responses. Br. J. Pharmacol. *153*, 191–199.

Pham, T.H.M., Okada, T., Matloubian, M., Lo, C.G., and Cyster, J.G. (2008). S1P1 Receptor Signaling Overrides Retention Mediated by Gαi-Coupled Receptors to Promote T Cell Egress. Immunity *28*, 122–133.

Pham, T.H.M., Baluk, P., Xu, Y., Grigorova, I., Bankovich, A.J., Pappu, R., Coughlin, S.R., McDonald, D.M., Schwab, S.R., and Cyster, J.G. (2010). Lymphatic endothelial cell sphingosine kinase activity is required for lymphocyte egress and lymphatic patterning. J. Exp. Med. *207*, 17–27.

Popova, T.G., Espina, V., Zhou, W., Mueller, C., Liotta, L., and Popov, S.G. (2014). Whole proteome analysis of mouse lymph nodes in cutaneous anthrax. PLoS One *9*.

Possot, C., Schmutz, S., Chea, S., Boucontet, L., Louise, A., Cumano, A., and Golub, R. (2011). Notch signaling is necessary for adult, but not fetal, development of RORγt+ innate lymphoid cells. Nat. Immunol. *12*, 949–958.

Powell, D.W., Pinchuk, I.V., Saada, J.I., Chen, X., and Mifflin, R.C. (2011). Mesenchymal Cells of the Intestinal Lamina Propria. Annu. Rev. Physiol. *73*, 213–237.

Del Prete, G., De Carli, M., Almerigogna, F., Giudizi, M.G., Biagiotti, R., and Romagnani, S. (1993). Human IL-10 is produced by both type 1 helper (Th1) and type 2 helper (Th2) T cell clones and inhibits

their antigen-specific proliferation and cytokine production. J. Immunol. *150*, 353–360.

Price, A.E., Liang, H.-E., Sullivan, B.M., Reinhardt, R.L., Eisley, C.J., Erle, D.J., and Locksley, R.M. (2010). Systemically dispersed innate IL-13-expressing cells in type 2 immunity. Proc. Natl. Acad. Sci. *107*, 11489–11494.

Qu, C., Edwards, E.W., Tacke, F., Angeli, V., Llodrá, J., Sanchez-Schmitz, G., Garin, A., Haque, N.S., Peters, W., Van Rooijen, N., et al. (2004). Role of CCR8 and other chemokine pathways in the migration of monocyte-derived dendritic cells to lymph nodes. J. Exp. Med. *200*, 1231–1241.

Quintin, J., Saeed, S., Martens, J.H.A., Giamarellos-Bourboulis, E.J., Ifrim, D.C., Logie, C., Jacobs, L., Jansen, T., Kullberg, B.J., Wijmenga, C., et al. (2012). Candida albicans infection affords protection against reinfection via functional reprogramming of monocytes. Cell Host Microbe *12*, 223–232.

Rahbar, E., Akl, T., Coté, G.L., Moore, J.E., and Zawieja, D.C. (2014). Lymph transport in rat mesenteric lymphatics experiencing edemagenic stress. Microcirculation *21*, 359–367.

Rajput, C., Cui, T., Han, M., Lei, J., Hinde, J.L., Wu, Q., Kelley Bentley, J., and Hershenson, M.B. (2017). RORα-dependent type 2 innate lymphoid cells are required and sufficient for mucous metaplasia in immature mice. Am. J. Physiol. - Lung Cell. Mol. Physiol. *312*, L983–L993.

Randolph, G.J., and Miller, N.E. (2014). Lymphatic transport of high-density lipoproteins and chylomicrons. J. Clin. Invest. *124*, 929–935.

Randolph, G.J., Angeli, V., and Swartz, M.A. (2005). Dendritic-cell trafficking to lymph nodes through lymphatic vessels. Nat. Rev. Immunol. *5*, 617–628.

Randolph, G.J., Ochando, J., and Partida-Sánchez, S. (2008). Migration of Dendritic Cell Subsets and their Precursors. Annu. Rev. Immunol. *26*, 293–316.

Randolph, G.J., Ivanov, S., Zinselmeyer, B.H., and Scallan, J.P. (2017). The Lymphatic System: Integral Roles in Immunity. Annu. Rev. Immunol. *35*, 31–52.

Reid, L., Meyrick, B., Antony, V.B., Chang, L.Y., Crapo, J.D., and Reynolds, H.Y. (2005). The mysterious pulmonary brush cell: A cell in search of a function. Am. J. Respir. Crit. Care Med. *172*, 136–139.

Reinisch, W., Sandborn, W., Danese, S., Cataldi, F., Hebuterne, X., Salzberg, B., Klopocka, M., Tarabar, D., Vanasek, T., Gregus, M., et al. (2015). 901a A Randomized, Multicenter Double-Blind, Placebo-Controlled Study of the Safety and Efficacy of Anti-MAdCAM Antibody PF-00547659 (PF) in Patients With Moderate to Severe Ulcerative Colitis: Results of the TURANDOT Study. Gastroenterology *148*, S-1193.

Reiss, Y., Proudfoot, A.E., Power, C.A., Campbell, J.J., and Butcher, E.C. (2001). CC Chemokine Receptor (CCR)4 and the CCR10 Ligand Cutaneous T Cell–attracting Chemokine (CTACK) in Lymphocyte Trafficking to Inflamed Skin. J. Exp. Med. *194*, 1541–1547.

Ricardo-Gonzalez, R.R., Van Dyken, S.J., Schneider, C., Lee, J., Nussbaum, J.C., Liang, H.E., Vaka, D., Eckalbar, W.L., Molofsky, A.B., Erle, D.J., et al. (2018). Tissue signals imprint ILC2 identity with anticipatory function. Nat. Immunol. *19*, 1093–1099.

Rockson, S.G. (2007). Molecular insights into the microvascular regulation of lymph formation. Lymphat. Res. Biol. *5*, 149.

Roediger, B., Kyle, R., Yip, K.H., Sumaria, N., Guy, T. V., Kim, B.S., Mitchell, A.J., Tay, S.S., Jain, R., Forbes-Blom, E., et al. (2013). Cutaneous immunosurveillance and regulation of inflammation by group 2 innate lymphoid cells. Nat. Immunol. *14*, 564–573.

Rosen, S.D. (2004). Ligands for L-Selectin: Homing, Inflammation, and Beyond. Annu. Rev. Immunol. *22*, 129–156.

Rosen, E.D., and Spiegelman, B.M. (2014). What we talk about when we talk about risk. The Lancet Psychiatry *1*, 95.

Rot, A., and von Andrian, U.H. (2004). Chemokines in innate and adaptive host defense: basic chemokinese grammar for immune cells. Annu. Rev. Immunol. *22*, 891–928.

Ruiter, B., Patil, S.U., and Shreffler, W.G. (2015). Vitamins A and D have antagonistic effects on expression of effector cytokines and gut-homing integrin in human innate lymphoid cells. Clin. Exp. Allergy *45*, 1214–1225.

Saeed, S., Quintin, J., Kerstens, H.H.D., Rao, N.A., Aghajanirefah, A., Matarese, F., Cheng, S.C., Ratter, J., Berentsem, K., Van Der Ent, M.A., et al. (2014). Epigenetic programming of monocyte-to-macrophage differentiation and trained innate immunity. Science (80-.). *345*.

Saenz, S.A., Noti, M., and Artis, D. (2010). Innate immune cell populations function as initiators and effectors in Th2 cytokine responses. Trends Immunol. *31*, 407–413.

Salimi, M., Barlow, J.L., Saunders, S.P., Xue, L., Gutowska-Owsiak, D., Wang, X., Huang, L.-C., Johnson, D., Scanlon, S.T., McKenzie, A.N.J., et al. (2013). A role for IL-25 and IL-33–driven type-2 innate lymphoid cells in atopic dermatitis. J. Exp. Med. *210*, 2939–2950.

Salmi, M., Alanen, K., Grenman, S., Briskin, M., Butcher, E.C., and Jalkanen, S. (2001). Immune cell trafficking in uterus and early life is dominated by the mucosal addressin MAdCAM-1 in humans. Gastroenterology *121*, 853–864.

Sanchez-Gurmaches, J., Hung, C.M., Sparks, C.A., Tang, Y., Li, H., and Guertin, D.A. (2012). PTEN loss in the Myf5 lineage redistributes body fat and reveals subsets of white adipocytes that arise from Myf5 precursors. Cell Metab. *16*, 348–362.

Sandborn, W.J., Colombel, J.F., Enns, R., Feagan, B.G., Hanauer, S.B., Lawrance, I.C., Panaccione, R., Sanders, M., Schreiber, S., Targan, S., et al. (2005). Natalizumab induction and maintenance therapy for Crohn's disease. N. Engl. J. Med. *353*, 1912–1925.

Sandborn, W.J., Feagan, B.G., Rutgeerts, P., Hanauer, S., Colombel, J.F., Sands, B.E., Lukas, M., Fedorak, R.N., Lee, S., Bressler, B., et al. (2013). Vedolizumab as induction and maintenance therapy for Crohn's disease. N. Engl. J. Med. *369*, 711–721.

Santambrogio, L. (2011). Immunology of the lymphatic system.

Sato, A. (2007). Tuft cells. Anat. Sci. Int. *82*, 187–199.

Sawicka, E., Dubois, G., Jarai, G., Edwards, M., Thomas, M., Nicholls, A., Albert, R., Newson, C., Brinkmann, V., and Walker, C. (2005). The Sphingosine 1-Phosphate Receptor Agonist FTY720 Differentially Affects the Sequestration of CD4 + /CD25 + T-Regulatory Cells and Enhances Their Functional Activity . J. Immunol. *175*, 7973–7980.

Scanlon, S.T., and McKenzie, A.N.J. (2012). Type 2 innate lymphoid cells: New players in asthma and allergy. Curr. Opin. Immunol. *24*, 707–712.

Scheiermann, C., Kunisaki, Y., Lucas, D., Chow, A., Jang, J.E., Zhang, D., Hashimoto, D., Merad, M., and Frenette, P.S. (2012). Adrenergic nerves govern circadian leukocyte recruitment to tissues. Immunity *37*, 290–301.

Scheiermann, C., Kunisaki, Y., and Frenette, P.S. (2013). Circadian control of the immune system. Nat. Rev. Immunol. *13*, 190–198.

Scheiermann, C., Gibbs, J., Ince, L., and Loudon, A. (2018). Clocking in to immunity. Nat. Rev. Immunol. *18*, 423–437.

Schenkel, J.M., and Masopust, D. (2014). Tissue-resident memory T cells. Immunity *41*, 886–897.

Schmid-Schonbein, G.W. (1990). Microlymphatics and lymph flow. Physiol. Rev. *70*, 987–1028.

Schneider, C., O'Leary, C.E., von Moltke, J., Liang, H.E., Ang, Q.Y., Turnbaugh, P.J., Radhakrishnan, S., Pellizzon, M., Ma, A., and Locksley, R.M. (2018). A Metabolite-Triggered Tuft Cell-ILC2 Circuit Drives Small Intestinal Remodeling. Cell 1–14.

Schneider, C., Lee, J., Koga, S., Ricardo-Gonzalez, R.R., Nussbaum, J.C., Smith, L.K., Villeda, S.A., Liang, H.E., and Locksley, R.M. (2019). Tissue-Resident Group 2 Innate Lymphoid Cells Differentiate by Layered Ontogeny and In Situ Perinatal Priming. Immunity *50*, 1425-1438.e5.

Schuijs, M.J., and Halim, T.Y.F. (2016). Group 2 innate lymphocytes at the interface between innate and adaptive immunity. Ann. N. Y. Acad. Sci. *1417*, 87–103.

Schwab, S.R., Pereira, J.P., Matloubian, M., Xu, Y., Huang, Y., and Cyster, J.G. (2005). Lymphocyte sequestration through S1P lyase inhibition and disruption of S1P gradients. Science (80-.). *309*, 1735–1739.

Scott, C.L., and Guilliams, M. (2018). Tissue Unit-ed: Lung Cells Team up to Drive Alveolar Macrophage Development. Cell *175*, 898–900.

Seale, P., Bjork, B., Yang, W., Kajimura, S., Chin, S., Kuang, S., Scimè, A., Devarakonda, S., Conroe, H.M., Erdjument-Bromage, H., et al. (2008). PRDM16 controls a brown fat/skeletal muscle switch. Nature *454*, 961–967.

Serafini, N., Klein Wolterink, R.G.J., Satoh-Takayama, N., Xu, W., Vosshenrich, C.A.J., Hendriks, R.W., and Di Santo, J.P. (2014). Gata3 drives development of RORγt+ group 3 innate lymphoid cells. J. Exp. Med. *211*, 199–208.

Serra, M., and Saba, J.D. (2010). Sphingosine 1-phosphate lyase, a key regulator of sphingosine 1-phosphate signaling and function. Adv. Enzyme Regul. *50*, 349–362.

Shamri, R., Grabovsky, V., Gauguet, J.M., Feigelson, S., Manevich, E., Kolanus, W., Robinson, M.K., Staunton, D.E., Von Andrian, U.H., and Alon, R. (2005). Lymphocyte arrest requires instantaneous induction of an extended LFA-1 conformation mediated by endothelium-bound chemokines. Nat. Immunol. *6*, 497–506.

Sharpe, A.H., and Pauken, K.E. (2018). The diverse functions of the PD1 inhibitory pathway. Nat. Rev. Immunol. *18*, 153–167.

Shimaoka, M., and Springer, T.A. (2003). Therapeutic antagonists and conformational regulation of integrin function. Nat. Rev. Drug Discov. *2*, 703–716.

Shimba, A., Cui, G., Tani-ichi, S., Ogawa, M., Abe, S., Okazaki, F., Kitano, S., Miyachi, H., Yamada, H., Hara, T., et al. (2018). Glucocorticoids Drive Diurnal Oscillations in T Cell Distribution and Responses by Inducing Interleukin-7 Receptor and CXCR4. Immunity *48*, 286-298.e6.

Shiow, L.R., Rosen, D.B., Brdickova, N., Xu, Y., An, J., Lanier, L.L., Cyster, J.G., and Matloubian, M. (2006). CD69 acts downstream of interferon-alpha/beta to inhibit S1P1 and lymphocyte egress from lymphoid organs. Nature *440*, 540–544.

Simoni, Y., Fehlings, M., Kløverpris, H.N., McGovern, N., Koo, S.L., Loh, C.Y., Lim, S., Kurioka, A., Fergusson, J.R., Tang, C.L., et al. (2017). Human Innate Lymphoid Cell Subsets Possess Tissue-Type Based Heterogeneity in Phenotype and Frequency. Immunity *46*, 148–161.

Singh, R.K., Gupta, S., Dastidar, S., and Ray, A. (2010). Cysteinyl leukotrienes and their receptors: Molecular and functional characteristics. Pharmacology *85*, 336–349.

Sinha, R.K., Park, C., Hwang, I.Y., Davis, M.D., and Kehrl, J.H. (2009). B Lymphocytes Exit Lymph Nodes through Cortical Lymphatic Sinusoids by a Mechanism Independent of Sphingosine-1-Phosphate-Mediated Chemotaxis. Immunity *30*, 434–446.

Somers, W.S., Shaw, G.D., and Camphausen, R.T. (2001). Insights into the molecular basis of leukocyte tethering and rolling revealed by structures of P- and E-selectin bound to SLeX and PSGL-1. Cell *105*, 971.

Spencer, S.P., Wilhelm, C., Yang, Q., Hall, J.A., Bouladoux, N., Boyd, A., Nutman, T.B., Urban, J.F., Wang, J., Ramalingam, T.R., et al. (2014). Adaptation of innate lymphoid cells to a micronutrient deficiency promotes type 2 barrier immunity. Science (80-.). *343*, 432–437.

Spiegel, S., and Milstien, S. (2011). The outs and the ins of sphingosine-1-phosphate in immunity. Nat. Rev. Immunol. *11*, 403–415.

Spits, H., Artis, D., Colonna, M., Diefenbach, A., Di Santo, J.P., Eberl, G., Koyasu, S., Locksley, R.M., McKenzie, A.N.J., Mebius, R.E., et al. (2013). Innate lymphoid cells-a proposal for uniform nomenclature. Nat. Rev. Immunol. *13*, 145–149.

Spooner, C.J., Lesch, J., Yan, D., Khan, A.A., Abbas, A., Ramirez-Carrozzi, V., Zhou, M., Soriano, R., Eastham-Anderson, J., Diehl, L., et al. (2013). Specification of type 2 innate lymphocytes by the transcriptional determinant Gfi1. Nat. Immunol. *14*, 1229–1236.

Squire, J.M., Chew, M., Nneji, G., Neal, C., Barry, J., and Michel, C. (2001). Quasi-periodic substructure in the microvessel endothelial glycocalyx: A possible explanation for molecular filtering? J. Struct. Biol. *136*, 239–255.

Steer, C.A., Martinez-Gonzalez, I., Ghaedi, M., Allinger, P., Mathä, L., and Takei, F. (2017). Group 2 innate lymphoid cell activation in the neonatal lung drives type 2 immunity and allergen sensitization. J. Allergy Clin. Immunol. *140*, 593-595.e3.

Stier, M.T., Zhang, J., Goleniewska, K., Cephus, J.Y., Rusznak, M., Wu, L., Van Kaer, L., Zhou, B., Newcomb, D.C., and Peebles, R.S. (2018). IL-33 promotes the egress of group 2 innate lymphoid cells from the bone marrow. J. Exp. Med. *215*, 263–281.

Sun, H., Liu, J., Zheng, Y.J., Pan, Y.D., Zhang, K., and Chen, J.F. (2014). Distinct chemokine signaling regulates integrin ligand specificity to dictate tissue-specific lymphocyte homing. Dev. Cell *30*, 61–70.

Sun, J.C., Beilke, J.N., and Lanier, L.L. (2009). Adaptive immune features of natural killer cells. Nature *457*, 557–561.

Sun, X.H., Copeland, N.G., Jenkins, N.A., and Baltimore, D. (1991). Id proteins Id1 and Id2 selectively inhibit DNA binding by one class of helix-loop-helix proteins. Mol. Cell. Biol. *11*, 5603–5611.

Suzukawa, M., Morita, H., Nambu, A., Arae, K., Shimura, E., Shibui, A., Yamaguchi, S., Suzukawa, K., Nakanishi, W., Oboki, K., et al. (2012). Epithelial Cell-Derived IL-25, but Not Th17 Cell-Derived IL-17 or IL-17F, Is Crucial for Murine Asthma. J. Immunol. *189*, 3641–3652.

Suzuki, K., Hayano, Y., Nakai, A., Furuta, F., Noda, M., and Kazuhiro Suzuki,1 Yuki Hayano,1 Akiko Nakai,1 Fumika Furuta,1 and Masaki Noda2, 3 (2016). Adrenergic control of the adaptive immune response by diurnal lymphocyte recirculation through lymph nodes. J. Exp. Med. *213*, 2567–2574.

Svensson, M., Marsal, J., Ericsson, A., Carramolino, L., Brodén, T., Márquez, G., and Agace, W.W. (2002). CCL25 mediates the localization to the small-intestinal mucosa Rapid Publication. J. Clin. Invest. *110*, 1113–1121.

Swain, S.L., Croft, M., Dubey, C., Haynes, L., Rogers, P., Zhang, X., and Bradley, L.M. (1996). From Naive to Memory T Cells. Immunol. Rev. *150*, 143–167.

Swartz, M.A., and Randolph, G.J. (2014). Introduction to the special issue on lymphangiogenesis in inflammation. Angiogenesis *17*, 323–324.

Tait Wojno, E.D., and Artis, D. (2012). Innate lymphoid cells: Balancing immunity, inflammation, and tissue repair in the intestine. Cell Host Microbe *12*, 445–457.

Takada, Y., Ye, X., and Simon, S. (2007). The integrins. Genome Biol. *8*.

Takatsu, K. (2011). Interleukin-5 and IL-5 receptor in health and diseases. Proc. Japan Acad. Ser. B Phys. Biol. Sci. *87*, 463–485.

Taliaferro, W.H., and Sarles, M.P. (1939). The cellular reactions in the skin, lungs and intestine of normal and immune rats after infection with nippostrongylus muris. J. Infect. Dis. *64*, 157–192.

Tammela, T., and Alitalo, K. (2010). Lymphangiogenesis: Molecular Mechanisms and Future Promise. Cell *140*, 460–476.

Tammela, T., Petrova, T. V., and Alitalo, K. (2005). Molecular lymphangiogenesis: New players. Trends Cell Biol. *15*, 434–441.

Targan, S.R., Feagan, B.G., Fedorak, R.N., Lashner, B.A., Panaccione, R., Present, D.H., Spehlmann, M.E., Rutgeerts, P.J., Tulassay, Z., Volfova, M., et al. (2007). Natalizumab for the Treatment of Active Crohn's Disease: Results of the ENCORE Trial. Gastroenterology *132*, 1672–1683.

Taylor, S., Huang, Y., Mallett, G., Stathopoulou, C., Felizardo, T.C., Sun, M.A., Martin, E.L., Zhu, N., Woodward, E.L., Elias, M.S., et al. (2017). PD-1 regulates KLRG1 + group 2 innate lymphoid cells. J. Exp. Med. *214*, 1663–1678.

Tchkonia, T., Thomou, T., Zhu, Y., Karagiannides, I., Pothoulakis, C., Jensen, M.D., and Kirkland, J.L. (2013). Mechanisms and metabolic implications of regional differences among fat depots. Cell Metab. *17*, 644–656.

Teijaro, J.R., Walsh, K.B., Cahalan, S., Fremgen, D.M., Roberts, E., Scott, F., Martinborough, E., Peach, R., Oldstone, M.B.A., and Rosen, H. (2011). Endothelial cells are central orchestrators of cytokine amplification during influenza virus infection. Cell *146*, 980–991.

Thio, C.L.P., Chi, P.Y., Lai, A.C.Y., and Chang, Y.J. (2018). Regulation of type 2 innate lymphoid cell–dependent airway hyperreactivity by butyrate. J. Allergy Clin. Immunol. *142*, 1867-1883.e12.

Tilney, N.L. (1971). Patterns of lymphatic drainage in the adult laboratory rat. J. Anat. *109*, 369–383.

Toki, S., Goleniewska, K., Reiss, S., Zhou, W., Newcomb, D.C., Bloodworth, M.H., Stier, M.T., Boyd, K.L., Polosukhin, V. V., Subramaniam, S., et al. (2016). The histone deacetylase inhibitor trichostatin A suppresses murine innate allergic inflammation by blocking group 2 innate lymphoid cell (ILC2) activation. Thorax *71*, 633–645.

Tomura, M., Yoshida, N., Tanaka, J., Karasawa, S., Miwa, Y., Miyawaki, A., and Kanagawa, O. (2008). Monitoring cellular movement in vivo with photoconvertible fluorescence protein "Kaede" transgenic mice. Proc. Natl. Acad. Sci. U. S. A. *105*, 10871–10876.

Townsend, M.J., Weinmann, A.S., Matsuda, J.L., Salomon, R., Farnham, P.J., Biron, C.A., Gapin, L., and Glimcher, L.H. (2004). T-bet regulates the terminal maturation and homeostasis of NK and Vα14i NKT cells. Immunity *20*, 477–494.

Tran, T.T., Yamamoto, Y., Gesta, S., and Kahn, C.R. (2008). Beneficial Effects of Subcutaneous Fat Transplantation on Metabolism. Cell Metab. *7*, 410–420.

Tso, P., Pitts, V., and Granger, D.N. (1985). Role of lymph flow in intestinal chylomicron transport. Am. J. Physiol. Liver Physiol. *249*, G21–G28.

Tsunemi, S., Iwasaki, T., Kitano, S., Imado, T., Miyazawa, K., and Sano, H. (2010). Effects of the novel immunosuppressant FTY720 in a murine rheumatoid arthritis model. Clin. Immunol. *136*, 197–204.

Turner, J.-E., Morrison, P.J., Wilhelm, C., Wilson, M., Ahlfors, H., Renauld, J.-C., Panzer, U., Helmby, H., and Stockinger, B. (2013). IL-9–mediated survival of type 2 innate lymphoid cells promotes damage control in helminth-induced lung inflammation. J. Exp. Med. *210*, 2951–2965.

Tyler, R.W., and Everett, N.B. (1972). Radioautographic study of cellular migration using parabiotic rats. Blood *39*, 249–266.

Veenstra, T.D., Conrads, T.P., Hood, B.L., Avellino, A.M., Ellenbogen, R.G., and Morrison, R.S. (2005). Biomarkers: Mining the Biofluid Proteome. Mol. Cell. Proteomics *4*, 409–418.

Vély, F., Barlogis, V., Vallentin, B., Neven, B., Piperoglou, C., Ebbo, M., Perchet, T., Petit, M., Yessaad, N., Touzot, F., et al. (2016). Evidence of innate lymphoid cell redundancy in humans. Nat. Immunol. *17*, 1291–1299.

Vermeire, S., Sandborn, W.J., Danese, S., Hébuterne, X., Salzberg, B.A., Klopocka, M., Tarabar, D., Vanasek, T., Greguš, M., Hellstern, P.A., et al. (2017). Anti-MAdCAM antibody (PF-00547659) for ulcerative colitis (TURANDOT): a phase 2, randomised, double-blind, placebo-controlled trial. Lancet *390*, 135–144.

Vestweber, D., and Blanks, J.E. (1999). Mechanisms That Regulate the Function of the Selectins and Their Ligands. Physiol. Rev. *79*, 181–213.

Vittet, D. (2014). Lymphatic collecting vessel maturation and valve morphogenesis. Microvasc. Res. *96*, 31–37.

Vivier, E., Van De Pavert, S.A., Cooper, M.D., and Belz, G.T. (2016). The evolution of innate lymphoid cells. Nat. Immunol. *17*, 790–794.

Vivier, E., Artis, D., Colonna, M., Diefenbach, A., Di Santo, J.P., Eberl, G., Koyasu, S., Locksley, R.M., McKenzie, A.N.J., Mebius, R.E., et al. (2018). Innate Lymphoid Cells: 10 Years On. Cell *174*, 1054–1066.

Vosshenrich, C. a J., García-Ojeda, M.E., Samson-Villéger, S.I., Pasqualetto, V., Enault, L., Richard-Le Goff, O., Corcuff, E., Guy-Grand, D., Rocha, B., Cumano, A., et al. (2006). A thymic pathway of mouse natural killer cell development characterized by expression of GATA-3 and CD127. Nat. Immunol. *7*, 1217–1224.

Walford, H.H., and Doherty, T.A. (2013). STAT6 and lung inflammation. Jak-Stat *2*, e25301.

Walker, J.A., and McKenzie, A.N.J. (2013). Development and function of group 2 innate lymphoid cells. Curr. Opin. Immunol. *25*, 148–155.

Walker, J.A., Oliphant, C.J., Englezakis, A., Yu, Y., Clare, S., Rodewald, H.R., Belz, G., Liu, P., Fallon, P.G., and McKenzie, A.N.J. (2015). Bcl11b is essential for group 2 innate lymphoid cell development. J. Exp. Med. *212*, 875–882.

Walker, J.A., Clark, P.A., Crisp, A., Barlow, J.L., Szeto, A., Ferreira, A.C.F., Rana, B.M.J., Jolin, H.E., Rodriguez-Rodriguez, N., Sivasubramaniam, M., et al. (2019). Polychromic Reporter Mice Reveal Unappreciated Innate Lymphoid Cell Progenitor Heterogeneity and Elusive ILC3 Progenitors in Bone Marrow. Immunity *51*, 104-118.e7.

Wallrapp, A., Riesenfeld, S.J., Burkett, P.R., Abdulnour, R.E.E., Nyman, J., Dionne, D., Hofree, M., Cuoco, M.S., Rodman, C., Farouq, D., et al. (2017). The neuropeptide NMU amplifies ILC2-driven allergic lung inflammation. Nature *549*, 351–356.

Wang, W., and Seale, P. (2016). Control of brown and beige fat development. Nat. Rev. Mol. Cell Biol. *17*, 691–702.

Wang, Y.-H., Angkasekwinai, P., Lu, N., Voo, K.S., Arima, K., Hanabuchi, S., Hippe, A., Corrigan, C.J., Dong, C., Homey, B., et al. (2007). IL-25 augments type 2 immune responses by enhancing the expansion and functions of TSLP-DC–activated Th2 memory cells. J. Exp. Med. *204*, 1837–1847.

Weber, B.N., Chi, A.W.S., Chavez, A., Yashiro-Ohtani, Y., Yang, Q., Shestova, O., and Bhandoola, A. (2011). A critical role for TCF-1 in T-lineage specification and differentiation. Nature *476*, 63–69.

Wensveen, F.M., Jelenčić, V., Valentić, S., Šestan, M., Wensveen, T.T., Theurich, S., Glasner, A., Mendrila, D., Štimac, D., Wunderlich, F.T., et al. (2015). NK cells link obesity-induced adipose stress to inflammation and insulin resistance. Nat. Immunol. *16*, 376–385.

Wilen, C.B., Lee, S., Hsieh, L.L., Orchard, R.C., Desai, C., Hykes, B.L., McAllaster, M.R., Balce, D.R., Feehley, T., Brestoff, J.R., et al. (2018). Tropism for tuft cells determines immune promotion of norovirus pathogenesis. Science (80-.). *360*, 204–208.

Wilhelm, C., Hirota, K., Stieglitz, B., Van Snick, J., Tolaini, M., Lahl, K., Sparwasser, T., Helmby, H., and Stockinger, B. (2011). An IL-9 fate reporter demonstrates the induction of an innate IL-9 response in lung inflammation. Nat. Immunol. *12*, 1071–1077.

Winer, D.A., Luck, H., Tsai, S., and Winer, S. (2016). The intestinal immune system in obesity and insulin resistance. Cell Metab. *23*, 413–426.

Wolber, F.M., Lowe, J.B., Stoolman, L.M., Curtis, J.L., Mály, P., Kelly, R.J., Smith, P., and Yednock, T.A. (1998). Endothelial selectins and α 4 integrins regulate independent pathways of T lymphocyte recruitment in the pulmonary immune response. J. Immunol. *161*, 4396–4403.

Wong, S.H., Walker, J.A., Jolin, H.E., Drynan, L.F., Hams, E., Camelo, A., Barlow, J.L., Neill, D.R., Panova, V., Koch, U., et al. (2012). Transcription factor RORα is critical for nuocyte development. Nat. Immunol. *13*, 229–236.

Woodberry, T., Suscovich, T.J., Henry, L.M., August, M., Waring, M.T., Kaur, A., Hess, C., Kutok, J.L., Aster, J.C., Wang, F., et al. (2005). α E β 7 (CD103) Expression Identifies a Highly Active, Tonsil-Resident Effector-Memory CTL Population . J. Immunol. *175*, 4355–4362.

Xu, B., Wagner, N., Pham, L.N., Magno, V., Shan, Z., Butcher, E.C., and Michie, S.A. (2003). Lymphocyte homing to bronchus-associated lymphoid tissue (BALT) is mediated by L-selectin/PNAd, α4β1 integrin/VCAM-1, and LFA-1 adhesion pathways. J. Exp. Med. *197*, 1255–1267.

Xu, W., Cherrier, D.E., Chea, S., Vosshenrich, C., Serafini, N., Petit, M., Liu, P., Golub, R., and Di Santo, J.P. (2019). An Id2RFP-Reporter Mouse Redefines Innate Lymphoid Cell Precursor Potentials. Immunity *50*, 1054-1068.e3.

Xue, L., Salimi, M., Panse, I., Mjösberg, J.M., McKenzie, A.N.J., Spits, H., Klenerman, P., and Ogg, G. (2014). Prostaglandin D 2 activates group 2 innate lymphoid cells through chemoattractant receptor-homologous molecule expressed on T H 2 cells. J. Allergy Clin. Immunol. *133*.

Yagi, R., Zhong, C., Northrup, D.L., Yu, F., Bouladoux, N., Spencer, S., Hu, G., Barron, L., Sharma, S., Nakayama, T., et al. (2014). The transcription factor GATA3 is critical for the development of all IL-7Rα-expressing innate lymphoid cells. Immunity *40*, 378–388.

Yang, D., Yang, W., Tian, Z., van Velkinburgh, J.C., Song, J., Wu, Y., and Ni, B. (2016a). Innate lymphoid cells as novel regulators of obesity and its-associated metabolic dysfunction. Obes. Rev. *17*, 485–498.

Yang, D., Han, Z., and Oppenheim, J.J. (2017). Alarmins and immunity. Immunol. Rev. *280*, 41–56.

Yang, J., Hu, S., Zhao, L., Kaplan, D.H., Perdew, G.H., and Xiong, N. (2016b). Selective programming of CCR10+ innate lymphoid cells in skin-draining lymph nodes for cutaneous homeostatic regulation. Nat. Immunol. *17*, 48–56.

Yang, Q., Monticelli, L.A., Saenz, S.A., Chi, A.W.S., Sonnenberg, G.F., Tang, J., De Obaldia, M.E., Bailis, W., Bryson, J.L., Toscano, K., et al. (2013a). T Cell Factor 1 Is Required for Group 2 Innate Lymphoid Cell

Generation. Immunity *38*, 694–704.

Yang, Q., Li, F., Harly, C., Xing, S., Ye, L., Xia, X., Wang, H., Wang, X., Yu, S., Zhou, X., et al. (2015). TCF-1 upregulation identifies early innate lymphoid progenitors in the bone marrow. Nat. Immunol. *16*, 1044–1050.

Yang, Y., Zhang, Y., Cao, Z., Ji, H., Yang, X., Iwamoto, H., Wahlberg, E., Lanne, T., Sun, B., and Cao, Y. (2013b). Anti-VEGF- and anti-VEGF receptor-induced vascular alteration in mouse healthy tissues. Proc. Natl. Acad. Sci. *110*, 12018–12023.

Yang, Z., Chen, M., Fialkow, L.B., Ellett, J.D., Wu, R., Brinkmann, V., Nadler, J.L., and Lynch, K.R. (2003). The immune modulator FYT720 prevents autoimmune diabetes in nonobese diabetic mice. Clin. Immunol. *107*, 30–35.

Yednock, T.A., Cannon, C., Fritz, L.C., Sanchez-Madrid, F., Steinman, L., and Karin, N. (1992). Prevention of experimental autoimmune encephalomyelitis by antibodies against a4b1 integrin. Lett. to Nat. *356*, 63–66.

Yokota, Y., Mansouri, A., Mori, S., Sugawara, S., Adachi, S., Nishikawa, S.I., and Gruss, P. (1999). Development of peripheral lymphoid organs and natural killer cells depends on the helix-loop-helix inhibitor Id2. Nature *397*, 702–706.

Yoshinaga, S.K., Whorlskey, J.S., Khare, S.D., Sarmiento, U., Guo, J., Horan, T., Shih, G., Zhang, M., Coccia, M.A., Kohno, T., et al. (1999). T-cell co-stimulation through B7RP-1 and ICOS. Nature *402*, 827–830.

Yu, J.C., Khodadadi, H., Malik, A., Davidson, B., Salles, É. da S.L., Bhatia, J., Hale, V.L., and Baban, B. (2018). Innate Immunity of Neonates and Infants. Front. Immunol. *9*, 1759.

Yu, X., Pappu, R., Ramirez-Carrozzi, V., Ota, N., Caplazi, P., Zhang, J., Yan, D., Xu, M., Lee, W.P., and Grogan, J.L. (2014). TNF superfamily member TL1A elicits type 2 innate lymphoid cells at mucosal barriers. Mucosal Immunol. *7*, 730–740.

Yu, Y., Wang, C., Clare, S., Wang, J., Lee, S.C., Brandt, C., Burke, S., Lu, L., He, D., Jenkins, N.A., et al. (2015). The transcription factor Bcl11b is specifically expressed in group 2 innate lymphoid cells and is essential for their development. J. Exp. Med. *212*, 865–874.

Yu, Y., Tsang, J.C.H., Wang, C., Clare, S., Wang, J., Chen, X., Brandt, C., Kane, L., Campos, L.S., Lu, L., et al. (2016). Single-cell RNA-seq identifies a PD-1hi ILC progenitor and defines its development pathway. Nature *539*, 102–106.

Zaiss, D.M.W., Gause, W.C., Osborne, L.C., and Artis, D. (2015). Emerging functions of amphiregulin in orchestrating immunity, inflammation, and tissue repair. Immunity *42*, 216–226.

Zhang, D.H., Cohn, L., Ray, P., Bottomly, K., and Ray, A. (1997). Transcription factor GATA-3 is differentially expressed in murine Th1 and Th2 cells and controls Th2-specific expression of the interleukin-5 gene. J. Biol. Chem. *272*, 21597–21603.

Zhang, P., Li, Y., Zhang, L.D., Wang, L.H., Wang, X., He, C., and Lin, Z.F. (2014). Proteome changes in mesenteric lymph induced by sepsis. Mol. Med. Rep. *10*, 2793–2804.

Zhao, Y., Liu, M., Chan, X.Y., Tan, S.Y., Subramaniam, S., Fan, Y., Loh, E., Chang, K.T.E., Tan, T.C., and Chen, Q. (2017). Uncovering the mystery of opposite circadian rhythms between mouse and human leukocytes in humanized mice. Blood *130*, 1995–2005.

Zhong, J., Sharma, J., Raju, R., Palapetta, S.M., Prasad, T.S.K., Huang, T.C., Yoda, A., Tyner, J.W., Van Bodegom, D., Weinstock, D.M., et al. (2014). TSLP signaling pathway map: A platform for analysis of TSLP-mediated signaling. Database *2014*, 1–8.

Zhou, W., Toki, S., Zhang, J., Goleniewksa, K., Newcomb, D.C., Cephus, J.Y., Dulek, D.E., Bloodworth, M.H., Stier, M.T., Polosuhkin, V., et al. (2016). Prostaglandin I2 signaling and inhibition of group 2 innate lymphoid cell responses. Am. J. Respir. Crit. Care Med. *193*, 31–42.

Zhu, J. (2018). Mysterious ILC2 tissue adaptation. Nat. Immunol. *19*, 2–4.

Ziegler, S.F. (2012). Thymic stromal lymphopoietin and allergic disease. J. Allergy Clin. Immunol. *130*, 845–852.

Ziegler, S.F., Roan, F., Bell, B.D., Stoklasek, T.A., Kitajima, M., and Han, H. (2013). The Biology of Thymic Stromal Lymphopoietin (TSLP) (Elsevier Inc.).

Zinkernagel, R.M. (2000). On immunological memory. Philos. Trans. R. Soc. B Biol. Sci. *355*, 369–371.

Zook, E.C., and Kee, B.L. (2016). Development of innate lymphoid cells. Nat. Immunol. *17*, 775.

Zook, E.C., Ramirez, K., Guo, X., van der Voort, G., Sigvardsson, M., Svensson, E.C., Fu, Y.X., and Kee, B.L. (2016). The ETS1 transcription factor is required for the development and cytokine-induced expansion of ILC2. J. Exp. Med. *213*, 687–696.

ANNEX

Matthieu Caubet[6]
Claire Laresche[2]
Francine Garnache-Ottou[1,3]
Philippe Saas[1,3]
Estelle Seilles[1,3]
François Aubin[1,7]

[1]*INSERM UMR 1098, University of Bourgogne Franche Comté, Besançon, France*
[2]*Department of Dermatology, University Hospital, Besançon, France*
[3]*Etablissement Français du Sang Bourgogne Franche Comte, Besançon, France*
[4]*Clinical Methodology Center, Besançon University Hospital, Besançon, France*
[5]*Department of Radiology, Besançon University Hospital, Besançon, France*
[6]*Department of Radiotherapy, Besançon University Hospital, Besançon, France*
[7]*EA3181, University of Bourgogne Franche Comté, Besançon, France*

Correspondence
François Aubin, Service de Dermatologie, Besançon Cedex, France.
Email: francois.aubin@univ-fcomte.fr

REFERENCES

[1] D. Castellana, F. Toti, J.-M. Freyssinet, *Thromb. Res.* **2010**, *125*(Suppl. 2), S84.
[2] H. Goubran, W. Sabry, R. Kotb, J. Seghatchian, T. Burnouf, *Transfus. Apher. Sci.* **2015**, *53*, 168.
[3] C. Laresche, F. Pelletier, F. Garnache-Ottou, T. Lihoreau, S. Biichlé, G. Mourey, P. Saas, P. Humbert, E. Seilles, F. Aubin, *J. Invest. Dermatol.* **2014**, *134*, 176.
[4] A. Willms, C. Müller, H. Julich, N. Klein, R. Schwab, C. Güsgen, I. Richardsen, S. Schaaf, M. Krawczyk, F. Lammert, D. Schuppan, V. Lukacs-Kornek, M. Kornek, Tumour-associated circulating microparticles: A novel liquid biopsy tool for screening and therapy monitoring of colorectal carcinoma and other epithelial neoplasia. *Oncotarget* **2016**, *7*, 30867.
[5] J. B. Kral, W. C. Schrottmaier, M. Salzmann, A. Assinger, *Transfus. Med. Hemother.* **2016**, *43*, 78.
[6] H. Shaker, A. S. Rothmeier, C. C. Kirwan, W. Ruf, *Thromb. Res.* **2016**, *140*(Suppl. 1), S172.
[7] P. Prandoni, A. Falanga, A. Piccioli, *Lancet Oncol.* **2005**, *6*, 401.
[8] S. Nomura, M. Niki, T. Nisizawa, T. Tamaki, M. Shimizu, *Biomark Cancer* **2015**, *7*, 51.

SUPPORTING INFORMATION

Additional Supporting Information may be found online in the supporting information tab for this article.

DATA S1 Extended information on experimental methods.
FIGURE S1 Analysis of circulating platelet-derived microparticles using NAVIOS™ cytometer
TABLE S1 Plasma levels of PMPs (μL−1) and STA-PPL (s) in patients with stage III and IV melanoma

Accepted: 23 February 2017
DOI: 10.1111/exd.13340

Analysis of the skin of mice humanized for the immune system

Abstract

Development of new immunotherapeutic strategies relies on the ability to activate the right cells at the right place and at the right moment and on the capacity of these cells to home to the right organ(s). Skin delivery has shown high potency for immunotherapeutic administration. However, an adequate in vivo model of human skin immunity is still a critical bottleneck. We demonstrated here that the skin of human immune system mice is colonized by human hematopoietic cells, mainly human T cells and that complementation with human antigen-presenting cells at the vaccination site allowed the induction of an immune response.

Abbreviations: APC, antigen-presenting cells; cDC, conventional dendritic cells; CLA, cutaneous lymphocyte antigen; hHPC, human hematopoietic progenitor cells; HIS, human immune system; MVA, modified vaccinia Ankara; pDC, plasmacytoid dendritic cells.

1 | BACKGROUND

The skin, the largest organ of the human body, is the first line of protection against pathogens, physical and chemical injuries. It is a major immunological organ with an important density of antigen-presenting cells (APC),[1] able to capture pathogens through endocytic pathways and exhibiting cross-presentation ability. In addition, the skin tissue contains a large pool of T cells, mostly memory T cells expressing the skin-homing marker CLA (cutaneous lymphocyte antigen) and displaying long-term immune protection capacity.[2,3] These are features highly desirable for induction of vaccination and tissue maintenance of immune protection. We previously demonstrated that delivery of vaccine via the skin allows for the generation of a potent CD8 T-cell response and the induction of a humoral

immune response in the mucosa.[4] However, the lack of an appropriate small animal model to study human skin immunity in vivo remains a major roadblock, which has been addressed by constructing mice humanized with human skin graft.[5] However, this mouse model is technically challenging to routinely establish. Alternatives exist with mice humanized for the human immune system (HIS).[6-8]

2 | QUESTIONS ADDRESSED

Human immune system mice represent an attractive tool to study ontogeny of cellular components of the human immune system in vivo. However, little is known about the skin compartment in these animals. Here, we investigated colonization of the skin of HIS mice by human hematopoietic cells in order to establish a preclinical model to investigate vaccination and immunotherapeutic application via the skin route.

3 | EXPERIMENTAL DESIGN

HLA-A2 transgenic NSG (NOD.Cg-Prkdc^{scid} Il2rg^{tm1Wjl} Tg(HLA-A2.1)1Enge/SzJ) mice were humanized (NSG-HLA-A2-HIS) with a single intra-hepatic injection of 0.5×10^5-1.5×10^5 HLA-A2$^+$CD34$^+$ human hematopoietic progenitor cells (hHPC) into sublethally irradiated newborn NSG-HLA-A2 mice (<5 days old). This led to a high-level engraftment of a human immune system with long-term maintenance capacity in vivo. NSG-HLA-A2-HIS mice were used as they demonstrated improved T-cell functionality after infection/immunization.

4 | RESULTS

We first evaluated by flow cytometry the level of human hematopoietic cell (hCD45$^+$) engraftment in the skin as compared to various organs of NSG-HLA-A2-HIS mice. We observed a high level of hCD45$^+$ engraftment in the spleen, liver, lymph node (Figure 1A) and thymus of the animals (data not shown). The lung and bone marrow exhibited good to intermediate level of human hCD45$^+$ cells engraftment (Figure 1A), whereas the vagina and intestine (data not shown) were moderately colonized by human hematopoietic cells. This data were confirmed by histology (Fig. S1). In comparison, the skin from the flank and the ear was moderately engrafted with human CD45$^+$ cells, which were mostly located in the dermis (Figure 1B,C). The engraftment efficiency of human cells in the skin was time-dependent, with increasing human cell density in the skin of older animals (23-26 weeks old, Figure 1C) as compared to younger ones (12-13 weeks old, Figure 1B).

The human cells observed in the skin of the animals as well as in other mucosal tissues (eg lung, vagina) were mainly human T cells (Figure 2A,B), and only few human APC, in contrast to human skin explants (Fig. S2). The human T cells present in the skin were composed for two-third of human CD4$^+$ T cells and one-third of human CD8$^+$ T cells, which were both predominantly of memory phenotype (Figure 2C), similarly to what is observed in human skin explants

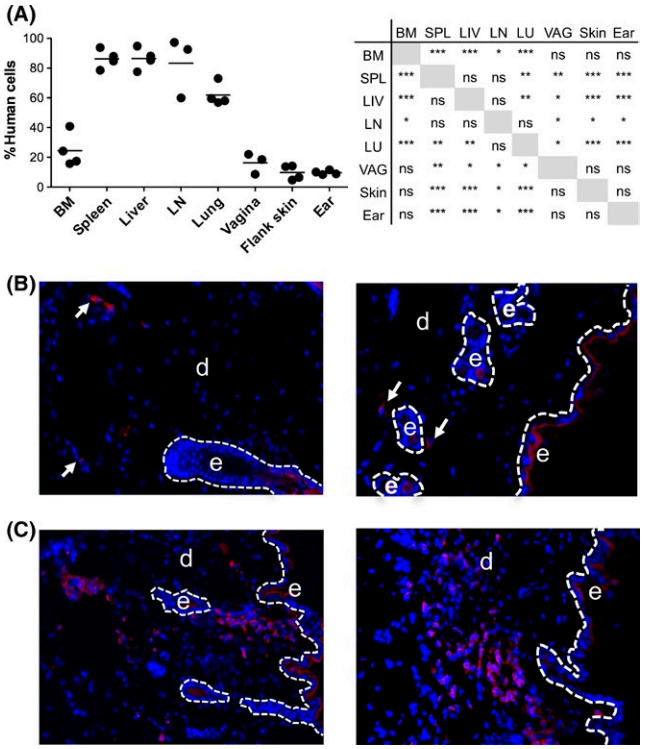

FIGURE 1 Colonization of the skin of humanized mice by human cells (A) The frequency of human CD45$^+$ cells was determined for NSG-HLA-A2-HIS mice (n=4) in various organs by flow cytometry. Each symbol corresponds to an individual animal. BM: bone marrow, LN: lymph node. The paired *t* test analysis is presented in the table (ns: not statistically significant, *<.05, **<.01, ***<.001). (B) Representative 5 μm flank skin cryosections labelled with DAPI (blue) and anti-human CD45 (red) of 2 HLA-A2^{Tg}-NSG-HIS mice of 14 weeks old and (C) 2 HLA-A2^{Tg}-NSG-HIS mice of 26 weeks old. Magnification ×10. The arrows indicate the rare human CD45$^+$ cells present in the skin of 14-week-old animals. e: epidermis, d: dermis

(Fig. S2) and the HIS mice lymphoid organs (Fig. S3). A high fraction (~80%) of these human T cells expressed CLA allowing them to reside in the skin (Fig. S3). Interestingly, human CD4$^+$ regulatory T cells (CD25^{++}FoxP3$^+$) were also identified in the skin of the animals at a frequency similar to the one observed in the spleen (Figure 2C).

We next immunized NSG-HLA-A2-HIS mice, intra-dermally, with MVA (Modified Vaccinia Ankara, 1 pfu/cell) or PBS control. No human T-cell response was detected by IFN-γ ELISPOT in the spleen of the animals (data not shown). Considering the size of the hAPC compartment in HIS mice and their critical role in the induction of T-cell responses, we speculated that hAPC density of at the site of administration (ie the skin) is potentially too low to optimally trigger T cells. We thus tested the capacity of human DC complementation in the skin of the NSG-HLA-A2-HIS mice,[9] deriving autologous human cDC from human CD14$^+$ cells isolated from the same cord blood than the hHPC used to reconstitute NSG-HLA-A2-HIS mice. Autologous umbilical cord blood CD14$^+$ monocytes were isolated by MACS and cultured for 3 days in presence of 50 ng/mL hGM-CSF and 5 ng/mL hIL-4. Autologous human monocyte-derived DC were loaded for

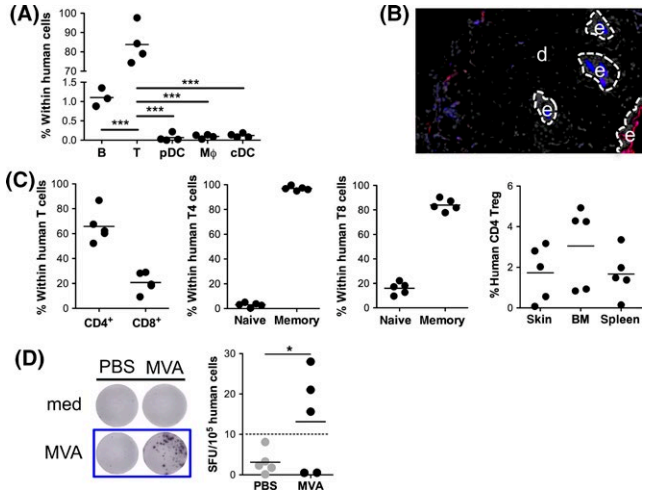

FIGURE 2 Human cells present in the skin of humanized mice and vaccination via intra-dermal route. (A) The frequency of different human cell subsets—B cells ($CD19^+$), T cells ($CD3^+$), pDC ($BDCA2^+HLADR^+$), monocytes (Mϕ, $CD14^+CD11c^+HLA\text{-}DR^+$), conventional DC (cDC, $CD11c^+CD14^-HLADR^+$)—in the skin of NSG-HLA-A2-HIS mice (26-30 weeks old, n=4) was determined by flow cytometry. Each symbol corresponds to an individual animal. ***P<.001 (paired t test). (B) Representative 5 µm flank skin cryosection of NSG-HLA-A2-HIS mouse of 26 weeks old labelled with DAPI (white), anti-human CD3 (blue) and anti-human HLA-DR (red). Magnification ×20. e: epidermis, d: dermis. (C) Analysis of the human $CD3^+$ cells in the skin of NSG-HLA-A2-HIS mice (n=5) by flow cytometry. The expression of CD45RA defined the naïve phenotype of the human T cells. (D) IFN-γ ELISPOT analysis of MVA-specific human T cells responses in the spleen of NSG-HLA-A2-HIS mice (32 weeks old) on day 7 after intra-dermal injection of 5×10^5 autologous human monocyte-derived DC loaded with MVA (1 pfu/cell) or PBS in the flank of the animals. Total splenocytes of MVA- or PBS-immunized NSG-HIS mice were incubated with medium (med) or MVA for 40 hours and analysed by ELISPOT assay. The graph represents the number of spot-forming unit (SFU) counted in the MVA stimulated well minus the ones counted in the medium stimulated well and according to the frequency of human $CD45^+$ cells in the spleen of each vaccinated animals. *P=.019 (chi-square test)

2 hours at 37°C with MVA or PBS. Next, NSG-HLA-A2-HIS mice were immunized intra-dermally in the flank with 0.5×10^6 matched human $CD14^+$-derived MVA- or PBS-loaded DC loaded. A human T-cell response was observed 7 days after immunization by IFN-γ ELISPOT in the spleen of the MVA-vaccinated animals (Figure 2D), with significantly more responder animals (3/5) than in the control group (0/5) (chi-square test, P=.019).

5 | CONCLUSIONS

We demonstrated here that the skin of HIS mice is colonized by human hematopoietic cells, mainly human T cells expressing CLA and exhibiting a memory phenotype. Complementation with human APC at the vaccination site allowed the induction of an immune response. This highlighted the potential of the HIS mice has an innovative preclinical model for human skin immunity as well as for prospective analysis of vaccination via skin route, and notably DC therapies. As such, this will also generate knowledge on understanding the early events following immunotherapeutic administration and support demands for in vivo biomodelling of the interaction of immunotherapeutic with the human immune system.

ACKNOWLEDGEMENTS

MC, MP, AJH, MD and AS performed research; DB and MM provided human materials. MC and BC designed the research, analysed data and wrote the manuscript. Dr Centlivre was supported by a FRM postdoctoral fellowship (SPF20121226281) and Dr Combadière received EU-FP7 CUTHIVAC (no. 241904) and FRM fundings. We thank Dr Morosan for animal facility and Dormeur Foundation, Vaduz, for providing AID EliSpot Reader and Cryostat HM550 apparatus and Dr Verrier for providing MVA.

CONFLICT OF INTERESTS

The authors declare they have no conflict of interests.

Keywords

antigen-presenting cells, human immune system mice, intra-dermal vaccination, route of administration, skin T cells

Mireille Centlivre[1,2]
Maxime Petit[1,2]
Andrew J. Hutton[1,2]
Mélody Dufossée[1,2]
David Boccara[1,2,3]
Maurice Mimoun[3]
Angèle Soria[1,2,4]
Béhazine Combadière[1,2]

[1]*UMR_S CR7, Centre d'Immunologie et des Maladies Infectieuses- Paris (CIMI-Paris), Sorbonne Universités, UPMC University Paris 06, Paris, France*
[2]*INSERM U1135, CIMI-Paris, Paris, France*
[3]*Service de Chirurgie Plastique, Reconstructrice, Esthétique, Centre de Brûlées, Hôpital Saint-Louis, Assistance Publique Hôpitaux de Paris (AP-HP), Paris, France*
[4]*Service de Dermatologie et Allergologie, Hôpital Tenon, Assistance Publique Hôpitaux de Paris (AP-HP), Paris, France*

Correspondence
Béhazine Combadière,
Centre d'Immunologie et des Maladies Infectieuses CIMI-Paris, Paris, France.
Email: behazine.combadiere@upmc.fr

REFERENCES

[1] T. S. Kupper, R. C. Fuhlbrigge, *Nat. Rev. Immunol.* **2004**, *4*, 211.
[2] R. A. Clark, *J. Invest. Dermatol.* **2010**, *130*, 362.

[3] S. N. Mueller, T. Gebhardt, F. R. Carbone, W. R. Heath, *Annu. Rev. Immunol.* **2013**, *31*, 137.
[4] C. Liard, S. Munier, M. Arias, A. Joulin-Giet , O. Bonduelle, D. Duffy, R. J. Shattock, B. Verrier, B. Combadiere, *Vaccine* **2011**, *29*, 6379.
[5] A. Soria, D. Boccara, L. Chonco, N. Yahia, M. Dufossee, S. Cardinaud, A. Moris, C. Liard, A. Joulin-Giet, M. Julithe, M. Mimoun, B. Combadiere, H. Perrin, *Exp. Dermatol.* **2014**, *23*, 850.
[6] N. Legrand, K. Weijer, H. Spits, *J. Immunol.* **2006**, *176*, 2053.
[7] A. Rongvaux, H. Takizawa, T. Strowig, T. Willinger, E. E. Eynon, R. A. Flavell, M. G. Manz, *Annu. Rev. Immunol.* **2013**, *31*, 635.
[8] L. D. Shultz, M. A. Brehm, J. V. Garcia-Martinez, D. L. Greiner, *Nat. Rev. Immunol.* **2012**, *12*, 786.
[9] G. Salguero, A. Daenthanasanmak, C. Münz, A. Raykova, C. A. Guzmán, P. Riese, C. Figueiredo, F. Länger, A. Schneider, L. Macke, B. S. Sundarasetty, T. Witte, A. Ganser, R. Stripeck, *J. Immunol.* **2014**, *192*, 4636.

SUPPORTING INFORMATION

Additional Supporting Information may be found online in the supporting information tab for this article.

Figure S1. Human cells engraftment in various organs of NSG-HLA-A2-HIS mice

Figure S2. Analysis of cell subsets in human skin explant

Figure S3. Analysis of human T cells in the lymphoid organs of NSG-A2-HIS mice

Accepted: 3 March 2017
DOI: 10.1111/exd.13342

Herpes simplex virus 1 and cytomegalovirus are associated with pemphigus vulgaris but not with pemphigus foliaceus disease

Abstract

Pemphigus vulgaris (PV) and pemphigus foliaceus (PF) are blistering autoimmune diseases that depend on interaction between genetic and environmental factors. Viral infections, like herpes simplex viruses 1 and 2 (HSV1/2), cytomegalovirus (CMV), Epstein-Barr virus and dengue virus, could trigger or exacerbate pemphigus. IgM and IgG antibodies against these viruses in serum from PV and PF, their relatives and controls were determined. HSV1/2 expression was evaluated by direct immunofluorescence (DIF) and qPCR in affected or not oral mucosa from PV patients compared with uninjured PF mucosa. IgG anti-HSV1 was higher in the PV group compared with all groups. IgG anti-CMV resulted higher in PV group compared with PF patients and PV relatives. HSV1 was confirmed by DIF and qPCR on oral samples from patients with PV. Lack of HSV1 expression in the oral mucosa of patients with PF corroborate that immunosuppressive therapy cannot be the main cause for HSV1 replication in PV disease.

1 | BACKGROUND

Pemphigus diseases involve production of autoantibodies against desmogleins (DSG), which cause acantholytic intra-epidermal blisters. The two main clinical forms of pemphigus are pemphigus vulgaris (PV), which affects the skin and mucous membranes by production of anti-DSG1 and anti-DSG3 antibodies, and pemphigus foliaceus (PF), which affects the skin by generation of anti-DSG1.[1–5]

The production of autoantibodies against DSG is well known, but the etiopathogenesis of pemphigus still requires elucidation, and depends on interaction between genetic and environmental factors.[6–9] Viral infections, like herpes simplex viruses 1 and 2 (HSV1/2), cytomegalovirus (CMV), Epstein-Barr virus (EBV) and dengue virus (DENV), could trigger or exacerbate pemphigus.[10–13]

2 | ADDRESSED QUESTIONS

Studies have related viral detection to the complications of pemphigus but have not recognized viruses as triggering agents. Conflicting results about the role of HSV in triggering pemphigus exist, making additional analysis to support this possible relationship necessary.

A large number of PV and PF cases are diagnosed in the northeastern region of the state of São Paulo each year.[8,9,14] We have investigated some viruses in patients with PV and compared them in patients with PF in this prevalent area for both PV and PF. We decided to study HSV1/2, CMV and EBV to confirm that these viruses are associated with pemphigus, mainly with PV.[15] We added DENV to our study because only a single report on PF exists,[13] and because dengue disease is endemic in our region.[16]

3 | EXPERIMENTAL DESIGN

This cross-sectional study comprised a convenience sample of patients with PV and PF attended at the outpatient clinic of the University Hospital of the Ribeirão Preto Medical School, University of São Paulo, Brazil, from January 1999 to December 2013. Diagnosis of PV and PF was based on clinical, histopathological and immunofluorescence features and on determination of autoantibodies against DSG1 and DSG3 with ELISA kits (MBL, Japan). This study also included

IMMUNOLOGY

Notch signaling in group 3 innate lymphoid cells modulates their plasticity

Sylvestre Chea,[1,2,3] Thibaut Perchet,[1,2,3] Maxime Petit,[1,2,3] Thomas Verrier,[3,4] Delphine Guy-Grand,[1] Elena-Gaia Banchi,[1,2,3] Christian A. J. Vosshenrich,[3,4] James P. Di Santo,[3,4] Ana Cumano,[1,2,3] Rachel Golub[1,2,3]*

The Notch signaling pathway is conserved throughout evolution, and it controls various processes, including cell fate determination, differentiation, and proliferation. Innate lymphoid cells (ILCs) are lymphoid cells lacking antigen receptors that fulfill effector and regulatory functions in innate immunity and tissue remodeling. Type 3 ILCs (ILC3s) reinforce the epithelial barrier and maintain homeostasis with intestinal microbiota. We demonstrated that the population of natural cytotoxicity receptor–positive (NCR$^+$) ILC3s in mice is composed of two subsets that have distinct developmental requirements. A major subset depended on the activation of Notch2 in NCR$^-$ ILC3 precursors in the lamina propria of the small intestine to stimulate expression of the genes encoding the transcription factors T-bet, RORγt, and aryl hydrocarbon receptor (AhR). Notch signaling contributed to the transition of NCR$^-$ cells into NCR$^+$ cells, the more proinflammatory subset, in a cell-autonomous manner. In the absence of Notch signaling, this subset of NCR$^-$ ILC3s did not acquire the gene expression profile of NCR$^+$ ILC3s. A second subset of NCR$^+$ ILC3s did not depend on Notch for their development or for increased transcription factor abundance; however, their production of cytokines and cell surface abundance of NCRs were decreased in the absence of Notch signaling. Together, our data suggest that Notch is a regulator of the plasticity of ILC3s by controlling NCR$^+$ cell fate.

INTRODUCTION

Innate lymphoid cells (ILCs) promote inflammatory responses and tissue homeostasis through the rapid secretion of effector cytokines at mucosal barriers and secondary lymphoid organs. These cells differentiate from a common lymphoid progenitor (CLP); however, unlike T cells or B cells, they are devoid of rearranged antigen-specific receptors. All ILCs require the transcriptional repressor Id2 (inhibitor of DNA binding 2) for their development (*1*–*3*). ILCs can be subdivided into three groups, which follow different developmental pathways and produce different cytokines (*4*). The transcriptional profiles of distinct ILC subsets in different tissues were analyzed in depth as part of the immunological genome project (*5*).

Group 1 ILCs consist of Eomes-positive conventional natural killer (cNK) cells and Eomes-negative ILC1s, secrete the inflammatory cytokine interferon-γ (IFN-γ), and require the transcription factor T-bet for proper development. ILC2s produce the cytokines interleukin-5 (IL-5) and IL-13 and are characterized by the expression of the transcription factors GATA3 and retinoic acid receptor–related orphan receptor α (RORα). The ILC3 group is heterogeneously composed of the fetal subset of lymphoid tissue inducer (LTi) cells (*6*) and the adult ILC3 subsets, which are mainly found at mucosal surfaces. All ILC3s depend on the transcription factor RORγt (which is encoded by *Rorc*) for their development and function and they produce IL-17 and IL-22 (*7*). In mice, adult ILC3s can be subdivided on the basis of the cell surface expression of the natural cytotoxicity receptor 1 (NCR1), NK protein 46 (NKp46), mostly found present on the surface of NK cells. The NKp46$^+$ (NCR$^+$) subset is characterized by the cell surface absence of the CC chemokine receptor 6 (CCR6) and produces both IL-22 and IFN-γ. The NKp46$^-$ (NCR$^-$) subset is composed of various subfractions that differently express combinations of CD4 and CCR6 on the cell surface. Adult NKp46$^-$ CCR6$^+$ cells consist of both CD4$^+$ and CD4$^-$ cells, which share several features with LTi cells and are also called LTi-like cells. The lineage relationship between adult ILC3 subsets and the molecular mechanisms that drive their development and effector functions have been under intense investigation (*8*–*15*). It was proposed that CCR6$^-$ and CCR6$^+$ ILC3s arise from distinct progenitors (*9*, *12*, *16*, *17*). Within the CCR6$^-$ population, T-bet–dependent ILC3s were identified as a source of NCR$^+$ cell precursors (*11*–*13*). ILC3s exhibit plasticity in vitro and in vivo, and environmental cues, such as microbiota and IL-7, stabilize these cells by maintaining RORγt abundance (*9*). The phenomenon of plasticity is recognized during the process of T cell differentiation, in which the phenotypic and functional characteristics of a given population are dependent on the milieu in which they are found. Several studies support the idea that Notch signaling is important for the generation of the NCR$^+$ ILC3 subset (*10*, *16*, *18*). It was also proposed that expression of the genes encoding T-bet and aryl hydrocarbon receptor (AhR) by the NCR$^-$ ILC3 subset is Notch-dependent (*12*, *13*); however, the potential role of the Notch pathway in adult ILC3s has not been directly analyzed in vivo (*10*–*13*, *19*).

The Notch pathway is involved in several developmental processes in different tissues. Upon receptor-ligand interaction, the Notch intracellular domain (NICD) translocates into the nucleus where it acts as a transcriptional cofactor together with recombining binding protein suppressor of hairless κ (RBP-Jκ). In T lymphocytes, the canonical Notch signaling pathway drives the expression of different target genes such as *Hes1*, *Tcf7*, and *Dtx1*, which respectively encode the transcription factor HES1, TCF1, and the DTX1 protein, which are all important for T cell development. Notch1 is especially implicated in various stages of T cell development by repressing B cell fate, whereas Notch2 signaling is essential for the generation of marginal zone B cells and for the development of CD11b$^+$ dendritic cells (DCs) in the spleen and intestine (*20*).

Here, we analyzed the distribution of adult ILC3 subsets in the lamina propria of mice deficient in Notch signaling through knockout of the genes encoding either Notch2 ($Il7r^{Cre/+}Notch2^{fl/fl}$ mice) or RBP-Jκ

[1]Lymphopoiesis Unit, Immunology Department, Institut Pasteur, 75015 Paris, France. [2]Université Paris Diderot, Sorbonne Paris Cité, Cellule Pasteur, 75015 Paris, France. [3]INSERM U1223, 75015 Paris, France. [4]Innate Immunity Unit, Immunology Department, Institut Pasteur, 75015 Paris, France.
*Corresponding author. Email: rachel.golub@pasteur.fr

(*Il7r*$^{Cre/+}$*Rbpj*$^{fl/fl}$ mice) under control of the *Il7r* promoter to ensure deletion at an early stage of lymphoid cell development or of mice that exhibit enhanced Notch signaling through expression of the constitutively active NICD under the control of the same promoter (*Il7r*$^{Cre/+}$*NICD* mice). We showed that the Notch pathway was essential for the generation of NCR$^+$ ILC3s. Competitive bone marrow reconstitution experiments indicated that the action of the Notch pathway was direct and cell-intrinsic. Mice that exhibited constitutively active Notch signaling in the earliest lymphoid progenitors showed an increased number not only of NCR$^+$ cells but also of NCR$^-$ ILC3s, which is compatible with a role for Notch in the differentiation of NCR$^+$ cells from an NCR$^-$ ILC3 subset. In contrast, mice that exhibited constitutively active Notch signaling at the later developmental NKp46$^+$ stage retained NCR$^+$ ILC3s that were indistinguishable from those of their littermate controls. We found that Notch acted on NCR$^-$ precursor cells by inducing expression of the genes encoding the transcription factors T-bet, AhR, and Gata3, thus enabling their differentiation into NCR$^+$ cells. A Notch-independent subset of NCR$^+$ ILC3s (around 20% of total NCR$^+$ ILC3s) was also identified, and these cells expressed *Tbx21* and Tcf7 independently of the Notch signaling pathway.

RESULTS

Notch signaling regulates intestinal NCR$^+$ ILC3s

To assess roles for the Notch pathway in ILC3 homeostasis, we generated *Il7r*$^{Cre/+}$*Rbpj*$^{fl/fl}$ mice, which have defective canonical Notch signaling in all lymphoid cells due to their lack of the transcriptional coactivator RBP-Jκ. We quantified the *Rbpj*-floxed alleles and determined that less than 1% of IL-7Rα$^+$ CLPs retained one *Rbpj* copy (fig. S1, A and B). In contrast, the *IL7Rα*$^{Cre/+}$ deletion in lymphoid-primed multipotent progenitors was restricted to a few *Rbpj* alleles. The Notch signaling pathway is essential for T cell development, which was blocked at the transitional stage between double-negative 1 (DN1) and DN2 cells (fig. S1, C and D) in *Il7r*$^{Cre/+}$*Rbpj*$^{fl/fl}$ mice; however, a few progenitors (less than 1%) escaped deletion and generated detectable peripheral T cells (fig. S1, C to F). When *Rbpj* was deleted at the hematopoietic stem cell stage in *Vav*$^{Cre/+}$*Rbpj*$^{fl/fl}$ mice, T cells were almost undetectable in the peripheral organs (fig. S1G).

We next assessed the effect of loss of Notch signaling on the composition of ILC subsets in the lamina propria of adult mice. cNK cells and ILC1s were defined by flow cytometric analysis as NK1.1$^+$NKp46$^+$ IL-7Rα$^-$ and NK1.1$^+$NKp46$^+$IL-7Rα$^+$ cells, respectively (Fig. 1A), whereas NCR$^+$ and NCR$^-$ ILC3s were defined as RORγt$^+$IL-7Rα$^+$NK1.1$^-$NKp46$^+$ and RORγt$^+$IL-7Rα$^+$NK1.1$^-$NKp46$^-$ cells, respectively (Fig. 1A). ILC1s and cNK cells represented less than 2% of the total number of lineage-negative (Lin$^-$) intestinal lamina propria cells, and their percentages and absolute numbers were similar in *Rbpj*-deficient and *Rbpj*-sufficient mice. We concluded that ILC1s were not affected, in terms of their total numbers or proportions, by the loss of Notch signaling (Fig. 1B).

We found that there was a 5- to 10-fold decrease in the number and percentage of NCR$^+$ ILC3s in *Rbpj*-deficient mice (0.8×10^4 cells, representing 1% of lamina propria Lin$^-$ cells) compared to those in *Rbpj*-sufficient or control *Il7r*$^{+/+}$ mice (~4×10^4 cells, representing 8%) (Fig. 1C). In contrast, the NCR$^-$ ILC3 subset was apparently unaffected by loss of *Rbpj* (~9×10^4 to 10×10^4 cells, representing 15 to 20%) (Fig. 1D), which suggests that neither the development nor the maintenance of this subset required Notch signaling in vivo. The phenotypic effect of the increased Sca1 abundance and decreased Thy1 abundance caused by the loss of Notch signaling was common to most ILC subsets, with the exception of cNK cells (Fig. 1, D and E). The increase in the abundance of the Ly49 CIFH marker, exclusively found in cNK cells, is compatible with the idea that NK cell precursors branch off from a common differentiation pathway before the other ILC lineages (*16*, *17*). In ILC3s deficient in Notch signaling, Thy1 quantities were decreased, whereas only NCR$^+$ ILC3s showed a substantial increase in the abundance of c-Kit, a receptor tyrosine kinase that responds to stem cell factor and induces the proliferation and differentiation of hematopoietic precursors (Fig. 1F). An important molecular sensor that detects "induced self" markers on cells in danger, the activating receptor NKG2D, was substantially less abundant in *Rbpj*-deficient cells; however, the difference in abundance was statistically significantly different only for the ILC1 and NCR$^+$ ILC3 subsets (Fig. 1, E and F). A comparison of the mean fluorescence intensity (MFI) of NKp46 showed that it was decreased in *Rbpj*-deficient NCR$^+$ ILC3s (fig. S1H). Moreover, NCR$^+$ ILC3s that were NKG2D$^+$ had substantially more NKp46 than did the NKG2D$^-$ subset (fig. S1I). The increased amounts of Sca1 were statistically significant in both the NCR$^+$ and NCR$^-$ ILC3 subsets from the *Rbpj*-deficient mice (Fig. 1F).

We previously reported that Notch2 is found early in ILC development (*19*). In contrast to T cell development, which is mainly dependent on Notch1, ILC3 differentiation could thus be Notch2-dependent. We generated *Il7r*$^{Cre/+}$*Notch2*$^{fl/fl}$ mice and found that the number of NCR$^+$ ILC3s was markedly reduced compared to those in *Il7r*$^{Cre/+}$*Notch2*$^{fl/+}$ mice (fig. S2A). Contrary to our findings with *Il7r*$^{Cre/+}$*Rbpj*$^{fl/+}$ mice, the decrease in the number of NCR$^+$ ILC3s was statistically significantly different in the *Il7r*$^{Cre/+}$*Notch2*$^{fl/+}$ mice (four times less than the number of cells in *Il7r*$^{Cre/+}$*Rbpj*$^{fl/+}$ mice), suggesting that *Notch2* haplodeficiency, which results in the reduced cell surface abundance of Notch2, was sufficient to reduce the absolute numbers of these ILCs. The absence of both *Notch2* alleles (in *Il7r*$^{Cre/+}$*Notch2*$^{fl/fl}$ mice) resulted in there being similar numbers of NCR$^+$ and NCR$^-$ cells to those found in the *Il7r*$^{Cre/+}$*Rbpj* mice. Similar to what was observed in the *Il7r*$^{Cre/+}$*Rbpj*$^{fl/fl}$ mice, no changes were found in the numbers of NCR$^-$ ILC3s or in the percentages or numbers of ILC1s after *Notch2* deletion (fig. S2A).

A residual population of NCR$^+$ ILC3s was still detectable in both *Il7r*$^{Cre/+}$*Notch2*$^{fl/fl}$ mice and *Il7r*$^{Cre/+}$*Rbpj*$^{fl/fl}$ mice, which might reflect incomplete Cre-mediated deletion in lymphoid progenitors. We therefore analyzed ILC3s in *Vav*$^{Cre/+}$*Rbpj*$^{fl/fl}$ mice in which peripheral T cells are undetectable, indicating complete inactivation of *Rbpj*. A small population of NCR$^+$ ILC3s was also present in these mice, which is suggestive of a Notch-independent pathway for the generation of this subset (fig. S2B). Overall, the intestinal ILC subsets in *Vav*$^{Cre/+}$*Rbpj*$^{fl/fl}$ mice mirrored those found in *Il7r*$^{Cre/+}$*Rbpj*$^{fl/fl}$ mice, with reduced numbers of NCR$^+$ cells, unchanged numbers of ILC1 and cNK subsets, and a small decrease in the number of NCR$^-$ ILC3s (Fig. 1B and fig. S2B). An increase in the abundance of Sca1 was maintained in the ILC1 and ILC3 subsets in *Vav*$^{Cre/+}$*Rbpj*$^{fl/fl}$ mice (fig. S2C); however, an increase in the abundance of Thy1 was observed only for the ILC1 subset (fig. S2C). Together, these results suggest that Notch signaling through Notch2 is essential for the development of appropriate numbers of NCR$^+$ cells, whereas a minor subset of NCR$^+$ ILC3s was derived through a Notch-independent pathway.

Loss of Notch signaling changes the secretive capacities of intestinal ILC3s

We next assessed whether loss of the Notch signaling pathway affected cytokine production by ILC3s and ILC1s. The abundances of mRNAs for *Il17a*, *Il17f*, *Il22*, *Csf2*, and *Ifnγ* were measured by quantitative reverse transcription polymerase chain reaction (qRT-PCR) analysis of mRNA extracted from ex vivo unstimulated ILCs sorted from the lamina propria (Fig. 2A). ILC1s did not have any T helper 17 cell cytokine family transcripts, whereas the abundance of *Ifnγ* mRNA was not affected by the loss of Notch signaling. NCR$^+$ and NCR$^-$ ILC3s from the *Il7r*$^{Cre/+}$*Rbpj*$^{fl/fl}$ mice

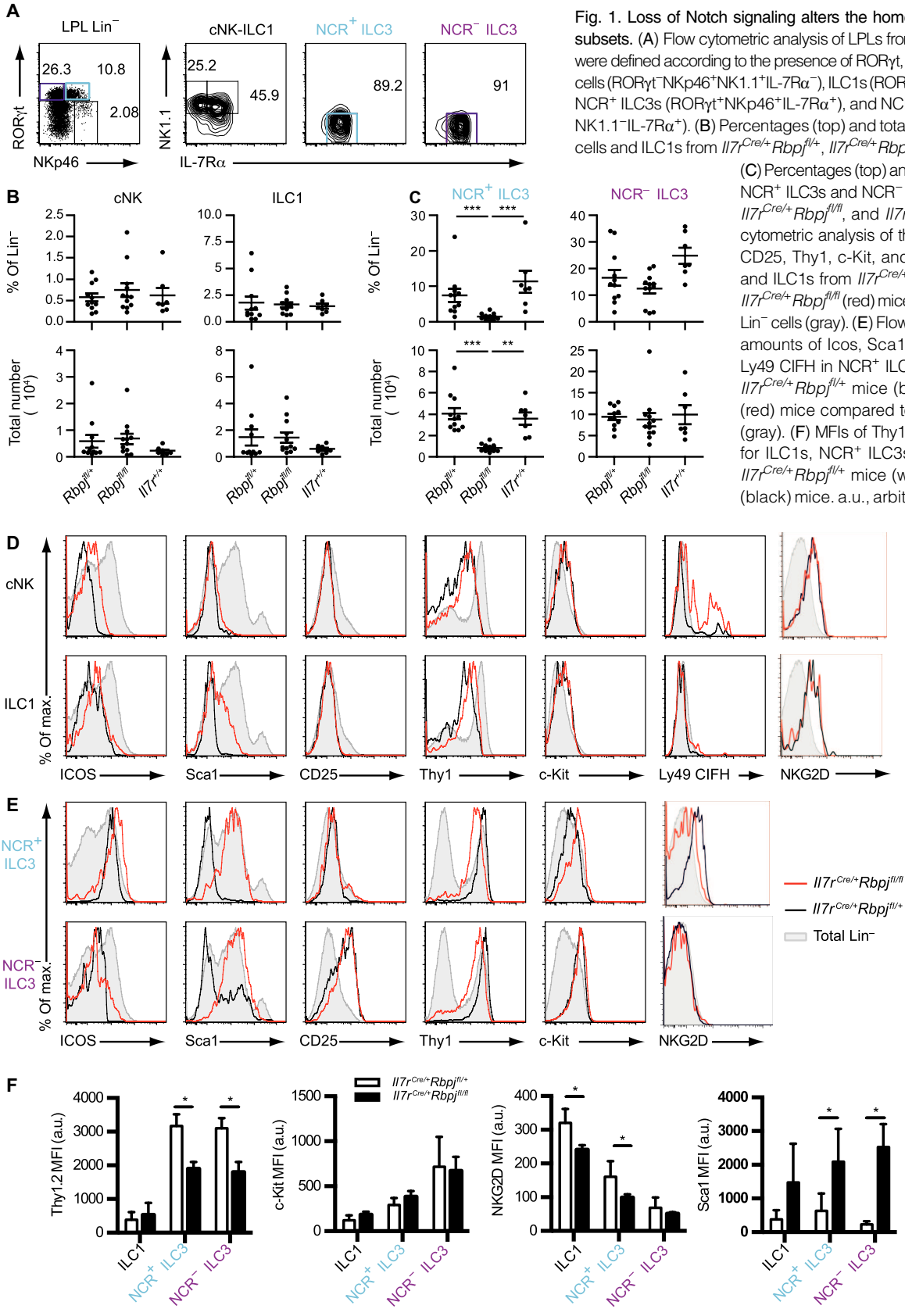

Fig. 1. Loss of Notch signaling alters the homeostasis of intestinal ILC3 subsets. (**A**) Flow cytometric analysis of LPLs from C57BL/6 mice. Lin⁻ cells were defined according to the presence of RORγt, IL-7Rα, and NKp46 as cNK cells (RORγt⁻NKp46⁺NK1.1⁺IL-7Rα⁻), ILC1s (RORγt⁻NKp46⁺NK1.1⁺IL-7Rα⁺), NCR⁺ ILC3s (RORγt⁺NKp46⁺IL-7Rα⁺), and NCR⁻ ILC3s (RORγt⁺NKp46⁻NK1.1⁻IL-7Rα⁺). (**B**) Percentages (top) and total numbers (bottom) of cNK cells and ILC1s from *Il7r*$^{Cre/+}$*Rbpj*$^{fl/+}$, *Il7r*$^{Cre/+}$*Rbpj*$^{fl/fl}$, and *Il7r*$^{+/+}$*Rbpj*$^{fl/+}$ mice. (**C**) Percentages (top) and total numbers (bottom) of NCR⁺ ILC3s and NCR⁻ ILC3s from *Il7r*$^{Cre/+}$*Rbpj*$^{fl/+}$, *Il7r*$^{Cre/+}$*Rbpj*$^{fl/fl}$, and *Il7r*$^{+/+}$*Rbpj*$^{fl/+}$ mice. (**D**) Flow cytometric analysis of the amounts of Icos, Sca1, CD25, Thy1, c-Kit, and Ly49 CIFH in cNK cells and ILC1s from *Il7r*$^{Cre/+}$*Rbpj*$^{fl/+}$ mice (black) and *Il7r*$^{Cre/+}$*Rbpj*$^{fl/fl}$ (red) mice compared to those in total Lin⁻ cells (gray). (**E**) Flow cytometric analysis of the amounts of Icos, Sca1, CD25, Thy1, c-Kit, and Ly49 CIFH in NCR⁺ ILC3s and NCR⁻ ILC3s from *Il7r*$^{Cre/+}$*Rbpj*$^{fl/+}$ mice (black) and *Il7r*$^{Cre/+}$*Rbpj*$^{fl/fl}$ (red) mice compared to those in total Lin⁻ cells (gray). (**F**) MFIs of Thy1, c-Kit, NKG2D, and Sca1 for ILC1s, NCR⁺ ILC3s, and NCR⁻ ILC3s from *Il7r*$^{Cre/+}$*Rbpj*$^{fl/+}$ mice (white) and *Il7r*$^{Cre/+}$ *Rbpj*$^{fl/fl}$ (black) mice. a.u., arbitrary units. Data are representative of at least three independent experiments with at least three mice of each genotype analyzed per experiment. Data in (B), (C), and (F) are means ± SEM of three independent experiments, with three mice of each genotype analyzed per experiment. Data points in (B) and (C) represent individual mice. $^{*}P < 0.05$, $^{**}P < 0.01$, $^{***}P < 0.001$ by Mann-Whitney test.

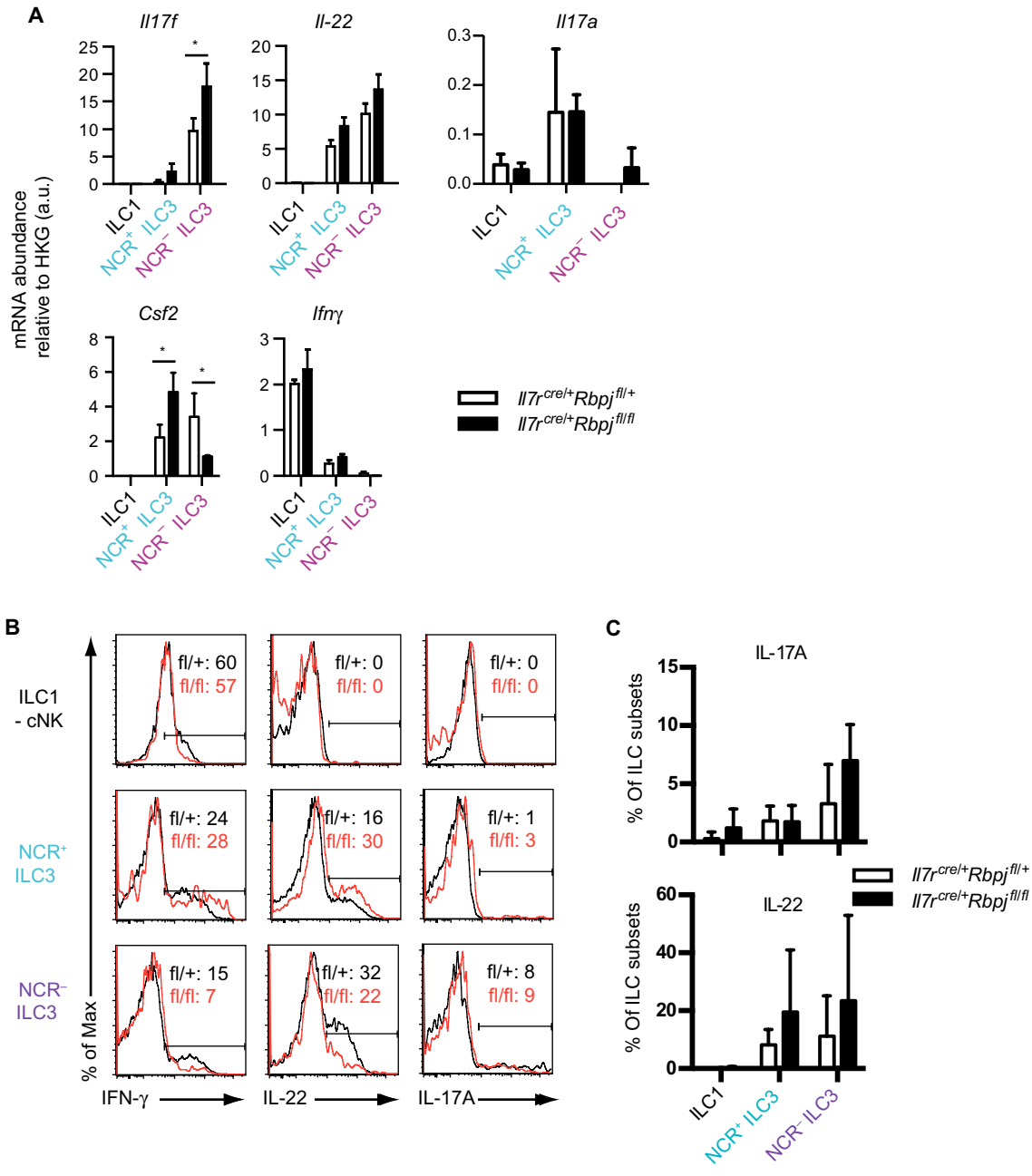

Fig. 2. Changes in the cytokine profiles of ILC3 subsets from mice deficient in Notch signaling. (A) qRT-PCR analysis of the relative steady-state abundances of *Il17f*, *Il22*, *Il17a*, *Csf2*, and *Ifnγ* mRNAs in ILC1, NCR$^+$ ILC3, and NCR$^-$ ILC3 subsets (as defined in Fig. 1A) from *Il7r*$^{Cre/+}$*Rbpj*$^{fl/+}$ mice (white) and *Il7r*$^{Cre/+}$*Rbpj*$^{fl/fl}$ mice (black). The abundances of the indicated mRNAs are presented relative to the average abundances of mRNAs of housekeeping genes (HKG). Data are means ± SEM of three independent experiments, with three mice of each genotype analyzed per experiment. *$P < 0.05$, **$P < 0.01$, ***$P < 0.001$ by Mann-Whitney test. (B) cNK-ILC1, NCR$^+$ ILC3, and NCR$^-$ ILC3 subsets isolated from *Il7r*$^{Cre/+}$*Rbpj*$^{fl/+}$ mice (black) and *Il7r*$^{Cre/+}$*Rbpj*$^{fl/fl}$ mice (red) were treated with PMA (left) or IL-23 (middle and right) and then were analyzed by flow cytometry to determine the relative abundances of IFN-γ (left), IL-22 (middle), and IL-17A (right). Numbers indicate the percentages of cells positive for the indicated cytokines. Data are representative of two independent experiments. (C) Analysis of the percentages of the indicated subsets of cells from *Il7r*$^{Cre/+}$*Rbpj*$^{fl/+}$ (white bars) and *Il7r*$^{Cre/+}$*Rbpj*$^{fl/fl}$ mice (black bars) that were positive for IL-17A (top) or IL-22 (bottom) in response to treatment with IL-23. Data are means ± SEM of two independent experiments, with two mice of each genotype analyzed per experiment. Analysis by Mann-Whitney test showed that there were no statistically significant differences among the groups.

had similar amounts of *Il22* and *Il17a* mRNAs to NCR$^+$ and NCR$^-$ ILC3s from control mice (Fig. 2A). The deficiency in *Rbpj* resulted in increased amounts of *Csf2* mRNA in NCR$^+$ ILC3s and decreased amounts in NCR$^-$ ILC3s, whereas *Il17f* mRNA was more abundant in the NCR$^-$ ILC3s from *Il7r*$^{Cre/+}$*Rbpj*$^{fl/fl}$ mice than in the NCR$^-$ ILC3s from control mice (Fig. 2A).

Under steady-state conditions, we observed differences in the abundances of *Il17f* and *Csf2* transcripts, which were statistically significantly increased in the NCR$^+$ subset (Fig. 2A). IFN-γ secretion was tested after activation of cells with phorbol 12-myristate 13-acetate (PMA), whereas the amounts of IL-17A and IL-22 proteins produced were tested by treating intestinal ILCs with IL-23. No differences in cytokine production were observed in ILC1s from either strain of mice (Fig. 2B), whereas *Rbpj*-deficient NCR$^+$ ILC3s produced substantially more IL-22 than did NCR$^+$ ILC3s from their littermate controls. NCR$^-$ ILC3s were the major producers of IL-17A irrespective of their genotype (Fig. 2, B and C). When we used a combination of IL-23 and PMA to activate intestinal lamina propria ILC3s (fig. S3A), we found that the NCR$^-$ ILC3 subset of the *Rbpj*-deficient mice produced more IL-22 than did the *Rbpj*-haploinsufficient mice. The abundance of *Il1r1* mRNA was substantially decreased in

NCR$^-$ subsets compared to that in NCR$^+$ subsets (fig. S3B). In conclusion, these data suggest that IL-22 production from ILC3s is increased by loss of the Notch signaling pathway.

Notch signals are cell-intrinsic during the differentiation of NCR$^-$ cells into NCR$^+$ ILC3s

To determine whether the decrease in the number of cells in the NCR$^+$ ILC3 subset of *Il7r*$^{Cre/+}$*Rbpj*$^{fl/fl}$ mice was a result of a direct or an indirect effect of the loss of Notch signaling, we analyzed competitive mixed bone marrow chimeric mice. The extent of reconstitution of ILCs and T cells was similar in both types of chimeras (Fig. 3). Wild-type competitor cells were more efficient at reconstitution than were both *Il7r*$^{Cre/+}$*Rbpj*$^{fl/+}$ and *Il7r*$^{Cre/+}$*Rbpj*$^{fl/fl}$ donor cells, because they were derived from mice deficient in one allele of *IL7Rα* (Fig. 3, A to D). This could be explained by the better proliferation and survival of both wild-type progenitor and mature cells that depend on IL-7R signaling. Hence, the reconstitution experiments were analyzed by first determining the overall percentages of the cells of interest and then by evaluating the ratio of reconstituted

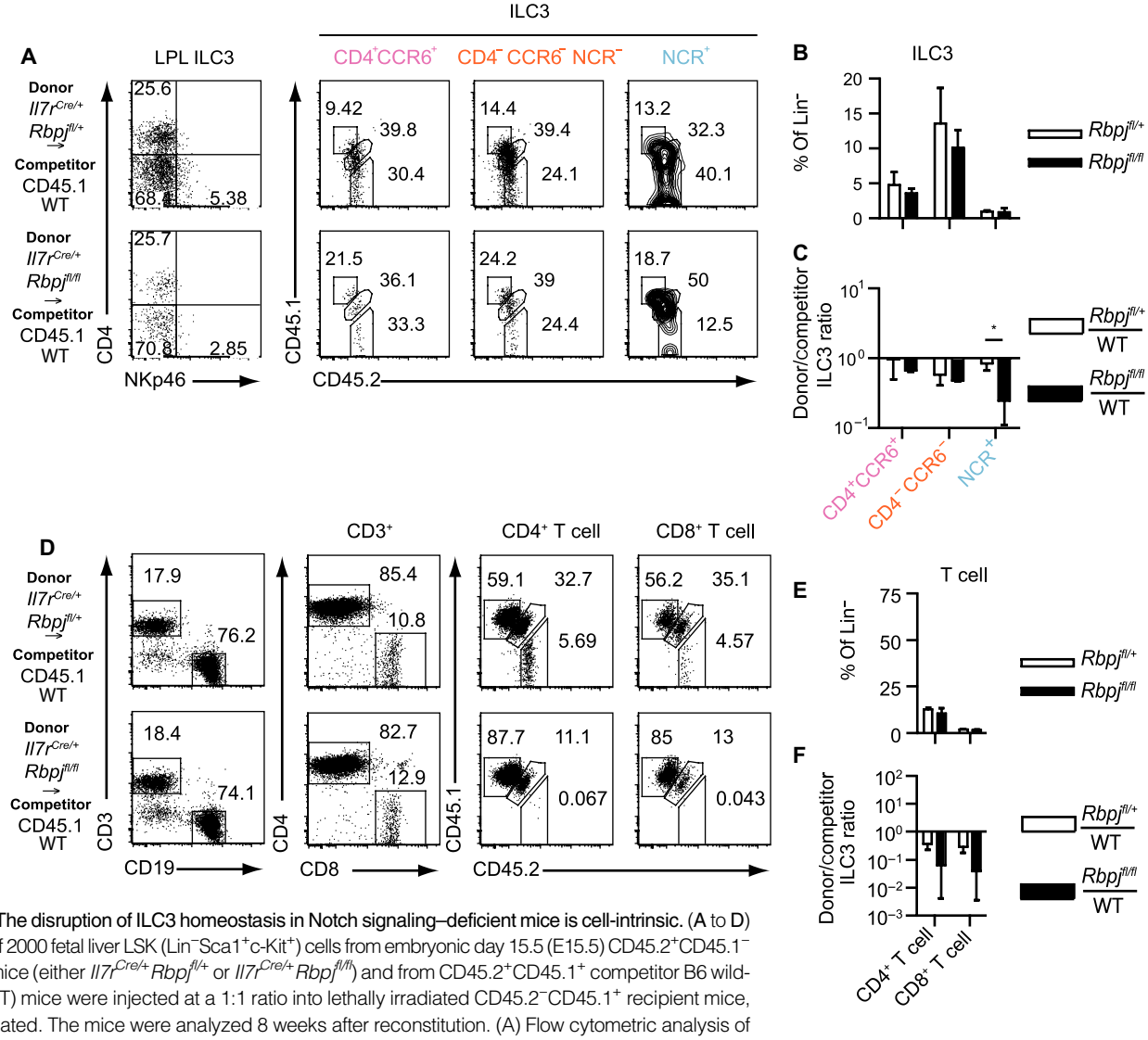

Fig. 3. The disruption of ILC3 homeostasis in Notch signaling–deficient mice is cell-intrinsic. (A to D) A total of 2000 fetal liver LSK (Lin$^-$Sca1$^+$c-Kit$^+$) cells from embryonic day 15.5 (E15.5) CD45.2$^+$CD45.1$^-$ donor mice (either *Il7r*$^{Cre/+}$*Rbpj*$^{fl/+}$ or *Il7r*$^{Cre/+}$*Rbpj*$^{fl/fl}$) and from CD45.2$^+$CD45.1$^+$ competitor B6 wild-type (WT) mice were injected at a 1:1 ratio into lethally irradiated CD45.2$^-$CD45.1$^+$ recipient mice, as indicated. The mice were analyzed 8 weeks after reconstitution. (A) Flow cytometric analysis of the ILC3s in the lamina propria of the indicated mice after reconstitution. LPL ILC3s were assigned on the basis of their cell surface expression of CD4, CCR6, and NKp46 into CD4$^+$CCR6$^+$ NCR$^-$ cells (pink), CD4$^-$CCR6$^-$ NCR$^-$ cells (orange), and CD4$^-$NKp46$^-$ NCR$^+$ cells (blue). (B) Percentages of donor ILC3 subsets from the lamina propria of both types of reconstituted mice [*Il7r*$^{Cre/+}$*Rbpj*$^{fl/+}$/WT (white); *Il7r*$^{Cre/+}$*Rbpj*$^{fl/fl}$/WT (black)]. (C) Donor/competitor ratios of ILC3 subsets [as defined in (A)] from mice reconstituted with *Il7r*$^{Cre/+}$*Rbpj*$^{fl/+}$/WT (white) or *Il7r*$^{Cre/+}$*Rbpj*$^{fl/fl}$/WT (black) cells. (D) Flow cytometric analysis of CD4$^+$ T cell (defined as CD3$^+$CD4$^+$) and CD8$^+$ T cell (defined as CD3$^+$CD8$^+$) subsets in the spleens of the indicated mice after reconstitution. (E) Percentages of donor CD4$^+$ T cell and CD8$^+$ T cell subsets from the lamina propria of both type of reconstituted mice [*Il7r*$^{Cre/+}$*Rbpj*$^{fl/+}$/WT (white); *Il7r*$^{Cre/+}$*Rbpj*$^{fl/fl}$/WT (black)]. (F) Donor/competitor ratios of CD4$^+$ T cell and CD8$^+$ T cell subsets [as defined in (C)] from mice reconstituted with *Il7r*$^{Cre/+}$*Rbpj*$^{fl/+}$/ WT (white) or *Il7r*$^{Cre/+}$*Rbpj*$^{fl/fl}$/WT (black) cells. Data are representative of two independent experiments, with four or five mice of each group analyzed per experiment. Data in (B) and (D) are means ± SEM. *P < 0.05, **P < 0.01, ***P < 0.001 by Mann-Whitney test.

cells between donor cells ($CD45.1^-CD45.2^+$) and competitor cells ($CD45.1^+CD45.2^+$). Similar to what was found in the $Rbpj^{fl/fl}$ mice, intestinal ILC3 subsets in the chimeric mice were differentially affected by the loss of Notch signaling (Fig. 3, A and B). *Rbpj*-deficient or *Rbpj*-sufficient hematopoietic progenitors made similar contributions to the $CD4^+CCR6^+$ and $CD4^-CCR6^-$ cells within the NCR^- ILC3 population; however, the size of the NCR^+ ILC3 population was statistically significantly reduced among the lymphoid cells derived from *Rbpj*-deficient progenitors as compared to that of *Rbpj*-sufficient progenitors (Fig. 3B). As expected, *Rbpj*-deficient progenitors were unable to reconstitute T cells (Fig. 3, C and D). Together, these results suggest that the mechanism for the decrease in the size of the NCR^+ population after inactivation of the Notch signaling pathway is cell-autonomous.

Intestinal NCR^+ ILC3s are derived from NCR^- precursors in a Notch signaling–dependent manner

Intestinal NCR^- ILC3s contain precursors of NCR^+ ILC3s (*11*–*13*, *19*). The NCR^- ILC3 subset is heterogeneous and can be subdivided on the basis of the cell surface expression of CD4 and CCR6. The $CCR6^+$ fraction is composed of $CD4^+$ and $CD4^-$ cells, whereas the $CCR6^-$ fraction is diverse and contains precursors that are potentially dependent on the Notch signaling pathway (*12*, *13*). We purified all three intestinal ILC3 subsets from $Il7r^{Cre/+}Rbpj^{fl/+}$ mice and $Il7r^{Cre/+}Rbpj^{fl/fl}$ mice (NCR^+, $CCR6^-NCR^-$, and $CD4^+CCR6^+NCR^-$) and analyzed the role of Notch signaling in their survival and differentiation (Fig. 4, A and B). The cell surface abundance of IL-7Rα was reduced on a fraction of $CCR6^-NCR^-$ cells isolated from the $Il7r^{Cre/+}Rbpj^{fl/fl}$ mice (Fig. 4A). The cells were then cultured for 4 days on control OP9 stromal cells or on OP9 cells that were transduced to express the Notch ligand delta-like 4 (OP9-DL4 cells) (Fig. 4, C and D). The $CD4^+CCR6^+NCR^-$ ILC3 subset was stable and insensitive to Notch signaling. Substantial differences were observed in the maintenance of NCR^+ cells under both conditions. Less NCR^+ cells were maintained either in the absence of Notch ligands (that is, when cultured on OP9 cells) or in cells from $Il7r^{Cre/+}Rbpj^{fl/fl}$ mice compared to their respective controls (Fig. 4D). Conversely, we found more frequently NCR^- cells after culture of sorted NCR^+ cells on OP9 cells (Fig. 4D), which suggested a role for Notch signaling in the maintenance of NKp46, but not RORγt or IL-7Rα in ILCs. When $CCR6^-NCR^-$ cells were cultured, most of them (~60%) maintained their phenotype (Fig. 4D). Moreover, NCR^+ cells obtained from Notch signaling–competent precursors were 1.5-fold more abundant in the presence of the Notch ligand than in its absence (Fig. 4D). The few NCR^+ cells that were obtained from Notch signaling–deficient precursors were insensitive to the presence of Notch ligands (Fig. 4D).

We then analyzed the abundances in the NCR^- and NCR^+ subsets of various transcripts that are direct targets of the Notch pathway or are important for the ILC developmental program. In contrast to *Tbx21*, the genes *Dtx1, Hes1*, and *Tcf7* could be considered to be Notch-inducible during ILC development (*21*). We found that mRNAs for these three genes were more abundant in the NCR^- cells than in the NCR^+ cells and were substantially decreased in the absence of Notch signaling, which suggests that the Notch pathway is active at the NCR^- stage (Fig. 4E). In contrast, the abundances of *Id2*, *Il7r*, and *Gata3* mRNAs were not statistically significantly different between the NCR^- and NCR^+ cells in the context of loss of Notch signaling (Fig. 4E and fig. S4). *Tbx21* mRNA was more abundant in NCR^+ cells than in the NCR^- ILC3s (Fig. 4E). In both cell populations, *Tbx21* mRNA was almost undetectable in the absence of Notch signaling. We also performed intracellular staining of ILC1s, NCR^-, and NCR^+ cells (Fig. 4F). Although T-bet was similarly low in abundance in all ILC3 subsets, confirming its essential role in the generation of NCR^+ cells, RORγt protein was substantially reduced in cells from the $Il7r^{Cre/+}Rbpj^{fl/fl}$ mice (Fig. 4G). These results suggest that two distinct pools of NCR^+ ILC3s differentiate in the lamina propria through *Rbpj*-dependent and *Rbpj*-independent pathways and that the Notch signaling pathway operates in NCR^- ILC3s by increasing not only the abundance of RORγt but also the expression of *Tcf7* and *Tbx21*.

Notch signaling directly stimulates the development of NCR^- ILC3 precursors into NCR^+ ILC3s

To complement our analyses of the role of the Notch signaling pathway on ILC3s, we generated mice with constitutive expression of the NICD in lymphoid cells ($Il7r^{Cre/+}NICD$ mice) (Fig. 5A). The percentages and total numbers of $CCR6^-NCR^-$ cells and NCR^+ ILC3s were statistically significantly increased in $Il7r^{Cre/+}NICD$ mice compared to those in the control mice, whereas the number of $CCR6^+NCR^-$ ILC3s remained unchanged (Fig. 5B). These results indicated that the Notch pathway was active in the $CCR6^-NCR^-$ cells. There was no increase in the mRNAs of proapoptotic genes in the absence of Notch signaling (fig. S5). Thus, we concluded that the absence of a large fraction of NCR^+ ILC3s in Notch signaling–deficient mice was not a result of increased apoptosis, but rather a low rate of differentiation. We did not detect the decreased expression of any gene encoding prosurvival factors in the absence of Notch signaling (fig. S5). On the contrary, the only difference detected in the absence of Notch signaling was the increase in expression of the prosurvival gene Bcl2 in NCR^- precursors (fig. S5). Hence, the increased numbers of ILC3s in the $Il7r\alpha^{Cre}Rosa26^{NICD/+}$ mice with constitutively active Notch signaling were likely not due to the increased survival of these cells.

We further tested whether Notch signaling also affected developing NCR^+ ILC3s by analyzing ILCs in the lamina propria of $Ncr1^{Cre/+}NICD$ mice, which constitutively express the active form of Notch in all cells expressing Ncr1 (NKp46). We found that all three ILC3 subsets were unchanged in percentages and numbers (Fig. 5, C and D). All subsets of ILC3s also had similar amounts of RORγt, NKp46, and IL-7Rα (fig. S6A). We concluded that the Notch signaling pathway had no effect on the survival of NCR^+ ILC3s. The MFI of NKp46 was increased in NCR^+ ILC3s expressing NICD, which is consistent with a role for Notch signaling in regulating the cell surface abundance of NKp46 (Fig. 5E), whereas the abundance of RORγt was unchanged in all ILC3 subsets (Fig. 5F). Furthermore, the total number of intestinal ILC1s was increased in the NICD-expressing mice (Fig. 5G). Because NICD had no effect on the ratio of NCR^+ ILC3s among total ILCs or the abundance of RORγt, we propose that constitutive activation of the Notch signaling pathway at the $NKp46^+$ stage increased the size of the ILC1 and cNK subsets independently of any potential ILC3 to ILC1 plasticity. Moreover, flow cytometric analysis of the cell surface amounts of both IL-7Rα and DX5 enabled the identification of ILC1s among total $NKp46^+NK1.1^+$ cells and tended to show that percentage of group 1 ILCs was decreased among ILC1s (fig. S6B). Together, these results support our conclusion that Notch has a direct role on the differentiation of NCR^- precursors into NCR^+ cells in the intestine, rather than modulating the survival or plasticity of $NKp46^+$ ILC3s.

In the absence of Notch signaling, the population of $CCR6^-NCR^-$ cells is devoid of Notch-dependent precursors of NCR^+ cells

We hypothesized that the maturation of NCR^- ILC3 precursors into NCR^+ ILC3s is blocked in the absence of canonical Notch signaling. Thus, we investigated the effect of loss of the Notch signaling pathway on the transcriptional profiles of different NCR^- ILC3 subsets. All NCR^- ILC3 subsets ($CD4^+CCR6^+$, $CD4^-CCR6^+$, and $CD4^-CCR6^-$) were present at comparable percentages and numbers in the lamina propria of *Rbpj*-deficient and *Rbpj*-haploinsufficient mice (Fig. 6, A and B). We then analyzed the

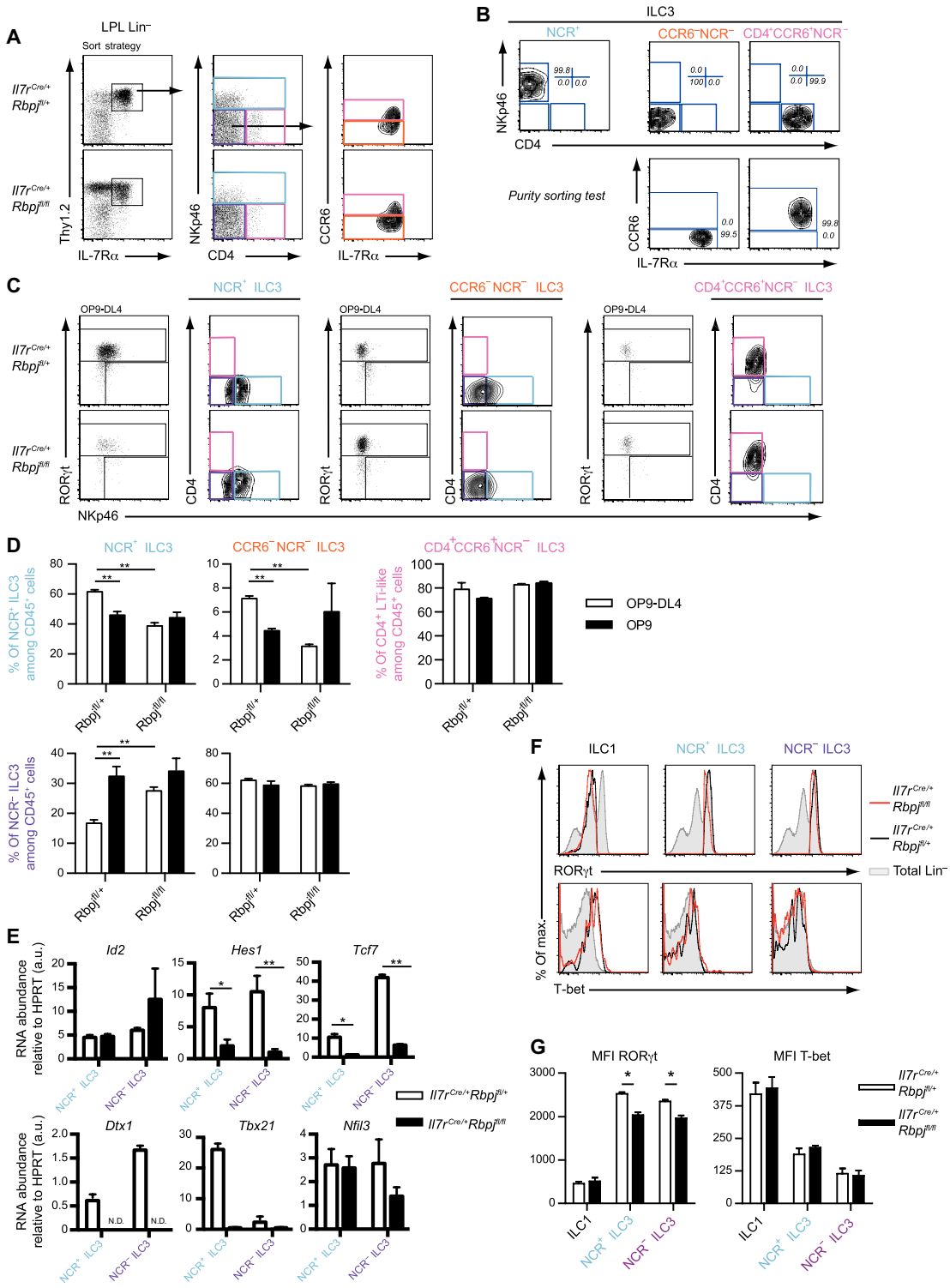

Fig. 4. Notch signaling contributes to the maintenance of NCR$^+$ ILC3s and the conversion of NCR$^-$ ILC3s into NCR$^+$ ILC3s. (**A**) Sorting strategy of NCR$^+$ ILC3s (blue; Lin$^-$ NK1.1$^-$KLRG1$^-$IL-7Rα$^+$ Thy1.2$^+$NKp46$^+$), CCR6$^-$ NCR$^-$ ILC3s (orange; Lin$^-$ NK1.1$^-$KLRG1$^-$IL-7Rα$^+$ Thy1.2$^+$NKp46$^-$CCR6$^-$), and CCR6$^+$ NCR$^-$ ILC3s (pink; Lin$^-$NK1.1$^-$KLRG1$^-$ IL-7Rα$^+$Thy1.2$^+$NKp46$^-$ CCR6$^+$) from *Il7r*$^{Cre/+}$ *Rbpj*$^{fl/+}$ mice (top) and *Il7r*$^{Cre/+}$*Rbpj*$^{fl/fl}$ mice (bottom). (**B**) Purity sorting test. After sorting, sorted cell populations were analyzed by flow cytometry for a second time to assess the purity of the cell populations, which was >99%. Data in (A) and (B) are representative of at least three experiments. (**C**) Flow cytometric analysis of the indicated ILC3 subsets isolated from *Il7r*$^{Cre/+}$*Rbpj*$^{fl/+}$ mice (top) and *Il7r*$^{Cre/+}$ *Rbpj*$^{fl/fl}$ mice (bottom) and cultured for 4 days on OP9-DL4 cells. Data are representative of four independent experiments. (**D**) Analysis of the indicated ILC3 subsets after culture on OP9-DL4 cells (white) or OP9 cells (black) expressed as a percentage of CD45$^+$ cells. Data are means ± SEM of four independent experiments. (**E**) qRT-PCR analysis of NCR$^+$ ILC3s and NCR$^-$ ILC3s isolated from *Il7r*$^{Cre/+}$ *Rbpj*$^{fl/+}$ mice (white) and *Il7r*$^{Cre/+}$*Rbpj*$^{fl/fl}$ mice (black). The abundances of the indicated mRNAs are presented relative to the average of those of the appropriate housekeeping genes. N.D., not detected. Data are means ± SEM of two independent experiments, with four mice of each genotype analyzed per experiment. HPRT, hypoxanthine-guanine phosphoribosyltransferase. (**F**) Flow cytometric analysis of the relative amounts of T-bet in ILC1s, NCR$^+$ ILC3s, and NCR$^-$ ILC3s isolated from *Il7r*$^{Cre/+}$*Rbpj*$^{fl/+}$ mice (black) and *Il7r*$^{Cre/+}$*Rbpj*$^{fl/fl}$ mice (red) compared to those in total Lin$^-$ cells (gray). Data are representative of three independent experiments. (**G**) Comparison of the MFIs of RORγt and T-bet in the indicated sorted cells isolated from *Il7r*$^{Cre/+}$ *Rbpj*$^{fl/+}$ mice (white) and *Il7r*$^{Cre/+}$ *Rbpj*$^{fl/fl}$ mice (black). Data are means ± SEM of three independent experiments, with two mice of each genotype analyzed per experiment. *P < 0.05, **P < 0.01, ***P < 0.001 by Mann-Whitney test.

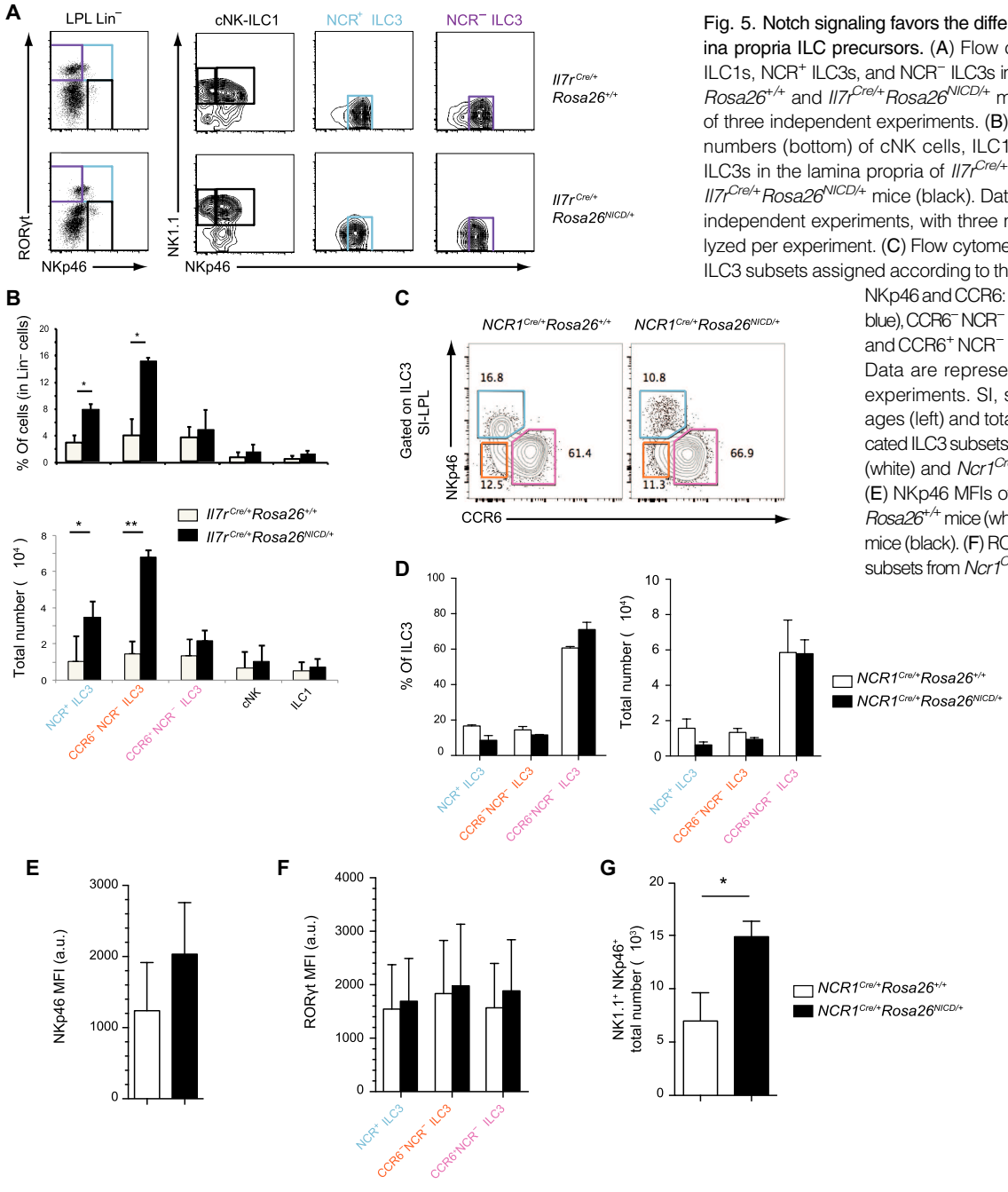

Fig. 5. Notch signaling favors the differentiation of ILC3s from lamina propria ILC precursors. (**A**) Flow cytometric analysis of cNK-ILC1s, NCR$^+$ ILC3s, and NCR$^-$ ILC3s in the lamina propria of *Il7r*$^{Cre/+}$*Rosa26*$^{+/+}$ and *Il7r*$^{Cre/+}$*Rosa26*$^{NICD/+}$ mice. Data are representative of three independent experiments. (**B**) Percentages (top) and total numbers (bottom) of cNK cells, ILC1s, NCR$^+$ ILC3s, and NCR$^-$ ILC3s in the lamina propria of *Il7r*$^{Cre/+}$*Rosa26*$^{+/+}$ mice (white) and *Il7r*$^{Cre/+}$*Rosa26*$^{NICD/+}$ mice (black). Data are means ± SEM of three independent experiments, with three mice of each genotype analyzed per experiment. (**C**) Flow cytometric analysis of the indicated ILC3 subsets assigned according to their cell surface expression of NKp46 and CCR6: NCR$^+$ ILC3s (NKp46$^+$CCR6$^-$; blue), CCR6$^-$ NCR$^-$ ILC3s (NKp46$^-$CCR6$^-$; orange), and CCR6$^+$ NCR$^-$ ILC3s (NKp46$^-$CCR6$^+$; pink). Data are representative of two independent experiments. SI, small intestine. (**D**) Percentages (left) and total numbers (right) of the indicated ILC3 subsets from *Ncr1*$^{Cre/+}$*Rosa26*$^{+/+}$ mice (white) and *Ncr1*$^{Cre/+}$*Rosa26*$^{NICD/+}$ mice (black). (**E**) NKp46 MFIs of NCR$^+$ ILC3s from *Ncr1*$^{Cre/+}$*Rosa26*$^{+/+}$ mice (white) and *Ncr1*$^{Cre/+}$*Rosa26*$^{NICD/+}$ mice (black). (**F**) RORγt MFIs of the indicated ILC3 subsets from *Ncr1*$^{Cre/+}$*Rosa26*$^{+/+}$ mice (white) and *Ncr1*$^{Cre/+}$*Rosa26*$^{NICD/+}$ mice (black). (**G**) Total numbers of cNK-ILC1s (NK1.1$^+$NKp46$^+$) from *Ncr1*$^{Cre/+}$*Rosa26*$^{+/+}$ mice (white) and *Ncr1*$^{Cre/+}$*Rosa26*$^{NICD/+}$ mice (black). Data in (D) to (G) are means ± SEM of two independent experiments, with two mice of each genotype analyzed per experiment. *$P < 0.05$, **$P < 0.01$, ***$P < 0.001$ by Mann-Whitney test.

transcriptional profiles, in Notch signaling–competent and Notch signaling–deficient cells, of a set of transcripts that includes transcription factors, chemokines, and cytokine receptors expressed in ILCs, as well as components of the Notch signaling pathway. We also analyzed ILC1s, CD4$^+$CCR6$^+$ ILC3s, and CD4$^-$CCR6$^+$ ILC3s and compared them to the NCR$^+$ and CCR6$^-$NCR$^-$ ILC3 subsets. Genes with low expression overall [less than 20-fold of that of *Tbp* (<3 mRNA molecules per cell) (*22*)] were removed from the analysis, and the abundances of all mRNAs were normalized to the average mRNA abundances of the housekeeping genes *Actb*, *Gapdh*, and *Hprt*.

Clustering of the samples and transcripts enabled the definition of gene signatures that characterized each subpopulation (Fig. 6C). ILC1s were separated from ILC3 subsets, whereas CD4$^+$CCR6$^+$ ILC3s clustered together with CD4$^-$CCR6$^+$ ILC3s, confirming their close relationship. Only for CCR6$^-$NCR$^-$ ILCs did cells from *Il7r*$^{Cre/+}$*Rbpj*$^{fl/fl}$ mice not cluster with cells from *Il7r*$^{Cre/+}$*Rbpj*$^{fl/+}$ mice, consistent with their dependence on Notch signaling. CCR6$^-$NCR$^-$ cells from *Il7r*$^{Cre/+}$*Rbpj*$^{fl/+}$ mice clustered with NCR$^+$ ILC3s, whereas cells from *Il7r*$^{Cre/+}$*Rbpj*$^{fl/fl}$ mice clustered with other NCR$^-$ ILC3 subsets. Target genes were identified as either decreased in expression (Fig. 6D, top) or increased in expression (Fig. 6D, bottom) with at least a 1.5-fold change in NCR$^+$ cells, CCR6$^-$NCR$^-$ ILC3s, and CCR6$^+$NCR$^-$ ILC3s from *Il7r*$^{Cre/+}$*Rbpj*$^{fl/fl}$ mice compared to haploinsufficient mice. CCR6$^-$NCR$^-$ ILC3s were the cells that showed the largest

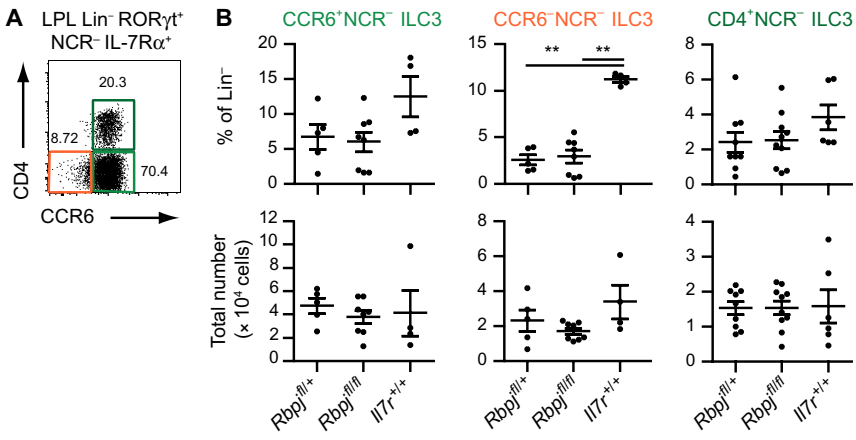

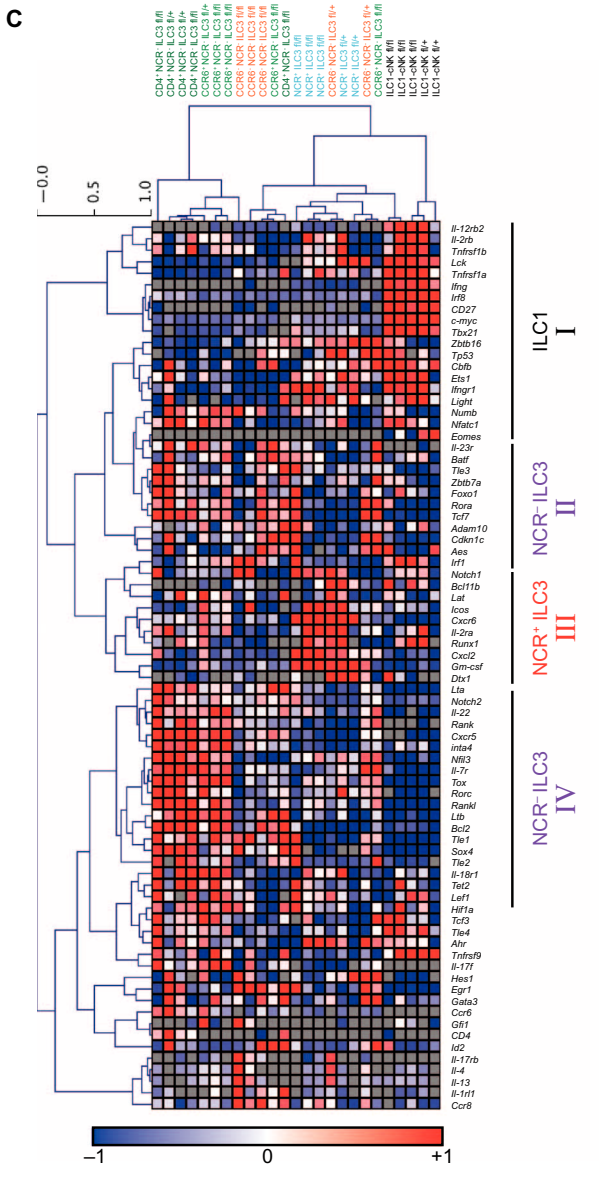

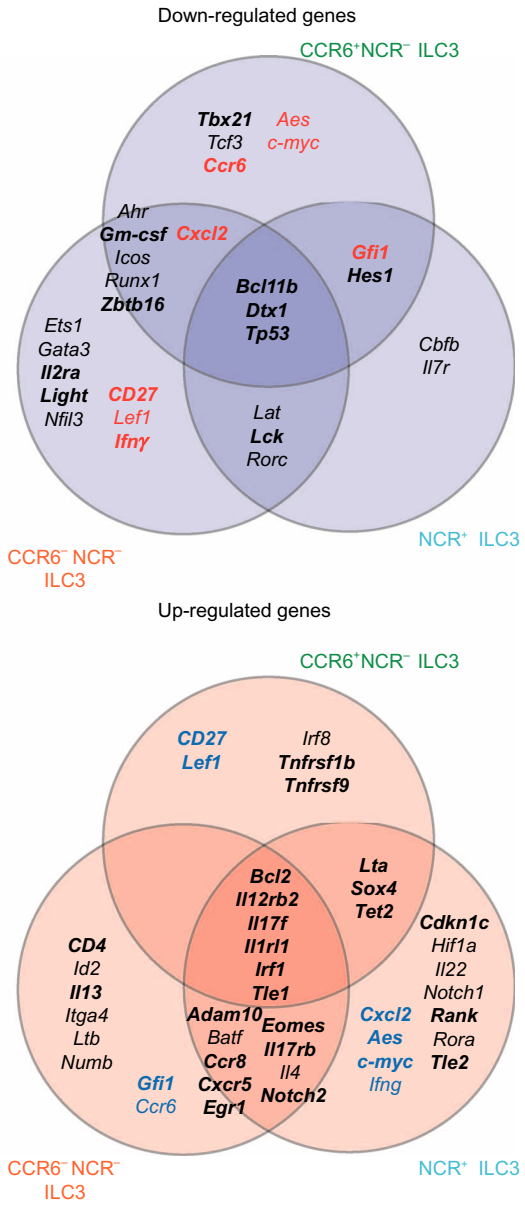

Fig. 6. The decrease in the number of NCR⁺ ILC3s in Notch signaling–deficient mice results from loss of the Notch-dependent RORγt⁺ subset. (A) Flow cytometric analysis of NCR⁻ ILC3 subsets from *Il7r*$^{+/+}$ *Rbpj*$^{fl/+}$ mice. All CD4⁺NCR⁻ ILC3s are CCR6⁺ (dark green), whereas CD4⁻NCR⁻ ILC3s are either CCR6⁺ (light green) or CCR6⁻ (orange). (B) Percentages (top) and total numbers (bottom) of the indicated NCR⁻ ILC3 subsets from *Il7r*$^{Cre/+}$ *Rbpj*$^{fl/+}$ mice, *Il7r*$^{Cre/+}$ *Rbpj*$^{fl/fl}$ mice, and *Il7r*$^{+/+}$ *Rbpj*$^{fl/+}$ mice. Each data point represents an individual mouse. Data are means ± SEM of at least three independent experiments, with two mice of each genotype analyzed per experiment. *$P < 0.05$, **$P < 0.01$, ***$P < 0.001$ by Mann-Whitney test. (C) Single-cell multiplex analysis of mRNA abundances in cNK-ILC1s, NCR⁺ ILC3s, and NCR⁻ ILC3s in the lamina propria of *Il7r*$^{Cre/+}$ *Rbpj*$^{fl/+}$ mice and *Il7r*$^{Cre/+}$ *Rbpj*$^{fl/fl}$ mice. Results are presented as relative to the average expression of housekeeping genes. After hierarchical clustering, data were median-centered and scaled for visualization (red, high expression; blue, low expression; gray, no expression). (D) Venn diagrams of the genes that were decreased in expression (top) and the genes that were increased in expression (bottom) in the indicated subsets of cells isolated from *Il7r*$^{Cre/+}$ *Rbpj*$^{fl/fl}$ mice compared to those in the same subsets isolated from *Il7r*$^{Cre/+}$ *Rbpj*$^{fl/+}$ mice. Genes with at least a 1.5-fold change in expression are listed, whereas those with at least a two-fold change in expression are in bold. Genes that are listed in colored text are either increased or decreased in expression in other cell populations. Data are representative of at least two independent experiments, with four mice of each genotype analyzed per experiment. *P* values from statistical analysis of the data in (D) are summarized in table S1.

number of genes that were decreased in expression (20 genes) compared to those in CCR6$^+$NCR$^-$ cells and NCR$^+$ cells, whereas increased gene expression was mainly found in NCR$^+$ ILC3s (29 genes) and CCR6$^-$NCR$^-$ ILC3s (23 genes).

Accordingly, most of the genes that were decreased in expression in the CCR6$^-$NCR$^-$ subset in the context of loss of Notch signaling were found in the NCR$^+$ ILC3 clusters (cluster III, 6 of 10 transcripts), including *Runx1*, *Bcl11b*, *Icos*, and *Dtx1*, and in ILC1 clusters (cluster I, 4 of 19 transcripts), including *Zbtb16*, *Ets1*, and *Nfil3*. On the other hand, increased gene expression was found in NCR$^-$ ILC3 clusters (clusters II and IV), including genes encoding cytokines (*Il17f* and *Ltb*) or cytokine and chemokine receptors (*Ccr6*, *Ccr8*, *Il17rb*, and *Cxcr5*). These results suggest that the transcriptional profile of CCR6$^-$NCR$^-$ cells from *Il7r*$^{Cre/+}$*Rbpj*$^{fl/+}$ mice was similar to that of NCR$^+$ ILC3s in haplosufficient mice and was completely different because of inactivation of Notch signaling. Conversely, many of the transcripts that were increased in abundance in CCR6$^-$NCR$^-$ cells from *Il7r*$^{Cre/+}$*Rbpj*$^{fl/fl}$ mice were shared with other NCR$^-$ ILC3 subsets. The expression of *Id2*, *Gata3*, *AhR*, and *Nfil3*, which are essential for the generation of helper-like ILCs, although present in all ILC subsets (*1*–*3*, *10*, *23*), was substantially decreased by the loss of Notch signaling in CCR6$^-$NCR$^-$ cells (fig. S7). *Nfil3* and the Notch-dependent gene *Gata3* were also reduced in expression, whereas the expression of *Tox*, which is important for ILC development (*24*), was not affected (Fig. 6D and fig. S7). *Zbtb16* [which encodes the PLZF (promyelocytic leukaemia zinc finger) protein] is transiently expressed by most ILCs in a Notch-dependent manner (*16*). Accordingly, we found that the expression of *Zbtb16* was decreased in all ILC3 subsets from *Il7r*$^{Cre/+}$*Rbpj*$^{fl/fl}$ mice and statistically significantly decreased in ILC1s (fig. S7).

Finally, we were interested in the expression patterns of *Rorc* and *Tbx21*, both of which are required for the development of NCR$^+$ ILC3s (*3*, *25*, *26*). *Rorc* expression in ILC3 subsets from *Il7r*$^{Cre/+}$*Rbpj*$^{fl/fl}$ mice was substantially reduced compared to that in ILC3 subsets from *Il7r*$^{Cre/+}$*Rbpj*$^{fl/+}$ mice. In comparison, T-bet was highly abundant in ILC1s, and, although it was also found in *Rbpj*-sufficient and *Rbpj*-deficient ILC3s, quantities of the T-bet protein did not exhibit a reduction in protein abundance that corresponded with *Tbx21* expression after loss of Notch signaling (Fig. 4, E to G). This apparent discrepancy might be explained by the low abundance of T-bet protein in ILC3s, which prevented its proper quantification (Fig. 4F). These results suggest that CCR6$^-$NCR$^-$ cells in which Notch signaling was lost could not give rise to NCR$^+$ ILC3s such that, in contrast to Notch signaling–competent cells, they had more genes with a similar transcriptional pattern to that found in CCR6$^+$CD4$^+$ and CCR6$^+$CD4$^-$NCR$^-$ cells. Hence, the Notch signaling pathway appeared to activate a complete transcriptional program that drove progression of the cells toward an NCR$^+$ fate.

DISCUSSION

Intestinal NCR$^-$ ILC3s contain the putative NCR$^+$ precursors previously suggested to be Notch-dependent (*10*–*13*). Intestinal ILC3s are both Notch1$^+$ and Notch2$^+$, whereas fibroblastic stromal cells in lymph nodes (*27*) and in intestinal Paneth cells (*28*) produce the Notch ligands. ILC3s are more abundant in the small intestine than in the colon (*9*), and a study showed a lower ratio of NCR$^+$ cells to NCR$^-$ cells in the colon compared to that in the small intestine (*29*).

Here, we demonstrated that the intestinal lamina propria is composed of at least two distinct pools of NCR$^+$ ILC3s that differ in their dependency on the Notch pathway. Both a major Notch-dependent and a minor (20%) Notch-independent subsets were found in mice in which the *Notch2* or *Rbpj* loci were ablated in hematopoietic progenitor cells (under either the *Il7r* or *Vav* promoters). These results suggest that the reduction in the number of NCR$^+$ ILC3s in *Rbpj*-deficient mice was Notch2-dependent, independent of bystander T cells, and cell-autonomous, which was confirmed by analysis of competitive mixed bone marrow chimeras. On the other hand, CCR6$^+$NCR$^-$ ILC3s, which were largely composed of LTi-like cells, were only mildly affected by the absence of Notch signaling. Thus, we propose a model for the Notch-dependent and Notch-independent differentiation of NCR$^+$ ILC3s (Fig. 7). We further obtained evidence for the segregation of Notch-dependent and Notch-independent NCR$^+$ subsets in vitro. The analysis of 93 transcripts showed that CCR6$^-$NCR$^-$ ILC3 precursors that clustered with NCR$^+$ cells in haplosufficient mice were more similar to LTi-like cells in the absence of Notch signaling. Hence, the specific effect of loss of Notch signaling in CCR6$^-$NCR$^-$ cells resulted in the absence of a subset that resembles NCR$^+$ cells.

The progression from NCR$^-$ toward NCR$^+$ cells is partly controlled by *AhR* (*10*) and T-bet (*11*–*13*). Accordingly, the Notch-independent NCR$^+$ subset that we identified still had *Tbx21* and *AhR* mRNAs, albeit at reduced amounts compared to those in the Notch-dependent cell subsets. Previous studies with *Tbx21*$^{-/-}$ mice revealed that the few T-bet–independent NCR$^+$ cells showed a reduction in RORγt abundance (*11*). Consistent with this finding, we observed substantial decreases in *Rorc* mRNA and RORγt protein in both NCR$^-$CCR6$^-$ cells and NCR$^+$ cells in Notch signaling–deficient mice, which suggests a role for Notch in activating the expression of both *Tbx21* and *Rorc*. Although *Dtx1* expression was undetectable, *Hes1*, *Tcf7*, *Zbtb16*, *Nfil3*, and *Gata3* transcripts were only partially reduced in abundance in the CCR6$^-$NCR$^-$ precursors, which suggests that their expression is regulated, in part, through an alternative pathway. Because our analyses were performed on populations rather than on single cells, the decreased expression of these genes may rather reflect the absence of the Notch-dependent precursors. Nonetheless, NCR$^+$ cells exhibited decreased amounts of *Hes1*, *Tcf7*, *Tbx21*, and *Rorc* transcripts in Notch signaling–deficient ILCs, which suggests that the Notch-independent generation of NCR$^+$ ILCs is compatible with reduced amounts of these transcripts.

Gata3 inhibits RORγt expression in ILC3s (*14*) and a 50% reduction in RORγt abundance is sufficient to promote the development of T-bet$^+$ NCR$^+$ ILC3s (*14*), presumably through derepression of *Gata3* expression. Because the expression of both *Gata3* and *Tbx21* was reduced in NCR$^-$ cells, the decrease in RORγt abundance appeared to be attributable to the loss of Notch signaling. In *Tbx21* haploinsufficient mice, NCR$^+$ ILC3s are decreased in number, and T-bet directly stimulates the expression of *Notch2*, but not *Notch1*, during the development of NKp46$^+$ ILCs (*13*). In our analysis, when Notch signaling was inactivated, both *Notch1* and *Notch2* transcripts were increased in abundance in NCR$^+$ ILC3s, although the abundance of T-bet was maintained. These results suggest that the Notch signaling pathway also regulates receptor abundance through a negative feedback loop.

It was proposed that Notch protein in ILC3s depends on AhR (*10*). Although decreased in abundance among the NCR$^-$ precursors, *AhR* transcripts were still present in Notch signaling–deficient cell populations, which could explain the maintenance of an AhR-dependent, IL-22–secreting CD4$^-$CCR6$^+$ population in normal numbers. It thus appears that the coordinated actions of RORγt, T-bet, Gata3, AhR, and Notch on the same target cells maintain the equilibrium between the NCR$^-$ and NCR$^+$ ILC3 subsets. When one of these coregulators is perturbed by environmental cues or pathologic conditions, the equilibrium shifts toward another subset, thus explaining the plasticity of ILC3s.

Experiments with NCR$^+$ cells in vitro showed that NKp46$^+$ ILC3s were more efficiently maintained in the presence rather than absence of Notch ligands, which suggests that Notch signaling is important for the cell surface expression of NKp46 or for maintaining it. Conversely, in Notch

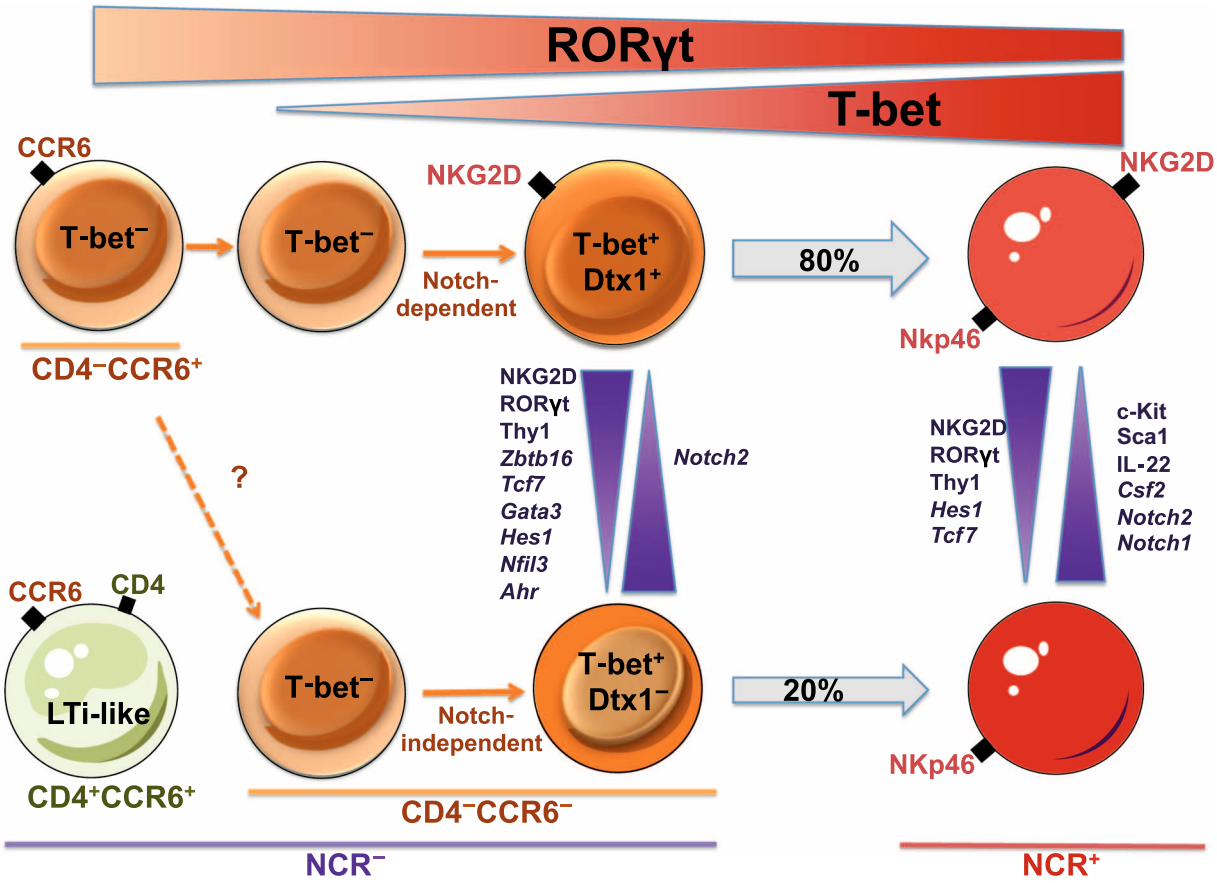

Fig. 7. Schematic representation of the differentiation of intestinal NCR$^+$ ILC3s. The recapitulative model shows that whereas 80% of the NCR$^+$ cells were derived from *Dtx1*$^+$ T-bet$^+$ precursors, the Notch-independent pool was derived from a *Dtx1*$^-$ T-bet$^+$ precursor and represents 20% of the total number of NCR$^+$ cells. The absence of Notch signaling is associated with decreased amounts of NKG2D, RORγt, and Thy1, as well as of Zbtb16, Tcf7, Gata3, Hes1, Nfil3, and AhR. Although the genes encoding most of these factors are Notch targets, the factors were decreased in abundance but were not absent in Notch-independent precursors. Similar to their NCR$^-$ precursors, the Notch-independent NCR$^+$ cells showed decreased amounts of similar proteins (including NKG2D, RORγt, Thy1, Tcf7, and Hes1). They also exhibited specific increases in c-Kit and Sca1 abundance. The transcripts for *Notch1* and *Notch2* were also both increased in abundance in Notch-independent NCR$^+$ cells. The Notch-independent NCR$^+$ cells expressed more *Csf2* transcripts under steady-state conditions and secreted more IL-22 before and after activation than did Notch-dependent NCR$^+$ cells. The CCR6$^+$ subset was added to the scheme as an early progenitor of Notch-dependent NCR$^+$ cells because a previous study showed that CD4$^-$CCR6$^+$ ILC3s can differentiate into NCR$^+$ ILC3s in a T-bet–dependent manner after culture in the presence of Notch ligands (that is, on OP9-DL1 cells) (*13*).

signaling–deficient conditions, the NK cell markers NKp46 and NKG2D were minimally abundant on the surface of NCR$^+$ cells. Other cell surface markers, such as Thy1, c-Kit, and Sca1, also changed their abundances on ILC3 populations when the Notch signaling pathway was lost, which implies that they are partially regulated by the Notch pathway. Transcripts of genes encoding pro- and antiapoptotic factors in ILC3s were similarly abundant in the presence or absence of Notch signaling, which suggests that NCR$^+$ cells do not undergo apoptosis in the absence of Notch. CCR6$^+$ NCR$^-$ ILC3s (LTi-like cells) appeared as a stable population, which was in comparison to NCR$^+$ ILC3s, which lost RORγt and produced IFN-γ, entering a state known as "ex-ILC3" (*9*, *12*). However, neither enhancement nor abrogation of the Notch signaling pathway alone was sufficient to drive the conversion of ILC3s to ILC1s. The increase in the number of NK cells in mice expressing NICD under the control of the *Ncr1* regulatory sequences was probably due to a specific action of Notch on ILC1s. This observation did not correlate with the transition from ILC3s to ILC1s, because the number of NCR$^+$ ILC3s was stable, the abundance of RORγt ILC3s was normal, and the ILC1 subset decreased as a percentage of group 1 ILCs.

In mice in which NICD was expressed at the earliest developmental stage of IL-7R$^+$ precursor, more NCR$^-$ cells received a Notch signal, and consequently, both the CCR6$^-$NCR$^-$ and NCR$^+$ populations were increased in number. In culture, NCR$^-$ cells that originated from NCR$^+$ cells were detected, and they were more frequent in the absence of Notch signaling, which suggests that NCR$^+$ cells may revert to NCR$^-$ cells in the absence of Notch signaling. However, no differences in NCR$^-$ cell numbers were found in vivo in the absence of Notch signaling. Hence, these results suggest that *Ncr1* is a direct target of Notch in ILC3s and is required to maintain the NCR$^+$ identity of the Notch-dependent cell subset. As observed in vitro, the cell surface expression of NKp46 could be transient on ILC3s, which implies that the NCR$^-$ cell population could contain some "ex-NCR$^+$" cells. Only a fate map mouse model tracing the NKp46$^+$ cells could determine whether the reversion of NCR$^+$ cells to NCR$^-$ ILC3s is a common event in the intestine. However, we consider

that process to be unlikely because a decrease in *Nkp46* expression in the absence of Notch signaling should have revealed an enrichment, rather than a reduction, of the NCR^+ transcriptional signature among the $CCR6^-NCR^-$ population in Notch signaling–deficient mice.

In comparison to previous studies, the mouse model reported here exhibits an inactivation of the Notch signaling pathway that is restricted to the lymphoid compartment and does not affect the Notch2-dependent DC subsets that deliver regulatory cytokines to ILCs. Under steady-state conditions, ILC3s support intestinal homeostasis through such diverse mechanisms as IL-22 secretion to control intestinal microbiota (*30*) or granulocyte-macrophage colony-stimulating factor secretion, which preserves the tolerogenic function of intestinal DCs (*31*). We report that Notch signaling–deficient ILC3 subsets have quantitative differences in their secretory capacities that could reinforce or challenge their steady-state functions. In Notch signaling–deficient ILC3 subsets, the production of IL-17F, IL-22, and Csf2 was increased compared to that of their Notch signaling–sufficient counterparts, whereas the production of IFN-γ was unaffected. Notch signaling–deficient NCR^+ ILC3s that also had lower amounts of cell surface NCR markers may have different functions during infection and inflammation. In conclusion, our study reveals that the Notch2 canonical signaling pathway regulates both the plasticity and function of adult ILC3s.

MATERIALS AND METHODS

Mice

Il7r^{Cre}*Rosa26*^{YFP} mice [provided by H.-R. Rodewald, German Cancer Research Center (*32*)] were crossed with *Rbpj*^{tm1Hon} mice (*33*) (*Il7r*$^{Cre/+}$*Rbpj*$^{fl/+}$*Rosa26*^{YFP}), Notch2 mice (*Il7r*$^{Cre/+}$*Notch2*$^{fl/+}$*Rosa26*^{YFP}) (*34*), or NICD mice (*Il7r*$^{Cre/+}$*Rosa26*$^{NICD/+}$) (*35*). *Vav*^{Cre} and *Ncr1*^{Cre}*Rosa26*$^{NICD/+}$ mice were from the laboratory of C.A.J.V. All animal experiments were approved by the Pasteur Institute Safety Committee in accordance with French Agriculture Ministry and the European Union guidelines.

Cell preparation

Fetal liver, bone marrow, thymic lobes, spleens, and lamina propria lymphocytes (LPLs) were harvested, dissociated, and resuspended in Hanks' balanced salt solution (HBSS) supplemented with 1% fetal calf serum (FCS; Gibco). Fetal liver, bone marrow, and spleen cells were depleted of Lin^+ cells by staining with biotinylated-conjugated antibodies specific for lineage markers [for bone marrow cells, these include CD3ε, CD5, CD8α, CD11c, CD19, Ter119, Gr-1, NK1.1, T cell receptor β (TCRβ), and TCRδ; for spleen cells, these include CD3ε, CD5, CD8α, CD19, Ter119, Gr-1, TCRβ, and TCRδ], followed by incubation with streptavidin microbeads (Miltenyi Biotec). Depletion was performed on LS MACS columns (Miltenyi Biotec) from which the negative fraction was recovered. To isolate LPLs, the small bowel was flushed with phosphate-buffered saline (PBS) and the conjunctive tissue and Peyer's patches were carefully removed. The intestine was opened and cut into 1-cm pieces. To eliminate epithelial cells and intraepithelial lymphocytes, these fragments were incubated at 37°C in 50 ml of RPMI 1640 (Gibco) containing 10% FCS and 10 mM Hepes buffer under strong agitation for 30 min, which was followed by vortex treatment for 4 min. For LPL isolation, the remaining fragments were incubated in identical medium to which was added type VIII collagenase (0.5 mg/ml; Sigma-Aldrich) and were shaken for 30 min at 37°C. To complete digestion, the suspension was repeatedly passed through a 10-ml syringe for 5 min and then filtered through a 40-μm cell strainer (BD Biosciences) and collected by centrifugation. The cell pellet was resuspended in 44% Percoll (GE Healthcare), laid over 67% Percoll, and centrifuged at 600*g* for 20 min at 20°C. Cells at the interface were collected, washed in HBSS containing 1% FCS, and recovered.

Flow cytometry and cell sorting

Flow cytometry data were acquired with a FACSCanto II or LSRFortessa flow cytometer (Becton Dickinson) and analyzed with FlowJo software (Tree Star). Dead cells were eliminated by exclusion with propidium iodide. Cells were stained intracellularly after permeabilization and fixation with Foxp3 Permeabilization/Fixation Concentrate and Diluent (eBioscience). Cells were then incubated for 5 min with DAPI (4′,6-diamidino-2-phenylindole; Invitrogen). LPL cells were purified with a FACSAria III (Becton Dickinson). Cells were recovered in tubes or in 96-well quantitative PCR (qPCR) plates for gene expression analysis.

Antibodies

All antibodies were from BD Biosciences, eBioscience, BioLegend, Cell Signaling Technology, or R&D Systems. Antibodies were biotinylated or conjugated to fluorochromes [fluorescein isothiocyanate, phycoerythrin (PE), PECy5, PerCPCy5.5, PECy7, allophycocyanin (APC), Alexa Fluor 647, APCCy7, Pacific Blue, BV421, eFluor450, V500, BV605, BV655, BV700, and BV786] and were specific for the following mouse antigens: Ly76 (TER119), Gr-1 (RB6-8C5), CD11c (HL3), CD3ε (145-2C11), CD5 (53-7.3), CD19 (6D5), NK1.1 (PK136), IL-7Rα (A7R34), c-Kit (2B8), Sca1 (D7), RORγt (AFKJS-9), $\alpha_4\beta_7$ (DATK32), Flt3 (A2F10), Ly6D (48-H4), CD8 (53-6.7), TCRβ (H57-597), TCRδ (GL3), CCR6 (29-2L17), CD4 (GK1.5), CD25 (PC61), CD44 (IM7), Thy1.2 (53-2.1), NKp46 (29A1.4), GATA3 (L50-823), ICOS (C398.4A), Ly49 CIFH (14B11), IFN-γ (XMG1.2), IL-22 (1H8PWSR), T-bet (eBio4B10), CD27 (LG.3A10), T1/ST2 (DIH9), CD45.1 (A20), CD45.2 (104), CD23 (B3B4), IL-17A (TC11.18H10.1), CD49a (HMa1), CD49b (DX5), NKG2D (CX5), and CD21 (7E9). Antibody against human Ki-67 (B56) was obtained from BD Pharmingen.

Cell culture

All experiments were performed in 96-well plates at 37°C and 5% CO_2 and in culture medium consisting of Opti-MEM, 10% (v/v) FCS, penicillin (100 U/ml), streptomycin (100 μg/ml), and 50 μM 2-mercaptoethanol (Gibco). OP9 and OP9-DL4 stromal cells were seeded into 96-well plates. The culture medium was supplemented with saturating amounts of c-Kit ligand, Flt3 ligand, IL-2, and IL-7. The presence of ILC3 subsets was determined by flow cytometric analysis of the expression of NKp46, RORγt, CCR6, and CD4 proteins among cultured cells after 4 days on OP9 or OP9-DL4 cells.

Chimeric reconstitution

Recipient Ly5.1 mice were sublethally irradiated (800 rad) before injection. Fetal liver progenitors (Lin^-IL-$7R\alpha^-$c-$Kit^{hi}Sca1^+$) cells were sorted from donor Ly5.2 or competitor Ly5.1 × Ly5.2 E15 embryos and then mixed at 1:1 ratio for injection. Additionally, protective congenic bone marrow cells (1×10^6 T cell–depleted Ly5.1 bone marrow cells) in PBS were also injected at the same time into the retro-orbital vein. Reconstituted mice were analyzed after 8 weeks. Cells from the recipient mice were $CD45.1^+CD45.2^-$, whereas competitor cells (wild-type B6) were $CD45.1^+CD45.2^+$, and *Rbpj*-deficient or *Rbpj*-sufficient donor cells were $CD45.1^-CD45.2^+$.

RT-PCR analysis

Cells were sorted in Buffer RLT (Qiagen) containing 2-mercaptoethanol (Sigma-Aldrich) and were frozen at −80°C. RNA was obtained with an RNeasy Micro Kit (Qiagen), and complementary DNA (cDNA) was

obtained with the PrimeScript RT Reagent Kit (Takara). A 7300 Real-Time PCR System (Applied Biosystems) and TaqMan technology (Applied Biosystems) or SYBR Green Technology (Qiagen) were used for qRT-PCR analysis. A bilateral unpaired Student's *t* test was used for statistical analysis. The following primers were from SABiosciences: *Il17f* (PPM05398E), *Il22* (PPM481A), and *Gapdh* (PPM02946E). The following primers were from Applied Biosystems: *Il1r1* (Mm_00434237_m1), *Il23r* (Mm_00519943_m1), *Csf2* (Mm_01290062_m1), *Ifnγ* (Mm_01168134_m1), *Casp3* (Mm_01195085_m1), *Casp9* (Mm_00516563_m1), *Bcl2* (Mm_00477631_m1), *Bcl2cl1* (Mm_00427783_m1), *Bcl2cl11* (Mm_00432359_m1), *Birc3* (Mm_01168413_m1), *Bik* (Mm_00476123_m1), *Hprt* (Mm_00446968_m1), and *Actb* (Mm_02619580_g1).

Multiplex RT-PCR analysis

Total RNA from the appropriate cell populations was extracted as previously described (*19*) and mixed in 10 μl of CellsDirect One-Step qRT-PCR Kit (Life Technologies), containing a mixture of diluted primers (0.05× final concentration; see table S1 for sequences). Preamplified cDNA (22 cycles) was obtained according to the manufacturer's instructions and was diluted 1:5 in TE buffer (pH 8; Ambion). The sample mixture was as follows: diluted cDNA (2.9 μl), Sample Loading Reagent (0.32 μl; Fluidigm), and either TaqMan Universal PCR Master Mix (3.5 μl; Applied Biosystems) or Solaris qPCR Low ROX Master Mix (3.5 μl; GE Dharmacon). The assay mixture was as follows: Assay Loading Reagent (Fluidigm) and either TaqMan (Applied Biosystems) or Solaris (GE Dharmacon). A 96.96 Dynamic Array integrated fluidic circuit (IFC; Fluidigm) was primed with control line fluid, and the chip was loaded with assays (either TaqMan or Solaris) and samples with an HX IFC controller (Fluidigm). The experiments were run on a Biomark HD (Fluidigm) for 40 cycles. Samples that did not express at least one of three housekeeping genes (*Actb*, *Gapdh*, or *Hprt*), and genes that were present in less than 5% of the wells (except for *Dtx1*, *Pax5*, *Ebf1*, and *Rag2*) were removed from the analysis. Gene expression was assessed by the $2^{\Delta Ct}$ method.

Statistical analysis

Statistical analysis was performed with the Mann-Whitney nonparametric test where appropriate. These tests were performed with Prism software (GraphPad). Graphs containing error bars show means ± SEM. Statistical significance is represented as follows: $*P < 0.05$, $**P < 0.01$, and $***P < 0.001$.

SUPPLEMENTARY MATERIALS

www.sciencesignaling.org/cgi/content/full/9/426/ra45/DC1

Fig. S1. *Rbpj* is efficiently deleted in IL-7Rα$^+$ CLPs by Cre recombinase.

Fig. S2. Notch2 signaling is specifically required for both NCR$^+$ and NCR$^-$ ILC3s.

Fig. S3. Analysis of cytokine secretion and receptors in *Il7r*$^{Cre/+}$*Rbpj*$^{fl/+}$ mice and *Il7r*$^{Cre/+}$*Rbpj*$^{fl/fl}$ mice.

Fig. S4. Expression of *Gata3* and *Il7ra* in ILC3 subsets in the presence or absence of Notch signaling.

Fig. S5. The expression of genes encoding proapoptotic proteins in ILC3 subsets is unchanged by the loss of Notch signaling.

Fig. S6. Analysis of ILC3 and ILC1 subsets in *Ncr1*$^{Cre/+}$*Rosa26*$^{NICD/+}$ mice.

Fig. S7. Analysis of transcription factors expressed in ILC3 and ILC1 subsets in *Il7r*$^{Cre/+}$*Rbpj*$^{fl/+}$ mice and *Il7r*$^{Cre/+}$*Rbpj*$^{fl/fl}$ mice.

Table S1. *P* values for the differential expression of 92 genes between the NCR$^+$, CCR6$^+$ NCR$^-$, and CCR6$^-$NCR$^-$ subsets of *Il7r*$^{Cre/+}$*Rbpj*$^{fl/+}$ mice and *Il7r*$^{Cre/+}$*Rbpj*$^{fl/fl}$ mice.

REFERENCES AND NOTES

1. Y. Yokota, A. Mansouri, S. Mori, S. Sugawara, S. Adachi, S.-I. Nishikawa, P. Gruss, Development of peripheral lymphoid organs and natural killer cells depends on the helix–loop–helix inhibitor Id2. *Nature* **397**, 702–706 (1999).
2. K. Moro, T. Yamada, M. Tanabe, T. Takeuchi, T. Ikawa, H. Kawamoto, J.-i. Furusawa, M. Ohtani, H. Fujii, S. Koyasu, Innate production of T_H2 cytokines by adipose tissue-associated c-Kit$^+$Sca-1$^+$ lymphoid cells. *Nature* **463**, 540–544 (2010).
3. N. Satoh-Takayama, S. Lesjean-Pottier, P. Vieira, S. Sawa, G. Eberl, C. A. J. Vosshenrich, J. P. Di Santo, IL-7 and IL-15 independently program the differentiation of intestinal CD3$^-$NKp46$^+$ cell subsets from Id2-dependent precursors. *J. Exp. Med.* **207**, 273–280 (2010).
4. N. Serafini, C. A. J. Vosshenrich, J. P. Di Santo, Transcriptional regulation of innate lymphoid cell fate. *Nat. Rev. Immunol.* **15**, 415–428 (2015).
5. M. L. Robinette, A. Fuchs, V. S. Cortez, J. S. Lee, Y. Wang, S. K. Durum, S. Gilfillan, M. Colonna; Immunological Genome Consortium, Transcriptional programs define molecular characteristics of innate lymphoid cell classes and subsets. *Nat. Immunol.* **16**, 306–317 (2015).
6. R. E. Mebius, P. Rennert, I. L. Weissman, Developing lymph nodes collect CD4$^+$CD3$^-$ LTβ$^+$ cells that can differentiate to APC, NK cells, and follicular cells but not T or B cells. *Immunity* **7**, 493–504 (1997).
7. G. Eberl, S. Marmon, M.-J. Sunshine, P. D. Rennert, Y. Choi, D. R. Littman, An essential function for the nuclear receptor RORγt in the generation of fetal lymphoid tissue inducer cells. *Nat. Immunol.* **5**, 64–73 (2004).
8. S. Sawa, M. Cherrier, M. Lochner, N. Satoh-Takayama, H. J. Fehling, F. Langa, J. P. Di Santo, G. Eberl, Lineage relationship analysis of RORγt$^+$ innate lymphoid cells. *Science* **330**, 665–669 (2010).
9. C. Vonarbourg A. Mortha, V. L. Bui, P. P. Hernandez, E. A. Kiss, T. Hoyler, M. Flach, B. Bengsch, R. Thimme, C. Hölscher, M. Hönig, U. Pannicke, K. Schwarz, C. F. Ware, D. Finke, A. Diefenbach, Regulated expression of nuclear receptor RORγt confers distinct functional fates to NK cell receptor-expressing RORγt$^+$ innate lymphocytes. *Immunity* **33**, 736–751 (2010).
10. J. S. Lee, M. Cella, K. G. McDonald, C. Garlanda, G. D. Kennedy, M. Nukaya, A. Mantovani, R. Kopan, C. A. Bradfield, R. D. Newberry, M. Colonna, AHR drives the development of gut ILC22 cells and postnatal lymphoid tissues via pathways dependent on and independent of Notch. *Nat. Immunol.* **13**, 144–151 (2012).
11. G. Sciumé, K. Hirahara, H. Takahashi, A. Laurence, A. V. Villarino, K. L. Singleton, S. P. Spencer, C. Wilhelm, A. C. Poholek, G. Vahedi, Y. Kanno, Y. Belkaid, J. J. O'Shea, Distinct requirements for T-bet in gut innate lymphoid cells. *J. Exp. Med.* **209**, 2331–2338 (2012).
12. C. S. N. Klose, E. A. Kiss, V. Schwierzeck, K. Ebert, T. Hoyler, Y. d'Hargues, N. Göppert, A. L. Croxford, A. Waisman, Y. Tanriver, A. Diefenbach, A T-bet gradient controls the fate and function of CCR6$^-$RORγt$^+$ innate lymphoid cells. *Nature* **494**, 261–265 (2013).
13. L. C. Rankin, J. R. Groom, M. Chopin, M. J. Herold, J. A. Walker, L. A. Mielke, A. N. J. McKenzie, S. Carotta, S. L. Nutt, G. T. Belz, The transcription factor T-bet is essential for the development of NKp46$^+$ innate lymphocytes via the Notch pathway. *Nat. Immunol.* **14**, 389–395 (2013).
14. C. Zhong, K. Cui, C. Wilhelm, G. Hu, K. Mao, Y. Belkaid, K. Zhao, J. Zhu, Group 3 innate lymphoid cells continuously require the transcription factor GATA-3 after commitment. *Nat. Immunol.* **17**, 169–178 (2016).
15. T. Ebihara, C. Song, S. H. Ryu, B. Plougastel-Douglas, L. Yang, D. Levanon, Y. Groner, M. D. Bern, T. S. Stappenbeck, M. Colonna, T. Egawa, W. M. Yokoyama, Runx3 specifies lineage commitment of innate lymphoid cells. *Nat. Immunol.* **16**, 1124–1133 (2015).
16. M. G. Constantinides, B. D. McDonald, P. A. Verhoef, A. Bendelac, A committed precursor to innate lymphoid cells. *Nature* **508**, 397–401 (2014).
17. C. S. N. Klose, M. Flach, L. Möhle, L. Rogell, T. Hoyler, K. Ebert, C. Fabiunke, D. Pfeifer, V. Sexl, D. Fonseca-Pereira, R. G. Domingues, H. Veiga-Fernandes, S. J. Arnold, M. Busslinger, I. R. Dunay, Y. Tanriver, A. Diefenbach, Differentiation of type 1 ILCs from a common progenitor to all helper-like innate lymphoid cell lineages. *Cell* **157**, 340–356 (2014).
18. S. H. Wong, J. A. Walker, H. E. Jolin, L. F. Drynan, E. Hams, A. Camelo, J. L. Barlow, D. R. Neill, V. Panova, U. Koch, F. Radtke, C. S. Hardman, Y. Y. Hwang, P. G. Fallon, A. N. J. McKenzie, Transcription factor RORα is critical for nuocyte development. *Nat. Immunol.* **13**, 229–236 (2012).
19. C. Possot, S. Schmutz, S. Chea, L. Boucontet, A. Louise, A. Cumano, R. Golub, Notch signaling is necessary for adult, but not fetal, development of RORγt$^+$ innate lymphoid cells. *Nat. Immunol.* **12**, 949–958 (2011).
20. K. L. Lewis, M. L. Caton, M. Bogunovic, M. Greter, L. T. Grajkowska, D. Ng, A. Klinakis, I. F. Charo, S. Jung, J. L. Gommerman, I. I. Ivanov, K. Liu, M. Merad, B. Reizis, Notch2 receptor signaling controls functional differentiation of dendritic cells in the spleen and intestine. *Immunity* **35**, 780–791 (2011).
21. E. V. Rothenberg, Transcriptional drivers of the T-cell lineage program. *Curr. Opin. Immunol.* **24**, 132–138 (2012).
22. E. E. Schmidt, U. Schibler, High accumulation of components of the RNA polymerase II transcription machinery in rodent spermatids. *Development* **121**, 2373–2383 (1995).
23. T. Hoyler, C. S. N. Klose, A. Souabni, A. Turqueti-Neves, D. Pfeifer, E. L. Rawlins, D. Voehringer, M. Busslinger, A. Diefenbach, The transcription factor GATA-3 controls cell fate and maintenance of type 2 innate lymphoid cells. *Immunity* **37**, 634–648 (2012).
24. C. R. Seehus, P. Aliahmad, B. de la Torre, I. D. Iliev, L. Spurka, V. A. Funari, J. Kaye, The development of innate lymphoid cells requires TOX-dependent generation of a common innate lymphoid cell progenitor. *Nat. Immunol.* **16**, 599–608 (2015).

25. N. Satoh-Takayama, C. A. J. Vosshenrich, S. Lesjean-Pottier, S. Sawa, M. Lochner, F. Rattis, J.-J. Mention, K. Thiam, N. Cerf-Bensussan, O. Mandelboim, G. Eberl, J. P. Di Santo, Microbial flora drives interleukin 22 production in intestinal NKp46$^+$ cells that provide innate mucosal immune defense. *Immunity* **29**, 958–970 (2008).
26. L. A. Mielke, J. R. Groom, L. C. Rankin, C. Seillet, F. Masson, T. Putoczki, G. T. Belz, TCF-1 controls ILC2 and NKp46$^+$RORγt$^+$ innate lymphocyte differentiation and protection in intestinal inflammation. *J. Immunol.* **191**, 4383–4391 (2013).
27. N. Fasnacht, H.-Y. Huang, U. Koch, S. Favre, F. Auderset, Q. Chai, L. Onder, S. Kallert, D. D. Pinschewer, H. R. MacDonald, F. Tacchini-Cottier, B. Ludewig, S. A. Luther, F. Radtke, Specific fibroblastic niches in secondary lymphoid organs orchestrate distinct Notch-regulated immune responses. *J. Exp. Med.* **211**, 2265–2279 (2014).
28. T. Sato, J. H. van Es, H. J. Snippert, D. E. Stange, R. G. Vries, M. van den Born, N. Barker, N. F. Shroyer, M. van de Wetering, H. Clevers, Paneth cells constitute the niche for Lgr5 stem cells in intestinal crypts. *Nature* **469**, 415–418 (2011).
29. C. Song, J. S. Lee, S. Gilfillan, M. L. Robinette, R. D. Newberry, T. S. Stappenbeck, M. Mack, M. Cella, M. Colonna, Unique and redundant functions of NKp46$^+$ ILC3s in models of intestinal inflammation. *J. Exp. Med.* **212**, 1869–1882 (2015).
30. G. F. Sonnenberg, D. Artis, Innate lymphoid cell interactions with microbiota: Implications for intestinal health and disease. *Immunity* **37**, 601–610 (2012).
31. A. Mortha, A. Chudnovskiy, D. Hashimoto, M. Bogunovic, S. P. Spencer, Y. Belkaid, M. Merad, Microbiota-dependent crosstalk between macrophages and ILC3 promotes intestinal homeostasis. *Science* **343**, 1249288 (2014).
32. S. M. Schlenner, V. Madan, K. Busch, A. Tietz, C. Läufle, C. Costa, C. Blum, H. J. Fehling, H.-R. Rodewald, Fate mapping reveals separate origins of T cells and myeloid lineages in the thymus. *Immunity* **32**, 426–436 (2010).
33. H. Han, K. Tanigaki, N. Yamamoto, K. Kuroda, M. Yoshimoto, T. Nakahata, K. Ikuta, T. Honjo, Inducible gene knockout of transcription factor recombination signal binding protein-J reveals its essential role in T versus B lineage decision. *Int. Immunol.* **14**, 637–645 (2002).
34. B. McCright, J. Lozier, T. Gridley, Generation of new *Notch2* mutant alleles. *Genesis* **44**, 29–33 (2006).
35. L. C. Murtaugh, B. Z. Stanger, K. M. Kwan, D. A. Melton, Notch signaling controls multiple steps of pancreatic differentiation. *Proc. Natl. Acad. Sci. U.S.A.* **100**, 14920–14925 (2003).

Acknowledgments: We thank A. Bandeira for the critical reading of the manuscript and S. Bechet for help with the illustrations. We acknowledge the Center for Human Immunology and the Cytometry Platform at Institut Pasteur for support. We thank H.-R. Rodewald (German Cancer Research Center) for the *Il7r*^{Cre}*Rosa26*^{YFP} mice. **Funding:** This work was supported by the Pasteur Institute, INSERM, Université Paris Diderot, and the Ministère de la Recherche (to S.C. and T.V.); the Association pour la Recherche sur le Cancer (to S.C. and R.G.); the REVIVE Future Investment Program and the Agence Nationale de la Recherche (ANR) (grant "Twothyme") (to A.C.); the Ligue Nationale contre le Cancer (to J.P.D.S. and T.V.); the ANR (grant "Myeloten") (to R.G.); and the Institut National du Cancer (grant "Role of the immune microenvironment during liver carcinogenesis") (to R.G.) and the Université Sorbonne Paris Cité (grant "Mucocell"). **Author contributions:** S.C. performed most of the experiments and analyzed the data; T.P. performed and analyzed experiments and prepared figures; M.P. performed and analyzed experiments; T.V. performed experiments with the *Ncr1*^{Cre}NICD mice; E.-G.B. performed the mouse genotyping; D.G.-G. supervised experiments with lamina propria cells and contributed to the writing of the manuscript; C.A.J.V. generated the *Ncr1*^{Cre} mice; J.P.D.S. and A.C. contributed to the writing of the manuscript; and R.G. directed the research, designed the experiments, analyzed the data, and wrote the manuscript. **Competing interests:** The authors declare that they have no competing interests.

Submitted 8 January 2016
Accepted 18 April 2016
Final Publication 3 May 2016
10.1126/scisignal.aaf2223
Citation: S. Chea, T. Perchet, M. Petit, T. Verrier, D. Guy-Grand, E.-G. Banchi, C. A. J. Vosshenrich, J. P. Di Santo, A. Cumano, R. Golub, Notch signaling in group 3 innate lymphoid cells modulates their plasticity. *Sci. Signal.* **9**, ra45 (2016).

Science Signaling

Notch signaling in group 3 innate lymphoid cells modulates their plasticity

Sylvestre Chea, Thibaut Perchet, Maxime Petit, Thomas Verrier, Delphine Guy-Grand, Elena-Gaia Banchi, Christian A. J. Vosshenrich, James P. Di Santo, Ana Cumano and Rachel Golub

Sci. Signal. **9** (426), ra45.
DOI: 10.1126/scisignal.aaf2223

Plasticity in innate lymphoid cell function

Like the T cells and B cells of the adaptive immune system, cells in the innate immune system are key to organismal health. Innate lymphoid cells (ILCs) are a heterogeneous type of innate immune cell that regulates immune responses and tolerance at mucosal surfaces, such as in the gut, by rapidly secreting cytokines. Group 3 ILCs (ILC3s) are characterized by the presence or absence of a cell surface natural cytotoxicity receptor (NCR). Two studies now provide evidence of heterogeneity and plasticity within ILC3s. Chea *et al.* found that a substantial proportion of mouse NCR^- ILC3s differentiated into NCR^+ ILC3s in response to stimulation of the receptor Notch2. In mice with defective Notch signaling specifically in lymphoid cells, NCR^+ ILC3s were reduced in number and showed impaired cytokine secretion. Viant *et al.* showed that Notch signaling was required for the maintenance of NCR^+ ILC3s. Furthermore, signaling by the cytokine transforming growth factor–β (TGF-β) antagonized Notch signaling, resulting in reduced numbers of NCR^+ ILC3s. Together, these studies indicate that ILC3 subset composition in vivo depends on the balance between different signals found in tissue microenvironments, which has implications for whether proinflammatory immune responses or immune tolerance will prevail.

Science Signaling (ISSN 1937-9145) is published by the American Association for the Advancement of Science, 1200 New York Avenue NW, Washington, DC 20005.

frontiers in Immunology

ORIGINAL RESEARCH
published: 07 June 2018
doi: 10.3389/fimmu.2018.01252

The Notch Signaling Pathway Is Balancing Type 1 Innate Lymphoid Cell Immune Functions

*Thibaut Perchet[1,2,3], Maxime Petit[1,2,3], Elena-Gaia Banchi[1,2,3], Sylvain Meunier[1,2,3], Ana Cumano[1,2,3] and Rachel Golub[1,2,3]**

[1] Unit for Lymphopoiesis, Department of Immunology, Pasteur Institute, Paris, France, [2] INSERM U1223, Paris, France, [3] Université Paris Diderot, Sorbonne Paris Cité, Cellule Pasteur, Paris, France

The Notch pathway is one of the canonical signaling pathways implicated in the development of various solid tumors. During carcinogenesis, the Notch pathway dysregulation induces tumor expression of Notch receptor ligands participating to escape the immune surveillance. The Notch pathway conditions both the development and the functional regulation of lymphoid subsets. Its importance on T cell subset polarization has been documented contrary to its action on innate lymphoid cells (ILC). We aim to analyze the effect of the Notch pathway on type 1 ILC polarization and functions after disruption of the RBPJk-dependent Notch signaling cascade. Indeed, type 1 ILC comprises conventional NK (cNK) cells and type 1 helper innate lymphoid cells (ILC1) that share Notch-related functional characteristics such as the IFNg secretion downstream of T-bet expression. cNK cells have strong antitumor properties. However, data are controversial concerning ILC1 functions during carcinogenesis with models showing antitumoral capacities and others reporting ILC1 inability to control tumor growth. Using various mouse models of Notch signaling pathway depletion, we analyze the effects of its absence on type 1 ILC differentiation and cytotoxic functions. We also provide clues into its role in the maintenance of immune homeostasis in tissues. We show that modulating the Notch pathway is not only acting on tumor-specific T cell activity but also on ILC immune subset functions. Hence, our study uncovers the intrinsic Notch signaling pathway in ILC1/cNK populations and their response in case of abnormal Notch ligand expression. This study help evaluating the possible side effects mediated by immune cells different from T cells, in case of multivalent forms of the Notch receptor ligand delta 1 treatments. In definitive, it should help determining the best novel combination of therapeutic strategies in case of solid tumors.

Keywords: Notch, innate lymphoid cells, liver, cancer, inflammation, transcription factors, cytotoxicity, molecular biology techniques

OPEN ACCESS

Edited by:
Antonio Francesco Campese, Sapienza Università di Roma, Italy

Reviewed by:
Gabrielle Belz, Walter and Eliza Hall Institute of Medical Research, Australia
Qi Yang, Albany Medical College, United States

***Correspondence:**
Rachel Golub
rachel.golub@pasteur.fr

Specialty section:
This article was submitted to Cancer Immunity and Immunotherapy, a section of the journal Frontiers in Immunology

Received: *13 March 2018*
Accepted: *18 May 2018*
Published: *07 June 2018*

Citation:
Perchet T, Petit M, Banchi E-G, Meunier S, Cumano A and Golub R (2018) The Notch Signaling Pathway Is Balancing Type 1 Innate Lymphoid Cell Immune Functions. Front. Immunol. 9:1252. doi: 10.3389/fimmu.2018.01252

INTRODUCTION

Type 1 innate lymphoid cells (ILC) are defined by the capacity to secrete IFNg and comprise at least two distinct subsets, type 1 helper innate lymphoid cells (ILC1) that are the tissue-resident counterparts of the circulating conventional NK (cNK) cells found in blood and in numerous tissues. ILC1 have been identified in liver, gut, salivary glands, skin, peritoneum, spleen, and uterus (1). cNK and ILC1 both express the receptors NKp46 and NK1.1 that distinguishes them from other ILC subsets.

ILC1 express markers of tissue residency with an immature CD49a$^+$CD49b$^-$ phenotype in the liver. cNK and ILC1s could be discriminated by the identity of T-box transcription factors they expressed. The T-box protein in T cells, T-bet, is encoded by the *Tbx21* gene involved in IFNg production. Another T-box transcription factor eomesodermin (Eomes) shares homology with T-bet. Mature cNK cells are T-bet$^+$ Eomes$^+$ and T-bet upregulation is induced during ILC differentiation in the liver. Studies in Eomes reporter mice showed that despite their immature phenotype, T-bet$^+$ hepatic ILC1 are not precursors of Eomes$^+$ cNK cells (2) and ILC1 and cNK lineages diverge early in ontogeny (3). There is limited information on the mechanisms inducing or repressing T-box transcription factors in different organs. Because *Tbx21* is a known potential target of the Notch canonical pathway, we investigated the role of the Notch signaling pathway on the differentiation and function of ILC1 and cNK cells residing in enterohepatic sites. The Notch pathway is highly conserved and regulates several aspects of development and differentiation (4, 5). Vertebrates express four different Notch receptors (Notch 1–4), which can engage five known ligands (Delta-like 1, 3, 4, Jagged 1, and 2) (6). The co-factor RBP-Jk and mastermind-like (MAML) mediate the signaling cascade of the canonical Notch pathway. Upon recognition of Notch ligands and after serial proteolytic cleavages, the Notch intracellular domain translocates to the nucleus where it binds to the transcription factor CSL/RBP-Jk, recruiting co-activator members of the MAML family, and enabling transcription of target genes (6, 7). Notch receptors are expressed in the hematopoietic cells with a well-known role of Notch1 signaling in regulating T versus B cell fate decisions (8). *In vitro* studies have shown that multipotent progenitors differentiate into T/cNK progenitors *via* the Notch1/Dll1 or Dll4 interaction; however, at later stages, Notch1 favor the T cell potential to the expense of cNK cells (9–11). It has been proposed that the Notch ligand Jagged2 promotes the development of cNK from murine hematopoietic progenitors (12). At later stages, Notch signaling has been implicated in the upregulation of KIR molecules (13) and in human peripheral cNK cells it increases IFNg secretion (14). cNK cells participate to immune surveillance of tumors and viral infection (15, 16). They are important cytotoxic players by the release of granules containing both perforin and granzyme B (GzmB) and by the production of inflammatory cytokines, such as IFNg and TNFa.

There is, however, limited information for a role of Notch pathway in ILC1 development and function. Single-cell transcriptional analyses of hepatic ILC1 and cNK showed that more than half of both cell types express Notch receptors. Moreover, gene expression analysis indicated a possible implication of the Notch signaling pathway on the heterogeneity of these populations. We therefore analyzed ILC1 in mice where the canonical Notch pathway is abrogated in all lymphoid lineages using a conditional knockout of RBP-Jk in cells expressing IL-7Ra, a receptor upregulated at the common lymphoid progenitor stage (11, 17). We found that both cNK and ILC1 are altered in the absence of the Notch signaling pathway. Hepatic and circulating ILC1 from Il7r^{Cre} Rbpj$^{F/F}$ mice showed decreased expression of CD49a and the ratio of cNK versus ILC1 were affected possibly due to a deregulation of proliferation/survival.

Considering that the Notch pathway activates Th1 type responses, we expected that the lack of Notch signaling would reduce inflammatory responses in type 1 ILC. Instead, we found that RBPJ deficiency enhanced the inflammatory and cytotoxic functions of the type 1 ILC subsets present in the enterohepatic region. Notably, we showed that T-bet was inhibited in RBPJ-deficient cells resulting in the upregulation of the complementary Eomes and of an inflammatory gene signature. Finally, we showed that RBPJ deficiency also increased the control of tumor proliferation at the early time-points due to the recruitment of highly inflammatory cNK cells. We conclude that Notch signaling, in type 1 ILC cells, prevents the over-expression of pro-inflammatory cytokines through the regulation of T-bet and Eomes expression.

MATERIALS AND METHODS

Mice

IL7r$^{+/+}$, IL7r$^{Cre/+}$ Rbpj$^{F/+}$, IL7r$^{Cre/+}$ Rbpj$^{F/F}$, Vav$^{Cre/+}$ Rbpj$^{F/+}$, Vav$^{Cre/+}$ Rbpj$^{F/F}$, IL7r$^{Cre/+}$ Notch2$^{F/+}$, and IL7r$^{Cre/+}$ Notch2$^{F/F}$ mice were bred in the animal facilities at Pasteur Institute, Paris. Mice were bred in accordance with Pasteur Institute guidelines in compliance with European animal welfare regulations, and all animal studies were approved by Pasteur Institute Safety Committee in accordance with French and European guidelines.

Cell Preparation

Bone marrow (BM), thymic lobes, spleens, and lamina propria lymphocytes (LPL) were harvested, dissociated, and resuspended in Hanks' balanced salt solution (HBSS) supplemented with 1% fetal calf serum (FCS; Gibco). To isolate LPL, the small bowel was flushed with phosphate-buffered saline (PBS), and the conjunctive tissue and Peyer's patches were carefully removed. The intestine was opened and cut into 1-cm pieces. To eliminate epithelial cells and intraepithelial lymphocytes, these fragments were incubated at 37°C in 50 ml of RPMI 1640 (Gibco) containing 10% FCS and 10 mM Hepes buffer under strong agitation for 30 min, which was followed by vortex treatment for 4 min. For LPL isolation, the remaining fragments were incubated in identical medium to which was added type VIII collagenase (0.5 mg/ml; Sigma-Aldrich) and were shaken for 30 min at 37°C. To complete digestion, the suspension was repeatedly passed through a 10-ml syringe for 5 min and then filtered through a 40-mm cell strainer (BD Biosciences) and collected by centrifugation. The cell pellet was resuspended in 44% Percoll (GE Healthcare), laid over 67% Percoll, and centrifuged at 600 *g* for 20 min at 20°C. Cells at the interface were collected, washed in HBSS containing 1% FCS, and recovered. Livers were harvested, dissociated, and resuspended in RPMI 1640 supplemented with 2% FCS. Cells were collected by centrifugation and resuspended in 44% Percoll. After centrifugation at 600 *g* for 20 min at 20°C, the cell pellet was washed in HBSS containing 1% FCS. Blood and portal vein blood (PVB) were harvested using a 1-ml syringe (BD Plastipak) and laid on Ficoll Paque Plus (GE Healthcare). After centrifugation at 600 *g* for 20 min at 20°C, the cell at the interface were washed in HBSS containing 1% FCS and recovered. Tumors were harvested and then washed with PBS, then separated into different tubes. The

tumors were resuspended in 2 ml of thermolysin (Liberase™, Roche Diagnostics, Mannheim, Germany) at 0.13 U/ml (concentrations as recommended by the manufacturer). Incubations were performed for 30 min at 37°C. Following incubation, the digestate was crushed and passed through a 70-µm filter and washed with RPMI supplemented with 10% FCS. Samples were centrifuged at 370 *g* for 7 min and resuspended in HBSS containing 1% FCS.

Flow Cytometry

Flow cytometry data were acquired with a LSRFortessa flow cytometer (Becton Dickinson) and analyzed with FlowJo software (Tree Star). Dead cells were eliminated by exclusion with propidium iodide. Cells were stained intracellularly after permeabilization and fixation with True Nuclear Transcription Factor Buffer Set (BioLegend). Cells were purified with a FACSAria III (Becton Dickinson) and recovered in tubes or in 96-well quantitative PCR (qPCR) plates for gene expression analysis.

Antibodies

All antibodies were from BD Biosciences, eBioscience, BioLegend, Cell Signaling Technology, or R&D Systems. Antibodies were biotinylated or conjugated to fluorochromes (fluorescein isothiocyanate, phycoerythrin, PECy5, PerCPCy5.5, PECy7, allophycocyanin, Alexa Fluor 647, APCCy7, Pacific Blue, BV421, eFluor450, V500, BV605, BV655, BV700, and BV786) and were specific for the following mouse antigens: Ly76 (TER119), Gr-1 (RB6-8C5), CD3e (145-2C11), CD19 (6D5), NK1.1 (PK136), IL-7Ra (A7R34), CD8 (53-6.7), TCRb (H57-597), TCRd (GL3), CD4 (GK1.5), Thy1.2 (53-2.1), NKp46 (29A1.4), IFNg (XMG1.2), CD27 (LG.3A10), CD45.2 (104), CD49a (HMa1), CD49b (DX5), Eomes (Dan11mag), TNFa (MP6-XT22), PD1 (29F.1A12), CD226 (10E5), Mac1 (M1/70), and GzmB (GB12).

RT-qPCR Analysis

Cells were sorted in Buffer RLT (Qiagen) containing 2-mercaptoethanol (Sigma-Aldrich) and were frozen at −80°C. RNA was obtained with an RNeasy Micro Kit (Qiagen), and complementary DNA (cDNA) was obtained with the PrimeScript RT Reagent Kit (Takara). A 7300 Real-Time PCR System (Applied Biosystems) and TaqMan technology (Applied Biosystems) or SYBR Green Technology (Qiagen) were used for qRT-PCR analysis. A bilateral unpaired Student's *t*-test was used for statistical analysis. The following primers were from SABiosciences: Ifng (Mm_01168134_m1), Eomes (Mm_01351984_m1), Tnfa (Mm_00443258_m1), GzmB (Mm_00442837_m1), Hprt (Mm_00446968_m1), and Actb (Mm_02619580_g1).

Tumor Injection

Cancer Hepa 1.6 cells were cultured in Opti-MEM with GlutaMAX (Gibco) containing 10% FCS (Gibco), 1% penicillin–streptomycin (Gibco), and 60 mM 2-mercaptoethanol (Sigma-Aldrich) and were maintained in a 37°C incubator (Thermo Scientific) with 5% CO_2. Cells were harvested, washed, and resuspended in PBS. 3×10^6 cells were injected subcutaneously in 150 µl of PBS. Mice were monitored every day and tumor growth was measured every 2/3 days.

T Cell Transfer

CD3 cells were isolated using magnetic microbead (Miltneyi Biotech, Bergisch Gladbach, Germany) from spleen of B6 wild-type mice. 3×10^6 purified CD3 positive cells were injected in 150 µl of PBS in host mice 3 days before Hepa1.6 injection.

Cytotoxicity Assay

Freshly isolated splenic cNK cells (Lin^- $CD45^+$ $CD4^-$ $NKp46^+$ $NK1.1^+$) were sorted to high purity (>98%) and used as effectors. Killing of the cNK-sensitive YAC-1 (European Collection of Cell Cultures) target cells was assessed using a fixable viability dye. Percentage specific of killing was calculated as: 100 × (experimental release − spontaneous release)/(total release − spontaneous release).

Single Cell Multiplex RT-qPCR

Cells were sorted in 96-well qPCR plates in 9 µl of a CellsDirect One-Step quantitative RT-PCR Kit (Life Technologies), containing mixtures of diluted primers (0.05× final concentration). Preamplified cDNA was obtained after reverse transcription (15 min at 40°C, 15 min at 50°C and 15 min at 60°C), and preamplification (22 cycles: 15 s at 95°C and 4 min at 60°C), and diluted 1:5 in TE pH8 Buffer (Ambion). Sample mix was as follows: diluted cDNA (2.9 µl), Sample Loading Reagent (0.29 µl; Fluidigm), TaqMan Universal PCR Master Mix (3.3 µl; Applied Biosystem), or Solaris quantitative PCR Low ROX Master Mix (3.3 µl; GE Dharmacon). The assay mix was as follows: Assay Loading Reagent (2.5 µl; Fluidigm) and TaqMan (2.5 µl; Applied Biosystem). A 48.48 dynamic array integrated fluidic circuit (IFC; Fluidigm) was primed with control line fluid, and the chip was loaded with assays (TaqMan) and samples using an HX IFC controller (Fluidigm). The experiments were run on a Biomark (Fluidigm) for amplification and detection (2 min at 50°C, 10 min for TaqMan reagents or 15 min for Solaris reagents at 95°C, 40 cycles: 15 s at 95°C and 60 s at 60°C).

Bioinformatic Analyses

For visualization, the dimensionality of the datasets was further reduced using the "Barnes-hut" approximate version of t-SNE. This was implemented using the Rtsne function from the Rtsne R package using 800 iterations and a perplexity setting that varied from 10 to 30 depending on the size of the dataset. PhenoGraph takes as input a matrix of N single-cell measurements and partitions them into subpopulations by clustering a graph that represents their phenotypic similarity. PhenoGraph builds this graph in two steps. First, it finds the k nearest neighbors for each cell (using Euclidean distance), resulting in N sets of k-neighborhoods. Second, it operates on these sets to build a weighted graph such that the weight between nodes scales with the number of neighbors they share. The Louvain community detection method is then used to find a partition of the graph that maximizes modularity. Given a dataset of N d-dimensional vectors, M distinct classes, and a vector providing the class labels for the first L samples, the PhenoGraph classifier assigns labels to the remaining N_L unlabeled vectors. First, a graph is constructed as described above. The classification problem then corresponds to the probability that a random walk originating

at unlabeled node x will first reach a labeled node from each of the M classes. This defines an M-dimensional probability distribution for each node x that records its affinity for each class.

Statistical Analysis

Statistical analysis was performed with the Student's *t*-test or two-way analysis of variance. The analysis was performed using Prism Software (GraphPad). Statistical significance is represented as follows: $*p < 0.05$, $**p < 0.01$, and $***p < 0.001$.

RESULTS

Four Distinct Populations of Type 1 ILC Are Defined in the Liver

Mutually exclusive expression of CD49a and CD49b separates the NKp46$^+$ NK1.1$^+$ population into ILC1 and cNK cells in the murine liver (**Figure 1A**). Purified single ILC1 and cNK cells were subjected to multiplex transcriptional analysis, as described (18). We analyzed 48 transcripts known or supposed to be expressed in type 1 ILC with some of them also being possible Notch pathway

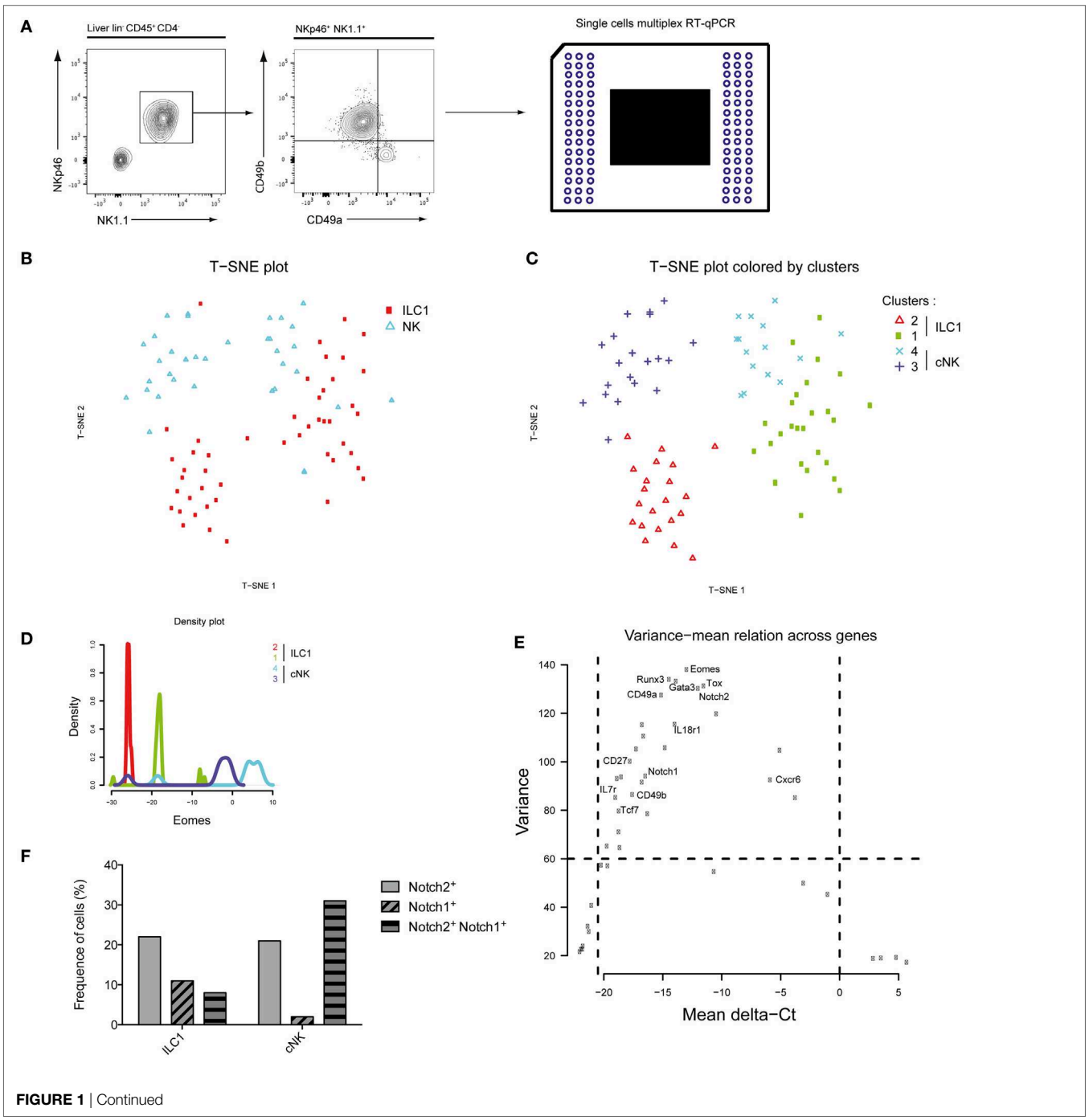

FIGURE 1 | Continued

FIGURE 1 | Group 1 innate lymphoid cell is composed of four distinct populations in the liver at homeostasis. **(A)** Single cells were sorted for transcriptomic analyses using the Biomark technology. Hepatic lineage negative CD45-positive cells (lin$^-$ CD45$^+$) were separated into type 1 helper innate lymphoid cells (ILC1) (CD4$^-$ NKp46$^+$ NK1.1$^+$ CD49a$^+$ CD49b$^-$) and conventional NK (cNK) cells (CD4$^-$ NKp46$^+$ NK1.1$^+$ CD49a$^-$ CD49b$^+$). **(B)** Application of t-SNE to single cells using 48 genes expression separates 48 ILC1 and 48 cNK into two distinct subsets. **(C)** Phenograph algorithm clustering performed and plotted on t-SNE graph, showing four different clusters among hepatic ILC1 and cNK. **(D)** Density plot of *Eomes* gene expression show four distinct types of expression among phenograph clusters of hepatic ILC1 and cNK. **(E)** The variance mean of delta Ct across expressed genes allows the selection of genes that are differentially expressed (variance > 60) with a significant expression (dCt from −20.5 to 0). **(F)** Frequency of hepatic ILC1 and cNK expressing Notch1 and/or Notch2. **(G)** Heatmap with unsupervised hierarchical clusters of gene selected in panel **(D)**.

targets. A t-SNE analysis of the data set indicated that both ILC1 and cNK cells were subdivided into two populations (**Figure 1B**), populations 1 and 2 for ILC1 and populations 3 and 4 for cNK (**Figure 1C**). Surprisingly, population 1 of ILC1 clustered closer to the cNK population 4 rather than to its ILC1 counterpart. Inversely, population 3 of cNK clustered closer to ILC1 population 2 (**Figure 1C**). We ascertained that cNK express high levels of Eomes transcripts and that ILC1 subsets had low expression levels (**Figure 1D**). Unexpectedly, Eomes gene expression is found as highly variable and different levels are observed for these four populations (**Figure 1E**). We then restricted our analysis to the genes that were the most variable (>60 of variance) and significantly expressed (mean values selection between 0 and −20) (**Figure 1E**). With *Eomes, Gata3, Tox, Notch2, Runx3*, and *Itga1* were among the most variable transcripts (**Figure 1E**). Notch receptors were expressed more frequently in cNK cells than in ILC1 (**Figure 1F**). Notch2$^+$ cells were more frequent than Notch1$^+$ cells (**Figure 1F**) and cells expressing both Notch1 and Notch2 transcripts represented 9% of ILC1 and 30% of cNK. It is interesting to notice that population 1 of Eomes^{lo} ILC1 was enriched in Notch expressing cells compared with Eomes$^-$ ILC1 (population 2). An unsupervised hierarchical cluster was constructed based on this restricted list of genes. The segregation of ILC1 and cNK into four different subsets was consistent with the t-SNE analysis (**Figure 1G**). The genes could be separated into two cluster signatures. The first comprises genes directly related to the Notch pathway (*Notch1, Gata3, Ahr, Tcf7, IL7ra*, and *c-myc*) and genes that define the identity of ILC1 versus cNK (CD49a, *Cd27*, and *Il7ra*). In the second cluster, *Notch2* together with *Cxcr6, Eomes*, CD49b, and *Il18r1* define the signature 2 and also cNK identity. Correlation heatmaps confirmed that most of genes among each signature are correlated (Figure S1A in Supplementary Material). A good correlation is shown between most genes of signature 1 with a strong correlated core for Tcf7, CD27, Rora, Klr5, Ahr, and Il7r (Figures S1A,B in Supplementary Material). A good correlation is described between Eomes, IL18r1, Tsc22d3, CD49b, and Tle4 for the signature 2 (Figure S1C in Supplementary Material). The data suggest that the Notch signaling pathway could play a role in the specification of the subsets of ILC1 and cNK in the liver.

RBPJ-Deficient Type 1 ILC Have Different Characteristics

We analyzed type 1 ILC (Lin$^-$ CD45$^+$ NK1.1$^+$ NKp46$^+$ cells) in Il7r^{Cre} Rbpj$^{F/F}$ mice to define the role of the canonical Notch signaling pathway in the maturation of this population (11). CD49a and CD49b expression that distinguishes hepatic ILC1 from cNK cells was tested in the spleen, BM, and thymus of Notch-competent and Notch-deficient mice (**Figure 2A**). In Notch-deficient mice, CD49a levels were decreased in most ILC1 while CD49b levels remained unchanged. Interestingly, a CD49a^{lo} CD49b$^-$ population appears in the circulation especially in the PVB (**Figure 2A**). Notch-deficient hepatic ILC1 showed decreased levels of CD49a (**Figure 2B**) and increased frequencies and absolute numbers (**Figure 2C**).

We then analyzed mice where the Notch signaling pathway was defective in hematopoietic cells (Vav^{Cre} Rbpj$^{F/F}$) or downstream of Notch2 (IL7r^{Cre} Notch2$^{F/F}$) (Figure S2A in Supplementary Material). In Notch2-deficient liver ILC (IL7r^{Cre} Notch2$^{F/F}$), CD49a and CD49b expression on type 1 ILC was unchanged contrasting with the decreased levels of CD49a in RBPJ-deficient ILC irrespective of whether deletion of RBPJ occurred in IL7r or in Vav-expressing cells (Figure S2B in Supplementary Material). Interestingly, while RBPJ deletion resulted in an increased frequency of ILC1, the Notch2 deletion induced an opposite effect with a decreased frequency of ILC1 suggesting non-redundant roles of Notch1 and Notch2 (Figure S2C in Supplementary Material) that was not due to differences in proliferation (Figure S3 in Supplementary Material). The analyses of Thy1 expression showed an increase from 10 to 50% in Notch-deficient cNK and to virtually 100% in Notch-deficient ILC1. Mac-1 expression among cNK showed a significant decrease (**Figures 2D,E**).

We have previously shown that type 1 ILC (Lin$^-$ NKp46$^+$ NK1.1$^+$ cells) in the intestinal lamina propria (LP) were not affected by RBPJ deletion (17). However, the changes in the expression levels of CD49a and CD49b described above led us to reevaluate the representation of the subsets of Notch-deficient type 1 ILC1 in the LP. In LP, CD49a and CD49b could not strictly separate ILC1 from cNK cells as numerous cells express both markers (**Figure 3A**). We designed a panel of surface markers that allowed the enrichment of NKp46$^+$ NK1.1$^+$ cells into Eomes$^-$ versus Eomes$^+$ subsets. Cells separated as CD226$^+$ CD49b$^-$ Mac1$^-$ are enriched for Eomes$^-$ ILC1 and CD226$^-$ CD49b$^+$ Mac1$^+$ cells are enriched into Eomes$^+$ cNK cells (**Figure 3A**). We found that Notch-deficient CD226$^+$ CD49b$^-$ Mac1$^-$ ILC1 comprises 15% of Eomes$^+$ cells whereas the enriched cNK subset is exclusively composed of Eomes$^+$ cells (**Figures 3A,B**). Similar to liver type 1 ILC all subsets in the LP have increased Thy1 levels (**Figure 3B**). Consistent with our previous observations, the absolute numbers of ILC1/cNK remained unchanged in RBPJ-deficient compared with control mice (**Figure 3C**). Altogether, these results indicated that the Notch signaling pathway was modulating several properties of the type 1 ILC including expression of transcription factors, integrins, and the capacity to circulate.

Type 1 ILC Functions Are Altered in RBPJ-Deficient Cells

We then assessed the functional properties of RBPJ-deficient hepatic ILC1 and cNK cells. We found that, after activation with PMA-ionomycin, TNFa and IFNg secretion by RBPJ-deficient

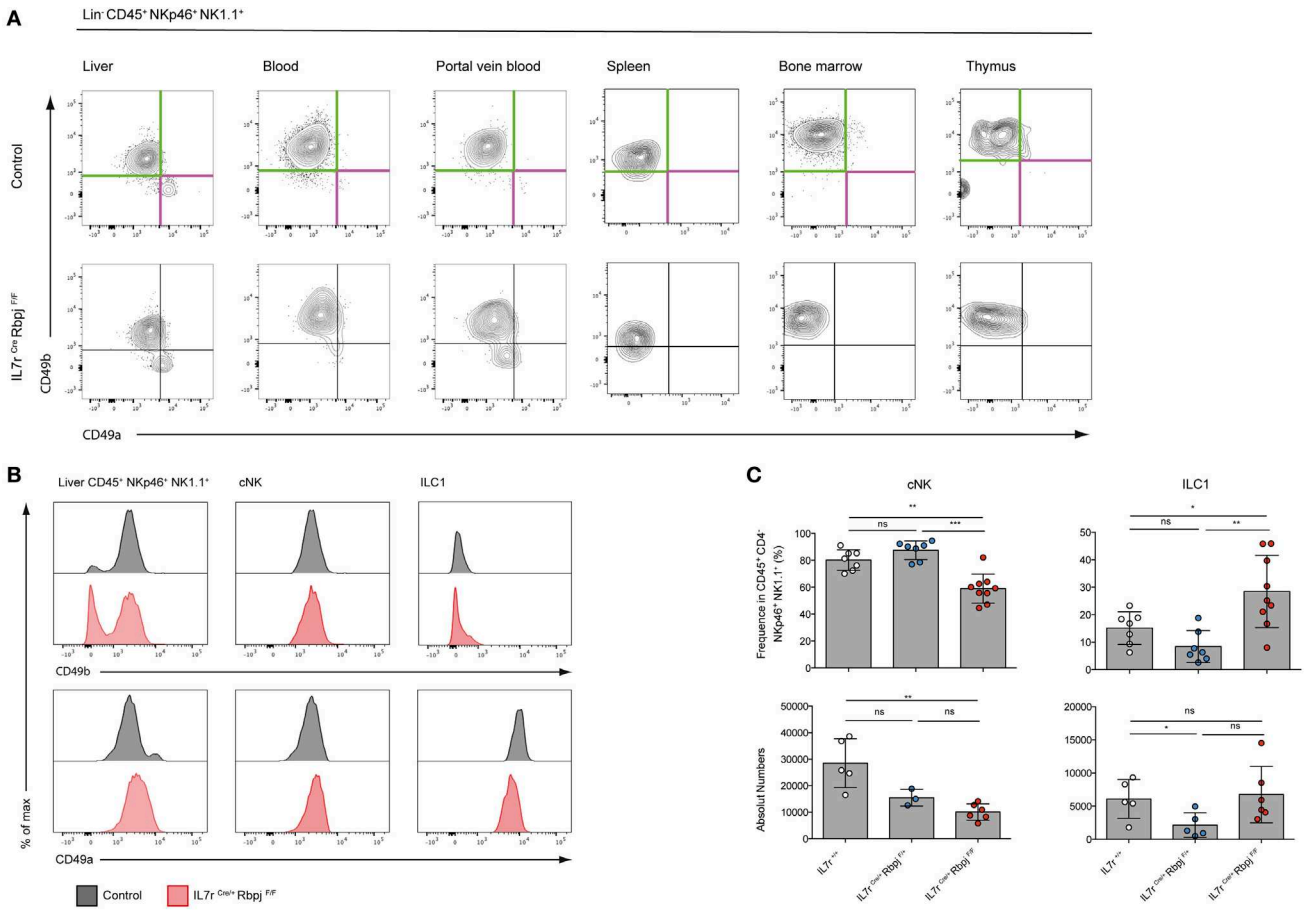

FIGURE 2 | Continued

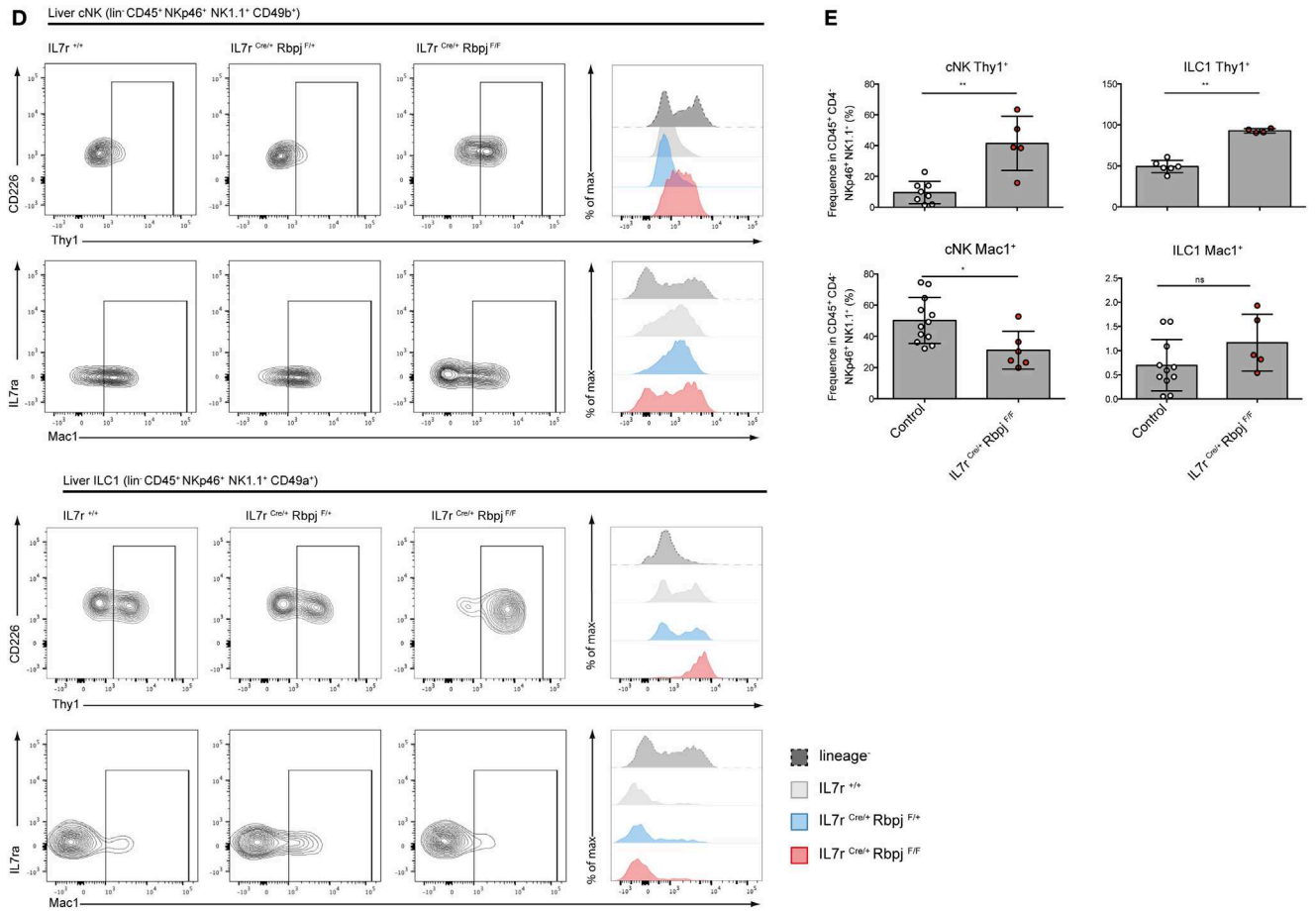

FIGURE 2 | Altered phenotype of NKp46$^+$ NK1.1$^+$ cells in IL7r^{Cre} Rbpj$^{F/F}$ mice. **(A)** Expression of CD49a (purple) and CD49b (green) in lin$^-$ CD45$^+$ NKp46$^+$ NK1.1$^+$ cells from the liver, blood, portal vein blood, spleen, bone marrow, and thymus of control IL7r^{Cre} Rbpj$^{F/+}$ mice (top panel) and IL7r^{Cre} Rbpj$^{F/F}$ mice (bottom panel). **(B)** Surface expression of CD49b (top panel) and CD49a (bottom panel) on total liver lin$^-$ CD45$^+$ NKp46$^+$ NK1.1$^+$ cells, hepatic conventional NK (cNK) and type 1 helper innate lymphoid cells (ILC1) in control IL7r^{Cre} Rbpj$^{F/+}$ mice (gray) and IL7r^{Cre} Rbpj$^{F/F}$ (red). **(C)** Frequency and absolute numbers of hepatic cNK and ILC1 in IL7r$^{+/+}$ (white), IL7r^{Cre} Rbpj$^{F/+}$ (blue), and IL7r^{Cre} Rbpj$^{F/F}$ (red) mice. **(D)** Surface expression of Thy1 and Mac1 on hepatic cNK (top panel) and ILC1 (bottom panel) in IL7r$^{+/+}$ (gray), IL7r^{Cre} Rbpj$^{F/+}$ (blue), and IL7r^{Cre} Rbpj$^{F/F}$ (red) mice. Lineage-negative cells were used as control for histograms (dashed gray). **(E)** Frequency of hepatic cNK and ILC1 expression of Thy1 (top panel) and Mac1 (bottom panel) in control IL7r^{Cre} Rbpj$^{F/+}$ mice (white) and IL7r^{Cre} Rbpj$^{F/F}$ (red).

ILC1 and cNK cells were more strongly increased compared with control cells (**Figure 4A**). TNFa was also more expressed by ILC1 than cNK, whereas IFNg was produced by most hepatic ILC1 and cNK, after Notch depletion. GzmB production by ILC1 remained unchanged while it was produced by few cNK Mac1$^+$, in absence of the Notch signaling pathway (**Figure 4A**). Similar to those from LP, hepatic RBPJ-deficient ILC1 comprise a fraction of Eomes$^+$ cells, whereas a subset of Eomes$^-$ Mac1$^-$CD49b$^+$ cells becomes more prominent among cNK cells. These differences in Eomes expression were also apparent in qRT-PCR (**Figure 4B**). Overall, the mRNA expression for *Tnfa, Gzmb*, and *Ifng* genes confirmed the increase of protein levels and high production of IFNg (**Figure 4B**). Similar experiments done in hepatic ILr7^{Cre} Notch2 $^{F/F}$ mice showed consistent increase of TNFa and IFNg production by Notch 2-deficient type 1 ILC (Figure S4 in Supplementary Material). RBPJ-deficient splenic NKp46$^+$NK1.1$^+$ cells showed significantly increased lytic abilities on YAC-1 mouse lymphoma cells (**Figure 4C**) that correlated with an increase frequency of cells capable to produce TNFa and IFNg (**Figure 4D**). To assess the *in vivo* functions of Notch-deficient type 1 ILC in inflammatory conditions, we used a model of liver damage with inflammation, immune infiltration, and fibrosis (19) induced by methionine-choline deficient (MCD) diet. Under MCD diet, RBPJ-deficient mice showed no differences in frequency of TNFa$^+$ and IFNg$^+$ cells (**Figure 4E**), in weight loss, and in the ratio of liver size versus body weight (**Figure 4F**). The levels of the circulating transaminase aspartate aminotransferase were also not different after 24 days of MCD diet (**Figure 4F**).

Taken together, these experiments indicated that RBPJ-deficient type 1 ILC had increased levels of inflammatory cytokines and increased cytotoxic activity that are not modified by a liver inflammatory inducing diet.

ILC1 and cNK Have Variations in Gene Expression After Abrogation of the Notch Signaling Pathway

To understand the role of Notch signaling pathway in ILC1 and cNK cells, we performed multiplex quantitative transcriptional analysis of 41 immune genes in these different populations from various organs. We used small numbers of cells (25 cells per subset) to reduce the averaging generated by population-level studies. We sorted the type 1 ILC populations of Notch-competent (Ctrl) and -deficient (Flox) mice in distinct organs according to the strategy outlined in **Figure 5A**.

We only analyzed samples expressing all three "housekeeping" genes and did an unsupervised hierarchical clustering analysis of the transcriptional profiles from 79 samples (**Figure 5B**). The population identity is indicated in the first line with a color code for cNK, ILC1 versus BM subsets of preNKP, iNK, and mNK cells. The genotype of the subset analyzed is indicated in the second line with a color code for Notch-competent (Ctrl-Blue) and Notch-deficient (Flox-Red) subsets and the third line indicates the tissue of origin.

The separation between the RBPJ-competent and -deficient samples was evident in most samples. Only, some splenic samples, exclusively composed of mature cNK cells, showed similar distribution of RBPJ-competent and -deficient subsets and clustered together with RBPJ-competent blood and RBPJ-deficient liver cNK samples. This indicates that RBPJ-deficient cNK cells from liver resemble cNK splenic subsets, insensitive to Notch inactivation. It also suggests that the canonical Notch pathway maintains an identity of cNK cells in liver, LP, mesenteric lymph

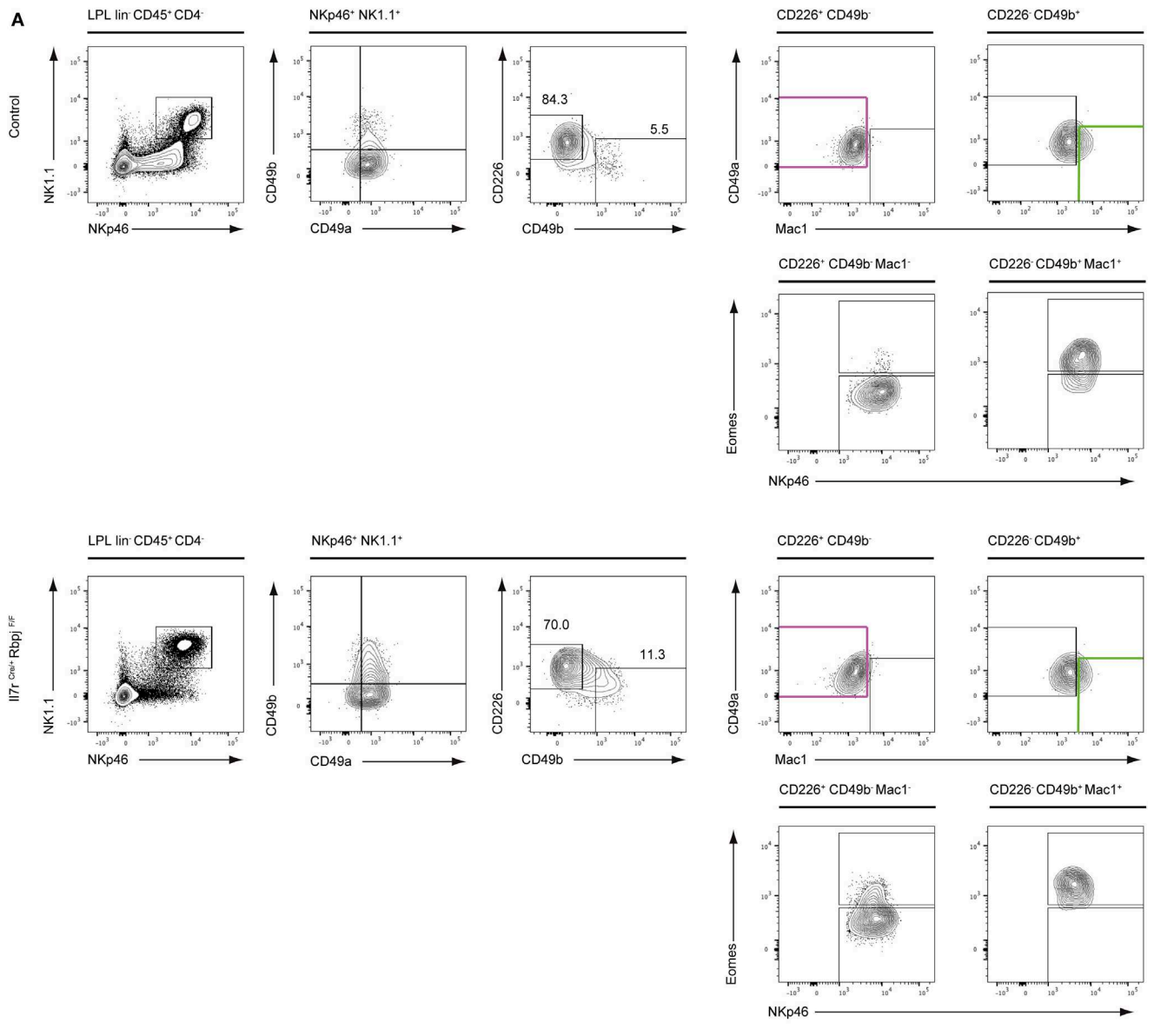

FIGURE 3 | Continued

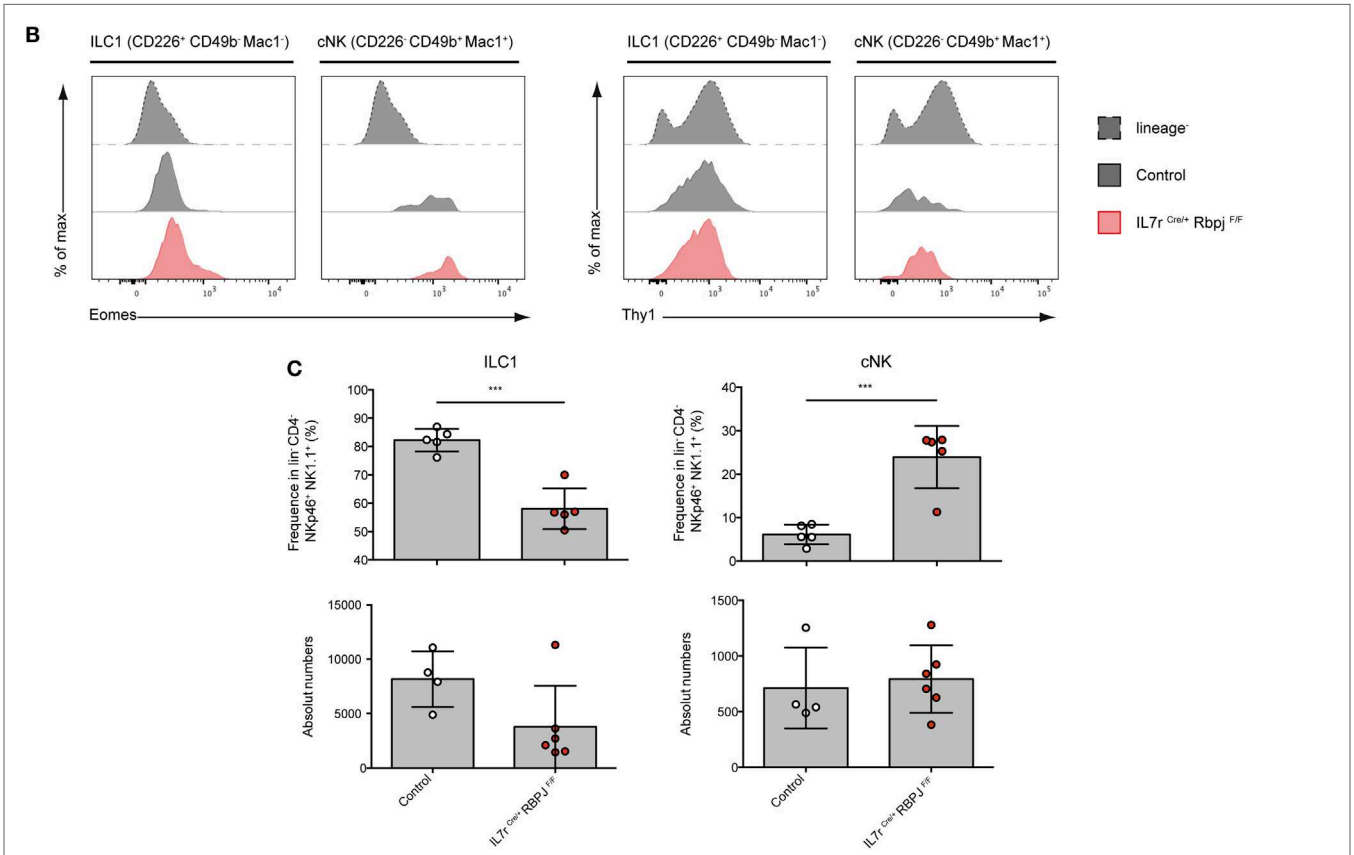

FIGURE 3 | Conventional NK (cNK) cells are increased in the lamina propria lymphocytes (LPL) of IL7r^{Cre} Rbpj$^{F/F}$ mice. **(A)** Flow cytometry of control IL7r^{Cre} Rbpj$^{F/+}$ mice (top panel) and IL7r^{Cre} Rbpj$^{F/F}$ LPL (bottom panel). Repartition of type 1 helper innate lymphoid cells (ILC1) (lin$^-$ CD45$^+$ CD4$^-$ NKp46$^+$ NK1.1$^+$ CD226$^+$ CD49b$^-$ CD49a$^+$ Mac1$^-$, in purple) and NK (lin$^-$ CD45$^+$ CD4$^-$ NKp46$^+$ NK1.1$^+$ CD49b$^+$ CD226$^-$ CD49a$^{-/+}$ Mac1$^+$, in green) in lamina propria (LP). **(B)** Eomesodermin (Eomes) and Thy1 expression in LP ILC1 and cNK in control IL7r^{Cre} Rbpj$^{F/+}$ mice (gray) and IL7r^{Cre} Rbpj$^{F/F}$ (red). Lineage-negative cells were used as control for expression (dashed gray). **(C)** Frequency and absolute numbers of LP ILC1 and cNK in control IL7r^{Cre} Rbpj$^{F/+}$ mice (white) and IL7r^{Cre} Rbpj$^{F/F}$ (red).

node (mLN), and PVB different from that found in the spleen and circulation.

Two subsets of BM iNK clustered with their Notch-deficient counterparts. Because all type 1 ILC and their precursors express *Tcf7* and these two samples express low levels of *Tcf7* and *Cd27*, we concluded that they contained few NK precursors. We decided not to eliminate them from the analysis, as they did not alter its global architecture of the hierarchy.

As discussed above, while surface expression of CD49a and CD49b separated hepatic ILC1 from cNK their separation by transcriptional profiling is less stringent. Indeed, even if most ILC1 subsets clustered together and separated from cNK, a few samples of hepatic ILC1 are interspersed with cNK cells. Notch-competent hepatic ILC1 subsets clustered with intestinal ILC1 and BM precursors (preNKp + iNK), whereas Notch-deficient hepatic ILC1 cluster together and were in the vicinity of mLN and intestinal LP cNK populations.

Our analysis allowed the separation of genes that varied with the activity of the Notch pathway. Genes in cluster 2 were upregulated and conversely genes in cluster 3 were dowregulated, in most Notch-deficient samples. We observe that interfering with the canonical Notch pathway in cNK cells of the enterohepatic axis led to the upregulation of *Eomes, Ly6c, Sell, Il18r1, Notch2, Tcf7, Cx3cr1, Cir1*, and *Cxcr6*. Nearly all were also upregulated in ILC1 subsets with the exception for *Sell* that is never found in this population. Despite being generally increased, *IL18r1* and *Tcf7* were undetectable in few ILC1 Notch-deficient samples illustrating a variable expression in this subset.

A group of genes related to ILC1 signature (*Il21r*, *Lnpp4b*, and *Tnfsf10*) were also upregulated in most Notch-deficient ILC1. *Itga1* was maintained in most hepatic RBPJ-deficient ILC1, although the BM and LPL cNK subsets silenced *Itga1* after RBPJ depletion. *Tnfsf10* expression was also downregulated after RBPJ depletion in cNK subsets. Other genes such as *IL12rb1*, *IL2ra*, and *Notch1* displayed increased expression after Notch depletion.

With the exception of *Tcf7* that was upregulated, most other known direct targets of the canonical Notch pathway comprising *Dtx1, Dtx3, Dtx3l, Zbtb16, Bcl2, Bik*, and *Tbx21* were silenced in Notch-deficient cells.

Genes implicated in apoptosis (*Bcl2l1*, *Crebbp*, and *Bcl2*) were down-modulated, whereas *Bcl2l11* showed increased expression in Notch-deficient cells.

Maml2, a co-activator of the Notch pathway, is decreased, whereas *Cir* a RBPJ co-repressor is upregulated, in RBPJ-deficient

cells. Splenic and circulating cNK subsets that were scattered within Notch-competent and -deficient genotypes did not express *Dtx1, Dtx3, Dtx3l, Crebbp, Bcl2, Zbtb16*, and *Tbx21*, thus appearing Notch independent. These subsets also did not express *Il21r, Tnf, Tnfsf10, Lnpp4b*, and *Tgfr2*.

To better visualize the genes that are co-modified by inactivation of the Notch pathway, we built a heatmap (Figure S5 in Supplementary Material) that clusters together genes that vary in a similar manner comparing RBPJ-proficient and -deficient cells. Gene enrichment analysis of the clusters thus obtained allowed identifying some hallmark for different pathways. *Il2ra*, *Eomes*, *IL18r1*, *Gzmb*, and *Sell* that are co-regulated belong to the inflammatory response genes and to those that are stimulated by Stat5 in response to IL2 stimulation. It is interesting to notice that these genes are related to *Notch2*, *Tcf7*, *Ly6c*, and the chemokine receptors *Cx3cr1* and *Cxcr6*.

A few genes at the bottom of the heatmap (*Tnfsf10, Bcl2*, and *Bcl2l1*) (Figure S5 in Supplementary Material) are also associated to the Stat5/IL2 pathway. Moreover, they correlated with genes implicated in the Notch signaling (*Notch1, Maml2, Crebbp, Dtx3*, and *Dtx3l*) and with Notch target genes (*Tbx21, Zbtb16*). *Itga2* correlated with *Notch1, Dtx3, Dtx3l*, and *Tbx21*, whereas *Itga1* correlated to *Dtx1*, *IL21r*, and *Ctbp2*.

We have previously observed after stimulation of RBPJ-deficient ILC1 subsets, a marked upregulation of *Tnfa* transcripts with similar levels for *Infa* and *Gzmb* (**Figure 4B**). However, in homeostatic conditions, *Tnfa, Ifng*, and *Gm-csf* transcripts were decreased in opposition to an increase for those coding *Gzmb*. Finally, we found that genes differentially regulated by the Notch pathway in type 1 ILC had a highly conserved binding site motif for NFAT and FOXO4. This suggests interactions between NFAT/FOXO4 and the Notch signaling pathway in regulating immune processes in these cells.

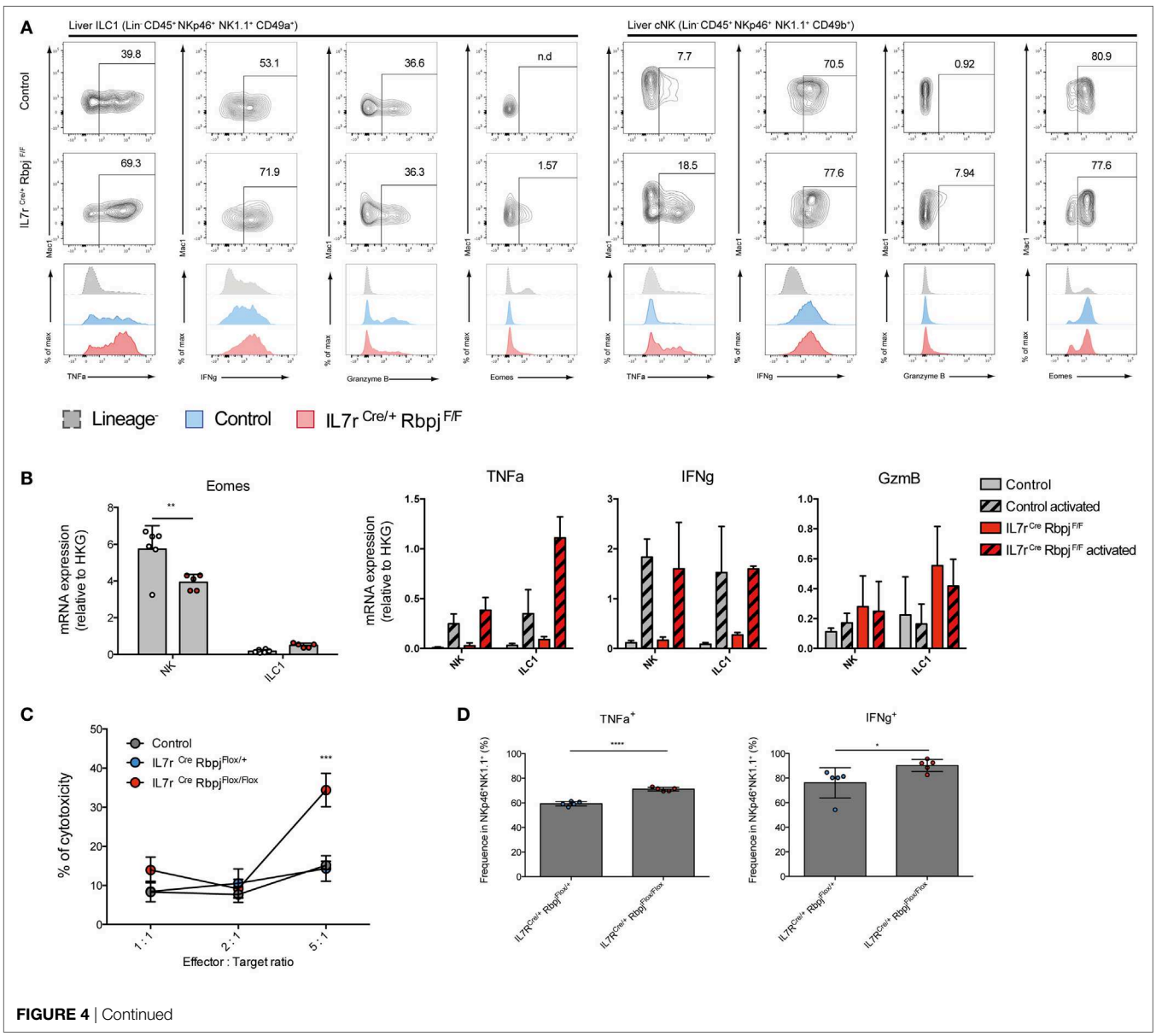

FIGURE 4 | Continued

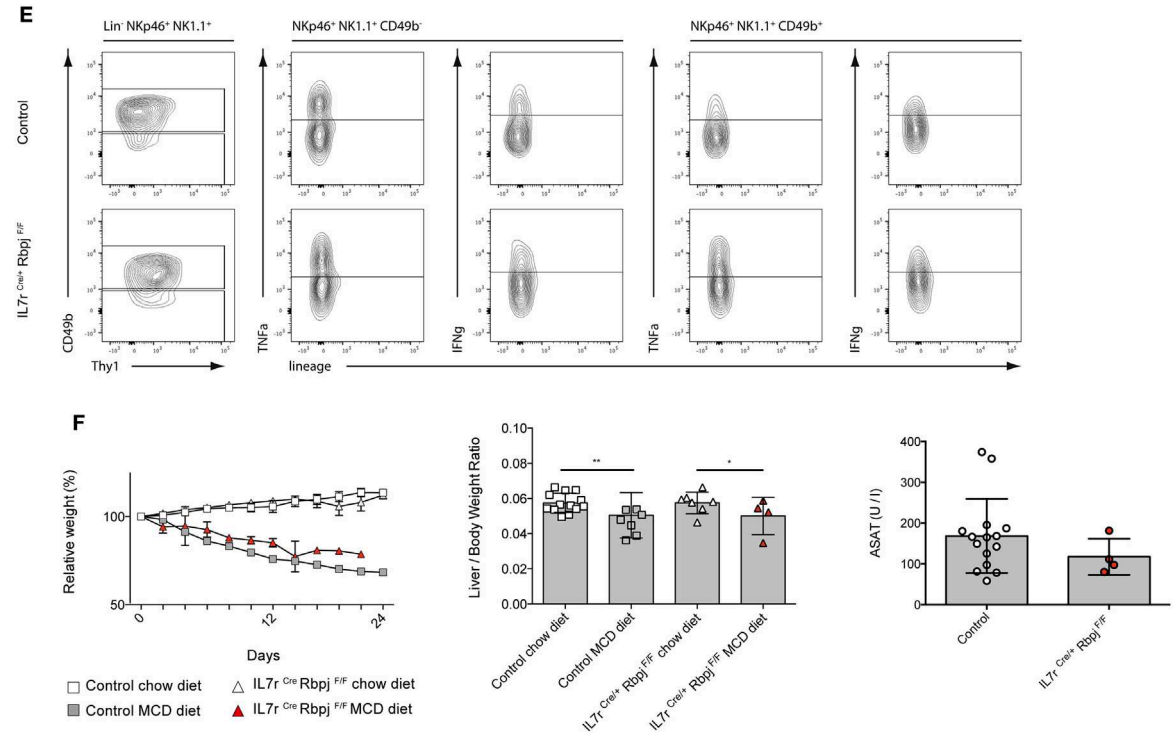

FIGURE 4 | Altered cytokine profile of NKp46$^+$ NK1.1$^+$ cells in IL7r^{Cre} Rbpj$^{F/F}$ mice. **(A)** Expression of TNFa, IFNg, granzyme B, and eomesodermin (Eomes) in hepatic type 1 helper innate lymphoid cells (ILC1) (left panel) and conventional NK (cNK) (right panel) of control IL7r^{Cre} Rbpj$^{F/+}$ mice (top panel) and IL7r^{Cre} Rbpj$^{F/F}$ mice (middle panel). Levels of expression were compared (bottom panel) between control IL7r^{Cre} Rbpj$^{F/+}$ mice (blue) and IL7r^{Cre} Rbpj$^{F/F}$ mice (red). Lineage-negative cells were used as control for surface expression (dashed gray). **(B)** Expression of *Eomes*, *Tnfa*, *Ifng*, and *Gzmb* mRNA in control IL7r^{Cre} Rbpj$^{F/+}$ mice (gray) and IL7r^{Cre} Rbpj$^{F/F}$ mice (red). For *Tnfa*, *Ifng*, and *Gzmb*, mRNA expression was also tested on activated cells (dashed histograms). **(C)** Splenic cNK cells killing capacity in control C57BL/6J (gray), IL7r^{Cre} Rbpj$^{F/+}$ (blue), and IL7r^{Cre} Rbpj$^{F/F}$ (red) mice. **(D)** Frequency of cNK expressing TNFa and IFNg during cytotoxicity assay. **(E)** Cytokine profile of hepatic ILC1 and NK cells in control IL7r^{Cre} Rbpj$^{F/+}$ (top panel) and IL7r^{Cre} Rbpj$^{F/F}$ mice (bottom panel) after methionine-choline deficient (MCD) diet. **(F)** Relative weight and liver/body weight ratio in control IL7r^{Cre} Rbpj$^{F/+}$, IL7r$^{+/+}$ Rbpj$^{F/+}$, and IL7r$^{+/+}$ Rbpj$^{F/+}$ mice (square) after chow (white) and MCD diet (gray) and in IL7r^{Cre} Rbpj$^{F/F}$ mice (triangles) after chow (white) and MCD diet (red). Aspartate aminotransferase (ASAT) levels of control IL7r^{Cre} Rbpj$^{F/+}$, IL7r$^{+/+}$ Rbpj$^{F/+}$, and IL7r$^{+/+}$ Rbpj$^{F/+}$ (white) and IL7r^{Cre} Rbpj$^{F/F}$ mice (red) after MCD diet.

RBPJ Deficiency Increases Type 1 ILC Control at the Initial Stages of Hepatic Tumor Development

To assess the effect of RBPJ deficiency on hepatic type 1 ILC function, we chose a model of hepatocellular carcinoma by injection a Hepa1–6 mouse liver cancer cell line. It was shown that cNK and T cells are important in the control of the tumors *via* IFNg and lytic granules (20). Three weeks after subcutaneous injection of Hepa1–6 cells, the area of the tumor was significantly increased in RBPJ-deficient mice compared with control mice (**Figure 6A**). Moreover, at 21 days post-transplantation, RBPJ-deficient mice showed no sign of tumor rejection while 50% of control mice were tumor free (**Figure 6B**). The analysis of the tumor-infiltrating cells indicated that CD49a$^+$ CD49b$^+$ cNK subset was only found in RBPJ-deficient animals (**Figure 6C**) that were more efficient than the conventional cNK subset in secreting GzmB and TNFa (**Figure 6C**). However, since RBPJ-deficient animals contain defective T cell subsets, they are not able to efficiently eliminate the tumors despite more cytotoxic cNK populations. Therefore, the tumor area difference between RBPJ-competent and -deficient mice starts around day 14 post-injection (**Figure 6A**). Consistent with a role of T cells in tumor rejection, we found infiltrated CD4$^+$ and CD8$^+$ T cells 14 days after injection in C57Bl6 mice (Figure S6 in Supplementary Material). T cells transferred resulted in the control of RBPJ-deficient mice tumor growth similar to that in Notch-competent mice (**Figures 6D,E**). Tumor-infiltrating cells were analyzed revealing a lower frequency of T cells and conversely a higher frequency of type 1 ILC in RBPJ-deficient mice compared with controls (**Figure 6E**). We showed that even if T cells secreting GzmB, TNFa, and IFNg were more numerous the cytotoxicity produced by cNK populations against the tumor was higher in RBPJ-deficient mice, even after T cell transfer (**Figure 6E**). Because RBPJ-deficient controlled better than RBPJ-competent mice the expansion of the tumor at early time points (**Figure 6A**), we analyzed the type 1 ILC composition and functions 5 days after tumor injection, a time point at which no infiltrating T cells could be detected. In RBPJ-deficient mice, the CD49a$^+$ subset was still absent but the intratumoral cNK cells were more prone to release GzmB, TNFa, and IFNg (**Figure 6F**). We propose that the canonical Notch signaling pathway is involved in the downregulation of cytotoxic capacities of specific cNK cell

A

Population name	ILC1	NK	NK	ILC1	ILC1	mNK/NK$^+$	NK	NK	NK	mNK/NK$^+$	iNK	iNK	preNKP
Sort strategy (Lin-)	CD226+ CD49a+ Mac1-	CD49b+ Mac1+ CD90-	CD49b+ Mac1+ CD90+	CD90-	CD90+	CD27+	CD27+ Mac1+	CD90-	CD90+	Mac1+	NKp46- CD49b- NK1.1+	NKp46- CD49b+ NK1.1+	NKp46- NK1.1- CD27+ CD127+
Blood	×	×	×	×	×	×	×	✓	✓	×	×	×	×
BM	×	×	×	×	×	✓	×	×	×	✓	✓	✓	✓
Liver	×	×	×	✓	✓	×	×	✓	✓	×	×	×	×
LP	✓	✓	✓	×	×	×	×	×	×	×	×	×	×
mLN	×	×	×	×	×	✓	×	×	×	✓	×	×	×
PVB	×	×	×	×	×	×	×	✓	✓	×	×	×	×
Spleen	×	×	×	×	×	✓	✓	×	×	✓	×	×	×

B

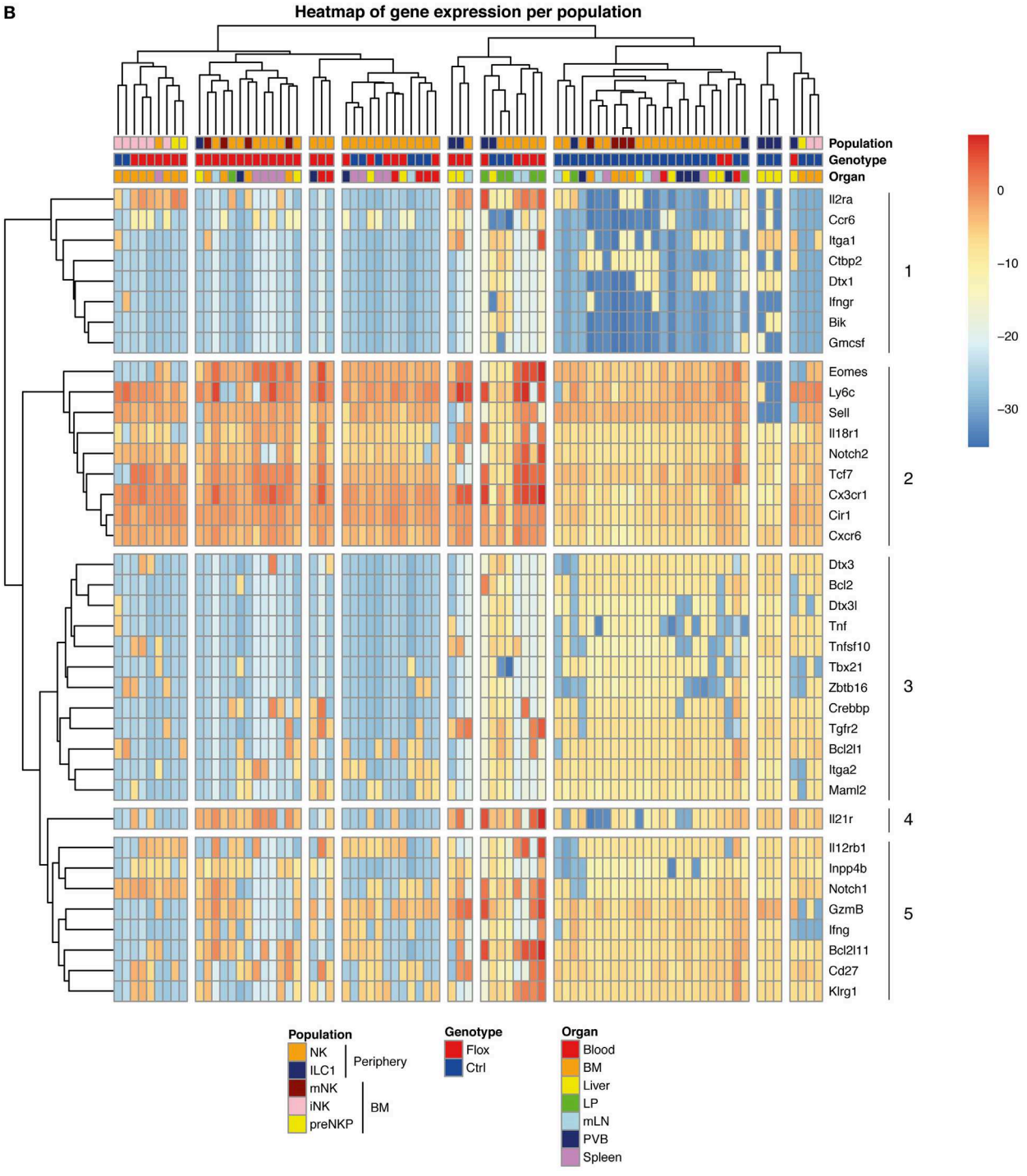

FIGURE 5 | Molecular signature heterogeneity of group 1 innate lymphoid cell (ILC) in IL7r^{Cre} Rbpj$^{F/+}$ and IL7r^{Cre} Rbpj$^{F/F}$ mice. **(A)** Sorting strategy of group 1 ILC cells in the different tissues **(B)** Heatmap of genes expression in group 1 ILC of IL7r^{Cre} Rbpj$^{F/+}$ and IL7r^{Cre} Rbpj$^{F/F}$ mice in blood, bone marrow (BM), liver, lamina propria (LP), mesenteric lymph nodes (mLN), portal vein blood (PVB), and spleen. Cluster of cells and genes were obtained using hierarchical clustering.

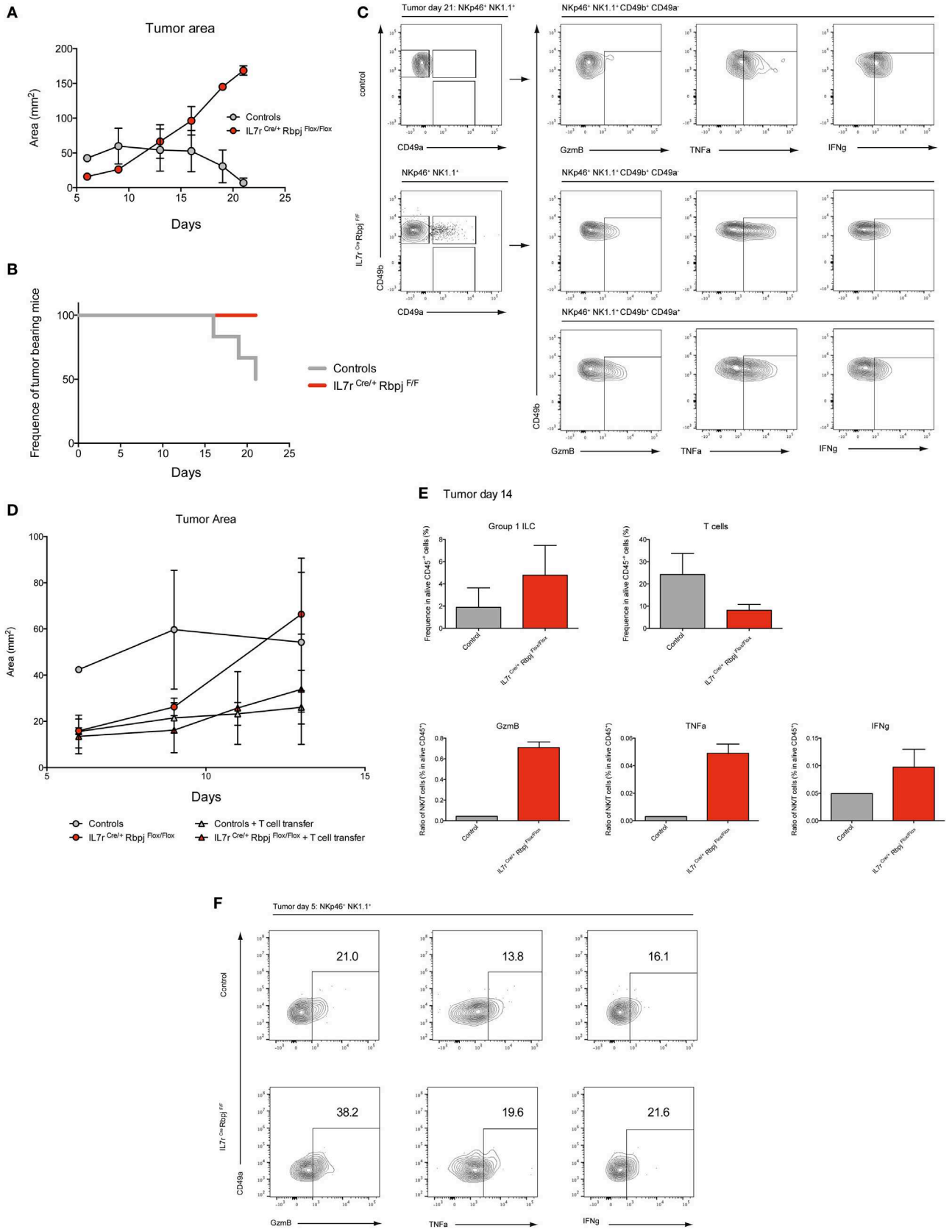

FIGURE 6 | Continued

FIGURE 6 | Notch signaling participates to early antitumoral activity. **(A)** Tumor area after subcutaneous injection of 3×10^6 Hepa1.6 cells in control IL7r^{Cre} Rbpj$^{F/+}$, IL7r$^{+/+}$ Rbpj$^{F/+}$, and IL7r$^{+/+}$ Rbpj$^{F/F}$ (gray) and IL7r^{Cre} Rbpj$^{F/F}$ mice (red). **(B)** Frequency of mice with a tumor after subcutaneous injection of 3×10^6 Hepa1.6 cells in control IL7r^{Cre} Rbpj$^{F/+}$, IL7r$^{+/+}$ Rbpj$^{F/+}$, and IL7r$^{+/+}$ Rbpj$^{F/F}$ (gray) and IL7r^{Cre} Rbpj$^{F/F}$ mice (red). 50% of control mice rejected the tumor after 21 days. **(C)** Group 1 innate lymphoid cell (ILC) tumor infiltrates in control IL7r^{Cre} Rbpj$^{F/+}$, IL7r$^{+/+}$ Rbpj$^{F/+}$, and IL7r$^{+/+}$ Rbpj$^{F/F}$ mice (top panel) and IL7r^{Cre} Rbpj$^{F/F}$ mice (bottom panel) 21 days after Hepa1.6 cells injection. **(D)** Tumor area after subcutaneous injection of 3×10^6 Hepa1.6 cells in control IL7r^{Cre} Rbpj$^{F/+}$, IL7r$^{+/+}$ Rbpj$^{F/+}$, and IL7r$^{+/+}$ Rbpj$^{F/F}$ (gray dot), IL7r^{Cre} Rbpj$^{F/F}$ mice (red dot), control IL7r^{Cre} Rbpj$^{F/+}$, IL7r$^{+/+}$ Rbpj$^{F/+}$, and IL7r$^{+/+}$ Rbpj$^{F/F}$ mice with T cell transfer (gray triangle) and IL7r^{Cre} Rbpj$^{F/F}$ mice with T cell transfer (red triangle). **(E)** Frequency of group 1 ILC and CD3-positive cells in tumor of control IL7r^{Cre} Rbpj$^{F/+}$, IL7r$^{+/+}$ Rbpj$^{F/+}$, and IL7r$^{+/+}$ Rbpj$^{F/F}$ (gray), IL7r^{Cre} Rbpj$^{F/F}$ mice (red) with T cell transfer 14 days after Hepa1.6 cells injection. Ratio of group 1 ILC on T cell expressing granzyme B (GzmB), TNFa, and IFNg. **(F)** Expression of GzmB, TNFa, and IFNg in group 1 ILC tumor infiltrates of IL7r^{Cre} Rbpj$^{F/+}$, IL7r$^{+/+}$ Rbpj$^{F/+}$, and IL7r$^{+/+}$ Rbpj$^{F/F}$ control (top panel) and IL7r^{Cre} Rbpj$^{F/F}$ mice (bottom panel) 5 days after Hepa1.6 cells injection.

subsets and also in the control of CD49a expression levels on recruited type 1 ILC populations.

DISCUSSION

In the liver, cNK and ILC1 are more heterogeneous than initially thought. Contrary to CD49b$^+$ cNK, resident hepatic ILC1 have been defined as Eomes$^-$ CD49a$^+$ CD49b$^-$ T-bet dependent (2, 21–24). We distinguished here two subsets of ILC1 and of cNK based on the expression of a limited set of transcripts. Surprisingly, Eomes transcripts were found expressed in one of the hepatic ILC1 subgroup and they were differentially expressed among cNK subsets. Differences in tissue ILC1 populations have been attributed to the environment, particularly in glands where ILC1 express both Eomes and T-bet (25). This made us consider the possibility that Eomes levels may be actively suppressed in hepatic ILC1. Since Eomes expression is repressed in T-bet$^+$ hepatic ILC1 (2), and that T-bet is a possible target of the Notch pathway, we investigated whether the Notch pathway acts on hepatic type 1 ILC.

Using single-cell transcriptomic analyses, we confirmed that nearly half of hepatic ILC1 and cNK cells expressed Notch receptors. We found that expression is heterogeneous as cells could either be Notch1$^+$, Notch2$^+$, or both. Hence, we suspected that the Notch signaling pathway could also play a role on different characteristics of type 1 ILC from other organs. Therefore, by selecting genes belonging to type 1 ILC developmental program and to the Notch signaling pathway, we designed a comparative transcriptomic study on numerous small populations of type 1 ILC subsets from diverse tissues. We showed that Notch pathway is actively operating in populations from most tissues, except for spleen where a substantial amount of cells was found to be Notch insensitive.

We found that RBPJ deficiency was associated with the reduction of the *Tbx21* gene expression in half hepatic ILC1 validating our hypothesis of the Notch pathway implication on hepatic subset specification and functions. We assume that T-bet might also be activated by other signaling pathways because the other half of ILC1 that are not expressing Notch receptors should have a path to upregulate T-bet. We observed identical changes of ILC1 and cNK transcriptional program in other organs. In a previous study, we reported that T-bet levels were maintained in type ILC1 in the intestinal LP (17). However, in our previous study, the Notch sensitive population was diluted among Notch insensitive cells masking the effect of the Notch signaling depletion. Therefore, to overcome this limitation, we used only 25 cells per population in this comparative transcriptomic assay. In the absence of the Notch signaling pathway, we also detected an increase of Eomes expression in ILC1 and cNK subsets both at transcriptional and protein levels. The presence of a new immature Eomes$^-$ cNK population in the liver diluted the Eomes transcript levels from the global population as observed in **Figure 4**. The expression of Eomes is probably due to the decrease of T-bet, as previously observed in T-bet-deficient cNK cells (2, 26). Moreover, T-bet$^-$ cNK cells fail to express Mac1 and maintain their CD27 levels (27, 28). Consistently, we observed a decrease of Mac1 expression in liver cNK cells and the presence of CD27$^+$ Mac1$^-$ immature subset. The presence of these immature subsets might be linked to the decrease of T-bet expression in type 1 ILC. It has been hypothesized that hepatic ILC1 depends on T-bet for their development, although no direct evidence has been provided. In our RBPJ-deficient model, it is possible that all Notch-dependent ILC1 subsets are absent because they are not able to differentiate *in situ*. This immature subset could therefore represent accumulating ILC1 precursors that could not progress to the T-bet$^+$ stage. On other hand, peripheral immature subsets could also represent accumulating immature cNK cells. It has been shown that environment could induce conversion between ILC1 and cNK (25, 29, 30). Our study illustrates a probable hepatic ILC1 differentiation into cNK where the absence of the Notch pathway leads to the induction of Eomes *via* the downregulation of its regulator T-bet. Consistent with this hypothesis, in T-bet-deficient mice, precursors in the BM show an increase of the immature CD27$^+$ and a decrease of the mature Mac1$^+$ populations (Figure S7 in Supplementary Material). Clustering of BM RBPJ-competent and -deficient subsets confirmed a role for Notch signaling in the early development of type 1 ILC. Even if T-bet levels are actively maintained low in BM cNK precursors, T-bet is expressed at the immature CD27$^+$ Mac1$^-$ stage. T-bet has been shown to control S1P5 expression which participates to cNK trafficking (31, 32). As in T-bet-deficient mice, we also found more cNK cells in the BM (Figure S7 in Supplementary Material) of RBPJ-deficient mice while their ratio were decreased to the expense of ILC1 in the periphery (32, 33). We proved that the increase of ILC1 was not due to excessive proliferation and propose that the Notch induced decrease of T-bet results in a reduced exit from the BM.

Notch1 and Notch2 were correlated to different set of genes in our study suggesting that Notch1 was related to CD49a expression, IL21r, IL12rb1. Modifications in integrin expression are observed mainly in ILC1 with a clear decrease of surface CD49a. CD49a is not changed in Notch2-deficient mice arguing that modulation of CD49a levels is a specific Notch1 related feature.

Hence, different Notch receptors could have different repercussions on the resulting subset especially if they are expressed at different frequencies. To consider whether Notch signaling could directly act on CD49a expression, we looked for potential binding sites for RBPJ in the promoter region of the itga1 gene (Figure S8 in Supplementary Material). Typical RBPJ-binding sequence (Figure S8A in Supplementary Material) was searched by screening the itga1 promoter region for a minimum of 5-mer motif. Three potential-binding sites were found suggesting a possible direct action of the Notch signaling pathway on the level of CD49a expression (Figure S8B in Supplementary Material). Due to the important proportion of type 1 ILC expressing Notch2 in the periphery and the superposition of the effects driven by RBPJ and Notch2 deficiency on enhanced effector functions, we suggest that Notch2 could be the main player in cell activation. Notch2 has been proposed as a central receptor for peripheral T cell maturation (34, 35). However, Notch1 could also control Eomes, perforin, and GzmB (36). Among others, Notch2 gene expression is correlated with the upregulation of Eomes, GzmB Cx3cr1, Ly6c, Il18r1, and IL2ra expression that constitute a hallmark of activated mature cNK cells. Increased expression of CX3CR1 was also described in T-bet-deficient mice (26) and is a marker of circulating peripheral cNK cells (37). Increased of Th1 cytokine receptors coupled with the increase of GzmB correspond to the phenotype of peripheral-activated cytotoxic cells. In our RBPJ-deficient model, type 1 ILC also increases their capacity to release IFNg and TNFa. The increase of Ly6C by RBPJ-deficient cNK cells is reminiscent of cells previously designated as peripheral resting inert mNK cells that could produce an effective and strong response in case of reactivation by cytokine stimuli (38). We suggest that maturation to the Ly6C^{hi} stage is linked to modification of T-bet/Eomes quantities driven by a deficiency in Notch signaling.

It was shown that Notch signaling impacts Th1 differentiation and cytotoxicity (34, 35, 39, 40). We found the opposite effect in type 1 ILC where the absence of the Notch signaling induces maturation of peripheral subsets toward a more "activated" state with enhanced cytotoxic functions. Nonetheless, our results are in agreement with other studies showing the maintenance of the Th1 response in Notch1/Notch2, RBPBJ-deficient, and MAML1 dominant-negative mice (41, 42).

Type 1 helper innate lymphoid cells and cNK cells are developmentally and functionally related and it has been suggested that cells can interconvert in certain conditions such as in a tumoral environment (25). In addition, dysregulations of the Notch signaling were described in diverse types of cancer where an oncogenic or tumor suppressive role depended on tissue type and particular microenvironments (43). In hepatocellular carcinoma, the implication of Notch signaling is currently under intense investigation (44).

To test antitumor ability of Notch-deficient cNK subsets, we used an *in vivo* hepatocellular carcinoma model. Hepa1–6 tumors grew slower at early phase when transplanted into Notch-deficient mice than into Notch-competent littermates thanks to an increase of intratumoral type 1 ILC frequency in RBPJ-deficient conditions. Moreover, deficient Notch signaling pathway leads to the presence of new CD49a^{+} cNK cells with a higher ability to release cytotoxic and inflammatory signals. Since in Notch-deficient mice, T cell subsets are reduced, this model is not ideal to compare later stages of tumor progression or regression. The progression of tumor area and analyses of intratumoral immune content in control animals allowed us to determine that tumors start to regress 2 weeks after hepatocellular carcinoma injections due to intratumoral effector T cells. The tumor regression is fast with already half of control littermates that have totally eradicated the tumor 3 weeks after injection. Hence, we decided to transfer T cells to both Notch-deficient and littermate controls to compare the tumor growth and analyze their immune compartment. As previously observed for early phase, RBPJ-deficient conditions allowed a better control of tumor growth until 10 days. To recover enough immune cells from the tumor, we did not extend our analysis over 2 weeks and observed that even after T cell transfer, type 1 ILC were more frequent and more cytotoxic in RBPJ-deficient animals. We concluded that inhibition of the Notch signaling pathway is beneficial for the early control of tumor growth by type 1 ILC. Other studies have shown that depending on Notch receptor and ligands identity, antagonistic effects could be found on tumor progression (45). Our study adds a stone by dissecting the regulation of important cytotoxic subsets implicated in the tumor immunosurveillance. Collectively, our data suggest that cNK cells unable to signal *via* the Notch pathway are more critical effector cells to restrain early carcinoma growth. These cells displayed features that resemble ILC1 but also mature reactivated cNK secreting higher amounts of cytotoxic and inflammatory cytokines. Tumor immunosurveillance studies using T-bet-deficient mice demonstrated that T-bet is essentially required at late stages of the immune response but is not crucial in primary tumors (26, 46, 47). Nonetheless, forced expression of Eomes in cNK cells was shown to decrease tumor growth and enhance survival (48). Hence, we propose that the Notch pathway in mature peripheral type 1 ILC represents a modulator of the inflammatory response. This is achieved by the regulation of T-bet versus Eomes expression and by regulating expression of pro/anti-apoptotic molecules, as observed on our comparative transcriptomic analyses. The Notch signaling pathway is also implicated in the regulation of the cNK cell-mediated tumor immunosurveillance. Hence, the tumoral environment could also temper the immune response *via* the regulation of Notch ligand expression.

Finally, we propose that the Notch signaling pathway as one of the extrinsic signals that control the intrinsic T-bet/Eomes balance. This pathway is implicated at multiple levels since T-bet/Eomes ratio are so important for cytotoxic lymphocyte differentiation and functions (49). Like TGF-β signaling that directs differentiation of salivary gland ILC1 through suppression of Eomes (25), we propose that the Notch signaling pathway participates to reduce Eomes levels in both cNK and ILC1, with a strong effect on hepatic ILC1. The spatio-temporal regulation of Notch receptor expression is participating to this equilibrium and enhances the complexity of the global picture.

ETHICS STATEMENT

Mice were bred in accordance with Pasteur Institute guidelines in compliance with European animal welfare regulations, and

all animal studies were approved by Pasteur Institute Safety Committee in accordance with French and European guidelines.

AUTHOR CONTRIBUTIONS

TP, SM, MP, and E-GB performed the experiments. RG, TP, and SM designed the experiments. RG, TP, AC, MP, SM, and E-GB analyzed the data. RG supervised the experiments and wrote the manuscript with the contribution of AC and TP.

ACKNOWLEDGMENTS

We thank C. A. J. Vosshenrich for YAC1 cells and help on the design of cytotoxic assays. We thank the Cytometry Core Facility and the Center for Human Immunology of Pasteur Institute for support. This work benefited from data assembled by the ImmGen consortium.

FUNDING

The work was supported by Pasteur Institute, Institut National de la Santé et de la Recherche Médicale (INSERM), the Ministère de la Recherche, Association pour la Recherche sur le Cancer, La Ligue Contre Le Cancer, Université Paris Diderot, the Institut National du Cancer Grant «Role of the immune microenvironment during liver carcinogenesis» and the USPC Grant «Mucocell», Agence Nationale de la Recherche (ANR) project Myeloten, the ANR Program REVIVE (Investment for the Future), the ANR project Twothyme, and by the Pasteur-Weizmann Foundation.

SUPPLEMENTARY MATERIAL

The Supplementary Material for this article can be found online at https://www.frontiersin.org/articles/10.3389/fimmu.2018.01252/full#supplementary-material.

FIGURE S1 | **(A)** Correlation heatmap of gene expression from transcripts of **Figure 1**. **G** using Spearman method. **(B)** Correlation heatmap of gene expression from transcripts of signature 1 from **Figure 1**. **G** using Spearman method. **(C)** Correlation heatmap of gene expression from transcripts of signature 2 from **Figure 1**. **G** using Spearman method. Levels of correlation are shown from blue (low level) to red (high level).

FIGURE S2 | **(A)** Flow cytometry of hepatic group 1 innate lymphoid cell in IL7r^{Cre} Notch2$^{F/F}$, Vav^{Cre} Rbpj$^{F/F}$ mice and their respective controls. **(B)** Mean fluorescence intensity of CD49a and CD49b in hepatic conventional NK (cNK) and type 1 helper innate lymphoid cells (ILC1) in control (white) and Vav^{Cre} Rbpj$^{F/F}$ (red) mice. **(C)** Frequency of hepatic ILC1 and cNK in IL7r^{Cre} Notch2$^{F/F}$, Vav^{Cre} Rbpj$^{F/F}$ mice, and their respective controls.

FIGURE S3 | **(A)** Frequency of hepatic type 1 helper innate lymphoid cells (ILC1) and conventional NK (cNK) in G0 (white), G1 (gray), and S/G2/M (black) phase. **(B)** T cells in the thymus were used as control of cell cycle.

FIGURE S4 | Expression of TNFa, IFNg, and granzyme B in hepatic type 1 helper innate lymphoid cells (ILC1) (left panel) and conventional NK (cNK) (right panel) of control IL7r^{Cre} Notch2$^{F/+}$ mice (top panel) and IL7r^{Cre} Notch2$^{F/F}$ mice (middle panel). Levels of expression were compared (bottom panel) between control IL7r^{Cre} Notch2$^{F/+}$ mice (blue) and IL7r^{Cre} Notch2$^{F/F}$ mice (red), Lineage-negative cells were used as control for expression (dashed black).

FIGURE S5 | Correlation heatmap of gene expression using Spearman method. Levels of correlation are shown from blue (low level) to red (high level).

FIGURE S6 | **(A)** Flow cytometry of T cell infiltrate from tumor at day 14. Intracellular granzyme B (GzmB), TNFa, and IFNg expression of T cells. **(B)** Frequency of T cells infiltrate in alive CD45$^+$ cells and frequency of T cells expressing GzmB, TNFa, and IFNg in alive CD45$^+$ cells.

FIGURE S7 | NK cells and NK progenitors (NKP) repartition in bone marrow (BM). **(A)** Flow cytometry of NKP (NKp46$^-$ NK1.1$^+$ CD49b$^{+/-}$), and NK cells (NKp46$^+$ NK1.1$^+$) in BM of control IL7r^{Cre} Rbpj$^{F/+}$ (top panel) and IL7r^{Cre} Rbpj$^{F/F}$ mice (bottom panel). **(B)** Frequency of NKP (NKp46$^-$ NK1.1$^-$ CD49b$^{+/-}$) and NK cells (NKp46$^+$ NK1.1$^+$) in BM of control IL7r^{Cre} Rbpj$^{F/+}$ (white) and IL7r^{Cre} Rbpj$^{F/F}$ mice (red). NKP were divided based on CD49b expression and NK cells were divided based on CD27 and Mac1 expression.

FIGURE S8 | **(A)** Consensus sequence for RBPJ-binding sites to promoter regions. **(B)** Location of 5-mer motifs for potential RBPJ binding sites along the itga1 (CD49a) promoter region. Different motifs are represented in different colors.

REFERENCES

1. Cortez VS, Colonna M. Diversity and function of group 1 innate lymphoid cells. *Immunol Lett* (2016) 179:19–24. doi:10.1016/j.imlet.2016.07.005
2. Daussy C, Faure F, Mayol K, Viel S, Gasteiger G, Charrier E, et al. T-bet and Eomes instruct the development of two distinct natural killer cell lineages in the liver and in the bone marrow. *J Exp Med* (2014) 211:563–77. doi:10.1084/jem.20131560
3. Constantinides MG, Gudjonson H, McDonald BD, Ishizuka IE, Verhoef PA, Dinner AR, et al. PLZF expression maps the early stages of ILC1 lineage development. *Proc Natl Acad Sci U S A* (2015) 112:5123–8. doi:10.1073/pnas.1423244112
4. Artavanis-Tsakonas S, Rand MD, Lake RJ. Notch signaling: cell fate control and signal integration in development. *Science* (1999) 284:770–6. doi:10.1126/science.284.5415.770
5. Sandy AR, Jones M, Maillard I. Notch signaling and development of the hematopoietic system. *Adv Exp Med Biol* (2012) 727:71–88. doi:10.1007/978-1-4614-0899-4_6
6. Mumm JS, Kopan R. Notch signaling: from the outside in. *Dev Biol* (2000) 228:151–65. doi:10.1006/dbio.2000.9960
7. Andersson ER, Sandberg R, Lendahl U. Notch signaling: simplicity in design, versatility in function. *Development* (2011) 138:3593–612. doi:10.1242/dev.063610
8. Deftos ML, Bevan MJ. Notch signaling in T cell development. *Curr Opin Immunol* (2000) 12:166–72. doi:10.1016/S0952-7915(99)00067-9
9. Benne C, Lelievre JD, Balbo M, Henry A, Sakano S, Levy Y. Notch increases T/NK potential of human hematopoietic progenitors and inhibits B cell differentiation at a pro-B stage. *Stem Cells* (2009) 27:1676–85. doi:10.1002/stem.94
10. Schmitt TM, Ciofani M, Petrie HT, Zuniga-Pflucker JC. Maintenance of T cell specification and differentiation requires recurrent notch receptor-ligand interactions. *J Exp Med* (2004) 200:469–79. doi:10.1084/jem.20040394
11. Chea S, Schmutz S, Berthault C, Perchet T, Petit M, Burlen-Defranoux O, et al. Single-cell gene expression analyses reveal heterogeneous responsiveness of fetal innate lymphoid progenitors to notch signaling. *Cell Rep* (2016) 14:1500–16. doi:10.1016/j.celrep.2016.01.015
12. DeHart SL, Heikens MJ, Tsai S. Jagged2 promotes the development of natural killer cells and the establishment of functional natural killer cell lines. *Blood* (2005) 105:3521–7. doi:10.1182/blood-2004-11-4237
13. Felices M, Ankarlo DE, Lenvik TR, Nelson HH, Blazar BR, Verneris MR, et al. Notch signaling at later stages of NK cell development enhances KIR expression and functional maturation. *J Immunol* (2014) 193:3344–54. doi:10.4049/jimmunol.1400534
14. Manaster I, Gazit R, Goldman-Wohl D, Stern-Ginossar N, Mizrahi S, Yagel S, et al. Notch activation enhances IFNgamma secretion by human peripheral blood and decidual NK cells. *J Reprod Immunol* (2010) 84:1–7. doi:10.1016/j.jri.2009.10.009
15. Yokoyama WM, Plougastel BF. Immune functions encoded by the natural killer gene complex. *Nat Rev Immunol* (2003) 3:304–16. doi:10.1038/nri1055

16. Cerwenka A, Lanier LL. Ligands for natural killer cell receptors: redundancy or specificity. *Immunol Rev* (2001) 181:158–69. doi:10.1034/j.1600-065X.2001.1810113.x
17. Chea S, Perchet T, Petit M, Verrier T, Guy-Grand D, Banchi EG, et al. Notch signaling in group 3 innate lymphoid cells modulates their plasticity. *Sci Signal* (2016) 9:ra45. doi:10.1126/scisignal.aaf2223
18. Perchet T, Chea S, Hasan M, Cumano A, Golub R. Single-cell gene expression using multiplex RT-qPCR to characterize heterogeneity of rare lymphoid populations. *J Vis Exp* (2017) 119:e54858. doi:10.3791/54858
19. Machado MV, Michelotti GA, Xie G, Almeida Pereira T, Boursier J, Bohnic B, et al. Mouse models of diet-induced nonalcoholic steatohepatitis reproduce the heterogeneity of the human disease. *PLoS One* (2015) 10:e0127991. doi:10.1371/journal.pone.0132315
20. Lin D, Lei L, Liu Y, Zhang Y, Hu B, Bao G, et al. Membrane IL1α inhibits the development of hepatocellular carcinoma via promoting T- and NK-cell activation. *Cancer Res* (2016) 76:3179–88. doi:10.1158/0008-5472.CAN-15-2658
21. Klose CSN, Flach M, Möhle L, Rogell L, Hoyler T, Ebert K, et al. Differentiation of type 1 ILCs from a common progenitor to all helper-like innate lymphoid cell lineages. *Cell* (2014) 157:340–56. doi:10.1016/j.cell.2014.03.030
22. Seillet C, Mielke LA, Amann-Zalcenstein DB, Su S, Gao J, Almeida FF, et al. Deciphering the innate lymphoid cell transcriptional program. *Cell Rep* (2016) 17:436–47. doi:10.1016/j.celrep.2016.09.025
23. Gordon SM, Chaix J, Rupp LJ, Wu J, Madera S, Sun JC, et al. The transcription factors T-bet and Eomes control key checkpoints of natural killer cell maturation. *Immunity* (2012) 36:55–67. doi:10.1016/j.immuni.2011.11.016
24. Sojka DK, Plougastel-Douglas B, Yang L, Pak-Wittel MA, Artyomov MN, Ivanova Y, et al. Tissue-resident natural killer (NK) cells are cell lineages distinct from thymic and conventional splenic NK cells. *Elife* (2014) 3:e01659. doi:10.7554/eLife.01659
25. Cortez VS, Ulland TK, Cervantes-Barragan L, Bando JK, Robinette ML, Wang Q, et al. SMAD4 impedes the conversion of NK cells into ILC1-like cells by curtailing non-canonical TGF-β signaling. *Nat Immunol* (2017) 18:995–1003. doi:10.1038/ni.3809
26. van Helden MJ, Goossens S, Daussy C, Mathieu AL, Faure F, Marçais A, et al. Terminal NK cell maturation is controlled by concerted actions of T-bet and Zeb2 and is essential for melanoma rejection. *J Exp Med* (2015) 212:2015–25. doi:10.1084/jem.20150809
27. Townsend MJ, Weinmann AS, Matsuda JL, Salomon R, Farnham PJ, Biron CA, et al. T-bet regulates the terminal maturation and homeostasis of NK and Valpha14i NKT cells. *Immunity* (2004) 20:477–94. doi:10.1016/S1074-7613(04)00076-7
28. Soderquest K, Powell N, Luci C, van Rooijen N, Hidalgo A, Geissmann F, et al. Monocytes control natural killer cell differentiation to effector phenotypes. *Blood* (2011) 117:4511–8. doi:10.1182/blood-2010-10-312264
29. Gao Y, Souza-Fonseca-Guimaraes F, Bald T, Ng SS, Young A, Ngiow SF, et al. Tumor immunoevasion by the conversion of effector NK cells into type 1 innate lymphoid cells. *Nat Immunol* (2017) 18:1004–15. doi:10.1038/ni.3800
30. Dadi S, Chhangawala S, Whitlock BM, Franklin RA, Luo CT, Oh SA, et al. Cancer immunosurveillance by tissue-resident innate lymphoid cells and innate-like T cells. *Cell* (2016) 164:365–77. doi:10.1016/j.cell.2016.01.002
31. Walzer T, Chiossone L, Chaix J, Calver A, Carozzo C, Garrigue-Antar L, et al. Natural killer cell trafficking in vivo requires a dedicated sphingosine 1-phosphate receptor. *Nat Immunol* (2007) 8:1337–44. doi:10.1038/ni1523
32. Jenne CN, Enders A, Rivera R, Watson SR, Bankovich AJ, Pereira JP, et al. T-bet-dependent S1P5 expression in NK cells promotes egress from lymph nodes and bone marrow. *J Exp Med* (2009) 206:2469–81. doi:10.1084/jem.20090525
33. Harms Pritchard G, Hall AO, Christian DA, Wagage S, Fang Q, Muallem G, et al. Diverse roles for T-bet in the effector responses required for resistance to infection. *J Immunol* (2015) 194:1131–40. doi:10.4049/jimmunol.1401617
34. Maekawa Y, Minato Y, Ishifune C, Kurihara T, Kitamura A, Kojima H, et al. Notch2 integrates signaling by the transcription factors RBP-J and CREB1 to promote T cell cytotoxicity. *Nat Immunol* (2008) 9:1140–7. doi:10.1038/ni.1649
35. Sugimoto K, Maekawa Y, Kitamura A, Nishida J, Koyanagi A, Yagita H, et al. Notch2 signaling is required for potent antitumor immunity in vivo. *J Immunol* (2010) 184:4673–8. doi:10.4049/jimmunol.0903661
36. Cho OH, Shin HM, Miele L, Golde TE, Fauq A, Minter LM, et al. Notch regulates cytolytic effector function in CD8+ T cells. *J Immunol* (2009) 182:3380–9. doi:10.4049/jimmunol.0802598
37. Grégoire C, Chasson L, Luci C, Tomasello E, Geissmann F, Vivier E, et al. The trafficking of natural killer cells. *Immunol Rev* (2007) 220:169–82. doi:10.1111/j.1600-065X.2007.00563.x
38. Omi A, Enomoto Y, Kiniwa T, Miyata N, Miyajima A. Mature resting Ly6C(high) natural killer cells can be reactivated by IL-15. *Eur J Immunol* (2014) 44:2638–47. doi:10.1002/eji.201444570
39. Maekawa Y, Tsukumo S, Chiba S, Hirai H, Hayashi Y, Okada H, et al. Delta1-Notch3 interactions bias the functional differentiation of activated CD4+ T cells. *Immunity* (2003) 19:549–59. doi:10.1016/S1074-7613(03)00270-X
40. Sun J, Krawczyk CJ, Pearce EJ. Suppression of Th2 cell development by Notch ligands Delta1 and Delta4. *J Immunol* (2008) 180:1655–61. doi:10.4049/jimmunol.180.3.1655
41. Amsen D, Blander JM, Lee GR, Tanigaki K, Honjo T, Flavell RA. Instruction of distinct CD4 T helper cell fates by different notch ligands on antigen-presenting cells. *Cell* (2004) 117:515–26. doi:10.1016/S0092-8674(04)00451-9
42. Tu L, Fang TC, Artis D, Shestova O, Pross SE, Maillard I, et al. Notch signaling is an important regulator of type 2 immunity. *J Exp Med* (2005) 202:1037–42. doi:10.1084/jem.20050923
43. Lobry C, Oh P, Aifantis I. Oncogenic and tumor suppressor functions of Notch in cancer: it's NOTCH what you think. *J Exp Med* (2011) 208:1931–5. doi:10.1084/jem.20111855
44. Geisler F, Strazzabosco M. Emerging roles of Notch signaling in liver disease. *Hepatology* (2015) 61:382–92. doi:10.1002/hep.27268
45. Lobry C, Oh P, Mansour MR, Look AT, Aifantis I. Notch signaling: switching an oncogene to a tumor suppressor. *Blood* (2014) 123:2451–9. doi:10.1182/blood-2013-08-355818
46. Werneck MB, Lugo-Villarino G, Hwang ES, Cantor H, Glimcher LH. T-bet plays a key role in NK-mediated control of melanoma metastatic disease. *J Immunol* (2008) 180:8004–10. doi:10.4049/jimmunol.180.12.8004
47. Peng BG, Liang LJ, He Q, Huang JF, Lu MD. Expansion and activation of natural killer cells from PBMC for immunotherapy of hepatocellular carcinoma. *World J Gastroenterol* (2004) 10:2119–23. doi:10.3748/wjg.v10.i14.2119
48. Gill S, Vasey AE, De Souza A, Baker J, Smith AT, Kohrt HE, et al. Rapid development of exhaustion and down-regulation of eomesodermin limit the antitumor activity of adoptively transferred murine natural killer cells. *Blood* (2012) 119:5758–68. doi:10.1182/blood-2012-03-415364
49. Zhang J, Marotel M, Fauteux-Daniel S, Mathieu AL, Viel S, Marçais A, et al. T-bet and Eomes govern differentiation and function of mouse and human NK cells and ILC1. *Eur J Immunol* (2018) 48:738–50. doi:10.1002/eji.201747299

Conflict of Interest Statement: The authors declare that the research was conducted in the absence of any commercial or financial relationships that could be construed as a potential conflict of interest.

Article

Cell Reports

Single-Cell Gene Expression Analyses Reveal Heterogeneous Responsiveness of Fetal Innate Lymphoid Progenitors to Notch Signaling

Graphical Abstract

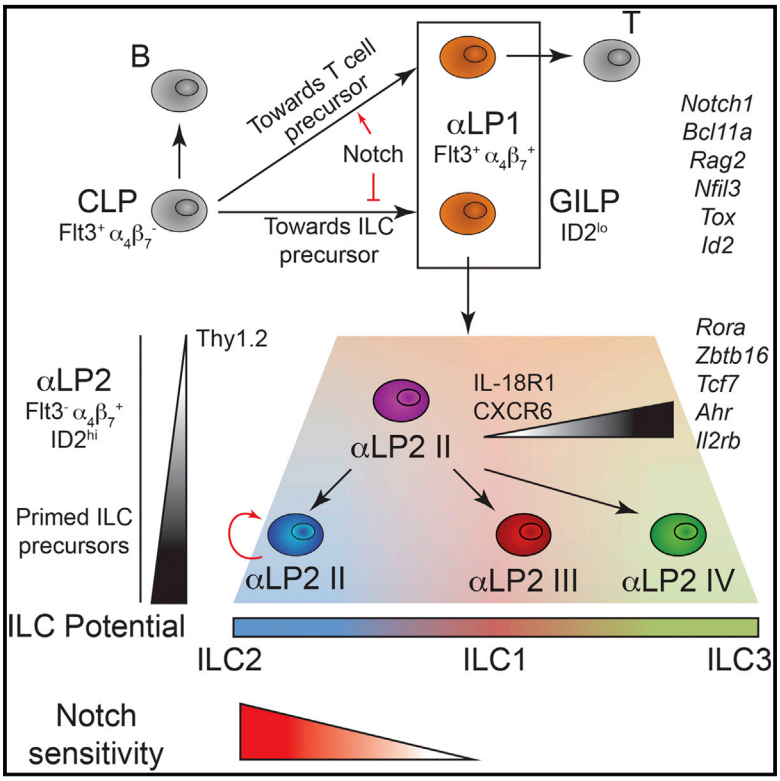

Highlights

- Global ILC progenitor and T precursors are found in the αLP1 compartment
- αLP2 compartment is heterogeneously composed of primed ILC precursors
- Notch signaling specifically acts on proliferation of an αLP2 ILC2 primed subset
- Constitutive NICD expression drives T cell development and restrains *Id2* expression

Authors

Sylvestre Chea, Sandrine Schmutz, Claire Berthault, ..., Hans-Reimer Rodewald, Ana Cumano, Rachel Golub

Correspondence

rachel.golub@pasteur.fr

In Brief

Molecular pathways and transcription factors involved in innate lymphoid cell (ILC) development are currently under intense investigation. Chea et al. now characterize different stages of ILC progenitors, from a global ILC progenitor (GILP) to committed ILC precursors, that are differentially sensitive to Notch signaling.

Chea et al., 2016, Cell Reports *14*, 1500–1516
February 16, 2016
http://dx.doi.org/10.1016/j.celrep.2016.01.015

CellPress

OPEN ACCESS
CellPress

Cell Reports
Article

Single-Cell Gene Expression Analyses Reveal Heterogeneous Responsiveness of Fetal Innate Lymphoid Progenitors to Notch Signaling

Sylvestre Chea,[1,2,3] Sandrine Schmutz,[1,4] Claire Berthault,[1,2,3] Thibaut Perchet,[1,2,3] Maxime Petit,[1,2,3] Odile Burlen-Defranoux,[1,2,3] Ananda W. Goldrath,[5] Hans-Reimer Rodewald,[6] Ana Cumano,[1,2,3] and Rachel Golub[1,2,3,*]

[1]Lymphopoiesis Unit, Immunology Department, Institut Pasteur, 75015 Paris, France
[2]University Paris Diderot, Sorbonne Paris Cité, Cellule Pasteur, 75013 Paris, France
[3]INSERM U1223, 75015 Paris, France
[4]Cytometry Platform, Institut Pasteur, 75015 Paris, France
[5]Molecular Biology Section, Division of Biological Sciences, University of California, San Diego, La Jolla, CA 92093, USA
[6]Division of Cellular Immunology, German Cancer Research Center, 69120 Heidelberg, Germany
*Correspondence: rachel.golub@pasteur.fr
http://dx.doi.org/10.1016/j.celrep.2016.01.015

SUMMARY

T and innate lymphoid cells (ILCs) share some aspects of their developmental programs. However, although Notch signaling is strictly required for T cell development, it is dispensable for fetal ILC development. Constitutive activation of Notch signaling, at the common lymphoid progenitor stage, drives T cell development and abrogates ILC development by preventing *Id2* expression. By combining single-cell transcriptomics and clonal culture strategies, we characterize two heterogeneous $\alpha_4\beta_7$-expressing lymphoid progenitor compartments. αLP1 (Flt3$^+$) still retains T cell potential and comprises the global ILC progenitor, while αLP2 (Flt3$^-$) consists of ILC precursors that are primed toward the different ILC lineages. Only a subset of αLP2 precursors is sensitive to Notch signaling required for their proliferation. Our study identifies, in a refined manner, the diversity of transitional stages of ILC development, their transcriptional signatures, and their differential dependence on Notch signaling.

INTRODUCTION

Innate lymphoid cells (ILCs) are a family of three groups (ILC1, ILC2, and ILC3) that rapidly respond to inflammatory signals by producing cytokines also involved in tissue homeostasis (Seillet et al., 2014). Group 1 is defined as distinct from conventional NK (cNK) cells and requires T-bet for its lineage specification (Bernink et al., 2013; Daussy et al., 2014; Fuchs et al., 2013; Klose et al., 2014). Group 2 expresses the transcription factors GATA3 and RORα (Hoyler et al., 2012; Klein Wolterink et al., 2013; Wong et al., 2012). Group 3 developmentally depends on the transcription factor RORγt and is composed of several distinct populations that emerge during ontogeny. During fetal life, only lymphoid tissue inducer (LTi) cells are present, and other ILC3 subsets appear after birth. LTi cells and their precursors are found in the fetal liver (FL) (Mebius et al., 2001). They are essential for the generation of secondary lymphoid tissues (Eberl et al., 2004) and express *Rorc*, which controls interleukin (IL)-17A and IL-22 production. LTi cells are CCR6$^+$c-Kit$^+$IL-7Ra^{hi} cells and are referred to as LTi_4 and LTi_0, depending on the expression of CD4 (Klose et al., 2013; Sawa et al., 2010). All ILCs initially derive from the common lymphoid progenitor (CLP) (Cherrier et al., 2012; Mebius et al., 2001; Possot et al., 2011; Wong et al., 2012; Yang et al., 2011b). A common feature to ILC commitment is the requirement for the transcriptional repressor regulator ID2 (Hoyler et al., 2012; Moro et al., 2010; Satoh-Takayama et al., 2010; Yokota et al., 1999), an inhibitor of E protein transcription factors. The current scheme of ILC development describes the global ILC (GILP) precursor as NFIL3$^+$TOX$^+$, which further becomes the ID2^{hi} common helper ILC precursor (CHILP) when cNK cell potential is lost (Constantinides et al., 2014; Klose et al., 2014; Seehus et al., 2015; Xu et al., 2015). After acquisition of *Zbtb16* expression, CHILP loses the capacity to differentiate into LTi cells, showing that LTi precursors stand at the bifurcation between GILP and CHILP (Constantinides et al., 2014).

The Notch pathway is conserved and involved in many biological processes (Hori et al., 2013). Activation of Notch receptors promotes their proteolysis, resulting in the release of the Notch intracellular domain (NICD), which enters the nucleus as a co-transcriptional factor with the DNA-binding protein RBP-Jκ (Recombination signal sequence-Binding Protein Jκ chain) (Hori et al., 2013). The activation of this canonical Notch signaling pathway is known to regulate the transcription of target genes (Iso et al., 2003). During hematopoiesis, the Notch pathway acts as a cell-fate switch between the lymphoid and myeloid lineages (Oh et al., 2013). Notch1 is essential for T cell development at the expense of B cell development (Han et al., 2002; Pui et al., 1999; Sambandam et al., 2005). Notch2 signaling is crucial to marginal zone B cells (Saito et al., 2003; Tanigaki et al., 2002) and to the development of CD11b$^+$ classical dendritic cells (cDCs) in spleen and intestine (Lewis et al., 2011; Satpathy et al., 2013).

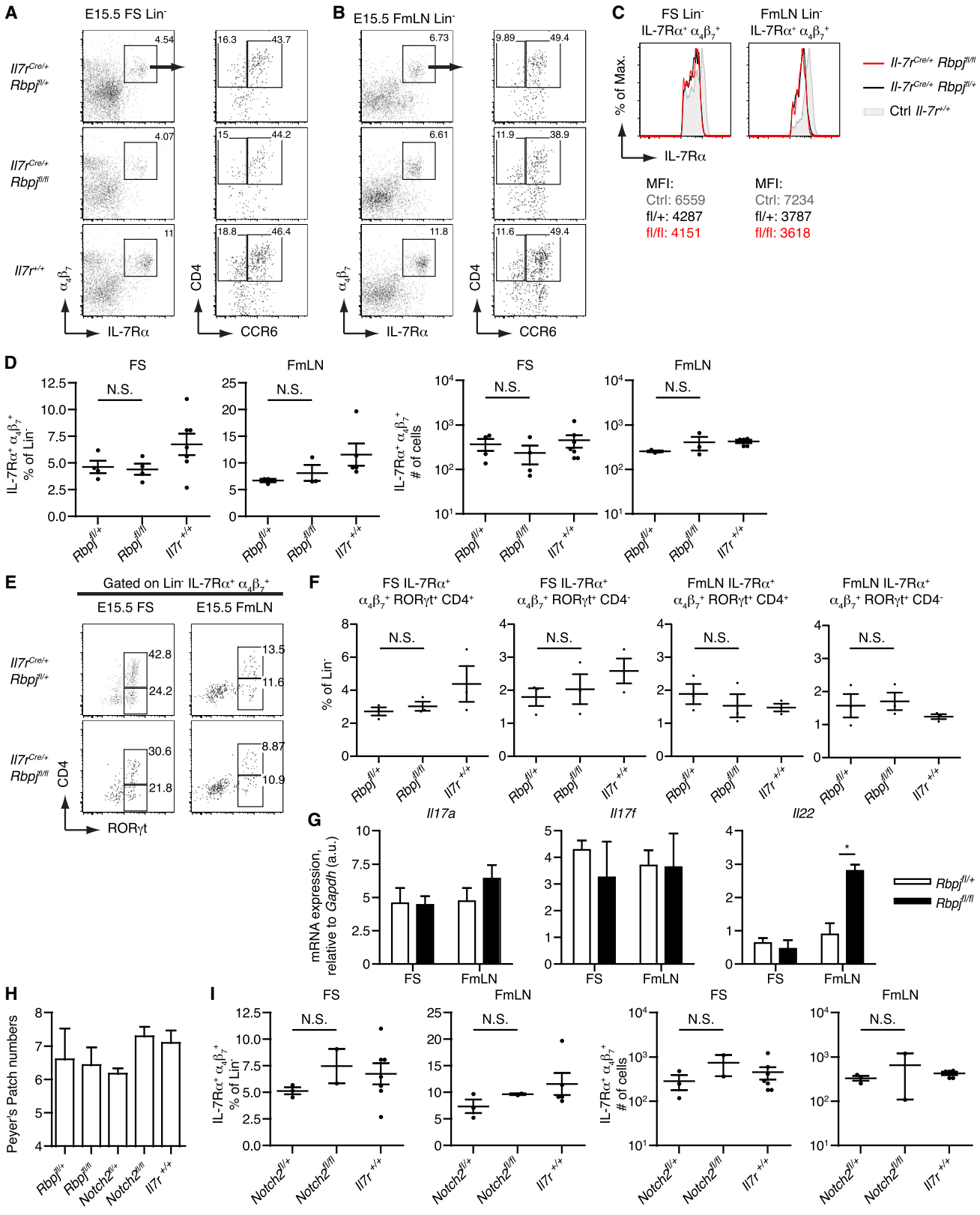

(legend on next page)

The relevance of the Notch pathway along ILC differentiation is still unresolved. Studies have supported the idea that the Notch pathway is necessary at a different branch point of adult ILC differentiation (Klose et al., 2013; Lee et al., 2012; Rankin et al., 2013). We recently suggested that Notch, although active, is not essential to the development of FL LTi cells (Possot et al., 2011), which was challenged by a report indicating that the Notch pathway blocks LTi development just before the expression of RORγt (Cherrier et al., 2012). Because both studies were performed in vitro, we developed mouse models to decipher the in vivo involvement of the Notch pathway during fetal LTi cell commitment and differentiation.

To delete the Notch pathway from the earliest stage of lymphoid progenitors, we used the *Il7r*^{Cre} mouse (Schlenner et al., 2010) combined with other mouse strains to either inactivate (*Rbpj*$^{fl/fl}$ and *Notch2*$^{fl/fl}$) or activate (*Rosa26*$^{loxP\text{-}Stop\text{-}loxP\text{-}NICD}$) Notch signaling. IL-7R is essential to drive lymphopoiesis and marks all lymphoid progenitors, as well as all ILCs, but not NK cells. IL-7 signaling provides the maintenance of lymphoid progenitors (Kondo et al., 1997) and is important for ILC development (Satoh-Takayama et al., 2010; Schmutz et al., 2009; Yoshida et al., 2002). Notch2 was previously shown to be more highly expressed in ILC precursors than Notch1 (Possot et al., 2011; Cherrier et al., 2012). In these mouse models, all the lymphoid progenitors and their progeny undergo Notch loss (or gain) of function. In parallel, we generated a double reporter *Id2*$^{yfp/+}$ *Cxcr6*$^{gfp/+}$ mouse to define diverse FL ID2$^+$ fractions of ILC precursors depending on the repartition of $\alpha_4\beta_7$, CXCR6, IL-18R1, and Thy1.2. We determined their hierarchy during ILC development and examined their equivalent in Notch-deficient embryos.

By targeting RBP-Jκ in lymphoid precursors, we report that canonical Notch signaling is unnecessary for LTi cell commitment and differentiation, and we showed that sustained Notch signaling is not blocking their development but rather promoting T cell development over any other lineages. In the periphery, Notch signaling modulates IL-22 levels in fetal mesenteric lymph node (FmLN) LTi cells. Finally, single-cell analysis of the expression of 81 mRNA transcripts revealed a hierarchy of differentiation, with heterogeneous fractions of lymphoid progenitors differentially enriched in ILC precursors. We demonstrate that Notch is only active on a sub-fraction mostly devoid of LTi fate. Notch signaling disruption changes the distribution of the ILC precursors and decreases the enrichment in *Hes1*$^+$/*Nfil3*$^+$ ILC precursors by regulating their proliferation. In conclusion, our study reveals the inherent cellular and developmental, context-dependent nature of canonical Notch signaling during fetal ILC commitment and differentiation.

RESULTS

Inactivation of the Notch Signaling Pathway Does Not Affect the Capacity of LTi Cells to Colonize the Lymph Node Anlagen but Alters Their Cytokine Production

We evaluated the in vivo role of Notch in the development of LTi cells in *Il7r*$^{cre/+}$*Rbpj*$^{fl/fl}$ and *Il7r*$^{Cre/+}$*Rbpj*$^{fl/+}$ embryos, where Notch signaling is inactivated in all lymphoid cells. All Lin$^-$ IL-7Rα$^+$ cells were yellow fluorescent protein positive (YFP$^+$), indicating that recombination efficiently occurred in all FL lymphoid precursors (Figure S1A). We also ascertain deletion of *Rbpj* using genomic PCR and detected less than 1% of failed *Rbpj* deletion (Figure S1B). A complete block at the DN1 (CD44$^+$CD25$^-$) stage was observed in the thymus of embryonic day (E)15.5 *Il7r*$^{Cre/+}$ *Rbpj*$^{fl/fl}$ but not in *Rbpj*$^{fl/+}$ embryos (Figure S1C). We analyzed lymphoid subsets of E15.5 fetal spleen (FS) and FmLNs in *Rbpj*-deleted embryos. $\alpha_4\beta_7^+$ progenitors (αLP) and LTi cells, as well as subfractions LTi_0 and LTi_4, were present in similar proportion and numbers after Notch inactivation (Figures 1A–1F). In all *Il7r*$^{Cre/+}$ embryos, the mean fluorescence intensity (MFI) for the IL7Rα was lower than in control *Il7r*$^{+/+}$ embryos (Figure 1C). We quantified their levels of *Il17a*, *Il17f*, and *Il22* transcripts. While *Il17a* and *Il17f* levels were identical, *Il22* mRNA levels were significantly higher in lymph node LTi cells after *Rbpj* deletion (Figure 1G). Moreover, in Notch-deficient mice, Peyer's patches formed in normal numbers (Figure 1H), and all types of peripheral lymph nodes were present, indicating that LTi cells' function as inducer cells is independent of Notch activation.

In peripheral LTi cells (FS and FmLN), *Notch2* is expressed in higher amounts than *Notch1* (Figure S1D). The inactivation of Notch signaling significantly interferes with the *Notch2* levels in lymphoid cells from the FmLNs (Figure S1D). No differences were observed for the frequency and total numbers of peripheral lymphoid progenitors from *Il7r*$^{cre/+}$*Notch2*$^{fl/fl}$ and *Il7r*$^{cre/+}$ *Notch2*$^{fl/+}$ embryos (Figure 1I). The distribution and phenotype of RORγt$^+$ LTi in both FS and FmLNs were also similar, indicating that these progenitors develop and migrate independently of Notch2 (Figures S1E and 1F).

In conclusion, although not required for the development, migration, and the functional property of secondary tissue

Figure 1. Notch Signaling Disruption Does Not Affect Peripheral Colonization of LTi Cells or LTi Function but Alters Cytokine Production

(A and B) Flow cytometry of FS (A) and FmLNs (B) for the presence of Lin$^-$ (Lin: CD3, CD11c, CD19, Ter119, Gr1, NK1.1) IL-7Rα$^+$, α4β7$^+$, and CD4 and CCR6 expression in those cells in Il7r$^{Cre/+}$ Rosa26YFP Rbpj$^{fl/+}$, Rbpj$^{fl/fl}$, or Il7r$^{+/+}$ embryos at E15.5.

(C and D) IL-7Rα MFI (C), percentages, and absolute numbers (D) of the different fractions analyzed in (A) and (B).

(E) Flow cytometry of E15.5 FS and FmLN Lin$^-$ IL-7Rα$^+$ $\alpha_4\beta_7^+$ cells for CD4 and RORγt expression.

(F) Percentages of IL-7Rα$^+$ $\alpha_4\beta_7^+$ RORγt$^+$ CD4$^+$ or CD4$^-$ cells of Lin$^-$ in FS or FmLN from *Il7r*$^{Cre/+}$ *Rosa26*^{YFP} *Rbpj*$^{fl/+}$, *Rbpj*$^{fl/fl}$, or *Il7r*$^{+/+}$ embryos at E15.5.

(G) RT qPCR analysis of *Il17a*, *Il17f*, and *Il22* in sorted Lin$^-$ IL-7Rα$^+$ $\alpha_4\beta_7^+$ cells from *Il7r*$^{Cre/+}$ *Rosa26*^{YFP}, *Rbpj*$^{fl/+}$, or *Rbpj*$^{fl/fl}$ E15.5 FS and FmLN after 3 hr of PMA (phorbol 12-myristate 13-acetate)/ionomycin activation. Results are presented relative to *Gapdh* (a.u.).

(H) Peyer's patch counts in adult Il7r$^{Cre/+}$ Rosa26^{YFP} Rbpj$^{fl/+}$, Rbpj$^{fl/fl}$, Notch2$^{fl/+}$, Notch2$^{fl/fl}$, and control Il7r$^{+/+}$ mice.

(I) Percentages and absolute numbers of E15.5 FS and FmLN Lin$^-$ IL-7Rα$^+$ $\alpha_4\beta_7^-$ CD4$^+$ *Il7r*$^{Cre/+}$ *Rosa26*^{YFP} *Notch2*$^{fl/+}$, *Notch2*$^{fl/fl}$, or control *Il7r*$^{+/+}$ mice.

Data are representative of at least three independent experiments (A, B, C, and E) ($n \geq 4$), three pooled independent experiments (D, F, and I) ($n = 3$), three independent experiments (G), or at least five pooled independent experiments (H) ($n \geq 5$). In (D), (F), and (I), each dot represents a single experiment. Statistical data show mean ± SEM. *$p < 0.05$ (unpaired Student's t test). N.S., not significant.

See also Figure S1.

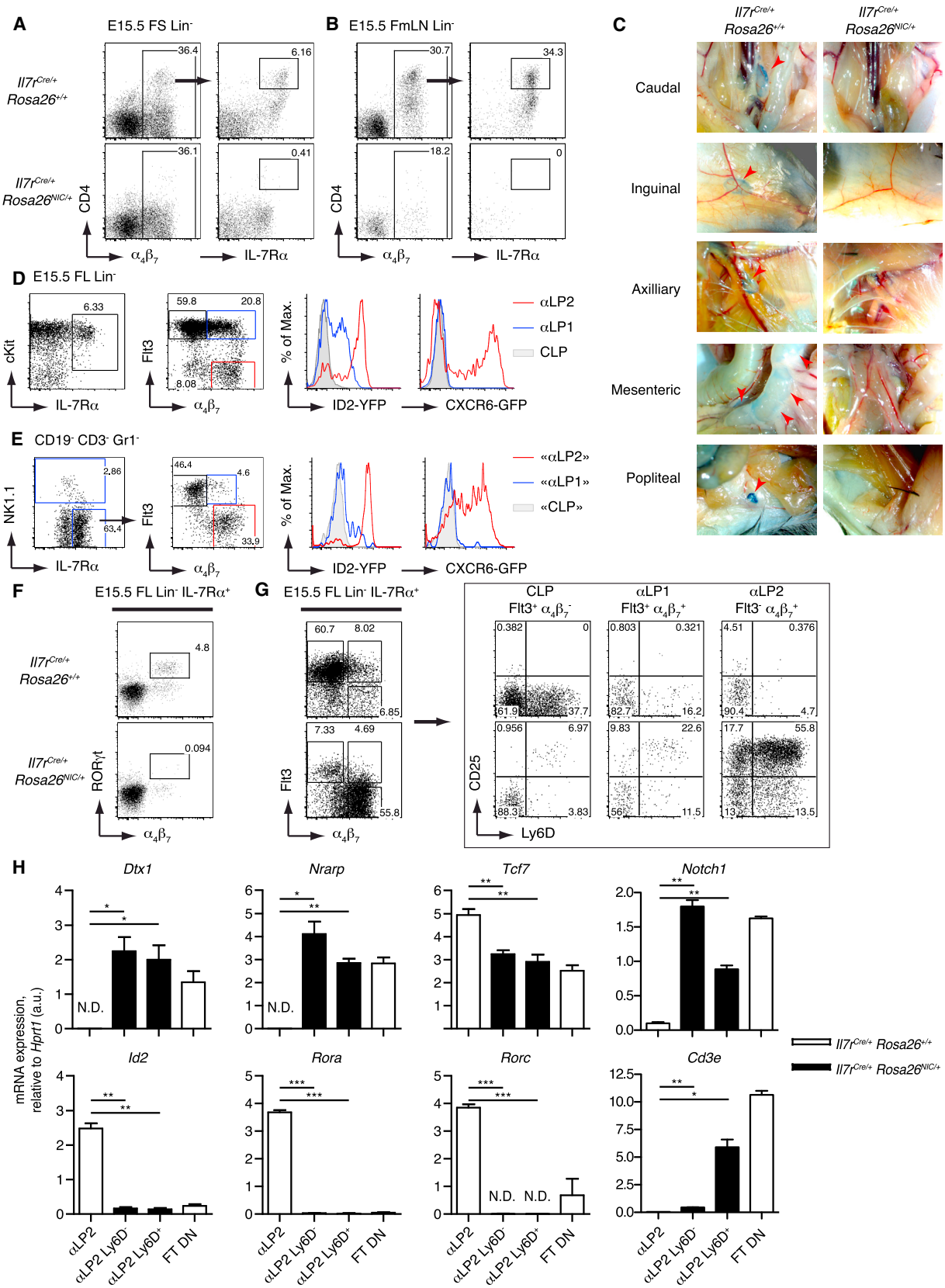

(legend on next page)

inducer, Notch activity only determines the profile of cytokine secretion of LTi cells in the periphery.

Constitutive Expression of the NICD Forces Lymphoid Precursors into T Cell Differentiation

Since Notch signaling is dispensable for the migration and function of LTi cells as secondary lymphoid organ inducers, we questioned whether persistent Notch signaling could modulate their functions and/or differentiation; therefore, we generated *Il7r*$^{Cre/+}$*Rosa26*^{NIC}, where Notch is constitutively active in lymphoid cells. In peripheral FS and FmLNs, RORγt$^+$ cells were undetectable (Figures 2A and 2B), and no lymph node were found in adult *Il7r*$^{Cre/+}$*Rosa26*^{NIC} mice (Figure 2C).

Analysis of the E15.5 *Id2*$^{yfp/+}$*Cxcr6*$^{gfp/+}$ FL compartment shows that CLPs (Flt3$^+\alpha_4\beta_7^-$) do not express YFP or GFP, whereas αLP, either Flt3$^+$ (named αLP1) or Flt3$^-$ (named αLP2), express different levels of ID2 (Figure 2D). αLP1 expressed intermediate levels of ID2, suggesting that the upregulation of ID2 begins within this subset. After short-term cultures, CLPs are able to give rise to both αLP1 and αLP2 fractions (Figure 2E). ID2 expression is detected in few αLP1 cells and in most αLP2 cells. Also, αLP2 expressed high levels of YFP contrary to the αLP1 fraction. In conclusion, αLP1 is a transitional stage between CLP and αLP2 with few ID2^{lo} progenitors. ID2^{hi} cells are highly represented in αLP2 (84.6%).

In embryos with constitutive Notch signaling activation, no $\alpha_4\beta_7^+$RORγt$^+$ cells could be detected in the FL (Figure 2F). Cells harboring a CLP phenotype were decreased, whereas those presenting an αLP2 phenotype were increased (Figure 2G). However, the αLP2 subset in *Il7r*$^{Cre/+}$*Rosa26*^{NIC} FL now comprises a majority of CD25$^+$Ly6D$^+$ cells not present in the control (Figure 2G), but resembling DN2-DN3 CD25$^+$Ly6D$^+$ from normal E15.5 thymocytes (data not shown). To determine whether the *Il7r*$^{Cre/+}$*Rosa26*^{NIC} αLP2 cells are composed of ID2$^+$ ILC progenitors or T cell progenitors, we quantified the expression of transcripts mutually exclusive to T cell progenitors (*Cd3e*, *Notch1*, *Dtx1*, *Nrarp*) or ILC progenitors (*Id2*, *Rora*, and *Rorc*) (Figure 2H). *Tcf7* is a possible target of the Notch pathway and is expressed by both T and ILC progenitors. The FL αLP2 fraction expressed undetectable levels of T cell-related gene mRNA in controls. However, both Ly6D$^-$ and Ly6D$^+$ αLP2 from *Il7r*$^{Cre/+}$*Rosa26*^{NIC} FL expressed these T cell progenitor transcripts but failed to express ILC transcripts (Figure 2H). We concluded that the constitutive activation of the Notch pathway committed all CLPs toward the T cell pathway.

Inactivation of the Notch Signaling Pathway Does Not Alter the Phenotype, Distribution, or Differentiation Capacities of FL Lymphoid Progenitors

We analyzed the development of lymphoid progenitors in FL from embryos with an inactive or functional canonical Notch pathway. In all embryos, lymphoid progenitors displayed a similar pattern of c-Kit, Sca1, Flt3, and $\alpha_4\beta_7$ expression (Figure 3A). The IL7Ra levels were similarly lower in all FL compartments that have only one IL7Ra allele (*Il7r*$^{Cre/+}$), compared to wild-type (WT) control (Figure 3B). However, concerning the αLP2 subset, the distribution of IL7Rα^{hi} cells may be different after notch disruption (Figure 3B). Numbers of lymphoid progenitors were consistently lower in mice with only one allele of the IL-7Rα (*Il7r*$^{Cre/+}$), although the percentages of Lin$^-$IL-7Rα$^+$ cells are similar and the representation of the different subsets within IL-7Rα$^+$ cells is unchanged. RORγt$^+$ cells represented a comparable subset of αLP2 in all genotypes (Figure 3A), and no statistical difference was detected in percentages and numbers of CLP, αLP1, αLP2, and LTip isolated from *Il7r*$^{Cre/+}$*Rbpj*$^{fl/fl}$ or littermate controls (*Il7r*$^{Cre/+}$*Rbpj*$^{fl/+}$) (Figure 3C).

We sorted the different precursor subsets (Figure S2A) and show that the level of *Notch1* transcripts decreases as differentiation into ILCs progresses from the CLP stage to the αLP2 stage, whereas *Notch2* transcripts reach maximal levels in αLP2 cells (Figure S2B). Because *Notch2*, but not *Notch1*, is highly expressed in ILC progenitors, and as non-canonical Notch signaling might operate in the absence of RBP-Jκ, we analyzed ILC development after *Notch2* deletion in lymphoid progenitors. Neither the phenotype, percentage, and numbers of FL lymphoid precursors (Figures S2C and S2D) nor T cell development (Figure S2E) were affected by the *Notch2* deletion.

Short-term cultures were performed to analyze the capacity of lymphoid progenitors to upregulate $\alpha_4\beta_7$ in the absence or presence of Notch signaling (Figure 3D). After 48 hr on OP9 stroma, around 35% of cultured CLPs expressed $\alpha_4\beta_7$ regardless of the genotypes. Upregulation of $\alpha_4\beta_7$ was also observed on OP9-DL4 for all genotypes (Figure 3E). Consistent with Notch deficiency, we observed the development of CD19$^+$ B cells on

Figure 2. Overexpression of the Notch Pathway Is Not Blocking the ILC Precursors at an Early Stage but Rather Instructs Strong T Cell Differentiation from Earliest Stages of the CLP

(A and B) Flow cytometry of E15.5 FS (A) and FmLN (B) for the presence of Lin$^-$IL-7Rα$^+\alpha_4\beta_7^+$CD4$^+$ cells in E15.5 *Il7r*$^{Cre/+}$*Rosa26*$^{+/+}$ or *Il7r*$^{Cre/+}$ *Rosa26*$^{NIC/+}$ embryos.

(C) Pictures of lymph nodes in adult *Il7r*$^{Cre/+}$*Rosa26*$^{+/+}$ or *Il7r*$^{Cre/+}$*Rosa26*$^{NIC/+}$ mice (6 to 10 weeks old), injected with China ink 2 hr prior to analysis.

(D) Flow cytometry of FL cells from *Id2*$^{YFP/+}$*Cxcr6*$^{GFP/+}$ E15.5 embryos. Lin$^-$IL-7Rα$^+$ is fractionated according to Flt3 and $\alpha_4\beta_7$ expression, and expression of ID2-YFP or CXCR6-GFP is assessed in CLP (filled gray, Flt3$^+\alpha_4\beta_7^-$), αLP1 (blue, Flt3$^+\alpha_4\beta_7^+$), and αLP2 (red, Flt3$^-\alpha_4\beta_7^+$) compartments.

(E) Short-term culture of 10,000 CLPs from E15.5 *Cxcr6*$^{GFP/+}$*Id2*$^{YFP/+}$ FL on OP9 cells for 3 days, with IL-7, cKitL, and Flt3L. Histogram shows ID2-YFP and CXCR6-GFP expression levels from in-vitro-generated CLP (filled gray), αLP1 (blue), or αLP2 (red) cells.

(F) Flow cytometry of E15.5 FL cells from *Il7r*$^{Cre/+}$*Rosa26*$^{+/+}$ or *Rosa26*$^{NIC/+}$ for LTip (Lin$^-$IL-7Rα$^+$RORγt$^+\alpha_4\beta_7^+$).

(G) Flow cytometry of E15.5 FL cells from *Il7r*$^{Cre/+}$*Rosa26*$^{+/+}$ or *Rosa26*$^{NIC/+}$. Each compartment, as defined in (D), is respectively analyzed for CD25 and Ly6D expression.

(H) RT qPCR analysis of various transcripts in αLP2 Ly6D$^-$ or αLP2 Ly6D$^+$ in *Il7r*$^{Cre/+}$*Rosa26*$^{NIC/+}$ (black) or αLP2 in *Il7r*$^{Cre/+}$*Rosa26*$^{+/+}$ (white) E15.5 FL, presented relative to *Hprt* (a.u.). Cells from *Il7r*$^{Cre/+}$*Rosa26*$^{+/+}$ E15.5 fetal thymus (FT DN) sorted as CD3$^-$CD4$^-$CD8$^-$CD44$^{hi}\alpha_4\beta_7^+$ were used as controls.

Data are representative of at least three independent experiments—(F), (G), and (H) from single FL each and (A), (B), and (D) from pooled organs—or three independent experiments (C) ($n \geq 3$ for each group), or three independent experiments with at least two wells per experiment (E). Statistical data show mean ± SEM. *$p < 0.05$; **$p < 0.01$; ***$p < 0.001$ (unpaired Student's t test). N.D., not detected.

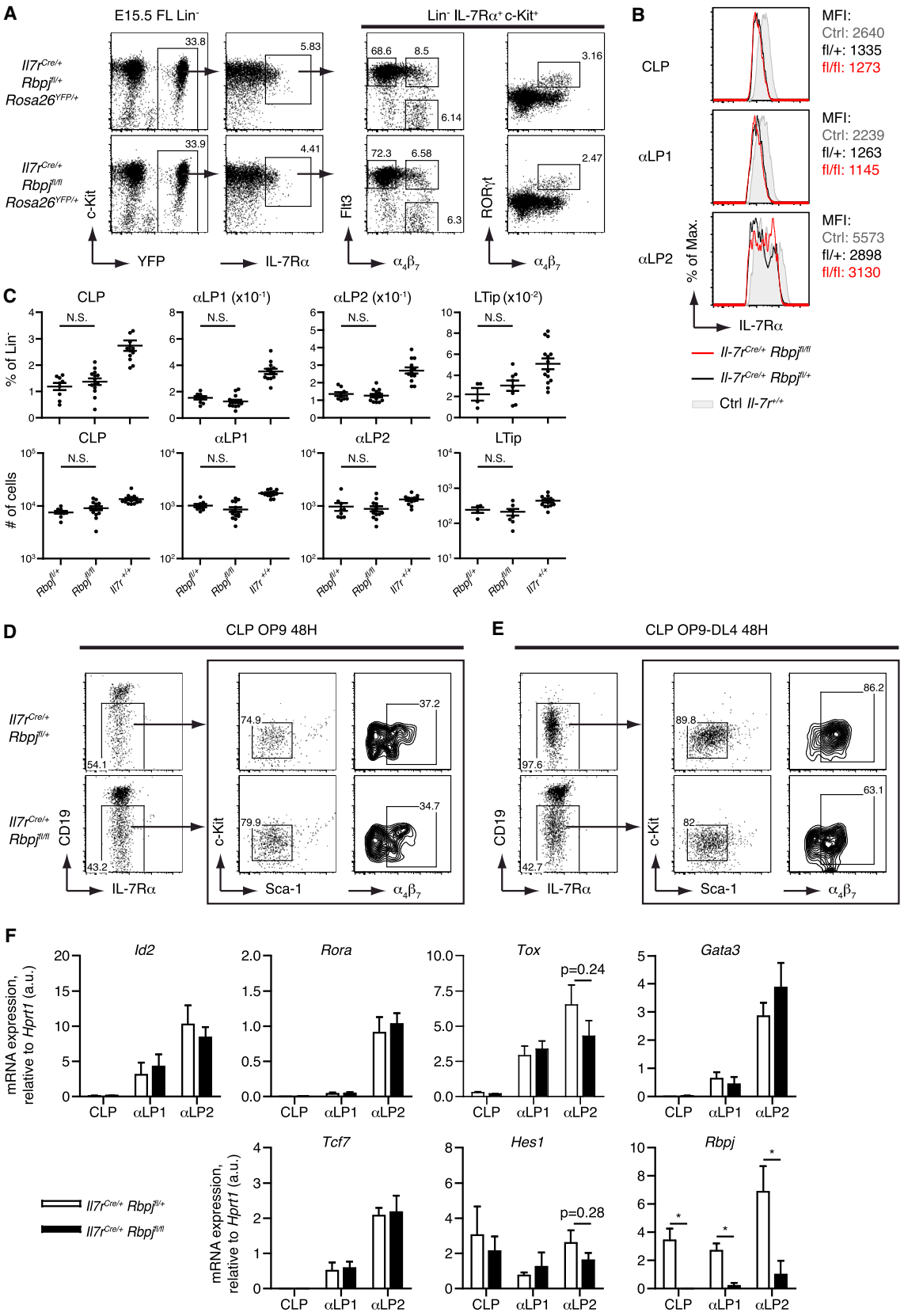

(legend on next page)

OP9-DL4 from CLPs isolated from *Il7r*$^{Cre/+}$*Rbpj*$^{fl/fl}$ embryos (Figure 3E). However, fewer progenitors have progressed to the $\alpha_4\beta_7^+$ stage in Notch-defective embryos.

The differentiation potential of αLP1 and αLP2 from Notch-deficient or Notch-competent embryos was tested after 8 days of culture. As expected, T cell differentiation potential was lost in Notch-deficient αLP1 cells, but not in their littermate controls, and the NK cell progeny increased proportionally to the loss of *Rbpj* alleles (Figure S2F). In αLP1 cells from *Il7r*$^{Cre/+}$*Rbpj*$^{fl/fl}$, $\alpha_4\beta_7$ expression was sustained, and similar proportions of RORγt$^+$ cells were obtained (Figures S2F and S2G). Because the αLP2 fraction already contains RORγt$^+$ cells, only the detection of NK cells was considered as differentiation.

Fetal lymphoid precursors and peripheral LTi cells express Notch receptors, and the ligand Delta1 was found in FL (Cherrier et al., 2012), suggesting a probable Notch activation of these cells. However, the Notch pathway abrogation did not impact on FL lymphoid progenitor numbers or phenotype. Hence, we examined whether Notch was activated by quantifying the mRNA expression of its key target genes (*Tcf7*, *Hes1*, *Gata3*, *Dtx1*, and *Nrarp*) and ILC transcripts (*Id2*, *Rora*, *Tox*) in E15.5 FL of *Il7r*$^{Cre/+}$*Rbpj*$^{fl/+}$ and *Rbpj*$^{fl/fl}$ embryos (Figure 3F). *Dtx1* and *Nrarp* were not expressed (data not shown). Except for *Rora* (only found in αLP2) and *Hes1* (also expressed in CLPs), the expression of most transcription factors analyzed begins at the αLP1 stage (Figure 3F). No statistical difference was detected in the expression levels of *Id2*, *Tcf7*, *Gata3* and *Rora* after the inactivation of the Notch pathway. We noticed a tendency for *Hes1* and *Tox* mRNA levels to decrease after disruption of the Notch pathway (Figure 3F).

In conclusion, the inactivation of the Notch pathway did not alter the capacity of FL lymphoid precursors to differentiate into ILCs. The Notch signaling pathway appears to be dispensable to generate and maintain the phenotype and distribution of FL lymphoid progenitors, including RORγt$^+$ LTip. However, it is probably implicated during the differentiation of specific ILC subsets, since some ILC-specific transcription factors tend to be decreased after Notch disruption. Hence, frequency and heterogeneity of αLP2 subsets may vary after disruption of the Notch pathway.

αLP2 Cells Have Heterogeneous Transcriptional Profiles at the Single-Cell Level

The heterogeneity of ILC progenitors drove us to develop a single-cell transcriptional analysis assay using the Biomark HD system to assess the effect of Notch signaling. The linearity, specificity, and efficiency of primers have been thoroughly tested (Figures S3A–S3E; Tables S1 and S2). We sorted single αLP1 and αLP2 cells from both Notch-competent and -deficient FL and analyzed the expression of 81 genes. Among the sorted single cells, only cells that expressed the three housekeeping genes (*Actb, Gapdh*, and *Hprt*) and more than 10% of the 81 selected genes were considered (Figure S4A). Analysis of single-cell transcriptional expression allowed the identification of common signatures and key gene signatures that distinguish αLP1 from αLP2 cells. αLP1 and αLP2 share expression of ILC transcription factors such as *Tox*, *Ets1*, *Id2*, and *Nfil3* and the absence of expression of specific B cell genes (*Pax5* or *Ebf1*) (Figure S4B). αLP1 cells are enriched in cells expressing *Notch1*, *Rag2*, and *Bcl11a*, which are characteristics of T cell progenitors. On the other hand, αLP2 cells mostly express *Zbtb16*, *Rora*, *Tcf7*, and *Il2rb* but have no expression of *Rag2* and *Bcl11a* (Figure S4C).

We have focused on the αLP2 subset analysis to avoid any T cell progenitor contaminant. After hierarchical clustering, we could define four clusters, based on the expression pattern of 43 discriminative genes regardless of the Notch deficiency. Using the Notch-competent condition as a control, we identified four groups of genes that could define specific transcriptional signatures (Figure 4A).

All clusters shared a core αLP2 gene signature composed of the expression of *Itga4*, *Ets1*, *Notch2*, *Rora*, *Foxo1*, *Hif1a*, *Nfatc1*, and *Zbtb16* (Figure 4B). Cluster I (αLP2 I) is substantially different from other clusters, as it has a halved *Id2*-expressing cell frequency, with lower expression levels of *Id2* by the few expressing cells (Figure S4D) and neither *Tox* nor *Tcf7* expression, which are key transcription factors required for ILC development. In contrast, almost all cells in clusters II, III, and IV expressed those genes, along with *Ahr, Il2rb*, and *Tnfrsf1a*. Furthermore, cluster I displays a unique gene signature distinct from that of ILCs (Figure 4C).

Further discrimination of cluster II from clusters III and IV is based on the expression of *Cxcr6* and *Il18r1* (Figure 4D). Key molecules for LTi cell function, such as *Lta*, *Ltb*, and *Cxcr5*, are also highly enriched in clusters III and IV. In contrast, cluster II is mostly characterized by the expression of transcription factors *Gata3*, *Nfil3*, and *Bcl11b*, suggesting enrichment in the ILC2 progenitor transcriptional profile. Interestingly, *Hes1*, a target of Notch signaling, was found at high frequency in cluster II, suggesting a possible Notch activity in this subset.

Finally, cluster III is enriched in cells expressing key NK genes such as transcription factors *Tbx21*, *Eomes*, *Irf1*, and *Irf8*, whereas cells expressing *Rorc*, *Bcl2*, and *Il1r1*, key features of LTi or LTip cells, constitute cluster IV (Figure 4E).

Figure 3. ILC3 FL Progenitors Are Maintained after In Vivo Disruption of the Notch Pathway

(A) Flow cytometry of E15.5 FL cells from *Il7r*$^{Cre/+}$ *Rosa26*^{YFP}, *Rbpj*$^{fl/+}$, or *Rbpj*$^{fl/fl}$ mice for the presence of CLP, αLP1, αLP2, and LTip cells.

(B and C) IL-7Rα MFI (B) and percentages and absolute numbers (C) of the different fractions analyzed in (A).

(D and E) Differentiation potential of E15.5 FL-derived CLP from *Il7r*$^{Cre/+}$ *Rosa26*^{YFP} *Rbpj*$^{fl/+}$ or *Rbpj*$^{fl/fl}$ mice cultured for 48 hr on OP9 (D) or OP9-DL4 (E) with Kit-L, Flt3-L, IL-2, and IL-7 (50 cells per well).

(F) RT qPCR analysis of various transcripts in CLP, αLP1, or αLP2 cells from *Il7r*$^{Cre/+}$ *Rosa26*^{YFP} *Rbpj*$^{fl/+}$ (white bars) or *Rbpj*$^{fl/fl}$ (black bars) E15.5 FL, presented relative to *Hprt* (a.u.).

Data are representative of at least four independent experiments (A–C; from single FL each, n ≥ 4), or at least six wells from two independent experiments (D and E), or from three pooled independent experiments (F). In (C), each dot represents a single FL. Statistical data show mean ± SEM. *p < 0.05 (unpaired Student's t test). Statistical data show mean ± SEM. *p < 0.05 (unpaired Student's t test). N.S., not significant.

See also Figure S2.

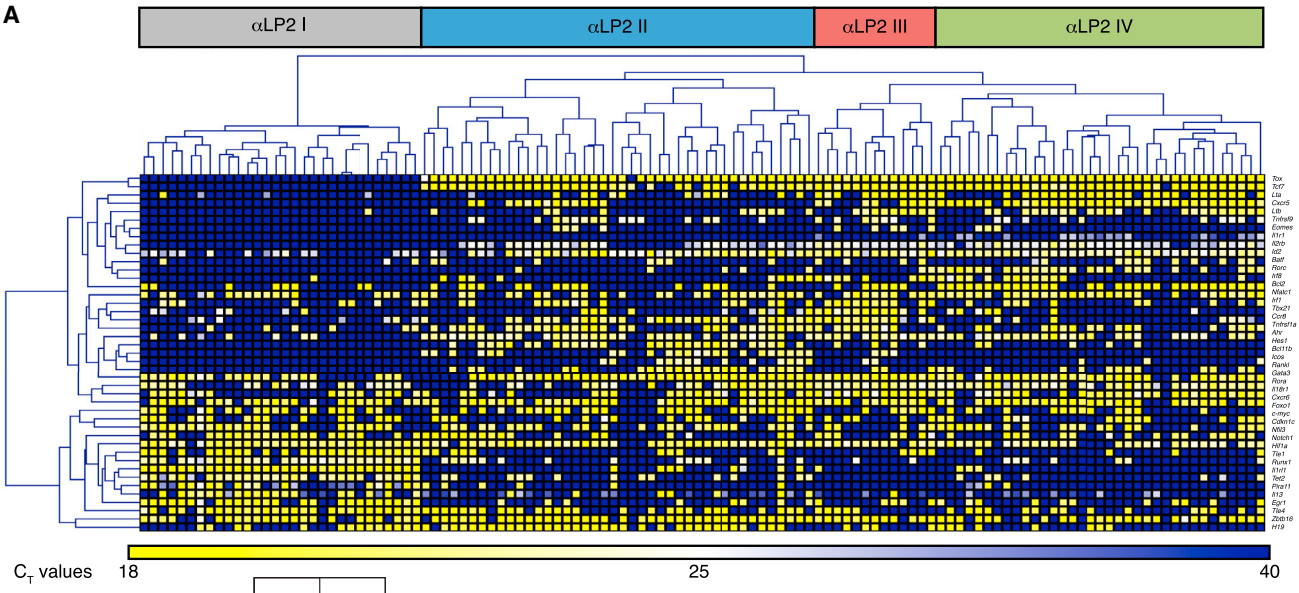

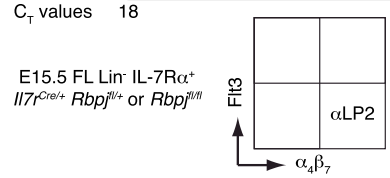

B Common αLP2 signature

	I	II	III	IV
Hif1a	100	93	100	79
Ets1	100	96	100	100
Foxo1	91	82	83	90
Notch2	91	93	100	100
Zbtb16	82	96	100	74
Rora	73	96	100	84
Itga4	73	96	100	100
Nfatc1	64	63	67	84
Bcl11a	0	3,7	0	0
Il23r	0	0	0	5,3
Cxcl2	0	7,4	0	5,3
Tnfrsf1b	0	0	0	0

C ILCp (II.III.IV) signature

	I	II	III	IV
Id2	46	93	100	100
Tox	0	100	100	100
Tcf7	0	82	100	100
Ahr	18	82	100	84
Il2rb	0	74	100	90
Tnfrsf1a	18	67	67	47
Batf	0	19	17	21
Pira11	64	11	0	16
Tle1	73	22	17	5.3
Egr1	73	22	17	26
Il13	73	44	17	42
Runx1	91	33	0	26
Tet2	91	33	0	21
Il1rl1	100	22	0	5.3
Notch1	91	37	50	42
Tle4	91	59	50	37

D ILC2p (II) vs III.IV signature

	I	II	III	IV
Il18r1	55	56	100	90
Cxcr6	27	52	100	79
Lta	9.1	33	83	68
Cxcr5	0	37	67	95
Ltb	0	22	50	63
Icos	0	26	33	5.3
Bcl11b	0	52	17	0
Gata3	0	56	33	32
Hes1	0	78	33	16
Ccr8	0	74	100	16
H19	27	93	67	11
c-myc	55	70	33	53
Nfil3	73	74	50	47

E NKp (III) vs LTip (IV) signature

	I	II	III	IV
Bcl2	36	41	50	84
Rorc	0	15	17	74
Il1r1	0	0	0	47
Eomes	0	7.4	50	11
Tnfrsf9	0	37	67	32
Cdkn1c	36	30	50	26
Irf8	9.1	15	83	42
Tbx21	18	22	83	16
Irf1	27	41	100	37

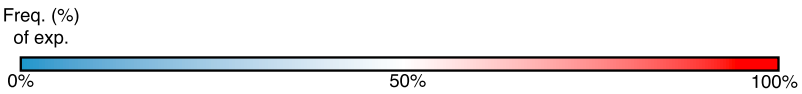

Figure 4. Single-Cell Transcriptional Analysis of FL αLP2

(A) RT qPCR analysis of single αLP2 from *Il7r*$^{Cre/+}$*Rbpj*$^{fl/+}$ or *Rbpj*$^{fl/fl}$ E15.5–E17.5 FL using the Biomark HD system. Each column represents a single cell, and each line represents a gene. Single cells are clustered, and four clusters are identified: αLP2 I (gray), αLP2 II (blue), αLP2 III (red), and αLP2 IV (green). Gradient represents the C_T value for each gene and each single cell (yellow = high expression, white = low expression, and dark blue = no expression; C_T > 40).

(legend continued on next page)

E15.5 FL lymphoid progenitors were tested for the presence of GATA3, T-bet, EOMES, and RORγt. Only GATA3$^+$ and RORγt$^+$ cells were detected in the αLP2 fraction (Figure S5A). Hence, the expression of both *Tbx21* and *Eomes* mRNA show that specific mature ILC genes already have an accessible chromatin at the precursor stage. GATA3 is known to be necessary for the development of ILC3 and then could be considered as an ILC progenitor transcription factor (Serafini et al., 2014). Clonal cultures on OP9 stromal cells of αLP2 RORγt$^+$ cells demonstrate that some RORγt-expressing cells could still be considered as ILC progenitors. Indeed, RORγt^{lo}IL-7Rα$^+$ cells retain the capacity to give rise to both NK (NK1.1$^+$) and ILC2 (ICOS^{hi}α$_4$β$_7{}^-$CD25$^+$RORγt$^-$) cells, contrary to RORγt^{hi}IL-7Rα$^+$ cells (Figures S5B–S5D). Moreover, frequencies of the progeny obtained from the clonal assay suggest that αLP2 RORγt^{lo} progenitors represent a heterogeneous compartment (Figure S5D). Hence, despite the expression of specific mature ILC transcripts, the FL αLP2 fraction is still heterogeneously composed of ILC progenitors.

In conclusion, we identified four subsets within the αLP2 fraction, each enriched in a specific ILC progenitor type. The clustering and the gene signatures suggest that the "αLP2 I" is enriched in *Id2*$^-$ cells, representing a population of non-T/B progenitors. The "αLP2 II" represents ILC precursors with an enrichment in ILC2 fate, whereas "αLP2 III" is mainly constituted of NK progenitor cells, and the "αLP2 IV" mainly consists of LTi progenitors.

Heterogeneity of αLP2 Cells Reveals Different Priming toward ILC Lineages

To discriminate αLP2 subsets as defined previously, Thy1.2 and IL-18R1 expression were analyzed jointly with CXCR6 and ID2 expression due to *Id2*$^{yfp/+}$ *Cxcr6*$^{gfp/+}$ embryos.

The heterogeneous levels of ID2 in the αLP2 compartment (Figure 2D) are in agreement with the single-cell assay showing diverse transcriptional levels of *Id2* gene expression (Figure 4C; Figure S4). All ID2$^-$ αLP2 cells are Thy1.2$^-$IL-18R1^{lo} (Figure 5A). ID2$^+$CXCR6$^-$ αLP2 cells are IL-18R1$^-$ and could be subdivided into Thy1.2$^-$ and Thy1.2$^+$. CXCR6$^+$ cells that are all ID2$^+$ also express IL-18R1 and Thy1.2 (Figure 5A). Hence, the combination of Thy1.2 and IL-18R1 enables the ex vivo subdivision of αLP2 subsets in embryos that are not tagged for ID2 or CXCR6 (Figure 5B). As observed in Figure 5C, the αLP2 II subset concerns Id2$^+$CXCR6$^-$ cells that could be isolated as IL-18R1$^-$ cells. The Id2$^+$CXCR6$^-$ subset is further separated into two main fractions depending on the expression of Thy1.2 (Figure 5B, Thy1.2$^+$IL-18R1$^-$ in blue and Thy1.2$^-$IL-18R1$^-$ in violet). Id2$^+$CXCR6$^+$ cells could be isolated as Thy1.2$^+$IL-18R1$^+$ cells and correspond to the αLP2 fractions III + IV. Finally, the Thy1.2$^-$IL-18R1$^+$ cells correspond to the αLP2 I cells.

We assessed the clonal in vitro potential of the CLP, αLP1, and αLP2 fractions (Figure 5C). After 8 days of culture on OP9-DL4, progeny cells were identified as either T progenitors (Lin$^-$ID2$^-$CD25$^+$) or ILCs (Lin$^-$ID2$^+$) that could be divided into NK1.1$^+$ ILC1, ICOS^{hi}α$_4$β$_7{}^-$ ILC2, or ICOS^{lo}α$_4$β$_7{}^{hi}$CXCR6^{hi} ILC3 (Figure 5D). αLP2 I barely gave rise to any cells in culture conditions promoting lymphoid development. CLP and αLP1 subsets have a clonal efficiency of 40%, whereas αLP2 II Thy1.2$^-$ or Thy1.2$^+$, III and IV have a clonal efficiency of 50% (Figure 5E). As suspected by the absence of Id2 gene expression and a specific gene signature, αLP2 I cells do not comprise ILC precursors.

CLPs mainly gave rise to T cells, with less than 5% of the progenitors that developed into ILCs alone. The αLP1 compartment retains T cell potential and could give rise to all ILC subsets, confirming our assumption from the transcriptome analysis that early ILC progenitors are represented in this fraction (Figure S3). All ILCs could be detected within single clones at very low frequencies (less than 7%, with or without T cells; Figure 5F). By using the sorting index, we observed that, among the αLP1 subset, ILC precursors are ID2^{med}α$_4$β$_7{}^{hi}$, whereas T progenitors are ID2$^-$α$_4$β$_7{}^+$ (data not shown). The αLP2 compartments, as previously reported, had no T cell potential (Possot et al., 2011). Interestingly, the subpopulations have distinctive ILC differentiation potentials (Figure 5G). No cell producing all ILC lineages could be detected at this frequency. Interestingly, each subpopulation preferentially gives rise to one ILC group. αLP2 II Thy1.2$^-$ cells mainly generate ILC1, as well as a fair proportion of ILC3. αLP2 II Thy1.2$^+$ cells preferentially give rise to ILC2. Finally, αLP2 III/IV cells are enriched in RORγt$^+$ cells and then are biased toward ILC3, but they may also differentiate into ILC1.

In conclusion, we report that the αLP1 compartment, which contains a frequent tripotent ILC lineage precursor, is upstream of the αLP2 compartment. This latter can be subdivided in three subsets according to the surface expression of IL-18R1 and Thy1.2, and these subsets are differentially primed for differentiation toward each ILC lineage.

Notch Deficiency Differentially Affects αLP2 Subsets

We included and compared the Notch-deficient cells to our single-cell analysis to assess the extent of Notch activity in these compartments. Principal-component analysis (PCA) shows that within each cluster, Notch-competent and Notch-deficient cells are overlapping, suggesting that the major key gene signatures could still be found in the absence of Notch (Figures 6A and 6B). We first studied the frequency of *Id2*$^+$ over *Id2*$^-$ progenitors in both genotypes and noticed that *Id2*$^-$ progenitors showed a 2-fold increase in αLP1 and αLP2 after disruption of the Notch pathway (Figures S6A and S6B). Moreover, there was a clear effect of Notch disruption on the αLP2 II subset that decreased from 43% to 26% within the αLP2 compartment. In contrast, αLP2 I was increased (from 17% to 34%), whereas percentages of NKp and LTip (αLP2 III and IV) remained unaffected (Figure 6C).

We further analyzed the expression pattern of αLP2 II to identify which genes are significantly affected by the deletion of Notch signaling in the remaining cells (Figures 6D and 6E). *Hes1* is a well-known target of the Notch signaling. As expected,

(B–E) Gene signatures of different clusters of *Il7r*$^{Cre/+}$*Rbpj*$^{fl/+}$ αLP2, presented as frequency of expression (red = high frequency; blue = low frequency). For (B), genes that were either expressed in the majority or minority of cells and that did not yield in discriminative profile were included.
Data are from two pooled experiments (n = 61 for *Il7r*$^{Cre/+}$*Rbpj*$^{fl/+}$ αLP2, and n = 55 for *Il7r*$^{Cre/+}$*Rbpj*$^{fl/fl}$ αLP2).
See also Figures S3 and S4.

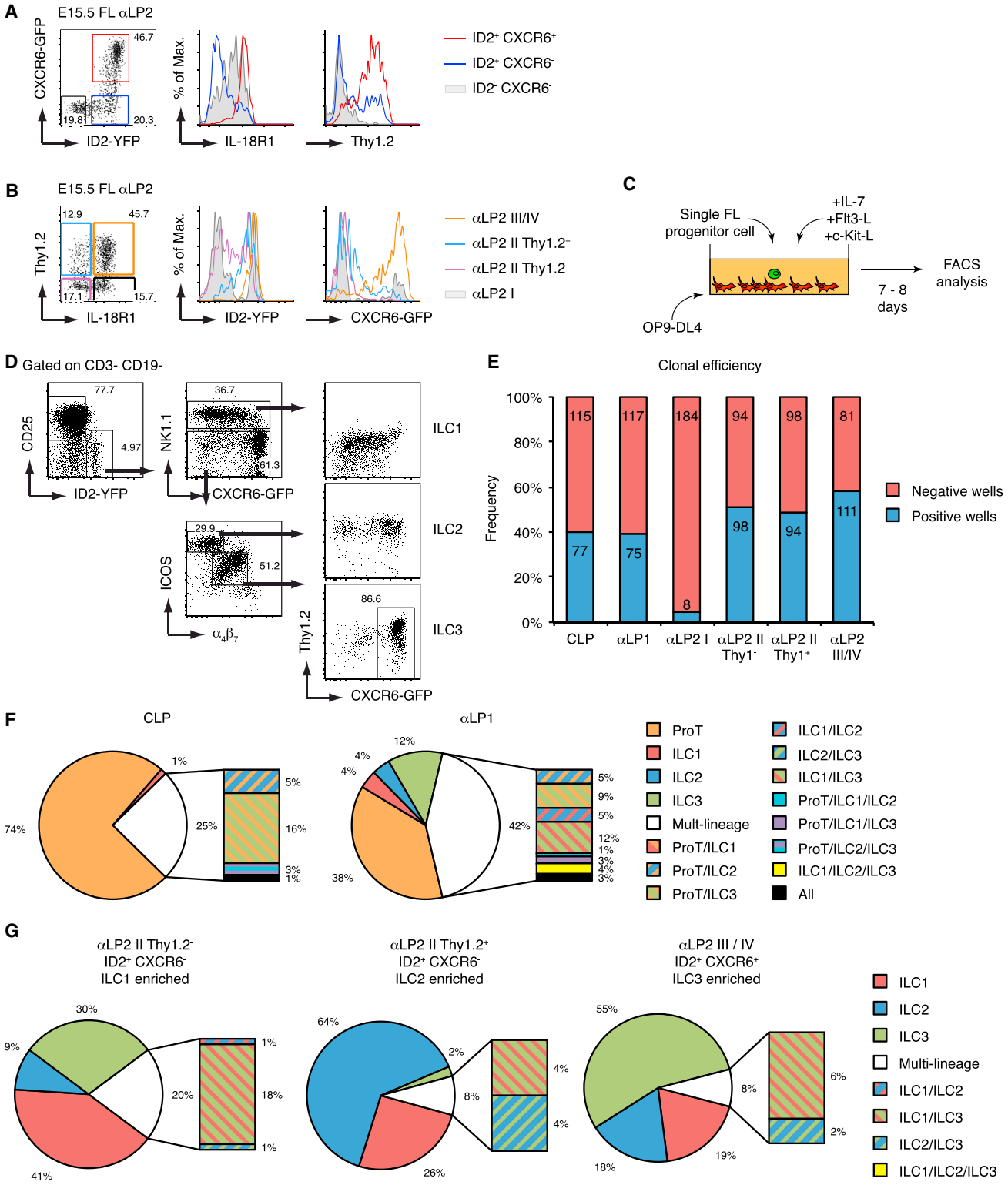

Figure 5. Heterogeneity of αLP2 Subsets Reveals Differential Priming toward ILC Lineages

(A) Flow cytometry of FL cells from *Id2*$^{yfp/+}$*Cxcr6*$^{gfp/+}$ E15.5 embryos. Subdivision of αLP2 according to ID2 and CXCR6 expression, and expression pattern of IL-18R1 and Thy1.2 in ID2^{-}CXCR6^{-} (filled gray), ID2^{+}CXCR6^{-} (blue), or ID2^{+}CXCR6^{+} (red) αLP2.

(B) Subdivision of αLP2 according to IL-18R1 and Thy1.2 expression, and expression pattern of ID2 and CXCR6 in αLP2 I (IL-18R1^{+}Thy1.2^{-}, filled gray), αLP2 II Thy1.2^{-} (IL-18R1^{-}Thy1.2^{-}, violet), αLP2 II Thy1.2^{+} (IL-18R1^{-}Thy1.2^{+}, blue), and αLP2 III/IV (IL-18R1^{+}Thy1.2^{+}, orange).

(legend continued on next page)

the frequency of *Hes1*-expressing cells is reduced from 78% to 47% in the cluster II after disruption of Notch signaling. In the αLP2 compartment, this frequency is decreased from 34% to 12%. Interestingly, *Nfil3* represents the transcription factor most sensitive to the Notch signaling disruption, with a decrease of *Nfil3*$^+$ cells from 74% to 33% of the αLP2 II subset. Milder decreases of gene expression frequencies are also observed for *c-myc*, *Egr1*, and *Cdkn1c*, which are all implicated in cell proliferation; *H19*, which is an oncofetal gene for a non-coding RNA; and *Rora*, which is a key factor of the αLP2 population.

The analysis of the combined expression of key transcription factors (*Rora*, *Gata3*, *Nfil3*, *Hes1*, and *Bcl11b*) uncovers the loss of all cells expressing this set of genes after disruption of the Notch signaling. The few *Tbx21*- or *Rorc*-expressing cells that remain in this subset did not present the same combinatorial diversity as those found in Notch-competent FL (Figure 6E). In conclusion, Notch signaling is active in subset II of the αLP2 compartment.

We analyzed the αLP2 compartments of Notch-competent and -deficient E15.5 FL (Figures 6F and 6G). As expected, no difference was observed in either αLP2 III/IV or αLP2 Thy1.2$^-$ populations after Notch signaling disruption, and the αLP2 I population was increased. In contrast, αLP2 II Thy1.2$^+$ was reduced by one third, confirming that the αLP2 subset is also Notch sensitive ex vivo.

Notch Signaling Acts on the Proliferation, but Not on the Differentiation, of the αLP2 II Thy1.2$^+$ Subset

Finally, we assessed whether Notch signaling could play a role in directing cells toward a given lineage. First, we cultured αLP1 (as control) and αLP2 fractions in short-term cultures with or without Notch inhibitor DAPT and analyzed the progeny, and then we measured their proliferation index (Figures 7A–7C). After 40 hr of culture, proliferation of αLP2 II Thy1.2$^-$ and the αLP2 III/IV subset was not significantly affected. The αLP1 subset gave rise to more ILC precursors in the presence of DAPT, since the development toward the T cell pathway is inhibited (Figure 7C). Only the αLP2 II Thy1.2$^+$ subset was affected by DAPT treatment, resulting in significantly less proliferation (Figure 7C).

We assessed whether Notch disruption would also affect the differentiation potential of each subset of αLP2 by clonal assays as previously described in Figure 5D. As expected, Notch-deficient αLP1 could not give rise to T cells (Figure S7A). αLP2 subsets have similar differentiation potential toward ILC1, ILC2, or ILC3, regardless of Notch signaling (Figure S7B). The differences of output frequencies for αLP2 cultures between WT (*Id2*$^{yfp/+}$ *Cxcr6*$^{gfp/+}$) and *Rbpj* transgenic embryos result from a distinct enrichment in Id2$^+$/CXCR6$^+$ cells among αLP2 fractions (Figure 5B). Indeed, since the αLP2II Thy1.2$^+$ subset still contains few CXCR6$^+$ progenitors in *Rbpj*$^{f/f}$ or *Rbpj*$^{f/+}$, they produce seven times more ILC3 than their WT counterparts devoid of CXCR6$^+$ cells, thanks to the GFP labeling (Figures 5D and S7B). We then compared the clonal efficiencies of αLP1 and αLP2 subsets between Notch-competent and -deficient progenitors. With the exception of the αLP2 II Thy1.2$^+$ subset that was reduced, no difference in the clonal efficiencies was observed for most αLP2 subsets (Figure 7D). Altogether, these results show that the proliferative capacity of the αLP2 II Thy1.2$^+$ compartment is modulated by Notch signaling.

DISCUSSION

By combining clonal in vitro cultures and single-cell gene expression analyses, we determined the pathway of differentiation from the CLP to the different ILC subsets. The combined use of Flt3 and α4β7 already defined CLP, αLP1, and αLP2 (Possot et al., 2011). Here, using ID2/CXCR6 reporter mice, we show that αLP1, while retaining T potential, comprises an all-ILC progenitor at a higher frequency than αLP2, mainly constituted of primed ILC precursors. Supporting this, aLP1 cells express mild levels of ID2. We propose that the GILP is phenotypically defined as Flt3$^+$ ID2^{med}*Tox*$^+$ CXCR6$^-$ in addition to the previous definition of $\alpha_4\beta_7$- and *Nfil3*-expressing cells (Xu et al., 2015). In the single-cell transcriptional analysis, the αLP1 subset encloses *Nfil3*$^+$*Id2*$^-$ cells with a transcriptional profile resembling that of *Nfil3*$^+$*Id2*^{med} cells committed to the ILC lineage. This observation is in accordance with the recent finding that NFIL3 directs the *Id2* expression through IL-7R signaling and control the ILC fate (Xu et al., 2015). However, formal confirmation of the capacity of NFIL3$^+$ cells to be ILC committed before expressing ID2 is still needed. From our single-cell experiment, we can assert that commitment toward the GILP takes place even earlier in the ID2$^+$ fraction of αLP1.

TOX is also an important transcription factor for ILC lineage, since it is found in both αLP1 and αLP2 signatures. TOX-deficient mice lack LTi cells and are devoid of lymph nodes and Peyer's patches, and overexpression of ID2 did not rescue cNK development (Aliahmad et al., 2010). According to a recent report (Seehus et al., 2015), TOX has a role in the early commitment to the ILC fate. Similarly, we show that it is mainly co-expressed with *Nfil3* and *Id2* in αLP1 cells and further maintained in the αLP2 cells.

The transition to the αLP2 stage is accompanied by the decrease of the Flt3 expression and the presence of CXCR6$^+$ cells, which mainly concerns ILC3 primed RORγt$^+$ cells (Possot

(C) Scheme of clonal culture conditions.

(D) Differentiation potential of FL progenitor cells from *Id2*$^{yfp/+}$*Cxcr6*$^{gfp/+}$ E15.5 embryos in conditions depicted in (C). Dot plots represents concatenation of all single wells from an experiment. Readout includes presence of T cell progenitors (CD25$^+$ID2$^-$), ILC1 (ID2$^+$NK1.1$^+$), ILC2 (ID2$^+$NK1.1$^-$ICOS$^{hi}\alpha_4\beta_7^-$), and ILC3 (ID2$^+$NK1.1$^-$ICOS$^{lo}\alpha_4\beta_7^+$CXCR6$^+$).

(E) Clonal efficiency, presented as frequency of positive (blue) and negative (red) wells for hematopoietic cells for each culture subset. Numbers indicate the number of wells that are positive or negative.

(F) Pie chart depicting all possible combinations of readouts after clonal culture of CLP and αLP1 cells. Percentages represent frequency of each combination among positive wells.

(G) Pie chart depicting all possible combinations of readouts after clonal culture of indicated αLP2 subsets. Percentages represent frequency of each combination among positive wells.

Data are representative of at least four independent experiments (A, B, and D) or are from four pooled independent experiments (E–G). In (D)–(G), 192 wells total for each population from four pooled experiments were analyzed.

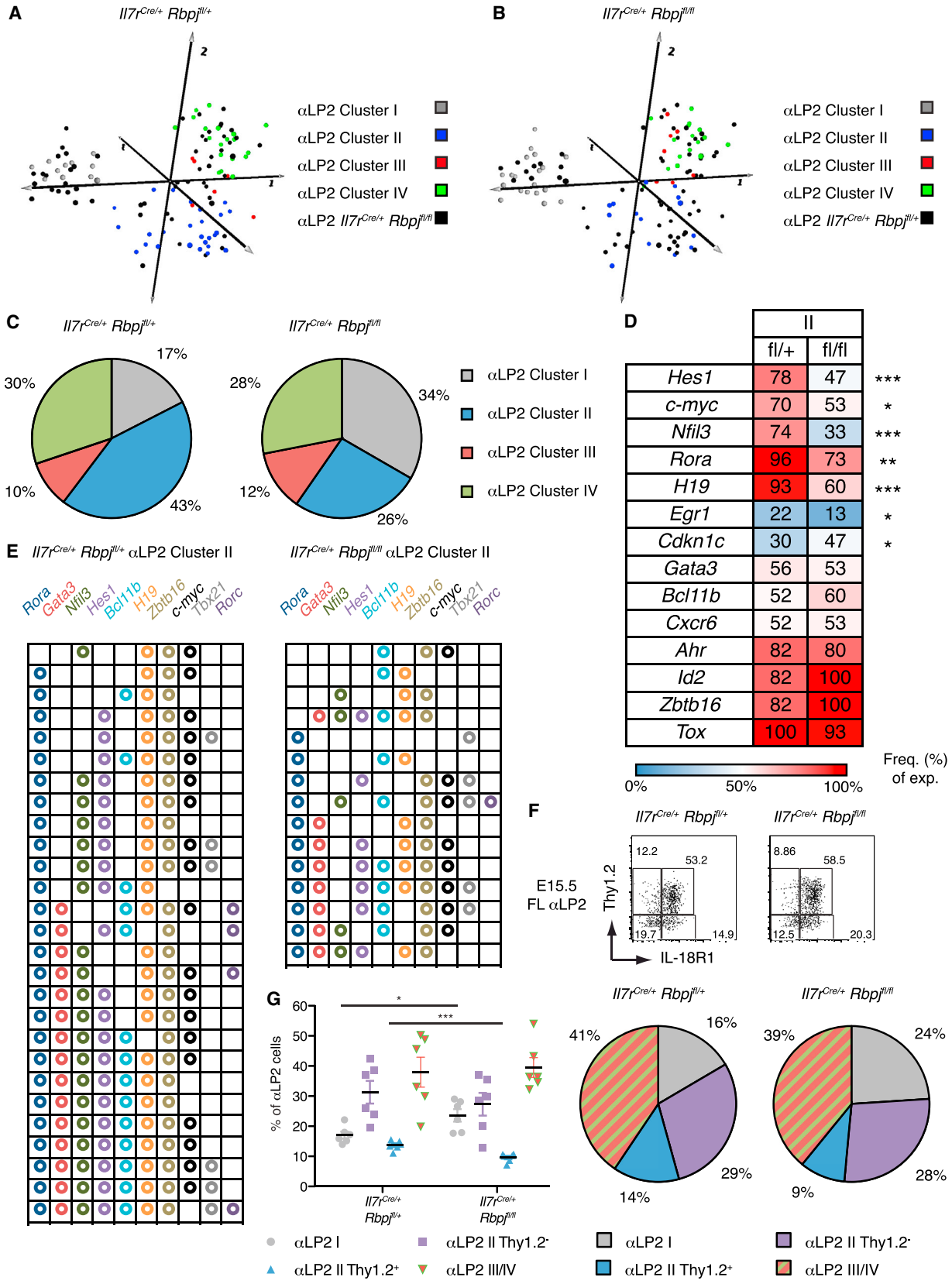

(legend on next page)

et al., 2011). This subset is highly heterogeneous and was separated into four populations thanks to the clustering analysis that displayed diverse enrichment for the expression of the 81 investigated genes. The αLP2 transcriptional signature is defined by the upregulation of ILC-specific markers such as *Notch2*, *Zbtb16*, *Rora*, *Tcf7*, and *Il2rb*. Cluster I contains *Id2*$^-$ progenitors with a quite specific profile different from that of other clusters. Despite the expression of *Nfil3*, these cells were essentially *Tox*$^-$*Tcf7*$^-$*Il2rb*$^-$ and could not differentiate into lymphoid progeny. Thus, we excluded this cluster from the ILC precursor analysis. Using different strategies (clonal cultures and single-cell transcriptomics), we separated subfractions of αLP2 that were already primed for ILC lineages. Transcriptional profiles matched the preferential priming. For example, αLP2 III/IV that is CXCR6$^+$ mainly give rise to ILC3 and, to some extent, ILC1, and it expresses Rorc (in protein and mRNA). It also expresses Tbx21 and Eomes transcripts.

Notch2 levels increase from CLP to αLP2 fraction, inversely to *Notch1* levels. Moreover, *Notch2* expression is maintained in peripheral LTi cells (Possot et al., 2011; Cherrier et al., 2012). Thus, we generated both *Notch2*- and *Rbpj*-deleted embryos in which the Notch pathway was conditionally deleted from the lymphoid progenitor stage, and we calculated that less than 1% of cells escaped the deletion.

CLP, αLP1, αLP2, and LTip fractions from FL were similar in percentage and numbers between Notch-deficient embryos and their control littermates, indicating that Notch signaling is not fundamental for their differentiation. In vitro cultures of Notch-deficient FL CLPs have demonstrated that they upregulate $\alpha_4\beta_7$ within 48 hr independently of Notch signaling. Similarly, the αLP1 and αLP2 precursors from both Notch-competent or -deficient embryos gave rise to identical progenies. A study suggested that Notch signaling must be interrupted after the $\alpha_4\beta_7^+$ stage, since constitutive active Notch signaling results in a block at this precursor stage (Cherrier et al., 2012). When we overexpressed NICD1 in all lymphoid progenitors, we observed accumulation of $\alpha_4\beta_7$ cells that were not *Id2*$^+$ progenitors but *Cd3e*$^+$*Notch1*$^+$ *Dtx1*$^+$ T progenitors. Hence, the absence of LTi cells in mice with a persistent Notch signaling does not result from an arrest at the ILC precursor stage but from an early conversion of lymphoid progenitors into T cell progenitors.

Transcriptional analyses showed that the Notch pathway is then active during ILC differentiation. Notch acts early in ILC development, since the frequency of *Id2*$^+$ progenitors was decreased from the αLP1 stage and to the same extent (more than two times) in the αLP2. This role of the Notch pathway could not be easily detected in vivo, since no marker is available to discern Id2$^+$ from Id2$^-$ cells. Moreover, the *Id2*$^-$ fraction compensated for the loss of *Id2*$^+$ cells in the αLP2 fraction.

ILC and T cells share developmental program similarities. Contrary to T cells, during ILC development, these commonly expressed genes are not significantly decreased after Notch disruption, with the exception of *Hes1*. *Nfil3* is importantly reduced after the Notch pathway disruption, suggesting a possible direct regulation of *Nfil3* by Notch in αLP2 II progenitors. Finally, the abrogation of the Notch pathway changes the distribution of ILC progenitor subsets with a complete loss of *Nfil3*$^+$*Gata3*$^+$*Rora*$^+$*Hes1*$^+$ cells that normally constitute the αLP2 cluster II. We also demonstrated that the Notch pathway is involved in the proliferation of the Thy1.2$^+$ subset of the cluster II, mainly enriched in ILC2 progenitors. Indeed, expression of genes considered as cell-cycle regulators were significantly modified in Notch-deficient embryos. *C-myc* and *Egr1* genes, considered as direct Notch targets in thymocytes, are also significantly decreased in the Thy1.2$^+$ αLP2 subset. These genes have been described as required for the proliferation and survival of thymocytes and downregulated upon inhibition of Notch expression (Dose et al., 2006; Schnell et al., 2006; Sharma et al., 2006). On the contrary, *Cdkn1c*, a negative regulator of cell proliferation and a target of the Notch pathway, is significantly increased in these Notch-deficient Thy1.2$^+$ ILC progenitors (Giovannini et al., 2012). These results are compatible with a study in which progenitors cultured on OP9DL4 gave rise to larger numbers of ILC2 than on OP9 cell lines (Yang et al., 2015).

In conclusion, we show that the Notch pathway is active in both αLP1 and αLP2 compartments, leading to changes in the transcriptional profile, abundance of *Id2*$^+$ progenitors, and proliferation of *Hes1*$^+$ progenitors in Notch-depleted, compared to Notch-competent, embryos. We defined new subsets that are differentially sensitive to the Notch pathway and clarify earlier contradictory in vitro observations. This comparative study indicates that, although it is not essential to the acquisition of $\alpha_4\beta_7$, CXCR6, and RORγt expression by LTip, the Notch pathway is active at different stages along ILC differentiation and in the peripheral pool of LTi cells.

Figure 6. Notch Signaling Disruption Differentially Affects Subsets of αLP2

(A and B) PCA of the single-cell data in Figure 4. Each cluster (identified in Figure 4A) is depicted according to the color key for *Il7r*$^{Cre/+}$*Rbpj*$^{fl/+}$ (A) or *Rbpj*$^{fl/fl}$ (B) αLP2.

(C) Pie charts show percentages of αLP2 I (gray), αLP2 II (blue), αLP2 III (red), or αLP2 IV (green) single cells from *Il7r*$^{Cre/+}$*Rbpj*$^{fl/+}$ (left) or *Rbpj*$^{fl/fl}$ (right) αLP2.

(D) Gene signatures differentially expressed in αLP2 II cells in *Il7r*$^{Cre/+}$*Rbpj*$^{fl/+}$ or *Rbpj*$^{fl/fl}$ FL, presented as frequency of expression (red = high frequency, blue = low frequency).

(E) Combination of expression pattern of selected genes in αLP2 II cells in *Il7r*$^{Cre/+}$*Rbpj*$^{fl/+}$ or *Rbpj*$^{fl/fl}$ FL. Each line represents a single cell, and each column represents the indicated gene.

(F and G) Flow cytometry of E15.5 FL cells from *Il7r*$^{Cre/+}$*Rbpj*$^{fl/+}$ or *Rbpj*$^{fl/fl}$ embryos for the presence of αLP2 subsets, according to IL-18R1 and Thy1.2 expression (F). In (G), percentages of each subset among αLP2 are represented in a dot plot, and pie charts depict the repartition and percentage of each subset in *Il7r*$^{Cre/+}$ *Rbpj*$^{fl/+}$ or *Rbpj*$^{fl/fl}$ αLP2.

Data are from two pooled independent experiments, (A)–(C) (n = 61 for *Il7r*$^{Cre/+}$*Rbpj*$^{fl/+}$ αLP2, and n = 55 for *Il7r*$^{Cre/+}$*Rbpj*$^{fl/fl}$ αLP2) and (D) and (E) (n = 27 for *Il7r*$^{Cre/+}$ *Rbpj*$^{fl/+}$ αLP2 II, and n = 15 for *Il7r*$^{Cre/+}$*Rbpj*$^{fl/fl}$ αLP2 II), are representative of at least four independent experiments (F), or are from four pooled independent experiments (G) (n = 6 single FL from E15.5 *Il7r*$^{Cre/+}$*Rbpj*$^{fl/+}$ or *Rbpj*$^{fl/fl}$ embryos). Statistical data show mean ± SEM. *p < 0.05; **p < 0.01; ***p < 0.001. Unpaired Student's t test was used in (G); chi-square test was used in (D).

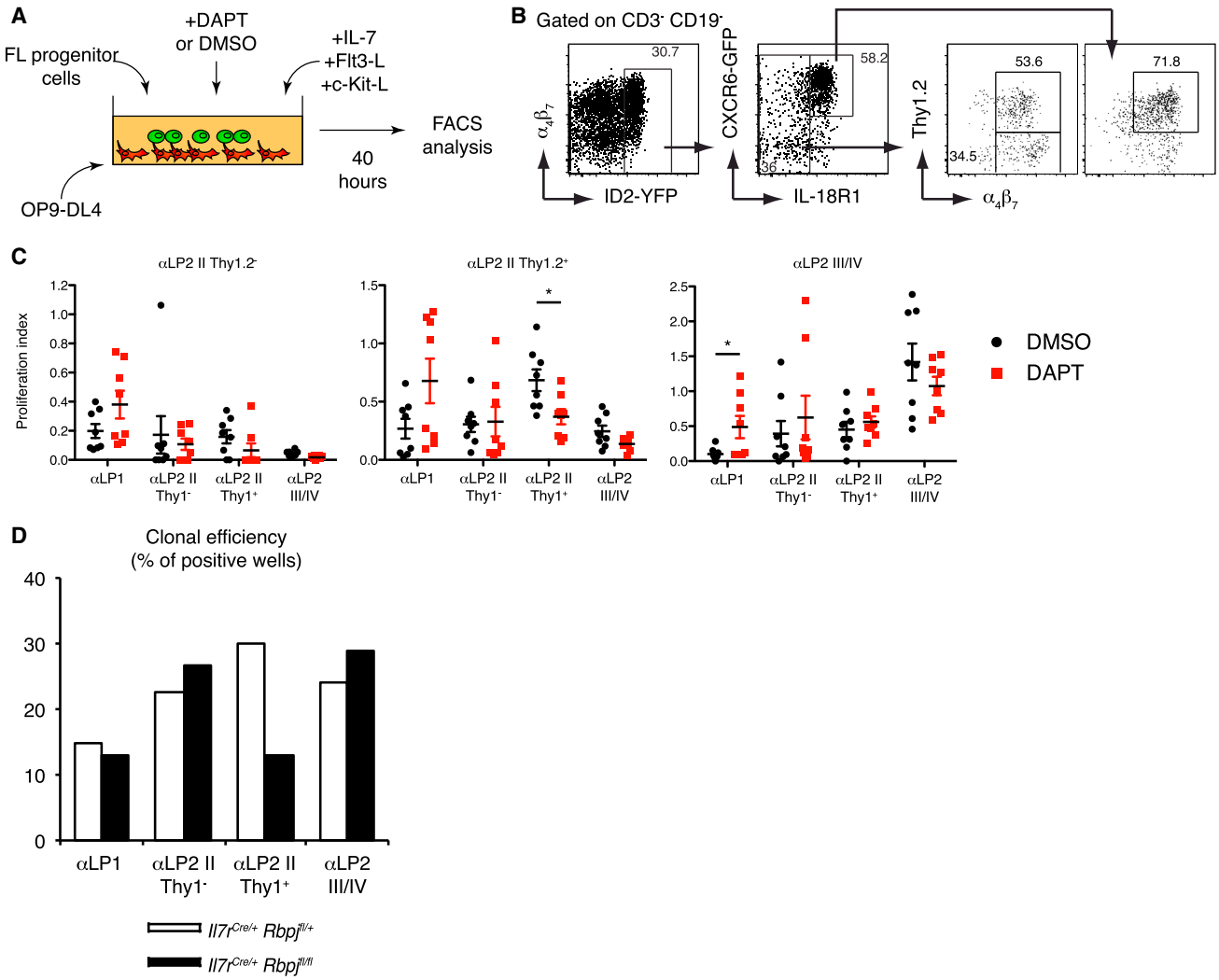

Figure 7. Effect of Notch Signaling on the Proliferation of αLP2 Subsets

(A) Scheme of short-term culture conditions.

(B) Short-term differentiation potential of FL-derived progenitor cells from E15.5 *Id2*$^{YFP/+}$*Cxcr6*$^{GFP/+}$ embryos in conditions depicted in (A). Dot plots represents concatenation of all wells from all populations in culture from an experiment. Cultured cells were analyzed for the presence of αLP2 II Thy1.2^{-}, αLP2 II Thy1.2^{+}, or αLP2 III/IV.

(C) Proliferation index of each subset of the αLP2 population (indicated above each graph) obtained after culture of the indicated αLP cells (indicated on the axis), cultured in the conditions described in (A), in DMSO (black circles) or DAPT (red squares). Proliferation is calculated on the number of cells of each population divided by the number of seeding cells (at least 50 cells in each condition).

(D) Clonal efficiency, presented as frequency of positive wells for each subset from isolated *Il7r*$^{Cre/+}$ *Rbpj*$^{fl/+}$ (white histograms) or *Rbpj*$^{fl/fl}$ E15.5 FL (black histograms). Data are representative of four independent experiments (A–C) or from four pooled independent experiments (D). In (D), each subset was cultured in clonal conditions with the following number of analyzed wells: *Il7r*$^{Cre/+}$*Rbpj*$^{fl/+}$ αLP1 (n = 240), αLP2 II Thy1.2^{-} (n = 240), αLP2 II Thy1.2^{+} (n = 170), αLP2 III/IV (n = 120); and *Il7r*$^{Cre/+}$*Rbpj*$^{fl/+}$ αLP1 (n = 264), αLP2 II Thy1.2^{-} (n = 232), αLP2 II Thy1.2^{+} (n = 137), and αLP2 III/IV (n = 186). In (C), each dot represents a single well from an experiment (two wells per experiment). Statistical data show mean ± SEM. *$p < 0.05$ (unpaired Student's t test).

See also Figure S7.

EXPERIMENTAL PROCEDURES

Mice

Il7r$^{Cre/+}$Rosa26^{YFP} mice (Schlenner et al., 2010) were crossed with Rbpj^{tm1Hon} (Il7r$^{Cre/+}$Rbpj$^{fl/+}$Rosa26^{YFP}), B6.129S-Notch2^{tm3Grid}/J (Il7r$^{Cre/+}$Notch2$^{fl/+}$Rosa26^{YFP}), or Gt(ROSA)26Sor$^{tm(Notch1)Dam}$ (Il7r$^{Cre/+}$Rosa26$^{Nic/+}$).

Id2$^{yfp/+}$*Cxcr6*$^{gfp/+}$ mice were obtained by crossing *Id2*$^{yfp/+}$ *mice* (Yang et al., 2011a) with *Cxcr6*$^{gfp/gfp}$ mice (The Jackson Laboratory). Rorct$^{tg(GFP)}$ mice were provided by G. Eberl. The time of the vaginal plug was considered E0.5. China ink was injected subcutaneously, and lymph nodes were analyzed 2 hr later. All animal experiments were approved by the Pasteur Institute Safety Committee in accordance with the French Ministry of Agriculture and the European Union (EU) guidelines.

Cell Preparation

Fetal organs were harvested, dissociated, and resuspended in Hank's balanced salt solution (HBSS) supplemented with 1% fetal calf serum (FCS) (Gibco). FL cells were depleted of lineage-positive cells by staining with

biotinylated-conjugated antibodies to lineage markers (CD3ε, CD19, CD11c, Ter119, Gr-1, NK1.1), followed by incubation with streptavidin microbeads (Miltenyi Biotec). Depletion was done on LS Columns (Miltenyi Biotec), from which the negative fraction was recovered.

Flow Cytometry and Cell Sorting

Flow cytometry data were acquired using a BD FACSCanto II or BD LSRFortessa (Becton Dickinson) and analyzed with FlowJo software (Tree Star). Dead cells were eliminated by propidium iodide exclusion. Cells were stained intracellularly after permeabilization and fixation with Foxp3 Transcription Factor Fixation/Permeabilization Concentrate and Diluent (eBioscience).

FL, FS, and FmLN cells were purified with a FACSAria III (Becton Dickinson). Cells were recovered in Eppendorf tubes or directly in 96-well qPCR plates for gene expression analysis.

Antibodies

All antibodies were from BD Biosciences, eBioscience, BioLegend, Cell Signaling Technology, or R&D Systems.

Antibodies either biotinylated or conjugated to various fluorochromes were used against the following mouse antigens: Ly76 (TER-119), Gr-1 (RB6-8C5), CD11c (HL3), CD3 (145-2C11), CD19 (6D5), NK1.1 (PK136), IL-7Rα (A7R34), c-Kit (2B8), Sca-1 (D7), RORγt (AFKJS-9), $\alpha_4\beta_7$ (DATK32), Flt3 (A2F10), CD8 (53-6.7), TCRβ (H57-597), CCR6 (29-2L17), CD4 (GK1.5), CD25 (PC61), CD44 (IM7), IL-18R1 (BG/IL18RA), and Thy1.2 (53-2.1).

Cell Culture

All experiments were done in 96-well plates at 37°C and 5% CO_2 and in culture medium consisting of OptiMEM, 10% (v/v) FCS, penicillin (100 U/ml), streptomycin (100 μg/ml) and 2-mercaptoethanol (5×10^{-7} M; GIBCO). OP9 and OP9-DL4 stromal cells were seeded into 96-well plates (1,000 cells per well). The culture medium was supplemented with saturating amounts of c-Kit ligand, Flt3 ligand, IL-2, and IL-7 made "in house." In some experiments, DAPT was added (20 μM, Sigma), with DMSO as control. CLP, αLP1, and αLP2 differentiation potentials were assayed by flow cytometry after 48 hr, 8 days, or 12 days of culture on OP9 or OP9-DL4 stroma.

RT-PCR

Cells were sorted in RLT Buffer (QIAGEN) and were frozen at −80°C. RNA was obtained with an RNeasy Micro Kit (QIAGEN), and cDNA was obtained with a PrimeScript RT Reagent Kit (Takara). A 7300 Real-Time PCR System (Applied Biosystems) and TaqMan technology (Applied Biosystems) or SYBRGreen technology (QIAGEN) were used for RT qPCR. A bilateral unpaired Student's t test was used for statistical analysis.

The following primers were from SABiosciences: *Il17a*, PPM03023A; *Il17f*, PPM05398E; *Il22*, PPM481A; and *Gapdh*, PPM02946E.

The following primers were from Applied Biosystems: *Gata3*, Mm00484683; *Id2*, Mm00711781; *Tox*, Mm00455231_m1; *Hes1*, Mm00468601_m1; *Hprt1*, Mm00446968; *Rbpj*, Mm01217627_g1; *Rora*, Mm01173766_m1; *Rorc*, Mm01261022_m1; *Dtx1*, Mm00492297_m1; *Nrarp*, Mm00482529_s1; *Tcf7*, Mm00493445_m1; *Notch1*, Mm00435249_m1; and *Notch2*, Mm00803069_m1.

The following primers were custom produced by Invitrogen: Cd3e forward: 5′-GCCTCAGAAGCATGATAAGC-3′/ Cd3e reverse: 5′- CCTTGGCCTTCCTATTCTTG-3′.

Biomark

Cells were sorted in 96-well qPCR plates in 10 μl of the CellsDirect One-Step qRT-PCR Kit (Thermo Fisher Scientific), containing a mix of diluted primers (0.05× final concentration; see Tables S1 and S2). Preamplified cDNA was obtained after reverse transcription (15′ at 40°C, 15′ at 50°C and 15′ at 60°C) and preamplification (22 cycles: 15″ at 95°C, 4′ at 60°C) and was diluted 1:5 in TE Buffer[pH 8] (Ambion). Sample mix was as follows: diluted cDNA (2.9 μl), Sample Loading Reagent (0.29 μl, Fluidigm), TaqMan Universal PCR Master Mix (3.3 μl, Applied Biosystems) or Solaris qPCR Low ROX Master Mix (3.3 μl, GE Dharmacon). Assay mix was as follows: Assay Loading Reagent (2.5 μl, Fluidigm), TaqMan (2.5 μl, Applied Biosystems) or Solaris (2.5 μl, GE Dharmacon). A 48.48 or 96.96 dynamic array integrated fluidic circuit (IFC; Fluidigm) was primed with control line fluid, and the chip was loaded with assays (either TaqMan or Solaris) and samples using an HX IFC controller (Fluidigm). The experiments were run on a Biomark HD (Fluidigm) for amplification and detection (2′ at 50°C, 10′ for TaqMan reagents or 15′ for Solaris reagents at 95°C, 40 cycles: 15″ at 95°C, 60″ at 60°C).

Samples that did not express at least one of three housekeeping genes (*Actb*, *Gapdh*, or *Hprt*) were removed from analysis. Data were processed through the MeV (MultiExperiment Viewer) Software (TM4). Hierarchical clustering was performed on C_T values of each gene analyzed from single cells, using uncentered Pearson's correlation with absolute distance and total linkage. PCA was performed to cluster samples.

Statistical Analyses

Statistical data show mean ± SEM. The chi-square test and unpaired Student's t test were used.

SUPPLEMENTAL INFORMATION

Supplemental Information includes seven figures and two tables and can be found with this article online at http://dx.doi.org/10.1016/j.celrep.2016.01.015.

AUTHOR CONTRIBUTIONS

S.C. and S.S. performed most experiments and analyzed data. C.B., T.P., and M.P. performed experiments. O.B.D. performed the mouse genotyping. H.R.R. and A.G. provided mouse lines. A.C. contributed to the writing. R.G. directed research, designed experiments, analyzed data, and wrote the manuscript with input from the coauthors.

ACKNOWLEDGMENTS

We thank A. Bendelac, J.Y. Bertrand, and D. Guy-Grand for critical reading. We are thankful to C. Possot to have started the breeding of the different mouse lines. We acknowledge the Center for Human Immunology and Cytometry platform at Institut Pasteur for support. This work was supported by the Institut Pasteur, INSERM, Université Paris Diderot, and by the Ministère de la Recherche (to S.C.), the Association pour la Recherche sur le Cancer (to S.C. and R.G.), the REVIVE Future Investment Program and the Agence Nationale de Recherche (ANR; grant "Twothyme" to A.C.), the Swiss National Science Foundation and Bourse Roux (to S.S.), ANR grant "Myeloten" (to R.G.), and the Institut National du Cancer (Role of the immune microenvironment during liver carcinogenesis, to R.G.).

Received: August 24, 2015
Revised: December 1, 2015
Accepted: January 2, 2016
Published: January 28, 2016

REFERENCES

Aliahmad, P., de la Torre, B., and Kaye, J. (2010). Shared dependence on the DNA-binding factor TOX for the development of lymphoid tissue-inducer cell and NK cell lineages. Nat. Immunol. *11*, 945–952.

Bernink, J.H., Peters, C.P., Munneke, M., te Velde, A.A., Meijer, S.L., Weijer, K., Hreggvidsdottir, H.S., Heinsbroek, S.E., Legrand, N., Buskens, C.J., et al. (2013). Human type 1 innate lymphoid cells accumulate in inflamed mucosal tissues. Nat. Immunol. *14*, 221–229.

Cherrier, M., Sawa, S., and Eberl, G. (2012). Notch, Id2, and RORγt sequentially orchestrate the fetal development of lymphoid tissue inducer cells. J. Exp. Med. *209*, 729–740.

Constantinides, M.G., McDonald, B.D., Verhoef, P.A., and Bendelac, A. (2014). A committed precursor to innate lymphoid cells. Nature *508*, 397–401.

Daussy, C., Faure, F., Mayol, K., Viel, S., Gasteiger, G., Charrier, E., Bienvenu, J., Henry, T., Debien, E., Hasan, U.A., et al. (2014). T-bet and Eomes instruct the development of two distinct natural killer cell lineages in the liver and in the bone marrow. J. Exp. Med. *211*, 563–577.

Dose, M., Khan, I., Guo, Z., Kovalovsky, D., Krueger, A., von Boehmer, H., Khazaie, K., and Gounari, F. (2006). c-Myc mediates pre-TCR-induced proliferation but not developmental progression. Blood *108*, 2669–2677.

Eberl, G., Marmon, S., Sunshine, M.J., Rennert, P.D., Choi, Y., and Littman, D.R. (2004). An essential function for the nuclear receptor RORgamma(t) in the generation of fetal lymphoid tissue inducer cells. Nat. Immunol. *5*, 64–73.

Fuchs, A., Vermi, W., Lee, J.S., Lonardi, S., Gilfillan, S., Newberry, R.D., Cella, M., and Colonna, M. (2013). Intraepithelial type 1 innate lymphoid cells are a unique subset of IL-12- and IL-15-responsive IFN-γ-producing cells. Immunity *38*, 769–781.

Giovannini, C., Gramantieri, L., Minguzzi, M., Fornari, F., Chieco, P., Grazi, G.L., and Bolondi, L. (2012). CDKN1C/P57 is regulated by the Notch target gene Hes1 and induces senescence in human hepatocellular carcinoma. Am. J. Pathol. *181*, 413–422.

Han, H., Tanigaki, K., Yamamoto, N., Kuroda, K., Yoshimoto, M., Nakahata, T., Ikuta, K., and Honjo, T. (2002). Inducible gene knockout of transcription factor recombination signal binding protein-J reveals its essential role in T versus B lineage decision. Int. Immunol. *14*, 637–645.

Hori, K., Sen, A., and Artavanis-Tsakonas, S. (2013). Notch signaling at a glance. J. Cell Sci. *126*, 2135–2140.

Hoyler, T., Klose, C.S., Souabni, A., Turqueti-Neves, A., Pfeifer, D., Rawlins, E.L., Voehringer, D., Busslinger, M., and Diefenbach, A. (2012). The transcription factor GATA-3 controls cell fate and maintenance of type 2 innate lymphoid cells. Immunity *37*, 634–648.

Iso, T., Kedes, L., and Hamamori, Y. (2003). HES and HERP families: multiple effectors of the Notch signaling pathway. J. Cell. Physiol. *194*, 237–255.

Klein Wolterink, R.G., Serafini, N., van Nimwegen, M., Vosshenrich, C.A., de Bruijn, M.J., Fonseca Pereira, D., Veiga Fernandes, H., Hendriks, R.W., and Di Santo, J.P. (2013). Essential, dose-dependent role for the transcription factor Gata3 in the development of IL-5+ and IL-13+ type 2 innate lymphoid cells. Proc. Natl. Acad. Sci. USA *110*, 10240–10245.

Klose, C.S., Kiss, E.A., Schwierzeck, V., Ebert, K., Hoyler, T., d'Hargues, Y., Göppert, N., Croxford, A.L., Waisman, A., Tanriver, Y., and Diefenbach, A. (2013). A T-bet gradient controls the fate and function of CCR6-RORγt+ innate lymphoid cells. Nature *494*, 261–265.

Klose, C.S., Flach, M., Möhle, L., Rogell, L., Hoyler, T., Ebert, K., Fabiunke, C., Pfeifer, D., Sexl, V., Fonseca-Pereira, D., et al. (2014). Differentiation of type 1 ILCs from a common progenitor to all helper-like innate lymphoid cell lineages. Cell *157*, 340–356.

Kondo, M., Weissman, I.L., and Akashi, K. (1997). Identification of clonogenic common lymphoid progenitors in mouse bone marrow. Cell *91*, 661–672.

Lee, J.S., Cella, M., McDonald, K.G., Garlanda, C., Kennedy, G.D., Nukaya, M., Mantovani, A., Kopan, R., Bradfield, C.A., Newberry, R.D., and Colonna, M. (2012). AHR drives the development of gut ILC22 cells and postnatal lymphoid tissues via pathways dependent on and independent of Notch. Nat. Immunol. *13*, 144–151.

Lewis, K.L., Caton, M.L., Bogunovic, M., Greter, M., Grajkowska, L.T., Ng, D., Klinakis, A., Charo, I.F., Jung, S., Gommerman, J.L., et al. (2011). Notch2 receptor signaling controls functional differentiation of dendritic cells in the spleen and intestine. Immunity *35*, 780–791.

Mebius, R.E., Miyamoto, T., Christensen, J., Domen, J., Cupedo, T., Weissman, I.L., and Akashi, K. (2001). The fetal liver counterpart of adult common lymphoid progenitors gives rise to all lymphoid lineages, CD45+CD4+CD3- cells, as well as macrophages. J. Immunol. *166*, 6593–6601.

Moro, K., Yamada, T., Tanabe, M., Takeuchi, T., Ikawa, T., Kawamoto, H., Furusawa, J., Ohtani, M., Fujii, H., and Koyasu, S. (2010). Innate production of T(H)2 cytokines by adipose tissue-associated c-Kit(+)Sca-1(+) lymphoid cells. Nature *463*, 540–544.

Oh, P., Lobry, C., Gao, J., Tikhonova, A., Loizou, E., Manent, J., van Handel, B., Ibrahim, S., Greve, J., Mikkola, H., et al. (2013). In vivo mapping of notch pathway activity in normal and stress hematopoiesis. Cell Stem Cell *13*, 190–204.

Possot, C., Schmutz, S., Chea, S., Boucontet, L., Louise, A., Cumano, A., and Golub, R. (2011). Notch signaling is necessary for adult, but not fetal, development of RORγt(+) innate lymphoid cells. Nat. Immunol. *12*, 949–958.

Pui, J.C., Allman, D., Xu, L., DeRocco, S., Karnell, F.G., Bakkour, S., Lee, J.Y., Kadesch, T., Hardy, R.R., Aster, J.C., and Pear, W.S. (1999). Notch1 expression in early lymphopoiesis influences B versus T lineage determination. Immunity *11*, 299–308.

Rankin, L.C., Groom, J.R., Chopin, M., Herold, M.J., Walker, J.A., Mielke, L.A., McKenzie, A.N., Carotta, S., Nutt, S.L., and Belz, G.T. (2013). The transcription factor T-bet is essential for the development of NKp46+ innate lymphocytes via the Notch pathway. Nat. Immunol. *14*, 389–395.

Saito, T., Chiba, S., Ichikawa, M., Kunisato, A., Asai, T., Shimizu, K., Yamaguchi, T., Yamamoto, G., Seo, S., Kumano, K., et al. (2003). Notch2 is preferentially expressed in mature B cells and indispensable for marginal zone B lineage development. Immunity *18*, 675–685.

Sambandam, A., Maillard, I., Zediak, V.P., Xu, L., Gerstein, R.M., Aster, J.C., Pear, W.S., and Bhandoola, A. (2005). Notch signaling controls the generation and differentiation of early T lineage progenitors. Nat. Immunol. *6*, 663–670.

Satoh-Takayama, N., Lesjean-Pottier, S., Vieira, P., Sawa, S., Eberl, G., Vosshenrich, C.A., and Di Santo, J.P. (2010). IL-7 and IL-15 independently program the differentiation of intestinal CD3-NKp46+ cell subsets from Id2-dependent precursors. J. Exp. Med. *207*, 273–280.

Satpathy, A.T., Briseño, C.G., Lee, J.S., Ng, D., Manieri, N.A., Kc, W., Wu, X., Thomas, S.R., Lee, W.L., Turkoz, M., et al. (2013). Notch2-dependent classical dendritic cells orchestrate intestinal immunity to attaching-and-effacing bacterial pathogens. Nat. Immunol. *14*, 937–948.

Sawa, S., Cherrier, M., Lochner, M., Satoh-Takayama, N., Fehling, H.J., Langa, F., Di Santo, J.P., and Eberl, G. (2010). Lineage relationship analysis of RORgammat+ innate lymphoid cells. Science *330*, 665–669.

Schlenner, S.M., Madan, V., Busch, K., Tietz, A., Läufle, C., Costa, C., Blum, C., Fehling, H.J., and Rodewald, H.R. (2010). Fate mapping reveals separate origins of T cells and myeloid lineages in the thymus. Immunity *32*, 426–436.

Schmutz, S., Bosco, N., Chappaz, S., Boyman, O., Acha-Orbea, H., Ceredig, R., Rolink, A.G., and Finke, D. (2009). Cutting edge: IL-7 regulates the peripheral pool of adult ROR gamma+ lymphoid tissue inducer cells. J. Immunol. *183*, 2217–2221.

Schnell, F.J., Zoller, A.L., Patel, S.R., Williams, I.R., and Kersh, G.J. (2006). Early growth response gene 1 provides negative feedback to inhibit entry of progenitor cells into the thymus. J. Immunol. *176*, 4740–4747.

Seehus, C.R., Aliahmad, P., de la Torre, B., Iliev, I.D., Spurka, L., Funari, V.A., and Kaye, J. (2015). The development of innate lymphoid cells requires TOX-dependent generation of a common innate lymphoid cell progenitor. Nat. Immunol. *16*, 599–608.

Seillet, C., Belz, G.T., and Mielke, L.A. (2014). Complexity of cytokine network regulation of innate lymphoid cells in protective immunity. Cytokine *70*, 1–10.

Serafini, N., Klein Wolterink, R.G., Satoh-Takayama, N., Xu, W., Vosshenrich, C.A., Hendriks, R.W., and Di Santo, J.P. (2014). Gata3 drives development of RORγt+ group 3 innate lymphoid cells. J. Exp. Med. *211*, 199–208.

Sharma, V.M., Calvo, J.A., Draheim, K.M., Cunningham, L.A., Hermance, N., Beverly, L., Krishnamoorthy, V., Bhasin, M., Capobianco, A.J., and Kelliher, M.A. (2006). Notch1 contributes to mouse T-cell leukemia by directly inducing the expression of c-myc. Mol. Cell. Biol. *26*, 8022–8031.

Tanigaki, K., Han, H., Yamamoto, N., Tashiro, K., Ikegawa, M., Kuroda, K., Suzuki, A., Nakano, T., and Honjo, T. (2002). Notch-RBP-J signaling is involved in cell fate determination of marginal zone B cells. Nat. Immunol. *3*, 443–450.

Wong, S.H., Walker, J.A., Jolin, H.E., Drynan, L.F., Hams, E., Camelo, A., Barlow, J.L., Neill, D.R., Panova, V., Koch, U., et al. (2012). Transcription factor RORα is critical for nuocyte development. Nat. Immunol. *13*, 229–236.

Xu, W., Domingues, R.G., Fonseca-Pereira, D., Ferreira, M., Ribeiro, H., Lopez-Lastra, S., Motomura, Y., Moreira-Santos, L., Bihl, F., Braud, V., et al. (2015). NFIL3 orchestrates the emergence of common helper innate lymphoid cell precursors. Cell Rep. *10*, 2043–2054.

Yang, C.Y., Best, J.A., Knell, J., Yang, E., Sheridan, A.D., Jesionek, A.K., Li, H.S., Rivera, R.R., Lind, K.C., D'Cruz, L.M., et al. (2011a). The transcriptional regulators Id2 and Id3 control the formation of distinct memory CD8+ T cell subsets. Nat. Immunol. *12*, 1221–1229.

Yang, Q., Saenz, S.A., Zlotoff, D.A., Artis, D., and Bhandoola, A. (2011b). Cutting edge: Natural helper cells derive from lymphoid progenitors. J. Immunol. *187*, 5505–5509.

Yang, Q., Li, F., Harly, C., Xing, S., Ye, L., Xia, X., Wang, H., Wang, X., Yu, S., Zhou, X., et al. (2015). TCF-1 upregulation identifies early innate lymphoid progenitors in the bone marrow. Nat. Immunol. *16*, 1044–1050.

Yokota, Y., Mansouri, A., Mori, S., Sugawara, S., Adachi, S., Nishikawa, S., and Gruss, P. (1999). Development of peripheral lymphoid organs and natural killer cells depends on the helix-loop-helix inhibitor Id2. Nature *397*, 702–706.

Yoshida, H., Naito, A., Inoue, J., Satoh, M., Santee-Cooper, S.M., Ware, C.F., Togawa, A., Nishikawa, S., and Nishikawa, S. (2002). Different cytokines induce surface lymphotoxin-alphabeta on IL-7 receptor-alpha cells that differentially engender lymph nodes and Peyer's patches. Immunity *17*, 823–833.

Hindawi Publishing Corporation
Mediators of Inflammation
Volume 2015, Article ID 368427, 15 pages
http://dx.doi.org/10.1155/2015/368427

Research Article

CXCR6 Expression Is Important for Retention and Circulation of ILC Precursors

Sylvestre Chea,[1,2,3] Cécilie Possot,[1,2,3] Thibaut Perchet,[1,2,3] Maxime Petit,[1,2,3] Ana Cumano,[1,2,3] and Rachel Golub[1,2,3]

[1]*Unité de Lymphopoièse, Département d'Immunologie, Institut Pasteur, 75015 Paris, France*
[2]*Université Paris Diderot, Sorbonne Paris Cité, Cellule Pasteur, Paris, France*
[3]*Inserm U668, Paris, France*

Correspondence should be addressed to Rachel Golub; rgolub@pasteur.fr

Received 12 June 2015; Accepted 10 August 2015

Academic Editor: Matthew R. Hepworth

Innate lymphoid cells are present at mucosal sites and represent the first immune barrier against infections, but what contributes to their circulation and homing is still unclear. Using $Rag2^{-/-}Cxcr6^{Gfp/+}$ reporter mice, we assessed the expression and role of CXCR6 in the circulation of ILC precursors and their progeny. We identify CXCR6 expressing ILC precursors in the bone marrow and characterize their significant increase in CXCR6-deficient mice at steady state, indicating their partial retention in the bone marrow after CXCR6 ablation. Circulation was also impaired during embryonic life as fetal liver from CXCR6-deficient embryos displayed decreased numbers of ILC3 precursors. When injected, fetal CXCR6-deficient ILC3 precursors also fail to home and reconstitute ILC compartments *in vivo*. We show that adult intestinal ILC subsets have heterogeneous expression pattern of CXCR6, integrin $\alpha_4\beta_7$, CD62L, CD69, and CD44, with ILC1 and ILC3 being more likely tissue resident lymphocytes. Intestinal ILC subsets were unchanged in percentages and numbers in both mice. We demonstrate that the ILC frequency is maintained due to a significant increase of ILC peripheral proliferation, as well as an increased proliferation of the *in situ* ILC precursors to compensate their retention in the bone marrow.

1. Introduction

The family of innate lymphoid cells (ILCs) concerns cells devoid of rearranged antigen receptors. It comprises conventional EOMES expressing NK (cNK) cells and the helper subsets composed of three groups (ILC1, ILC2, and ILC3) in analogy with the T-helper cell nomenclature [1]. ILC1 designates the group of T-bet expressing cells that are producing the IFNγ whereas ILC2 includes RORα/GATA3 dependent cells producing type Th2 cytokines. ILC3 includes different subsets that are all RORγt dependent and produce IL-17 and/or IL-22 (for review, see [2]). In the intestine, the ILC3 populations constantly interact with the microbiota, dietary compounds, epithelial factors, and cytokines to preserve the epithelial barrier integrity. IL-22 producing cells from the ILC3 group mainly concerns the subset that expresses the NK cell receptor NKp46 (termed NCR^+ ILC3). In mice, this intestinal subset has been shown to protect against infection with the pathogen *Citrobacter rodentium* [3–5]. NCR^+ ILC3 cells are $CCR6^-$ and do not produce IL-17A. They are rare in cryptopatches compared to $CD4^+$ ILC3 (LTi–like) cells that express CCR6 and produce IL-17A. This LTi–like subset is the adult counterpart of the LTi cells present during fetal life and is crucial for the development of lymph nodes (LN) and Peyer's patches. A third subset of double negative ($CD4^-$ $NKp46^-$) ILC3 is also present in the lamina propria. It is usually denominated by NCR^-ILC3 [6–8]. Intestinal ILC2 populations are crucial against parasitic infections [9–11] and may also be implicated in the regulation of gut homeostasis by limiting the inflammation [12].

The migration of lymphocytes to specific tissues is driven by the upregulation of adhesion and chemokine receptors. The T lymphocytes are imprinted with specific trafficking programs that are currently well known [13]. However, little is known concerning the circulation of ILC and their progenitors. All ILC groups derive from a bone marrow

(BM) precursor that expresses the ID2 transcription factor and the common γ chain of the interleukin 2 receptor [2]. Initial steps of ILC development start in the bone marrow. Intestinal lamina propria and spleen could also support the late stages of ILC differentiation, especially for the ILC3 lineage since precursors are unable to upregulate RORγt in the bone marrow [14]. Using mice bearing a targeted insertion of a GFP-reporter into the *Cxcr6* locus (*Cxcr6*$^{Gfp/+}$ mice) [15], we have previously shown that a subset of ILC precursors both in the adult bone marrow and fetal liver expresses CXCR6 [14]. CXCR6 has also been described as expressed by most of the ILC intestinal subsets [16]. Homing and trafficking are achieved by a specific combination of adhesion molecules and chemokine receptors, and CXCR6 expression could be critical and correlated with differential homing and/or function of ILC subsets. It has been shown, for example, that hepatic NK cells rely on CXCR6 expression for the persistence of memory NK cells [17]. Hence, we decided to evaluate the role of CXCR6 in the circulation of both ILC progenitors and ILC subsets.

In this study, we assess the effect of CXCR6 deficiency on ILC precursors and ILC subsets from the bone marrow, intestinal lamina propria (LP), and mesenteric lymph nodes (mLN). The effect of CXCR6 loss could be analyzed using the *Rag2*$^{-/-}$ *Cxcr6*$^{Gfp/Gfp}$ mouse model since the GFP reporter insertion simultaneously inactivates the corresponding *Cxcr6* allele [15], and *Rag2* deletion ensures a proper ILC analysis devoid of T-cell contamination. We have observed an increased percentage of bone marrow CXCR6$^+$ ILC precursors without any concomitant proliferation of those precursors, nor loss of differentiation potential, which suggests active bone marrow retention of ILC precursors after the CXCR6 loss. Similarly, CXCR6 contributes to circulation of fetal ILC3 precursors in the fetal liver (FL) as CXCR6-deficient fetal livers were partially depleted of ILC3 precursors. Using injection and reconstitution analysis, we show that CXCR6 is required for circulation of ILC3 precursors to intestinal LP or liver.

We show that pattern expression of CXCR6 and integrin $\alpha_4\beta_7$ and egress or circulation markers such as CD62L, CD69, and CD44 among ILC are heterogeneous and only intestinal ILC1 and ILC3 subsets were more likely to be tissue resident ILC populations. Finally, we show that CXCR6-deficiency does not alter the homeostatic balance of intestinal ILC subsets. However, those subsets were seeded and enriched in dividing and recently divided cells when CXCR6 deficiency occurs. The bone marrow derived ILC progenitor was similarly highly active and proliferative in CXCR6-deficient intestinal lamina propria, showing that this high proliferative state compensates retention of the bone marrow precursors.

2. Materials and Methods

2.1. Mice. *Rag2*$^{-/-}$ *Cxcr6*$^{+/+}$, *Rag2*$^{-/-}$ *Cxcr6*$^{Gfp/+}$, *Rag2*$^{-/-}$ *Cxcr6*$^{Gfp/Gfp}$, *Cxcr6*$^{Gfp/+}$ *Id2*$^{Yfp/+}$, and Ly5.1 *Rag2*$^{-/-}$ $\gamma c^{-/-}$ mice were bred in the animal facilities at Pasteur Institute, Paris. Mice were cared for in accordance with Pasteur Institute guidelines in compliance with European animal welfare regulations, and all animal studies were approved by Pasteur Institute Safety Committee in accordance with French and European guidelines.

2.2. Cell Preparation. Bone marrows (BM) were flushed out of femurs and tibias; mesenteric lymph nodes (mLN), fetal livers (FL), and fetal spleens (FS) were mechanically dissociated to obtain cell suspensions. Additionally, BM red blood cells were lysed by incubation with ammonium chloride-potassium bicarbonate solution. Cells from BM, mLN, and FL were magnetically depleted of Lin$^+$ cells via staining with biotin labeled antibodies to lineage markers, followed by the use of Streptavidin MicroBeads (Miltenyi).

Small intestine was washed from its contents by PBS injection, and Peyer's patches, if present, were removed. After being cut open longitudinally, small intestine was cut in 1 cm fragments. Fragments of small intestine were incubated 30 min at 37° and 5% CO_2 in RPMI medium (Gibco) plus 20% fetal calf serum (FCS), HEPES buffer (10 μM, Sigma-Aldrich), and then vortexed thoroughly for 4 minutes for removal of epithelial cells and intraepithelial lymphocytes. Remaining fragments of small intestine were incubated 30 min at 37° and 5% CO_2 in RPMI medium plus 20% FCS, HEPES Buffer (10 μM), and collagenase type VIII (250 μg/mL, Sigma) for the isolation of LP lymphocytes. Cell suspension was centrifuged, resuspended in a 40% solution of Percoll (GE Healthcare), and underlaid with a 75% solution of Percoll. After centrifugation 20 min at 600 g, cells were collected at the 40–75% interface.

All cells were then collected in cold HBSS (Gibco) plus 1% FCS. Cell suspensions were counted on Malassez cell, and dead cells were excluded using Trypan Blue.

2.3. Flow Cytometry. After antibody staining, cells were washed and dead cells were excluded by Propidium Iodide staining (250 ng/mL, Sigma-Aldrich). Cells were stained intracellularly using Foxp3 Permeabilzation/Fixation Kit according to manufacturers notice (eBiosciences). Cells were then incubated for 5 min with DAPI (4,6-diamidino-2-phenylindole, 2 μg/mL, Life Technologies), and washed prior to cell acquisition. FACSCanto II and LSR Fortessa (BD Biosciences) were used for flow cytometry acquisition, with Diva6 software (BD Biosciences), and analyzed with FlowJo v8 software (TreeStar). For visual purposes, only 8000 events maximum are shown in each FACS dot plot.

Cells were purified with a FACSAria III sorter (BD Biosciences). Cells were recovered in PBS for cell injection, or OPTIMEM (Gibco) plus 10% FCS for cell culture.

2.4. Antibodies. Streptavidin was coupled to PECy5. The following antibodies were either biotinylated or coupled to fluorochromes (Alexa488, PerCPCy5.5, PE, PECy7, APC, Alexa 660, APCCy7, BV421, eFluor 450, HZ V500, BV605, BV650, BV711, BV786): Ly76 (TER-119), Gr-1 (RB6-8C5), CD11c (HL3), CD3ε (145-2C11), CD19 (6D5), CD8α (53-6.7), CD5 (53-7.3), TCRβ (H57-597), TCR$\gamma\delta$ (GL-3), NK1.1 (PK136), NKp46 (29A1.4), IL-7Rα (A7R34), c-Kit (2B8), Sca-1 (D7), $\alpha_4\beta_7$ (DATK32), Flt3 (A2F10), CD4 (GK1.5), CD45.2

(104), Thy1.2 (53-2.1), ICOS (C398.4A), CD62L (MEL-14), CD69 (H1.2F3), CD44 (IM7), RORγt (AFKJS-9 or Q31-378), Gata3 (L50-823), human/mouse Ki67 (B56).

Lineage cocktails consisted of

BM: CD3ε, CD5, CD8, CD11c, CD19, TCRβ, TCRγδ, Ter119, Gr1, and NK1.1,

FL and FS: CD3ε, CD11c, CD19, Ter119, Gr1, and NK1.1,

MLN and LPL: CD3ε, CD5, CD8, CD11c, CD19, TCRβ, TCRγδ, Ter119, and Gr1.

All antibodies were purchased from BD Biosciences, eBiosicences, or Biolegend.

2.5. Cell Culture. OP9-DL4 stromal cells were plated one day prior to culture experiment in culture medium: OPTIMEM, 10% FCS, β-Mercaptoethanol (500 μM, Gibco), penicillin (5 U/mL, Gibco), and streptomycin (5 μg/mL, Gibco). Bone marrow precursors were FACS sorted in 400 μL of culture medium and plated on OP9-DL4 cells at 20 cells per well. Medium was complemented with in-lab produced cytokines (IL-7, c-KitL and Flt3-L). Cells were cultured for 10 days at 37°C and 5% CO_2 and then harvested and stained for analysis.

2.6. In Vivo Reconstitution. Ly5.1 *Rag2*$^{-/-}\gamma c^{-/-}$ mice were nonlethally irradiated (900 rad) at least 4 hours prior to cell injection. Between 1000 and 2000 Lin$^-$ CD4^{hi} IL-7Rα$^+$ CXCR6$^+$ cells from fetal spleens obtained from either E15.5 *Cxcr6*$^{Gfp/+}$ or *Cxcr6*$^{Gfp/Gfp}$ embryos were sorted in 100 μL of PBS, and retroorbital injection was performed. Mice were analyzed 4 weeks after injection.

2.7. Statistical Analysis. All data were submitted to Student's unpaired bilateral t-test. Data were deemed significantly different when $^{*}p < 0.05$, $^{**}p < 0.01$, or $^{***}p < 0.005$.

3. Results

3.1. CXCR6-Deficient ILC Precursors Are Retained in the Bone Marrow. We first characterized the BM lymphoid precursor compartments by crossing and analyzing adult *Id2*$^{Yfp/+}$ *Cxcr6*$^{Gfp/+}$ bone marrow cells [15, 18]. As previously described [14, 19, 20], Lin$^-$ IL-7Rα$^+$ compartment comprises ILC2 precursors (ILC2P) that are Sca-1^{hi} c-Kit^{lo} and lymphoid Sca-1$^{-/lo}$ c-Kit^{med} precursors that are divided into common lymphoid progenitors (CLP; Flt3$^+$ $\alpha_4\beta_7{}^-$) and $\alpha_4\beta_7$ expressing lymphoid precursors (Flt3$^-$ $\alpha_4\beta_7{}^+$). The latter expresses ID2 (thus representing ILC precursors or ILCP), as well as ILC2P compartment whereas CLP cells have no expression of ID2. We observe that ILCP and ILC2P comprised both CXCR6$^+$ and CXCR6$^-$ fractions (Figure 1(a)). CXCR6^{hi} cells are only found in ILC2P fraction (up to 60%).

To confirm the ILC potential of the two different ILCP subsets (CXCR6$^+$ and CXCR6$^-$), we cultured them on OP9-DL4 stromal cell lines with cytokines to promote cell survival and differentiation (IL-7, c-KitL, and Flt3-L) and analyzed their progeny after 10 days of culture. We confirmed that both CXCR6$^+$ and CXCR6$^-$ ILCP cells were able to give rise to ILC1 (ID2$^+$ NKp46$^+$ NK1.1$^+$), ILC3 (ID2$^+$ NKp46$^-$ NK1.1$^-$ IL-7Rα$^+$ RORγt$^+$), and ILC2 (ID2$^+$ NKp46$^-$ NK1.1$^-$ IL-7Rα$^+$ RORγt$^-$) cells (Figure 1(b)). Interestingly, all ILCs that were obtained expressed variable levels of CXCR6. ILC1 progeny cells were distributed between CXCR6$^-$ and CXCR6^{hi} levels, with a majority of CXCR6^{int} cells, regardless of their progenitor (CXCR6$^+$ or CXCR6$^-$ ILCP), showing that ILC1 could acquire or loose CXCR6 expression. Amongst remaining non-ILC1 cells, all cells are ID2$^+$ and are enriched in CXCR6^{hi} cells (up to 77%), but for a smaller fraction that is CXCR6$^-$. Because in our previous work, we showed that all RORγt$^+$ cells (which represent between 30% and 50% in NK1.1$^-$ NKp46$^-$ fraction after culture of ILCP, Figure 1(b)) were comprised of CXCR6^{hi} cells, and the remaining ID2$^+$ IL-7Rα$^+$ ILC2 cells are both CXCR6^{hi} and CXCR6$^-$, recapitulating the phenotype of *ex vivo* bone marrow ILC2P.

We analyzed then the contribution of CXCR6 to different lymphoid precursor compartments, using *Rag2*$^{-/-}$ *Cxcr6*$^{+/+}$ (wt), *Cxcr6*$^{Gfp/+}$ (HZ), or *Cxcr6*$^{Gfp/Gfp}$ (KO) mice. As expected, CLP compartment that does not express CXCR6 was not affected by *Cxcr6* deletion either in frequency or in numbers. No difference was observed for total numbers of ILCP and ILC2P in CXCR6-deficient bone marrow (Figure 2(a)). Levels of CXCR6-GFP between HZ and KO mice were not different (Figure 2(b)). However, when looking at the enrichment in CXCR6 expressing cells, a significant increase of CXCR6$^+$ precursors is detected in both ILCP and ILC2P subsets (Figure 2(c)). ILCP from both HZ and KO mice were able to give rise to cNK/ILC1 cells (NK1.1$^+$ NKp46$^+$ T-bet$^+$ EOMES$^{+/-}$), ILC2 (NK1.1$^-$ NKp46$^-$ GATA-3$^+$ RORγt$^-$), and ILC3 (NK1.1$^-$ NKp46$^-$ GATA-3$^-$ RORγt$^+$), showing that their differentiation potential was not affected by CXCR6-deficiency (Figure 2(d)). This increase in CXCR6$^+$ precursors was not due to a particular proliferative behavior of bone marrow precursors in CXCR6-deficient conditions. The lymphoid precursor subsets display similar frequency of both Ki67$^+$ and DAPI$^+$ cells in CXCR6-deficient and competent bone marrow (Figures 2(e) and 2(f)).

Overall, our results show that, in CXCR6-deficient mice, a fraction of ILC precursors that still expresses GFP but no functional CXCR6 protein under the control of *Cxcr6* promoter is retained in the bone marrow. This confinement to the bone marrow concerns both ILCP and committed ILC2P and indicates that CXCR6 contributes to cell egress of all ILC subsets from the bone marrow.

3.2. CXCR6 Contributes to Fetal ILC3 and ILC3 Precursor Circulation. Our previous work has shown that fetal ILC3 precursors were found during embryonic development in the fetal liver (FL) at embryonic day E15.5, among CXCR6 expressing progenitors [14]. Similarly, to address the contribution of CXCR6 to ILC3 circulation during embryonic development, we analyzed E15.5 FL for the ILC3 precursor compartment, defined as Lin$^-$ c-Kit$^+$ IL-7Rα$^+$ RORγt$^+$ (Figure 3(a)) in *Cxcr6*$^{+/+}$ (wt), *Cxcr6*$^{Gfp/+}$ (HZ), or

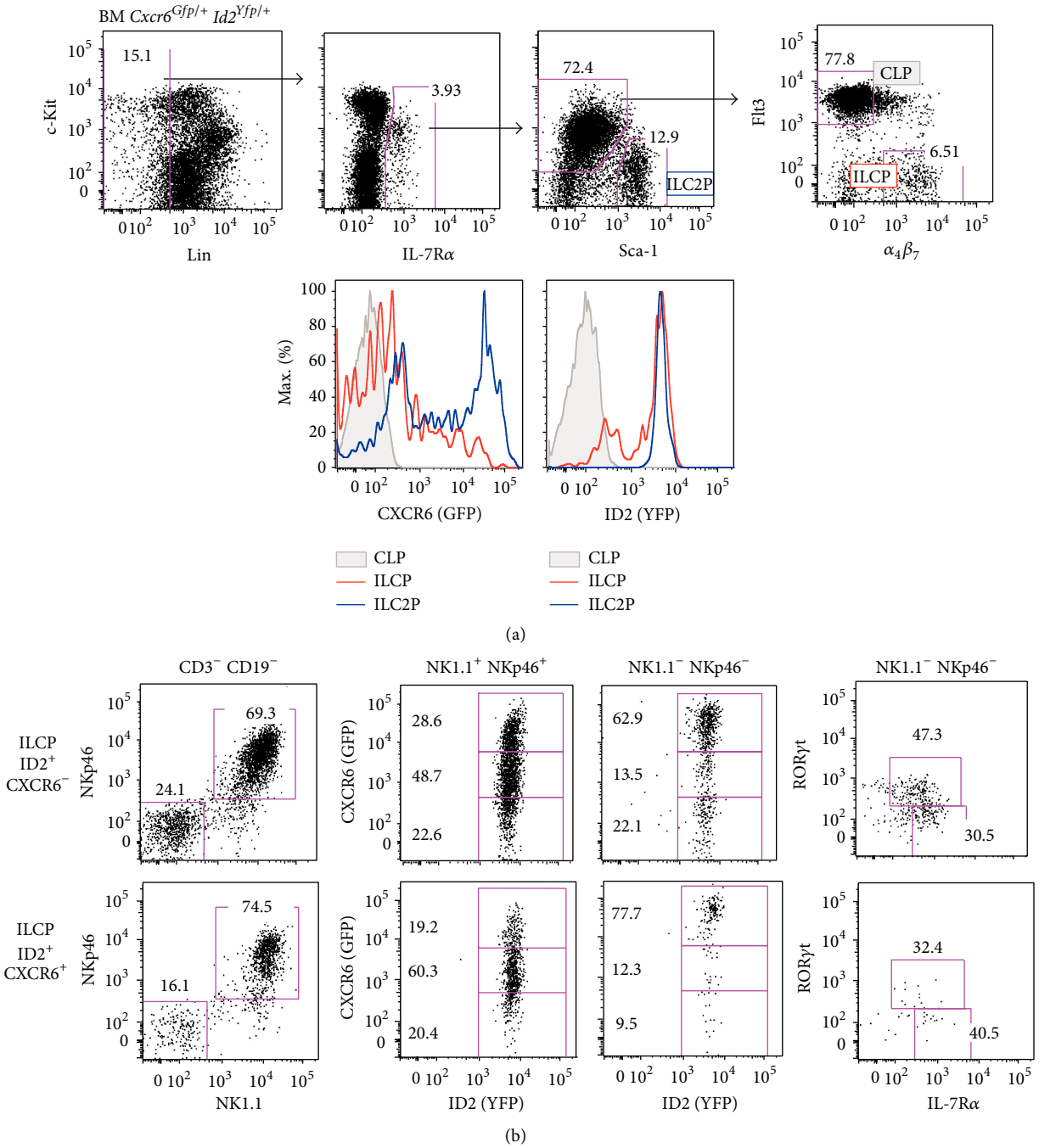

Figure 1: ILCP and ILC2P in the bone marrow heterogeneously express CXCR6. (a) Flow cytometry of lineage depleted (Lin: CD3ε, CD5, CD8, CD11c, CD19, TCRβ, TCR$\gamma\delta$, Ter119, Gr1, and NK1.1) adult bone marrow (BM) from *Cxcr6*$^{Gfp/+}$ *Id2*$^{Yfp/+}$ mice. Among Lin$^-$ IL-7Rα^+ compartments are defined: CLP (filled gray, c-Kit^{lo} Sca-1$^{-/lo}$ Flt3$^+$ $\alpha_4\beta_7^-$), ILCP (red, c-Kit^{lo} Sca-1$^{-/lo}$ Flt3$^-$ $\alpha_4\beta_7^+$), and ILC2P (blue, c-Kit$^-$ Sca-1^{hi}). Each compartment is analyzed for CXCR6-GFP and ID2-YFP expression (bottom histograms). (b) Cell culture of BM ILCP, selected as ID2$^+$ CXCR6$^-$ (upper panels) or ID2$^+$ CXCR6$^+$ (lower panels). Each population is sorted and cultured at 20 cells per well on OP9-DL4 stromal cells with IL-7, c-KitL, and Flt3L for 10 days and analyzed by flow cytometry. Indicated obtained progenies were analyzed for ID2-YFP, CXCR6-GFP, RORγt, and IL-7Rα expression. Results are representative of at least 3 experiments each ((a): $n > 5$), or 2 experiments ((b), at least 4 wells of each condition).

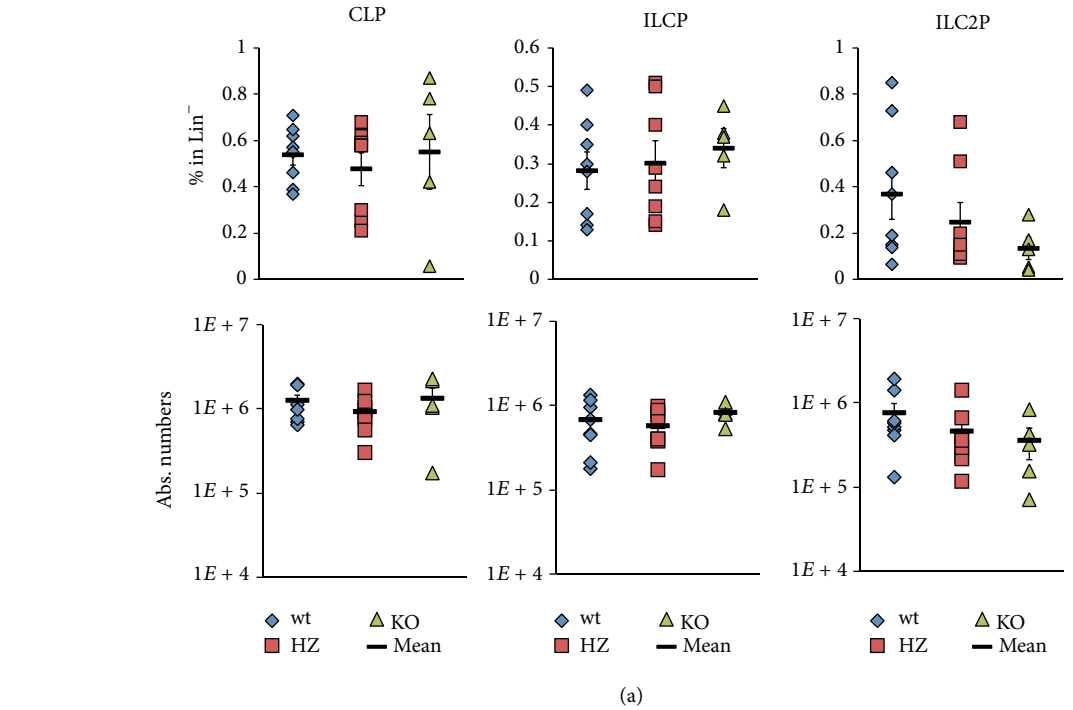

(a)

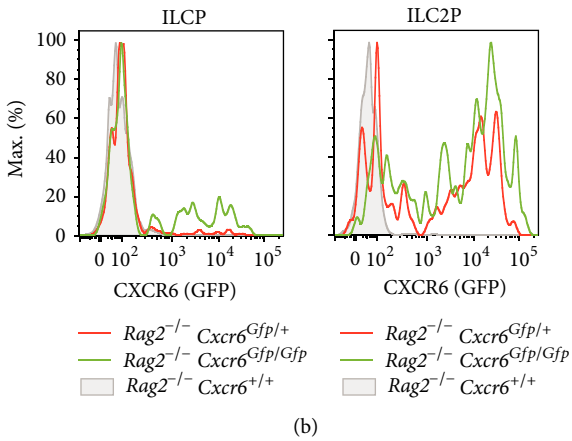

(b)

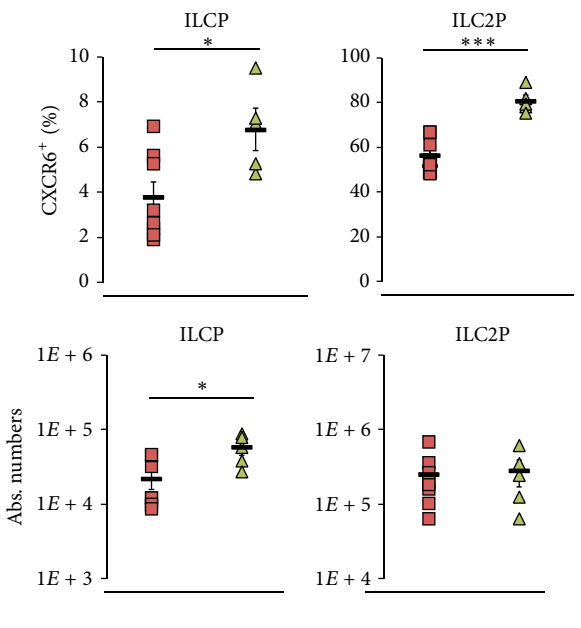

(c)

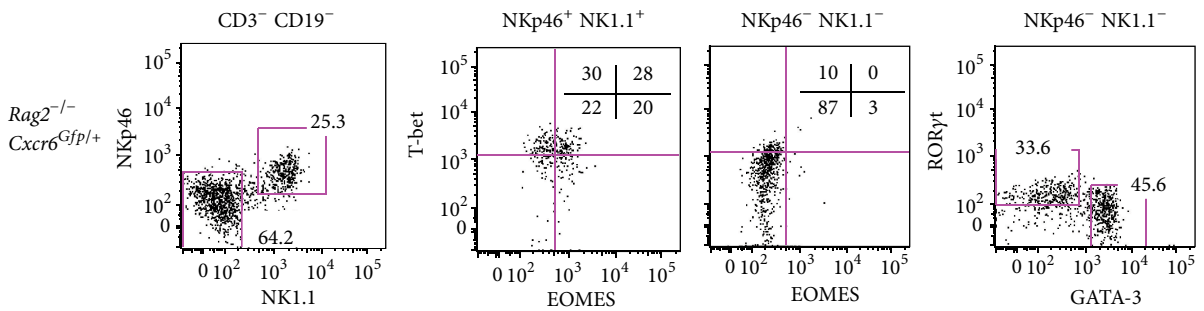

Figure 2: Continued.

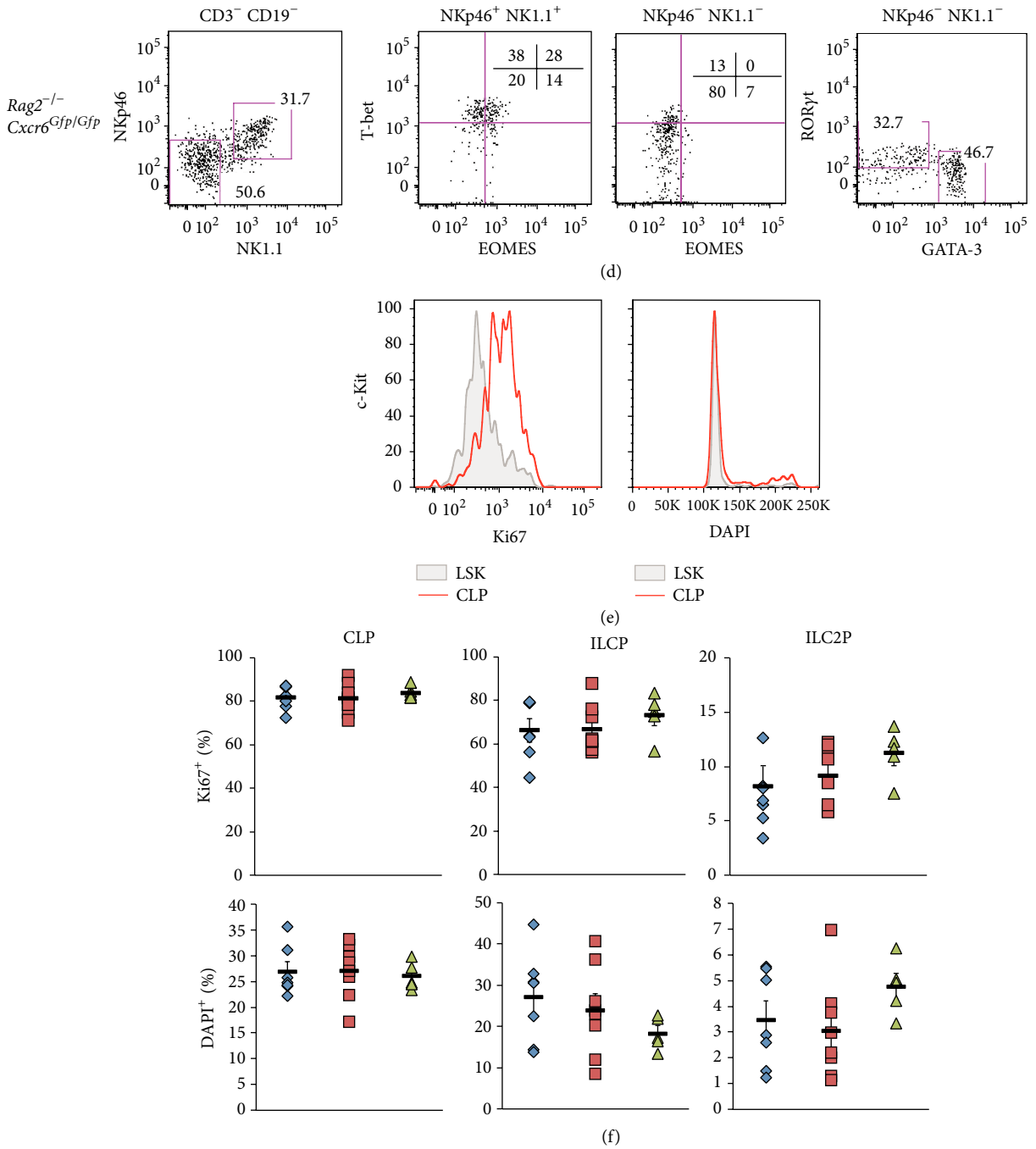

Figure 2: CXCR6-deficient precursors are retained in the bone marrow. (a) Percentages in Lin$^-$ (upper panels) and absolute numbers (lower panels) of BM CLP, ILCP, and ILC2P as defined in Figure 1(a) from *Rag2*$^{-/-}$ *Cxcr6*$^{+/+}$ (wt, blue losange), *Cxcr6*$^{Gfp/+}$ (HZ, red square), or *Cxcr6*$^{Gfp/Gfp}$ (KO, green triangle) adult mice. (b) Histograms depicting levels of CXCR6-GFP in ILCP (left panel) or ILC2P (right panel) from *Rag2*$^{-/-}$ *Cxcr6*$^{+/+}$ (filled gray), *Cxcr6*$^{Gfp/+}$ (red line), or *Cxcr6*$^{Gfp/Gfp}$ (green line) bone marrows. (c) Percentages of CXCR6$^+$ cells (upper panels) and absolute numbers of (lower panels) BM ILCP (left panels) and ILC2P (right panels) in *Rag2*$^{-/-}$ *Cxcr6*$^{Gfp/+}$ (HZ, red square) or *Cxcr6*$^{Gfp/Gfp}$ (KO, green triangle) adult mice. (d) Cell culture of BM ILCP from *Rag2*$^{-/-}$ *Cxcr6*$^{Gfp/+}$ (upper panels) or *Cxcr6*$^{Gfp/Gfp}$ (lower panels) adult mice. Each population is sorted and cultured at 20 cells per well on OP9-DL4 stromal cells with IL-7, c-KitL, and Flt3-L for 7 days and analyzed by flow cytometry. Indicated obtained progenies were analyzed for T-bet, EOMES, RORγt, and GATA-3 expression. (e) Histograms of BM LSK cells (filled gray, selected as Lin$^-$ IL-7Rα$^-$ c-Kit^{hi} Sca-1$^+$) and CLP (red line) for Ki67 expression and DAPI levels. (f) Percentages of Ki67$^+$ cells (upper panels) and DAPI$^+$ cells (lower panels) among BM CLP, ILCP, and ILC2P in *Rag2*$^{-/-}$ *Cxcr6*$^{+/+}$ (wt, blue losange), *Cxcr6*$^{Gfp/+}$ (HZ, red square), or *Cxcr6*$^{Gfp/Gfp}$ (KO, green triangle) adult mice. Data are representative of at least 3 experiments ((b), (e): $n > 5$), or are from one experiment ((d), at least 4 wells of each conditions), or are from 3 pooled experiments ((a), (c), (f), wt: $n = 8$, HZ: $n = 8$, KO: $n = 5$). In ((a), (c), (f)), each dot represents a single mouse. Statistical data are displayed with mean and SEM (Student's unpaired bilateral test, $^*p < 0.05$; $^{**}p < 0.01$; $^{***}p < 0.005$).

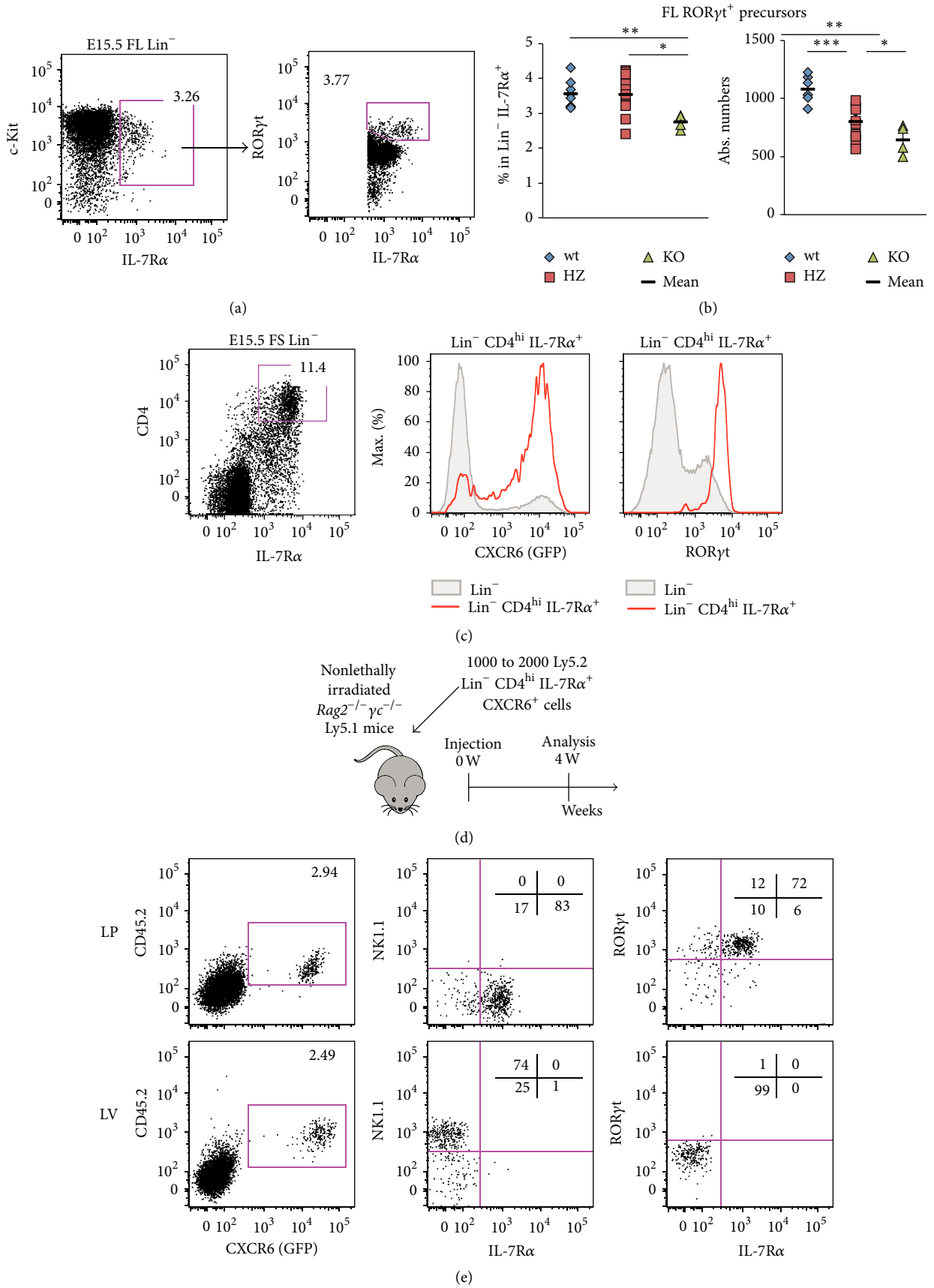

Figure 3: Continued.

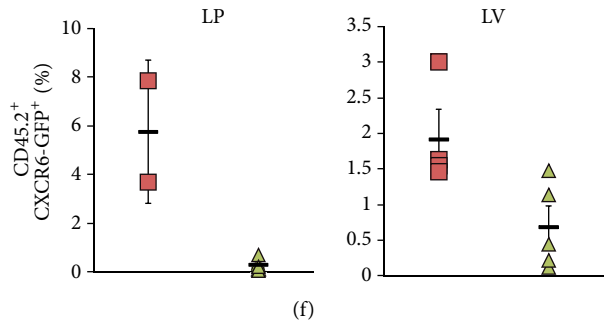

Figure 3: CXCR6 contributes to fetal ILC3 and ILC3 precursor circulation. (a) Flow cytometry of lineage depleted (Lin: CD3ε, CD11c, CD19, Ter119, Gr1, NK1.1) E15.5 fetal liver (FL). ILC3 precursors are defined as Lin$^-$ IL-7Rα^+ c-Kit^{med} RORγt$^+$. (b) Percentages of Lin$^-$ IL-7Rα^+ c-Kit^{med} (left panel) and absolute numbers (right panel) of FL ILC3 precursors as defined in Figure 2(a) in FL from *Cxcr6*$^{+/+}$ (wt, blue losange), *Cxcr6*$^{Gfp/+}$ (HZ, red square) or *Cxcr6*$^{Gfp/Gfp}$ (KO, green triangle) E15.5 embryos. (c) Flow cytometry of Lin$^-$ compartment fetal spleen (FS) from *Cxcr6*$^{Gfp/+}$ E15.5 embryos. Lin$^-$ CD4^{hi} IL-7Rα^+ cells (red) and total Lin$^-$ cells (filled gray) are analyzed for CXCR6-GFP (left histogram) and RORγt (right histogram). (d) Scheme depicting injection and reconstitution experiment. (e) Analysis of reconstitution experiment. 1000 to 2000 Ly5.2 Lin$^-$ CD4^{hi} IL-7Rα^+ CXCR6$^+$ cells were injected in nonlethally irradiated *Rag2*$^{-/-}\gamma c^{-/-}$ Ly5.1 mice. Recipients were killed 4 weeks after injection and intestinal lamina propria (LP, upper panels) and liver (LV, lower panels) were analyzed by flow cytometry. (f) Percentages of reconstitution experiment as explained in Figures 2(d) and 2(e) using *Cxcr6*$^{Gfp/+}$ (HZ, red squares) or *Cxcr6*$^{Gfp/Gfp}$ (KO) E15.5 embryos in intestinal LP (left panel) or LV (right panel). Results are representative of at least 3 experiments each ((a), (c): $n > 5$), or are from 3 pooled experiments ((b), wt: $n = 6$, HZ: $n = 10$, KO: $n = 4$), or are from at least 2 pooled experiments ((e), (f), LP HZ: $n = 2$, LP KO: $n = 5$, LV HZ: $n = 4$, LV KO: $n = 5$). In ((b), (f)), each dot represents a single mouse. Statistical data are displayed with mean and SEM (Student's unpaired bilateral test, $^*p < 0.05$; $^{**}p < 0.01$).

Cxcr6$^{Gfp/Gfp}$ (KO) E15.5 FL (Figure 3(b)). We show that frequencies of ILC3 precursors and absolute numbers were significantly reduced, though not totally absent, in KO embryos compared to both HZ and wt embryos (Figure 3(b)).

We next addressed directly the circulation capacities of such CXCR6 expressing ILC3 precursors during adult life. Fetal spleen (FS) Lin$^-$ CD4^{hi} IL-7Rα^+ cells are highly enriched in CXCR6 expressing cells and are almost all RORγt$^+$ (Figure 3(c)). Among those cells, we purified the CXCR6$^+$ fraction from either *Cxcr6*$^{Gfp/+}$ or *Cxcr6*$^{Gfp/Gfp}$ Ly5.2 embryos and injected them into nonlethally irradiated *Rag2*$^{-/-}\gamma c^{-/-}$ Ly5.1 mice. Reconstitution for ILC1 and ILC3 compartments in the intestinal lamina propria (LP) and liver (LV) was analyzed 4 weeks after injection (Figure 3(d)). Among donor CD45.2$^+$ cells, LP is mainly composed of NK1.1$^-$ IL-7Rα^+ RORγt$^+$ ILC3 cells, whereas LV mainly reconstitutes NK1.1$^+$ IL-7Rα^- ILC1 cells (Figure 3(e)). Interestingly, all reconstituting cells expressed high levels of CXCR6. We clearly observe that CXCR6-deficient progenitor cells fail to reconstitute peripheral compartments, as compared to *Cxcr6*$^{Gfp/+}$ injected ILC3 precursors (Figure 3(f)).

In conclusion, CXCR6 highly contributes to fetal ILC3 precursors and ILC3 circulation, especially towards the intestine and the liver.

3.3. Intestinal ILC Compartments Have Heterogeneous Expression of CXCR6 and Egress Markers. CXCR6 is heterogeneously expressed by ILC subtypes. By analyzing *Rag2*$^{-/-}$ *Cxcr6*$^{Gfp/+}$ intestinal LP, we show that ILC1 are all CXCR6^{hi} and the diverse ILC3 subsets express different levels of CXCR6, with LTi-like cells expressing lower levels than NCR$^+$ and NCR$^-$ ILC3 subsets. In contrast, cNK are all CXCR6$^-$, and intestinal ILC2 subsets were separated into a large CXCR6$^-$ and a smaller CXCR6$^+$ fraction (Figure 4(a)).

We further analyzed expression of egress or retention markers such as CD62L, CD69, and CD44, as well as CXCR6 and integrin $\alpha_4\beta_7$ in intestinal LP and also mesenteric lymph nodes (mLN) ILC populations (Figures 4(b) and 4(c)). All ILC subsets expressed CD44 in all organs. Most of the CD62L$^+$ mLN cells belong to the ILC1-cNK subset. In the LP, these cells largely become CD62L$^-$ as their ILC2 and ILC3 intestinal counterparts. Only intestinal ILC2 subsets were CD69^{lo}, whereas intestinal ILC1-cNK and all ILC3 subsets were CD69$^+$, suggesting less retention of ILC2 cells in the tissue [21, 22]. In contrast, all mLN ILC subsets were CD69$^-$. CXCR6-GFP expression pattern in mLN ILC subsets is similar to what could be observed in LP ILC subsets (Figure 4(a)). Finally, integrin $\alpha_4\beta_7$ was only detected in ILC2 subset but not in other ILC subsets in both LP and mLN (Figure 4(c)).

In conclusion, only intestinal ILC1 and ILC3 subsets that express high levels of both CXCR6 and CD69 are more likely to be tissue resident ILC populations.

3.4. Normal Intestinal ILC1 and ILC3 Compartments in CXCR6-Deficient Mice Are Compensated by Higher Proliferative Capacities of Respective ILC Compartments and of an In Situ Progenitor Cell. We confirmed that, in CXCR6-deficient mice, there was no impact on the repartition of the different ILC subsets at homeostasis, except for cNK-ILC1 that are significantly (but slightly only) increased in CXCR6-deficient LP (Figure 5(a)), in line with previous publications [16]. Overall, the balance of intestinal ILC subsets was not majorly affected, as we observed similar repartitions between wt, HZ, and KO mice. Intestinal ILC are mainly composed of

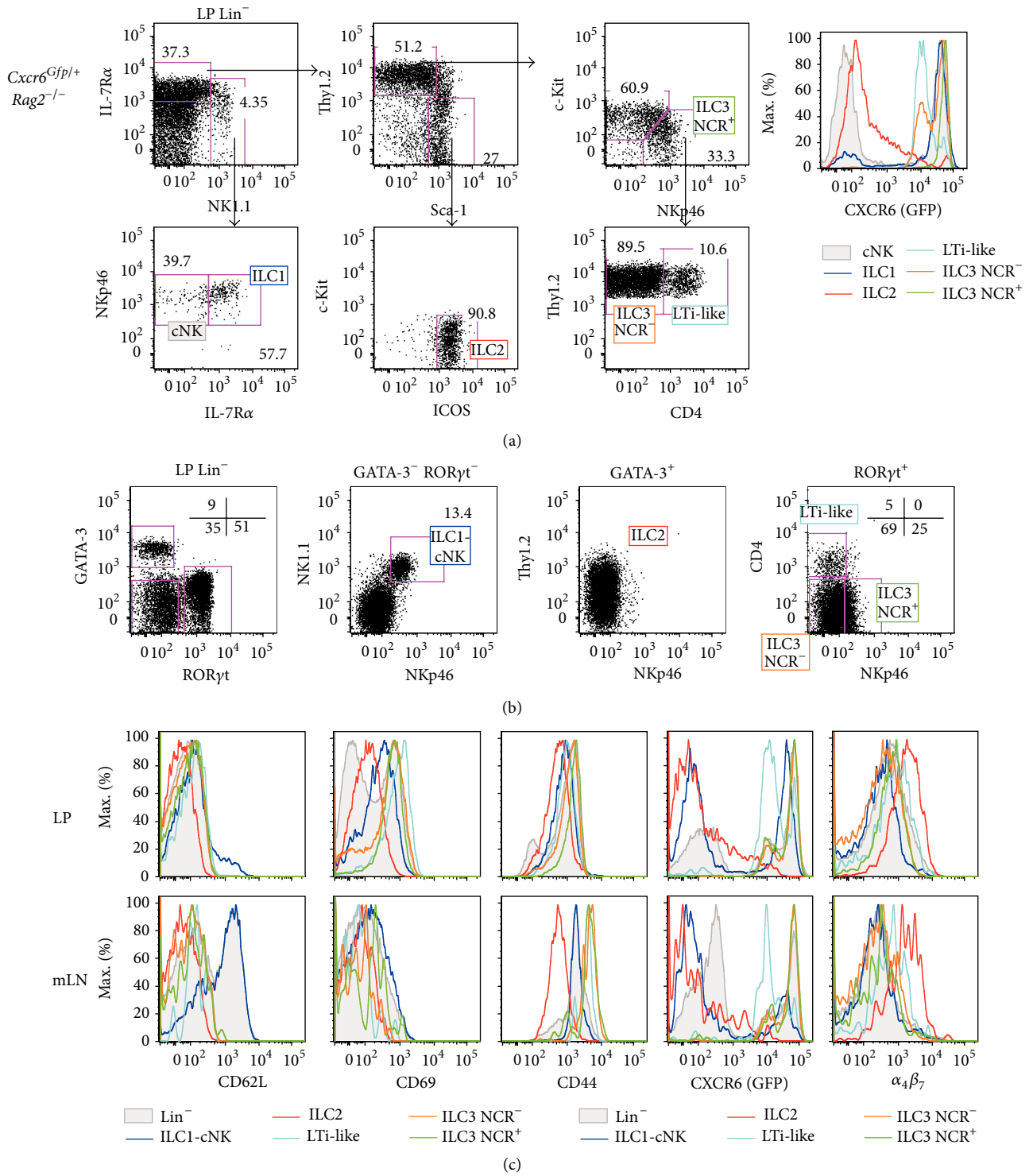

Figure 4: Intestinal ILC compartments have heterogeneous expression of CXCR6 and egress markers. (a) Flow cytometry of Lin$^-$ (Lin: CD3ε, CD5, CD8, CD11c, CD19, TCRβ, TCR$\gamma\delta$, Ter119, and Gr1) adult intestinal LP from *Rag2*$^{-/-}$ *Cxcr6*$^{Gfp/+}$ mice. ILC subsets are defined as cNK (filled gray, Lin$^-$ NK1.1$^+$ NKp46$^+$ IL-7Rα^-), ILC1 (blue, Lin$^-$ NK1.1$^+$ NKp46$^+$ IL-7Rα^-), ILC2 (red, Lin$^-$ NK1.1$^-$ Thy1.2$^{-/lo}$ Sca-1^{hi} c-Kit$^-$ ICOS^{hi}), ILC3 NCR$^+$ (green, Lin$^-$ NK1.1$^-$ Thy1.2^{hi} Sca-1$^{-/lo}$ c-Kit$^-$ NKp46$^+$), ILC3 NCR$^-$ (orange, Lin$^-$ NK1.1$^-$ Thy1.2^{hi} Sca-1$^{-/lo}$ c-Kit^{med} NKp46$^+$ CD4$^-$), and LTi-like (light blue, Lin$^-$ NK1.1$^-$ Thy1.2^{hi} Sca-1$^{-/lo}$ c-Kit^{med} NKp46$^+$ CD4$^+$). Each compartment is analyzed for CXCR6-GFP expression. (b) Flow cytometry of Lin$^-$ adult intestinal LP from *Rag2*$^{-/-}$ *Cxcr6*$^{Gfp/+}$ mice. ILC subsets are defined as ILC2 (red, Lin$^-$ GATA-3$^+$ RORγt$^-$), ILC3 NCR$^+$ (green, Lin$^-$ GATA-3$^-$ RORγt$^+$ NKp46$^+$ CD4$^-$), ILC3 NCR$^-$ (orange, Lin$^-$ GATA-3$^-$ RORγt$^+$ NKp46$^-$ CD4$^-$), LTi-like (light blue, Lin$^-$ GATA-3$^-$ RORγt$^+$ NKp46$^-$ CD4$^+$), and ILC1-cNK (blue, Lin$^-$ GATA-3$^-$ RORγt$^-$ NKp46$^+$ NK1.1$^+$). (c) Histograms depicting levels of CD62L, CD69, CD44, CXCR6-GFP, and $\alpha_4\beta_7$ in Lin$^-$ (filled gray) or ILC subsets (as defined in Figure 3(b)) in adult LP (upper panels) or mesenteric lymph nodes (mLN, lower panels) from *Rag2*$^{-/-}$ *Cxcr6*$^{Gfp/+}$ mice. Results are representative of at least 3 experiments each ((a), (b), (c): $n > 5$).

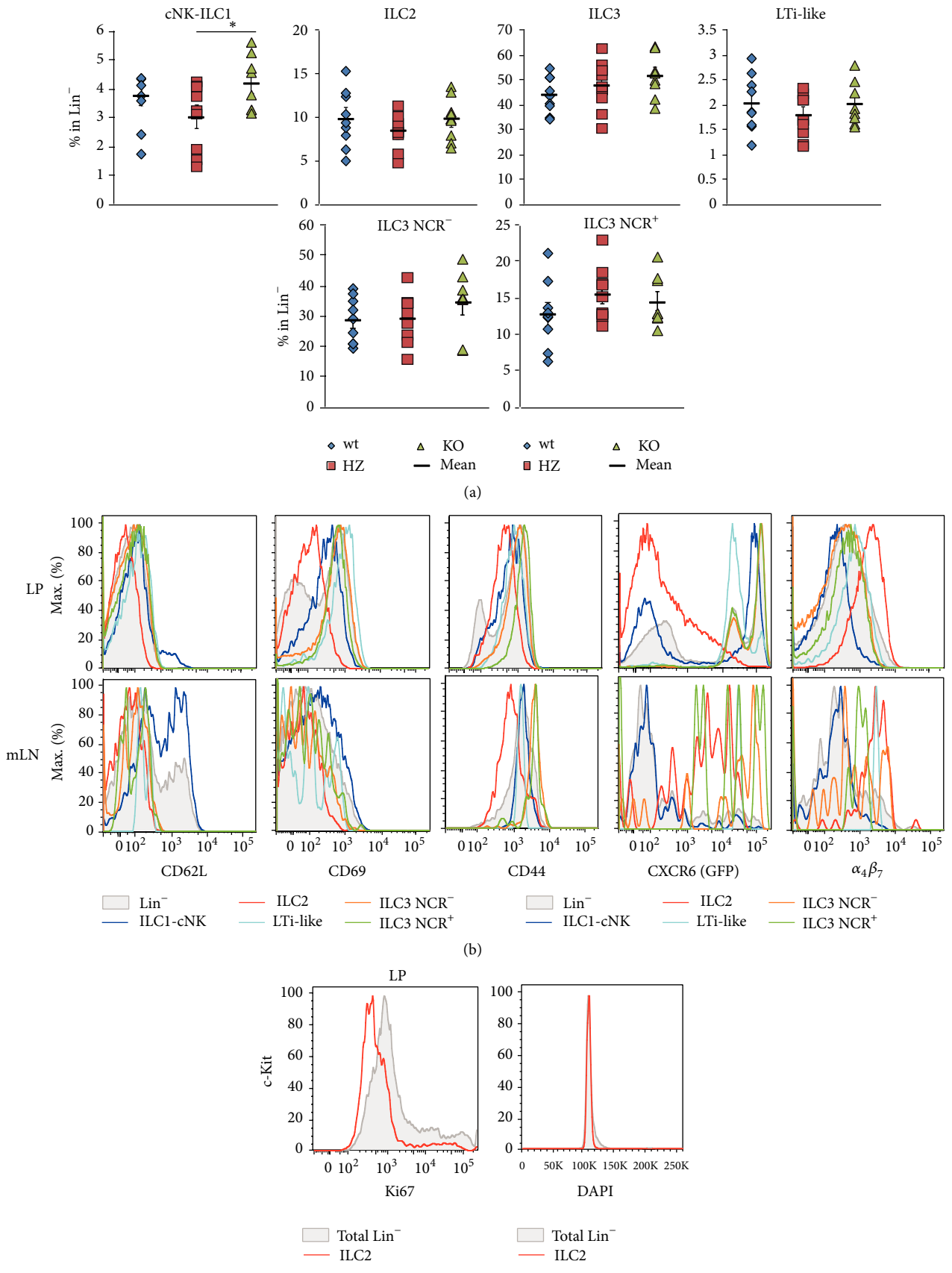

Figure 5: Continued.

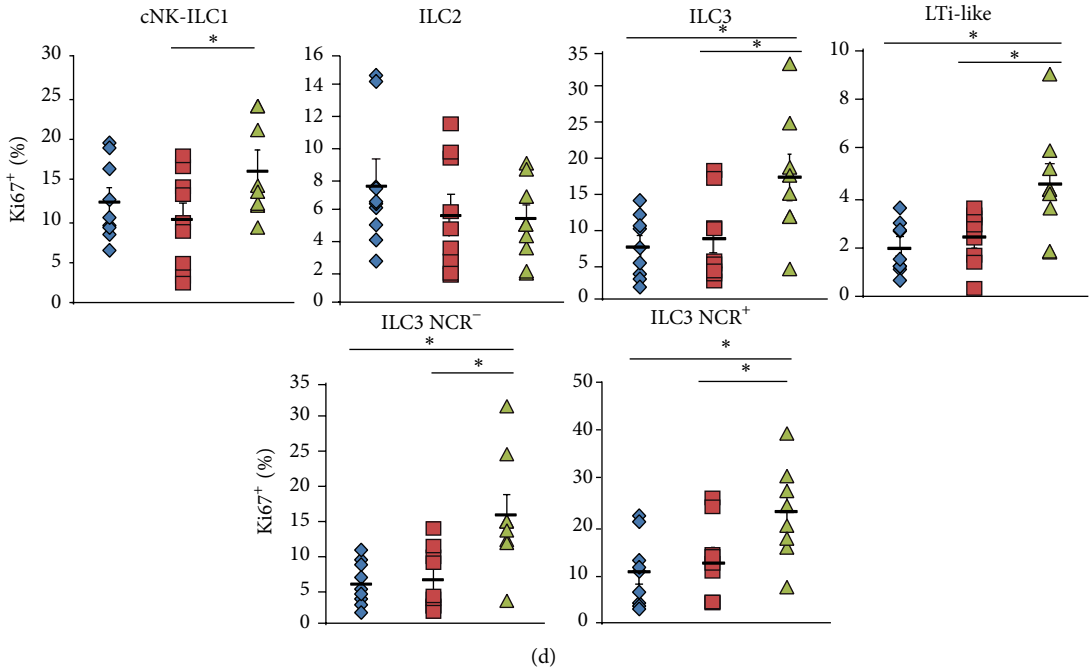

(d)

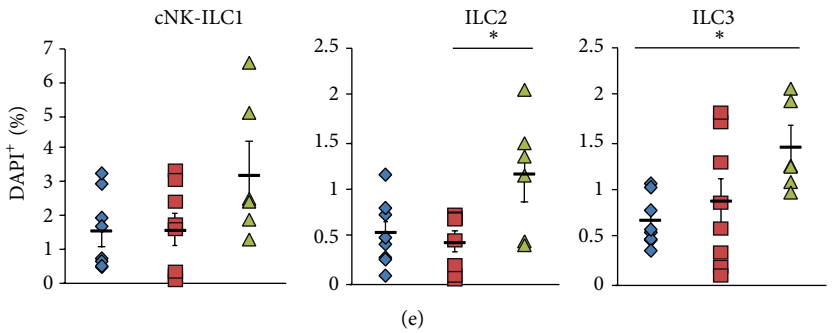

(e)

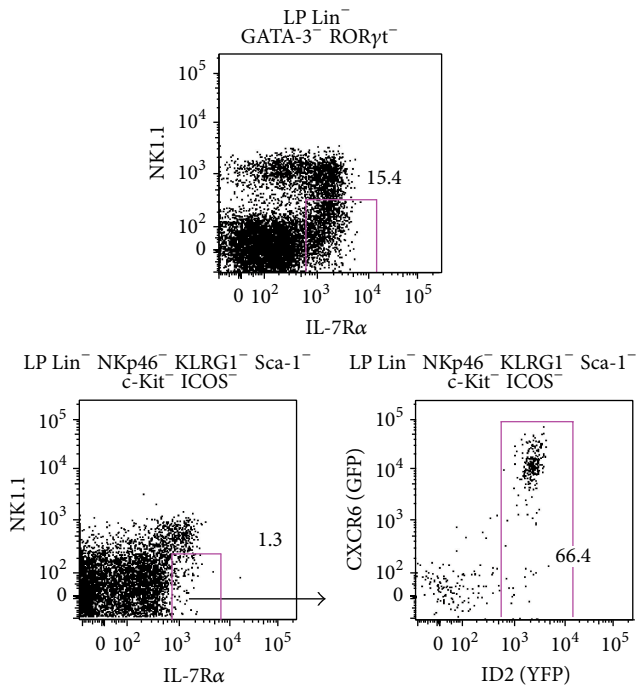

(f)

Figure 5: Continued.

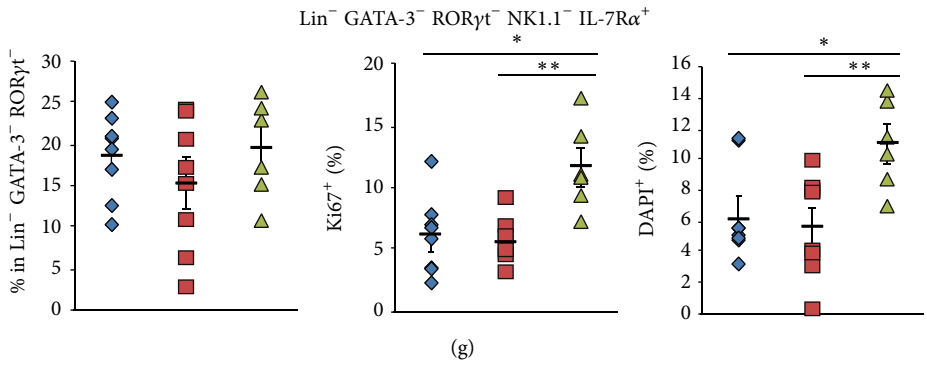

Figure 5: Normal intestinal ILC compartments in CXCR6-deficient mice are compensated by higher proliferative capacities of *in situ* progenitor cell. (a) Percentages of ILC subsets in Lin$^-$ (as defined in Figure 3(b)) in adult LP from *Rag2*$^{-/-}$ *Cxcr6*$^{+/+}$ (wt, blue losange), *Cxcr6*$^{Gfp/+}$ (HZ, red square), or *Cxcr6*$^{Gfp/Gfp}$ (KO, green triangle) adult mice. (b) Histograms depicting levels of CD62L, CD69, CD44, CXCR6-GFP, and $\alpha_4\beta_7$ in Lin$^-$ (filled gray) or ILC subsets (as defined in Figure 3(b)) in adult LP (upper panels) or mesenteric lymph nodes (mLN, lower panels) from *Rag2*$^{-/-}$ *Cxcr6*$^{Gfp/Gfp}$ mice. (c) Histograms of total LP Lin$^-$ cells (filled gray) or ILC2 cells (red line) for Ki67 expression and DAPI levels. ((d), (e)) Percentages of Ki67$^+$ cells (d) and DAPI$^+$ cells (e) among ILC subsets (as defined in Figure 4(b)) in LP from *Rag2*$^{-/-}$ *Cxcr6*$^{+/+}$ (wt, blue losange), *Cxcr6*$^{Gfp/+}$ (HZ, red square), or *Cxcr6*$^{Gfp/Gfp}$ (KO, green triangle) adult mice. (f) Flow cytometry of LP *in situ* ILCP (upper panel) and CXCR6-GFP and ID2-YFP expression of LP *in situ* ILCP (lower panels) from *Cxcr6*$^{Gfp/+}$ *Id2*$^{Yfp/+}$ mice. (g) Percentages of IL-7Rα^+ precursors in Lin$^-$ (left), Ki67$^+$ (middle), and DAPI$^+$ (right) cells among IL-7Rα^+ precursors in LP from *Rag2*$^{-/-}$ *Cxcr6*$^{+/+}$ (wt, blue losange), *Cxcr6*$^{Gfp/+}$ (HZ, red square), or *Cxcr6*$^{Gfp/Gfp}$ (KO, green triangle) adult mice. Results are from 3 pooled experiments ((a), (c), (d): wt: $n = 9$, HZ: $n = 9$, KO: $n = 8$) or from 2 pooled experiments ((e), (f), GF, wt: $n = 8$, HZ: $n = 8$, KO: $n = 6$) or are representative of 3 experiments (b). In ((a), (d), (e), (g)), each dot represents a single mouse. Statistical data are displayed with mean and SEM (Student's unpaired bilateral test, $^*p < 0.05$; $^{**}p < 0.01$).

45% to 50% of ILC3 (with a minority of 2% of LTi-like cells, roughly 15% of ILC3 NCR$^+$ cells, and mainly ILC3 NCR$^-$ cells), then a subsequent part of ILC2 (10%), and a minority of cNK-ILC1 cells (3% to 4%) (Figure 5(a)).

Similar to HZ mice, we tested CD69, CD62L, CD44, CXCR6-GFP, and integrin $\alpha_4\beta_7$ expression among ILC subsets in LP and mLN from KO mice. We show that the expression pattern of those markers was not significantly perturbed by CXCR6-deficiency (Figure 5(b)).

Then, we tested whether each of the ILC subsets was similarly distributed between the different stages of proliferation (Figure 5(c)). We defined that there was an important increase (up to two fold increase) in Ki67$^+$ cells amongst cNK-ILC1 and all ILC3 subsets between HZ or wt control and CXCR6-deficient conditions (Figures 5(c) and 5(d)). In contrast, the Ki67$^+$ frequency of ILC2 cells remained unchanged. Additionally, DAPI staining showed that all ILC subsets were enriched in cells that were in S-G2-M stages (i.e., DAPI$^+$) in the CXCR6-deficient condition (Figure 5(e)). These results show that intestinal ILC1 and ILC3 compartments, and to a certain extent ILC2, were seeded with dividing DAPI$^+$ and active recently divided Ki67$^+$ cells, after CXCR6 ablation.

We analyzed the putative *in situ* intestinal ILC precursor fraction that is isolated as Lin$^-$ NKp46$^-$ NK1.1$^-$ GATA3$^-$ RORγt$^-$ IL-7Rα^+ cells (Figure 5(f)). This fraction, gated using surrogate markers as described to identify ILC subsets in *Cxcr6*$^{Gfp/+}$ *Id2*$^{Yfp/+}$ mice (as in Figure 4(a)), expresses CXCR6 and ID2 (Figure 5(f)). No difference in the frequency of those cells is observed, but they were significantly enriched in both Ki67$^+$ (active G1-S-G2 cells) and DAPI$^+$ (dividing S-G2-M cells) in CXCR6-deficient intestines (Figure 5(g)). This result determines that this compartment is highly active in the CXCR6-deficient mice and contributes to proliferation, thus differentiation to seed the respective mature ILC compartments.

In conclusion, these results show that *in situ* intestinal ILC precursor cells compensate a defect in homing to the intestine by homeostatically proliferating and result in a proper balance of diverse ILC compartments.

4. Discussion

ILCs share numerous characteristics with the T-helper cell subsets and we considered that they might have similarities in their trafficking features even if they do not have to encounter antigen. For naïve T lymphocytes, it was demonstrated that the intestinal homing marker $\alpha_4\beta_7$ is upregulated after their activation in the mLN [23]. For the ILC lineage, this intestinal homing marker is already expressed by their precursors in the bone marrow. Moreover, CXCR6 was also shown to be expressed by the most mature fraction of $\alpha_4\beta_7^+$ medular ILC precursors. Hence, CXCR6 may represent one of the chemokine receptors important for the egress and homing of ILC precursors. We decided to study the role of CXCR6 by comparing diverse features of ILC populations between *Cxcr6*$^{Gfp/+}$ and *Cxcr6*$^{Gfp/Gfp}$ mice in steady state conditions. We crossed our mouse models to obtain *Rag2*$^{-/-}$ *Cxcr6*$^{Gfp/+}$ and *Rag2*$^{-/-}$ *Cxcr6*$^{Gfp/Gfp}$ mice since most studies of ILC function count on *Rag2*$^{-/-}$ mice to avoid an important contamination of T cells.

The determination of CXCR6 expression fractions among the ID2$^+$ ILC precursors was performed using *Cxcr6*$^{Gfp/+}$

Id2$^{Yfp/+}$ double reporter mice and showed that the ILCP (Lin$^-$ IL-7Rα^+ Sca-1$^{-/lo}$ c-Kit^{med} Flt3$^-$ $\alpha_4\beta_7{}^+$) and ILC2P (Lin$^-$ IL-7Rα^+ Sca-1^{hi} c-Kit^{lo}) subsets are inversely enriched into CXCR6$^+$ precursors, with few CXCR6$^+$ cells among ILCP and a substantial fraction of CXCR6$^+$ cells among ILC2P.

Here, we showed that deficiency of the chemokine receptor CXCR6 leads to increased number of all bone marrow CXCR6-GFP ILC precursors in homeostatic conditions. This observation suggested that CXCR6 could either regulate the proliferation of ILCP/ILC2P or could be implicated in the egress of those precursors to the peripheral organs. Hence, we analyzed the proliferative status of the bone marrow progenitors and demonstrated that CXCR6 is not implicated in the proliferation of these progenitor pools but participates in their specific egress. Thus, we further analyzed how the CXCR6 expression affects the steady-state number of the different ILC subsets *in vivo* in the periphery. Intestinal lamina propria was analyzed for the repartition of the different ILC compartments in absence of CXCR6. Despite the retention of ILC precursors in the bone marrow, we observed comparable frequencies for mature ILC2 and ILC3 intestinal subsets between *Rag2*$^{-/-}$ *Cxcr6*$^{Gfp/+}$ and *Rag2*$^{-/-}$ *Cxcr6*$^{Gfp/Gfp}$ littermates. Hence, under homeostatic conditions, the deficiency in CXCR6 does not affect the distribution of ILC2 and ILC3 subsets in the intestine as also recently shown using CXCR6-deficient mice [16].

The absence of difference in ILC frequencies, at steady state, suggested that CXCR6 was not required for the development or tissue homing of ILC [16]. However, since we observed that the ILC precursors are partially retained in the bone marrow and previously showed their homing to the periphery for final differentiation towards the ILC3 lineage [14], we suspected CXCR6 as a specific chemokine receptor for initiating the ILCP egress and homing. Then, we decided to check for the seeding and frequency of this progenitor compartment in the periphery. No decrease in the frequency of this progenitor was observed. By analyzing its homeostatic *in situ* proliferation, we proved that increased proliferation of this progenitor in the intestine is one explanation for the normal distribution of ILC subsets in CXCR6-deficient mice despite the partial bone marrow retention.

We also used the combination of Ki67/DAPI to examine the mature ILC subsets and showed that, in CXCR6-deficient mice, all ILC subsets are more frequent in proliferation or in active state in the intestine. ILC subsets in the intestinal LP were already shown to be more activated than ILCs in other tissues, probably because of their constant exposure to varied environmental signals [24]. The analyses of intestinal Ki67$^+$ ILC subsets demonstrated that both recent proliferative ILC1 and ILC3 subsets stay in the intestine in CXCR6 deficient mice whereas ILC2 tends to leave the organ since no increase of Ki67$^+$ ILC2 cells was detected in CXCR6-deficient intestines. This result is consistent with the observation that intestinal ILC2 subsets express lower levels of the resident marker CD69 and lower levels of CXCR6 than ILC3 subsets. It has been previously shown that, in the intestinal lamina propria, the diverse ILC3 subsets express CXCR6 at different levels with higher levels for the NCR$^+$ ILC3 subset [25]. We found similar results in *Rag2*$^{-/-}$ *Cxcr6*$^{Gfp/+}$ intestines where the GFP expression is the highest in NCR$^+$ ILC3 and in most NCR$^-$ ILC3 cells and lower in both CD4$^+$ LTi-like ILC3 and a small NCR$^-$ ILC3 subset. In infectious conditions, a specific reduction of NCR$^+$ ILC3 subset was shown in CXCR6-deficient mice [25]. Indeed, *Citrobacter rodentium* infection challenges have recently defined that CXCR6 may highly contribute to the localization of NCR$^+$ ILC3 subsets and its capacity to eliminate the bacterial load. The CXCR6 ligand (CXCL16) is expressed in the intestine by a specific population of CX3CR1$^+$ DC cells [26] and was reported to be crucial for NCR$^+$ ILC3 stimulation and production of IL-22 [25]. However, the regulation of ILC function could be different depending on the ILC subset since numerous types of cells, such as epithelial cells, monocytes, and macrophages, also express CXCL16.

CXCR6 is also important for circulation of ILC3 and ILC3P in the embryo since we observed a significant decrease of RORγt$^+$ cells in the fetal liver of CXCR6-deficient mice. We already assessed the effect of CXCR6 deficiency in ILC3 fetal differentiation and demonstrated that CXCR6 deficiency does not affect ILC3 differentiation during embryogenesis [14]. Since *Cxcr6*$^{Gfp/Gfp}$ mice possess normal development of Peyer's patches and lymph nodes [14, 25], the homing of ILC3P is not impaired. However, circulation of these progenitors could be affected. Indeed, RORγt$^+$ cells are rare in the fetal liver and could be considered as partly derived from the circulation. Hence, we suspected an important role of CXCR6 for the recirculation of ILC3 precursors and ILC3 subsets. We demonstrated by reconstitution assays that, in absence of CXCR6 expression, ILC3P are unable to correctly reach the peripheral organs contrary to CXCR6-competent precursors. Reconstitutions were performed using i.v. injection suggesting that recirculation via the blood circuit is altered in absence of CXCR6 expression.

A study using Kaede transgenic mice demonstrated a constitutive trafficking of ILC from the gut to the mLN where LTi like-cells ILC3 migration was dependent on CCR7 in contrary to other ILC subsets [27]. The predominance of some ILC3 over other ILC subsets was already described in LN and it was observed that, in lymphopenic mLN, the ILC frequencies are altered [27], so we decided to look for ILC homing markers expression in both CXCR6 competent and deficient mLN but not for ILC respective repartition. We found that markers are maintained after CXCR6 loss and determined that ILCs were mainly trafficking between the intestine and mLN since they were all CD44$^+$ CD69$^-$ in mLN. All ILC subsets except some ILC1 were clearly negative for CD62L, showing no preferential circulation through lymphoid organs.

In conclusion, we provide here new data on the role of CXCR6 during circulation of ILC progenitors and ILC populations at steady state. ILC precursors that are deficient for CXCR6 are retained in the bone marrow and only few of them could reach the blood and colonize peripheral lymphoid organs to continue their maturation. However, we demonstrated that homeostatic proliferation is increased in these CXCR6 deficient animals to compensate for the

reduction of seeding precursors resulting in normal ILC subset distribution. Future studies concerning the function of this receptor during inflammation and infection should now take into account the importance of this receptor on ILC recirculation capacities.

Conflict of Interests

The authors declare that there is no conflict of interests regarding the publication of this paper.

Acknowledgments

The authors thank A. Goldrath for providing $Id2^{Yfp/+}$ mouse strain. This study is supported by the Ministère de la recherche (Sylvestre Chea, Thibaut Perchet), Association pour la Recherche sur le Cancer (Sylvestre Chea, Rachel Golub), Institut Pasteur (Ana Cumano), Université Paris Diderot (Rachel Golub, Sylvestre Chea, Thibaut Perchet), Institut National de la Santé et de la Recherche Médicale (Ana Cumano), Institut National du Cancer (Rachel Golub, Maxime Petit), and the Agence Nationale de Recherches (Rachel Golub).

References

[1] H. Spits, D. Artis, M. Colonna et al., "Innate lymphoid cells—a proposal for uniform nomenclature," *Nature Reviews Immunology*, vol. 13, no. 2, pp. 145–149, 2013.

[2] H. Spits and T. Cupedo, "Innate lymphoid cells: emerging insights in development, lineage relationships, and function," *Annual Review of Immunology*, vol. 30, pp. 647–675, 2012.

[3] N. Satoh-Takayama, C. A. J. Vosshenrich, S. Lesjean-Pottier et al., "Microbial flora drives interleukin 22 production in intestinal $NKp46^+$ cells that provide innate mucosal immune defense," *Immunity*, vol. 29, no. 6, pp. 958–970, 2008.

[4] Y. Zheng, P. A. Valdez, D. M. Danilenko et al., "Interleukin-22 mediates early host defense against attaching and effacing bacterial pathogens," *Nature Medicine*, vol. 14, no. 3, pp. 282–289, 2008.

[5] G. F. Sonnenberg, L. A. Monticelli, M. M. Elloso, L. A. Fouser, and D. Artis, "$CD4^+$ lymphoid tissue-inducer cells promote innate immunity in the gut," *Immunity*, vol. 34, no. 1, pp. 122–134, 2011.

[6] S. Buonocore, P. P. Ahern, H. H. Uhlig et al., "Innate lymphoid cells drive interleukin-23-dependent innate intestinal pathology," *Nature*, vol. 464, no. 7293, pp. 1371–1375, 2010.

[7] C. S. N. Klose, E. A. Kiss, V. Schwierzeck et al., "A T-bet gradient controls the fate and function of $CCR6^-RORγt^+$ innate lymphoid cells," *Nature*, vol. 494, no. 7436, pp. 261–265, 2013.

[8] S. Sawa, M. Cherrier, M. Lochner et al., "Lineage relationship analysis of RORgammat+ innate lymphoid cells," *Science*, vol. 330, no. 6004, pp. 665–669, 2010.

[9] K. Moro, T. Yamada, M. Tanabe et al., "Innate production of T_H2 cytokines by adipose tissue-associated $c\text{-}Kit^+Sca\text{-}1^+$ lymphoid cells," *Nature*, vol. 463, no. 7280, pp. 540–544, 2010.

[10] D. R. Neill, S. H. Wong, A. Bellosi et al., "Nuocytes represent a new innate effector leukocyte that mediates type-2 immunity," *Nature*, vol. 464, no. 7293, pp. 1367–1370, 2010.

[11] A. E. Price, H.-E. Liang, B. M. Sullivan et al., "Systemically dispersed innate IL-13-expressing cells in type 2 immunity," *Proceedings of the National Academy of Sciences of the United States of America*, vol. 107, no. 25, pp. 11489–11494, 2010.

[12] A. M. Owyang, C. Zaph, E. H. Wilson et al., "Interleukin 25 regulates type 2 cytokine-dependent immunity and limits chronic inflammation in the gastrointestinal tract," *Journal of Experimental Medicine*, vol. 203, no. 4, pp. 843–849, 2006.

[13] D. Guy-Grand, P. Vassalli, G. Eberl et al., "Origin, trafficking, and intraepithelial fate of gut-tropic T cells," *The Journal of Experimental Medicine*, vol. 210, no. 11, article 2493, 2013.

[14] C. Possot, S. Schmutz, S. Chea et al., "Notch signaling is necessary for adult, but not fetal, development of $RORγt^+$ innate lymphoid cells," *Nature Immunology*, vol. 12, no. 10, pp. 949–958, 2011.

[15] F. Geissmann, T. O. Cameron, S. Sidobre et al., "Intravascular immune surveillance by CXCR6+ NKT cells patrolling liver sinusoids," *PLoS Biology*, vol. 3, no. 4, Article ID e113, 2005.

[16] M. L. Robinette, A. Fuchs, V. S. Cortez et al., "Transcriptional programs define molecular characteristics of innate lymphoid cell classes and subsets," *Nature Immunology*, vol. 16, no. 3, pp. 306–317, 2015.

[17] S. Paust, H. S. Gill, B.-Z. Wang et al., "Critical role for the chemokine receptor CXCR6 in NK cell-mediated antigen-specific memory of haptens and viruses," *Nature Immunology*, vol. 11, no. 12, pp. 1127–1135, 2010.

[18] C. Y. Yang, J. A. Best, J. Knell et al., "The transcriptional regulators Id2 and Id3 control the formation of distinct memory $CD8^+$ T cell subsets," *Nature Immunology*, vol. 12, no. 12, pp. 1221–1229, 2011.

[19] C. S. N. Klose, M. Flach, L. Möhle et al., "Differentiation of type 1 ILCs from a common progenitor to all helper-like innate lymphoid cell lineages," *Cell*, vol. 157, no. 2, pp. 340–356, 2014.

[20] W. Xu, R. G. Domingues, D. Fonseca-Pereira et al., "NFIL3 orchestrates the emergence of common helper innate lymphoid cell precursors," *Cell Reports*, vol. 10, no. 12, pp. 2043–2054, 2015.

[21] L. R. Shiow, D. B. Rosen, N. Brdičková et al., "CD69 acts downstream of interferon-α/β to inhibit $S1P_1$ and lymphocyte egress from lymphoid organs," *Nature*, vol. 440, no. 7083, pp. 540–544, 2006.

[22] A. J. Bankovich, L. R. Shiow, and J. G. Cyster, "CD69 suppresses sphingosine 1-phosophate receptor-1 (S1P1) function through interaction with membrane helix 4," *Journal of Biological Chemistry*, vol. 285, no. 29, pp. 22328–22337, 2010.

[23] D. J. Campbell and E. C. Butcher, "Rapid acquisition of tissue-specific homing phenotypes by $CD4^+$ T cells activated in cutaneous or mucosal lymphoid tissues," *Journal of Experimental Medicine*, vol. 195, no. 1, pp. 135–141, 2002.

[24] E. A. Kiss, C. Vonarbourg, S. Kopfmann et al., "Natural aryl hydrocarbon receptor ligands control organogenesis of intestinal lymphoid follicles," *Science*, vol. 334, no. 6062, pp. 1561–1565, 2011.

[25] N. Satoh-Takayama, N. Serafini, T. Verrier et al., "The chemokine receptor CXCR6 controls the functional topography of interleukin-22 producing intestinal innate lymphoid cells," *Immunity*, vol. 41, no. 5, pp. 776–788, 2014.

[26] P. Ancuta, K.-Y. Liu, V. Misra et al., "Transcriptional profiling reveals developmental relationship and distinct biological functions of CD16+ and CD16- monocyte subsets," *BMC Genomics*, vol. 10, article 403, 2009.

[27] E. C. Mackley, S. Houston, C. L. Marriott et al., "CCR7-dependent trafficking of RORγ^+ ILCs creates a unique microenvironment within mucosal draining lymph nodes," *Nature Communications*, vol. 6, article 5862, 2015.

nature immunology

Evidence of innate lymphoid cell redundancy in humans

Frédéric Vély[1,2,20], Vincent Barlogis[3,20], Blandine Vallentin[3,20], Bénédicte Neven[4–7,20], Christelle Piperoglou[1,2], Mikael Ebbo[1,8], Thibaut Perchet[9,10], Maxime Petit[9,10], Nadia Yessaad[11], Fabien Touzot[5,12], Julie Bruneau[5,13], Nizar Mahlaoui[4–7], Nicolas Zucchini[14], Catherine Farnarier[2], Gérard Michel[3], Despina Moshous[4–7], Stéphane Blanche[4–7], Arnaud Dujardin[15], Hergen Spits[16], Jörg H W Distler[17], Andreas Ramming[17], Capucine Picard[4–7,18], Rachel Golub[9,10], Alain Fischer[4–7,19,21] & Eric Vivier[1,2,21]

Innate lymphoid cells (ILCs) have potent immunological functions in experimental conditions in mice, but their contributions to immunity in natural conditions in humans have remained unclear. We investigated the presence of ILCs in a cohort of patients with severe combined immunodeficiency (SCID). All ILC subsets were absent in patients with SCID who had mutation of the gene encoding the common γ-chain cytokine receptor subunit IL-2Rγ or the gene encoding the tyrosine kinase JAK3. T cell reconstitution was observed in patients with SCID after hematopoietic stem cell transplantation (HSCT), but the patients still had considerably fewer ILCs in the absence of myeloablation than did healthy control subjects, with the exception of rare cases of reconstitution of the ILC1 subset of ILCs. Notably, the ILC deficiencies observed were not associated with any particular susceptibility to disease, with follow-up extending from 7 years to 39 years after HSCT. We thus report here selective ILC deficiency in humans and show that ILCs might be dispensable in natural conditions, if T cells are present and B cell function is preserved.

ILCs include natural killer (NK) cells and three other main subsets, ILC1, ILC2 and ILC3, referred as to 'helper-like ILCs'[1–3]. Since their discovery, ILCs have been shown to contribute to wound healing and defense against infection, and studies have revealed critical aspects of their differentiation. However, much of the role of ILCs remains to be elucidated, particularly given the diversity of these cells, which adds to the complexity of their analysis.

Unlike T cells and B cells, ILCs do not express antigen-specific receptors derived from gene rearrangements dependent on RAG recombinases. Other than that major difference in their recognition repertoire, the ILC and T cell subsets display striking similarities, as ILC1s, ILC2s and ILC3s are driven by the transcription factors T-bet, GATA-3 and RORγt, respectively, and produce the cytokines IFN-γ (ILC1s), interleukin 5 (IL-5) and IL-13 (ILC2s), and IL-17 and IL-22 (ILC3s)[1–3]. In addition, NK cells are driven by the transcription factors Eomes and T-bet, can be cytolytic and produce interferon-γ (IFN-γ), like $CD8^+$ T cells. Such similarity of features has led to the suggestion that ILCs are the innate counterparts of T cells[1–3]. During the course of evolution, two highly parallel systems have thus emerged, with ILCs mimicking the effector profile of T cell subsets. However, it remains unclear how these two systems are integrated in natural conditions in humans.

In mice, all ILCs are generated by a transcription-factor-Id2-dependent pathway from a common lymphoid progenitor, which initially differentiates into a common ILC precursor. The common ILC precursors differentiate into three precursors and give rise to three different lineages: NK-cell precursors, lymphoid-tissue-inducer-cell precursors, and common-helper-innate-lymphoid-cell precursors. Common-helper-innate-lymphoid-cell precursors express the transcription factor PLZF and give rise to the ILC1, ILC2 and ILC3 subsets. Lymphoid-tissue-inducer cells are essential for the development of secondary lymphoid organs, such as lymph nodes and Peyer's patches in mice. In contrast, ILC differentiation in humans is less well understood[4]. NK-cell progenitors with a $Lin^-CD34^+CD38^+CD123^-CD45RA^+CD7^+CD10^+CD127^-$ phenotype have been found in the bone marrow, cord blood and tonsils[5]. These cells differentiate exclusively into NK cells and are unable to generate ILC2, ILC3 or other lineages. ILC3 progenitors have been identified in human tonsils

[1]Aix Marseille Université, CNRS, INSERM, CIML, Marseille, France. [2]APHM, Hôpital de la Conception, Service d'Immunologie, Marseille, France. [3]APHM, Hôpital de la Timone, Service d'Hématologie et Oncologie Pédiatrique, Marseille, France. [4]APHP, Hôpital Universitaire Necker-Enfants Malades, Centre de Référence Déficits Immunitaires Héréditaires, Paris, France. [5]Université Paris Descartes–Sorbonne Paris Cité, Institut Imagine, Paris, France. [6]INSERM, Paris, France. [7]APHP, Hôpital Universitaire Necker-Enfants Malades, Unité d'Immunologie-Hématologie et Rhumatologie Pédiatrique, Paris, France. [8]APHM, Hôpital de la Timone, Service de Médecine Interne, Marseille, France. [9]Institut Pasteur, Unité de Lymphopoièse, INSERM, Paris, France. [10]Université Paris Diderot, Sorbonne Paris Cité, Cellule Pasteur, Paris, France. [11]MI-mAbs consortium, Aix-Marseille University, Marseille, France. [12]APHP, Hôpital Necker-Enfants Malades, Biotherapy Unit, Paris, France. [13]APHP, Hôpital Necker-Enfants Malades, Service d'anatomopathologie, Paris, France. [14]BD Biosciences, Le Pont-de-Claix, France. [15]Innate-Pharma, Marseille, France. [16]Academic Medical Center at the University of Amsterdam, Arizona Amsterdam, the Netherlands. [17]Department of Internal Medicine, Rheumatology & Immunology, University of Erlangen-Nuremberg, Erlangen, Germany. [18]APHP, Hôpital Necker-Enfants Malades, Study Center of Immunodeficiencies, Paris, France. [19]College de France, Paris, France. [20]These authors contributed equally to this work. [21]These authors jointly directed this work. Correspondence should be addressed to A.F. (alain.fischer@aphp.fr) or E.V. (vivier@ciml.univ-mrs.fr).

Received 29 March; accepted 3 August; published online 12 September 2016; corrected after print 19 October 2016; doi:10.1038/ni.3553

and intestinal lamina propria but not in the bone marrow, thymus or peripheral blood[6]. A Lin$^-$CD34$^+$CD45RA$^+$CD117$^+$IL-1R1$^+$RORγt$^+$ progenitor population expressing Id2 has been shown to give rise *in vitro* to all ILCs, including NK cells, but not other leukocyte lineages[7]. This RORγt$^+$ progenitor is present selectively in the tonsils, lymph nodes and spleen but not in the peripheral blood, bone marrow, umbilical cord blood or thymus[7].

SCID is a life-threatening condition that affects infants and is characterized by defective T cell development associated with various deficiencies of other cell lineages, such as NK cells, B cells and myeloid cells[8,9]. Patients present with profound abnormalities in immunity that lead to severe recurrent and fatal infections. The life-threatening nature of SCID requires treatment by allogeneic HSCT or gene therapy to resolve the immunodeficiency syndrome[9–11]. HSCT often requires that the patients be treated with a conditioning regimen to induce myeloablation and hence favors engraftment. Some patients with SCID who have mutation of *IL2RG* or autosomal-recessive mutation of *JAK3*. Both these types of mutation result in a complete block in the development of T cells and NK cells[12]. We delineated here the differentiation and function of human ILCs by analyzing these cells in patients with SCID resulting from mutation of *IL2RG* or *JAK3*, before and after treatment by allogeneic HSCT. We found that these patients were ILC deficient before HSCT and continued to display ILC deficiency after HSCT in the absence of myeloablation. No particular susceptibility to disease was observed in these patients. Together with published findings of mice[13,14], these results provide evidence for possible redundancy of the protective immunological function of ILCs in the presence of a functional adaptive immune system.

RESULTS

Circulating ILCs in healthy children and adults

The ILC1, ILC2 and ILC3 subsets are present mainly as sedentary cells in tissues, in which they can be maintained by self-renewal[15]. Nevertheless, cells of these ILC subsets are detectable in human peripheral blood[16–18]. Using a panel of conventional lineage markers (lineage (Lin): CD3, CD19, CD14, TCRαβ, TCRγδ, CD94, CD16, FcεRI, CD34, CD123 and CD303) and cell-surface expression of CD127, CD117 and CRTH2, we identified the ILC1 subset as Lin$^-$CD127$^+$CD117$^-$CRTH2$^-$ cells, the ILC2 subset as Lin$^-$CD127$^+$CRTH2$^+$ cells and the ILC3 subset as Lin$^-$CD127$^+$CD117$^+$CRTH2$^-$ cells, among the circulating lymphocytes. NK cells were classically defined as CD3$^-$CD56$^+$ lymphocytes (**Fig. 1a**). All ILC subsets were detected in the peripheral blood of healthy children (6–18 years) and adults (**Fig. 1b**,**c**, **Table 1** and **Supplementary Table 1**). NK cells were by far the most abundant circulating ILCs (with a median of 215 × 10^3 cells per ml in healthy children and 265 × 10^3 cells per ml in adults); the total number of ILCs was only 3.8 × 10^3 cells per ml in healthy children and 1.6 × 10^3 cells per ml in adults (**Fig. 1b**,**c**, **Table 1** and **Supplementary Table 1**). The number and frequency of helper-like ILCs among peripheral blood lymphocytes decreased with age (**Fig. 1b**), whereas this trend was not observed for NK cells (**Fig. 1c**). We also investigated whether there was any association between the number of circulating ILC1s and that of circulating ILC2s or ILC3s in healthy subjects and whether there was an effect of the subject's sex on these values. In accordance with the common origin of helper-like ILCs, there was a strong positive correlation between the absolute number of ILC2s and that of ILC3s in children and adults and there was a weak or moderate positive relationship for ILC1s and other ILCs (**Supplementary Fig. 1**). However, there was no difference related to the subjects' sex (data not shown). Consistent with the greater number of ILCs in children, the abundance of ILCs was greater in umbilical cord blood than in the peripheral blood of children or adults (**Fig. 1d**). The ILC1, ILC2 and ILC3 subsets in the circulation or cord blood displayed an equivalent frequency of total helper-like ILCs, and this distribution remained stable across age groups (**Fig. 1e**). Together, these results established normal values for human circulating ILCs under natural conditions that were consistent with those reported previously for adults[19], and they paved the way for comparisons with data of circulating ILCs for patients with various pathological conditions.

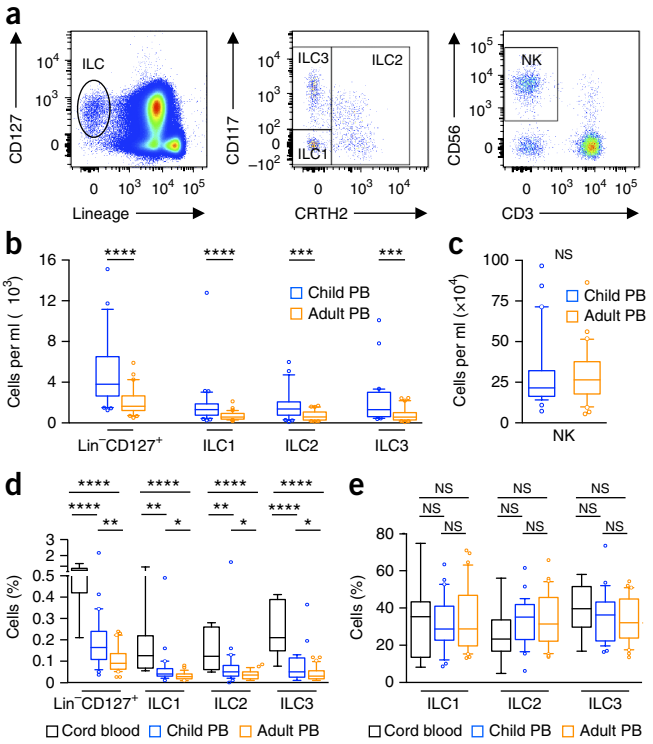

Figure 1 Normal abundance of ILCs in the peripheral blood of healthy pediatric and adult subjects. (**a**) Flow cytometry of cells in the peripheral blood of healthy humans, defining ILCs within the CD45$^+$ lymphocyte gate as Lin$^-$CD127$^+$ cells (with a lineage 'cocktail' of antibodies to CD3, CD19, CD14, TCRαβ, TCRγδ, CD94, CD16, FcεRI, CD34, CD123 and CD303) (left), and identifying the ILC subsets as CD117$^-$CRTH2$^-$ cells (ILC1), CRTH2$^+$ cells (ILC2) and CD117$^+$CRTH2$^-$ cells (ILC3) among the Lin$^-$CD127$^+$ gated at left (middle), and NK cells as CD3$^-$CD56$^+$ cells in the CD45$^+$ lymphocyte gate (right). (**b**,**c**) Quantification of ILCs (Lin$^-$CD127$^+$), ILC1s, ILC2s and ILC3s (**b**) and NK cells (defined as in **a**) (**c**) in the peripheral blood (PB) of healthy children (n = 29) and adults (n = 30) (key). (**d**,**e**) Frequency of ILC1s, ILC2s and ILC3s among lymphocytes (**d**) or helper-like ILCs (**e**) in cord blood or in the peripheral blood of healthy children and adults (key). Each symbol (**b**–**e**) represents an outlier (error bars, 10th and 90th percentiles). NS, not significant ($P > 0.05$); *$P < 0.05$, **$P < 0.01$, ***$P < 0.001$ and ****$P < 0.0001$ (Mann-Whitney test). Data are from one experiment representative of more than 60 independent experiments with similar results (**a**), or 29 (children) or 30 (adults) or 7 (cord blood) experiments with one subject in each (**b**–**e**).

Lack of circulating ILCs in SCID with JAK3 deficiency

The ILC1, ILC2 and ILC3 subsets are dependent on IL-7, whereas NK cells are dependent on IL-15 (ref. 20). The IL-7 and IL-15 signals are integrated via IL-2Rγ and JAK3. NK-cell deficiency is a known hallmark of typical cases of deficiency in IL-2Rγ or JAK3 (ref. 12). We therefore assessed the presence of other ILCs in patients with SCID who had genetic deficiency in this pathway. Our cohort comprised 28 patients with SCID (12 deficient in IL-2Rγ, 9 deficient in JAK3,

Table 1 Distribution and quantification of peripheral blood ILC subsets in healthy subjects

	NK cell		ILC1		ILC2		ILC3	
	Frequency	Cells (per µl)	Frequency	Cells (per ml)	Frequency	Cells (per ml)	Frequency	Cells (per ml)
Children	8.3% (4.9–17.0%)	215 (141–714)	30% (12–55%)	1303 (387–3116)	32% (17–45%)	1348 (88–3214)	34% (20–52%)	1047 (380–3199)
Adults	12.6% (6.4–24.6%)	265 (98–514)	29% (15–63%)	468 (249–1218)	31% (15–54%)	585 (153–1566)	32% (18–52%)	513 (180–2186)

Frequency of NK cells in the lymphocyte gate, frequency of ILC subsets in the ILC gate, and absolute number of NK cells (per µl) and ILC subsets (per ml) in the peripheral blood of healthy children ($n = 29$) and adults ($n = 30$), compiled from flow cytometry as in **Figure 1** and presented as median values (10th and 90th percentiles in parentheses). Data are representative of one experiment per donor.

and 7 deficient in RAG1 or RAG2) and 6 control subjects (**Table 2** and **Supplementary Table 1**). Among these 28 patients with SCID, we were able to monitor circulating ILCs before HSCT in 5 patients and after HSCT in 20 patients (**Table 2** and **Supplementary Table 1**). Before HSCT, no circulating ILCs were detected in the peripheral blood of three of patients with SCID who had JAK3 deficiency (patients P19, P20 and P21) (**Fig. 2**). These data were consistent with the absence of tonsils and palpable lymph nodes shown before in patients with SCID[8,21,22] and suggested an absence of the lymphoid-tissue-inducer subset of ILCs in patients with this condition. In contrast, the ILC compartment was phenotypically normal in patients with RAG1 deficiency (patients C11 and C12) (**Supplementary Fig. 2**), consistent with the lack of a requirement for RAG-dependent DNA-recombination events in the development of ILCs in mice[2,3,23–25].

ILC deficiency in SCID treated with non-myeloablative HSCT

We studied patients with SCID who were deficient in IL-2Rγc or JAK3 ($n = 18$; P1–P18) and had undergone HSCT 7–39 years before the ILC analysis, with mild myeloablation or no myeloablation (except for P4), and analyzed the reconstitution of ILCs in these patients (**Table 2** and **Supplementary Table 1**). This cohort consisted of 7 children (P1–P7) and 11 adults (P8–P18) with mutation of *IL2RG* (12 patients) or *JAK3* (6 patients). We also analyzed circulating or tissue-resident ILCs in 6 patients with SCID who had mutation of *RAG1* or *RAG2* that resulted in selective impairment in the development of T cells and B cells and who underwent HSCT after myeloablation (C1, C2, C10, C11 and C13). T cell reconstitution was observed in both groups of patients[26] (**Fig. 3**). In almost all patients with SCID of the first group who underwent HSCT without myeloablation, our analysis

Table 2 Clinical characteristics of patients

Subject	Diagnosis	Samples after HSCT		Age at HSCT (years)	Time between HSCT & ILC evaluation (years)	Donor origin	Conditioning regimen	T cell depletion	ATG (mg/kg)	Time between HSCT & final chimerism evaluation (years)	Final chimerism evaluation	
		Blood	Tissue								Lymphoid	Myeloid
P1	γC	+	+	0.7	12.8	MMRD	0	CD34 pos	0	1.8	1	2
P2	JAK3	+	–	0.6	10.8	MMRD	0	CD34 pos	10	0.7	1	3
P3	γC	+	+	0.6	10.6	MMRD	0	CD34 pos	10	1	1	2
P4	JAK3	+	–	0.4	10.5	MMRD	Bu 16 + Cy 200	CD34 pos	10	10.5	1	1
P5	γC	+	+	0.33	10.4	MMRD	0	CD34 pos	5	10	1	2
P6	γC	+	–	0.75	8.7	PRD	0	0	0	ND	ND	ND
P7	JAK3	+	–	0.6	7.0	MSD	0	0	0	2.4	1	2
P8	γC	+	–	0.1	39.4	PRD	0	0	0	27.8	1	2
P9	JAK3	+	–	1.1	30.3	MMRD	Bu 8 + Cy 200	E-ros	10	18.1	1	2
P10	JAK3	+	–	0.8	32.3	MMRD	0	E-ros	0	8.6	1	2
P11	JAK3	+	+	0.6	29.7	PRD	0	0	0	25	1	2
P12	γC	+	–	0.6	27.5	MMRD	Bu 8 + Cy 200	mAb	0	3.9	1	2
P13	γC	+	–	0.15	26.3	MMRD	Bu 8 + Cy 200	mAb	0	16.7	1	2
P14	γC	+	+	0.5	23.0	PRD	0		0	11.0	1	2
P15	γC	+	+	0.7	22.2	MMRD	Bu 8 + Cy 200	mAb	0	9.9	1	2
P16	γC	+	+	1.2	20.1	MMRD	0	mAb	0	8.9	1	2
P17	γC	+	–	0.5	21.4	MMRD	Bu 8 + Cy 200	mAb	0	2.3	1	2
P18	γC	+	–	0.8	17.4	MMRD	0	CD34 pos	0	6.2	1	2
C1	RAG1	+	–	0.6	8.5	UUCB	Bu 12.8 + Cy 200	CD34 pos	7.5	4.4	1	1
C2	RAG1	+	–	0.9	10.5	MMRD	Bu 16 + Cy 200	CD34 pos	10	2	1	1
C3	ALL	+	–	0.5	4.4	UUCB	Bu 12 + Cy 200	CD34 pos	7.5	4.4	1	1
C4	SAA	+	–	0.7	5.2	MUD	Flu 120 + Cy 200	CD34 pos	7.5	6.4	1	1
C5	ALL	+	–	6.5	5.3	UUCB	Flu 75 + Cy 120 + TBI	CD34 pos	0	4.7	1	1
C6	AML	+	–	6.8	13.5	MSD	Bu 14 + Cy 200	CD34 pos	0	11.7	1	1
C7	ALL	+	–	5.4	12.7	UUCB	Cy 120 + TBI	CD34 pos	0	12.5	1	1
C8	SAA	+	–	9.5	8.2	MSD	Cy 200	CD34 pos	12.5	8.3	1	1
C9	RAG1	–	+	0.33	ND	PRD	0	0	0	ND	ND	ND
C10	RAG2	–	+	0.55	ND	MMRD	Bu 12.8 + Cy 200	CD34 pos	10	0.4	1	1
C11	RAG1	–	+	0.33	4.1	MMRD	Bu 16 + Flu + TT	CD34 pos	10	0.3	NA	1
C13	RAG1	–	+	0.15	ND	MMRD	Bu 16 + Cy 200	CD34 pos	10	0.2	NA	1

Characteristics of pediatric (P1–P7) and adult (P8–P18) patients with SCID, and patients with complete donor chimerism (C1–C13), for whom ILCs were evaluated after grafting; C12, P19, P20 and P21 are not included here because their ILCs were evaluated only before transplantation. Patients were diagnosed as having mutation of *IL2RG* (γC), *JAK3* (JAK3), *RAG1* (RAG1) or *RAG2* (RAG2), or acute lymphoblastic leukemia (ALL), acute myeloid leukemia (AML) or severe aplastic anemia (SAA). Donor origins of the transplanted tissue include mismatched-related donor (MMRD), 'pheno-related donor' (PRD; related donor with more than one compatible HLA haplotype but not genetically identical), umbilical cord blood from an unrelated donor (UUCB), matched unrelated donor (MUD) or matched sibling donor (MSD). Conditioning regimens provided before transplantation included no conditioning (0), busulfan (BU; mg per kg body weight (total dose)), cyclophosphamide (Cy; mg per kg body weight (total dose)), fludarabine (Flu; mg per m^2 of skin (total dose)), total body irradiation (TBI) or thiotepa (TT). Patient samples also underwent depletion of T cells via positive selection of $CD34^+$ cells (CD34 pos) or negative selection by mAb (mAb), or E-rosetting (E-ros), or no depletion of T cells (0). The final chimerism is defined as donor chimerism (1), host myeloid chimerism (2) or mixed myeloid chimerism (3). ND, not done; NA, not applicable (no lymphocyte reconstitution at chimerism evaluation).

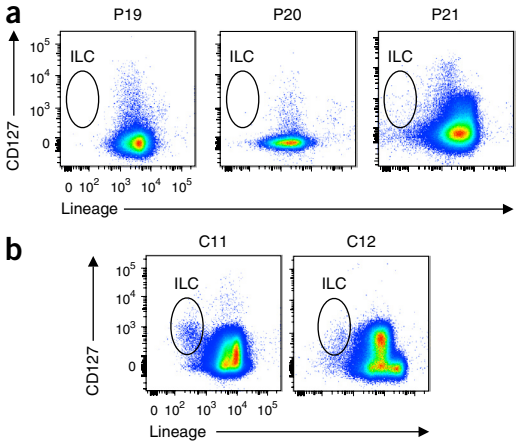

Figure 2 Severe ILC lymphopenia in patients with SCID who have mutation of *JAK3*. Flow cytometry of cells from patients with SCID and mutation of *JAK3* (P19, P20 and P21) (**a**) or *RAG1* (C11 and C12) (**b**), assessed before HSCT (control), showing ILC staining (as in **Fig. 1a**). Data are representative of one experiment per subject.

revealed a highly specific split chimerism, with the T cells of donor origin and the other leukocyte subsets of host origin[27] (**Table 2**). In the patients with SCID who had mutation of *RAG1* or *RAG2*, long-term analysis revealed complete donor chimerism (**Table 2**), which provided evidence of donor HSC engraftment. The ILC2 and ILC3 subsets were barely detectable in the peripheral blood of pediatric patients (**Fig. 3a**) or adult patients (**Fig. 3b**) with SCID who had mutation of *IL2RG* or *JAK3* and were undergoing HSCT. Consistent with published studies[26], circulating NK cells were either undetectable or present in only very low numbers in all of these patients (**Fig. 3**). Similarly, ILC1s were generally undetectable, but a small number of ILC1s were present in a few children and adults (**Fig. 3**). However, a large number of ILC1s were present in one child who was otherwise healthy (P1) and one adult with chronic lung infections (P12) (**Fig. 3**). Human ILC1s are highly heterogeneous, and published findings indicate that ILC1s include cells that synthesize transcripts encoding variable regions of the T cell antigen receptor[28,29] and other molecules typically expressed by T cells, such as CD4, CD5, CD6, CD28 and CD27 (refs. 29,30). Indeed, most of the ILC1s in HSCT-treated patients with SCID and healthy control subjects were $CD5^+$ (**Supplementary Fig. 3**). These results suggested that a substantial fraction of these ILC1s might have belonged to the T cell lineage and that the number of true ILC1s that reconstituted HSCT-treated patients with SCID might have been even lower than that estimated by the classic $Lin^-CD127^+CD117^-CRTH2^-$ cell-surface-phenotype analysis. Nevertheless, our results showed that patients with SCID who had mutation of *IL2RG* or *JAK3* continued to display ILC deficiency after HSCT in the absence of myeloablation.

One obvious limitation of the analysis above was the lack of data on tissue-resident ILCs. We obtained skin and gut biopsies from patients with SCID who had mutation of *IL2RG* or *JAK3* and were treated with non-myeloablative HSCT (patients P1, P3, P5, P11, P14 and P16) and generated paraffin-embedded and frozen tissue sections from the biopsies (**Table 2**). With the exception of the biopsies of P3, these biopsies were performed 1–10 years after HSCT. We assessed the presence of all $NKp46^+$ cell subsets of ILCs (i.e., NK cells[2], tissue-resident $CD127^-$ ILC1s[31] and NCR^+ ILC3s[2]) in these samples on the basis of positive staining for the activating receptor NKp46 and an absence of expression of the invariant signaling protein CD3ε. This analysis was made possible by the generation of a monoclonal antibody to human NKp46 screened for its reactivity to paraffin-embedded tissues. In these tissues, $NKp46^+$ ILCs were not detected or were barely detectable in three of the patients we assessed (**Fig. 4a**). We also analyzed frozen sections of gut biopsies from two patients (P1 and P3); in P3, T cells ($CD3^+$) were detected but no cell-associated NKp46 staining was detectable, in contrast to the results obtained for control sections (**Supplementary Fig. 4**).

We also sought to analyze ILC2s in tissue sections corresponding to those assessed for $NKp46^+$ ILCs. However, the consensus marker for ILC2s, CRTH2, could not be used for analysis of tissue sections due to the lack of reliable reagent. An alternative involved reliance on immunofluorescence staining based on the $CD3^-CD11b^-ICOS^+ST2^+$ and

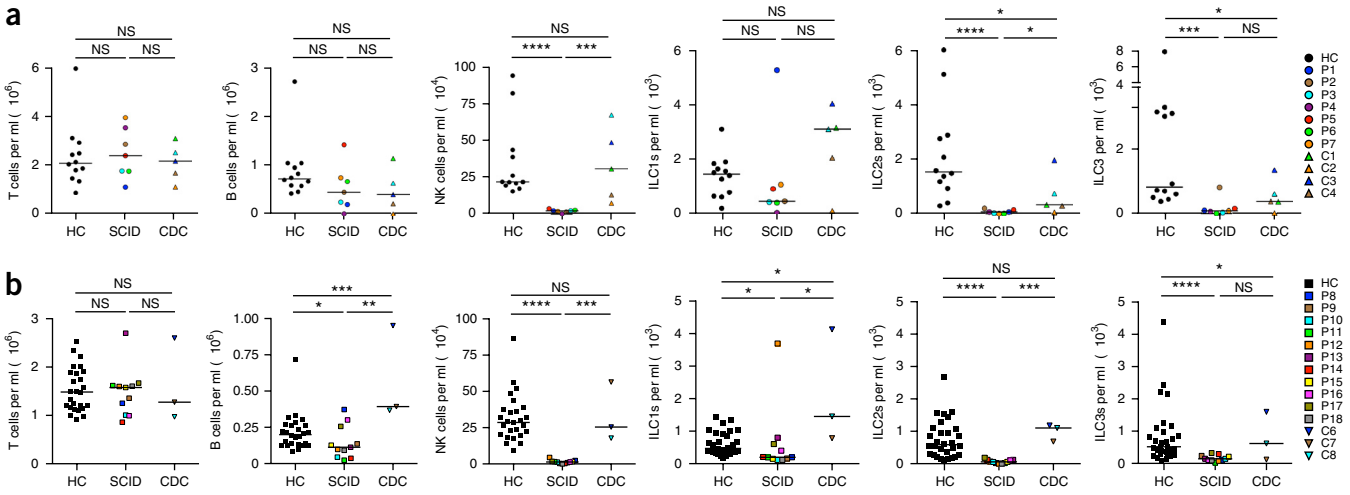

Figure 3 Long-term ILC lymphopenia in HSCT-treated patients with SCID. Absolute number of $CD3^+$ T cells, $CD19^+$ B cells and $CD3^-CD56^+$ NK cells or ILC subsets in the peripheral blood of 6- to 14-year-old healthy control subjects (HC; $n = 12$), patients with SCID who have mutation of *IL2RG* or *JAK3* (SCID; $n = 7$) and patients with complete donor chimerism (CDC; $n = 5$) (**a**) or of healthy adult control subjects ($n = 26$), adult patients with SCID who have mutation of *IL2RG* or *JAK3* ($n = 11$) and adult patients with complete donor chimerism ($n = 3$). (**b**) Each symbol represents an individual donor (patient identifiers (key) correspond to those in **Tables 2** and **3**); small horizontal lines indicate the median. $^*P < 0.05$, $^{**}P < 0.01$, $^{***}P < 0.001$ and $^{****}P < 0.0001$ (Mann-Whitney test). Data are representative of one experiment per subject.

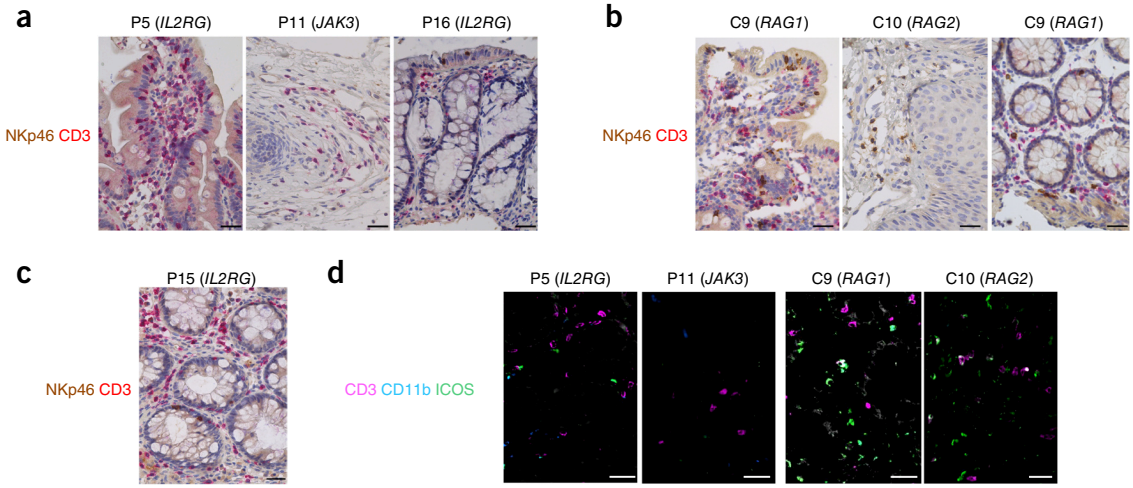

Figure 4 Intestinal and skin ILCs in HSCT-treated patients with SCID. (**a**) Microscopy of tissue sections from patients with SCID who were treated with non-myeloablative HSCT, stained as $CD3^-NKp46^+$ to identify tissue-resident $NKp46^+$ ILCs: duodenum from P5 (*IL2RG* mutation) (left), skin from P11 (*JAK3* mutation) (middle) and colon from P16 (*IL2RG* mutation) (right), at 10 years (P5), 18 years (P11) or 5.5 years (P16) after HSCT. (**b**) Microscopy of tissue sections from patients who were treated with HSCT (stained as in **a**): duodenum (left) or colon (right) from C9 (*RAG1* mutation) and skin from C10 (*RAG2* mutation) (middle), at 15 months (C9) or 4 months (C10) after HSCT. (**c**) Microscopy of a section of duodenum from a patient with SCID (P15; *IL2RG* mutation) at 15 months after treatment with myeloablative HSCT (stained as in **a**). (**d**) Microscopy of tissue sections from patients with SCID (colon from P5 and skin from P11 (as in **a**); colon from C9 and skin from C10 (as in **b**)), stained as $CD3^-CD11b^-ICOS^+$ to identify ILC2s. Scale bars, 50 µm. Data are representative of two experiments per subject.

$Lin^-CD34^-ST2^+IL\text{-}17RB^+KLRG1^+$ phenotypes, as described before[32]. However, the density of expression of the IL-33 receptor ST2 varies with ILC2 activation[33]; therefore, ST2 expression did not seem as reliable as CRTH2 staining was for the identification of circulating ILC2s. We thus used the $CD3^-CD11b^-ICOS^+$ phenotype to evaluate the presence of ILC2s in gut and skin. In these tissues, ILC2s were barely detectable in sections from patients with SCID who had mutation of *IL2RG* or *JAK3* and were treated with non-myeloablative HSCT (**Fig. 4d**). We drew similar conclusions by analysis of $Lin^-CD34^-KLRG1^+$ staining (data not shown). The specificity of our staining protocols was confirmed by the absence of detectable staining in tissues of cytopenic patients with SCID who had mutation of *RAG1* (C11 and C13), obtained 3 months after failure of HSCT performed in myeloablative conditions (**Supplementary Fig. 5**). Thus, patients with SCID who had mutation of *IL2RG* or *JAK3* were deficient in circulating and tissue-resident ILCs, and this deficiency persisted after non-myeloblative HSCT.

ILC reconstitution in myeloablative HSCT

A question that can be raised from the results reported above is whether ILC reconstitution might no longer happen in post-natal life in patients with mutation of *IL2RG* or *JAK3*. Only one patient with SCID in this study who had mutation of *IL2RG* underwent myeloablative HSCT (P4) (**Table 2**). ILC reconstitution was not observed in the peripheral blood of this patient (P4) (**Fig. 3a**), which indicated that if myeloablation were one of the factors involved in the reconstitution of circulating ILCs in HSCT-treated patients with SCID, it was not the only parameter. However, partial tissue-resident reconstitution of ILCs was observed in patients treated with HSCT under mild myeloablative conditions (results for patient P15 presented here; **Fig. 4c**). We also analyzed long-term reconstitution (>4 years) of all subsets of circulating ILCs in patients undergoing myeloablative HSCT for acute lymphoblastic leukemia ($n = 3$), acute myelogenous leukemia ($n = 1$), aplastic anemia ($n = 2$) or SCID with *RAG1* mutation ($n = 2$). All these patients displayed complete donor chimerism (**Table 2**). In these settings, NK cells, ILC1s, ILC2s and ILC3s were detected (**Fig. 3**). The number of these cells in blood was heterogeneous, particularly for ILC1s (**Fig. 3**). For ILC2s and ILC3s, the number of cells in the blood was lower than that of age-matched controls for the pediatric patients (**Fig. 3a**) but was normal (ILC2) or close to normal (ILC3) in adults (**Fig. 3b**). As expected, complete reconstitution of NK cells was observed in pediatric and adult patients (**Fig. 3**). Thus, long-term reconstitution of circulating ILCs after HSCT was observed in these myeloablative conditions. In addition, $NKp46^+$ ILCs and ILC2s were readily observed in tissues from patients treated with myeloablative HSCT, as illustrated by the analysis of skin biopsies from a patient with SCID who had mutation of *RAG2* (C10) and was treated with myeloablative HSCT (**Fig. 4b**,**d**). Thus, ILCs were reconstituted postnatally. Therefore, ILC reconstitution occurred in humans after the transplantation of allogeneic hematopoietic grafts, but these cells developed only in myeloablative conditions. As a control, tissue-resident gut ILCs were observed in a patient with SCID who had mutation of *RAG1* (C9) but was treated with 'pheno-related' HSCT (related donor with more than one compatible HLA haplotype but not genetically identical) under non-myeloablative conditions (**Fig. 4b**,**d**). Our data also showed that the precursors of all ILC subsets were present in human bone marrow and cord blood, the two sources of hematopoietic cells used for HSCT for the patients with SCID in our cohort (**Table 2**).

ILC reconstitution in mouse HSCT

To further ascertain the lack of tissue-infiltrating ILCs in HSCT-treated patients, we used mouse models to mimic HSCT in myeloablative and non-myeloablative conditions. $CD45.2^+$ bone marrow LSK ($Lin^-Sca1^+cKit^+$) progenitors were sorted as both $Flt3^{int}$ multipotent progenitors and as $Flt3^+$ lymphoid-primed multipotent progenitors (**Supplementary Fig. 6a**) and were injected into sub-lethally irradiated or non-irradiated alymphoid $CD45.1^+$ *Rag2*$^{-/-}$*Il2rg*$^{-/-}$mice. At 3 weeks after HSCT, ILC populations from the liver, lungs and intestine of the recipient mice were analyzed. Lung ILC2 ($Lin^-Gata3^+CD127^+ICOS^+ST2^+$) populations were observed in all irradiated mice but were undetectable in all non-irradiated mice (**Fig. 5** and **Supplementary Fig. 6b**).

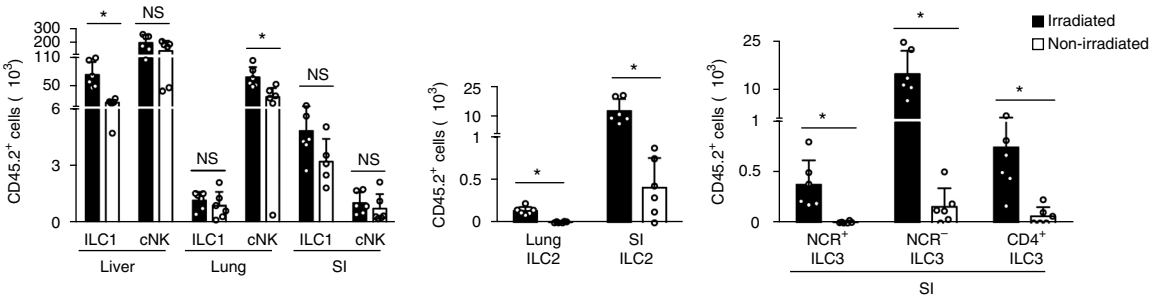

Figure 5 Reconstitution of ILCs after engraftment of adult multipotent progenitor cells into *Rag2*$^{-/-}$*Il2rg*$^{-/-}$ mice. Absolute number of cells in various ILC populations (horizontal axes) in the liver, lungs and small intestine (SI) of irradiated and non-irradiated (key) *Rag2*$^{-/-}$*Il2rg*$^{-/-}$ (CD45.1$^+$) recipient mice reconstituted with multipotent progenitors sorted (as in **Supplementary Fig. 6**) from the bone marrow of C57BL/6J (CD45.2$^+$) adult donor mice, analyzed by flow cytometry: donor-derived (CD45.2$^+$) hematopoietic populations were separated from their host (CD45.1$^+$) counterparts through the use of the congenic markers CD45.1 and CD45.2; ILC1s and NK cells from the lungs were identified as NKp46$^+$NK1.1$^+$IL-7Rα$^+$ and NKp46$^+$NK1.1$^+$IL-7Rα$^-$, respectively; ILC2s from the lungs were identified as Lin$^-$Gata3$^+$ IL-7Rα$^+$ cells co-expressing ICOS and ST2; ILC1s and NK cells from the liver were identified by expression of CD49a and CD49b, respectively, on NKp46$^+$NK1.1$^+$ populations; NK cell, ILC1, ILC2 and ILC3 populations from the lamina propria of the small intestine (SILP) were identified by expression of CD3, CD19, Thy1, CD4, NKp46, NK1.1, CD49a, CD49b, KLRG1, RORγt, Gata3 and IL-7Rα. Each symbol represents an individual mouse. *$P < 0.02$ (Mann-Whitney test). Data are representative of two experiments with three mice per condition (mean and s.d.).

Similarly, intestinal ILC2s (Lin$^-$CD127$^+$Gata3$^+$KLRG1$^+$) and intestinal NCR$^+$ ILC3s (Lin$^-$Thy1$^+$CD127$^+$NKp46$^+$RORγt$^+$), NCR$^-$ ILC3s (Lin$^-$Thy1$^+$CD127$^+$CD4$^-$NKp46$^-$RORγt$^+$) and lymphoid-tissue-inducer-like ILC3s (Lin$^-$Thy1$^+$CD127$^+$CD4$^+$NKp46$^-$RORγt$^+$) underwent reconstitution in the intestinal lamina propria of irradiated mice but were barely detectable in non-irradiated mice (**Fig. 5** and **Supplementary Fig. 6c**). Thus, reconstitution of ILC2s and ILC3s was effective in all sub-lethally irradiated recipients but not in non-irradiated recipient mice. The reconstitution was much more effective for ILC1s and NK cells than for ILC2s or ILC3s in non-myeloablative conditions, as intestinal lamina propria ILC1s (Lin$^-$NKp46$^+$NK1.1$^+$CD49a$^+$CD49b$^-$) and NK cells (Lin$^-$NKp46$^+$NK1.1$^+$CD49a$^-$CD49b$^+$) of donor origin were equally present in both irradiated mice and non-irradiated mice (**Fig. 5** and **Supplementary Fig. 6c**). Although liver ILC1s (Lin$^-$NKp46$^+$NK1.1$^+$CD49a$^+$CD49b$^-$) were detected in irradiated mice, they were lower in abundance in non-myeloablative conditions (**Fig. 5** and **Supplementary Fig. 6d**). Similarly, lung NK cells (Lin$^-$NKp46$^+$NK1.1$^+$CD127$^-$) underwent reconstitution in non-myeloablative conditions, but this was not as efficient as their reconstitution in irradiated mice (**Fig. 5** and **Supplementary Fig. 6b**). Nonetheless, circulating NK cells (Lin$^-$NKp46$^+$NK1.1$^+$CD49a$^-$CD49b$^+$) were detected in the recipient mice reconstituted in

Table 3 Clinical follow-up

Subject	Iv Ig	Common warts	Severe HPV	ENT infection	Diarrhea	Respiratory sequelae	Other
P1	1	0	0	1	1[a]	0	0
P2	0	0	0	0	0	0	0
P3	1	1	0	0	0	0	Pancreatic insufficiency
P4	0	0	0	0	0	0	0
P5	1	0	0	0	1	0	Hepatic granulomatous disease, IBD-like disease, onychomycosis
P6	0	1	1	0	0	0	0
P7	0	1	0	0	0	0	0
P8	1	0	0	0	0	0	0
P9	0	1	1	0	0	0	0
P10	0	0	0	1	0	0	0
P11	0	1	0	0	0	0	Epilepsy
P12	1	0	0	0	0	1	0
P13	1	0	0	0	0	0	Pheochromocytoma
P14	0	1	0	0	0	0	0
P15	1	0	0	0	0	0	0
P16	1	0	0	0	0	0	0
P17	0	1	0	0	0	0	0
P18	1	1	0	1	0	1	0
C1	0	0	0	0	0	0	0
C2	1[b]	0	0	0	0	0	0
C3	0	0	0	0	0	0	0
C4	0	0	0	0	0	0	0
C5	0	0	0	0	0	0	0
C6	0	0	0	0	0	0	0
C7	0	0	0	0	0	0	Mediastinal lymphoma after HSCT
C8	0	0	0	0	0	0	0

Clinical follow up of pediatric (P1–P7) and adult (P8–P18) patients with SCID, and patients with complete donor chimerism (C1–C8), from 2 years after HSCT until time of publication, presented as parameters that were present (1) or absent (0); P19, P20 and P21 are not included because their ILCs were evaluated before transplantation. Intravenous immunoglobulin (IVIG) indicates immunoglobulin replacement. Severe infection with human papilloma virus (HPV) is defined as more than 30 cutaneous lesions during at least 2 years. 'ENT infection' indicates infections of the ears, nose and throat. Respiratory sequelae include infection or disease.
[a]The inflammatory bowel disease (IBD)-like disease in this patient improved after a 'boost' of depletion of unconditioned T cells 2 years after HSCT. [b]This patient had no B cell reconstitution after monoclonal antibodies to the B cell–specific surface antigen CD20 were given for the treatment of autoimmune hemolytic anemia.

non-myeloablative conditions (data not shown), which indicated that the presence of ILCs in peripheral blood correlated with the presence of tissue-resident ILCs. The absence of ILC2 and ILC3 chimerism in non-myeloablative conditions in these mice supported the data obtained for HSCT-treated patients with SCID and suggested an inability of common-helper-innate-lymphoid-cell precursors in humans and in mice to fully differentiate into the appropriate niches, as they might compete with endogenous progenitors in these niches. This mechanism for the restriction of donor HSC engraftment by occupancy of niches by host HSCs was supported by data showing that the clearance of HSC niches via antibody treatment leads to efficient transplantation[34].

Human ILC deficiency is not associated with disease

In HSCT-treated patients with SCID, we observed no increase, relative to normal values, in non-conventional T-cell subsets, such as γδ T cells or $V_{\alpha}24^{+}V_{\beta}11^{+}$ NKT cells that could compensate for the absence of ILCs on the basis of similarities in effector function (**Supplementary Fig. 7a**,**b**). The almost total absence of ILCs in these patients thus provided us with a highly informative situation for evaluating the function of ILCs in natural conditions in humans. Notably, this situation of persistent ILC deficiency had no major clinical consequences over very long periods of follow-up (7–39 years) (**Table 3**). This cohort of patients was no more prone to infection or inflammation than were those undergoing HSCT for other types of SCID with or without myeloablation[26,35] (**Table 3**). Growth and quality of life were similar in these groups of patients (**Table 3**). A higher-than-normal incidence of infection with human papillomavirus leading to chronic disease has been observed in HSCT-treated patients with SCID who have mutation of *IL2RG* or *JAK3* (ref. 36). However, no association was detected between infection with this virus and the absence of NK cells[36] or other ILCs (**Table 3**). Instead, these data fit with the hypothesis that infection with this virus is controlled by IL-2Rγ- or JAK3-dependent signaling in keratinocytes rather than in lymphocytes[37,38]. Nine patients with SCID in our cohort who had mutation of *IL2RG* or *JAK3* required immunoglobulin replacement because of residual B cell deficiency due to impaired signaling via the cytokine receptors IL-21R and IL-4R in B cells with mutation of *IL2RG* or *JAK3* (ref. 39) (**Table 3**). The pattern of ILC detection in the blood was similar for these patients and for the other patients of the cohort (**Table 3**). ILCs thus seemed to be dispensable in humans with a functional adaptive immune system, which supported the proposal of redundancy between ILCs and adaptive lymphocytes in humans in natural conditions.

DISCUSSION

We aimed here to contribute to the understanding of ILC differentiation and function in humans in natural conditions. We focused our analysis on a cohort of patients with SCID who were deficient in T cells, B cells and NK cells and had deficiency in JAK3 or IL-2Rγ and showed that these patients lacked all ILC subsets. These results are consistent with the strict dependence of ILC1s, ILC2s, ILC3s and NK cells on IL-7 or IL-15 (refs. 40–42).

The patients in our cohort with SCID and mutation of *JAK3* or *IL2RG* underwent allogeneic HSCT, which could be performed in the absence of myeloablation due to the absence of allogeneic immune responses in the recipients. In these HSCT protocols, split chimerism was generally observed, with development of T cells from the transplanted donor cells and the other lineages remaining of host origin[27]. Progenitor T cells are thought to persist in the long term in the absence of donor HSC engraftment[27,43]. In this setting, no reconstitution of blood NK cells, ILC2s or ILC3s was observed. In tissues, a marked reduction in the abundance of $NKp46^{+}$ ILCs and ILC2 was also observed. Thus, patients with SCID who had mutation of *IL2RG* or *JAK3* continued to display ILC deficiency after HSCT in the absence of myeloablation. However, there was a trend for a better reconstitution of the ILC1 subset that even expanded in a few patients (2 of 18 patients in our study). Among the ILC subsets, the ILC1 subset is still not well defined. In particular, it is possible that some of these ILC1s might correspond to activated T cells with low expression of the complex of CD3 invariant signaling proteins and the T cell antigen receptor. The cell-surface expression of not only CD5 but also CD4, CD28 and CD3 and expression of transcripts encoding the T cell antigen receptor is consistent with this hypothesis[28–30]. The lack of a robust consensual definition of ILC1 phenotype is most probably one of the factors that leads to the apparent heterogeneity of ILC1s.

In contrast to the results reported above, circulating and tissue ILCs were detected in most patients of our cohort who underwent HSCT with myeloablation, consistent with published reports showing an early wave of NK cells[44] and slow, incomplete helper-like ILC reconstitution[16] in these settings. The partial nature of the reconstitution of circulating ILCs in these patients makes it impossible to rule out the possibility that ILC precursors or differentiated ILCs seed various anatomical sites throughout the body during embryonic development, with subsequent maintenance by self-renewal *in situ*, which would contribute to the production of tissue-resident ILCs after birth[15,45]. In this hypothesis, ILCs could have the following two distinct anatomical and temporal origins: yet-to-be-identified organs during embryonic life; and bone marrow after birth and in stress conditions such as HSCT. This 'dual-ILC' system would parallel the observation of the layered system composed of tissue-resident macrophages that originate mainly from yolk-sac progenitor cells and of macrophages that originate from bone-marrow hematopoietic stem cells[46]. Nevertheless, our data indicated that ILCs can be reconstituted postnatally. Those data were supported by similar results obtained in our mouse model of HSCT.

ILCs are seen as sentinels and local guardians of tissue function, and many immunological functions have been attributed to them, mostly on the basis of experimental challenges in mice or *in vitro* experiments with human cells[1]. However, the small number of genes selectively expressed by ILCs or ILC subsets[28] and the consequent lack of mouse models with selective targeting of ILC subsets has hindered attempts to delineate the selective contribution of these cells to immunological defense *in vivo*[47]. The much lower abundance of subsets of circulating and tissue-resident ILCs in transplanted patients with SCID with mutation of *IL2RG* or *JAK3*, with the exception of rare cases of ILC1 reconstitution, has provided an informative model with which to assess the role of ILCs in natural conditions in humans. It was clear from our study that these major ILC deficiencies appeared to be clinically silent, in contrast to the severe clinical conditions associated with deficiency in T cells and B cells. Thus, ILCs appear to be redundant, at least in the context of modern medicine and hygiene, which provides an alternative view of their immunological function. Further very long-term evaluation, beyond 40 years, will nevertheless be needed to determine whether redundancy of T cells, NK cells and ILCs is maintained in older patients. Our findings are supported by the redundancy of ILC3s and T cells in protection against intestinal infection of mice with *Citrobacter rodentium*[13,14]. They are also consistent with case reports of impaired NK-cell effector function without apparent clinical immunodeficiency in humans[48]. Notably, NK cells have been shown to contribute to tumor immunosurveillance; however, our cohort was too small to address this possibility. Given the similarities between ILCs and T cells in terms of transcription-factor expression, cytokine secretion and localization, ILCs are probably 'substituted'

by T cells rather than by B cells. Redundant mechanisms that ensure a robust immune response might have led to the selection of features common to ILCs and T cells. Our data indicating that ILCs are part of a multi-layered protective arsenal of immune cells suggest that it would be useful to elucidate the role of ILCs in patients with various genetic or acquired conditions that compromise adaptive immunity, including patients on immunosuppressive therapy. Depletion of circulating ILCs has been reported in patients infected with human immunodeficiency virus who are not receiving early antiretroviral therapy, but the effect of this lack of ILCs on immunodeficiency and the underlying mechanisms remain unknown[19]. Further investigation of the role of ILCs in these conditions, as well as during embryonic life, early childhood and old age, will be essential for full understanding of ILC biology.

ILCs have also been shown to have a role in reproduction. Indeed, the uterine ILC population, including NK cells, expands during pregnancy, and these cells have been reported to regulate placental development and fetal growth in humans and mice[49]. However, two female JAK3-deficient patients included in our study had no signs of fertility disorders and had healthy babies with a normal birth weight and no other pathological symptoms following pregnancies free of adverse clinical events. Therefore, ILCs seem to be dispensable for human reproduction in natural conditions.

METHODS

Methods and any associated references are available in the online version of the paper.

Note: Any Supplementary Information and Source Data files are available in the online version of the paper.

ACKNOWLEDGMENTS

We thank all patients and their families for participating in the study; C. Bonnafous and N. Anceriz (Innate-Pharma) for monoclonal antibody to NKp46; F. Suarez (Paris), N. Schleinitz (Marseille) and Y. Bertrand (Lyon) for enrolling patients in the study; and the Laboratory of Hematology (P.E. Morange, Marseille) for sample storage. Supported by the European Research Council (THINK Advanced Grant for the E.V. laboratory), the Ligue Nationale contre le Cancer (Equipe Labellisée; E.V. laboratory), institutional grants from INSERM, CNRS and Aix-Marseille University to CIML (E.V. laboratory), the Institut Universitaire de France (E.V.), the European Research Council (Pidimmune Advanced Grant for the A.F. laboratory), institutional grants from INSERM, Paris Descartes University and Collège de France (A.F. laboratory), Investissements d'Avenir Instituts Hospitaliers Universitaires (A.F. laboratory), institutional grants from Institut Pasteur, INSERM, Université Paris Diderot and the Agence Nationale de la Recherche ("Myeloten"; R.G. group), the Institut National du Cancer (R.G. group) and Université Sorbonne Paris Cité ("Mucocell"; R.G. group).

AUTHOR CONTRIBUTIONS

F.V., A.F. and E.V. devised and supervised the study, designed the research, and wrote the manuscript, with the help of the other co-authors; V.B., B.V. and B.N. designed the research, performed experiments and analyzed the data; C. Pip., T.P., M.P., N.Y., F.T., J.B., J.H.W.D., A.R. and R.G. performed the experiments and analyzed the data; and M.E., N.M., N.Z., C.F., G. M., D.M., S.B., A.D., H.S. and C. Pic. provided key expertise, reagents or samples.

COMPETING FINANCIAL INTERESTS

The authors declare competing financial interests: details are available in the online version of the paper.

1. Klose, C.S. & Artis, D. Innate lymphoid cells as regulators of immunity, inflammation and tissue homeostasis. *Nat. Immunol.* **17**, 765–774 (2016).
2. Spits, H. *et al.* Innate lymphoid cells—a proposal for uniform nomenclature. *Nat. Rev. Immunol.* **13**, 145–149 (2013).
3. Eberl, G., Colonna, M., Di Santo, J.P. & McKenzie, A.N. Innate lymphoid cells. Innate lymphoid cells: a new paradigm in immunology. *Science* **348**, aaa6566 (2015).
4. Juelke, K. & Romagnani, C. Differentiation of human innate lymphoid cells (ILCs). *Curr. Opin. Immunol.* **38**, 75–85 (2016).
5. Renoux, V.M. *et al.* Identification of a human natural killer cell lineage-restricted progenitor in fetal and adult tissues. *Immunity* **43**, 394–407 (2015).
6. Montaldo, E., Juelke, K. & Romagnani, C. Group 3 innate lymphoid cells (ILC3s): origin, differentiation, and plasticity in humans and mice. *Eur. J. Immunol.* **45**, 2171–2182 (2015).
7. Scoville, S.D. *et al.* A progenitor cell expressing transcription factor RORγt generates all human innate lymphoid cell subsets. *Immunity* **44**, 1140–1150 (2016).
8. Buckley, R.H. Molecular defects in human severe combined immunodeficiency and approaches to immune reconstitution. *Annu. Rev. Immunol.* **22**, 625–655 (2004).
9. Fischer, A., Hacein-Bey-Abina, S. & Cavazzana-Calvo, M. Gene therapy for primary adaptive immune deficiencies. *J. Allergy Clin. Immunol.* **127**, 1356–1359 (2011).
10. Gennery, A.R. *et al.* Transplantation of hematopoietic stem cells and long-term survival for primary immunodeficiencies in Europe: entering a new century, do we do better? *J. Allergy Clin. Immunol.* **126**, 602–610 (2010).
11. Buckley, R.H. Transplantation of hematopoietic stem cells in human severe combined immunodeficiency: longterm outcomes. *Immunol. Res.* **49**, 25–43 (2011).
12. Fischer, A. Primary immunodeficiency diseases: an experimental model for molecular medicine. *Lancet* **357**, 1863–1869 (2001).
13. Rankin, L.C. *et al.* Complementarity and redundancy of IL-22-producing innate lymphoid cells. *Nat. Immunol.* **17**, 179–186 (2016).
14. Song, C. *et al.* Unique and redundant functions of NKp46$^+$ ILC3s in models of intestinal inflammation. *J. Exp. Med.* **212**, 1869–1882 (2015).
15. Gasteiger, G., Fan, X., Dikiy, S., Lee, S.Y. & Rudensky, A.Y. Tissue residency of innate lymphoid cells in lymphoid and nonlymphoid organs. *Science* **350**, 981–985 (2015).
16. Munneke, J.M. *et al.* Activated innate lymphoid cells are associated with a reduced susceptibility to graft-versus-host disease. *Blood* **124**, 812–821 (2014).
17. Hazenberg, M.D. & Spits, H. Human innate lymphoid cells. *Blood* **124**, 700–709 (2014).
18. Vallentin, B. *et al.* Innate lymphoid cells in cancer. *Cancer Immunol. Res.* **3**, 1109–1114 (2015).
19. Kløverpris, H.N. *et al.* Innate lymphoid cells are depleted irreversibly during acute HIV-1 infection in the absence of viral suppression. *Immunity* **44**, 391–405 (2016).
20. Huntington, N.D., Carpentier, S., Vivier, E. & Belz, G.T. Innate lymphoid cells: parallel checkpoints and coordinate interactions with T cells. *Curr. Opin. Immunol.* **38**, 86–93 (2016).
21. Buckley, R.H. *et al.* Human severe combined immunodeficiency: genetic, phenotypic, and functional diversity in one hundred eight infants. *J. Pediatr.* **130**, 378–387 (1997).
22. Stephan, J.L. *et al.* Severe combined immunodeficiency: a retrospective single-center study of clinical presentation and outcome in 117 patients. *J. Pediatr.* **123**, 564–572 (1993).
23. McKenzie, A.N., Spits, H. & Eberl, G. Innate lymphoid cells in inflammation and immunity. *Immunity* **41**, 366–374 (2014).
24. Diefenbach, A., Colonna, M. & Koyasu, S. Development, differentiation, and diversity of innate lymphoid cells. *Immunity* **41**, 354–365 (2014).
25. Artis, D. & Spits, H. The biology of innate lymphoid cells. *Nature* **517**, 293–301 (2015).
26. Neven, B. *et al.* Long-term outcome after hematopoietic stem cell transplantation of a single-center cohort of 90 patients with severe combined immunodeficiency. *Blood* **113**, 4114–4124 (2009).
27. Fischer, A. *et al.* Severe combined immunodeficiency. A model disease for molecular immunology and therapy. *Immunol. Rev.* **203**, 98–109 (2005).
28. Robinette, M.L. *et al.* Transcriptional programs define molecular characteristics of innate lymphoid cell classes and subsets. *Nat. Immunol.* **16**, 306–317 (2015).
29. Björklund, A.K. *et al.* The heterogeneity of human CD127$^+$ innate lymphoid cells revealed by single-cell RNA sequencing. *Nat. Immunol.* **17**, 451–460 (2016).
30. Roan, F. *et al.* CD4$^+$ group 1 innate lymphoid cells (ILC) form a functionally distinct ilc subset that is increased in systemic sclerosis. *J. Immunol.* **196**, 2051–2062 (2016).
31. Fuchs, A. *et al.* Intraepithelial type 1 innate lymphoid cells are a unique subset of IL-12- and IL-15-responsive IFN-γ-producing cells. *Immunity* **38**, 769–781 (2013).
32. Wohlfahrt, T. *et al.* Type 2 innate lymphoid cell counts are increased in patients with systemic sclerosis and correlate with the extent of fibrosis. *Ann. Rheum. Dis.* **75**, 623–626 (2016).
33. Koyasu, S. Inflammatory ILC2 cells: disguising themselves as progenitors? *Nat. Immunol.* **16**, 133–134 (2015).
34. Czechowicz, A., Kraft, D., Weissman, I.L. & Bhattacharya, D. Efficient transplantation via antibody-based clearance of hematopoietic stem cell niches. *Science* **318**, 1296–1299 (2007).
35. Railey, M.D., Lokhnygina, Y. & Buckley, R.H. Long-term clinical outcome of patients with severe combined immunodeficiency who received related donor bone marrow

transplants without pretransplant chemotherapy or post-transplant GVHD prophylaxis. *J. Pediatr.* **155**, 834–840.e1 (2009).
36. Laffort, C. *et al.* Severe cutaneous papillomavirus disease after haemopoietic stem-cell transplantation in patients with severe combined immune deficiency caused by common gammac cytokine receptor subunit or JAK-3 deficiency. *Lancet* **363**, 2051–2054 (2004).
37. Goldschmidt, M.H. *et al.* Severe papillomavirus infection progressing to metastatic squamous cell carcinoma in bone marrow-transplanted X-linked SCID dogs. *J. Virol.* **80**, 6621–6628 (2006).
38. Nishio, H., Matsui, K., Tsuji, H., Tamura, A. & Suzuki, K. Immunolocalisation of the janus kinases (JAK) signal transducers and activators of transcription (STAT) pathway in human epidermis. *J. Anat.* **198**, 581–589 (2001).
39. Recher, M. *et al.* IL-21 is the primary common γ chain-binding cytokine required for human B-cell differentiation in vivo. *Blood* **118**, 6824–6835 (2011).
40. Huntington, N.D. *et al.* IL-15 trans-presentation promotes human NK cell development and differentiation in vivo. *J. Exp. Med.* **206**, 25–34 (2009).
41. Satoh-Takayama, N. *et al.* IL-7 and IL-15 independently program the differentiation of intestinal CD3$^-$NKp46$^+$ cell subsets from Id2-dependent precursors. *J. Exp. Med.* **207**, 273–280 (2010).
42. Kang, J. & Coles, M. IL-7: the global builder of the innate lymphoid network and beyond, one niche at a time. *Semin. Immunol.* **24**, 190–197 (2012).
43. Cavazzana-Calvo, M. *et al.* Long-term T-cell reconstitution after hematopoietic stem-cell transplantation in primary T-cell-immunodeficient patients is associated with myeloid chimerism and possibly the primary disease phenotype. *Blood* **109**, 4575–4581 (2007).
44. Ruggeri, L., Aversa, F., Martelli, M.F. & Velardi, A. Allogeneic hematopoietic transplantation and natural killer cell recognition of missing self. *Immunol. Rev.* **214**, 202–218 (2006).
45. Fan, X. & Rudensky, A.Y. Hallmarks of Tissue-Resident Lymphocytes. *Cell* **164**, 1198–1211 (2016).
46. Perdiguero, E.G. & Geissmann, F. The development and maintenance of resident macrophages. *Nat. Immunol.* **17**, 2–8 (2016).
47. Bando, J.K. & Colonna, M. Innate lymphoid cell function in the context of adaptive immunity. *Nat. Immunol.* **17**, 783–789 (2016).
48. Parry, D.A. *et al.* A homozygous STIM1 mutation impairs store-operated calcium entry and natural killer cell effector function without clinical immunodeficiency. *J. Allergy Clin. Immunol.* **137**, 955–957 (2016).
49. Boulenouar, S. *et al.* The residual innate lymphoid cells in NFIL3-Deficient mice support suboptimal maternal adaptations to pregnancy. *Front. Immunol.* **7**, 43 (2016).

ONLINE METHODS

Patients and healthy control subjects. Patients were treated by allogeneic HSCT in the Immuno-Hematology Department of Necker Children's Hospital (Paris, France) or in the Pediatric Hematology and Oncology Department of Timone Enfants Hospital (Marseille, France). The cells transplanted were obtained from mismatched related donors (19 patients), phenotypically matched related donors (5 patients), unrelated umbilical cord blood (4 patients), matched unrelated donors (1 patient) or matched sibling donors (3 patients). The characteristics of the patient and the HSCT are provided in **Table 2** and **Supplementary Table 1**. Clinical events and the personal variables of the patients were assessed retrospectively, with data collected during annual visits to the outpatient clinic. All clinical events present 2 years after HSCT or occurring thereafter were recorded, together with the timing, severity, and outcome of these events. Chimerism was determined on total blood or sorted cell lineages, by XY-fluorescence *in situ* hybridization or by the polymerase chain reaction amplification of short tandem repeats. For each cell lineage, mixed chimerism was defined as the presence of 10–90% donor-derived cells. Blood samples were obtained with consent from patients or families in the context of routine follow-up. In order to minimize variability, exclusion criteria were established. Thus, healthy controls had no infections or current diseases (for example, hematological, systemic, cardiac or renaldisease). All children were admitted to the Department of Pediatric Surgery of the Timone Hospital (Marseille) during programmed hospitalizations before minor surgery procedure as undescended testes, circumcision or frenulum surgery. These healthy controls were referred to the outpatient clinics of Conception Hospital (Marseille) for diagnostic blood testing. They underwent routine blood testing before minor elective surgery. Cord blood were collected from siblings of patients treated for hematological malignancies. When these cord blood units were not compatible with the recipient, parents and guardians have signed an informed consent for studies on these samples before destruction. This study was performed according French rules (Art. L. 1243-1 et Art. L. 1245-2 du Code de la Santé Publique). All patients provided written informed consent for participation, including possible inclusion in genetic studies, and the study was approved by the local ethics committee of the Hôpital Necker (Paris) and the Hôpital de la Timone (Marseille). The characteristics of the patients, including age and sex, are presented in **Supplementary Table 1**.

Cell preparation and flow cytometry. Human blood samples were centrifuged on a Ficoll gradient to obtain a preparation enriched in peripheral blood mononuclear cells (PBMCs), which was then frozen, as previously described[50]. T lymphocytes and B lymphocytes were quantified with 6-Color BD Multitest and BD Trucount technologies, according to the manufacturer's instructions (Becton Dickinson, San Diego, USA). The monoclonal antibodies (mAbs) used to analyze human cells are provided in **Supplementary Table 2**. Data were acquired with a FACSCanto II cytometer (T/B/NK subsets) or a Fortessa X20 cytometer (helper-like ILC subsets), both from Becton Dickinson. Data were analyzed with FlowJo software.

Immunofluorescence and immunohistochemistry of tissue sections. Human intestine and skin biopsy specimens were isolated from HSCT-treated patients with SCID with *IL2RG* or *JAK3* mutations and control subjects. For immunofluorescence, samples were thoroughly washed in PBS and embedded in optimum cutting temperature compound, frozen in a bath of isopentane cooled on dry ice, and cut into 8-µm-thick sections. Before staining, sections were fixed by incubation in cold acetone for 10 min before saturation. Human NKp46 staining was then performed with polyclonal goat anti-human NKp46 antibody, followed by Alexa488-conjugated donkey anti-goat secondary antibody (**Supplementary Table 2**). Human CD3ε staining was performed with a mouse anti-human Alexa647-conjugated mAb (**Supplementary Table 2**). DAPI was used to counterstain the nucleus. After staining, the slides were allowed to dry and mounted in Prolong Gold for examination under a Leica SP5 confocal microscope (Leica). Images were processed with Leica LAS Lite and Adobe Photoshop software. For ILC2 immunohistochemistry, paraffin-embedded sections of gut and skin biopsy samples from patients and controls were incubated with goat anti-ICOS, mouse anti-CD3, rat anti-CD11b and Pacific Blue-labeled anti-lineage markers (Lin; CD3, CD14, CD16, CD19, CD20 and CD56) (**Supplementary Table 2**). The following secondary antibodies were used: Dylight-conjugated chicken anti-rat 350, Alexa-Fluor-labeled donkey anti-goat 594, -goat anti-rabbit 660, -donkey anti-mouse 647 and donkey anti-rabbit 488 (**Supplementary Table 2**). Toluidine Blue staining was performed according to standard protocols using a working solution with a pH between 2.0 and 2.5. Six randomly chosen high-power fields at 200-fold magnification per patient or healthy volunteer were evaluated by two experienced researchers in a blinded manner. For NKp46$^+$ ILC immunohistochemistry, paraffin embedded sections of gut and skin biopsy samples from patients and controls were double stained automatically with Leica Bond Max autostainer (Leica Biosystem). Antibody used were polyclonal anti-CD3 (DAKO; **Supplementary Table 2**) and anti-NKp46 (clone 8E5B Innate Pharma, Marseille, France). A full characterization of the 8E5B mAb will be published elsewhere.

Reconstitution experiments in mice. All mice were C57/BL6/J females used between 6 and 9 weeks of age. *Rag2*$^{-/-}$*Il2rg*$^{-/-}$ mice bearing the CD45.1 congenic marker were used as recipients in the reconstitution experiments. CD45.2$^+$ hematopoietic progenitors from the bone marrow of C57BL/6 congenic mice were sorted and injected intravenously in the retro-orbital sinus of sub-lethally irradiated (500 rads, cesium source) or non-irradiated *Rag2*$^{-/-}$ *Il2rg*$^{-/-}$ recipient mice. CD45.2$^+$Lin$^-$Sca1$^+$cKit$^+$Flt3^{int} cells (multipotent progenitors) and Lin$^-$Sca1$^+$cKit$^+$Flt3^{hi} cells (lymphoid-primed multipotent progenitors) were mixed for the bone marrow grafts transplanted into sub-lethally irradiated and non-irradiated CD45.1$^+$ *Rag2*$^{-/-}$*Il2rg*$^{-/-}$ host mice. Recipients received 7×10^3 adult hematopoietic progenitors, and reconstitution was analyzed 3 weeks after transplantation. The recipient livers, lungs and intestines (lamina propria and intra-epithelial lymphocytes) were analyzed by flow cytometry for the presence of donor (CD45.2$^+$) or recipient (CD45.1$^+$) lymphoid cell populations.

Statistical analysis. Statistical analyses were performed with Prism 5 (GraphPad Software, San Diego, CA).

50. Tomasello, E. *et al.* Mapping of NKp46$^+$ cells in healthy human lymphoid and non-lymphoid tissues. *Front. Immunol.* **3**, 344 (2012).

doi:10.1038/ni.3553

Corrigendum: Evidence of innate lymphoid cell redundancy in humans

Frédéric Vély, Vincent Barlogis, Blandine Vallentin, Bénédicte Neven, Christelle Piperoglou, Thibaut Perchet, Maxime Petit, Nadia Yessaad, Fabien Touzot, Julie Bruneau, Nizar Mahlaoui, Nicolas Zucchini, Catherine Farnarier, Gérard Michel, Despina Moshous, Stéphane Blanche, Arnaud Dujardin, Hergen Spits, Jörg H W Distler, Andreas Ramming, Capucine Picard, Rachel Golub, Alain Fischer & Eric Vivier

***Nat. Immunol.* 17, 1291–1299 (2016); published online 12 September 2016; corrected after print 19 October 2016**

In the version of this article initially published, author Mikael Ebbo was missing from the author list. The correct list is as follows: Frédéric Vély[1,2,20], Vincent Barlogis[3,20], Blandine Vallentin[3,20], Bénédicte Neven[4–7,20], Christelle Piperoglou[1,2], Mikael Ebbo[1,8], Thibaut Perchet[9,10], Maxime Petit[9,10], Nadia Yessaad[11], Fabien Touzot[5,12], Julie Bruneau[5,13], Nizar Mahlaoui[4–7], Nicolas Zucchini[14], Catherine Farnarier[2], Gérard Michel[3], Despina Moshous[4–7], Stéphane Blanche[4–7], Arnaud Dujardin[15], Hergen Spits[16], Jörg H W Distler[17], Andreas Ramming[17], Capucine Picard[4–7,18], Rachel Golub[9,10], Alain Fischer[4–7,19,21] & Eric Vivier[1,2,21]. The correct affiliation list ends as follows: [8]APHM, Hôpital de la Timone, Service de Médecine Interne, Marseille, France. [9]Institut Pasteur, Unité de Lymphopoièse, INSERM, Paris, France. [10]Université Paris Diderot, Sorbonne Paris Cité, Cellule Pasteur, Paris, France. [11]MI-mAbs consortium, Aix-Marseille University, Marseille, France. [12]APHP, Hôpital Necker-Enfants Malades, Biotherapy Unit, Paris, France. [13]APHP, Hôpital Necker-Enfants Malades, Service d'anatomopathologie, Paris, France. [14]BD Biosciences, Le Pont-de-Claix, France. [15]Innate-Pharma, Marseille, France. [16]Academic Medical Center at the University of Amsterdam, Arizona Amsterdam, the Netherlands. [17]Department of Internal Medicine, Rheumatology & Immunology, University of Erlangen-Nuremberg, Erlangen, Germany. [18]APHP, Hôpital Necker-Enfants Malades, Study Center of Immunodeficiencies, Paris, France. [19]College de France, Paris, France. [20]These authors contributed equally to this work. [21]These authors jointly directed this work. The correct Author Contributions section ends as follows: "…and M.E., N.M., N.Z., C.F., G. M., D.M., S.B., A.D., H.S. and C. Pic. provided key expertise, reagents or samples."

In addition, the description of patient C9 was incorrect in the text and legend for Figure 4b,d. The correct text (in the final paragraph of the fourth subsection of Results) is as follows: "In addition, NKp46$^+$ ILCs and ILC2s were readily observed in tissues from patients treated with myeloablative HSCT, as illustrated by the analysis of skin biopsies from a patient with SCID who had mutation of *RAG2* (C10) and was treated with myeloablative HSCT (Fig. 4b,d)…. As a control, tissue-resident gut ILCs were observed in a patient with SCID who had mutation of *RAG1* (C9) but was treated with 'pheno-related' HSCT (related donor with more than one compatible HLA haplotype but not genetically identical) under non-myeloablative conditions (Fig. 4b,d). The correct Figure 4b,d legend is as follows: "(b) Microscopy of tissue sections from patients who were treated with HSCT (stained as in a): duodenum (left) or colon (right) from C9 (*RAG1* mutation) and skin from C10 (*RAG2* mutation) (middle), at 15 months (C9) or 4 months (C10) after HSCT.…(d) Microscopy of tissue sections from patients with SCID (colon from P5 and skin from P11 (as in a); colon from C9 and skin from C10 (as in b))…."

Also, a label was missing under Figure 1d, far left; that should be labelled as 'Lin$^-$CD127$^+$'.

Finally, the description of lung NK cells in the final paragraph of Results was incorrect; that text should read as follows: "Similarly, lung NK cells (Lin$^-$NKp46$^+$NK1.1$^+$CD127$^-$) underwent reconstitution…." These errors have been corrected in the PDF and HTML versions of this article.

Article

Immunity

An Id2^{RFP}-Reporter Mouse Redefines Innate Lymphoid Cell Precursor Potentials

Highlights

- A highly sensitive *Id2*-reporter strain allows identification of ILC precursors
- Id2+ ILCPs harbor multi-potent NK and/or ILC precursors at the clonal level
- *Id2*$^{+}$*Zbtb16*$^{+}$ ILCPs retain substantial conventional NK-cell potential

Authors

Wei Xu, Dylan E. Cherrier, Sylvestre Chea, ..., Pentao Liu, Rachel Golub, James P. Di Santo

Correspondence

wei_xuxx@fudan.edu.cn (W.X.), james.di-santo@pasteur.fr (J.P.D.S.)

In Brief

Several transcription factors orchestrate innate lymphoid cell (ILC) development. By using a highly sensitive *Id2*^{RFP}-reporter mouse model, Xu et al. identify multi-potent ILC precursors that redefine branchpoints in ILC development.

Xu et al., 2019, Immunity *50*, 1054–1068
April 16, 2019
https://doi.org/10.1016/j.immuni.2019.02.022

CellPress

CellPress

Immunity
Article

An Id2^{RFP}-Reporter Mouse Redefines Innate Lymphoid Cell Precursor Potentials

Wei Xu,[1,2,3,7,*] Dylan E. Cherrier,[1,2,4,7] Sylvestre Chea,[2,5] Christian Vosshenrich,[1,2] Nicolas Serafini,[1,2] Maxime Petit,[2,4,5] Pentao Liu,[6] Rachel Golub,[2,5] and James P. Di Santo[1,2,8,*]

[1]Innate Immunity Unit, Institut Pasteur, Paris 75724, France
[2]Inserm U1223, Institut Pasteur, Paris 75724, France
[3]Department of Immunology, Shanghai Medical College, Fudan University, Shanghai 200032, China
[4]Paris Diderot University, Sorbonne Paris Cité, Paris 75013, France
[5]Lymphopoiesis Unit, Institut Pasteur, Paris 75724, France
[6]Li Ka Shing Faculty of Medicine, University of Hong Kong, Hong Kong, China
[7]These authors contributed equally
[8]Lead Contact
*Correspondence: wei_xuxx@fudan.edu.cn (W.X.), james.di-santo@pasteur.fr (J.P.D.S.)
https://doi.org/10.1016/j.immuni.2019.02.022

SUMMARY

Innate lymphoid cell (ILC) development proposes that ILC precursors (ILCPs) segregate along natural killer (NK) cell versus helper cell (ILC1, ILC2, ILC3) pathways, the latter depending on expression of *Id2*, *Zbtb16*, and *Gata3*. We have developed an *Id2*-reporter strain expressing red fluorescent protein (RFP) in the context of normal *Id2* expression to re-examine ILCP phenotype and function. We show that bone-marrow ILCPs were heterogeneous and harbored extensive NK-cell potential *in vivo* and *in vitro*. By multiplexing Id2^{RFP} with Zbtb16^{CreGFP} and Bcl11b^{tdTomato} strains, we made a single-cell dissection of the ILCP compartment. In contrast with the current model, we have demonstrated that *Id2*$^+$*Zbtb16*$^+$ ILCPs included multi-potent ILCPs that retained NK-cell potential. Late-stage ILC2P and ILC3P compartments could be defined by differential *Zbtb16* and *Bcl11b* expression. We suggest a revised model for ILC differentiation that redefines the cell-fate potential of helper-ILC-restricted *Zbtb16*$^+$ ILCPs.

INTRODUCTION

Innate lymphoid cells (ILCs) are characterized by their lack of antigen receptors and prompt reaction to signals from infected or injured tissues. Like T and B lymphocytes from the adaptive immune system, lymphocytes of the innate immune system are important players in immune responses and tolerance at mucosal barriers. ILCs have been recently re-classified into five groups (natural killer cells, NK cells; ILC1s; ILC2s; ILC3s; and lymphoid tissue inducer [LTi] cells) based on their functional outputs and expression of key transcription factors (TFs) that mirror adaptive CD8$^+$ (cluster of differentiation 8$^+$) and CD4$^+$ T cells (reviewed in Vivier et al., 2018). Although both ILC1s and conventional NK cells express T-box transcription factor (T-bet) and are capable of producing interferon-γ (IFN-γ) and tumor necrosis factor (TNF), NK cells also express Eomesodermin (Eomes) and Eomes-dependent perforin and granzymes that promote granule-dependent cytotoxic functions. ILC2s consist of cells that express the transcription factor GATA3 and are potent producers of T helper 2 (Th2)-cell-associated cytokines such as interleukin (IL)-5, IL-9, and IL-13. ILC3s are heterogeneous but uniformly express the transcription factor RORγt (RAR-related orphan receptor gamma). This group comprises CCR6$^+$CD4$^{+/-}$ and CD49a$^+$NKp46$^{+/-}$ ILC3 subsets that secrete Th17-cell-associated cytokines IL-22 or IL-17 upon activation. LTi cells are related to ILC3s but exert their function during fetal development through promotion of lymphoid-tissue organogenesis (reviewed in Cording et al., 2014).

ILCs share their developmental origins with adaptive lymphocytes (reviewed in Zook and Kee, 2016; Serafini et al., 2015). All ILC subsets are derived from common lymphoid progenitors (CLPs) in the fetal liver and adult bone marrow (BM). It is proposed that the developmental program of ILCs is similar to that of T cells, in which CLPs differentiate into specific ILC lineages by progressive loss of alternative lineage potentials. Multiple ILC-lineage-restricted progenitors downstream of CLPs have been identified. The earliest common ILC precursor (CILCP) is thought to reside in the CD135 (Flt3)$^-$α4β7$^+$ progenitor population, which still retains some T cell potential (Yu et al., 2014). The acquisition of chemokine receptor CXCR6 (C-X-C motif chemokine receptor 6) was shown to be concurrent with the loss of T cell potential in these precursors (Possot et al., 2011; Yu et al., 2014), although CXCR6 is not required for the generation of this population (Chea et al., 2015). A common helper-ILC progenitor (CHILP) has been identified using Id2^{GFP}-reporter mice (Klose et al., 2014). Id2-expressing CHILPs can give rise to all helper ILCs but fail to differentiate into killer NK cells. A distinct ILC precursor (ILCP) marked by transient expression of *Zbtb16* (encoding promyelocytic leukemia zinc finger [PLZF], a TF previously associated with NKT-cell development) has also been described (Constantinides et al., 2014). These *Zbtb16*$^+$ ILCPs fail to generate LTi and NK cells but can still generate other helper ILCs. A phase of multi-lineage priming was shown to occur in these ILCPs with co-expression of genes for different ILC lineages (Ishizuka et al., 2016). It was proposed that the final

commitment to one of the ILC lineages is influenced by external and internal signals that gradually turn off the alternative developmental programs. Despite the identification of several developmental intermediate cells along ILC-differentiation pathways, the precise stages where specific lineage programs are enabled, as well as the underlying mechanisms that restrict helper versus killer lineages, are still poorly understood (Cherrier et al., 2018; Serafini et al., 2015). This is in part due to the different model systems used (TF reporters), the varying culture conditions used to demonstrate ILCP potential, and the lack of a uniform phenotype to define ILCs that have been generated from ILCPs *in vitro* or *in vivo*.

Several TFs have been shown to be essential for early ILC differentiation, including *Nfil3*, *Tox*, *Tcf7*, and *Id2*, whose expression is initiated immediately downstream of CLPs (Ishizuka et al., 2016; Seillet et al., 2016). Loss of these factors differentially affects the generation of ILC precursors, as well as that of mature ILCs (Seehus et al., 2015; Seillet et al., 2016; Xu et al., 2015; Yang et al., 2015; Yu et al., 2014). Both *Id2* and *Tox* are required for the organogenesis of lymphoid tissues (Aliahmad et al., 2010; Yokota et al., 1999), indicating their overlapping functions in LTi-cell development during the fetal period. ID2 belongs to the family of helix-loop-helix (HLH) proteins that can form heterodimers with E proteins, thereby preventing their transcriptional activities (Kee, 2009). Inhibitor of DNA-binding (ID) proteins and E proteins play important roles in determining the cell fate in the immune system. Id2 is constitutively expressed in all ILC subsets and is indispensable for their development (Cherrier et al., 2012; Moro et al., 2010; Satoh-Takayama et al., 2010; Yokota et al., 1999). ID2 is recognized as a key regulator for establishing the ILC fate, because loss of EBF1 (early B cell factor 1), a repressor of ID2, in B cell progenitors leads to the development of ILCs and T cells (Nechanitzky et al., 2013). These findings argue for the existence of Id2-expressing lymphoid progenitors with common T and ILC potential. However, the $Id2^+$ progenitors identified using previously described Id2-reporter mice have not been shown to possess potentials for all ILC lineages and in some cases specifically lacked NK-cell potential (Jackson et al., 2011; Klose et al., 2014; Yang et al., 2011). These results contrasted with the fact that ID2 was required for normal NK-cell development (Yokota et al., 1999; Boos et al., 2007) and had been shown to be expressed in NK-committed precursors (NKPs) (Carotta et al., 2011; Rosmaraki et al., 2001), although NKPs and immature NK cells still developed in $Id2^{-/-}$ mixed-background mice, presumably due to upregulation of *Id3* expression (Boos et al., 2007). As such, $Id2^+$ CHILPs have been generally considered as a heterogeneous population that includes progenitors for ILC1s, ILC2s, and/or ILC3s, but not for conventional NK cells (reviewed in Diefenbach et al., 2014; Yang and Bhandoola, 2016).

Here, we developed an $Id2^{RFP}$-reporter mouse model and identified a complex repertoire of Id2-expressing ILC progenitors that includes common progenitors to both helper- and killer-ILC lineages. Single-cell transcriptional analysis revealed the marked heterogeneity of the ILCP population, which harbored subsets that differentially expressed *Zbtb16* and *Bcl11b*. These ILCP subsets were then further characterized using mice bearing combinations of $Id2^{RFP}$, $Zbtb16^{GFPcre}$, and $Bcl11b^{tdTomato}$ reporters. Through *in vitro* and *in vivo* assays, we could show that *Zbtb16* expression was associated with loss of ILC3 potential but not NK-cell potential, whereas *Bcl11b* expression appeared to identify an ILC2-committed progenitor, independent of *Zbtb16* expression. As such, our results redefine the cell-fate potential of putative helper-ILC-restricted $Zbtb16^+$ ILCPs as multi-potent CILCPs. In addition, TF multiplexing provides a powerful approach to identify the earliest common ILC and NK-cell progenitors as they emerge from CLPs.

RESULTS

An $Id2^{RFP}$-Reporter Strain Identifies BM NK and ILC Progenitors

To facilitate the study of Id2-expressing cells, we generated $Id2^{RFP}$-reporter mice that harbor an internal ribosome entry site monomeric red fluorescent protein (IRES-mRFP) cassette downstream of the 3′ translated region within exon 2 of the *Id2* gene ($Id2^{RFP}$) (Figure 1A). As expected, RFP was highly expressed in all ILC subsets, including splenic NK cells, liver NK cells and ILC1s, lung ILC2s, and different intestinal ILC3 subsets (Figures 1B and 1C). In contrast, RFP was poorly expressed in splenic $CD4^+$ and $CD8^+$ T cells and was not detected in B cells (Figure 1C). This pattern of RFP expression in innate and adaptive lymphocytes mirrored that of endogenous *Id2* mRNA, as shown by qRT-PCR (Figure 1D). Finally, no obvious differences in ILC development were noted in $Id2^{RFP/+}$ or $Id2^{RFP/RFP}$ mice compared with wild-type (WT) mice (data not shown). Together, these results demonstrate that $Id2^{RFP}$ mice faithfully report on *Id2* expression within major lymphocyte subsets and that the $Id2^{RFP}$ allele is functional.

A previous study of NK-cell development used an $Id2^{GFP}$ reporter in which the GFP cassette replaced one *Id2*-encoding allele (Klose et al., 2014; Rawlins et al., 2009). In this report, *Id2* was not expressed until the refined NK-cell precursor (rNKP) stage during NK-cell development, and only a small subset of the committed NK-cell progenitors expressed *Id2*. Using $Id2^{RFP}$ mice, we observed that the vast majority of rNKP cells and more than half of the pre-NKP cells expressed RFP (Figure 1E), whereas BM CLPs were Id2 negative, as shown previously (Constantinides et al., 2014; Fathman et al., 2011; Ramirez et al., 2012). These results suggest that early Id2 expression within the earliest-defined NK cells is associated with emergence of this innate lymphocyte subset from CLPs.

It was previously shown that fractions of pre-NKP and rNKP cells share phenotypic properties (*Zbtb16* and $\alpha4\beta7$ expression) with $Lin^-CD135^-\alpha4\beta7^+$ lymphoid precursors that can generate NK cells and all helper ILCs (Constantinides et al., 2015; Yu et al., 2014). We therefore examined *Id2* expression in BM ILC progenitors from $Id2^{RFP}$ mice. We found that 70% of $Lin^-CD117^+CD135^-\alpha4\beta7^+CD25^-$ BM ILCPs (which we will refer to as ILCPs) expressed RFP, whereas CLPs and the few $CD135^+\alpha4\beta7^+$ cells did not (Figure 2A; data not shown). By comparison, the subsets of relatively mature ILC2s present in BM and splenic NK cells also were clearly RFP^+ (Constantinides et al., 2014; Hoyler et al., 2012; Yu et al., 2016), although these subsets showed reduced RFP fluorescence (Figures 2A–2C).

We next made a side-by-side comparison of the previously described $Id2^{GFP}$ reporter (Klose et al., 2014; Rawlins et al., 2009) and our $Id2^{RFP}$-reporter strains. When comparing GFP and RFP expression on total BM cells, notable differences

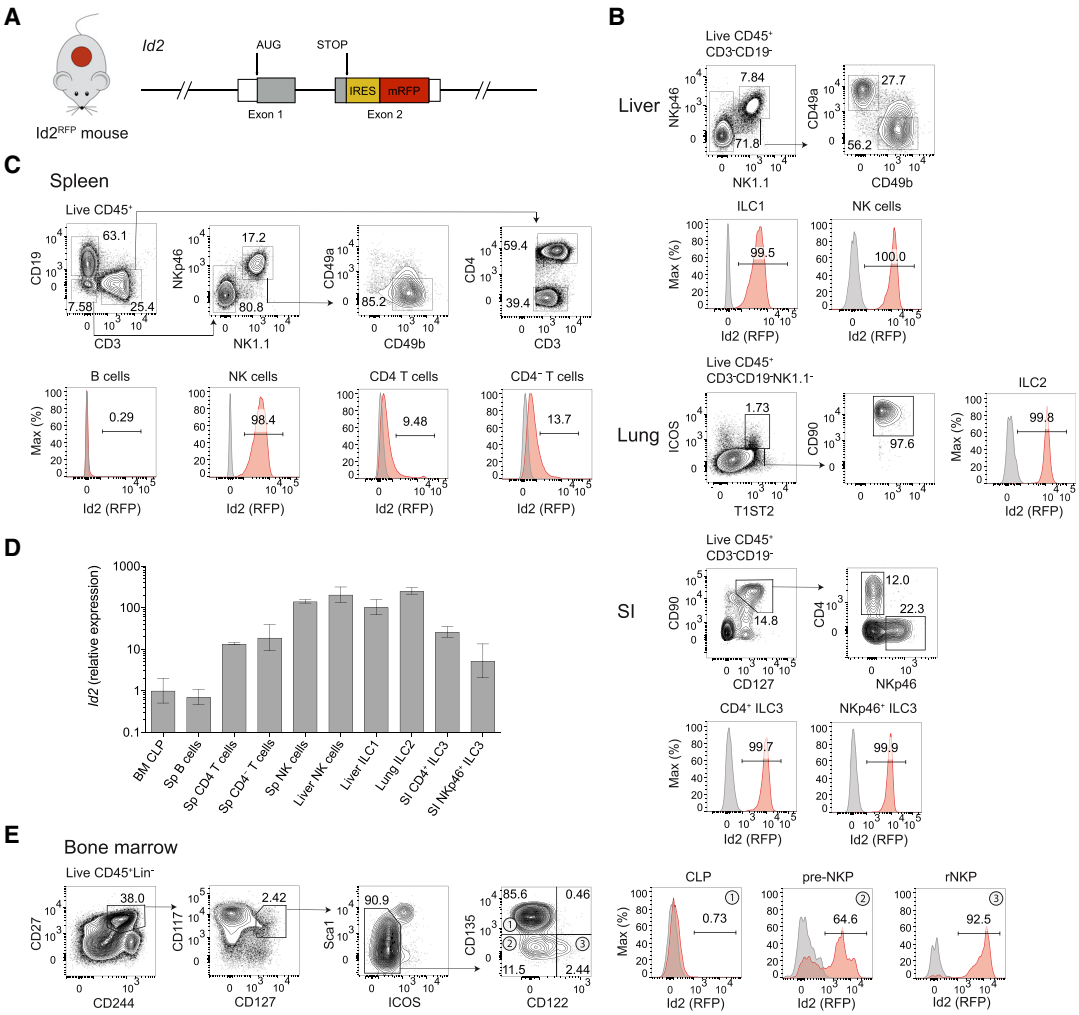

Figure 1. Characterization of *Id2*^{RFP} Reporter Mice

(A) Schematic representation of the genetic modification engineered in Id2^{RFP}-reporter mice.

(B and C) RFP expression in innate lymphoid cells isolated from (B) liver, lung and small intestine (SI), and (C) spleen of C57BL/6 (gray) and Id2^{RFP} (red) mice. Data are from one experiment representative of two independent experiments.

(D) Quantitative PCR analysis of *Id2* expression in precursor and mature cell subsets in Id2^{RFP} mice. *Id2* expression has been normalized to *Hprt* expression and to expression in CLPs. n = 3; error bars represent the standard deviation.

(E) RFP expression in BM lymphoid progenitor cells. Data are from one experiment representative of three independent experiments. Please also see Figure S1.

were observed, with the Id2^{RFP} reporter allowing detection of a larger fraction of cells with a higher mean fluorescence intensity (Figure S1A). The improved sensitivity of the Id2^{RFP} reporter over the Id2^{GFP} reporter was also apparent when comparing Id2 expression (as revealed by GFP or RFP) on gated NK cells, ILCPs, and pre-NKP cells (Figure S1B). Analysis of Id2^{GFP} × Id2^{RFP} double-reporter mice revealed that RFP^{+} cells co-expressed GFP, indicating that both reporters were active in the same cells. Together, these results indicate that our Id2^{RFP} reporter provides a highly sensitive tool to characterize *Id2*-expressing cells, including BM ILCPs.

We further compared selected cell-surface markers of Id2^{RFP} ILCPs with mature NK cells, BM CLPs, and BM ILC2s. ILCPs expressed CD244 (2B4) similarly to CLPs and NK cells, whereas KLRG1 (killer cell lectin-like receptor G1) expression was restricted to NK cells and a subset of BM ILC2s (Figure 2C). These different subpopulations showed distinct CD117 (c-Kit) and CD90 (Thy1) expression patterns (Figure 2C).

We next compared transcriptional profiles of Id2^{RFP} ILCPs to CLPs, ILC2s, and NK cells using qRT-PCR. We confirmed high amounts of *Id2* mRNA in ILCPs, ILC2Ps, and NK cells, whereas *Notch1* and *Rag2* transcripts (which are essential for B and T cell development) were very low in all subsets compared to CLPs (Figure 2D). Id2^{RFP} ILCPs expressed *Il7r* at comparable amounts to CLPs, suggesting a dependence on IL-7 signaling for ILCP emergence from lymphoid progenitors. Id2^{RFP} ILCPs expressed *Ets1*, a key transcription factor for NK and ILC2 development (Zook et al., 2016; Ramirez et al., 2012; Zook and Kee, 2016), as well as *Gata3*, which is required for the generation of ILC2s and ILC3s (Hoyler et al., 2012; Serafini et al., 2014). The

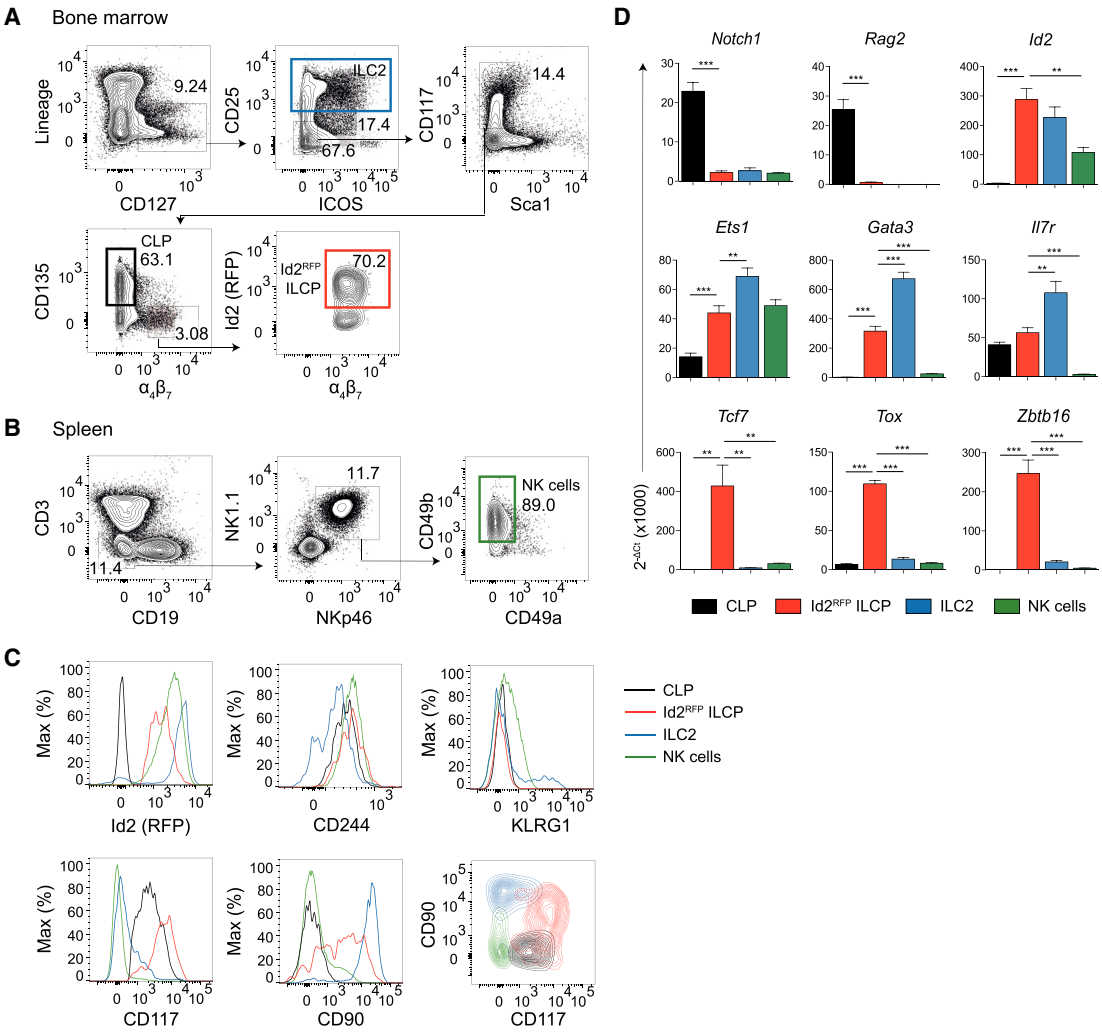

Figure 2. Characterization of *Id2*$^{+}$ BM ILCPs

(A) Flow cytometry analysis of BM ILC2s, CLPs, and ILC precursors. Data are from one experiment representative of three independent experiments.

(B) Flow cytometry analysis of splenic NK cells.

(C) Flow cytometry analysis of surface markers on CLPs, Id2^{RFP} ILCPs, ILC2s, and splenic NK cells. Data are from one experiment representative of two independent experiments.

(D) qRT-PCR analysis of TF transcripts in CLPs, Id2^{RFP} ILCPs, ILC2s, and splenic NK cells. Gene expression has been normalized to *Actb* expression. n = 6; error bars represent the standard error of the mean; *p < 0.05, **p < 0.01, ***p < 0.001, Student's t test. Please also see Figure S1.

transcription factors *Tcf7*, *Tox*, and *Zbtb16*, previously shown to mark ILC commitment (Constantinides et al., 2014; Seehus et al., 2015; Yang et al., 2015), were also highly expressed in Id2^{RFP} ILCPs but were not expressed or expressed at very low amounts in CLPs, ILC2s, or NK cells (Figure 2D). Taken together, these results validate our Id2^{RFP}-reporter mouse model that can be used to interrogate the biological properties of NK-cell progenitors and ILC progenitors, as well as mature ILC subsets in different tissues.

Id2^{+} ILCPs Harbor Common Progenitors to All ILC Lineages, Including NK Cells

In the current model of ILC development, Lin^{-}CD117^{+} CD135^{-}α4β7^{+}CD25^{-} ILCPs are considered the earliest ILC progenitors downstream of CLPs (Serafini et al., 2015; Zook and Kee, 2016), although a fraction of these cells still retain some T-cell-differentiation potential (Possot et al., 2011). As Id2 functions to block E-protein activity that is essential for T and B cell development, Id2 up-regulation is generally associated with the loss of T and B potential and the establishment of ILC fate. Our findings of Id2^{RFP} expression in a subset of BM ILCPs and in pre-NKPs (Figures 1E and 2A) led us to ask whether these subsets harbored committed progenitors for helper ILCs and/or killer NK cells and to assess their potential for other lymphoid lineages.

We first interrogated the capacity of Id2^{RFP} ILCPs to generate diverse lymphocyte subsets *in vivo*. We transferred purified CLPs or ILCPs into sub-lethally-irradiated *Rag2*$^{-/-}$*Il2rg*$^{-/-}$ recipient mice (Figure 3A). Donor-derived cells were analyzed in different organs by flow cytometry 5 weeks after transfer. As

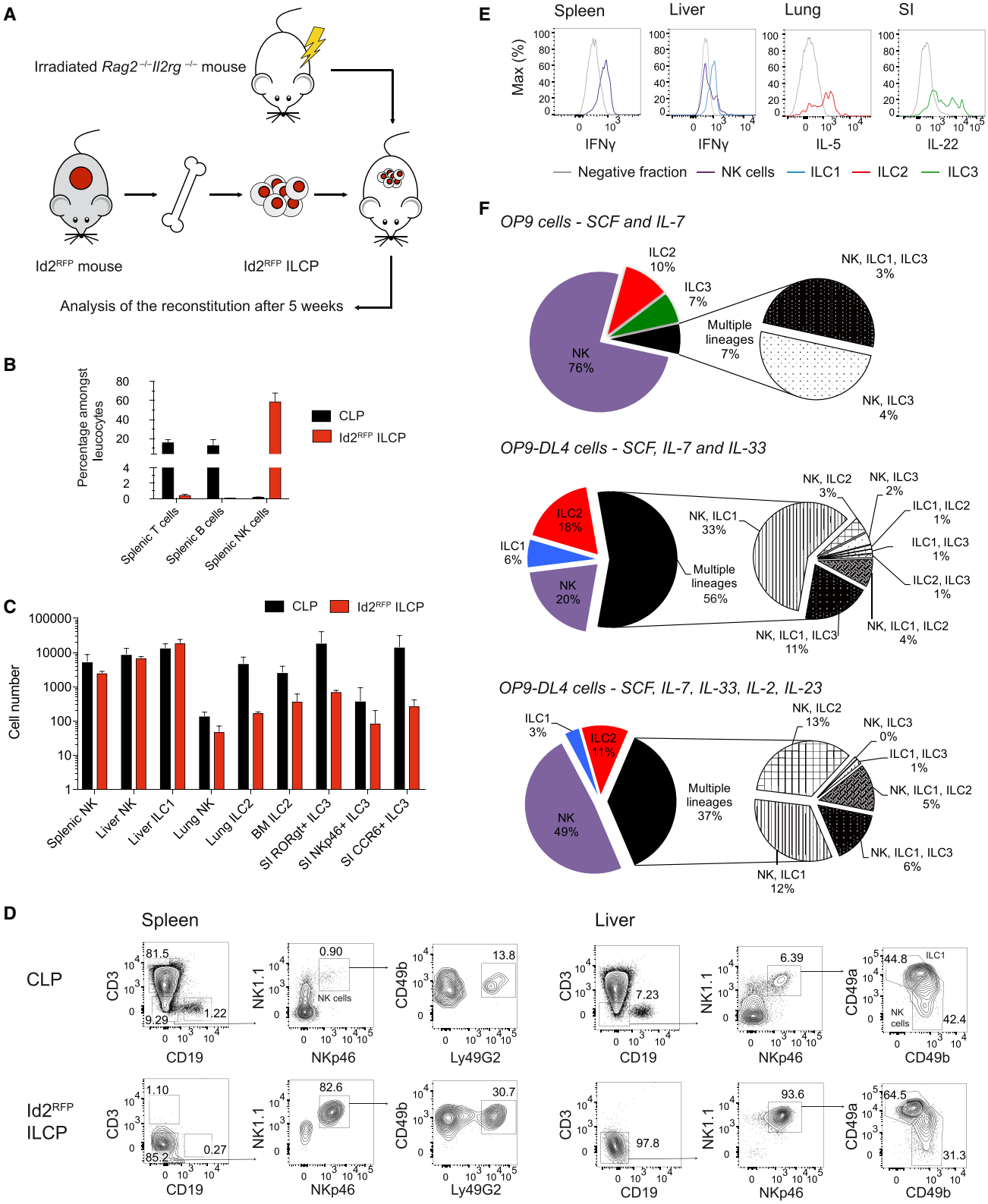

Figure 3. *Id2*$^{+}$ ILCPs Give Rise to All ILC Subsets

(A) Schematic representation of Id2^{RFP} ILCPs adoptive transfer to alymphoid *Rag2*$^{-/-}$*Il2rg*$^{-/-}$ mice.

(B and C) Reconstitution of splenic T, B, and NK cell compartments (B) and ILC compartments (C) in mice adoptively transferred with CLPs or *Id2*$^{+}$ ILCPs. n = 2–5; error bars represent standard error of the mean.

(legend continued on next page)

expected (Klose et al., 2014; Possot et al., 2011), both CLPs and Id2^{RFP} ILCPs could give rise to diverse helper-ILC subsets (including CD49a$^+$ ILC1s, ILC2s, and ILC3s; see Figure S2 for additional *in vivo* gating strategies), whereas CLPs could also give rise to T and B lymphocytes (Figures 3B and 3C). However, we also clearly detected conventional NK cells (expressing CD49b and Ly49 inhibitory receptors for major histocompatibility complex [MHC] class I) after transfer of Id2^{RFP} ILCPs (Figure 3B–3D). This result demonstrates that BM ILCPs detected using Id2^{RFP} mice harbored precursors for conventional NK cells at the population level. In contrast, such NK-cell precursors were not revealed using the Id2^{GFP}-reporter strain (Klose et al., 2014). *In-vivo*-generated NK cells and ILCs appeared functional because they were capable of producing signature cytokines after *in vitro* stimulation (Figure 3E). Our results confirm that Id2^{RFP} CD135$^-\alpha4\beta7^+$ cells harbor ILC precursors but also identify a precursor with NK-cell potential within this subset.

Generation of NK cells and ILCs *in vivo* from Id2^{RFP} ILCPs might be due to the presence of an NK-cell-committed precursor. Alternatively, a common NK-cell and ILC precursor (CILCP) that can give rise to both killer NK cells and helper ILCs could explain these findings. In order to distinguish between these possibilities, we characterized the *in vitro* lineage potential of Id2^{RFP} ILCPs. Previous reports have shown that culturing lymphoid precursors on OP9 stromal cells that do or do not express the Notch ligand Delta-like 1 could support T, NK, and helper ILC differentiation *in vitro*, depending on the cytokine milieu (Cherrier et al., 2012; Possot et al., 2011; Wong et al., 2012). Using bulk culture, we found that Id2^{RFP} ILCPs generated non-B-cell and non-T-cell populations that included not only all helper-ILC subsets but also Eomes$^+$ conventional NK cells (Figures S3A and S3B). In contrast, culture of RFP$^-$ Lin$^-$CD135$^-\alpha4\beta7^+$CD25$^-$ cells generated CD3$^+$ T cells on OP9-DL4 stroma (Figure S3A), consistent with earlier work showing that acquisition of $\alpha4\beta7$ expression by lymphoid progenitors is associated with loss of B but not T cell potential (Yoshida et al., 2001; Possot et al., 2011). Finally, *in vitro* potential from WT (non-transgenic) and Id2^{RFP} ILCPs were comparable (Figure S3C), confirming that the modified allele in Id2^{RFP} mice does not impact ILCP populations.

We further assessed the clonal heterogeneity of cell-fate potential within Id2^{RFP} ILCPs. Single ILCPs were sorted and co-cultured with OP9 or OP9-DL4 stromal cells using different cytokine combinations. The generation of various ILC subsets was assessed by flow cytometry analysis 2 weeks later. NK cells were defined as NK1.1$^+$NKp46$^+$Eomes$^+$T-bet$^+$ cells, ILC1s as NK1.1$^+$NKp46$^+$Eomes$^-$T-bet$^+$ cells, ILC2s as GATA3^{hi}CD25$^+$ ICOS$^+$ cells, and ILC3s as NKp46$^{+/-}$RORγt$^+$ cells (Figure S3B). These studies revealed several properties of Id2^{RFP} ILCPs. First, single-cell cultures of Id2^{RFP} ILCPs invariably gave rise to both single and mixed colonies of NK cells, ILC1s, ILC2s, and ILC3s (Figure 3F). This demonstrated that Id2^{RFP} ILCPs were heterogeneous and comprised multi-potent (capable of generating two or more ILC and/or NK-cell progeny) and uni-potent progenitors. Second, we found fewer colonies containing ILC2s in cultures with OP9 than in those with OP9-DL4 stromal cells (7.4% versus 28.9%), consistent with previous reports that Notch signaling is important for ILC2 generation (Wong et al., 2012). There were also more mixed-lineage ILC colonies generated in the presence of Notch ligands, suggesting that Notch signaling may be necessary to maintain or promote differentiation of multi-potent ILC precursors, as has been shown for human ILCPs (Lim et al., 2017). Third, RORγt$^+$ ILC3s were generated from Id2^{RFP} ILCPs, although these occurred at low frequency, possibly due to sub-optimal conditions for ILC3 development or expansion. Finally, a large subset of Id2^{RFP} ILCPs appeared to have robust NK-cell-lineage potential, independent of the cytokine milieu present in the cultures. These appeared mainly as uni-potent NK-cell precursors, consistent with Id2^{RFP} expression in pre-NKPs and rNKPs (Figure 1E). Nevertheless, many wells with mixed ILC lineages also harbored NK cells, indicating the presence of multi-potent Id2-expressing precursors that can give rise to both NK cells and ILCs that had not been previously appreciated (Klose et al., 2014).

Single-Cell Analysis Reveals Potential ILCP Transcriptional Trajectories

To further understand the molecular basis for the functional heterogeneity of Id2^{RFP} ILCPs, we performed single-cell transcriptional analysis by multiplex qRT-PCR. We sorted single ILCPs and CLPs from the BM of Id2^{RFP} mice and assessed the expression of 44 genes encoding TFs and surface markers that are associated with lymphoid-cell development (see Table S1). We compared these profiles with those derived from BM-resident ILC2s.

Unsupervised hierarchical clustering analysis revealed that Id2^{RFP} ILCPs had a distinct gene-expression profile compared to those of CLPs or ILC2s (Figure 4A). Four distinct clusters could be identified: cluster 1 and cluster 2 were formed by ILC2s and CLPs, respectively, whereas Id2^{RFP} ILCPs segregated into distinct clusters 3 and 4 (Figures 4A and 4B). Transcriptional signatures for cluster 2 included the cell-surface markers *CD27*, *Il7r*, and *Itga4*, as well as *Notch1*, *Rag2*, *Bcl11a*, *Runx1*, and *Ets1*, which characterize the molecular mechanisms driving CLP differentiation into the T and B cell lineages (Figure 4B). ILC-lineage-specific genes, including *Id2*, *Gata3*, *Rorc*, *Tbx21*, and *Eomes*, were not expressed in cluster 2. In contrast, cluster 1 demonstrated the expected expression signature of ILC2s, which included several TFs (*Id2*, *Rora*, *Gata3*, and *Est1*) and cell surface receptors (*Il2ra*, *Icos*, and *Il1rl1*).

Concerning Id2^{RFP} ILCPs, clusters 3 and 4 expressed the core ILC TF signature, including *Id2*, *Rora*, *Gata3*, and *Ets1*, but, unlike ILC2, also highly expressed *Tcf7*, *Tcf12*, *and Tox*. Id2^{RFP} ILCPs in clusters 3 and 4 expressed a diversity of cytokine receptors, including *Il18r1* and *Il2b* (Figure 4B), that are key drivers of NK-cell development (Hoshino et al., 1999; Suzuki et al., 1997),

(D) Spleen and liver flow cytometry analysis for ILC1s in mice adoptively transferred with CLPs or Id2^{RFP} ILCPs. Data are from one experiment representative of three independent experiments.

(E) Cytokine production of ILC subsets in mice reconstituted with Id2^{RFP} ILCPs.

(F) *In vitro* differentiation of ILCPs on OP9 or OP9-DL4 cells. Cells were cultured for 15 days with SCF and IL-7 alone or with IL-33 and/or IL-2 and IL-23. Please also see Figures S2 and S3.

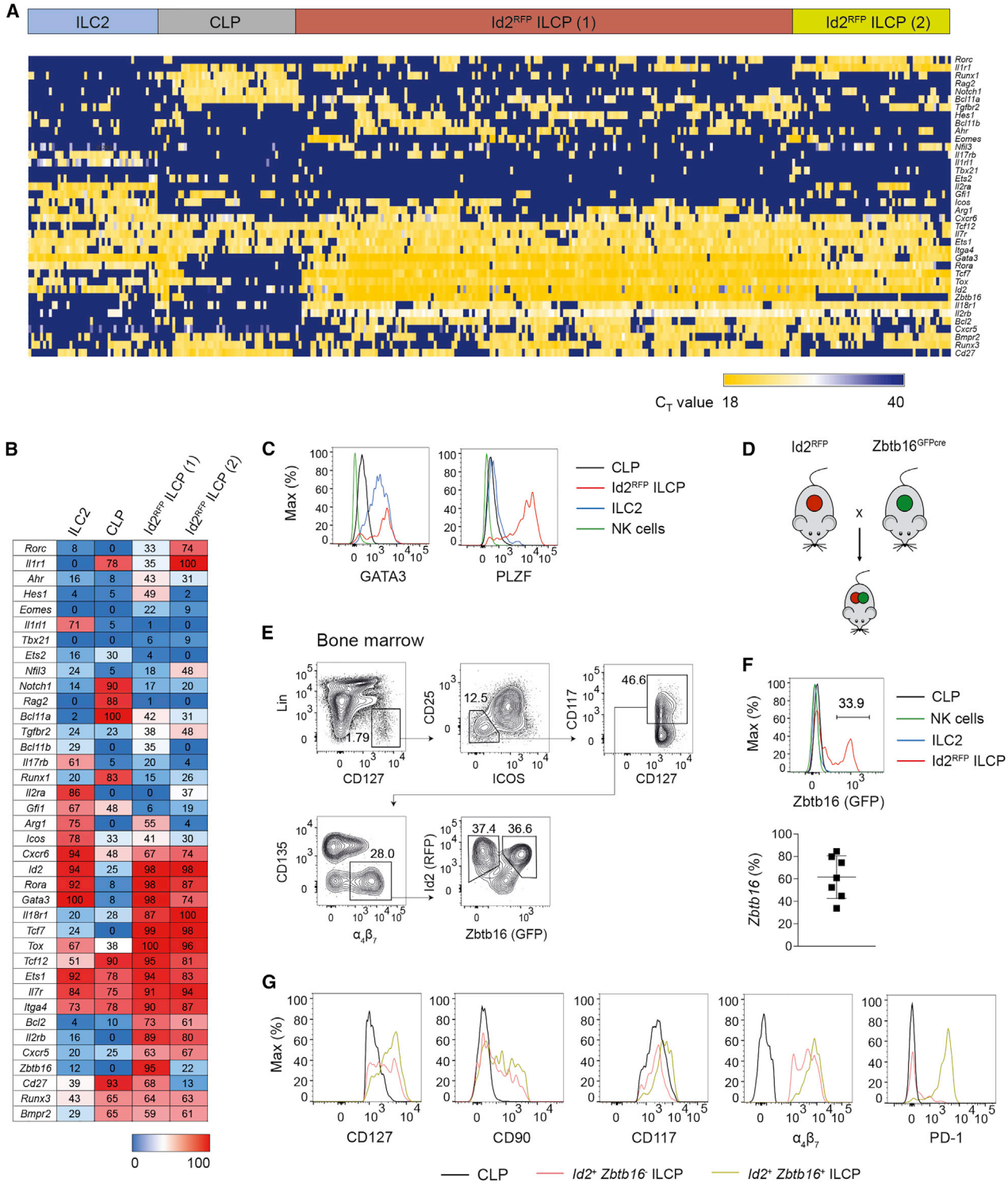

Figure 4. *Zbtb16* Expression Defines Two Subsets of *Id2*$^+$ ILCPs

(A) Single-cell multiplex qPCR ordered by hierarchical clustering of BM CLPs, *Id2*$^+$ ILCPs, and ILC2s.

(B) Percentage of single cells expressing genes of interest within CLPs, Id2^{RFP} ILCPs, and ILC2s.

(C) Fluorescence-activated cell sorting (FACS) analysis of TF expression on CLPs, *Id2*$^+$ ILCPs, ILC2s, and splenic NK cells. Data are from one experiment representative of two independent experiments.

(D) Generation of Id2^{RFP}Zbtb16^{GFPcre} double-reporter mice.

(E) Flow cytometry gating strategy for BM *Id2*$^+$*Zbtb16*$^+$ ILCPs. Data are from one experiment representative of three independent experiments.

(legend continued on next page)

although ILC1 and NK-cell transcription factors *Tbx21* and *Eomes* were mostly absent. Segregation of ILCPs in cluster 3 from those in cluster 4 was driven by the expression of *Il1r1* and *Rorc*, whereas essentially all cells in cluster 3 expressed *Zbtb16* (encoding PLZF), previously reported to identify ILCPs (Constantinides et al., 2014). Analysis of GATA3 and PLZF proteins confirmed the differential expression of these TFs in CLPs, Id2^{RFP} ILCPs, and ILC2s (Figure 4C). Taken together, the single-cell transcriptional analyses identified two closely related subsets within Id2^{RFP} ILCPs with markedly different expressions of transcription factor *Zbtb16*.

NK Lineage Potential Is Largely Retained in Id2^{+}Zbtb16^{+} ILCPs

Zbtb16-expressing cells represented about 75% of the total ILCP population in our single-cell transcriptional analysis and, as noted above, 90% of these cells expressed *Il2rb* and *Il18r1* (Figure 4B). Although a previous study showed that PLZF^{+} BM progenitors lacked NK potential (Constantinides et al., 2014), our results suggested that ILCPs expressing both Id2 and Zbtb16 might generate NK cells given the proper environmental signals. To address this hypothesis, we intercrossed Id2^{RFP} and Zbtb16^{GFPcre} strains to generate double-reporter mice (Figure 4D). Analysis of BM progenitors from Id2^{RFP}Zbtb16^{GFPcre} mice demonstrated that a fraction (ranging from 30% to 80%) of Id2^{RFP} ILCPs co-expressed Zbtb16-driven GFP (Figure 4E and 4F). The *Id2*$^{+}$*Zbtb16*$^{-}$ and *Id2*$^{+}$*Zbtb16*$^{+}$ subsets showed comparable *Id2* expression, whereas *Id2*$^{+}$*Zbtb16*$^{+}$ cells expressed higher amounts of $\alpha4\beta7$, CD117, CD127, and CD90 (Figure 4G). Moreover, we confirmed preferential expression of the inhibitory receptor PD-1 (Seillet et al., 2016; Yu et al., 2016) within the *Id2*$^{+}$*Zbtb16*$^{+}$ ILCPs (Figure 4G).

We next compared the capacity of these *Zbtb16*-expressing ILCP subsets to further differentiate *in vivo*. *Id2*$^{+}$*Zbtb16*$^{-}$ and *Id2*$^{+}$*Zbtb16*$^{+}$ ILCPs were purified from Id2^{RFP}Zbtb16^{GFPcre} mice and transferred into *Rag2*$^{-/-}$*Il2rg*$^{-/-}$ hosts. Both populations generated exclusively ILC and NK-cell progeny and lacked potential for B, T, or myeloid cells. Similar to results previously reported for *Zbtb16*$^{+}$ ILCPs (Constantinides et al., 2014), *Id2*$^{+}$ *Zbtb16*$^{+}$ ILCPs gave rise to multiple ILC lineages (ILC1, ILC2, and ILC3) in different tissues (Figure 5A). However, NK cells expressing inhibitory Ly49 receptors were clearly detected in the spleen and Eomes^{+} or CD49b^{+} NK cells were detected in the liver (Figure 5B), although CD49a^{+} ILC1s dominated in the latter, as expected (Constantinides et al., 2014). A similar pattern was observed after transfer of *Zbtb16*$^{-}$ ILCPs (Figure 5A and 5B). Taken together, these results confirm that BM *Id2*$^{+}$*Zbtb16*$^{+}$ ILCPs can give rise to ILC1s, ILC2s, and ILC3s *in vivo* (Constantinides et al., 2014) but also demonstrate that *Id2*$^{+}$*Zbtb16*$^{+}$ ILCPs retain NK-lineage potential.

We further characterized Id2^{RFP}Zbtb16^{GFPcre} progenitors using clonal assays. Single *Id2*$^{+}$*Zbtb16*$^{+}$ ILCPs were purified and cultured on OP9 or OP9-DL4 stromal cells, and the development of different ILC subsets was determined by flow cytometry as above. We found that *Id2*$^{+}$*Zbtb16*$^{+}$ ILCPs generated colonies of single or mixed ILC lineages (Figure 5C), confirming previous studies (Constantinides et al., 2014). To our surprise, many single-cell cultures of *Id2*$^{+}$*Zbtb16*$^{+}$ ILCPs also harbored NK cells (Figure 5C; Table S2). Nearly 80% of the wells derived from *Id2*$^{+}$ *Zbtb16*$^{+}$ ILCPs contained Eomes^{+} NK cells, which was comparable to results using unfractionated ILCPs (85.2%) (Figure 3F; Table S2). In contrast, the percentage of mixed-lineage colonies derived from *Id2*$^{+}$*Zbtb16*$^{+}$ ILCPs was lower than that obtained with total ILCPs (13.9% from *Id2*$^{+}$*Zbtb16*$^{+}$ ILCPs versus 37.1% from *Id2*$^{+}$ ILCPs), and the frequencies of colonies containing ILC1s or ILC3s were also reduced, in agreement with a more restricted lineage potential of *Id2*$^{+}$*Zbtb16*$^{+}$ ILCPs. Phenotypic analysis of the NK cells generated from *Id2*$^{+}$*Zbtb16*$^{+}$ ILCPs confirmed their cytotoxic potential (Figure 5D).

Id2, Zbtb16, and Bcl11b Transcripts Define Lineage Restriction of ILC Progenitors

To better understand the relationship between *Id2*$^{+}$*Zbtb16*$^{-}$ and *Id2*$^{+}$*Zbtb16*$^{+}$ ILCP subsets, we performed multiplex qRT-PCR for gene-expression analysis of the two populations. Single CLPs, *Id2*$^{+}$*Zbtb16*$^{-}$ and *Id2*$^{+}$*Zbtb16*$^{+}$ ILCPs were purified from Id2^{RFP}Zbtb16^{GFPcre} BM and 44 lymphoid genes were examined as described above. Using unsupervised hierarchical clustering, we found that *Id2*$^{+}$*Zbtb16*$^{+}$ ILCPs and *Id2*$^{+}$*Zbtb16*$^{-}$ cells were closely related but could be distinguished (Figure 6A). As expected, the expression of *Zbtb16* was restricted to *Id2*$^{+}$*Zbtb16*$^{+}$ ILCPs. The expression of several ILC-related genes, including *Id2*, *Tox*, *Tcf7*, *Gata3*, and *Rora*, gradually increased from *Id2*$^{+}$ *Zbtb16*$^{-}$ to *Id2*$^{+}$*Zbtb16*$^{+}$ ILCPs. These results implied a close developmental relationship between the *Id2*$^{+}$*Zbtb16*$^{-}$ and *Id2*$^{+}$ *Zbtb16*$^{+}$ ILCPs. Accordingly, short-term culture of *Id2*$^{+}$*Zbtb16*$^{-}$ ILCPs generated a discrete subset of *Zbtb16*$^{+}$ cells (Figure 6B) consistent with previous studies (Constantinides et al., 2014).

In addition to *Zbtb16*, we identified several genes that were enriched in *Id2*$^{+}$*Zbtb16*$^{+}$ ILCPs, including *Bcl11b*, a TF essential for ILC2 development (Califano et al., 2015; Yu et al., 2015); *Arg1*, a urea cycle enzyme that marks ILC precursors in the fetal gut and plays a key role in regulating ILC2 functions (Bando et al., 2015; Monticelli et al., 2016); and *Hes1*, a downstream target of Notch signaling (Ohtsuka et al., 1999). Conversely, we found that *Rorc*, a pivotal transcription factor for the generation of ILC3 lineages, as well as *Il1r1* and *Il2ra*, receptor subunits required for IL-1β and IL-2 signaling, respectively, were preferentially expressed in *Id2*$^{+}$*Zbtb16*$^{-}$ ILCPs.

The reduced frequency of *Rorc* and *Il1r1* transcripts in the *Id2*$^{+}$*Zbtb16*$^{+}$ ILCPs led us to speculate that these cells may have lower ILC3-lineage potential than *Id2*$^{+}$*Zbtb16*$^{-}$ ILCPs. To test this possibility, we cultured *Id2*$^{+}$*Zbtb16*$^{-}$ and *Id2*$^{+}$*Zbtb16*$^{+}$ ILCPs on OP9 or OP9-DL4 stromal cells and compared their differentiation capacity *in vitro*. Indeed, few ILC3s were generated from *Id2*$^{+}$*Zbtb16*$^{+}$ ILCPs, whereas RORγt^{+} ILC3s were detected

(F) GFP expression in CLPs, Id2^{RFP} ILCPs, ILC2s, and splenic NK cells of Id2^{RFP}Zbtb16^{GFPcre} mice (top) and percentage of Zbtb16^{GFP} expression in *Id2*$^{+}$ ILCPs (n = 7) (bottom).

(G) Flow cytometry analysis of surface marker expression on CLPs and *Id2*$^{+}$*Zbtb16*$^{-}$ and *Id2*$^{+}$*Zbtb16*$^{+}$ ILCPs. Data are from one experiment representative of two independent experiments.

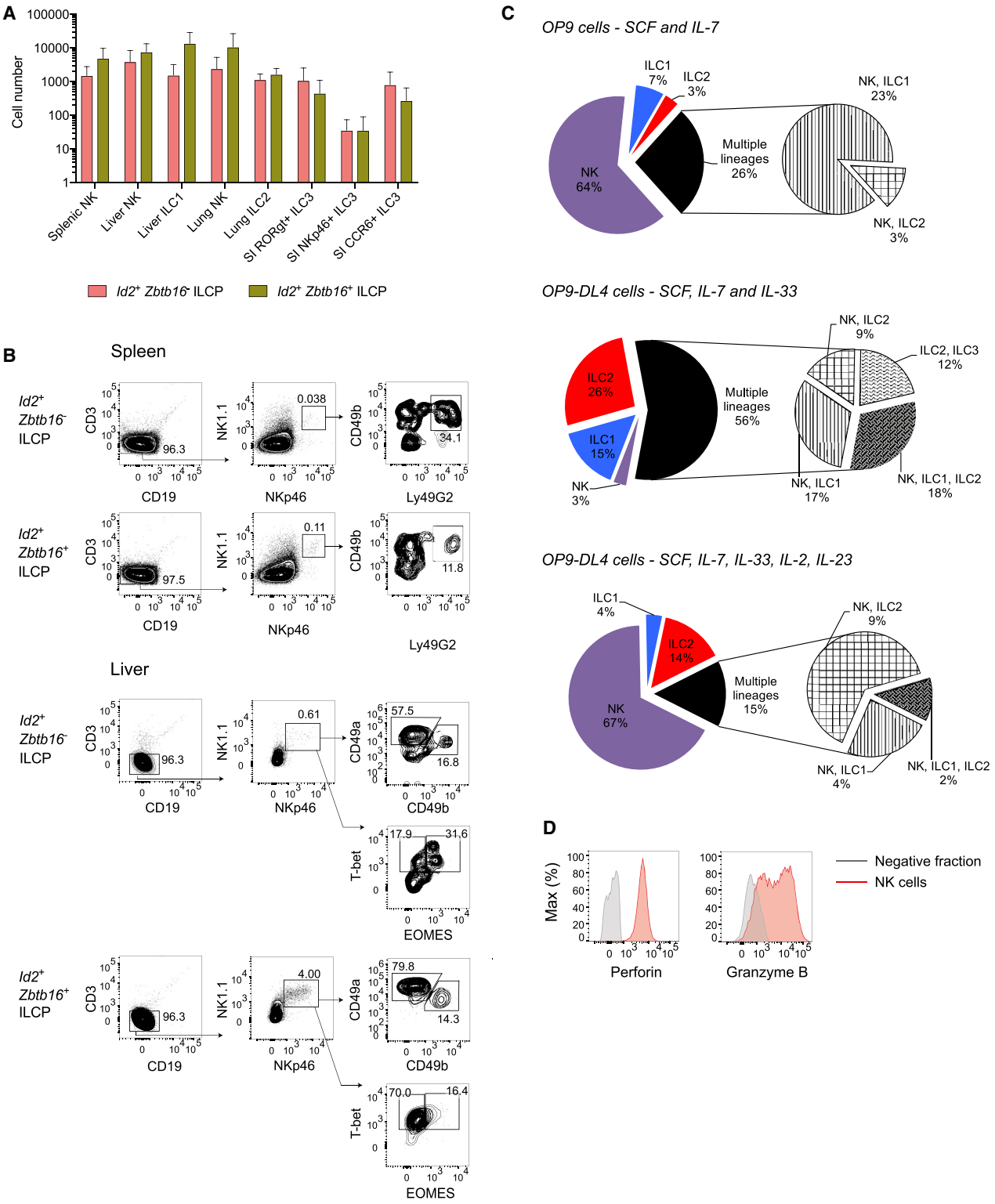

Figure 5. *Id2*$^{+}$*Zbtb16*$^{+}$ ILCPs Retain NK-Cell Potential

(A) Reconstitution of ILC compartments in mice adoptively transferred with *Id2*$^{+}$*Zbtb16*$^{-}$ or *Id2*$^{+}$*Zbtb16*$^{+}$ ILCPs (n = 4; error bars represent standard error of the mean).

(B) Spleen and liver FACS analysis for ILC1s in mice adoptively transferred with *Id2*$^{+}$*Zbtb16*$^{-}$ or *Id2*$^{+}$*Zbtb16*$^{+}$ ILCPs. Data are from one experiment representative of two independent experiments.

(legend continued on next page)

in cultures derived from *Id2*$^{+}$*Zbtb16*$^{-}$ ILCPs (Figure 6C) with little effect of enforced Notch signaling. These RORγt^{+} ILC3s also expressed CCR6, a chemokine receptor expressed by LTi cells, and were NKp46^{-} (Figure 6C). Together, these data demonstrated that *Zbtb16* expression in ILC precursors is associated with progressive loss of capacity to generate the ILC3 lineage, especially CCR6^{+} ILC3s.

The transcription factor *Bcl11b* was proposed as a global early ILCP marker that is further up-regulated in ILC2-restricted precursors and required for ILC2 development (Califano et al., 2015; Yu et al., 2015). Our single-cell multiplex gene-expression data revealed that *Bcl11b* is expressed in a subset of *Id2*$^{+}$ ILCPs and preferentially expressed in *Id2*$^{+}$*Zbtb16*$^{+}$ ILCPs. To further explore the function of these different *Id2*$^{+}$ ILCPs subsets, we intercrossed Bcl11b^{tdTomato} (Li et al., 2010) and Id2^{RFP}Zbtb16^{GFPcre} mice to generate Id2^{RFP}Zbtb16^{GFPcre} Bcl11b^{tdTomato} triple-reporter mice. Analysis of the BM progenitor cells from these mice showed that *Zbtb16* and *Bcl11b* expression divided Id2^{RFP} ILCPs into four discrete subsets: *Zbtb16*$^{-}$*Bcl11b*$^{-}$, *Zbtb16*$^{+}$*Bcl11b*$^{-}$, *Zbtb16*$^{+}$*Bcl11b*$^{+}$, and *Zbtb16*$^{-}$*Bcl11b*$^{+}$ ILCPs (Figure 7A).

We next compared the expression of several cell-surface markers of BM progenitors or ILC2s among these four subsets. Although all comparably expressed CD27, CD117, and CD90 (Figure 7B), PD-1 was strictly expressed by *Zbtb16*$^{+}$ ILCPs regardless of *Bcl11b* expression, and none of the subsets expressed CD25, which characterizes late-stage ILC2 differentiation. A fraction of *Zbtb16*$^{-}$*Bcl11b*$^{-}$ ILCPs expressed RORγt and lower amounts of CD27 compared to other subsets (Figure 7C), in accordance with the transcriptional profile of *Id2*$^{+}$*Zbtb16*$^{-}$ ILCPs (Figure 6A). To compare the developmental potential of these four Id2^{RFP} ILCPs subsets, we bulk cultured purified *Zbtb16*$^{-}$*Bcl11b*$^{-}$, *Zbtb16*$^{+}$*Bcl11b*$^{-}$, *Zbtb16*$^{+}$*Bcl11b*$^{+}$, and *Zbtb16*$^{-}$*Bcl11b*$^{+}$ ILCPs on OP9-DL4 stromal cells with cytokines and characterized their progeny. *Bcl11b*-expressing ILCPs, regardless of *Zbtb16* expression, grew poorly in IL-7 and stem cell factor (SCF) (Figure S3D). When IL-33 was added to the cultures, robust ILC2 growth was observed (Figures 7D and 7E), indicating that these cells were highly enriched in ILC2 precursors, consistent with previous reports (Califano et al., 2015; Yu et al., 2015). In contrast, *Zbtb16*$^{+}$*Bcl11b*$^{-}$ ILCPs could generate NK cells, ILC1s, and ILC2s but only few ILC3s. Only *Zbtb16*$^{-}$*Bcl11b*$^{-}$ ILCPs could give rise to all three ILC lineages (ILC1, ILC2, and ILC3) as well as NK cells (Figures 7D and 7E). Clonal analyses confirmed these findings (Figure 7F). Thus, *Zbtb16*$^{-}$*Bcl11b*$^{-}$ ILCPs harbor the earliest BM Id2^{RFP} ILCPs that can generate all ILC and NK-cell lineages.

DISCUSSION

Using a highly sensitive Id2^{RFP}-reporter mouse model, we have characterized heterogeneous progenitor populations in adult BM that include ILCPs and NK-cell-restricted precursors (NKPs). These Id2^{RFP} ILCPs are comprised of both multi-potent (giving rise to multiple ILC lineages, including conventional NK cells) and uni-potent precursors, with potential for a single ILC group or for conventional NK cells. By multiplexing our Id2^{RFP} reporter with existing TF reporters (Zbtb16^{GFPcre} and Bcl11b^{tdTomato}), we could simultaneously assess the impact of three key transcription factors (*Id2*, *Zbtb16*, and *Bcl11b*) to ILC development and uncover the substantial phenotypic and functional heterogeneity of Id2^{RFP} ILCPs. Through single-cell qPCR analysis and *in vitro* clonal assays, we could redefine the earliest common ILCPs downstream of the common lymphoid progenitor and clarify the contribution of several TFs at the different stages of ILC development. Based on these results, we propose a revised scheme of murine BM ILC and NK-cell differentiation that markedly contrasts with the current helper versus killer model (Figure S4).

The Id2^{RFP} reporter used in this study provided a key tool to dissect ILCP diversity due to robust and distinct fluorescence properties. Compared with the previously described Id2^{GFP} mice used to identify CHILPs (Klose et al. 2014), our Id2^{RFP} reporter has brighter fluorescence, which allowed for the identification of a larger fraction of *Id2*-expressing cells in the BM. Because RFP can be spectrally separated from GFP, YFP, and tdTomato fluorochromes using standard flow cytometers, we could take advantage of multiplexed fluorescent reporters to isolate distinct ILCP subpopulations that differentially expressed three key transcription factors required for ILC development. This allowed us to perform an in-depth phenotypic, transcriptomic, and functional analysis of Id2^{RFP} ILCP subsets both *in vivo* and *in vitro*. Importantly, we used standardized and widely accepted criteria for identifying mature ILC subsets derived from these different ILCPs. This was a critical issue because previous reports have not always used the same defining markers for NK cells and ILC progeny of ILCPs (Constantinides et al., 2014; Klose et al., 2014), leading to some question about the precursor-product relationship of ILCPs with mature ILC and NK cells.

Based on studies using Id2^{GFP} mice, Klose et al. (2014) identified an ILCP population (CHILPs) that could give rise *in vitro* and *in vivo* to several ILC subsets (Eomes^{-} ILC1, ILC2, and ILC3) but not to conventional Eomes^{+} NK cells. The authors proposed a killer versus helper model of ILC and NK-cell development from CLPs in which NK cells emerge prior to the *Id2*$^{+}$ CHILP stage, although other ILC subsets are CHILP derived. The authors also suggested that early NK-cell development was relatively Id2 independent because only low amounts of GFP were detected in NKPs from *Id2*^{GFP} mice (Klose et al., 2014). In contrast, we have provided evidence for *Id2*-expressing lymphoid progenitors in Id2^{RFP} mice with potential for all ILC lineages, including NK cells. These differences may be explained by the better discrimination of these rare cells in Id2^{RFP} mice, allowing for isolation of multi-potent ILCPs and NKPs. Single-cell assays demonstrate that ILCPs can generate both conventional

(C) *In vitro* differentiation of *Id2*$^{+}$*Zbtb16*$^{+}$ ILCPs on OP9 or OP9-DL4 cells. Cells were cultured during 15 days with SCF and IL-7 or with IL-33 and/or IL-2 and IL-23. (D) Analysis of perforin and granzyme B expression in NK cells derived from bulk culture of 200 *Id2*$^{+}$*Zbtb16*$^{+}$ ILCPs. Cells were cultured during 7 days on OP9 cells with SCF and IL-7 and supplemented for 1 day with IL-12 and IL-15. Data are from one experiment representative of two independent experiments, each including technical triplicates.

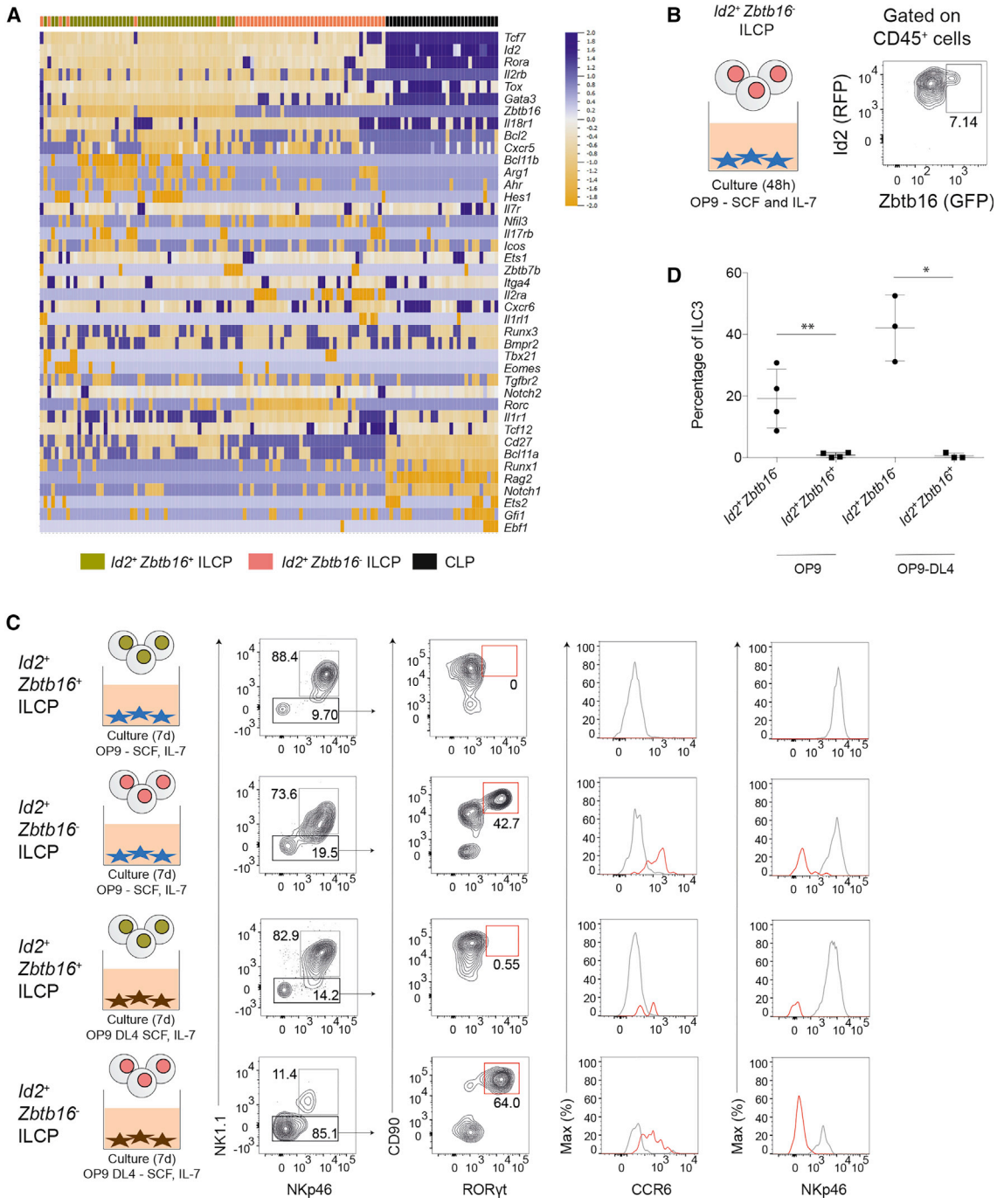

Figure 6. *Id2*$^+$*Zbtb16*$^+$ ILCPs Derive from *Id2*$^+$*Zbtb16*$^-$ Cells with Loss of ILC3 Potential

(A) Single-cell multiplex qPCR ordered by hierarchical clustering of BM CLPs and *Id2*$^+$*Zbtb16*$^-$ and *Id2*$^+$*Zbtb16*$^+$ ILCPs.

(B) RFP and GFP expression on *Id2*$^+$*Zbtb16*$^-$ ILCPs cultured for 48 h on OP9 cells with SCF and IL-7. Data are from one experiment representative of three independent experiments.

(C) Flow cytometry analysis for ILC3s after culture of *Id2*$^+$*Zbtb16*$^-$ ILCPs and *Id2*$^+$*Zbtb16*$^+$ ILCPs or 7 days on OP9 or OP9-DL4 cells with SCF and IL-7. Data are from one experiment representative of two independent experiments, each including technical duplicates.

(D) Percentage of ILC3s among CD45$^+$ cells after 7 days' culture of *Id2*$^+$*Zbtb16*$^-$ and *Id2*$^+$*Zbtb16*$^+$ ILCPs on OP9 or OP9-DL4 cells with SCF and IL-7. n = 3 or 4; error bars represent standard error of the mean; *p < 0.1, **p < 0.05, Mann-Whitney U test.

Eomes$^+$ NK cells and different ILC subsets, providing evidence for a common ILC and NK-cell progenitor that expresses *Id2*. Our results argue against the notion of separate "branches" of killer-NK-cell and helper-ILC development that are *Id2* independent and *Id2* dependent, respectively. Rather, we envisage a model of *Id2*-mediated suppression of adaptive B and T cell

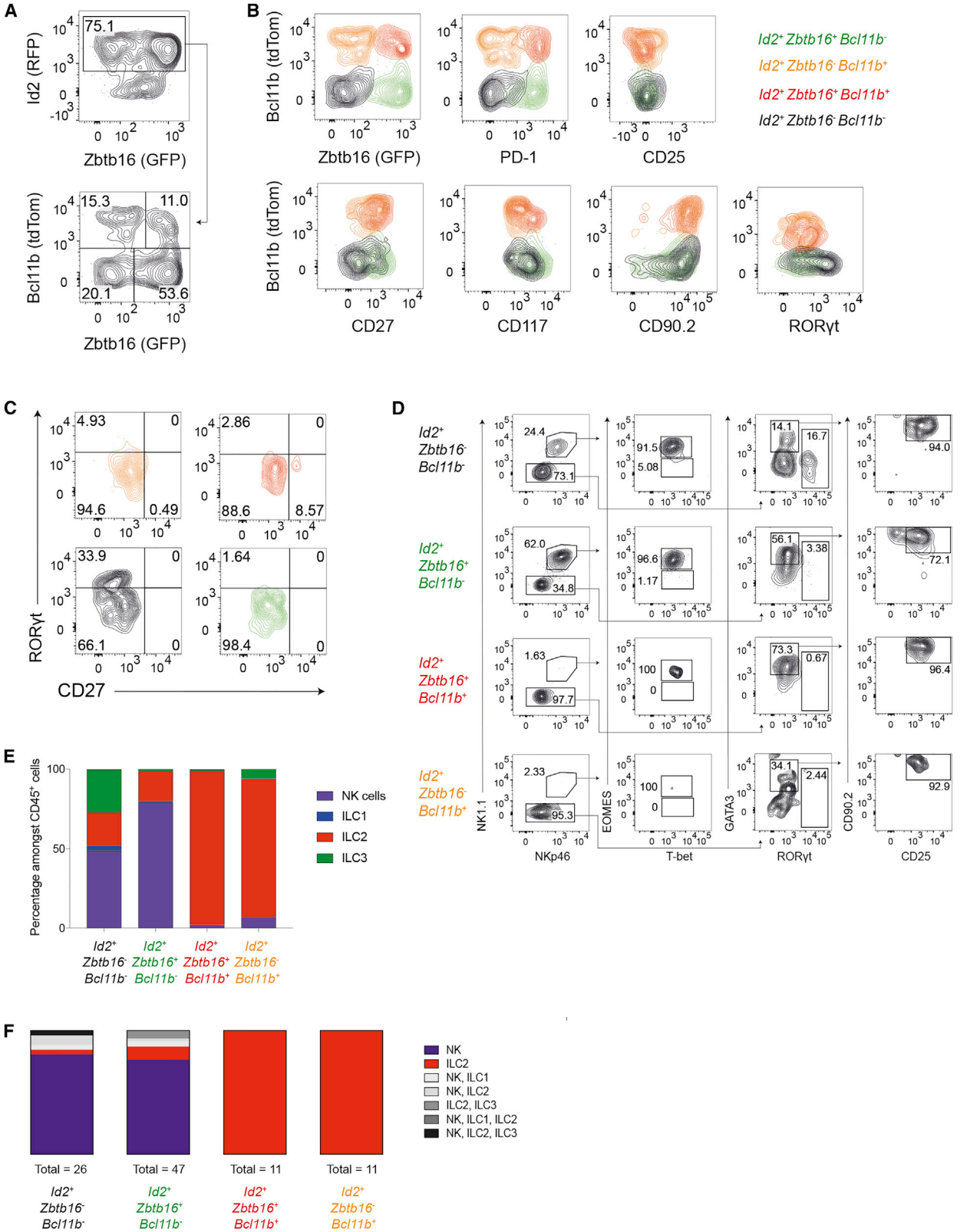

Figure 7. *Bcl11b* Marks Emergence of an ILC2-Restricted Precursor

(A) Flow cytometry characterization of Lin$^-$CD127$^+$CD25$^-$ICOS$^-$CD117$^+$CD135$^-$$\alpha_4\beta_7^+$ cells from Id2^{RFP}Zbtb16^{GFPcre}Bcl11b^{tdTomato} mice.

(B) Flow cytometry analysis of surface marker and transcription factor expression on Id2^{RFP} ILCPs according to their expression of *Zbtb16* and *Bcl11b*.

(legend continued on next page)

development from CLPs that is associated with emergence of CILCPs and NK-cell precursors (Figure S4). This revised model places committed NK-cell progenitors (Fathman et al. 2011; Rosmaraki et al., 2001) downstream of CILCPs.

Previous studies using Zbtb16^{GFPCre} reporter mice identify a PLZF$^+$ ILCP (Constantinides et al., 2014) that shows a phenotypic and functional overlap with *Id2*$^+$ CHILPs (Klose et al., 2014). *Zbtb16*$^+$ ILCPs could give rise to ILC1s, ILC2s, and NKp46$^+$ ILC3s but not to conventional NK cells or CD4$^+$ LTi-like ILC3s. A model has been proposed whereby PLZF expression in ILCPs was associated with reduced generation of NK cells and CCR6$^+$ CD4$^+$ ILC3s. It was therefore of great interest to better understand the complexity of these different ILCP populations through analysis of Id2^{RFP}Zbtb16^{CreGFP} double-reporter mice. As expected (Constantinides et al., 2014), we found that *Id2*$^+$*Zbtb16*$^+$ ILCPs could robustly generate ILC1 and ILC2 subsets and showed strongly reduced potential for CCR6$^+$ ILC3s (LTi-like ILC3s). Moreover, we found that *Id2*$^+$*Zbtb16*$^+$ ILCPs gave rise to conventional NK cells both *in vitro* and *in vivo*, suggesting that these precursors retained substantial NK-cell-lineage potential. Generation of Eomes$^+$ NK-cell-containing clones was obtained from *Id2*$^+$*Zbtb16*$^+$ ILCPs, and these cells harbored Eomes-dependent cytotoxic molecules (perforin and granzyme B) after growth *in vitro*. Importantly, NK cells derived from *Id2*$^+$*Zbtb16*$^+$ ILCPs *in vivo* expressed markers of mature conventional NK cells (Ly49 receptors, CD49b) that were not expressed by ILC1s. These results indicate that PLZF expression in ILCPs is compatible with conventional NK-cell development, in contrast with the current models (Diefenbach et al., 2014; Constantinides et al., 2014). It is possible that NK-cell progeny from *Zbtb16*$^+$ ILCPs were not detected because Eomes staining was not performed in the previous study (Constantinides et al., 2014). The molecular mechanisms that promote NK-cell development from ILCPs remain unclear, although it is interesting to speculate that this process might be controlled in an analogous fashion to that which operates during intrathymic CD8-lineage determination (via cytokine-driven survival and expansion) (Cherrier et al., 2018).

By multiplexing *Id2*, *Zbtb16*, and *Bcl11b* reporters, we could confirm previous reports that identified early *Bcl11b* expression and ILC2 differentiation (Califano et al., 2015; Yu et al., 2015). The precise stage at which up-regulation of Bcl11b occurs to commit ILCPs to the ILC2 fate was not known. By studying Id2^{RFP}Zbtb16^{GFPcre}Bcl11b^{tdTomato} triple-reporter mice, we could demonstrate complexity in the ILCP compartment that raised additional questions concerning the progressive stages of ILC differentiation. We found that *Bcl11b* expression was enriched for ILC2 fate in *Id2*$^+$ ILCPs but that this process appeared independent of *Zbtb16* expression. A sequential model of ILC2 differentiation (*Zbtb16*$^+$*Bcl11b*$^-$ → *Zbtb16*$^+$*Bcl11b*$^+$ → *Zbtb16*$^-$*Bcl11b*$^+$) would accommodate the data and be consistent with previous fate-mapping studies (Constantinides et al., 2014), although *Zbtb16*-independent pathways may also exist. Further studies will be required to understand the inter-relationships between PLZF- and BCL11B-dependent ILC differentiation.

Analysis of Id2^{RFP}Zbtb16^{GFPcre}Bcl11b^{tdTomato} mice also demonstrated that in ILC3s, especially CCR6$^+$ ILC3s (LTi-like cells), differentiation was highly enriched in *Id2*$^+$*Zbtb16*$^-$*Bcl11b*$^-$ ILCPs. In contrast, expression of either *Zbtb16* or *Bcl11b* was associated with loss of ILC3 potential. As such, our results suggest that ILC3 emergence from *Id2*$^+$ ILCPs may represent one of the earliest branch points in ILC development, which separates ILC3 (via up-regulation of *Rorc*) from ILC1, ILC2, or NK-cell (via up-regulation of *Zbtb16*) pathways, which was also observed during fetal ILC differentiation (Ishizuka et al., 2016). Understanding the signals that instruct expression of these critical TFs should shed light on how these unique innate effector cells are generated and may lead to approaches that can promote their development in diverse disease settings.

STAR★METHODS

Detailed methods are provided in the online version of this paper and include the following:

- KEY RESOURCES TABLE
- CONTACT FOR REAGENT AND RESOURCE SHARING
- METHOD DETAILS
  - Mice
  - Cell Isolation
  - Flow Cytometric Analysis
  - Cell Culture
  - *In Vivo* Adoptive Transfer
  - Biomarker Analysis and qRT-PCR
- QUANTIFICATION AND STATISTICAL ANALYSIS

SUPPLEMENTAL INFORMATION

Supplemental Information can be found with this article online at https://doi.org/10.1016/j.immuni.2019.02.022.

ACKNOWLEDGMENTS

We thank Albert Bendelac for providing Zbtb16^{GFPCre} mice, Andreas Diefenbach for providing Id2^{GFP} mice, and Ana Cumano for providing OP9 and OP9-DL4 cells. We are grateful to Francina Langa-Vives and Franck Bourgade for their help with the generation of Id2^{RFP} mice and the CB-UTechS platform for cytometry support. We thank all the members of the Innate Immunity Unit for helpful discussions. D.E.C. is supported by the French Ministry of Higher Education, Research and Innovation. The Innate Immunity Unit is supported by grants from the Institut National de la Santé et de la Recherche Médicale (INSERM), Institut Pasteur, the Agence National pour le Recherche (ANR),

(C) Flow cytometry analysis of RORγt and CD27 expression on Id2^{RFP} ILCPs according to their expression of *Zbtb16* and *Bcl11b*. Data are from one experiment representative of two independent experiments.

(D) Flow cytometry analysis for mature ILCs after bulk culture of *Id2*$^+$*Zbtb16*$^-$*Bcl11b*$^-$, *Id2*$^+$*Zbtb16*$^+$*Bcl11b*$^-$, *Id2*$^+$*Zbtb16*$^+$*Bcl11b*$^+$, or *Id2*$^+$*Zbtb16*$^-$*Bcl11b*$^+$ ILCPs for 7 days on OP9 cells with SCF, IL-7, and IL-33. Data are from one experiment representative of three independent experiments.

(E) Percentage of mature ILC subsets among CD45$^+$ cells for (D).

(F) *In vitro* differentiation of single *Id2*$^+$*Zbtb16*$^-$*Bcl11b*$^-$, *Id2*$^+$*Zbtb16*$^+$*Bcl11b*$^-$, *Id2*$^+$*Zbtb16*$^+$*Bcl11b*$^+$, or *Id2*$^+$*Zbtb16*$^-$*Bcl11b*$^+$ ILCPs on OP9 cells. Cells were cultured during 15 days with SCF, IL-7, and IL-33. Please also see Figure S3.

and the European Research Council (ERC) under the European Union's Horizon 2020 research and innovation program (695467 – ILC_REACTIVITY).

AUTHOR CONTRIBUTIONS

W.X. and D.E.C. designed, performed, and analyzed experiments and wrote the manuscript; S.C. and M.P. analyzed the Biomark experiments; C.V. and R.G. helped edit the manuscript; N.S. performed experiments and helped prepare figures; P.L. provided Bcl11b^{tdTom} mice; and J.P.D. designed and directed the study and wrote the manuscript.

DECLARATION OF INTERESTS

The authors declare no competing interests.

Received: July 12, 2018
Revised: January 3, 2019
Accepted: February 25, 2019
Published: March 26, 2019

REFERENCES

Aliahmad, P., de la Torre, B., and Kaye, J. (2010). Shared dependence on the DNA-binding factor TOX for the development of lymphoid tissue-inducer cell and NK cell lineages. Nat. Immunol. *11*, 945–952.

Bando, J.K., Liang, H.E., and Locksley, R.M. (2015). Identification and distribution of developing innate lymphoid cells in the fetal mouse intestine. Nat. Immunol. *16*, 153–160.

Boos, M.D., Yokota, Y., Eberl, G., and Kee, B.L. (2007). Mature natural killer cell and lymphoid tissue-inducing cell development requires Id2-mediated suppression of E protein activity. J. Exp. Med. *204*, 1119–1130.

Califano, D., Cho, J.J., Uddin, M.N., Lorentsen, K.J., Yang, Q., Bhandoola, A., Li, H., and Avram, D. (2015). Transcription Factor Bcl11b Controls Identity and Function of Mature Type 2 Innate Lymphoid Cells. Immunity *43*, 354–368.

Carotta, S., Pang, S.H.M., Nutt, S.L., and Belz, G.T. (2011). Identification of the earliest NK-cell precursor in the mouse BM. Blood *117*, 5449–5452.

Chea, S., Possot, C., Perchet, T., Petit, M., Cumano, A., and Golub, R. (2015). CXCR6 Expression Is Important for Retention and Circulation of ILC Precursors. Mediators Inflamm. *2015*, 368427.

Cherrier, M., Sawa, S., and Eberl, G. (2012). Notch, Id2, and RORγt sequentially orchestrate the fetal development of lymphoid tissue inducer cells. J. Exp. Med. *209*, 729–740.

Cherrier, D., Serafini, N., and Di Santo, J.P. (2018). Innate Lymphoid Cell Development: A T Cell Perspective. Immunity *48*, 1091–1103.

Colucci, F., Soudais, C., Rosmaraki, E., Vanes, L., Tybulewicz, V.L., and Di Santo, J.P. (1999). Dissecting NK cell development using a novel alymphoid mouse model: investigating the role of the c-abl proto-oncogene in murine NK cell differentiation. J. Immunol. *162*, 2761–2765.

Constantinides, M.G., McDonald, B.D., Verhoef, P.A., and Bendelac, A. (2014). A committed precursor to innate lymphoid cells. Nature *508*, 397–401.

Constantinides, M.G., Gudjonson, H., McDonald, B.D., Ishizuka, I.E., Verhoef, P.A., Dinner, A.R., and Bendelac, A. (2015). PLZF expression maps the early stages of ILC1 lineage development. Proc. Natl. Acad. Sci. USA *112*, 5123–5128.

Cording, S., Medvedovic, J., Cherrier, M., and Eberl, G. (2014). Development and regulation of RORγt(+) innate lymphoid cells. FEBS Lett. *588*, 4176–4181.

Diefenbach, A., Colonna, M., and Koyasu, S. (2014). Development, differentiation, and diversity of innate lymphoid cells. Immunity *41*, 354–365.

Fathman, J.W., Bhattacharya, D., Inlay, M.A., Seita, J., Karsunky, H., and Weissman, I.L. (2011). Identification of the earliest natural killer cell-committed progenitor in murine bone marrow. Blood *118*, 5439–5447.

Hoshino, K., Tsutsui, H., Kawai, T., Takeda, K., Nakanishi, K., Takeda, Y., and Akira, S. (1999). Cutting edge: generation of IL-18 receptor-deficient mice: evidence for IL-1 receptor-related protein as an essential IL-18 binding receptor. J. Immunol. *162*, 5041–5044.

Hoyler, T., Klose, C.S.N., Souabni, A., Turqueti-Neves, A., Pfeifer, D., Rawlins, E.L., Voehringer, D., Busslinger, M., and Diefenbach, A. (2012). The transcription factor GATA-3 controls cell fate and maintenance of type 2 innate lymphoid cells. Immunity *37*, 634–648.

Ishizuka, I.E., Chea, S., Gudjonson, H., Constantinides, M.G., Dinner, A.R., Bendelac, A., and Golub, R. (2016). Single-cell analysis defines the divergence between the innate lymphoid cell lineage and lymphoid tissue-inducer cell lineage. Nat. Immunol. *17*, 269–276.

Jackson, J.T., Hu, Y., Liu, R., Masson, F., D'Amico, A., Carotta, S., Xin, A., Camilleri, M.J., Mount, A.M., Kallies, A., et al. (2011). Id2 expression delineates differential checkpoints in the genetic program of CD8α+ and CD103+ dendritic cell lineages. EMBO J. *30*, 2690–2704.

Kee, B.L. (2009). E and ID proteins branch out. Nat. Rev. Immunol. *9*, 175–184.

Klose, C.S.N., Flach, M., Möhle, L., Rogell, L., Hoyler, T., Ebert, K., Fabiunke, C., Pfeifer, D., Sexl, V., Fonseca-Pereira, D., et al. (2014). Differentiation of type 1 ILCs from a common progenitor to all helper-like innate lymphoid cell lineages. Cell *157*, 340–356.

Li, P., Burke, S., Wang, J., Chen, X., Ortiz, M., Lee, S.-C., Lu, D., Campos, L., Goulding, D., Ng, B.L., et al. (2010). Reprogramming of T cells to natural killer-like cells upon Bcl11b deletion. Science *329*, 85–89.

Lim, A.I., Li, Y., Lopez-Lastra, S., Stadhouders, R., Paul, F., Casrouge, A., Serafini, N., Puel, A., Bustamante, J., Surace, L., et al. (2017). Systemic Human ILC Precursors Provide a Substrate for Tissue ILC Differentiation. Cell *168*, 1086–1100.e10.

Monticelli, L.A., Buck, M.D., Flamar, A.-L., Saenz, S.A., Tait Wojno, E.D., Yudanin, N.A., Osborne, L.C., Hepworth, M.R., Tran, S.V., Rodewald, H.-R., et al. (2016). Arginase 1 is an innate lymphoid-cell-intrinsic metabolic checkpoint controlling type 2 inflammation. Nat. Immunol. *17*, 656–665.

Moro, K., Yamada, T., Tanabe, M., Takeuchi, T., Ikawa, T., Kawamoto, H., Furusawa, J., Ohtani, M., Fujii, H., and Koyasu, S. (2010). Innate production of T(H)2 cytokines by adipose tissue-associated c-Kit(+)Sca-1(+) lymphoid cells. Nature *463*, 540–544.

Nechanitzky, R., Akbas, D., Scherer, S., György, I., Hoyler, T., Ramamoorthy, S., Diefenbach, A., and Grosschedl, R. (2013). Transcription factor EBF1 is essential for the maintenance of B cell identity and prevention of alternative fates in committed cells. Nat. Immunol. *14*, 867–875.

Ohtsuka, T., Ishibashi, M., Gradwohl, G., Nakanishi, S., Guillemot, F., and Kageyama, R. (1999). Hes1 and Hes5 as notch effectors in mammalian neuronal differentiation. EMBO J. *18*, 2196–2207.

Possot, C., Schmutz, S., Chea, S., Boucontet, L., Louise, A., Cumano, A., and Golub, R. (2011). Notch signaling is necessary for adult, but not fetal, development of RORγt(+) innate lymphoid cells. Nat. Immunol. *12*, 949–958.

Ramirez, K., Chandler, K.J., Spaulding, C., Zandi, S., Sigvardsson, M., Graves, B.J., and Kee, B.L. (2012). Gene deregulation and chronic activation in natural killer cells deficient in the transcription factor ETS1. Immunity *36*, 921–932.

Rawlins, E.L., Clark, C.P., Xue, Y., and Hogan, B.L.M. (2009). The Id2+ distal tip lung epithelium contains individual multipotent embryonic progenitor cells. Development *136*, 3741–3745.

Rosmaraki, E.E., Douagi, I., Roth, C., Colucci, F., Cumano, A., and Di Santo, J.P. (2001). Identification of committed NK cell progenitors in adult murine bone marrow. Eur. J. Immunol. *31*, 1900–1909.

Satoh-Takayama, N., Lesjean-Pottier, S., Vieira, P., Sawa, S., Eberl, G., Vosshenrich, C.A.J., and Di Santo, J.P. (2010). IL-7 and IL-15 independently program the differentiation of intestinal CD3-NKp46+ cell subsets from Id2-dependent precursors. J. Exp. Med. *207*, 273–280.

Seehus, C.R., Aliahmad, P., de la Torre, B., Iliev, I.D., Spurka, L., Funari, V.A., and Kaye, J. (2015). The development of innate lymphoid cells requires TOX-dependent generation of a common innate lymphoid cell progenitor. Nat. Immunol. *16*, 599–608.

Seillet, C., Mielke, L.A., Amann-Zalcenstein, D.B., Su, S., Gao, J., Almeida, F.F., Shi, W., Ritchie, M.E., Naik, S.H., Huntington, N.D., et al. (2016). Deciphering the Innate Lymphoid Cell Transcriptional Program. Cell Rep. *17*, 436–447.

Serafini, N., Klein Wolterink, R.G.J., Satoh-Takayama, N., Xu, W., Vosshenrich, C.A.J., Hendriks, R.W., and Di Santo, J.P. (2014). Gata3 drives development of RORγt+ group 3 innate lymphoid cells. J. Exp. Med. *211*, 199–208.

Serafini, N., Vosshenrich, C.A., and Di Santo, J.P. (2015). Transcriptional regulation of innate lymphoid cell fate. Nat. Rev. Immunol. *15*, 415–428.

Suzuki, H., Duncan, G.S., Takimoto, H., and Mak, T.W. (1997). Abnormal development of intestinal intraepithelial lymphocytes and peripheral natural killer cells in mice lacking the IL-2 receptor beta chain. J. Exp. Med. *185*, 499–505.

Vivier, E., Artis, D., Colonna, M., Diefenbach, A., Di Santo, J.P., Eberl, G., Koyasu, S., Locksley, R.M., McKenzie, A.N.J., Mebius, R.E., et al. (2018). Innate Lymphoid Cells: 10 Years On. Cell *174*, 1054–1066.

Wong, S.H., Walker, J.A., Jolin, H.E., Drynan, L.F., Hams, E., Camelo, A., Barlow, J.L., Neill, D.R., Panova, V., Koch, U., et al. (2012). Transcription factor RORα is critical for nuocyte development. Nat. Immunol. *13*, 229–236.

Xu, W., Domingues, R.G.G., Fonseca-Pereira, D., Ferreira, M., Ribeiro, H., Lopez-Lastra, S., Motomura, Y., Moreira-Santos, L., Bihl, F., Braud, V., et al. (2015). NFIL3 orchestrates the emergence of common helper innate lymphoid cell precursors. Cell Rep. *10*, 2043–2054.

Yang, Q., and Bhandoola, A. (2016). The development of adult innate lymphoid cells. Curr. Opin. Immunol. *39*, 114–120.

Yang, C.Y., Best, J.A., Knell, J., Yang, E., Sheridan, A.D., Jesionek, A.K., Li, H.S., Rivera, R.R., Lind, K.C., D'Cruz, L.M., et al. (2011). The transcriptional regulators Id2 and Id3 control the formation of distinct memory CD8+ T cell subsets. Nat. Immunol. *12*, 1221–1229.

Yang, Q., Li, F., Harly, C., Xing, S., Ye, L., Xia, X., Wang, H., Wang, X., Yu, S., Zhou, X., et al. (2015). TCF-1 upregulation identifies early innate lymphoid progenitors in the bone marrow. Nat. Immunol. *16*, 1044–1050.

Yokota, Y., Mansouri, A., Mori, S., Sugawara, S., Adachi, S., Nishikawa, S., and Gruss, P. (1999). Development of peripheral lymphoid organs and natural killer cells depends on the helix-loop-helix inhibitor Id2. Nature *397*, 702–706.

Yoshida, H., Kawamoto, H., Santee, S.M., Hashi, H., Honda, K., Nishikawa, S., Ware, C.F., Katsura, Y., and Nishikawa, S.-I. (2001). Expression of alpha(4) beta(7) integrin defines a distinct pathway of lymphoid progenitors committed to T cells, fetal intestinal lymphotoxin producer, NK, and dendritic cells. J. Immunol. *167*, 2511–2521.

Yu, X., Wang, Y., Deng, M., Li, Y., Ruhn, K.A., Zhang, C.C., and Hooper, L.V. (2014). The basic leucine zipper transcription factor NFIL3 directs the development of a common innate lymphoid cell precursor. eLife *3*, 945–952.

Yu, Y., Wang, C., Clare, S., Wang, J., Lee, S.C., Brandt, C., Burke, S., Lu, L., He, D., Jenkins, N.A., et al. (2015). The transcription factor Bcl11b is specifically expressed in group 2 innate lymphoid cells and is essential for their development. J. Exp. Med. *212*, 865–874.

Yu, Y., Tsang, J.C.H.H., Wang, C., Clare, S., Wang, J., Chen, X., Brandt, C., Kane, L., Campos, L.S., Lu, L., et al. (2016). Single-cell RNA-seq identifies a PD-1^{hi} ILC progenitor and defines its development pathway. Nature *539*, 102–106.

Zook, E.C., and Kee, B.L. (2016). Development of innate lymphoid cells. Nat. Immunol. *17*, 775–782.

Zook, E.C., Ramirez, K., Guo, X., van der Voort, G., Sigvardsson, M., Svensson, E.C., Fu, Y.X., and Kee, B.L. (2016). The ETS1 transcription factor is required for the development and cytokine-induced expansion of ILC2. J. Exp. Med. *213*, 687–696.

STAR★METHODS

KEY RESOURCES TABLE

REAGENT or RESOURCE	SOURCE	IDENTIFIER
Antibodies		
Anti-mouse CD3	BioLegend	Cat# 100241; RRID: AB_2563945
Anti-mouse CD19	BD Biosciences	Cat# 563333; RRID: AB_2738141
Anti-mouse NKp46	eBiosciences	Cat# 12-3351-82; RRID: AB_1210743
Anti-mouse NK1.1	BioLegend	Cat# 108724; RRID: AB_830871
Anti-mouse CD49a	BD Biosciences	Cat# 562115; RRID: AB_11153117
Anti-mouse CD49b	BioLegend	Cat# 108912; RRID: AB_492880
Anti-mouse CD4	BD Biosciences	Cat# 553047; RRID: AB_394583
Anti-mouse ICOS	BioLegend	Cat# 313524; RRID: AB_2562545
Anti-mouse T1/ST2	BD Biosciences	Cat# 566312; RRID: AB_2744490
Anti-mouse CD90	BD Biosciences	Cat# 564365; RRID: AB_2734760
Anti-mouse CD127	eBiosciences	Cat# 25-1271-82; RRID: AB_469649
Anti-mouse CD25	eBiosciences	Cat# 12-0251-82; RRID: AB_465607
Anti-mouse CD27	BD Biosciences	Cat# 561245; RRID: AB_10611853
Anti-mouse CD244	BD Biosciences	Cat# 553306; RRID: AB_394770
Anti-mouse CD117	BD Biosciences	Cat# 563160; RRID: AB_2722510
Anti-mouse Sca1	eBiosciences	Cat# 56-5981-82; RRID: AB_657836
Anti-mouse CD135	eBiosciences	Cat# 46-1351-82; RRID: AB_10733393
Anti-mouse CD122	eBiosciences	Cat# 48-1222-82; RRID: AB_2016697
Anti-mouse α4β7	eBiosciences	Cat# 17-5887-80; RRID: AB_1210578
Anti-mouse KLRG1	eBiosciences	Cat# 17-5893-82; RRID: AB_469469
Anti-mouse Ly49G2	eBiosciences	Cat# 46-5781-82; RRID: AB_1834437
Anti-human/mouse GATA3	eBiosciences	Cat# 46-9966-42; RRID: AB_10804487
Anti-mouse PLZF	BD Biosciences	Cat# 563490; RRID: AB_2738238
Anti-mouse PD1	BioLegend	Cat# 135223; RRID: AB_2563522
Anti-mouse Perforin	eBiosciences	Cat# 12-9392-82; RRID: AB_466243
Anti-human/mouse Granzyme	BioLegend	Cat# 515408; RRID: AB_2562196
Anti-mouse RORgt	BD Biosciences	Cat# 562684; RRID: AB_2651150
Anti-mouse CCR6	BioLegend	Cat# 129819; RRID: AB_2562513
Anti-mouse EOMES	eBiosciences	Cat# 50-4875-82; RRID: AB_2574227
Anti-mouse TBET	eBiosciences	Cat# 25-5825-82; RRID: AB_11042699
Anti-mouse IFNg	BD Biosciences	Cat# 557724; RRID: AB_396832
Anti-mouse IL-5	eBiosciences	Cat# 12-7052-82; RRID: AB_763587
Anti-mouse IL-22	eBiosciences	Cat# 12-7221-82; RRID: AB_10597428
FcR Blocking Reagent, mouse	Miltenyi Biotec	Cat# 130-092-575
Chemicals, Peptides, and Recombinant Proteins		
Streptavidin	BD Biosciences	Cat# 554063
Fixable viability dye	eBiosciences	Cat# 65-0866-18
Anti-Biotin MicroBeads UltraPure	Miltenyi Biotec	Cat# 130-105-637
Percoll	GE Healthcare	Cat# 17-0891-01
Liberase TL Research Grade	Roche	Cat# 05401020001
DNAse I	Roche	Cat# 10104159001
Penicillin-Streptomycin (5,000 U/mL)	Thermo Fischer	Cat# 15070-063
2-Mercaptoethanol	Thermo Fischer	Cat# 31350-010

(*Continued on next page*)

Continued

REAGENT or RESOURCE	SOURCE	IDENTIFIER
Opti-MEM Reduced Serum Medium, GlutaMAX Supplement	Thermo Fischer	Cat# 51985034
Mouse IL-7, research grade	Miltenyi Biotec	Cat# 130-094-066
Mouse IL-33, research grade	Miltenyi Biotec	Cat# 130-112-961
Mouse SCF, premium grade	Miltenyi Biotec	Cat# 130-101-693
Mouse IL-23, research grade	Miltenyi Biotec	Cat# 130-096-676
Mouse IL-2, research grade	Miltenyi Biotec	Cat# 130-094-055
Experimental Models: Cell Lines		
Mouse: OP9	Institut Pasteur	Cat# CRL-2749
Mouse: OP9-DL4	Institut Pasteur	N/A
Experimental Models: Organisms/Strains		
Mouse: Zbtb16GFPcre	U. Chicago	Constantinides et al., 2014
Mouse: Bcl11btdTomato	Sanger Institute	Li et al., 2010
Mouse: Rag2$^{-/-}$ Il2rg$^{-/-}$	Institut Pasteur	Colucci et al., 1999
Mouse: Id2RFP	Institut Pasteur	N/A
Mouse: C57BL6/J	Institut Pasteur	N/A
Mouse: Id2GFP	Charité Berlin	Rawlins et al., 2009
Oligonucleotides		
Taqman gene primers for Biomark analysis	This paper	See Table S1
Software and Algorithms		
Flow Jo_v10	FlowJo	https://www.flowjo.com/
Prism 7	Prism-Graphpad	https://www.graphpad.com

CONTACT FOR REAGENT AND RESOURCE SHARING

Further information and requests for resources and reagents should be directed to and will be fulfilled by the Lead Contact, James Di Santo (james.di-santo@pasteur.fr).

METHOD DETAILS

Mice

Mice were bred in dedicated facilities of the Institut Pasteur. Id2^{RFP} mice were generated by genOway (Lyon, FR) by insertion of an IRES-mRFP cassette downstream of the STOP codon in 3′ UTR region of *Id2* exon 2 using homologous recombination in C57BL/6 ESCs. Correctly targeted ESCs were microinjected into Balb/c blastocysts to generate chimeric mice and germline transmission was verified after breeding with C57BL/6 females. Zbtb16^{GFPcre} (Constantinides et al., 2014), Bcl11b^{tdTomato} (Li et al., 2010), Id2^{GFP} (Rawlins et al., 2009) and *Rag2*$^{-/-}$*Il2rg*$^{-/-}$ mice (Colucci et al., 1999) were on the C57BL/6 background. Procedures involving mice were previously approved by local Animal Ethics Committees and registered with the French authorities.

Cell Isolation

Lymphocyte preparations from spleen and LNs were prepared using 70 μm strainers. BM cells were collected by either flushing or crushing bones. Lungs were minced and incubated 30 min at 37oC with agitation in HBSS with 5mM EDTA, 10mM HEPES and 5% FBS followed by 1 hr digestion with collagenase D (5 mg/ml; Roche) and DNase I (0.1 mg/ml; Roche) in RPMI, 5% FBS with 10 mM HEPES. Sequentially cells were purified by centrifugation 30 min at 2400 rpm in 40/80 Percoll (Sigma) gradient. Small intestines were cut, washed with PBS 1 × 5 mM EDTA 15 min at 37oC with agitation. IELs were removed using a 100 μm cell strainer, the remaining pieces were digested 30 min at 37oC with agitation in RPMI with 10 mM HEPES and 5% FBS, collagenase D (5mg/ml; Roche) and DNase I (0.1 mg/ml; Roche). Sequentially cells were purified by centrifugation 30 min at 2400 rpm in 40/80 Percoll gradient. Livers were smashed and cells were purified by centrifugation 30 min at 2400 rpm in 35% Percoll.

Flow Cytometric Analysis

Cells were stained for surface markers for 30 min at 4°C, except for CCR6 (37°C for 15 min then at 4°C for 15 min). Transcription factors were analyzed after cell fixation in either 4% PFA in PBS (20 min at 4°C) or using a commercial fixative according to manufacturer's instructions (eBioscience). Antibodies used in this study are listed in the Key Resources Table. Labeled cells were analyzed using a Fortessa flow cytometer (BD Biosciences) or sorted using a FACSAria III. The data were analyzed with FlowJo software.

Cell Culture

Cells were cultured using flat-bottom 96-well plates previously coated with 1000 OP9 or OP9-DL4 stromal cells in 10% FCS, 50 U penicillin (Invitrogen), 50 mg/mL streptomycin (Invitrogen), 50 mM β-mercaptoethanol (Invitrogen). Stem Cell Factor (20 ng/mL), IL-7 (20 ng/mL), IL-33 (10 ng/mL), IL-23 (10 ng/mL), IL-2 (10 ng/mL), IL-15 (10 ng/mL) or IL-12 (10 ng/mL) were added in the medium when specified. Half of the medium was removed and replaced by fresh medium every 3 days. Visible clones were analyzed by flow cytometry after 10-14 days.

In Vivo Adoptive Transfer

After dissection of femur, tibia, and pelvis, the bones were crushed, and cell suspensions were filtered through 100uM sieves before red cell depletion. Lin^+ cells were depleted using biotin-coupled antibodies and anti-Biotin MicroBeads (Miltenyi Biotec), in accordance with the manufacturer's indications. Lineage cocktail included TCRβ, TCRγδ, CD3ε, CD8, CD19, B220, NK1.1, CD11b, CD11c, Gr-1, CD115 and Ter119 (for clone details, see Table S3). Sorted lymphoid progenitors (CLP, ILCP subsets) were retro-orbitally injected into sub-lethally irradiated 5-week-old *Rag2*$^{-/-}$*Il2rg*$^{-/-}$ mice. 800 ILCPs (unfractionated *Id2*$^+$, *Id2*$^+$*Zbtb16*$^+$, *Id2*$^{+-}$ *Zbtb16*$^-$) or 2000 CLP were injected into each recipient. After 5 weeks, recipient mice were sacrificed and organs were collected for analysis.

Biomarker Analysis and qRT-PCR

For Biomark analysis, cells were sorted in 96-well qPCR plates in 10 μl of the Cells Direct One-Step qRT-PCR Kit (Thermo Fisher Scientific), containing a mix of diluted primers (0.05× final concentration; see Table S1). Pre-amplified cDNA was obtained after reverse transcription and pre-amplification, and was diluted 1:5 in TE Buffer, pH 8 (Ambion). Sample mix was prepared as follows: diluted cDNA (2.9 μl), Sample Loading Reagent (0.29 μl, Fluidigm), TaqMan Universal PCR Master Mix (3.3 μl, Applied Biosystems). Assay mix was as follows: Assay Loading Reagent (2.5 μl, Fluidigm), TaqMan (2.5 μl, Applied Biosystems). A 48.48 dynamic array integrated fluidic circuit (IFC; Fluidigm) was primed with control line fluid, and the chip was loaded with assays (TaqMan) and samples using an HX IFC controller (Fluidigm). The experiments were run on a Biomark HD (Fluidigm) for amplification and detection (2′ at 50°C, 10′ at 95°C, 40 cycles: 15′′ at 95°C, 60′′ at 60°C). Heatmaps of two-dimensional hierarchical clustering analysis were performed by Qlucore Omics Explorer software. For qRT-PCR, cells were sorted in RLT Buffer (QIAGEN), RNA was obtained with the RNeasy Micro Kit (QIAGEN), and cDNA was obtained using SuperScript III Reverse Transcriptase (Invitrogen). A 7300 Real-Time PCR System (Applied Biosystems) and Solaris primers (GE Dharmacon) were used.

QUANTIFICATION AND STATISTICAL ANALYSIS

Statistic tests were performed using Prism software. Variance equality was tested using an F-test. Samples were there analyzed using Student's t tests or Mann-Whitney U tests (for samples that did not follow a normal distribution) as indicated.

Annual Review of Immunology

New Molecular Insights into Immune Cell Development

Ana Cumano,[1,2] Claire Berthault,[1,2] Cyrille Ramond,[1] Maxime Petit,[1,2] Rachel Golub,[1,2] Antonio Bandeira,[1,2] and Pablo Pereira[1,2]

[1]Unité Lymphopoïèse, Département d'Immunologie, INSERM U1223, Institut Pasteur, 75724 Paris CEDEX 15, France; email: ana.cumano@pasteur.fr, claire.berthault@inserm.fr, pablo.pereira-esteva@pasteur.fr

[2]Cellule Pasteur, Université Paris Diderot, Sorbonne Paris Cité, 75015 Paris, France

Annu. Rev. Immunol. 2019. 37:497–519

The *Annual Review of Immunology* is online at immunol.annualreviews.org

https://doi.org/10.1146/annurev-immunol-042718-041319

Keywords

lymphoid progenitors, lineage commitment, innate lymphoid cells, fetal liver, thymus-settling progenitors, transcriptional signatures

Abstract

During development innate lymphoid cells and specialized lymphocyte subsets colonize peripheral tissues, where they contribute to organogenesis and later constitute the first line of protection while maintaining tissue homeostasis. A few of these subsets are produced only during embryonic development and remain in the tissues throughout life. They are generated through a unique developmental program initiated in lympho-myeloid-primed progenitors, which lose myeloid and B cell potential. They either differentiate into innate lymphoid cells or migrate to the thymus to give rise to embryonic T cell receptor–invariant T cells. At later developmental stages, adaptive T lymphocytes are derived from lympho-myeloid progenitors that colonize the thymus, while lymphoid progenitors become specialized in the production of B cells. This sequence of events highlights the requirement for stratification in the establishment of immune functions that determine efficient seeding of peripheral tissues by a limited number of cells.

INTRODUCTION

HSC: hematopoietic stem cell

CLP: common lymphoid progenitor

DC: dendritic cell

Hematopoiesis is the process resulting in the constant blood cell production that, in mammals, occurs in the fetal liver (FL) and adult bone marrow or in the thymus (for T cell production). It involves a highly hierarchical progression that ultimately depends on the differentiation of a rare cell with multilineage differentiation potential that is capable of maintaining blood cell production throughout life. This cell type, the hematopoietic stem cell (HSC), differentiates in a unidirectional manner such that once it is triggered, reversion into a more immature stage does not occur under physiologic conditions (1, 2). The process of multilineage differentiation requires hierarchical developmental progression and stepwise choices between two or more alternative pathways of differentiation at specific points, designated lineage commitment (see the sidebar titled Attributes of Hematopoietic Progenitors and the sidebar titled Models of Cell Lineage Commitment).

The Weissman laboratory were pioneers in identifying two key progenitor cells: the common myeloid progenitor (CMP) (3), which has lost all lymphoid potential, further developing into erythrocyte-megakaryocyte progenitors or into granulocyte-monocyte progenitors, and the common lymphoid progenitor (CLP) (4), which is identified by the expression of the interleukin-7 receptor alpha chain (IL-7Rα or CD127) and has lost myeloid, erythroid, and megakaryocyte potential. However, dendritic cells (DCs) (5) can be produced from both CMPs (6) and CLPs (although having lost the capacity to generate granulocytes and monocytes, the latter retain the potential to generate some DC subsets) (7). Therefore, the potential to generate DCs needs to be

ATTRIBUTES OF HEMATOPOIETIC PROGENITORS

Lineage Priming

The expression of lineage-specific transcripts in cells that will eventually become engaged in that pathway of differentiation is designated lineage priming, e.g., expression of *Il7r* transcripts in multipotent LMPPs. Transcripts are usually detected at lower levels than those in the lineage the particular gene is specific for, and this is taken as a sign of the accessibility of the locus for transcription.

Lineage Bias

Lineage bias is the partial loss of differentiation potential in the direct progeny of a multipotent cell. It indicates that the probability that a fraction of differentiating cells will generate a particular lineage has decreased. It is important to distinguish lineage-biased cells from a heterogeneous population comprising cells of multiple origins. Thus, the term lineage bias should only be used when a lineage relationship has been established, e.g., loss of myeloid potential in FLT3^{hi} LMPPs.

Lineage Commitment

The engagement of a progenitor in a given pathway of differentiation is lineage commitment. This process is normally irreversible in physiologic conditions. For example, commitment to the B lineage pathway is marked by the expression of *Pax5*, which also blocks alternative pathways of differentiation (129).

Cell Fate

The destiny of a cell is its fate. In lymphocyte-committed progenitors, randomness of the antigen receptor rearrangement results in cells that either become mature lymphocytes or fail to produce a functional receptor. Fate can be reversed when progenitors successively attempt different rearrangements (130).

MODELS OF CELL LINEAGE COMMITMENT

Instructive Models

Instructive models postulate that environmental signals are determinants in lineage commitment. In these models it is the availability of cues delivered by neighboring cells that regulates commitment and fate. In an extreme example, a multipotent cell interacting with a stromal cell expressing high amounts of IL-7 would become a lymphocyte, whereas if the stromal cell expressed colony-stimulating factor 1 (CSF-1), also designated macrophage-colony-stimulating factor (M-CSF), it would become a macrophage (103, 131).

Selective/Permissive Models

Selective/permissive models postulate that lineage commitment occurs by a cell-autonomous process. Fluctuation in the expression of key transcripts in multipotent cells, resulting from asymmetric cell division, will eventually lead to the activation of a transcriptional network required for engagement in a given differentiation pathway (132). This fluctuation can be modeled by the Waddington landscape, which was recently revised to accommodate combinations of selective and instructive processes (133). In contrast to instructive models, in these models survival or expansion signals from the environment determine not commitment but fate. This implies that in selective/permissive models the committed cells that failed to receive trophic signals die, whereas instructive models allow progression without cell loss.

distinguished from the potential to generate other myeloid cells to properly assign differentiation capacities to progenitors.

The discovery of these two complementary progenitor cells, CMPs and CLPs, suggested that lineage commitment progressed through a succession of binary decisions where lymphoid versus myelo-erythroid commitment occurred early in differentiation. Furthermore, single-cell transcriptional analysis showed a significant level of expression of erythroid- and megakaryocyte-associated, but also of granulocyte- and monocyte-associated, transcripts in uncommitted CMPs and even in HSCs (8). It was only when granulocyte and monocyte or erythroid and megakaryocyte potentials were segregated that mutually exclusive expression of associated transcripts occurred.

This simple binary decision–based scheme was challenged by the identification of a cell type designated lympho-myeloid-primed progenitor (LMPP). LMPPs were defined as lineage-negative (Lin^-), Sca-1^+, c-kit $(CD117)^+$ (LSK) cells (9, 10) that have lost erythrocyte and megakaryocyte potentials. Their position in the hematopoietic hierarchy is intermediate, between that of HSCs and CLPs. The identification of LMPPs contributed to the complex field of hematopoietic lineage commitment, with two basic notions: (*a*) Differentiation of hematopoietic progenitors likely occurs through a succession of discrete events rather than by a sudden change in differentiation potential; and (*b*) lymphoid lineage commitment is also preceded by low expression levels of lymphoid-specific transcripts in otherwise multipotent cells, a process designated lineage priming (11) (see the sidebar titled Attributes of Hematopoietic Progenitors).

Lymphocytes are leukocytes that comprise T, B, and innate lymphoid cells (ILCs). They are the major cellular component of the immune system, protect organisms against pathogens, and have a general role in tissue homeostasis (12). The essential roles of *E2a* (13), *Ebf1* (14), and *Pax5* (15) in B cell differentiation; those of delta-like 4 (*Dll4*) (16), *Gata3* (17), and *Tcf7* in T cell production (18); and that of DNA-binding protein inhibitor 2 (*Id2*), which blocks E-box protein function (19) in ILC development, have been well characterized. B cell development relies on upregulation of *E2a*, which is required for expression of transcription factors *Ebf1* and *Pax5*, at the transition from CLP

LMPP: lympho-myeloid-primed progenitor

LSK cell: lineage-negative (Lin^-), Sca-1^+, c-kit $(CD117)^+$ cell

ILC: innate lymphoid cell

TCR: T cell receptor

to pro-B cells. It is *Pax5* expression that determines B lineage commitment and loss of the potential to generate alternative lineages. IL-7 is essential at this stage to ensure the expansion of B lineage cells in mice, albeit not in humans. E2A is also important to maintain NOTCH1 expression in hematopoietic progenitors that migrate to the thymus, where they encounter high levels of the NOTCH1 ligand DLL4. Following NOTCH activation *Gata3* and *Tcf7* are upregulated and T cell progenitors initiate a developmental program that progresses through the CD4 and CD8 double negative (DN) stages 1 ($CD44^+CD25^-$c-kit^+), 2 ($CD44^+CD25^+$c-kit^+), 3 ($CD44^-CD25^+$), and 4 ($CD44^-CD25^-$) before the stage of CD4/CD8 double positive cells, where selection for T cell receptor (TCR) specificity occurs. IL-7 and KIT-ligand promote the expansion of DN1 and DN2 thymocytes, and in the absence of both cytokines the thymus is virtually empty (20). Increasing expression of *Id2* in some progenitors in the fetal liver or bone marrow inactivates E2A, blocking B and T cell differentiation and therefore restricting the cells to the ILC pathway.

It remains unclear, however, what signals drive the expression of these different proteins in a given progenitor, or in other words, what the molecular basis for lineage priming and subsequent commitment is. In this review we summarize present knowledge of the origin of hematopoietic lineages, the initial differentiation events that drive multipotent cells into the lymphoid lineage, and whether T/ILC versus B cell commitment in FL follows a preestablished, cell-autonomous program or signals from the environment to engage in a given differentiation pathway.

GENERATION OF HEMATOPOIETIC CELLS

Primitive Hematopoiesis Generates Definitive Hematopoietic Cells, but Not Hematopoietic Stem Cells

The first hematopoietic cells differentiate in the yolk sac blood islands of the mammalian embryo (21). They contain megakaryocytes and a majority of erythrocytes that, like those in fish and birds, do not enucleate and, unlike their adult counterparts, express embryonic hemoglobin. For these reasons they were designated primitive erythrocytes. The yolk sac harbors mature macrophages of maternal origin around embryonic day 8 (E8), and later monopotent macrophage progenitors followed by erythro-myeloid progenitors (22). Both types of progenitors express c-kit but not CD45, differentiate into myeloid cells including $F4/80^+CX_3CR1^+$ macrophages, and migrate out of the yolk sac to form populations of tissue-resident macrophages that, depending on the tissues, can persist throughout adult life (23). At these early stages of development lymphocyte progenitors are not detected in the yolk sac.

It is only after E9.5–10 that circulating multipotent progenitors can be detected in mice (24, 25). The anatomic sites where HSCs are generated are beyond the scope of this review; therefore, we refer exclusively to HSC production in the consensus sites: the dorsal aorta [aorta, gonads, and mesonephros (AGM) region] (26, 27) and the omphalomesenteric (vitellin) and umbilical arteries (28). Other potential sites of HSC generation include the yolk sac (29), the placenta (30), and the allantois (31).

Irrespective of the HSC anatomic origin there are two important notions to retain. (*a*) The entire pool of HSCs or their immediate progenitors is generated during a short window of time (in the mouse embryo between E9 and E11) in major blood vessels and in close association with endothelial cells. They are highly proliferative, rapidly enter circulation, and home to the FL, the major hematopoietic organ in the embryo (32, 33). Using an inducible *Runx1* lineage tracer model, Nishikawa and colleagues showed that a single induction of the lineage tracer at E9.5 labels nearly all adult HSCs, indicating that de novo HSC production does not occur after mid-gestation (34). (*b*) The properties and behavior of fetal and adult HSCs are distinct. Emerging pre-HSCs or immature HSCs show multipotency when tested in clonal in vitro assays, but unlike their adult

counterparts, they are inefficient in repopulating the hematopoietic system in transplantation assays into adult recipients, a classic criterion used to define HSCs. One reason for their poor reconstitution ability is the absence of MHC-I molecules, which makes them a target for natural killer (NK) cells. This can be partially overcome by using NK-deficient *Rag2*$^{-/-}$/$\gamma c^{-/-}$ mice as recipients (35, 36). Therefore, embryonic hematopoietic cells cannot be probed in assays similar to those used for adult HSCs (37). When immature HSCs further develop in an organ culture, they rapidly acquire functional properties of adult HSCs (33, 36). Consequently, the emerging HSC progenitors can expand and engage in differentiation (in the AGM, FL, or elsewhere) prior to maturation into functional adult-type HSCs.

Rag: recombination-activating gene

DETC: dendritic epidermal T cells

LTi cell: lymphoid tissue–inducer cell

TSP: thymus-settling progenitors

Fetal Versus Adult Hematopoiesis

Major differences distinguish adult (bone marrow) from embryonic (FL) hematopoiesis. The most evident is the highly proliferative HSC compartment in FL (38), which sharply contrasts with mostly quiescent bone marrow HSCs (39, 40). FL and bone marrow progenitors react differently to estrogens and to IFN-α (41), although both are sensitive to glucocorticoids (42). HSCs from both origins can generate all major blood cell populations; however, a number of innate-type lymphoid cells, i.e., dendritic epidermal T cells (DETCs) (43), lymphoid tissue–inducer (LTi) cells (44), and a subset of IL-17-producer γδ T cells (45), can only differentiate from embryonic HSCs. B1 B cells (46, 47) were also initially described as being exclusively of fetal origin. However, recent evidence indicates that B1 cells can also originate from adult HSCs (48, 49); that they derive from the same progenitors as B2 cells; and that expression of LIN28B (50), an RNA-binding protein progressively lost by HSCs in the bone marrow, regulates the capacity to generate B1 versus B2 cells. This and other molecular constraints (51) explain why the fetal precursors are better at generating B1 cells than their adult counterparts.

DETCs develop in the fetal thymus, express an invariant Vγ5Vδ1 TCR, and migrate to the skin (52). Interestingly, not only were adult progenitors unable to differentiate into DETCs in a fetal thymus, but fetal progenitors also failed to generate DETCs in an adult environment, suggesting a role for environmental cues essential for the survival or expansion of these cells (43). A mutation of a butyrophilin gene family member (*Btnl*) occurring in an FVB mouse substrain (FVB/Tac) provided evidence that a protein expressed by thymic epithelia and keratinocytes is essential for the development of DETCs. This gene was designated selection and upkeep of intraepithelial T cells 1 (*Skint-1*) (53). The *Btnl* gene family members are heterogeneously expressed in different species; e.g., *Skint-1* is a pseudogene in humans, who lack DETCs. Other *Btnl* members (*Btnl1* and *Btnl6* in the mouse and *BTNL3* and *BTNL8* in humans) drive the activation of γδ T cell subsets in the intestine (54). The presence of *Skint-1* in the thymus induces *Tbx21* and IFN-γ production through the expression of *Egr3* diverting Vγ5Vδ1 T cells away from a default Th17 differentiation pathway (55). This result also suggests a correlation between TCR specificity and phenotype, although a direct association between *Btnl* gene products and the TCR has not been formally demonstrated.

LYMPHOCYTE PROGENITORS

Historic Perspective

The identification of CLPs both in the adult bone marrow (4) and in FL (56) was undisputed evidence that lymphocytes share a common restricted progenitor. It seemed, then, logical to think that they were the thymus-settling progenitors (TSPs), and this throughout life. However, this notion was challenged by the finding, in mid-gestation embryos, of T and NK cell–restricted

Flt3: fms tyrosine kinase 3

progenitors in circulation (57) and in the fetal spleen (58), and reports identifying T/NK cell common progenitors in FL suggested that lineage restriction occurs before homing to the thymus (59). Fetal thymic organ cultures colonized by single cells (60, 61) led to the conclusion that FL lymphoid progenitors comprise a surprisingly high frequency of pre-T or pre-B cell progenitors, but not both. Conditions favoring T cell differentiation (NOTCH signaling) (62) are incompatible with those favoring B cell development. For both T and B cells to be found in the same assay, progenitors must expand before engaging in either the T- or the B-differentiation pathway, which is unlikely to occur in cells with limited self-renewal capacity, such as CLPs. Despite this caveat, Kawamoto et al. (60) and Katsura (61) were the first to conclude that T cell commitment occurs prior to B cell commitment during embryonic development. A monoclonal antibody recognizing the A isoform of paired immunoglobulin-like receptors (PIR-A) labeled a prethymic progenitor in the FL that lacked B and myeloid potential but retained T, NK, and DC potential (63). Progenitors with similar properties were also found in the FL from mice mutant for *Hes1*, a major effector protein of the NOTCH signaling pathway. Altogether, these data suggest that restriction into the T, NK, and DC pathways of differentiation (and consequently the loss of B and myeloid potentials) occurs in FL, in a NOTCH signaling–independent manner.

Early Lymphoid Progenitors

The phenotypic characterization of LMPPs was based on their higher expression of FLT3 (also designated as FLK2 or CD135) protein tyrosine kinase receptor when compared to multipotent progenitors. Their survival and/or expansion depends on FLT3 ligand (64, 65). FLT3 expression gradually increases from HSCs to CLPs, forming a continuum. Therefore, LMPPs do not form a distinct population recognizable by flow cytometry (10). Moreover, expression levels of FLT3 and IL-7Rα, which distinguish LMPPs from CLPs, vary with exposure to their respective ligands (66, 67), which induces the internalization of the receptor-ligand complex. A Rag-GFP knock-in strain enabled the definition of early lymphoid progenitors (ELPs), corresponding to 3–5% of the LMPPs. ELPs have a robust lymphoid potential, with only residual myeloid differentiation capacity (68, 69). These properties suggested that ELPs are an intermediate population between LMPPs and CLPs, although it cannot be excluded that a fraction of the originally defined ELPs are CLPs that internalized the IL-7R/IL-7 complex.

In bone marrow, all available evidence indicates that LMPPs are derived from HSCs, as the hierarchical relationship between both populations has been firmly established (70). However, this might not be the case during embryonic development. Progenitors with the potential to generate myeloid and lymphoid cells and resembling bone marrow LMPPs by phenotype and function were isolated from the yolk sac prior to the detection of HSC activity (before E12.5) (25). This observation was taken as evidence for an early, stage-restricted, HSC-independent pathway of lymphoid development. Virtually all HSC activity in the adult bone marrow can be traced back to emerging hematopoietic progenitors between E9.5 and E10.5 that do not exhibit adult HSC reconstituting capacity (34, 36). These newly generated cells extensively proliferate and can differentiate into lineage-restricted progenitors prior to acquiring the capacity to reconstitute adult irradiated recipients (33). Therefore, the identification of a lineage-restricted progenitor cell before detection of long-term reconstituting activity (starting at E12.5) should not be taken as evidence for their independent origin from HSCs or their immediate precursors.

An *Flt3* lineage tracer mouse model revealed a hematopoietic progenitor displaying similar function and phenotype as HSCs, except for a history of FLT3 expression and a singular capacity to preferentially generate lymphocytes, in particular B1 cells and DETCs (71). This progenitor appeared endowed with self-renewal capacity but was not found in the adult bone marrow, thus suggesting that tissue-resident lymphocytes are generated by a transient fetal HSC subset. Of

notice, transient HSCs expressed *Rag1*, *Rag2*, *Ccr9*, and *Il7r* genes, which are essential for lymphocyte development and usually only found in LMPPs and CLPs. This work raised the possibility that, at the onset of hematopoiesis, lymphoid-associated genes could be expressed in a subset of HSCs capable of long-term reconstitution upon transplantation, a concept that is, however, difficult to reconcile with their transient nature. Further studies are required to clarify to what extent this progenitor differs from bona fide lymphoid-primed LMPPs.

Il7r: interleukin 7 receptor α chain

PLZF: promyelocytic leukemia zinc finger protein; encoded by *Zbtb16*

The Common Lymphoid Progenitor

According to its original definition, the bone marrow CLP is a Lin^- cell that, different from LMPPs, expresses IL-7Rα and lower levels of c-kit and Sca-1 (4). In FL, most Lin^-IL-7Rα^+ cells are detected in the c-kit^{hi} compartment, a phenotypic peculiarity that generated some confusion in the field. Clonal assays testing the differentiation potential demonstrated that most multipotent lymphoid progenitors (endowed with B, T, and NK cell potential but lacking myeloid potential) expressed high levels of c-kit, thus contrasting with the c-kit^{lo} adult bone marrow CLP (**Supplemental Figure 1**).

Supplemental Material >

The fetal CLP compartment is heterogeneous, comprising a population of integrin $\alpha_4\beta_7$–expressing cells with LTi, T, and DC potential that have lost the capacity to generate B cells (72–74) (**Figure 1**). A small subset of $\alpha_4\beta_7^-$ CLPs that have lost FLT3 expression exhibit clonogenic B and NK differentiation potential but have lost T cell potential in vitro and in vivo (75). These progenitors show a moderate upregulation of *Id2* and *Id3* that partially inhibits *E2a* activity, leading to the downregulating NOTCH1 expression. Consistent with this idea, $FLT3^-$ CLPs in $Id2^{-/-}/Id3^{+/-}$ embryos partially recover T cell differentiation potential. A similar population was described in an independent report as a B cell–committed progenitor (76). The in vivo transplantation assay used by these authors (sublethal irradiated wild-type mice) did not allow detection of the NK potential, which requires transplantation into $Rag^{-/-}\gamma c^{-/-}$ mice.

ILCs are a heterogeneous group of mononucleated cells; most of them are tissue-resident cells that rapidly secrete cytokines in response to a variety of stimuli, ensuring homeostasis (77). They comprise conventional NK (cNK) cells, group 1 ILCs (ILC1s) (secreting Th1 cytokines and expressing *Tbx21*), ILC2s (secreting Th2 cytokines and expressing *Gata3*), ILC3s (secreting Th17 cytokines and expressing *Rorc*), and, in the embryo, also LTi cells. They do not express clonally distributed antigen receptors and are therefore *Rag* independent. Fetal and adult ILCs differentiate from CLPs (78, 79) through the upregulation of $\alpha_4\beta_7$ expression concomitant to the loss of B cell potential. Further expression of CXCR6 and loss of FLT3 mark the loss of T cell potential (78).

GFP expression in an *Id2* reporter mouse model defined the common helper ILC precursor (CHILP) in adult $\alpha_4\beta_7^+$ CLPs. CHILPs comprise a heterogeneous population able to generate all ILCs, including LTi cells but not cNK cells (80). A mouse line that reports and traces *Zbtb16*-expressing cells marked a majority of mature ILCs but only a small fraction of cNK and LTi cells, thus defining the ILC precursor (ILCP) as a $PLZF^+\alpha_4\beta_7^+FLT3^-$ CLP (81).

Overall, B, T and innate lymphoid cells, which also comprise cNK cells, derive from restricted progenitors in fetal liver that have lost myeloid, erythroid, and megakaryocyte differentiation potentials.

THE TRANSCRIPTIONAL PROFILE OF COMMON LYMPHOID PROGENITORS

ILC Precursors

Innate cell development initiates with the expression of *Id2*, which inhibits E-box transcription factors (82). High levels of ID2 expression coincide with the loss of cNK potential (80),

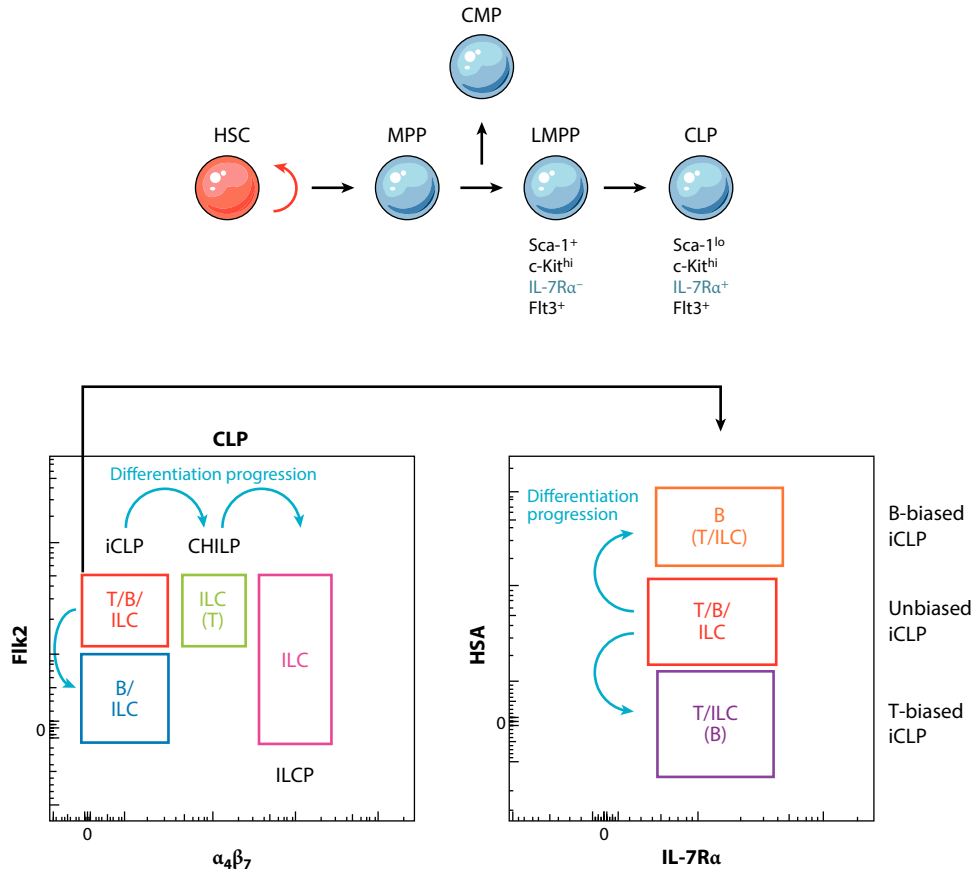

Figure 1

Hematopoietic development in the embryo. The red arrow indicates self-renewal capacity; blue arrows indicate differentiation progression. Colored characters in the plots indicate differentiation potential; characters within brackets indicate residual differentiation potential in biased populations. Abbreviations: CHILP, common helper ILCP; CLP, common lymphoid progenitor; CMP, common myeloid progenitor; HSC, hematopoietic stem cell; iCLP, immature CLP; ILC, innate lymphoid cell; ILCP, ILC precursor; LMPP, lympho-myeloid-primed progenitor; MPP, multipotent progenitor.

and subsequent upregulation of *Zbtb16* is concomitant to the loss of LTi potential (81). The transcriptional profile expressed in ILCPs includes *Id2*, *Tcf7* (83, 84), *Gata3* (85, 86), *Tox* (87), and *Zbtb16*. Inactivation of any of these genes profoundly affects the development of all ILC lineages. *Nfil3* is transitionally expressed before *Id2*, and it is important for ILC commitment (88, 89).

The expression of *Gata3* and *Tcf7* is essential for T cell development in the thymus, where they are regulated by NOTCH1 signaling (12). By contrast, NOTCH signaling appears to be dispensable for the expression of both transcription factors in ILCPs and $\alpha_4\beta_7$, which marks bias in differentiation toward the ILC pathway in FL (78, 90, 91). Only a subset of $\alpha_4\beta_7$ CLPs primed for the expression of ILC2 genes was affected by the inactivation of the NOTCH pathway (90).

Single-cell transcriptional and differentiation potential analyses confirmed that the fetal LTi cell precursor separates from the ILCP and that the CHILP could be considered as their

common precursor (89). Importantly, the transcriptional programs for ILC1s, ILC2s, and ILC3s were initiated in cells that maintain multi-ILC potential and could be found coexpressed before being segregated (89), a process that usually occurs in the periphery (92, 93). Only LTi progenitors did not appear to transit through a stage of multilineage priming.

HSA: heat-stable antigen

"To B or Not to B" Lineage Segregation Model

Analyses of the differentiation potential of CLPs undertaken by multiple laboratories indicated that close to 60% of the Lin$^-$IL-7Rα^+c-kit$^+$Sca-1^{lo} cells in FL retain the capacity to generate the three main lymphoid lineages, T, B, and ILC [FLT3$^+\alpha_4\beta_7^-$ and designated hereafter as immature CLP (iCLP)] (74, 78, 94, 95). To understand the molecular events that preceded lineage commitment, this population was further subdivided according to expression of heat-stable antigen (HSA, also known as CD24). A majority of iCLPs expressed intermediate levels (HSA^{int}), and two smaller subsets expressed higher and lower levels of HSA (HSA^{hi} and HSA^{lo}) (95). This heterogeneity in HSA expression correlated with different biases in the capacity to generate the three lymphoid lineages (**Figure 1**). HSA^{int} iCLPs retained a robust T, B, and NK (taken here as surrogate of ILC) potential, whereas HSA^{hi} iCLPs exhibited a robust B but low T and NK potentials, and conversely, HSA^{lo} iCLPs were efficient in T and NK cell assays but had poor B cell potential. Therefore, B- versus T/ILC-biased progenitors could be discriminated within iCLPs in FL by the expression of HSA, and loss of B cell differentiation potential could occur outside the thymus.

Short-term cultures suggested that HSA^{int} iCLPs are the direct progeny of LMPPs and that HSA^{int} iCLPs generate HSA^{hi} or HSA^{lo} iCLPs. $\alpha_4\beta_7^+$ CLPs are the progeny of HSA^{int} iCLPs, although it could not be clearly established whether or not they transit through the HSA^{lo} iCLP compartment before acquiring $\alpha_4\beta_7$ expression.

A genome-wide microarray analysis revealed a transcriptional signature of the three HSA iCLPs and of the $\alpha_4\beta_7^+$FLT3$^+$ ILC–biased population. HSA^{hi}, B-biased iCLPs expressed B-lineage genes (*Ebf1*, *Pax5*, *Vpreb*, *Foxo1*, *Pou2af1*, *Rag1*, and *Ly6d*), and unexpectedly, they also differentially expressed *Hes1* in the absence of any other known target of the NOTCH signaling pathway (95). The ILC-biased population expressed ILC-related transcripts previously mentioned (*Tcf7*, *Id2*, *Gata3*, *Tox*, *Nfil3*, *Nkg7*, and *Rorc*), whereas *Zbtb16*, *Lta/Ltb*, and *Cxcr5* were not found differentially expressed. Consistent with their lack of B cell differentiation potential, these cells show the lowest expression of *Ebf1* and *Rag1* but also of *Notch1*, consistent with their reduced capacity to generate T cells (30% lower than in $\alpha_4\beta_7^-$ iCLPs). HSA^{int} iCLPs showed differential expression of few transcripts; one is the latrophilin-like G protein–coupled receptor *Eltd1*, which is highly expressed in HSCs and gradually downregulated as differentiation progresses (**https://www.immgen.org**). The expression of *Eltd1* will be taken here as a sign of undifferentiation or of ontogenic distance from the HSCs.

HSA^{lo} iCLPs that exhibited T- and ILC-biased differentiation potentials showed differential expression of *Cd7* (96), *Cdh17*, *Pira11*, *Pira1*, *Ccr9* (97, 98), and *Glis3*. Some of these transcripts were also found expressed in adult TSPs and were associated with T cell differentiation (**https://www.immgen.org**). For example, *Cd7* is highly expressed in ETPs and in some subsets of T cells; *Ccr9* is involved in the thymic migration of hematopoietic progenitors. *Pira11* and *Pira1* are not expressed in adult T progenitors but are associated with DC progenitors. Both related gene products are identified by a monoclonal antibody and were previously described as markers of fetal progenitors with T and ILC potential (63). Nonetheless, none of the transcripts detected in adult TSPs and required for T cell differentiation [including *Hes1*, *Nrarp*, *Tcf7*, *Gata3*, and *Dtx1* (only upregulated in adult DN3 thymocytes)] were overexpressed, indicating that HSA^{lo} iCLPs were not engaged in the T cell–differentiation pathway.

The main conclusion to be taken from these experiments is that at the earliest stages of fetal hematopoiesis, lymphoid progenitors either engage in the B cell pathway of differentiation (with concomitant expression of *E2a*, *Ebf1*, and *Pax5*) or lose B cell potential, appearing as T/ILC-restricted cells that only in the thymus engage in the T cell–differentiation pathway, triggered by NOTCH signaling. Accordingly, the numbers of HSA^{lo} iCLPs, their transcriptional profile, and their low capacity to generate B cells were indistinguishable in the presence and in the absence of NOTCH signaling (91, 95), consistent with previous independent observations (63).

Lineage Priming Occurs in Unbiased CLPs

At the single-cell level, many HSA^{int} iCLPs express transcripts from the B- and/or T/ILC-biased signatures. However, *Pira11* is seldom (<10% of the cells) coexpressed with *Ebf1*, and consistent with this, $PIRA/B^{+}HSA^{int}$ iCLPs have lost B cell potential (95). Less than 20% of iCLPs show no signs of lineage priming, indicating that B, T, or ILC signature transcripts are coexpressed in cells that maintain the capacity to generate all three lymphoid lineages. Expression of the B or T signature is highest in the respective biased population, whereas significantly lower levels are found in cells that express both signature transcripts. This observation suggests a Waddington landscape effect where expression of low levels of transcripts specific for multiple signatures precedes a stabilized state of expression of only one signature and where upregulation of transcripts of one signature correlates with lineage bias (see the sidebar titled Attributes of Hematopoietic Progenitors).

Analyses of the frequency and levels of expression of *Eltd1*, the marker of immature cells, confirmed conclusions based on short-term cultures, namely that LMPPs (100% of cells expressing *Eltd1*) differentiate into HSA^{int} iCLPs (50%) that give rise to HSA^{lo}- and HSA^{hi}-biased iCLPs (20% of which express *Eltd1*). Only 10% of $\alpha_4\beta_7^{+}$ CLPs show *Eltd1* expression, suggesting that they might not derive directly from HSA^{int} cells but could have transited through a stage as HSA^{lo} iCLPs. This possibility is compatible with the finding that HSA^{lo} iCLPs also express low levels of transcripts belonging to the ILC signature.

Interestingly, *Pira11* expression also defines two populations of $\alpha_4\beta_7^{+}$ CLPs (**Figure 2**): One, similar to HSA^{lo} iCLPs, expresses PIRA/B, *Cd7*, and *Ccr9* but also expresses the highest levels of the ILC signature genes *Id2*, *Tox*, *Tcf7*, and *Rorc* and, therefore, appears to be the direct progeny of T/ILC-biased iCLPs in the ILC-differentiation pathway; another expresses neither PIRA/B nor significant levels of any T/ILC-biased signature transcript and also shows low expression of ILC signature genes. They also express less *Id2* and more *Eltd1* than $PIRA/B^{+}\alpha_4\beta_7^{+}$ CLPs, raising the possibility that they are direct progenies of HSA^{int} iCLPs (**Figures 2** and **3**).

The low expression levels of *Notch1* and *Ebf1* in $\alpha_4\beta_7^{+}$ CLPs is compatible with their partial loss of T and complete loss of B cell potentials. *E2a* expression, a direct target of *Id2*, can regulate the expression of *Notch1* and *Ebf1* (99).

However, the finding that $PIRA/B^{-}$ $\alpha_4\beta_7^{+}$ CLPs express low levels of both *Notch1* and *Id2* indicates that signals other than those mediated by *Id2* upregulation are involved in the loss of T cell potential in ILCPs.

Altogether, these data indicate that expression of *Pira11* marks cells that have lost B cell potential but retain both T and ILC potential in FL lymphoid progenitors.

Loss of B and Myeloid Potential Occurs in LMPPs

$FLT3^{hi}$ FL LMPPs (corresponding to the 10% LSK cells expressing the highest levels of FLT3) exhibited a pattern of gene expression very similar to that detected in HSA^{int} iCLPs. Particularly

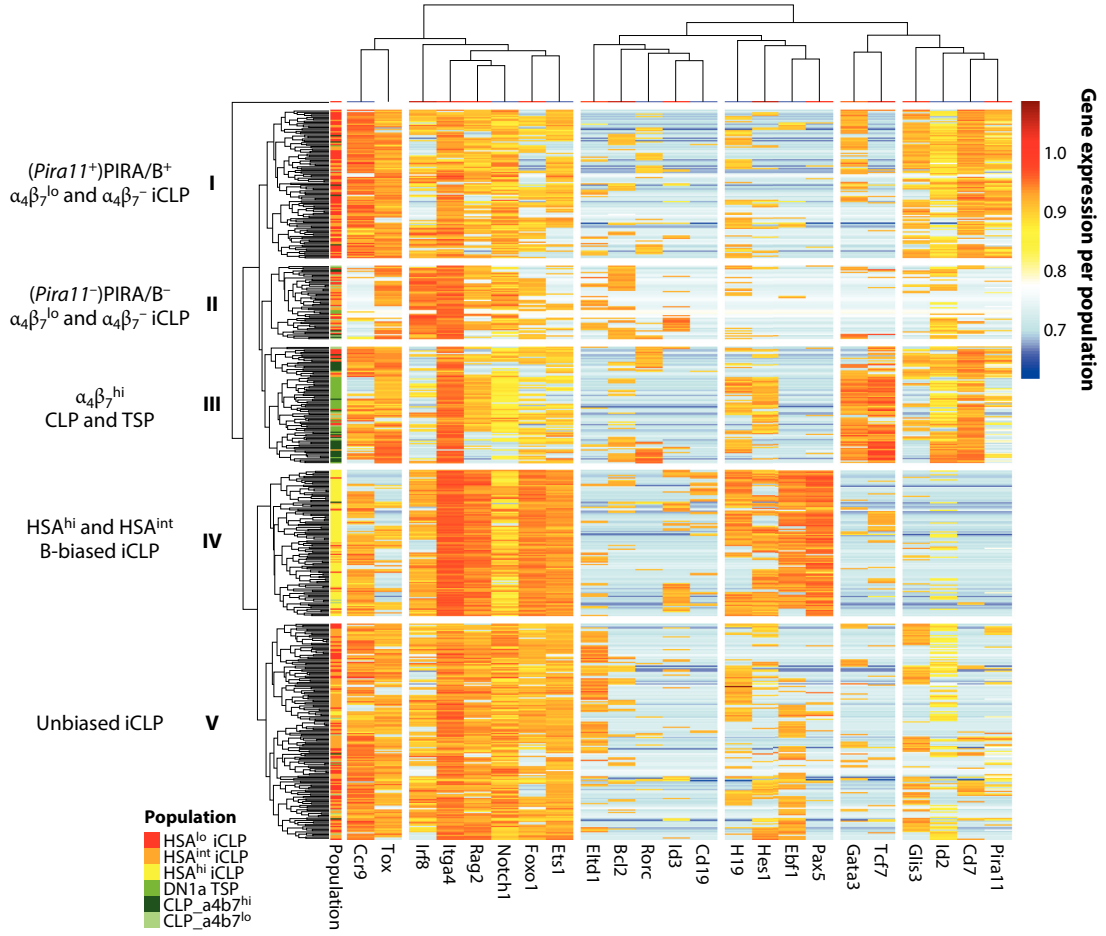

Figure 2

PIRA/B marks the expression of a T/ILC-biased signature. Unsupervised hierarchical clustering (heat map) of FL CLP subsets and DN1a thymocytes based on levels (Ct values) of expression of the signature transcripts published in Reference 95, normalized for actin-b expression (see also **Supplemental Figure 2**). Five clusters were defined: I, PIRA/B$^+$ $\alpha_4\beta_7{}^{lo}$ and $\alpha_4\beta_7{}^-$ CLPs (*Pira11*, *Cd7*, *Id2*, *Glis3*, *Ccr9*); II, PIRA/B$^-$ $\alpha_4\beta_7{}^+$ and $\alpha_4\beta_7{}^-$ CLPs (*Ccr9*$^-$, *Id3*, *Bcl2*, *Id2*^{lo}); III, $\alpha_4\beta_7{}^{hi}$ CLPs and DN1a thymocytes (including a few $\alpha_4\beta_7{}^-$ CLPs) (*Pira11*, *Cd7*, *Id2*, *Glis3*, *Tcf7*, and *Gata3*); IV, HSA^{hi} and HSA^{int} B-biased CLPs (*Ebf1*, *Pax5*, *Hes1*, and *H19*); and V, unbiased CLPs (*Eltd1*). Abbreviations: CLP, common lymphoid progenitor; Ct, cycle threshold; FL, fetal liver; ILC, innate lymphoid cell.

striking was the high expression of *Il7r* mRNA found in more than 90% of LMPPs. By contrast, FLT3^{hi} LMPPs isolated from *Il7*-deficient mice no longer expressed transcripts of the B-biased signature, and less than 20% expressed *Il7r* (95). This observation indicated that a large fraction of FLT3^{hi} LMPPs, comprising previously described populations such as ELPs, are contaminated with CLPs that internalized the IL-7R and, therefore, were designated LMPPs by phenotype. Consistent with this interpretation, the levels of *Il7r* in LMPPs from wild-type embryos were twofold higher than those found in *Il7*-deficient embryos, although still twofold lower than those found in CLPs. *Eltd1* expression in wild-type LMPPs was also intermediate, between that found in *Il7*-deficient LMPPs and that in unbiased iCLPs (**Supplemental Figure 3**). Similarly, cells expressing low levels of FLT3 could contaminate HSC populations in several experimental situations.

Supplemental Material >

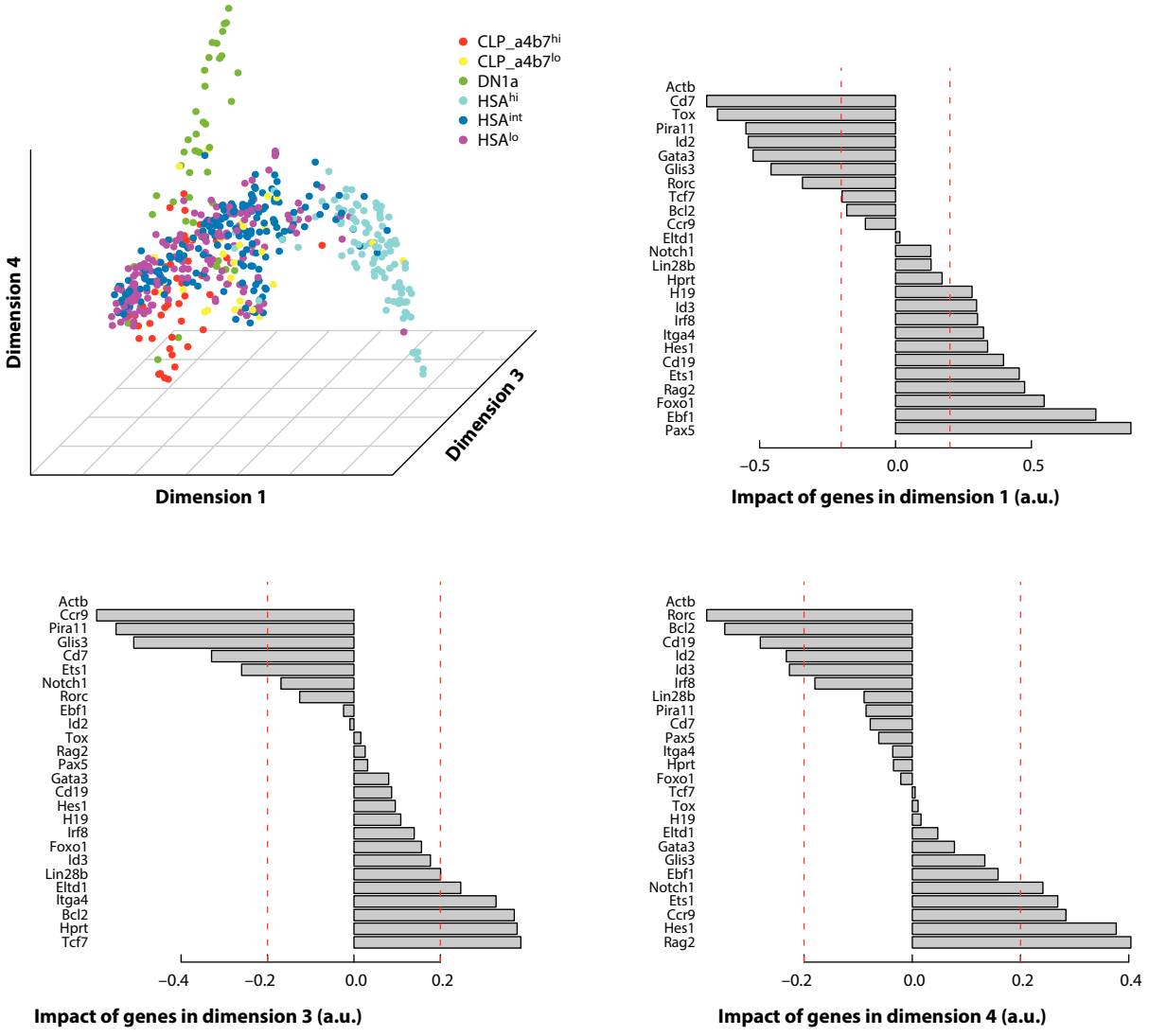

Figure 3

3-D diffusion plot of the development of fetal lymphoid cells. Diffusion plot was constructed with the R package "destiny," with the gene expression data shown in **Figure 2**. Shown are a representation of the dimensions 1, 3, and 4 and the normalized expression values in arbitrary units (a.u.) of the genes that impacted each of these dimensions. Abbreviations: CLP, common lymphoid progenitor; DN1a, double negative 1 thymocytes; HSA, heat-stable antigen.

There are two important implications from the above experiments: (*a*) The expression of the B lineage signature occurs concomitantly with that of *Il7r*, and (*b*) the "not B" signature expressed by cells restricted to the T/ILC-differentiation pathways was already found in LMPPs before *Il7r* expression. Therefore, the transcriptional priming for the B or T/ILC signatures occurs asynchronously, at two different developmental stages, and B versus T/ILC lineage commitment appeared as a nonbinary choice.

A large fraction (close to 45%) of FLT3^{hi} LMPPs from *Il7*-deficient mice expressed T/ILC-biased transcripts including *Pira11*. PIRA/B^{+} LMPPs exhibited lower potential to generate B

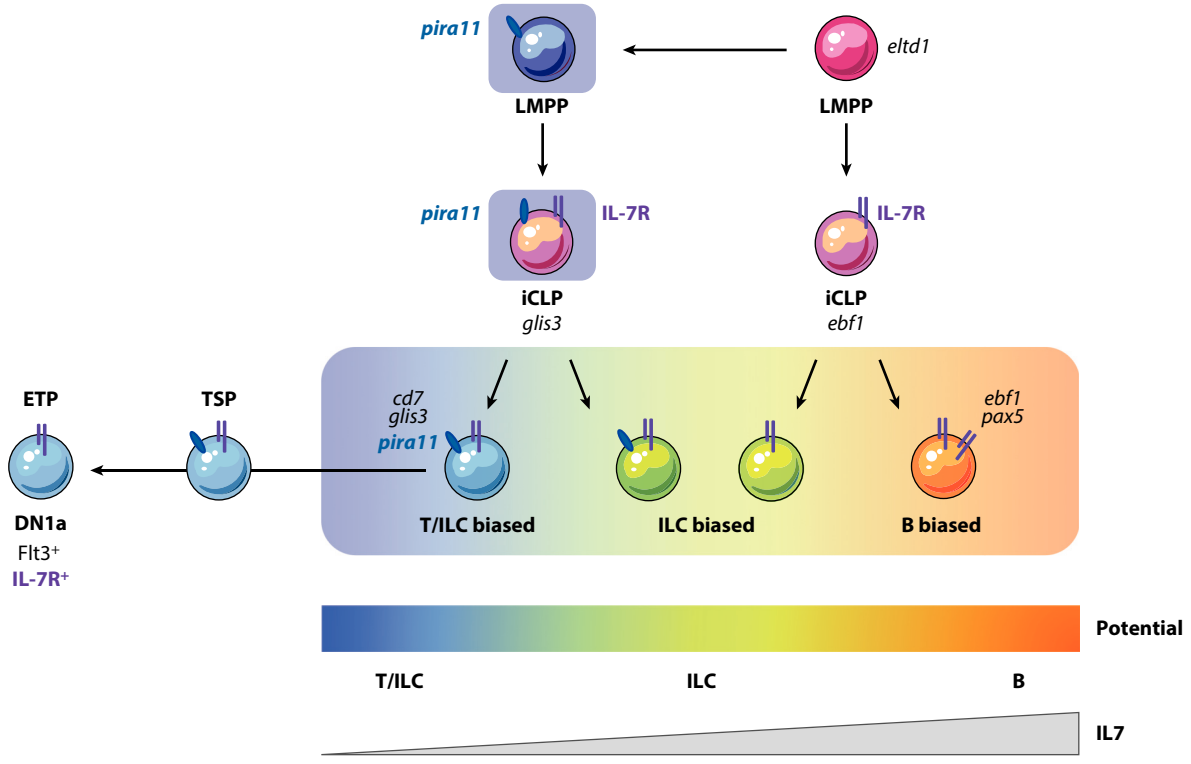

Figure 4

Lymphoid development in fetal liver. Abbreviations: ETP, early thymic progenitor; iCLP, immature common lymphoid progenitor; ILC, innate lymphoid cell; LMPP, lympho-myeloid-primed progenitor; TSP, thymus-settling progenitor.

and myeloid cells than their PIRA/B$^-$ counterparts (95). This result established that, in FL, loss of B cell and myeloid differentiation potentials occurs in PIRA/B$^+$ LMPPs that rapidly generate HSA^{int} and HSA^{lo} iCLPs in short-term cultures. This suggests that embryonic CLPs derive from two distinct LMPPs. One expresses PIRA/B, shows restricted potential to generate the T/ILC lineages before *Il7r* expression, and differentiates into PIRA/B-expressing HSA^{int} and HSA^{lo} iCLPs. These progenitors will either migrate to the thymus as TSPs or progress to generate ILC-biased CLPs. The second LMPP subset loses myeloid potential only after *Il7r* expression, can generate T cells, B cells, and ILCs, and differentiates into HSA^{int}, HSA^{hi}, and HSA^{lo} iCLPs and into $\alpha_4\beta_7^+$ CLPs but will not generate T/ILC-biased progenitors (**Figure 4**).

ROLE OF CYTOKINES IN LYMPHOID COMMITMENT

An Instructive Role of IL-7?

The concomitant expression of *Il7r* and of the B-biased transcripts in CLPs suggested that IL-7 signaling was intimately linked to B cell commitment. Different laboratories have studied a possible instructive role of IL-7 in the choice of a B cell–differentiation pathway in recent years. Adult, but not fetal, B cell development was drastically affected in *Il7*-deficient mice in which B cell progenitors were totally absent in the bone marrow (6 weeks after birth) (100). Consequently,

TSLP: thymic stromal lymphopoietin

these mice showed a reduction of 90% in the number of peripheral B cells, but B1 and marginal zone B cells were overrepresented, suggesting that fetal lymphopoiesis is less dependent on IL-7 signaling than its adult counterpart. Consistent with this notion, CLPs that were reduced in the bone marrow appeared normal in the FL of *Il7*-deficient mice. Only the combined *IL7* and *Flt3l* deficiencies resulted in the virtual absence of FL lymphopoiesis. Altogether, these observations indicated that a strict dependence on IL-7 for B cell production occurs only after the transition from fetal to adult hematopoiesis (around 6 weeks of age) (101, 102).

Instructive versus selective/permissive roles of cytokines in hematopoiesis (103) have been difficult to test because the experimental designs are complex, both instructive and selective processes may coexist, and any of them may predominate at different stages of development (see the sidebar titled Models of Cell Lineage Commitment).

In the absence of IL-7, bone marrow CLPs were reduced in number and most progenitors had lost B cell potential and maintained intact T and NK potential. These results indicate that the absence of IL-7 was affecting not the survival of CLPs but rather the maintenance of the B cell developmental program (104). The lack of B cell potential was accompanied by low levels of expression of *Ebf1*, essential for B lymphopoiesis, and IL-7 signaling regulated the expression of *Ebf1* (105). Consistent with these observations, Ly6D$^+$ bone marrow CLPs (with a B cell–biased differentiation potential) were virtually absent in the bone marrow of *Il7*-deficient mice, and the few remaining cells had multilineage differentiation potential (NK and DC) (106). These experiments suggested that IL-7 signaling regulated the expression of *Ebf1*, thus modulating B cell commitment. Apparently against this notion, a model of *Stat5* deficiency could be complemented with overexpression of the antiapoptotic survival protein BCL2 (107). However, due to the development of an autoimmune syndrome early in life, most mice in this experimental setup were analyzed before 6 weeks of age and, therefore, before the transition to adult hematopoiesis and before lymphopoiesis becomes strictly dependent on IL-7. Moreover, the CRE-recombinase that deleted *Stat5* might not be efficiently expressed in the LMPP-to-CLP transition because it was expressed under the control of the *Rag1* regulatory sequences.

More recently, the analysis of a comprehensive combination of overexpression and inactivation mouse models for *Il7* and *Flt3l* indicated that the latter is important for the expansion and survival of FLT3$^+$ LSK cells whereas the former functions as a survival factor, but not as a growth factor, for *Ebf1*-expressing cells prior to the upregulation of CD19. Only CD19$^+$ B cell progenitors were induced to proliferate when exposed to IL-7 (108). The above experiments suggested that neither of these two factors has a strict inductive role in lineage commitment and highlighted the difficulties in deciphering the mechanisms of action of hematopoietic cytokines in physiologic conditions.

IL-7, but Not FLT3L or TSLP, Determines the Number and the Frequency of Biased CLPs

IL-7 signaling differs in the FL-biased CLP subsets. The B-biased HSA^{hi} iCLPs expressed more IL-7Rα and less KIT than the other subsets and were more efficient in phosphorylating STAT5 after IL-7 stimulation. By contrast, HSA^{lo} and HSA^{int} iCLPs expressed similar levels of IL-7Rα, but the phosphorylation of STAT5 was less efficient in HSA^{int} and barely detectable in T-biased HSA^{lo} iCLPs. Consistent with this, the numbers of B-biased HSA^{hi} iCLPs were severely reduced whereas the number of T-biased HSA^{lo} iCLPs was significantly increased and the total number of iCLPs was unchanged in the absence of IL-7. In the absence of detectable differences in the rate of cell death, these results are suggestive of an instructive rather than a permissive/selective role

of IL-7 in iCLP biased populations. Moreover, although the numbers of unbiased iCLPs were similar to those of wild type, in the absence of IL-7 the frequency of cells expressing the B lineage signature (*Ebf1*) was decreased and that of cells with the T/ILC-biased signature was significantly increased (95).

Although IL-7 might also promote the survival of selected iCLP subsets, two arguments were in favor of an instructive rather than a selective/permissive mechanism of IL-7: (*a*) The two transcriptional signatures in unbiased iCLPs are represented differently, and (*b*) the increase in the absolute numbers of T/ILC-biased iCLPs was associated with the decrease in B-biased iCLPs. In support of this view, unbiased PIRA/B$^-$ iCLPs developed in vitro into $\alpha_4\beta_7{}^+$ and PIRA/B$^+$ CLPs in the absence of IL-7, whereas in its presence, fewer $\alpha_4\beta_7{}^+$ and PIRA/B$^+$ but more HSA^{hi} B-biased iCLPs were generated. No effect in the representation of the biased subsets and of their respective transcriptional signatures was observed in the absence of *Flt3l* compared to wild-type mice or in *Tslp/Il7* double-deficient compared to *Il7*-deficient embryos.

Although the results above argue for a role of IL-7 in controlling FL T/ILC- and B-biased cell numbers, *Il7*-deficient mice have reduced but significant pro-B cell production during fetal and neonatal life. In addition, cells expressing *Ebf1*, although reduced in frequency, were still detected in *Il7*-deficient FL, indicating that IL-7 is not involved in the induction of *Ebf1* expression, but rather in the stabilization and possibly potentiation of the B signature. Consistent with this view, LMPPs from *Il7*-deficient mice upregulated *Ebf1* expression in vitro even in the presence of the JAK3 inhibitor tofacitinib. This result is compatible with the hypothesis that *Ebf1* is induced in CLPs concomitant to the IL-7Rα chain, but independent of IL-7 signaling, in a cell-autonomous manner.

Availability of IL-7 Determines the Presence of T/ILC-Biased CLPs in Fetal Liver

In adult bone marrow, CLPs contain two major subsets, $\alpha_4\beta_7{}^+$, ILC-biased cells that have lost B cell potential (78) and a larger fraction of Ly6D$^+$ (a marker not detected before E15 in FL) B-biased progenitors. Ly6D$^+$ CLPs comprise HSA^{int} and HSA^{hi} CLPs that also generate NK cells but that, similar to HSA^{hi} iCLPs in FL, have poor T cell potential (109, 110). HSA^{lo} iCLPs are not detected in bone marrow, single-cell differentiation potential assays failed to detect T/ILC-biased cells in bone marrow CLPs, and the T/ILC-biased signature defined in FL was not detected in bone marrow. A kinetic analysis indicated that HSA^{lo} iCLPs are frequent between E11 and E14 and are no longer detected by E15 and thereafter (95). By contrast, HSA^{hi} iCLPs are undetectable up to E13 and sharply increase at later developmental stages, following an inverted kinetics. The increased numbers of HSA^{lo} and decreased numbers of HSA^{hi} iCLPs in FL of *Il7*-deficient embryos suggested that the representation of these subsets is directly linked with IL-7 availability. Consistent with this view, IL-7 mRNA expression by FL nonhematopoietic cells was fivefold higher at E15 than at E11. Consistent with this observation, E11 FL showed no detectable B lineage signature expressed in unbiased iCLPs, but more than 50% of these cells expressed the T/ILC-associated transcriptional signature. Therefore, the HSA^{lo} T/ILC-biased compartment is transient, is only present at early stages of FL hematopoietic development, and is strictly associated with IL-7 availability.

Circulating embryonic CLPs are composed of $\alpha_4\beta_7{}^+$, ILC-biased cells and of HSA^{lo}, T/ILC-biased iCLPs that express the highest levels of the chemokine receptor CCR9, which is essential for thymic colonization. The transient population of HSA^{lo} iCLPs that has lost B cell potential could, therefore, represent an embryonic wave of TSPs.

THYMUS COLONIZATION

A First Wave of T/ILC-Restricted Lymphoid Progenitors

After the onset of thymus colonization, the analysis of thymocytes at different developmental stages indicated that at E12 the predominant population expresses c-kit and CD44 but lacks CD25 expression, markers that define early thymic progenitors (ETPs). The majority of E12 ETPs expressed the IL-7Rα chain, FLT3, and low levels of CD24 (HSA^{lo}) (111, 112), thus resembling by phenotype T/ILC-biased HSA^{lo} iCLPs. This population was the first to become undetectable in thymic organ cultures, indicating that in the absence of peripheral input, this is the first subset to get exhausted and, therefore, the first to enter the thymus. Consistent with this view, it was also the first population to decrease in frequency as development progressed in vivo. This population lacked detectable B cell and myeloid differentiation potential and was very efficient in generating T cells, NK cells, and DCs in clonal assays. Altogether, these observations suggest that they were derived from the only subset of progenitors with similar properties, the FL HSA^{lo} iCLPs. Similar to FL and circulating $PIRA/B^{+}HSA^{lo}$ iCLPs that expressed the highest levels of *Ccr9*, virtually all E13 TSPs expressed a FL T/ILC0-biased signature that included *Pira11*, *Cd7*, *Ccr9*, and *Glis3*. In addition, TSPs upregulated *Gata3*, *Tcf7*, *Hes1*, and *Dtx1*, likely the first signs of the activation of the NOTCH signaling pathway (113).

The lack of B and myeloid potential in E13 TSPs could result from the activation of the NOTCH signaling pathway instructing T cell differentiation in a dominant manner. Against this argument is the finding that although the levels of DLL1 and DLL4 increase during development (114), B and myeloid potential are readily detectable in TSPs after E16 (115). Moreover, transcriptional analysis of TSPs from E13 and E18 (see below) indicated that only the latter express Sca-1 (Ly6A) present in LMPPs but absent in FL CLPs (**Supplemental Figure 4**).

Supplemental Material >

Two Waves of Thymus-Settling Progenitors

The first wave of colonizing progenitors is first detected at E12 and persists up to E15, at which time virtually no TSPs can be detected. This wave comprises quickly differentiating cells that do not self-renew and accounts for fewer than 1,000 cells in the mouse (111).

After E16, a new wave of TSPs expresses high levels of Sca-1 (not detected in CLPs); high levels of L-Selectin (CD62L), previously reported to be expressed in adult TSPs (116); and high levels of the undifferentiation marker *Eltd1* (**Supplemental Figure 4**). In addition, they display a robust B and myeloid differentiation potential, indicating that this new wave of TSPs originates from the less-differentiated LMPPs (111, 115). Several properties distinguish the progeny of both waves: (*a*) Only the first wave can generate Vγ5Vδ1 DETC precursors and Vγ6Vδ1 IL-17-producing γδ T cells; (*b*) thymocytes from the first wave do not proliferate extensively but rapidly differentiate into $CD3^{+}$ T cells, whereas those from the second wave undergo several rounds of division before T cell differentiation; and (*c*) the progenitors from the first but not those from the second wave express transcripts related to the ILC pathway of differentiation.

CONCLUDING REMARKS

The picture that emerges indicates that in mammals thymic immigration is not a continuous process but, similar to the process in birds, progresses in waves (117, 118). The results indicating that the initial thymic migrants are lymphoid-restricted progenitors without residual B and myeloid differentiation potential are in line with reports showing embryonic circulating T/NK-restricted progenitors (57) are also found in the spleen (58) and FL (119). These progenitors

can be isolated by their expression of PIRA/B (63) (**Figure 4**). Later in development and after birth, however, T/NK-restricted progenitors are rarely reported and PIRA/B-expressing cells no longer mark restriction to the T cell–differentiation pathway. By contrast, postnatal TSPs are more frequently identified as multipotent cells that retain B and myeloid potential (115, 120, 121).

The finding that the thymus is colonized at the onset of fetal hematopoiesis by a lymphoid progenitor and later by a multipotent cell reconciles most reports in the literature (122). It is, however, not compatible with recent findings indicating that before thymus formation only multipotent cells are found in the vicinity of the thymus anlage (123). This report, however, provides limited evidence that the cells thus characterized are the progenitors of the first T cells.

At present, it is difficult to assess whether the adult thymus is colonized by LMPPs, CLPs, or both, because cells entering the thymus each day are rare (calculated to be five cells) (124) and, therefore, difficult to identify. Several observations favor an adult colonization of the thymus by multipotent LMPPs: (*a*) Thymus colonization by bone marrow LMPPs is more efficient than colonization by CLPs, although Ly6D$^+$ progenitors that are the majority of bone marrow CLPs and are B biased have not been eliminated from the analysis, conferring an obvious advantage to LMPPs (125); (*b*) in contrast to LMPPs, CLPs are not found in circulation (126); and (*c*) adult ETPs have robust myeloid potential (120, 121), although the myeloid differentiation assay was done in the presence of DLL4, which also reveals myeloid potential in bone marrow CLPs that have limited in vivo myeloid contribution (7, 127).

Based on *Il7r* tracing it has been argued that adult CLPs are the TSPs. In that experimental setup, however, a small but sizable fraction of ETPs did not have a history of *Il7r* expression, which would be compatible with LMPPs being the thymus-colonizing cells, if TSPs correspond, as predicted, to less than 10% of DN1 thymocytes (7). The lack, in this report, of an analysis of the TSP compartment precludes a formal conclusion.

The conventional T cells produced by the first wave of TSPs were rapidly outnumbered in vivo by T cells from the second wave (111), indicating that the major contribution from the first TSPs to the immune function is the production of innate T cell subsets and probably ILCs, known to be important in shaping the thymic architecture (128). We propose that the initial phases of the development of the immune system are dominated by hematopoietic progenitors poised to produce ILCs and innate-type cells that follow embryo-specific developmental pathways regulated in an environment characterized by low availability of IL-7 (**Figure 4**). The subsequent phases are characterized by a transition to environments (bone marrow) where cytokine production is stable and where IL-7 availability directs IL-7Rα-expressing cells into the B cell pathway of differentiation. In such an environment, T cell production is ensured by the exit from the bone marrow of LMPPs, prior to IL-7Rα expression, which will colonize the thymus. This will ensure that IL-7 signaling will not impact on thymic progenitors before they enter the thymus and respond to thymic IL-7, which is essential for T cell development. Therefore, the adult CLPs appear devoted to generate B cells and ILCs but not T cells, indicating that CLPs are possibly not the progenitors of all lymphocytes. In this scenario, we hypothesize that ILC differentiation is ensured by an early or strong expression of *Id2* that counterbalances the effects of IL-7 driving B cell differentiation. In embryonic lymphopoiesis, molecular priming and bias to T/ILC pathways occur in LMPPs, indicating that throughout life, T versus B lineage choice takes place in progenitors that are at different stages of differentiation, and therefore it is not a binary choice. It is thus tempting to speculate that the core molecular events that determine the production of embryonic T cells and ILCs occur in LMPPs. Therefore, a better understanding of LMPP phenotypic and transcriptional heterogeneity will be necessary to understand the mechanisms that govern the production of these increasingly important embryonic cell types.

DISCLOSURE STATEMENT

The authors are not aware of any affiliations, memberships, funding, or financial holdings that might be perceived as affecting the objectivity of this review.

ACKNOWLEDGMENTS

We thank members of the A.C. laboratory for many fruitful discussions.

This work was financed by the Pasteur Institute, INSERM, ANR (grant Twothyme) for A.C. and (grant Myeloten) R.G. and by REVIVE Future Investment Program and Pasteur-Weizmann Foundation through grants to A.C. We apologize to all colleagues that contributed to the field and whose work could not be cited here due to limitation in space availability.

LITERATURE CITED

1. Weissman IL, Anderson DJ, Gage F. 2001. Stem and progenitor cells: origins, phenotypes, lineage commitments, and transdifferentiations. *Annu. Rev. Cell Dev. Biol.* 17:387–403
2. Höfer T, Busch K, Klapproth K, Rodewald HR. 2016. Fate mapping and quantitation of hematopoiesis in vivo. *Annu. Rev. Immunol.* 34:449–478
3. Akashi K, Traver D, Miyamoto T, Weissman IL. 2000. A clonogenic common myeloid progenitor that gives rise to all myeloid lineages. *Nature* 404:193–97
4. **Kondo M, Weissman IL, Akashi K. 1997. Identification of clonogenic common lymphoid progenitors in mouse bone marrow. *Cell* 91:661–72**
5. Liu K, Nussenzweig MC. 2010. Origin and development of dendritic cells. *Immunol. Rev.* 234:45–54
6. Traver D, Akashi K, Manz M, Merad M, Miyamoto T, et al. 2000. Development of CD8α-positive dendritic cells from a common myeloid progenitor. *Science* 290:2152–54
7. Schlenner SM, Madan V, Busch K, Tietz A, Läufle C, et al. 2010. Fate mapping reveals separate origins of T cells and myeloid lineages in the thymus. *Immunity* 32:426–36
8. Miyamoto T, Iwasaki H, Reizis B, Ye M, Graf T, et al. 2002. Myeloid or lymphoid promiscuity as a critical step in hematopoietic lineage commitment. *Dev. Cell* 3:137–47
9. Adolfsson J, Borge OJ, Bryder D, Theilgaard-Mönch K, Astrand-Grundström I, et al. 2001. Upregulation of Flt3 expression within the bone marrow $Lin^{-}Sca1^{+}c\text{-}kit^{+}$ stem cell compartment is accompanied by loss of self-renewal capacity. *Immunity* 15:659–69
10. **Adolfsson J, Månsson R, Buza-Vidas N, Hultquist A, Liuba K, et al. 2005. Identification of $Flt3^{+}$ lympho-myeloid stem cells lacking erythro-megakaryocytic potential: a revised road map for adult blood lineage commitment. *Cell* 121:295–306**
11. **Månsson R, Hultquist A, Luc S, Yang L, Anderson K, et al. 2007. Molecular evidence for hierarchical transcriptional lineage priming in fetal and adult stem cells and multipotent progenitors. *Immunity* 26:407–19**
12. Rothenberg EV. 2014. Transcriptional control of early T and B cell developmental choices. *Annu. Rev. Immunol.* 32:283–321
13. Bain G, Robanus Maandag EC, te Riele HP, Feeney AJ, Sheehy A, et al. 1997. Both E12 and E47 allow commitment to the B cell lineage. *Immunity* 6:145–54
14. Lin H, Grosschedl R. 1995. Failure of B-cell differentiation in mice lacking the transcription factor EBF. *Nature* 376:263–67
15. Busslinger M. 2004. Transcriptional control of early B cell development. *Annu. Rev. Immunol.* 22:55–79
16. Koch U, Fiorini E, Benedito R, Besseyrias V, Schuster-Gossler K, et al. 2008. Delta-like 4 is the essential, nonredundant ligand for Notch1 during thymic T cell lineage commitment. *J. Exp. Med.* 205:2515–23
17. Rothenberg EV, Moore JE, Yui MA. 2008. Launching the T-cell-lineage developmental programme. *Nat. Rev. Immunol.* 8:9–21
18. De Obaldia ME, Bhandoola A. 2015. Transcriptional regulation of innate and adaptive lymphocyte lineages. *Annu. Rev. Immunol.* 33:607–42

4. Identification of a restricted lymphoid progenitor in bone marrow.

10. Identification of a progenitor population primed for lymphoid gene expression.

11. Evidence for transcriptional lineage priming in hematopoietic progenitors.

19. Zook EC, Kee BL. 2016. Development of innate lymphoid cells. *Nat. Immunol.* 17:775–82
20. Rodewald HR, Ogawa M, Haller C, Waskow C, DiSanto JP. 1997. Pro-thymocyte expansion by c-kit and the common cytokine receptors γ chain is essential for repertoire formation. *Immunity* 6:265–72
21. Cumano A, Godin I. 2007. Ontogeny of the hematopoietic system. *Annu. Rev. Immunol.* 25:745–85
22. Bertrand JY, Jalil A, Klaine M, Jung S, Cumano A, Godin I. 2005. Three pathways to mature macrophages in the early mouse yolk sac. *Blood* 106:3004–11
23. Gomez Perdiguero E, Klapproth K, Schulz C, Busch K, Azzoni E, et al. 2015. Tissue-resident macrophages originate from yolk-sac-derived erythro-myeloid progenitors. *Nature* 518:547–51
24. Godin I, Cumano A. 2002. The hare and the tortoise: an embryonic haematopoietic race. *Nat. Rev. Immunol.* 2:593–604
25. Böiers C, Carrelha J, Lutteropp M, Luc S, Green JC, et al. 2013. Lymphomyeloid contribution of an immune-restricted progenitor emerging prior to definitive hematopoietic stem cells. *Cell Stem Cell* 13:535–48
26. Cumano A, Dieterlen-Lievre F, Godin I. 1996. Lymphoid potential, probed before circulation in mouse, is restricted to caudal intraembryonic splanchnopleura. *Cell* 86:907–16
27. Medvinsky A, Dzierzak E. 1996. Definitive hematopoiesis is autonomously initiated by the AGM region. *Cell* 86:897–906
28. de Bruijn MF, Speck NA, Peeters MC, Dzierzak E. 2000. Definitive hematopoietic stem cells first develop within the major arterial regions of the mouse embryo. *EMBO J.* 19:2465–74
29. Yoder MC, Hiatt K, Dutt P, Mukherjee P, Bodine DM, Orlic D. 1997. Characterization of definitive lymphohematopoietic stem cells in the day 9 murine yolk sac. *Immunity* 7:335–44
30. Gekas C, Dieterlen-Lièvre F, Orkin SH, Mikkola HK. 2005. The placenta is a niche for hematopoietic stem cells. *Dev. Cell* 8:365–75
31. Caprioli A, Minko K, Drevon C, Eichmann A, Dieterlen-Lièvre F, Jaffredo T. 2001. Hemangioblast commitment in the avian allantois: cellular and molecular aspects. *Dev. Biol.* 238:64–78
32. Bertrand JY, Giroux S, Golub R, Klaine M, Jalil A, et al. 2005. Characterization of purified intraembryonic hematopoietic stem cells as a tool to define their site of origin. *PNAS* 102:134–39
33. Taoudi S, Gonneau C, Moore K, Sheridan JM, Blackburn CC, et al. 2008. Extensive hematopoietic stem cell generation in the AGM region via maturation of VE-cadherin$^+$CD45$^+$ pre-definitive HSCs. *Cell Stem Cell* 3:99–108
34. Samokhvalov IM, Samokhvalova NI, Nishikawa S. 2007. Cell tracing shows the contribution of the yolk sac to adult haematopoiesis. *Nature* 446:1056–61
35. Cumano A, Ferraz JC, Klaine M, Di Santo JP, Godin I. 2001. Intraembryonic, but not yolk sac hematopoietic precursors, isolated before circulation, provide long-term multilineage reconstitution. *Immunity* 15:477–85
36. Kieusseian A, Brunet de la Grange P, Burlen-Defranoux O, Godin I, Cumano A. 2012. Immature hematopoietic stem cells undergo maturation in the fetal liver. *Development* 139:3521–30
37. Müller AM, Medvinsky A, Strouboulis J, Grosveld F, Dzierzak E. 1994. Development of hematopoietic stem cell activity in the mouse embryo. *Immunity* 1:291–301
38. Morrison SJ, Hemmati HD, Wandycz AM, Weissman IL. 1995. The purification and characterization of fetal liver hematopoietic stem cells. *PNAS* 92:10302–6
39. Passegué E, Wagers AJ, Giuriato S, Anderson WC, Weissman IL. 2005. Global analysis of proliferation and cell cycle gene expression in the regulation of hematopoietic stem and progenitor cell fates. *J. Exp. Med.* 202:1599–611
40. Wilson A, Laurenti E, Oser G, van der Wath RC, Blanco-Bose W, et al. 2008. Hematopoietic stem cells reversibly switch from dormancy to self-renewal during homeostasis and repair. *Cell* 135:1118–29
41. Jassinskaja M, Johansson E, Kristiansen TA, Åkerstrand H, Sjöholm K, et al. 2017. Comprehensive proteomic characterization of ontogenic changes in hematopoietic stem and progenitor cells. *Cell Rep.* 21:3285–97
42. Igarashi H, Kouro T, Yokota T, Comp PC, Kincade PW. 2001. Age and stage dependency of estrogen receptor expression by lymphocyte precursors. *PNAS* 98:15131–36

43. Ikuta K, Kina T, MacNeil I, Uchida N, Peault B, et al. 1990. A developmental switch in thymic lymphocyte maturation potential occurs at the level of hematopoietic stem cells. *Cell* 62:863–74
44. Eberl G, Marmon S, Sunshine MJ, Rennert PD, Choi Y, Littman DR. 2004. An essential function for the nuclear receptor RORγt in the generation of fetal lymphoid tissue inducer cells. *Nat. Immunol.* 5:64–73
45. Haas JD, Ravens S, Düber S, Sandrock I, Oberdörfer L, et al. 2012. Development of interleukin-17-producing γδ T cells is restricted to a functional embryonic wave. *Immunity* 37:48–59
46. Hayakawa K, Hardy RR, Herzenberg LA, Herzenberg LA. 1985. Progenitors for Ly-1 B cells are distinct from progenitors for other B cells. *J. Exp. Med.* 161:1554–68
47. Herzenberg LA. 2000. B-1 cells: the lineage question revisited. *Immunol. Rev.* 175:9–22
48. Düber S, Hafner M, Krey M, Lienenklaus S, Roy B, et al. 2009. Induction of B-cell development in adult mice reveals the ability of bone marrow to produce B-1a cells. *Blood* 114:4960–67
49. Lam KP, Rajewsky K. 1999. B cell antigen receptor specificity and surface density together determine B-1 versus B-2 cell development. *J. Exp. Med.* 190:471–77
50. Kristiansen TA, Jaensson Gyllenbäck E, Zriwil A, Björklund T, Daniel JA, et al. 2016. Cellular barcoding links B-1a B cell potential to a fetal hematopoietic stem cell state at the single-cell level. *Immunity* 45:346–57
51. Montecino-Rodriguez E, Fice M, Casero D, Berent-Maoz B, Barber CL, Dorshkind K. 2016. Distinct genetic networks orchestrate the emergence of specific waves of fetal and adult B-1 and B-2 development. *Immunity* 45:527–39
52. Allison JP, Havran WL. 1991. The immunobiology of T cells with invariant γδ antigen receptors. *Annu. Rev. Immunol.* 9:679–705
53. Boyden LM, Lewis JM, Barbee SD, Bas A, Girardi M, et al. 2008. Skint1, the prototype of a newly identified immunoglobulin superfamily gene cluster, positively selects epidermal γδ T cells. *Nat. Genet.* 40:656–62
54. Di Marco Barros R, Roberts NA, Dart RJ, Vantourout P, Jandke A, et al. 2016. Epithelia use butyrophilin-like molecules to shape organ-specific γδ T cell compartments. *Cell* 167:203–18.e17
55. Turchinovich G, Hayday AC. 2011. Skint-1 identifies a common molecular mechanism for the development of interferon-γ-secreting versus interleukin-17-secreting γδ T cells. *Immunity* 35:59–68
56. Mebius RE, Miyamoto T, Christensen J, Domen J, Cupedo T, et al. 2001. The fetal liver counterpart of adult common lymphoid progenitors gives rise to all lymphoid lineages, $CD45^+CD4^+CD3^-$ cells, as well as macrophages. *J. Immunol.* 166:6593–601
57. Rodewald HR, Kretzschmar K, Takeda S, Hohl C, Dessing M. 1994. Identification of pro-thymocytes in murine fetal blood: T lineage commitment can precede thymus colonization. *EMBO J.* 13:4229–40
58. Carlyle JR, Zúñiga-Pflücker JC. 1998. Requirement for the thymus in αβ T lymphocyte lineage commitment. *Immunity* 9:187–97
59. Douagi I, Colucci F, Di Santo JP, Cumano A. 2002. Identification of the earliest prethymic bipotent T/NK progenitor in murine fetal liver. *Blood* 99:463–71
60. Kawamoto H, Ikawa T, Ohmura K, Fujimoto S, Katsura Y. 2000. T cell progenitors emerge earlier than B cell progenitors in the murine fetal liver. *Immunity* 12:441–50
61. Katsura Y. 2002. Redefinition of lymphoid progenitors. *Nat. Rev. Immunol.* 2:127–32
62. Schmitt TM, Zúñiga-Pflücker JC. 2002. Induction of T cell development from hematopoietic progenitor cells by delta-like-1 in vitro. *Immunity* 17:749–56
63. Masuda K, Kubagawa H, Ikawa T, Chen CC, Kakugawa K, et al. 2005. Prethymic T-cell development defined by the expression of paired immunoglobulin-like receptors. *EMBO J.* 24:4052–60
64. Mackarehtschian K, Hardin JD, Moore KA, Boast S, Goff SP, Lemischka IR. 1995. Targeted disruption of the *flk2/flt3* gene leads to deficiencies in primitive hematopoietic progenitors. *Immunity* 3:147–61
65. Sitnicka E, Bryder D, Theilgaard-Mönch K, Buza-Vidas N, Adolfsson J, Jacobsen SEW. 2002. Key role of flt3 ligand in regulation of the common lymphoid progenitor but not in maintenance of the hematopoietic stem cell pool. *Immunity* 17:463–72
66. Noguchi M, Nakamura Y, Russell SM, Ziegler SF, Tsang M, et al. 1993. Interleukin-2 receptor gamma chain: a functional component of the interleukin-7 receptor. *Science* 262:1877–80

63. A subset of fetal liver progenitors identified by a surface marker appears T cell committed.

67. Turner AM, Lin NL, Issarachai S, Lyman SD, Broudy VC. 1996. FLT3 receptor expression on the surface of normal and malignant human hematopoietic cells. *Blood* 88:3383–90
68. Yokota T, Kouro T, Hirose J, Igarashi H, Garrett KP, et al. 2003. Unique properties of fetal lymphoid progenitors identified according to RAG1 gene expression. *Immunity* 19:365–75
69. Yokota T, Huang J, Tavian M, Nagai Y, Hirose J, et al. 2006. Tracing the first waves of lymphopoiesis in mice. *Development* 133:2041–51
70. Sawai CM, Babovic S, Upadhaya S, Knapp DJHF, Lavin Y, et al. 2016. Hematopoietic stem cells are the major source of multilineage hematopoiesis in adult animals. *Immunity* 45:597–609
71. Beaudin AE, Boyer SW, Perez-Cunningham J, Hernandez GE, Derderian SC, et al. 2016. A transient developmental hematopoietic stem cell gives rise to innate-like B and T cells. *Cell Stem Cell* 19:768–83
72. Mebius RE, Streeter PR, Michie S, Butcher EC, Weissman IL. 1996. A developmental switch in lymphocyte homing receptor and endothelial vascular addressin expression regulates lymphocyte homing and permits $CD4^+$ $CD3^-$ cells to colonize lymph nodes. *PNAS* 93:11019–24
73. Yoshida H, Honda K, Shinkura R, Adachi S, Nishikawa S, et al. 1999. IL-7 receptor $alpha^+$ $CD3^-$ cells in the embryonic intestine induces the organizing center of Peyer's patches. *Int. Immunol.* 11:643–55
74. Yoshida H, Kawamoto H, Santee SM, Hashi H, Honda K, et al. 2001. Expression of $\alpha_4\beta_7$ integrin defines a distinct pathway of lymphoid progenitors committed to T cells, fetal intestinal lymphotoxin producer, NK, and dendritic cells. *J. Immunol.* 167:2511–21
75. Pereira de Sousa A, Berthault C, Granato A, Dias S, Ramond C, et al. 2012. Inhibitors of DNA binding proteins restrict T cell potential by repressing Notch1 expression in Flt3-negative common lymphoid progenitors. *J. Immunol.* 189:3822–30
76. Karsunky H, Inlay MA, Serwold T, Bhattacharya D, Weissman IL. 2008. $Flk2^+$ common lymphoid progenitors possess equivalent differentiation potential for the B and T lineages. *Blood* 111:5562–70
77. Spits H, Artis D, Colonna M, Diefenbach A, Di Santo JP, et al. 2013. Innate lymphoid cells—a proposal for uniform nomenclature. *Nat. Rev. Immunol.* 13:145–49
78. Possot C, Schmutz S, Chea S, Boucontet L, Louise A, et al. 2011. Notch signaling is necessary for adult, but not fetal, development of $ROR\gamma t^+$ innate lymphoid cells. *Nat. Immunol.* 12:949–58
79. Cherrier M, Sawa S, Eberl G. 2012. Notch, Id2, and RORγt sequentially orchestrate the fetal development of lymphoid tissue inducer cells. *J. Exp. Med.* 209:729–40
80. Klose CSN, Flach M, Möhle L, Rogell L, Hoyler T, et al. 2014. Differentiation of type 1 ILCs from a common progenitor to all helper-like innate lymphoid cell lineages. *Cell* 157:340–56
81. Constantinides MG, McDonald BD, Verhoef PA, Bendelac A. 2014. A committed precursor to innate lymphoid cells. *Nature* 508:397–401
82. Yokota Y, Mansouri A, Mori S, Sugawara S, Adachi S, et al. 1999. Development of peripheral lymphoid organs and natural killer cells depends on the helix-loop-helix inhibitor Id2. *Nature* 397:702–6
83. Yang Q, Li F, Harly C, Xing S, Ye L, et al. 2015. TCF-1 upregulation identifies early innate lymphoid progenitors in the bone marrow. *Nat. Immunol.* 16:1044–50
84. Mielke LA, Groom JR, Rankin LC, Seillet C, Masson F, et al. 2013. TCF-1 controls ILC2 and $NKp46^+ROR\gamma t^+$ innate lymphocyte differentiation and protection in intestinal inflammation. *J. Immunol.* 191:4383–91
85. Yagi R, Zhong C, Northrup DL, Yu F, Bouladoux N, et al. 2014. The transcription factor GATA3 is critical for the development of all IL-7Rα-expressing innate lymphoid cells. *Immunity* 40:378–88
86. Serafini N, Klein Wolterink RG, Satoh-Takayama N, Xu W, Vosshenrich CA, et al. 2014. Gata3 drives development of $ROR\gamma t^+$ group 3 innate lymphoid cells. *J. Exp. Med.* 211:199–208
87. Aliahmad P, de la Torre B, Kaye J. 2010. Shared dependence on the DNA-binding factor TOX for the development of lymphoid tissue-inducer cell and NK cell lineages. *Nat. Immunol.* 11:945–52
88. Seillet C, Mielke LA, Amann-Zalcenstein DB, Su S, Gao J, et al. 2016. Deciphering the innate lymphoid cell transcriptional program. *Cell Rep.* 17:436–47
89. Ishizuka IE, Chea S, Gudjonson H, Constantinides MG, Dinner AR, et al. 2016. Single-cell analysis defines the divergence between the innate lymphoid cell lineage and lymphoid tissue-inducer cell lineage. *Nat. Immunol.* 17:269–76

78. Innate lymphoid cells derive from common lymphoid progenitors through a Notch-independent mechanism.

90. Chea S, Schmutz S, Berthault C, Perchet T, Petit M, et al. 2016. Single-cell gene expression analyses reveal heterogeneous responsiveness of fetal innate lymphoid progenitors to Notch signaling. *Cell Rep.* 14:1500–16
91. Chea S, Perchet T, Petit M, Verrier T, Guy-Grand D, et al. 2016. Notch signaling in group 3 innate lymphoid cells modulates their plasticity. *Sci. Signal* 9:ra45
92. Bando JK, Liang HE, Locksley RM. 2015. Identification and distribution of developing innate lymphoid cells in the fetal mouse intestine. *Nat. Immunol.* 16:153–60
93. Cherrier DE, Serafini N, Di Santo JP. 2018. Innate lymphoid cell development: a T cell perspective. *Immunity* 48:1091–103
94. Lai AY, Kondo M. 2008. T and B lymphocyte differentiation from hematopoietic stem cell. *Semin. Immunol.* 20:207–12
95. Berthault C, Ramond C, Burlen-Defranoux O, Soubigou G, Chea S, et al. 2017. Asynchronous lineage priming determines commitment to T cell and B cell lineages in fetal liver. *Nat. Immunol.* 18:1139–49
96. Lee DM, Schanberg LE, Fleenor DE, Seldin MF, Haynes BF, Kaufman RE. 1996. The mouse CD7 gene: identification of a new element common to the human CD7 and mouse Thy-1 promoters. *Immunogenetics* 44:108–14
97. Uehara S, Grinberg A, Farber JM, Love PE. 2002. A role for CCR9 in T lymphocyte development and migration. *J. Immunol.* 168:2811–19
98. Desanti GE, Jenkinson WE, Parnell SM, Boudil A, Gautreau-Rolland L, et al. 2011. Clonal analysis reveals uniformity in the molecular profile and lineage potential of $CCR9^{+}$ and $CCR9^{-}$ thymus-settling progenitors. *J. Immunol.* 186:5227–35
99. Ikawa T, Kawamoto H, Goldrath AW, Murre C. 2006. E proteins and Notch signaling cooperate to promote T cell lineage specification and commitment. *J. Exp. Med.* 203:1329–42
100. Carvalho TL, Mota-Santos T, Cumano A, Demengeot J, Vieira P. 2001. Arrested B lymphopoiesis and persistence of activated B cells in adult interleukin $7^{-/-}$ mice. *J. Exp. Med.* 194:1141–50
101. Vosshenrich CA, Cumano A, Müller W, Di Santo JP, Vieira P. 2004. Pre-B cell receptor expression is necessary for thymic stromal lymphopoietin responsiveness in the bone marrow but not in the liver environment. *PNAS* 101:11070–75
102. Sitnicka E, Brakebusch C, Martensson IL, Svensson M, Agace WW, et al. 2003. Complementary signaling through flt3 and interleukin-7 receptor alpha is indispensable for fetal and adult B cell genesis. *J. Exp. Med.* 198:1495–506
103. Rieger MA, Hoppe PS, Smejkal BM, Eitelhuber AC, Schroeder T. 2009. Hematopoietic cytokines can instruct lineage choice. *Science* 325:217–18
104. Dias S, Silva H Jr., Cumano A, Vieira P. 2005. Interleukin-7 is necessary to maintain the B cell potential in common lymphoid progenitors. *J. Exp. Med.* 201:971–79
105. Kikuchi K, Lai AY, Hsu C-L, Kondo M. 2005. IL-7 receptor signaling is necessary for stage transition in adult B cell development through up-regulation of EBF. *J. Exp. Med.* 201:1197–203
106. Tsapogas P, Zandi S, Åhsberg J, Zetterblad J, Welinder E, et al. 2011. IL-7 mediates Ebf-1-dependent lineage restriction in early lymphoid progenitors. *Blood* 118:1283–90
107. Malin S, McManus S, Cobaleda C, Novatchkova M, Delogu A, et al. 2010. Role of STAT5 in controlling cell survival and immunoglobulin gene recombination during pro-B cell development. *Nat. Immunol.* 11:171–79
108. von Muenchow L, Alberti-Servera L, Klein F, Capoferri G, Finke D, et al. 2016. Permissive roles of cytokines interleukin-7 and Flt3 ligand in mouse B-cell lineage commitment. *PNAS* 113:E8122–30
109. Inlay MA, Bhattacharya D, Sahoo D, Serwold T, Seita J, et al. 2009. Ly6d marks the earliest stage of B-cell specification and identifies the branchpoint between B-cell and T-cell development. *Genes Dev.* 23:2376–81
110. Mansson R, Zandi S, Welinder E, Tsapogas P, Sakaguchi N, et al. 2010. Single-cell analysis of the common lymphoid progenitor compartment reveals functional and molecular heterogeneity. *Blood* 115:2601–9

95. Asynchronous B and T cell transcriptional priming determines lineage divergence in fetal liver.

111. Ramond C, Berthault C, Burlen-Defranoux O, de Sousa AP, Guy-Grand D, et al. 2014. Two waves of distinct hematopoietic progenitor cells colonize the fetal thymus. *Nat. Immunol.* 15:27–35

112. Porritt HE, Rumfelt LL, Tabrizifard S, Schmitt TM, Zúñiga-Pflücker JC, Petrie HT. 2004. Heterogeneity among DN1 prothymocytes reveals multiple progenitors with different capacities to generate T cell and non-T cell lineages. *Immunity* 20:735–45

113. Weber BN, Chi AW, Chavez A, Yashiro-Ohtani Y, Yang Q, et al. 2011. A critical role for TCF-1 in T-lineage specification and differentiation. *Nature* 476:63–68

114. Abramson J, Anderson G. 2017. Thymic epithelial cells. *Annu. Rev. Immunol.* 35:85–118

115. Luc S, Luis TC, Boukarabila H, Macaulay IC, Buza-Vidas N, et al. 2012. The earliest thymic T cell progenitors sustain B cell and myeloid lineage potential. *Nat. Immunol.* 13:412–19

116. Perry SS, Wang H, Pierce LJ, Yang AM, Tsai S, Spangrude GJ. 2004. L-selectin defines a bone marrow analog to the thymic early T-lineage progenitor. *Blood* 103:2990–96

117. Coltey M, Jotereau FV, Le Douarin NM. 1987. Evidence for a cyclic renewal of lymphocyte precursor cells in the embryonic chick thymus. *Cell Differ.* 22:71–82

118. Jotereau FV, Le Douarin NM. 1982. Demonstration of a cyclic renewal of the lymphocyte precursor cells in the quail thymus during embryonic and perinatal life. *J. Immunol.* 129:1869–77

119. Douagi I, Vieira P, Cumano A. 2002. Lymphocyte commitment during embryonic development, in the mouse. *Semin. Immunol.* 14:361–69

120. Bell JJ, Bhandoola A. 2008. The earliest thymic progenitors for T cells possess myeloid lineage potential. *Nature* 452:764–67

121. Wada H, Masuda K, Satoh R, Kakugawa K, Ikawa T, et al. 2008. Adult T-cell progenitors retain myeloid potential. *Nature* 452:768–72

122. Bhandoola A, von Boehmer H, Petrie HT, Zúñiga-Pflücker JC. 2007. Commitment and developmental potential of extrathymic and intrathymic T cell precursors: plenty to choose from. *Immunity* 26:678–89

123. Luis TC, Luc S, Mizukami T, Boukarabila H, Thongjuea S, et al. 2016. Initial seeding of the embryonic thymus by immune-restricted lympho-myeloid progenitors. *Nat. Immunol.* 17:1424–35

124. Ceredig R, Bosco N, Rolink AG. 2007. The B lineage potential of thymus settling progenitors is critically dependent on mouse age. *Eur. J. Immunol.* 37:830–37

125. Allman D, Sambandam A, Kim S, Miller JP, Pagan A, et al. 2003. Thymopoiesis independent of common lymphoid progenitors. *Nat. Immunol.* 4:168–74

126. Schwarz BA, Bhandoola A. 2004. Circulating hematopoietic progenitors with T lineage potential. *Nat. Immunol.* 5:953–60

127. Richie Ehrlich LI, Serwold T, Weissman IL. 2011. In vitro assays misrepresent in vivo lineage potentials of murine lymphoid progenitors. *Blood* 117:2618–24

128. Roberts NA, White AJ, Jenkinson WE, Turchinovich G, Nakamura K, et al. 2012. Rank signaling links the development of invariant γδ T cell progenitors and Aire^{+} medullary epithelium. *Immunity* 36:427–37

129. Nutt SL, Heavey B, Rolink AG, Busslinger M. 1999. Commitment to the B-lymphoid lineage depends on the transcription factor Pax5. *Nature* 401:556–62

130. Pereira P, Boucontet L, Cumano A. 2012. Temporal predisposition to αβ and γδ T cell fates in the thymus. *J. Immunol.* 188:1600–8

131. Hoppe PS, Schwarzfischer M, Loeffler D, Kokkaliaris KD, Hilsenbeck O, et al. 2016. Early myeloid lineage choice is not initiated by random PU.1 to GATA1 protein ratios. *Nature* 535:299–302

132. Teschendorff AE, Enver T. 2017. Single-cell entropy for accurate estimation of differentiation potency from a cell's transcriptome. *Nat. Commun.* 8:15599

133. Ferrell JE. 2012. Bistability, bifurcations, and Waddington's epigenetic landscape. *Curr. Biol.* 22:R458–66

111. In the mouse embryo the thymus is colonized by two different waves of hematopoietic progenitors.

115. Neonatal thymus–settling cells are multipotent lympho-myeloid-primed progenitors.

Annual Review of Immunology
Volume 37, 2019

Contents

Sixty Years of Discovery
David Baltimore 1

Neuro–Immune Cell Units: A New Paradigm in Physiology
Cristina Godinho-Silva, Filipa Cardoso, and Henrique Veiga-Fernandes 19

Tuft Cells—Systemically Dispersed Sensory Epithelia Integrating Immune and Neural Circuitry
Claire E. O'Leary, Christoph Schneider, and Richard M. Locksley 47

Neuroinflammation During RNA Viral Infections
Robyn S. Klein, Charise Garber, Kristen E. Funk, Hamid Salimi, Allison Soung, Marlene Kanmogne, Sindhu Manivasagam, Shannon Agner, and Matthew Cain 73

Antigen Receptor Function in the Context of the Nanoscale Organization of the B Cell Membrane
Michael R. Gold and Michael G. Reth 97

The Platelet Napoleon Complex—Small Cells, but Big Immune Regulatory Functions
Craig N. Morrell, Daphne N. Pariser, Zachary T. Hilt, and Denisse Vega Ocasio 125

Emerging Cellular Therapies for Cancer
Sonia Guedan, Marco Ruella, and Carl H. June 145

Cancer Neoantigens
Ton N. Schumacher, Wouter Scheper, and Pia Kvistborg 173

Origin, Organization, Dynamics, and Function of Actin and Actomyosin Networks at the T Cell Immunological Synapse
John A. Hammer, Jia C. Wang, Mezida Saeed, and Antonio T. Pedrosa 201

The Antibody Response to *Plasmodium falciparum*: Cues for Vaccine Design and the Discovery of Receptor-Based Antibodies
Joshua Tan, Luca Piccoli, and Antonio Lanzavecchia 225

Self-Awareness: Nucleic Acid–Driven Inflammation and the Type I Interferonopathies
Carolina Uggenti, Alice Lepelley, and Yanick J. Crow 247

The Myeloid Cell Compartment—Cell by Cell
Kevin Bassler, Jonas Schulte-Schrepping, Stefanie Warnat-Herresthal, Anna C. Aschenbrenner, and Joachim L. Schultze 269

Fine-Tuning Cytokine Signals
Jian-Xin Lin and Warren J. Leonard 295

Purine Release, Metabolism, and Signaling in the Inflammatory Response
Joel Linden, Friedrich Koch-Nolte, and Gerhard Dahl 325

Double-Stranded RNA Sensors and Modulators in Innate Immunity
Sun Hur 349

The Microbiome and Food Allergy
Onyinye I. Iweala and Cathryn R. Nagler 377

Disease Tolerance as an Inherent Component of Immunity
Rui Martins, Ana Rita Carlos, Faouzi Braza, Jessica A. Thompson, Patricia Bastos-Amador, Susana Ramos, and Miguel P. Soares 405

Nonclassical Monocytes in Health and Disease
Prakash Babu Narasimhan, Paola Marcovecchio, Anouk A.J. Hamers, and Catherine C. Hedrick 439

CD8 T Cell Exhaustion During Chronic Viral Infection and Cancer
Laura M. McLane, Mohamed S. Abdel-Hakeem, and E. John Wherry 457

New Molecular Insights into Immune Cell Development
Ana Cumano, Claire Berthault, Cyrille Ramond, Maxime Petit, Rachel Golub, Antonio Bandeira, and Pablo Pereira 497

Tissue-Resident T Cells and Other Resident Leukocytes
David Masopust and Andrew G. Soerens 521

Using T Cell Receptor Repertoires to Understand the Principles of Adaptive Immune Recognition
Philip Bradley and Paul G. Thomas 547

CRISPR-Based Tools in Immunity
Dimitre R. Simeonov and Alexander Marson 571

Gut Microbiota Regulation of T Cells During Inflammation and Autoimmunity
Eric M. Brown, Douglas J. Kenny and Ramnik J. Xavier 599